TN
690
.P94
v.9
c.1

PROGRESS IN MATERIALS SCIENCE

Incorporating

Progress in Metal Physics Volumes 1 - 8

Volume 9

Editor

BRUCE CHALMERS, D.Sc., Ph.D.

Division of Engineering and Applied Physics, Harvard University,
Cambridge, Mass., U.S.A.

PERGAMON PRESS

OXFORD . LONDON . NEW YORK . PARIS

1961

PERGAMON PRESS LTD.
Headington Hill Hall, Oxford
4 & 5 *Fitzroy Square, London, W.*1
PERGAMON PRESS INC.
122 *East 55th Street, New York* 22, *N.Y.*
1404 *New York Avenue N.W., Washington* 5, *D.C.*
PERGAMON PRESS S.A.R.L.
24 *Rue des Écoles, Paris V^e^*
PERGAMON PRESS G.m.b.H.
Kaiserstrasse 75, *Frankfurt-am-Main*

VOL.
9
1961

Copyright
©
1961
PERGAMON PRESS LTD.

Library of Congress Card Number 49–50107

Set in Times New Roman 10/12pt. and
made and printed in Great Britain at Page Bros. (Norwich) Ltd.

CONTENTS

PAGE

1. NUCLEAR MAGNETIC RESONANCE IN METALS 1

T. J. Rowland
Metals Research Laboratories,
Union Carbide Metals Company,
Niagara Falls, New York.

2. THE EFFECT OF TEMPERATURE AND ALLOYING ADDITIONS ON THE DEFORMATION OF METAL CRYSTALS 93

R. W. K. Honeycombe
Department of Metallurgy,
University of Sheffield, England.

3. EFFECTS OF ENVIRONMENT ON MECHANICAL PROPERTIES OF METALS 131

Irvin R. Kramer
Martin Company, Baltimore, Maryland.
and *Louis J. Demer.*
University of Arizona, Tucson, Arizona.

4. THE HYDROGEN EMBRITTLEMENT OF METALS 201

P. Cotterill
Metallurgy Department
Battersea College of Technology, London.

5. THE STRUCTURE AND PROPERTIES OF SOLID SOLUTIONS .. 305

J. M. Sivertsen and M. E. Nicholson
Department of Metallurgy,
University of Minnesota.

CONTENTS OF PREVIOUS VOLUMES IN THE PROGRESS IN METAL PHYSICS SERIES

AUTHOR INDEX 379

SUBJECT INDEX 387

VOL.
9
1961

AUTHORS' INDEX

ABELL, D. F. 90
ABOAV, D. A. 96, 97, 115, 127
ACHTER, M. P. 191, 192, 199
ADAMS, M. A. 108, 115, 122, 128, 143, 144, 149, 150, 196
AKSENOV, S. I. 90
ALBRECHT, W. H. 260, 300
ALEXANDER, B. H. 129
ALFRED, L. 377
ALLEN, K. A. 198
ALLEN, N. P. 100, 101, 121, 128
ANDERSON, A. G. 89, 91
ANDERSON, J. S. 267, 268, 300
ANDRADE, E. N. DA C. 96, 97, 111, 112, 115, 127, 128, 133, 138, 145, 149, 157, 177, 179, 180, 181, 185, 196, 197, 198, 199
ANDREW, E. R. 76, 86, 89
ANDREW, K. F. 260, 299, 300
ANDROES, G. M. 87, 91
ANTAL, J. 375
ARDLEY, G. W. 125, 129
ARMBRUSTER, M. 230, 298
ARP, V. 89
ATKINSON, H. 350, 377
AUBMANN, A. B. 198
AVERBACH, B. L. 298, 323, 324, 325, 326 *n.*, 329, 330, 331, 333, 343, 344, 345, 346, 347, 348, 349, 374, 375, 377
AVERBUCH, P. 83, 90
AXON, H. 326, 327, 328, 375
AZOU, D. 235, 299

BACON, G. 378
BAKARIAN, P. W. 120, 129
BALDWIN, W. M. JR. 163, 164, 197, 257, 276, 278, 279, 283, 300
BARDEEN, J. 23, 87
BARNES, R. 377
BARNES, R. G. 91
BARNETT, W. J. 299
BARRER, R. M. 297
BARRETT, C. S. 89, 120, 128, 161, 162, 197, 337, 338, 376
BARSON, F. 377
BASINSKI, Z. S. 114, 115, 120, 122, 129
BASTIEN, D. 235, 299
BATTERMAN, 351 *n.*
BEAVER, W. W. 198
BECHOLD, J. H. 298
BECK, P. 356, 377
BECKMAN, 362
BEERWALD, A. 165, 198
BEEVERS, C. J. 130
BEHRINGER, R. E. 89
BELL, R. L. 121, 129
BELL, W. A. 299
BENEDEK, G. B. 88
BENEDICKS, C. 190, 199
BENNETT, D. G. 197
BENNETT, J. A. 197
BENNETT, W. D. G. 299
BENNINGER, H. H. 197
BENTON, A. F. 211, 298
BERGER, A. G. 90
BERGER, L. W. 250, 299
BERGNER, E. 276, 300
BERSOHN, R. 88
BETHE, 305
BEVINGTON, C. F. D. 300
BIBB, A. E. 301
BILBY, B. A. 127, 144, 196, 229, 298, 341, 376
BIOLOBZHESKII, A. V. 197
BIONDI, M. A. 87
BENEDEK, G. B. 87
BLACHMAN, A. G. 91
BLAKEY, R. E. 267, 268, 300
BLANDIN, A. 40, 82, 88, 90
BLEWITT, T. 377
BLEWITT, T. H. 115, 128
BLIN, J. 374
BLIN-STOYLE, R. J. 89
BLOCH, F. 70, 77, 86
BLOEMBERGEN, N. 22, 44, 46, 49, 58, 67, 68, 72, 76, 78, 79, 85, 86, 87, 88, 89, 90, 378
BLUMBERG, W. E. 82, 90
BOAS, W. 99, 118, 127, 129
BOHM, H. V. 87, 323
BOLEF, D. I. 89
BOLLMANN, 338
BORIE, B. 330
BORISOV, V. S. 197
BOUTON, G. M. 197
BRADSHAW, F. 343, 377
BRAGDON, R. W. 299
BRAGG, L. 333, 375
BRAME, D. R. 152, 153, 197
BRICK, R. M. 100, 121, 129, 130, 165, 198
BRICOT, I. 123, 129

BROOKS, 2. 37
BROOKS, H. 336, 375
BROWN, D. F. 119, 128, 151, 196
BROWN, J. T. 257, 300
BROWN, R. M. 89
BROWNE, M. 88, 89
BRUEGGEMAN, W. C. 198
BRUNIG, K. 277, 300
BURGESS, J. H. 89
BURKE, E. C. 120, 129
BURKE, J. E. 90, 300
BURTE, H. M. 253, 255, 256, 299, 300
BUTTERWORTH, J. 82, 90
BUZZARD, R. W. 299

CABBLE, G. M. JR. 197
CAHN, R. W. 121, 124, 129
CARLSEN, K. M. 125, 129
CARNEY, D. 299
CARRUTHERS, R. C. 298
CARVER, T. R. 74, 87, 89
CATALANO, E. 88
CHALMERS, B. 137, 152, 196, 197
CHANG, H. C. 222, 223, 298
CHANG, P. L. 299
CHAPMAN, A. C. 63, 72, 88, 89
CHEN, N. K. 101, 129, 162, 197
CHENG, C. 355, 377
CHIOU, C. 126, 127, 130
CHURCHMAN, A. T. 100, 119, 129
CLAREBROUGH, 95 *n.*, 111 *n.*
CLARK, D. S. 109, 129
CLARKE, D. S. 298
CLAUSS, A. 192, 199, 279, 300
CLEAVES, H. E. 299
CLOGSTON, D. M. 90
COCHARDT, A. 341, 374
COCHARDT, A. W. 162, 163, 197
COFFIN, F. D. 160, 197
COHEN, M. 33, 66, 68, 88, 322, 325, 333, 338, 359, 373, 375, 376
COHEN, M. H. 38, 88, 90
COLE, H. 377
COLES, B. R. 89, 365, 370, 377
COLTMAN, R. R. 115, 128
CONRAD, H. 99, 100, 116, 117, 122, 128, 129
COOPER, L. N. 23, 87
COOPER, W. A. 168, 198
CORVILLE, N. L. 298
COTTRELL, A. H. 89, 108, 109, 113, 114, 115, 122, 124, 128, 129, 135, 136, 137, 144, 150, 181, 182, 183, 184, 185, 196, 226, 228, 229, 298, 301, 335, 336, 340, 341, 342, 376
COTTRELL, C. L. M. 299
COX, J. J. 101, 121, 130
CRACKNELL, A. 299
CRAIGHEAD, C. M. 242, 246, 251, 254, 255, 256, 259, 283, 299
CRITTENDEN, E. C. 87
CRUSSARD, C. 332, 375
CUBICCIOTTI, D. 300
CUPP, C. R. 206, 297
CURRAN, J. K. 197
CUTHILL, J. R. 160, 197

DANNE, A. 377
DARKEN, L. S. 377
DAS, M. P. 88
DAS, T. P. 91
DAVIES, W. 267, 270, 271, 272, 273, 274, 275, 374
DAVIS, R. S. 152, 197
DAVIS, W. 374
DEANE, A. H. 300
DE BERGEUIN, F. 90
DE GENNES, H. 276
DEKARTOVA, 198
DE KAZINSKY, F. 234, 235, 238, 299
DEMARCO, J. J. 351, 352, 377
DEMER, L. J. 188, 189, 199
DE MORTON, M. E. 235, 236, 299
DENT, B. M. 166, 198
DERUYTERRE, A. 118, 129
DESORBO, 343 *n.*
DEXTER, D. L. 335, 376
DICKINSON, W. C. 86
DIEHL, J. 96, 98, 111, 115, 128
DIENES, G. 377
DOBRY, A. 169, 198
DOLAN, T. J. 197
DOWNING, J. 333
DRAIN, L. E. 38, 87
DUBE, C. A. 129
DUBRISSAY, R. 169, 198
DUMUR, I. 378
DUPRE, A. 165, 198
DUSHMAN, S. 208, 276, 277, 284, 297

EASTWOOD, L. W. 297
EDELSON, B. I. 162, 197
EDWARDS, J. O. 198
EDWARDS, R. K. 300, 333
EDWARDSON, STURE, 102, 103, 128
EISINGER, J. 90
ELCOCK, E. 356, 377
ELLINGER, F. 268, 300
ELLIOTT, H. A. 221, 298
ELLIOTT, J. 368, 377
ENGARDT, R. D. 91
ESHELBY, J. D. 89, 223, 298, 327, 332, 375
EVANS, E. 372, 375
EVANS, T. 152, 153, 197
EYRING, H. 210, 298

VOL.
9
1961

FAHRENHORST, W. 118, 129
FAST, J. D. 207, 217, 218, 297
FEDERIGHI, 343 *n.*
FEHER, G. 87
FELD, B. 88
FELTHAM, P. 114, 120, 128
FERGUSON, L. 197
FERMI, E. 87
FISHER, J. C. 108, 128, 134, 196
FISHER, J. E. 126, 129, 342, 376
FLEISCHER, R. L. 137, 196
FLINN, P. 348, 372, 375
FLYNN, C. P. 90
FORESTIER, H. 192, 199, 279, 300
FORM, G. W. 163, 164, 197
FORRESTER, A. T. 87
FORT, T. 198
FOWLER, R. H. 210, 298
FOX, H. W. 192, 199
FRANK, F. C. 223, 298
FRANKENBURG, W. G. 211, 297
FRICKE, W. G. JR. 198
FRIEDEL, J. 37, 82, 88, 90, 106, 111, 115, 128, 309, 311, 312, 313, 314, 315, 316, 318, 319, 321, 322, 327, 332 333, 368, 374, 375, 378
FROHLICH, F. 88
FROST, B. R. T. 300
FROST, P. D. 300
FUMI, F. 335, 375

GAGER, W. B. 90
GARFUNKEL, M. P. 87
GARSTENS, M. A. 89
GARSTONE, J. 97, 98, 103, 106, 108, 112, 114, 123, 128, 140, 141, 148, 196
GATES, J. E. 300
GAYLER, M. L. 376
GEIBEL, 362
GEIL, G. W. 298
GENSAMER, M. 133, 154, 196, 197
GERRITSEN, A. 367, 378
GIBB, F. D. R. 299
GIBB, P. D. R. 299, 300
GIBBONS, D. F. 136, 196
GIBBS, J. W. 166, 167. 198
GILMAN, J. J. 100, 121, 128, 129, 133, 139, 140, 144, 145, 146, 147, 150, 151, 152, 154, 159, 196, 197, 224, 225, 298
GLADSTONE, S. 210, 298
GLEN, J. W. 133, 196
VON GÖLER, F. 102, 103, 124, 128
GOODINGS, D. A. 90
GORTER, G. J. 78, 87
GORYUNOV, YU, V. 198
GOSSARD, A. C. 80, 90
GOTTA, A. 300
GOUGH, H. J. 191, 198, 199
GRAHAM, T. P. 91
GRANT, N. J. 222, 223, 298, 299
GREENOUGH, G. B. 118, 129, 154, 155, 197
GREENWOOD, G. W. 224, 298
GREENWOOD, J. NEILL, 191, 199
GREETHAM, G. 112, 114, 123, 125, 126, 129, 140, 141, 148, 196
GRIFFITHS, A. A. 220, 221, 234, 298
GRISWOLD, T. W. 89
GRIVET, D. 89
GROUER, H. J. 198
GUERON, J. 300
GUINIER, A. 374
GULBRANSEN, E. A. 260, 299, 300
GUTOWSKY, H. S. 48, 86, 87

HAASEN, P. 96, 97, 115, 116, 122, 127
HAESZNER, F. 123, 129
HAGEN, H. 300
HÄGG, R. M. 241, 260, 299, 300
HAHN, E. L. 78, 86, 88
HALL, E. O. 199
HALL, M. N. A. 261, 300
HAMMOND, R. A. F. 197
HAMMOND, R. H. 87, 88
HANCOCK, N. 377
HANNA, S. S. 90
HANSEN, W. W. 70, 86
HARE, E. F. 199
HARGREAVES, 95 *n.*, 111 *n.*
HARPER, S. 136, 137, 181, 182, 183, 184, 185, 196
HARRISON, W. N. 160, 197
HART, E. W. 126, 129, 342, 376
HARVEY, W. E. 197
HARWELL, R. H. 198
HASLEM, M. E. 198
HASS, W. P. A. 91
HEAD, A. K. 138, 153, 196
HEBEL, L. C. 24, 87
HEBERLE, J. 90
HEINE, V. 23, 38, 87, 88, 90, 91, 373, 375, 376
HEITLER, W. 78, 90
HENDERSON, C. 97, 111, 112, 128, 138, 145, 150, 196
HENRY, W. 316, 375, 377
HERBSTEIN, F. 330 *n.*, 345, 347, 349, 377
HERRING, C. 87, 198
HEWITT, R. R. 87, 90
HIBBARD, W. R. 120, 124, 129
HILTON-SMITH, 169, 187
HINTON, K. 378
HIRSCH, P. B. 114 *n.*, 122, 127, 128, 130, 338, 342, 350, 377
HOARE, F. E. 87, 356, 359, 377
HOBSON, J. D. 299
HOFER, 298

HOGAN, H. L. 197
HOLCOMB, D. F. 48, 78, 89
HOLMES, D. 377
HONEYCOMBE, R. W. K. 97, 98, 103, 106, 108, 112, 114, 119, 123, 125, 128, 129, 130, 140, 141, 148, 151, 196
HOPKINS, B. E. 100, 128
HORNE, G. T. 101, 130, 338
HOWELL, F. M. 197
HROSTOWSKI, H. J. 88
HUANG, K. 316, 330, 375
HUBER, H. 300
HUBER, O. J. 300
HUGHES, D. G. 91
HULTGREN, R. 333
HULTSCH, R. A. 91
HUME-ROTHERY, W. 89, 219, 281, 291, 298, 305, 306, 310, 312, 313, 326, 327, 328, 331, 374, 375
HUNTER, M. S. 198
HUNTER, S. C. 89, 376
HURD, D. T. 298

INGLIS, C. E. 220, 298

JACCARINO, V. 90
JACKSON, L. R. 198
JACOBS, I. 372, 378
JAFFEE, R. I. 242, 244, 246, 250, 251, 254, 255, 256, 259, 283, 299, 300
JAMESON, R. E. 104, 105, 106, 128
JAMES, J. H. 198
JAOUL, B. 123, 129
JAUMOT, F. 376
JEFFREY, H. 119, 129
JEFFRIES, C. D. 86
JENNINGS, L. 377
JILLSON, D. C. 96, 129
JOFFÉ, A. F. 136, 196
JOHNS, I. S. 300
JOHNSON, H. H. 236, 237, 239, 255, 258, 280, 293, 295, 299.
JOHNSON, R. P. 343 *n.*
JOHSON, O. 300
JONES, H. 34, 38. 88, 90, 305, 312, 313, 331 *n.*, 359 *n.*, 374
JONES, R. V. 90
JONES, W. H. JR. 91

KAMBE, K. 68, 89
KAMINOW, I. P. 90
KARNOP, R. 125, 129
KARPENKO, G. V. 133, 198
KASUYA, T. 365, 377
KAUFFMAN, J. 374
KAUFMANN, A. R. 121, 129
KAWAKAMI, M. 333
KAYA, 369
KEEPING, E. 374
KEESOM, W. 377
KELLY, A. 126, 127, 130
KEMSLEY, D. S. 173, 198
KENNEDY, E. M. JR. 163, 197
KERZE, F. 129
KIMURA, H. 342, 343, 376
KING, R. 138, 139, 144, 147, 151, 152, 196
KINGDOM, K. H. 212, 298
KIP, A. F. 87, 89
KIRSCHFELD, L. 300
KITTEL, C. 51, 53, 86, 88, 89, 378
KJELDASS, T. JR. 87
KLEIN, M. P. 90, 91
KLEMENS, P. G. 376
KLEPPA, O. 317, 318, 319, 320, 321, 322, 323, 343, 375
KLINKERBERGER, V. W. 184, 185, 199
KNIGHT, W. D. 8. 9, 17, 18, 30, 53, 70, 74, 86, 87, 88, 89, 90, 91
KOEHLER, J. S. 114, 120, 128
KOHN, W. 87, 91
KOI, Y, 90
KOMAR, S. 377
KOPFERMANN, H. 87
KOROVSKII, SH. YA. 199
KORRINGA, J. 24, 78, 79, 87, 378
KOSTER, G. 308, 323, 374
KOUVELITES, J. 356, 377
KRAMER, J, 169, 186, 188, 189, 195, 198, 199
KRUSCHWITZ, H. W. JR. 299, 300
KUBASCHEWSKI, O. 374, 375
KUBO, R. 88
KUHLMANN-WILSDORF, D. 119, 128, 342, 376
KUNZ, F. W. 301
KURGANOV, G. V. 197
KURNAKOW, 362
KUSHIDA, T. 87, 88

LAIDLER, K. J. 210, 218, 298
LAMB, W. E. 86, 88
LANDAU, L. 87
LANE, C. T. 378
LANGE, H. 112, 114, 128, 149, 196
LANGMUIR, I. 208, 210, 212, 298
LAWSON, A. W. 332, 359 *n.*, 375
LAZARUS, D. 343 *n.*
LEE, A. T. 100, 121, 130
LEE, P. 311 *n.*
LEGVOLD, S. 366, 367, 377
LENNARD-JONES, J. E. 166, 198
LENNING, G. A. 242, 243, 245, 246, 251, 254, 255, 256, 259, 283, 299

VOL.
9
1961

LEVESQUE, P. 300
LEVINE, E. D. 104, 105, 128
LEVINE, O. 198
LEVY, R. A. 89
LI, C. H. 374
LICHTMAN, V. I. 133, 170, 171, 172, 173, 196, 198, 199
LINDE, J. O. 102, 103, 105, 128, 363, 364, 377, 378
LINDELL, B. O. 128
LIPPMAN, G. 175, 198
LIPSETT, F. R. 138, 139, 147, 151, 152, 196
LIPSON, H. 376
LIU, T. S. 249, 299
LOCK, J. 357, 358, 377
LOCK, J. M. 87
LOELIGER, H. R. 87
LOGAN, H. L. 163, 197
LOMER, W. 354, 355, 376, 377
LÜCKE, K. 112, 114, 118, 128, 129, 149, 184, 185, 196, 199
LUMSDEN, J. 332, 375
LURIO, A. 90, 91
LUSTMAN, B. 129

MADDIN, R. 101, 124, 129, 342, 376
MADER, S. 111, 119, 128
MAHNCKE, H. A. 169, 198
MAIR, B. J. 375
MAKIN, M. J. 115, 129, 138, 196, 199, 377
MALLETT, M. W. 260, 261, 264, 265, 265, 268, 269, 270, 297, 300
MANNING, G. K. 272, 297
MARCH, N. 311 *n.*, 377
MAREZIO, M. 331, 375
MARSH, L. L. 272, 274, 275, 297
MARSHALL, W. 354, 355, 377
MARTIN, D. C. 299
MARTIN, E. 277, 300
MARTIN, S. L. 300
MARTIN, S. L. H. 261, 300
MASING, G. 112, 118, 128, 129, 177, 178, 184, 185, 195, 198, 199
MASKREY, J. T. 300
MASLENNIKOV, 172, 198
MASSALSKI, 338
MASUDA, Y. 26, 73, 86, 89, 91
MATHEWS, D. H. 300
MATHEWSON, C. H. 98, 99, 120, 124, 128, 129
MATTHEWS, J. C. 87, 356, 355, 377
MATTHIAS, B. T. 88, 90
MATTHIESSEN, 305, 362
MATTRAW, H. C. 267, 300
MAYS, J. M. 88
MEAKIN, J. D. 114, 120, 128
MEHL, R. F. 101, 130, 375
MEISSNER, J. 124, 129
MENES, M. 89
MENTER, J. W. 199
MESHII, M. 376
METZGER, M. 159, 160, 197
MEYER, A. 378
MEYERING, J. 374
MEYERS, W. R. 87
MILFORD, F. J. 90
MILLER, P. 375
MITCHELL, A. H. 79, 90
MOORE, 233
MORGAN, H. W. 86
MORISSET, P. 163, 197
MORITZ, H. 231, 298
MORLET, J. G. 236, 237, 238, 239, 240, 241, 255, 258, 280, 282, 292, 293, 295, 299
MORSE, R. W. 87
MOTT, N. F. 88, 108, 125, 127, 129, 130, 224, 298, 305, 311 *n.*, 317, 323, 336, 342, 352, 359, 361 *n.*, 363, 364, 365, 370, 371, 374, 375, 376, 377
MUHLENKAMP, G. T. 262, 263, 272 297, 300
MULFORD, R. N. R. 268, 300
MÜLLER-WARMUTH, W. 90
MURPHY, W. 333
MYLER, W. S. 299

MCCALL, D. W. 88
MCCLURE, 331 *n.*
MCGARVEY, B. R. 86, 87
MCGILL, R. M. 198
MCGUIRE, J. C. 300
MCHENRY, H. T. 199
MCLEAN, D. 377
MCLENNAN, J. E. 101, 128
MCQUILLAN, A. D. 241, 242, 243, 299
MCSHARRY, J. J. 299, 300

NABANO, F. R. N. 89
NABARRO, F. R. N. 41, 88, 108, 125, 127, 130, 342, 376
NAKAYAMA, 369
NARBORO, F. R. N. 223, 298
NACHTRIEB, N. H. 88
NASH, R. R. 104, 105, 128
NAUMOV, F. N. 197
NEWTON, A. S. 300
NICHOLAS, J. 310
NICHOLSON, R. 377
NIKISHOV, A. S. 197
NOGGLE, T. S. 120, 128
NORBERG, R. E. 48, 78, 89
NOTTORF, R. M. 300
NOWICK, A. S. 333, 375

NUTTALL, W. H. 168, 198
NUTTING, J. 377

OLLOM, J. F. 68, 89
OLSEN, L. O. 87
ORGEL, L. E. 86
ORIANI, R. 317, 332, 333, 375
OROWAN, E. 129, 166, 198, 221, 298
ORR, R. 333
OSSWALD, E. 103, 104, 124, 128
OTTER, F. 378
OVERHAUSER, A. W. 74, 78, 89, 90, 370, 378
OWEN, E. A. 89, 326, 328, 375
OWEN, J. 82, 88, 89

PACKARD, M. 70, 86
PAIGE, H. 198
PAKE, G. E. 48, 76, 86, 90
PARKER, E. 376
PARKER, E. R. 158, 159, 192, 197, 199, 335, 342, 376
PATTERSON, M. 339 *n.*
PAULI, W. 19, 87
PAULING, L. 62, 90
PAXTON, H. W. 137, 196
PEARSON, S. 343, 377
PEARSON, W. B. 329, 375
PEIERLS, R. E. 376
PERLOW, G. J. 90
PETCH, N. J. 224, 228, 234, 235, 238, 298 299, 300, 301
PETER, M. 90
PFEIL, L. B. 205, 231, 297
PFUTZENREUTER, A. 177, 178, 198
PHILLIPS, A. 165, 198
PHILLIPS, D. J. 177, 178, 179, 199
PICKUS, M. R. 158, 159, 192, 197, 199
PIERCY, G. R. 124, 129
PIETTE, L. H. 87
PINES, B. J. 332, 375
PINES, D. 19, 78, 79, 87, 90, 323, 377
PIPPARD, A. B. 23, 87, 323, 325, 338, 375, 376, 378
PLANKENHORN, W. J. 197
PLUSQUELLBEC, J. 299
POBEREskin, M. 300
POMERANTZ, M. 30, 87, 88, 91
PORTIS, A. M. 80, 90
POULIS, N. J. 87, 91
POUND, R. V. 8, 46, 70, 76, 86, 87, 89
POWELL, 367
PRATT, G. 377
PRESTON, R. S. 90
PROBST, H. B. 199
PRUTTON, C. F. 169, 198
PRY, R. H. 126, 129, 376
PURCELL, E. M. 11, 46, 76, 86, 90

QUARRELL, A. G. 224, 298

RAECHLE, R. 375
RAFFELSIEFER, J. 112, 128
RAMSEY, N. F. 14, 86
RANDALL, R. F. Y. 157, 177, 179, 180, 181, 197, 199
RANSLEY, C. E. 215 217, 218, 298
RAYNE, J. 356, 377
RAYNOR, G. V. 63, 89, 219, 281, 291, 298, 306, 307, 312, 313, 326, 328, 329, 331, 374, 375
READ, T. A. 139, 140, 144, 145, 146, 152, 159, 160, 161, 196, 197
REDFIELD, A. G. 72, 77, 78, 80, 86, 88, 89, 91
REDMAN, J. K. 115, 128
REED-HILL, R. E. 120, 129
REES, A. L. G. 261, 300
REHBINBER, P. A. 133, 170, 173, 174, 176, 185, 190, 194, 196, 198, 199
REIF, F. 33, 66, 68, 87, 88
RHINES, N. F. 207, 218, 297
RHODERICK, E. H. 89
RHODES, P. 89, 377
RICHMOND, J. C. 160, 197
RIMAI, L. 85, 88
RIPLING, E. J. 257, 258, 299
ROBERT, C. 90
ROBERTS, B. W. 278, 279, 297, 329, 330, 344, 377
ROBERTS, C. S. 298
ROBERTS, J. K. 298
ROBERTS, L. 359, 360, 377
ROBERTSON, W. D. 99, 100, 116, 117, 120, 128, 129, 162, 197
ROGERS, H. C. 236, 280, 299, 377
ROGERS, M. C. 278, 279, 297
ROSCOE, R. 133, 136, 138, 145, 196
ROSI, F. D. 98, 99, 114, 119, 128, 129, 141, 142, 148, 149, 196
ROWLAND, T. J. 86, 87, 88, 89, 90
ROZHANSKII, V. N. 185, 198, 199
RUDERMAN, M. A. 51, 86
RUDMAN, P. 331, 333, 345, 346, 348, 374, 375
RUNDLE, R. E. 267, 300
RUSSELL, B. 375
RUSSELL, H. W. 198
RYDER, D. A. 154, 155, 197
RYLSKI, O. Z. 206, 245, 247, 250, 253, 254, 297

SACHS, G. 102, 103, 124, 125, 128, 129
SACK, R. A. 220, 298
SALKOVITZ, E. 378
SAMPSON, E. G. 197

VOL.
9
1961

Sandle, W. J. 90
Sarles, L. R. 87
Sato, M. 199
Satterthwaite, C. B. 87
Savage, E. G. 197
Sawatzky, A. 376
Schawlow, A. L. 88
Schindler, A. 370, 378
Schmid, E. 95, 99, 100, 117, 118, 120, 127, 128, 129
Schmitt, R. 372, 378
Schoek, G. 376
Schrieber, D. 123, 129
Schrieffer, J. R. 23, 87
Schröder, K. 118, 129
Schumacher, R. T. 87, 91
Schwarpe, A. D. 262, 263, 300
Schwartz, C. M. 261, 262, 264, 265, 266, 297, 300
Seabrook, J. B. 299
Sears, G. W. 297
Sebisty, J. J. 198
Seeger, A. 95, 98, 106, 107, 111, 114, 115, 119, 121, 125, 127, 128, 129, 334, 336, 337, 338, 339, 376
Seigle, L. 333
Seith, 217, 298
Seitz, F. 88, 305, 375
Serebrennikan, B. V. 197
Seybolt, A. U. 90
Seymour, E. F. W. 63, 88, 89
Shahinian, P. 191, 199
Shapiro, S. 161, 197
Shaw, C. H. 378
Sheely, W. F. 104, 105, 128
Sherrill, F. A. 104, 105, 106, 128
Shipko, F. J. 241, 299
Shreider, A. V. 197
Shull, C. 349, 351, 352, 353, 377, 378
Shulman, N. 267, 268, 300
Shulman, R. G. 53, 67, 88, 89
Shuttleworth, R. 166, 198
Sidhu, S. S. 300
Siebel, G. 100, 117, 128
Sieverts, A. 230, 231, 276, 277, 298, 300
Silcox, J. 342, 377
Sims, C. E. 233, 299
Sivertsen, J. M. 376
Slater, J. 305, 306, 323, 374
Slichter, C. P. 24, 47, 73, 74, 87, 88, 89, 90
Slifkin, L. 343 *n.*
Smallman, R. 338, 339, 376, 377
Smith, C. S. 87, 300
Smith, D. P. 214, 215, 232, 285, 297
Smith, E. 100, 119, 129
Smith, F. C. 198
Smith, H. A. 198
Smith, J. 378
Smithells, C. J. 206, 211, 212, 217, 218, 297, 298
Sneddon, I. 311 *n.*
Snowden, K. O. 191, 199
Sogo, P. B. 86
Sommerfeld, A. 20, 87
Sopwith, D. G. 191, 198, 199
Sosin, A. 128
Spedding, F. 377
Spedding, F. H. 300
Speiser, R. 217, 298
Spokas, J. J. 47, 88
Spretnak, J. W. 217, 298
Stables, P. 299
Stade, C. H. 128
Staubwasser, W. 113, 114, 128
Steinberg, M. A. 249, 299
Stevens, K. 352, 359, 370, 371, 377
Stickley, G. W. 197
Stokes, R. J. 113, 114, 122, 128
Street, R. 378
Stroh, A. N. 223, 224, 298
Sugawara, T. 82, 90
Suhl, H. 90
Sukenik, H. J. 89
Sully, A. H. 299
Sumner, C. G. 168, 198
Suzuki, H. 104, 105, 108, 109, 110, 112, 120, 128, 150, 165, 196, 198, 376
Svensson, 362
Swalin, R. 377
Sweetland, E. D. 158, 197, 199
Sykes, C. 299

Takamura, J. 137, 138, 147, 148, 151, 196
Takeuchi, S. 112, 128, 196
Taylor, A. 378
Taylor, H. S. 211, 298
Taylor, J. W. 217, 298
Teeters, D. R. 88
Tegart, W. J. M. 127
Teller, E. 78, 90
Teviotdale, A. 377
Thomas, G. 130, 377
Thompson, D. 377
Thompson, N. 177, 178, 179, 199
Thomson, R. 341, 376
Thornton, P. R. 114 *n.*, 122, 128, 130, 342, 377
Tighe, N. J. 161, 197
Tiller, W. A. 111, 128
Tingle, E. D. 169, 198
Tomita, K. 88
Torrey, H. C. 49, 86, 89
Townes, C. H. 87, 88
Treaftis, 343 *n.*
Troiano, A. R. 236, 237, 239, 255, 258, 280, 293, 295, 299

TRUMBORE, F. 333
TRZECIAK, M. J. 268, 269, 270, 300
TSUJIMURA, A. 90
TUER, G. L. 121, 129
TURNBULL, 343 *n.*

VAN der LUGT, W. 82, 91
VAN VLECK, J. H. 43, 88
VARLEY, J. O. 316, 375
VAUGHAN, H. G. 235, 236, 299
VEGARD, L. 326, 375
VEHSE, W. E. 91
VINCENT, D. H. 90
VOGEL, F. L. 100, 129
VOLKOFF, G. M. 88
VOLMER, M. 210, 298
VON BATCHELDER, F. 375
VOSKO, S. H. 91
VREELAND, T. 298

WADSWORTH, N. J. 191, 199
WAGNER, C. 305, 332, 375
WALCHLI, H. E. 86
WALKER, C. 374, 375
WALKER, C. B. 331, 375
WALLING, J. 356, 377
WANNIER, G. 308, 374
WAREKOIS, E. 338, 339, 376
WARF, J. C. 300
WARREN, B. 326, 329, 330, 338, 339, 343, 344, 345, 376, 377
WASHBURN, J. 376
WASSERMAN, G. 120, 129
WATKINS, G. D. 8, 59, 89
WEAVER, H. E. 87
WEAVER, H. E. JR. 86
WEBB, M. B. 91
WEBB, W. W. 341, 376
WECHSLER, M. 343, 377
WEERTS, J. 103, 124, 128, 129
WEI, C. 355, 377
WEIL, J. A. 88
WEIMAN, A. L. 160, 197
WEINBERG, D. 88
WEINER, L. C. 133, 154, 156, 157, 196, 197
WEISS, R. 350, 377
WEISS, R. J. 351, 352, 370, 377
WENSTROM, E. K. 170, 173, 176, 190, 198, 199
WERNICK, J. H. 90
WERT, C. A. 376
WESSEL, E. T. 226, 227, 298
WEST, G. W. 91
WESTMACOTT, K. 338, 339, 376, 377
WHELAN, M. J. 130 338
WHITE, G. 366, 378
WHITE, T. A. 211, 298
WIEDERSICH, H. 376
WILKINSON, M. 349, 351, 352, 377, 378
WILLIAMS, 233
WILLIAMS, C. 197
WILLIAMS, D. A. 300
WILLIAMS, D. N. 250, 299
WILLIAMS, F. S. 198
WILSDORF, H. 119, 128
WINTER, J. M. 90
WOMELDORPH, W. J. 197
WOOD, D. S. 109, 129, 298
WOODS, S. 368, 378
WYLUDA, B. J. 88, 89

YAFFE, L. 300
YARZHEMSKAYA, N. I. 197
YOSIDA, K. 82, 87, 88, 378
YOUNG, A. P. 262, 266, 300
YUKIMOTO, Y. 90

ZACHARISSEN, W. H. 268, 300
ZAKOSCHIKOVA, 190, 199
ZAPFE, G. 298
ZAPFFE, C. A. 198 231, 232, 233, 299
ZEMANY, P. D. 297
ZEMCZUZNY, 362
ZENER, C. 41, 88, 222, 224, 298
ZISMAN, W. A. 169, 198, 199
ZOGRITSENKA, Z. I. 197

VOL.
9
1961

SUBJECT INDEX

Abnormal after effects in metals 133, 161
Absolute intensity of x-ray diffraction lines 350
Adsorption isotherm 208
Adsorption on metals 166
Anchoring of dislocations 150, 154
Anisotropic Knight shift 25, 33, 75
Antishielding factor 32
Asymmetric absorption curve 72
Atomic diffusion 75
  size factor 325

Bending of metals 133
Bond states 306, 309
Brillouin zone theory 34
Brittle fracture in metals 219
Brittle temperature 155
Bulk susceptibility 19

Carbon in steel 235
Ceramic coatings on metals 164
Characteristic time of lattice vibrations 22
Charge density near impurity 37
Chemisorption 210
Chemi-adsorption on metals 172
Cleavage cracks 224
Clustering in alloys 341
Cold-worked metals 58, 83
Composition inhomogeneity broadening 40
Coulomb self energy 308
Crack formation in metals 135
Creep effects in metals 157
Creep properties of metals 133
Critical crack velocities 225
Critical shear stress 95
  effect of temperature 97, 105
  in pure metals 106
  in solid solutions 108
Curie point 363
Curie–Weiss law 370
Current alloy theories 34

Damping behaviour of metals 133
Defects in lattice 54, 69
Deformation, of alloys 125
  of body-centred cubic metals 100
  of face-centred cubic metal 97
  of hexagonal close-packed metals 99
  of surface films 152
Delayed failure 232
Detection schemes for N.M.R. 70
Diffuse scattering of x-rays 329, 333, 343
Diffusion 45
  of hydrogen in metals 217, 258
  narrowing of N.M.R. absorption lines 84
Dipolar broadening 43, 50, 75, 80, 84
Dislocations 56, 59, 69
Dislocation locking 101, 109
Ductility and strength of metals 163
Ductile-to-brittle transition 219, 225

Effective defect size 60
Effect of alloying elements on critical shear stress 101
  of electrolytes on metals 165, 173, 180
  of metal films on critical resolved shear stress 136
  of films on polycrystalline metals 190
  of particle size on resonance absorption 72
Effective Q 76
Elastic stain energy 308, 325, 332
Electrical resistance of alloys 350, 359
Electro chemical factor 310
Electron-coupled interactions 49, 53
Electron spin, resonance 20, 73
  susceptibility 24
Electronic structure of solid solutions 350
Electronic specific heat 20, 350, 355
Electronic energy bands in metals 306
Endothermic occlusion 207, 212, 230
Exchange interaction parameter 51
Exchange-coupling constant 83
Exchange polarization 81
Exothermic occlusion 208, 213

Fatigue of metals 133, 164
Fermi surface in copper 323
Fermi–Thomas approximation 311
Ferromagnetic metals 80
  ordering 367
Filling factor 71
Flow stress in pure metals 106
Formation of lattice defects 335
Fracture of metals 154
Friedel theory 84, 311, 323

Gas permeation through metals 207
Griffith–Orowan mechanisms 223

Griffith theory of fracture 219, 234
Gyromagnetic ratio 24

Hardening in solid solutions 108
Henry's model of a solid solution 316
Huang effects 334
Hume-Rothery rules 310, 313
Hybrid states 368
Hydrogen–Chromium system 277
Hydrogen
  embrittlement, of body-centred cubic metals 276, 280
    in metals 284
    of steel 231, 257
  in iron 230, 240
  in solid solution 214
 -metal relationships 206
 -molybdenum system 277
 -niobium system 276
 -tantalum system 276
 -tungsten system 277
 -vanadium system 276
Hyperfine structure constant 19

Image forces 153
Imperfections in metals 75
Interaction, of hydrogen with dislocations 235
  of lattice defects 335
Intercrystalline fracture 219
Intergranular fracture 222
Intermediate d-states 363
Intermediate phases in alloys 39
Intermetallic compounds, 42, 67, 82
Internal friction in metals 133, 161
Interstitial atoms 336
Interstitial solution of hydrogen 236
Ionic attraction in solid solutions 308
Ionic repulsion in solid solutions 308
Isobar 208
Isotere 208

Kink bands 148
Knight Shift, in alloys 34, 81
  in pure metals 17, 21, 81
Korringa relation 24, 49, 81

Langmuir's isotherm 210
Lattice distortion 75
Lattice spacing 325
Lattice strain 83
Liquid alloys 84

Matthiessen's rule 360, 363
Meissner effect 23
Microscopic deformation of metals 151
Microstructure of solid solutions 335
Motional narrowing of N.M.R. absorption lines 45, 84

Necking 219
Neutron diffraction studies on alloys 367
Nitrogen in steel 235
Nuclear magnetic susceptibility 77

Ordered lattices 28, 69
Oxide films on metals 134

Paramagnetic susceptibility 19
Phase boundaries 22, 38, 75
Physical adsorption 208
Physical properties of solid solutions 350
Planar pressure theory 232
Plastic flow 96, 134
Polarization of conduction electrons 41
Polycrystalline samples 74
Powder samples, N.M.R. line shape 25
Precipitation 69
Pseudo-dipolar broadening 52
Pseudo-hydrides 208
Pure quadrupole resonance 33

Quadrupole effects in alloys 34, 59, 65, 68
Quadrupole interactions in imperfect crystals 53
Quadrupole perturbations 27

Radiation damage 69
Rehbinder effect 170
Residual resistance in alloys 341, 360
Resonance position, temperature dependence, volume dependence 20
Rigid band approx. 38, 313

Satellite lines 29, 55, 65, 75
Screened charge model 36
Screw dislocations 151
Short range order in alloys 108, 341, 344
Shielding factor 31
Sievert's law 207, 212
Skin depth 72
Slip bands in metal crystals 119, 134
Small angle scattering 343
Soap films on metals 169, 186
Solid solutions 36, 58, 307
Solute atom-defect interaction in solid solutions 340
Spin
  -disorder scattering 352, 363, 369
  echoes 78
  exchange polarization 82
  flipping 78
  lattice relaxation time 23, 24, 68, 78
  broadening 48
Spin–spin broadening 43
Spurious line broadening in N.M.R. 71
Stacking faults 108, 334
  energies 337

VOL. 9 1961

Static fatigue 232
Strain rate effects 150
of metals 342
Strength of oxide films 136
Stress–strain curve and films on metals 145
Stress–strain curves, for alloys 123
in metals, temperature dependence 111
Structural disorder 334
Structure of solid solutions 334
Super conductors 22, 75
Super lattice 309
Surface alloy layers 141
Surface active agents 165
Surface free energy of metals 166
Surface Frank–Read source 134

Tensile properties of metals 133
Theory of stress–strain curves in metals 121
Thermochemistry of solid solutions 317
Thin film microscopy 127
Titanium alloys 250, 255
Transition probability 76
Twinning in metals 144

Unpaired electron spin 26
Uranium–hydrogen system 267
Valence effects, in alloys 83
Varley's model of a solid solution 317
Vegard's law 328
Virtual 3*d* states 82
Voids in metals 282
von Laue diffuse scattering 329

Wavefunctions of transition metal alloys 368
Width and shape of resonance absorption 42
Work hardening 134, 148

X-ray emission spectroscopy 371
lattice spacings 326

Yield points in face-centred cubic metals 101

Zero point vibrations 22

VOL.
9
1961

CONTENTS OF PREVIOUS VOLUMES IN THE PROGRESS IN METAL PHYSICS SERIES

OL.
9
961

VOLUME 1

Progress in the Theory of Alloys G. V. RAYNOR
Theory of Dislocations A. H. COTTRELL
Crystal Boundaries R. KING and B. CHALMERS
Age Hardening of Metals G. C. SMITH
Hardening Response of Steels E. H. BUCKNALL and W. STEVEN
Preferred Orientation in Non-Ferrous Metals T. L. RICHARDS
Diffusion of Metals in Metals A. D. LE CLAIRE

VOLUME 2

Order-Disorder Changes in Alloys H. LIPSON
Rate Process in Physical Metallurgy I. I. BETCHERMAN
Anisotropy in Metals W. BOAS and J. K. MACKENZIE
Developments in Magnesium Alloys H. G. WARRINGTON
Internal Strains and Recrystallization R. W. CAHN
Researches on the Polygonization of Metals A. GUINIER and J. TENNEVIN
Polygonization in Strongly Deformed Metals C. CRUSSARD, F. AUBERTIN, B. JAOUL and G. WYON

VOLUME 3

Crystallography of Transformations J. S. BOWLES and C. S. BARRETT
Properties of Metals at Low Temperatures D. K. C. MacDONALD
Recent Advances in the Electron Theory of Metals N. F. MOTT
Twinning R. CLARK and G. B. CRAIG
Ferromagnetism URSULA M. MARTIUS
Quantitative X-ray Diffraction Observations on Strained Metal Aggregates G. B. GREENHOUGH
Recrystallization and Grain Growth J. E. BURKE and D. TURNBULL
Structure of Crystal Boundaries B. CHALMERS

VOLUME 4

Internal Friction in Metals A. S. NOWICK
The Mechanism of Oxidation of Metals and Alloys at High Temperatures KARL HAUFFE
Gases in Metals C. R. CUPP
The Theory of Sintering G. A. GEACH
Theory of Dislocations A. H. COTTRELL
Diffusion in Metals A. LE CLAIRE
Nucleation J. H. HOLLOMON and D. TURNBULL

VOLUME 5

The Fracture of Metals N. J. PETCH
Geometrical Aspects of the Plastic Deformation of Metal Single Crystals R. MADDIN and N. K. CHEN
The Structure of Liquid Metals B. R. T. FROST
Report of Precipitation H. K. HARDY and T. J. HEAL
Solidification of Metals URSULA M. MARTIUS

VOLUME 6

The Effect of Hydrostatic Pressure on the Electrical Resistivity of Metals A. W. LAWSON
The Filamentary Growth of Metals H. K. HARDY
The Austenite : Pearlite Reaction R. F. MEHL and W. C. HAGEL
Recent Advances in Knowledge Concerning the Process of Creep in Metals A. H. SULLY
The Mechanism of Evaporation O. KNACKE and I. N. STRANSKI
Mosaic Structure P. B. HIRSCH

VOL.
9
1961

VOLUME 7

Equilibrium, Diffusion and Imperfections in Semiconductors J. N. HOBSTETTER
The Physical Metallurgy of Titanium Alloys R. I. JAFFEE
Thermodynamics and Kinetics of Martensitic Transformations LARRY KAUFMAN and MORRIS COHEN
The Stored Energy of Cold Work A. L. TITCHENER and M. B. BEVER
The Properties of Metals at Low Temperatures H. M. ROSENBERG

VOLUME 8

Work Hardening of Metals L. M. CLAREBROUGH and M. E. HARGREAVES
Grain Boundaries in Metals F. WEINBERG
X-ray Studies of Deformed Metals B. E. WARREN
Substructures in Crystals Grown from the Melt C. ELBAUM
Defects in Pure Metals W. M. LOMER

OL.
9
961

VOL.
9
1961

PROGRESS IN MATERIALS SCIENCE VOLUME 9
(INCORPORATING PROGRESS IN METAL PHYSICS)
GENERAL EDITOR: BRUCE CHALMERS

Nuclear Magnetic Resonance in Metals

by
T. J. ROWLAND
Metals Research Laboratories, Union Carbide Metals Company,
Niagara Falls, New York.

PERGAMON PRESS
OXFORD · LONDON · NEW YORK · PARIS

PERGAMON PRESS LTD.
Headington Hill Hall, Oxford
4 & 5 *Fitzroy Square, London, W.*1

PERGAMON PRESS INC.
122 *East* 55*th Street, New York* 22, *N.Y.*
Statler Center 640, 900 *Wilshire Boulevard,*
Los Angeles, California

PERGAMON PRESS S.A.R.L.
24 *Rue des Écoles, Paris V*[e]

PERGAMON PRESS G.m.b.H.
Kaiserstrasse 75, *Frankfurt-am-Main*

VOL.
9
1961

Copyright
©
1961
PERGAMON PRESS LTD.

Library of Congress Card Number 49-50107

Set in Times New Roman 10/12pt. and
made and printed in Great Britain at Page Bros. (Norwich) Ltd.

PROGRESS IN MATERIALS SCIENCE

(INCORPORATING PROGRESS IN METAL PHYSICS)

PUBLISHER'S NOTE

THE twelve years that have elapsed since the publication of the first volume of PROGRESS IN METAL PHYSICS has seen a great increase in the rate of publication of papers in this, as in most other fields of science, and realization that the physics of metals is an important part of, but not the whole of, the science of materials, a field of considerable practical and theoretical importance.

It is becoming extremely difficult, if it is not already impossible, for most scientists to keep up-to-date in their own and closely related fields by reading all the relevant original papers; one approach to the solution of this problem is the provision of adequate up-to-date critical review articles. For these reasons the Editor and the Publisher of PROGRESS IN METAL PHYSICS have decided to broaden the subject matter to include the whole of the field of the Science of Materials, and, in order to ensure maximum availability, to publish each article as a separate entity; thus, an individual subscriber need no longer purchase a whole volume in order to obtain some of the articles. This new procedure will make it possible to publish each article within five months of its receipt by the Editor.

VOL.
9
1961

NUCLEAR MAGNETIC RESONANCE IN METALS

Contents

I. Introduction 3

II. Discussion of Resonance Parameters 5
A. Shape and Width 6
B. Intensity 8
C. Position 8

III. Atomistic View of Resonance in Metals 10
A. Nuclear Magnetic Resonance Absorption and Relaxation—General Comments 10
B. Resonance Position in Metals and Alloys 17
1. Knight Shift in Pure Metals 17
2. Temperature and Volume Dependence of the Resonance Position 20
3. The Anisotropic Knight Shift in Pure Metals 25
4. Quadrupole Perturbations of the Nuclear Resonance in Pure Metals 27
4a. First-Order Quadrupole Effects in Pure Metals or Ordered Lattices 28
4b. Second-Order Effects in Pure Metals or Ordered Lattices 31
4c. Summary of Quadrupole Perturbations in Ordered Structures 32
5. Pure Quadrupole Resonance 33
6. The Knight Shift in Alloys. 34
C. Width and Shape of Resonance Absorption 42
1. Dipolar Broadening 43
2. Motional Narrowing 45
3. Spin-Lattice Relaxation Time Broadening 48
4. Electron-Coupled Interactions Between Nuclear Spins 49
5. Electron-Coupled Interactions Between Nuclear Spins and Ion Cores 53
D. Intensity of Resonance Absorption and Discussion of Quadrupole Interactions in Imperfect Crystals 53
1. Quadrupole Broadening of the Magnetic Resonance 54
2a. First-Order Quadrupole Effects 56
2b. Second-Order Quadrupole Effects 58
3. Discussion of Experimental Work 58
3a. Quadrupole Effects in Cold-Worked Metals 58
3b. Quadrupole Effects in Alloys 59
4. Miscellaneous Effects of Quadrupole Interactions 67
5. Summary of Quadrupole Effects 69

IV. Miscellaneous Topics and Experimental Methods 69
A. Remarks on Experimental Techniques 69
B. Influence of Particle Size on the Resonance Absorption in Conductors 72
C. Derivation of Absorption Line Shapes for Polycrystalline Samples 74
D. Summary and Comments 75

CONTENTS

APPENDIX A	76
APPENDIX B	78
NOTE ADDED IN PROOF	80
REFERENCES	86

VOL.
9
1961

NUCLEAR MAGNETIC RESONANCE IN METALS

T. J. Rowland

I. Introduction

Nuclear magnetic resonance has developed since its discovery[1, 2] in 1945 into a technique which not only has provided the nuclear physicist with much fundamental information but also has given new insights into the physics of atoms and molecules in the gaseous, liquid, and solid states.[3] Theoretical understanding of matter had advanced to the point where immediate advantage could be taken of this new type of information; consequently, the use of magnetic resonance techniques has increased rapidly. This is especially true in the field of chemistry because theory and experiment could be compared using relatively well understood simple molecules with small numbers of atoms. The uses of nuclear resonance have multiplied and the techniques have become more specialized until each application of the tool has become practically a field in itself. Many metal physicists would be dismayed at the prospect of determining the structure of a porcupine quill from its X-ray pattern, and quite similarly, they may find it difficult to interpret the nuclear resonance pattern of nicotine to gain structural information. In fact, the probability is great that the equipment used to obtain the resonance properties of a metal would not be immediately suitable for work on organic molecules. Although the fundamental interactions between nuclei and between electrons and nuclei are the same regardless of the state of matter involved, these interactions are useful in interpreting specific resonance measurements only when the theory is appropriately specialized with regard to the electronic structure and state of internal motion of the matter. It is the purpose of the present paper to summarize the experimental results and theory as they pertain to metals.

The data resulting from nuclear magnetic resonance experiments are often expressed as a rate of energy absorption versus the absorption frequency. The available information is contained in the descriptive parameters of the resonance absorption line, namely its position, width, shape and intensity. These parameters are, of course, commonly used to characterize a spectral line. In the case of nuclear resonance, they depend upon the electric and magnetic fields at the positions of the nuclei; these fields are, in turn, determined by the local atomic configurations and conduction electron density around the nuclei. It is then of considerable importance to attach a unique interpretation to the change in parameters which occurs when a metal undergoes a change of structure or composition.

When nuclear resonance can be observed, it proves to be well suited to the study of imperfections of many types, as well as mass diffusion and electronic changes of a subtle nature. Examples of these applications will form an appreciable proportion of the present paper. Specific topics to which resonance techniques have been applied include the working of metals and the subsequent annealing process. These have been found to affect the intensity of the resonance line while changing the width and shape in only a minor fashion and the position not at all. Alloying, or a heat treatment which induces atomic rearrangement of the constituents of an alloy, will in general influence all of the parameters although in specific cases it often happens that the most pronounced changes are in the position or intensity of the line. Much also can be learned about metals from studies which are of less obvious importance metallurgically, such as the effects of pressure or temperature on the resonance. Hydrostatic pressure on the metal has been found to shift the position of the resonance leaving the other parameters essentially unchanged, and temperature changes can cause the width to change drastically under some circumstances.

VOL.
9
1961

Our understanding of the electronic properties of metals has benefited from resonance studies because the conduction electron density in the metal is a determining factor of the position of the absorption line. This relatively new field of investigation has thus gained the attention both of those who are attempting to formulate a better theory of metals and of those who are interested primarily in the mechanical properties of metals, especially in the cases where these properties appear to be intimately related to the defect structure of the metal. The latter interest derives from the fact that dislocations and point imperfections are known to affect the resonance parameters if they are present in sufficient number.

The capability of nuclear resonance to probe the internal electronic configurations in a metal appears great; however, there are also many obstacles to the general application of resonance, some of which are insurmountable. This is not an experimental method which can be applied to any solid with fair confidence of obtaining useful information; on the contrary, the properties of the atomic nuclei are of the utmost importance, and in the majority of instances these properties determine the material on which experiments must be performed. Also, the method is not particularly "sensitive" in the sense of being able to detect, directly, small quantities of an element or compound, and for that reason it has not been used for analytical work on metals.

Section II is devoted to an introduction to the quantities measured in, or derived from, nuclear magnetic resonance experiments. Each of the absorption parameters mentioned above will be discussed in more detail regarding its quantitative measurement and its usefulness for a specific investigation, without regard for its microscopic derivation. Section III will include a more detailed exposition of the mechanisms which are responsible for the position, width, shape and intensity of observed nuclear resonance absorption lines.

A final section will call attention to those features of experimental technique which have themselves been the subject of research and which must be considered if one is to avoid complicating the measurements unnecessarily, or to correct for these complications when they are unavoidable.

II. Discussion of Resonance Parameters

Nuclear magnetic resonance spectroscopy of metals, like other types of absorption spectroscopy (optical, ultra-violet), depends on the selective absorption of radiation over a range of frequencies. The functional dependence of absorption on frequency is determined by the composition, structure and temperature of the metal, and in a direct manner by the magnetic field in which it is placed. It will be assumed in the balance of this section that the metal sample is immersed in a strong magnetic field, e.g 10,000 G. The apparatus used to detect the absorption must be capable of supplying radiation of the proper frequency, and also of measuring

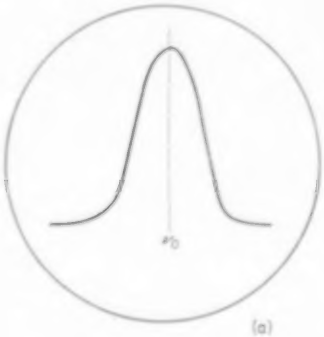

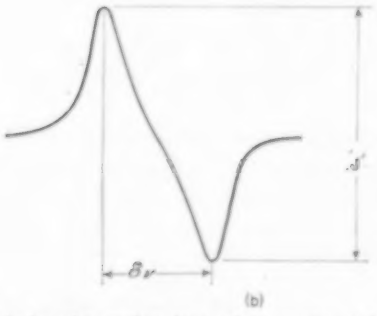

Fig. 1a. A tracing of the absorption line of pure aluminium metal at room temperature. The ordinate is proportional to the rate energy is absorbed. The abscissa is frequency.

Fig. 1b. An absorption derivative curve of aluminium illustrating the definition of width $\delta\nu$ and amplitude J' used throughout the text. $\delta\nu$ is in units of frequency, J' is proportional to the maximum slope of the curve in 1a.

the quantity absorbed. The amount of energy absorbed by a specific nuclear species is usually small outside of a very narrow resonance region where it is enhanced by several orders of magnitude. Confining attention to this relatively narrow region of the radio frequency spectrum, perhaps 100 kc/s wide centred at 10 Mc/s, a few typical absorption lines will be considered with regard to their characterization in terms of experimental measurements.

The resonance of pure aluminium metal as it appears on an oscilloscope is shown in Fig. 1a. More frequently, an absorption line is seen as a recorder trace which, because of the detection method most often employed, displays the *derivative* of the line (Fig. 1b). In fact, resonance data are so commonly obtained in derivative form that reference to *line width* or *amplitude* most often means from maximum to minimum of the derivative curve as $\delta\nu$ and J' of Fig. 1b. Other typical absorption lines and their derivatives are shown in Fig. 2. The abscissa in these figures is frequency and the ordinate is in

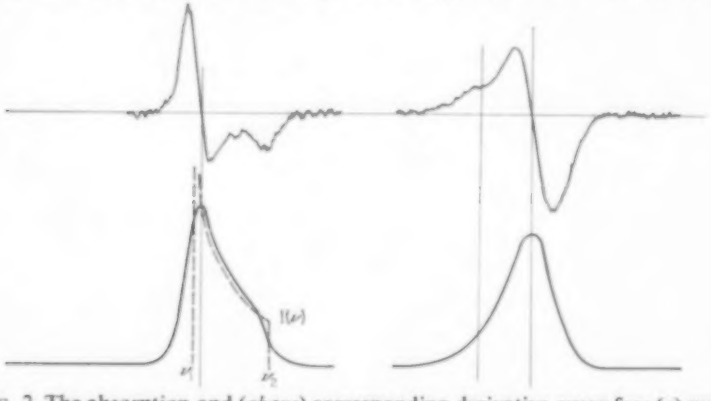

FIG. 2. The absorption and (*above*) corresponding derivative curve for: (*a*) pure cadmium powder and (*b*) silver–0·61 atomic per cent tin alloy powder, both observed at about 11,300 G. and room temperature. The traces illustrate the resonance behaviour of (*a*) non-cubic metals of spin 1/2 and (*b*) alloys of low impurity concentration. Nuclei near the impurity cause the small bump in the derivative curve of 2b.

arbitrary amplitude units. Although many shapes may be encountered, Figs. 1 and 2 illustrate many of the important aspects one needs to consider. A brief description of the experimental procedure used to obtain the recorded derivative curves from the more basic absorption of radio frequency energy is given in Section IV.

A. *Shape and Width*

The symmetry of the resonance is one of its most easily observed and significant features, revealing immediately whether or not its *shape function* $g(\nu)$ has a centre of symmetry. Considering first a resonance symmetric about a frequency ν_0 such as that in Fig. 1, the shape is often approximated analytically by one or the other of two bell-shaped curves, the Gaussian, for

which $g(\nu)$ is proportional to $\exp[-2(\nu-\nu_0)^2/\delta\nu^2]$, or the Lorentzian, for which $g(\nu) \propto [1+4(\nu-\nu_0)^2/3\delta\nu^2]^{-1}$. Actually, these seldom provide a precise representation of an experimental line shape, but they are easily handled expressions and have some theoretical justification. The Gaussian (which is closely approximated by many metals at temperatures well below their melting points) can be expected to result from the randomness of the nuclear spin orientations of the nuclei in the sample, while the Lorentzian is a good approximation if processes limiting the lifetime of the nuclear states are involved. The lifetime can in fact be estimated by using the uncertainty principle in the form $\Delta E \Delta t \gtrsim \hbar$. If $\Delta E = h\delta\nu$ then the lifetime against transition is about $1/2\pi\delta\nu$, i.e. approximately the inverse of the line width. In the description of any *symmetrical* line, it is customary to quote $\delta\nu$ (cf. Fig. 1); this interval between the extreme slopes of the absorption line can be measured accurately and easily and it conveys the idea of width fairly well. It has little fundamental significance; its popularity as a form of stating data is due to the detection method which has come to be standard, as mentioned before, and to the fact that for a Gaussian line, $\delta\nu$ is simply twice the root mean square width (root second moment) of the line, i.e. $\delta\nu = 2[\overline{(\Delta\nu)^2}]^{\frac{1}{2}}$. The experimental second moment, defined by $\overline{(\Delta\nu)^2} = \int_0^\infty (\nu-\nu_0)^2\, g(\nu)\mathrm{d}\nu$, $\int_0^\infty g(\nu)\mathrm{d}\nu = 1$, is of fundamental significance since a theoretical value for it can be calculated independently of experiment from first principles.

For the asymmetric line in Fig. 2a, a *width* is usually not stated in the same form. The appearance of this absorption suggests that it is composed of an assembly of symmetric resonance absorptions which are distributed according to the dotted curve $I(\nu)$. Here $I(\nu)\mathrm{d}\nu$ is proportional to the number of nuclei which would absorb energy in the frequency range from ν to $\nu + \mathrm{d}\nu$ in the absence of the symmetric broadening. It is necessary in this case to estimate the width of the symmetric component lines, and then to determine the shape of the distribution function $I(\nu)$ and possibly the end frequencies ν_1 and ν_2 of the absorption region defined by $I(\nu)$. If the function $I(\nu)$ is known, as it frequently is, these end frequencies satisfactorily describe the resonance as it would appear in the absence of symmetric broadening. The asymmetric line is thus always described by quoting the width of its symmetric component as described in the preceding paragraph, and enough information to define completely the function $I(\nu)$.

The nuclear absorption lines discussed above correspond to the imaginary part of the nuclear susceptibility; the real part gives rise to nuclear dispersion (see Appendix A). Both convey the same fundamental information; however, an important aspect of the dispersion to the present topic of line shape is that voltage proportional to the dispersion is sometimes inadvertently mixed with the absorption signal. This can happen because of improperly adjusted apparatus or because of "skin effects" occurring in metals. The latter topic is considered in Section IV.

B. *Intensity*

The intensity of an absorption line characterized by a shape function $g(\nu)$ is $K\int_0^\infty g(\nu)\mathrm{d}\nu = K$, where K is determined by the number of nuclei contributing, the square of the matrix element for the transition, and other factors characteristic of the resonant nuclear species (see Appendix A). A change in the width of $g(\nu)$ not accompanied by a change in shape will, of course, change the amplitude J' which we should like to use as a measure of intensity. In order to compensate for this when determining the integrated intensity we note that since $g(\nu)$ is normalized, its maximum value $g(\nu_{\max})$ is proportional to $(\delta\nu)^{-1}$, and its maximum slope is proportional to $(\delta\nu)^{-2}$. The peak to peak amplitude of the observed derivative, J', is then proportional to $K(\delta\nu)^{-2}$ and consequently the total intensity K is proportional to $J'(\delta\nu)^2$. In comparing the intensities of a number of alloys the shape of a line may be practically constant so that the product $J'(\delta\nu)^2$ provides a good measure of relative intensity. When the width is constant, the J' values alone satisfactorily determine the intensity, which is then often presented as $g(\nu_{\max})$ after being suitably standardized to a constant number of nuclei present in the sample and corrected for apparatus sensitivity.

Because of the difficulty of maintaining all of the experimental parameters constant during measurements on a series of alloys or worked material, some method of calibrating the intensity scale is always used. Each complete intensity measurement consists of observing both the resonance of the sample under observation *and* a reference signal provided either electrically or in the form of a standard sample whose resonance is recorded. The electrical "dummy" signal is generally used with the resonance absorption equipment of the type designed by POUND, KNIGHT and WATKINS,[4] and both methods have been used with nuclear induction equipment of the Bloch type.[5, 177] In the latter case, the electrical signal is more difficult to arrange but still has practical advantages over the "standard sample" which for convenience should have a strong resonance close to, but not overlapping, the resonance being studied. The calibration signal resulting from either of these procedures is used to standardize all data of a series by dividing each measured amplitude J' by its accompanying calibration signal amplitude. The latter may vary due to changes in circuit parameters of the detecting equipment, or other extraneous causes, but the quotient is, of course, independent of these changes provided they do not occur between the recording of the sample and standard signals. The symbol J will be reserved for this normalized amplitude.

C. *Position*

The position of the resonance in a metal is of exceptional importance because it is partially determined by the electron density and wave functions in the metal. The position of the resonance of a nucleus in a magnetic field in the absence of all electron–nuclear and nuclear–nuclear interactions, is a fundamental property of the atomic nucleus. It is the presence of interactions

with other nuclei and electrons which results in the experimentally observed position and which brings about the change of the resonance from an infinitesimally wide "spike" as a function of frequency, to the interesting resonance structure actually observed.

The position of a symmetric absorption is naturally understood to mean its centre frequency ν_0, while for any more complicated shape, some unique point may be chosen (generally the readily measurable zero of the derivative) which does indeed locate the resonance but which needs to be accompanied by a discussion of the shape in order to fully describe the positions of the component resonances which comprise the observed absorption. For the asymmetric line of an alloy (Fig. 2b) the position of the zero of the derivative is essentially unchanged from that of the pure metal which has a symmetric absorption; the marked changes distinguishing the resonance of the alloy from that of the pure metal must be expressed in terms of a shape function and a symmetrical width.

The position of the nuclear resonance in a metal is usually stated in the form of a shift from the resonance of the same isotope in a non-conducting reference substance, both materials being in the same magnetic field. In a typical measurement of line position, the nuclear resonance frequency ν_r of the reference nuclei in a compound or an aqueous solution containing a compound of the element under investigation is determined. The resonance frequency ν_0 of the same nuclear species in the metal is also determined in the same external magnetic field. The frequency difference, $\nu_0 - \nu_r$, is known as the Knight shift in consideration of its discoverer, W. D. Knight. It occurs because of the unpaired electron spins present in the metal in the magnetic field and can be a measure of the number of unbalanced spins. Ideally, the measurement should be made on the metal with all of its conduction electron spins paired, and again on the metal as it actually is when in a magnetic field. This has not been possible in practice, and the former condition has been approximated by a judiciously chosen chemical compound. An uncertainty in the true Knight shift arises because of differences in the positions of the resonances of the various possible reference compounds. These so-called *chemical shifts* thus limit the accuracy to which the Knight shift can be

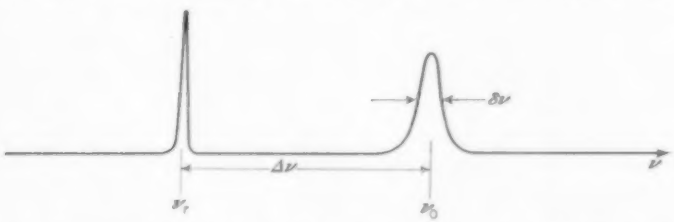

FIG. 3. Absorption lines of the same isotope in a non-conducting reference compound and in a metal in the same external magnetic field. The resonance frequency in the metal ν_0 is greater than ν_r because the magnetic field at the nuclei in the metal is larger than it is in the insulator; both ν_0 and ν_r are directly proportional to field strength.

determined by experiment. In addition to having all electrons paired an adequate reference compound should provide no second order paramagnetic contribution to the chemical shielding.[7] The latter condition implies the desirability of using a compound of high structural symmetry.[8] Paramagnetic impurities in the solution containing the reference compounds can also lead to small errors[9] in the determination of the Knight shift. The metal and reference samples can be held in the detection apparatus simultaneously or interchanged, whichever is more convenient, provided there is adequate assurance that if the separate samples are interchanged, the magnetic field impressed on each sample is the same. Figure 3 is a diagram of absorption versus frequency; $\Delta\nu = \nu_0 - \nu_r$ is marked as the difference in the centre frequencies of the two symmetric resonances.

III. Atomistic View of Resonance in Metals

A. *Nuclear Magnetic Resonance Absorption and Relaxation—General Comments*

In the present context, a metal is visualized as a space lattice of nuclei composing the *spin system*, so called because the nuclei possess spin, or, more accurately, spin angular momentum.* Each nucleus with non-zero spin, also has a magnetic dipole moment given by $\mu = \gamma\hbar I$, where γ is the gyromagnetic ratio, $\hbar$ is Planck's constant divided by 2π, and I is the nuclear spin quantum number which can have one of the values 1/2, 1, 3/2, . . . as shown in Column 7 of Table 1 on page 14. The nuclear spin and moment are intrinsic properties as characteristic of a particular nuclear species as its mass and charge. The nucleons (protons and neutrons) comprising the nuclei each have a spin and moment directly comparable to the more familiar analogous properties of the electron; however, their contribution to the observed total moment of a nucleus is not a straightforward vector sum of the component moments but includes contributions from their orbital motions within the nucleus. Fortunately it is not necessary to understand the origin of nuclear moments to use them as probes of the internal electric and magnetic fields of matter. Since the moments cannot be computed we rely upon experiment to supply the values of both μ and I. The spin I is most often determined by means of hyperfine structure measurements in optical spectra, microwave spectra, paramagnetic spectra or molecular beams. These methods can also be used to determine the magnetic moments; however, nuclear resonance techniques, upon which the present article is based, usually provide the most accurate method. It is known that nuclei with odd mass number, A, have nuclear spin quantum numbers I which take only the odd half-integral values, 1/2, 3/2, . . . and that nuclei with even A and odd Z (nuclear charge) have integral values of I. The most stable nuclei are those

* It is not necessary for a nucleus to have spin angular momentum and, indeed, all nuclei for which *both* the nuclear charge and mass number are even have none. The subject of this paper presupposes that we are considering nuclei with non-zero spins.

for which both A and Z are even and thus for which $\mu = 0$, and the least stable nuclei (which are accordingly rare in nature) are those for which A is even and Z is odd. We find, therefore, that the spins of nearly all nuclei with which we will be concerned are odd half-integral numbers (cf. Table 1), a fact of significance in predicting the resonance behaviour of some metals and alloys. Nuclei with spin equal to or greater than 1 may also have a nuclear electric quadrupole moment Q. This is associated with the deviation of the shape of the nucleus from that of a sphere, a positive quadrupole moment indicating an elongation of the nucleus along the angular momentum axis. PURCELL[10] discusses the action of the electric field on the quadrupole moment in a very illuminating manner. Electric dipole moments and magnetic quadrupole moments can be shown to be zero. Higher order multipole moments, the existence of which can be argued on the basis of parity,[3] have negligibly small interaction energies with the fields existing in solids and do not need to be considered in the present study.

The phenomenon of nuclear magnetic resonance lends itself to a wide variety of equivalent descriptions. In the interest of clarity and consistency one of these has been chosen as the framework for the discussions of this paper. The decision to use the "optical" approach[11] is based on its ability readily to embrace the perturbation theory and thus provide a good phenomenological picture of the interactions in solids. Also, the terminology is thought to be somewhat simpler to introduce than that commonly used to discuss the Bloch nuclear induction technique or the various bridge detection methods frequently used.[12] All of these steady state methods which employ continuous radio frequency excitation differ slightly in concept from the experiments utilizing pulsed radio frequency power to excite the nuclear transitions, the so-called spin-echo and free precession experiments.[13, 14] To compare these methods in the body of the text, would needlessly encumber the reader with the nomenclature and details of various experimental approaches. It should, however, be recognized that each one represents a method of obtaining resonance data, the correct interpretation of which, in terms of nuclear interactions, must be the same for all.

In every application of nuclear resonance, energy is transferred from a radio frequency circuit to a nuclear spin system immersed in a strong uniform magnetic field of strength H_0. In practice, this is a sample of perhaps 1 cm^3 of metal contained in a coil of wire which is between the pole faces of a suitable magnet. The energy transfer is the result of induced transitions among the energy levels of the spin system. For each spin, characterized by $I\hbar$ and μ (the maximum components in the direction of H_0 of angular momentum and magnetic moment, respectively) there are $(2I + 1)$ possible orientations, each corresponding to an energy level of the nuclear magnet in the magnetic field. The difference in energy of adjacent levels is $h\nu_0 = \mu H_0/I$. (See the left-hand side of Fig. 5.) Transitions between the adjacent levels are allowed by the selection rules governing the process, and upon the application of an oscillating magnetic field of frequency ν_0, both stimulated emission and

absorption will occur. An expression for the net rate of absorption and a somewhat more quantitative description the process are given in Appendix A. These processes correspond to changes of $+1$, -1, respectively, in the magnetic quantum number m which labels the various allowed levels. m can take on the values $I, I-1, \ldots, -I$, the energy of the m^{th} level being $-m\mu_z H_0/I$. If a net absorption of energy from the radiation field is to occur, it is essential that transitions of the type ($\Delta m = -1$) predominate. This can be the case only if there is an excess of spins in the lower energy states, a condition which will be attained if there is some way by which the spin system can interact with its surroundings and come to thermal equilibrium. At equilibrium, the population of the $2I+1$ levels will be governed by the Boltzmann factor, $\exp(m\mu_z H_0/I\,kT)$, and the required surplus of nuclei in the lower energy states will have been established. Here T is absolute temperature and k is the Boltzmann constant. If the contact between the spin system and the lattice (the thermal reservoir) is poor, then clearly the absorption process is going to disturb this equilibrium. A steady application of radiation will cause a dwindling of the excess population which existed in the lower states and thus will tend to equalize the populations. Since the net number of absorptive transitions is directly proportional to the excess population of the lower state, the absorption of power from the radio frequency circuit will dwindle accordingly and the resonance absorption is said to be undergoing *saturation*. If the radio frequency excitation is now switched off, the spin system will be found to regain its equilibrium energy distribution, not instantaneously, but through a gradual approach, the rate of which is characterized by the spin-lattice relaxation time T_1. For metals at room temperature, this time is of the order of 1 to 10 milliseconds.

The foregoing discussion presupposed that some coupling between the nuclei of the spin system existed; otherwise it could hardly have been treated as an entity with internal equilibrium. No strictly analogous operational definition of the *spin–spin* relaxation time T_2' can be given, but its qualitative interpretation is similar. If one portion of the spin system were subjected to radiation and thus became locally heated or saturated, its excess energy would be spread through the spin system by a spin-diffusion process.[15b] The essential difference in concept here is that distance through the lattice must be involved when spin–spin interactions are considered. In the process of spin-diffusion, the nuclear magnets can be thought of as passing their *orientation* from one to the other in a manner similar to ordinary mass diffusion, except that no atomic motion occurs in the spin-diffusion process. The equations for heat or mass diffusion apply to spin diffusion if the appropriate diffusion constant is used. In this case, the diffusing quantity is the probability of unbalanced spin.

Another symbol T_2, often found in the literature, is used as a parameter characterizing the resonance line width. Since the shape function $g(\nu)$ is normalized $\left(\int_0^\infty g(\nu)\mathrm{d}\nu = 1\right)$, broadening of a resonance line is reflected in

$g(\nu)$ as a decrease in its maximum value $g(\nu_{max})$. For reasons now primarily of historical importance, we have the definition $T_2 = \frac{1}{2}\, g(\nu_{max})$. This definition brought an internal consistency to the notation used by the two independent groups responsible for the early work on the nuclear absorption [10, 11] and nuclear induction [17, 1] methods of observing the properties of nuclei. For any reasonable bell-shaped curve, T_2 turns out to be approximately $1/\pi\delta\nu$, and thus is sometimes referred to simply as the inverse line width. T_2 approximates the lifetime of the nuclear state which was estimated in Section II-A to be about $1/2\pi\delta\nu$. A more thorough discussion of T_2 involves the various sources of line width which are to be considered below in more detail (Section III-C and Appendix B).

In summary, the nuclear resonance consists of an absorption of radio frequency energy by the nuclei of the metal and the subsequent loss of this energy to the lattice, where it appears as an inconsiderable quantity of heat. The frequency at which the resonance occurs is given by the resonance condition

$$\nu_0 = \mu H_0/Ih = (\gamma/2\pi)\, H_0 \quad . \quad . \quad . \quad . \quad . \quad . \quad (1)$$

where γ, the gyromagnetic ratio, is the ratio of the nuclear dipole moment μ to the nuclear angular momentum Ih and H_0 is the magnetic field at the nucleus.

Although exceedingly simple in form, Eqn. (1) has several implications worthy of emphasis. It is clearly a relationship existing between the magnetic field *at the nucleus*, and the observed resonance frequency only. It depends in no way upon the material in which the nuclei are contained. The opportunity exists, therefore, to observe the resonances of a particular isotope in several compounds, or in metals, and to compare them to study the internal magnetic fields of these solids. Any differences in external applied field H_{ext} necessary to cause the resonance to fall at the same frequency each time must be a result of the internal magnetic field in the solid (or liquid or gas). The internal fields are usually less than one per cent of the main field H_{ext}. Of significance, therefore, is the fact that according to (1) we can measure either the frequency or the field to arrive at the same conclusions about the internal magnetic field of the solid. Frequency can be measured to very high accuracy (one part in 10^6 is not difficult) and, therefore, even 0·01 per cent changes in it can usually be measured with good accuracy. In any case, whichever quantity one is in a position to measure more accurately and easily can be used. Suppose that at fixed frequency, ν_0, we observe two resonances successively, first that of a metal, then that of some reference compound. This, of course, requires that we change the external magnetic field from one value to the other in order to bring the centre of the resonance to frequency ν_0 for each substance. If an external field H_m allows the resonance condition to be satisfied for a metal, it will be found that another field strength H_r is necessary to satisfy it in the reference compound. It is $\Delta H = H_r - H_m$ which is practically equivalent to the measurement of $\Delta\nu =$

$\nu_0 - \nu_r$ mentioned at the end of the previous section. It should be noticed that this "change of variable" has the effect of reflecting shifted resonances through the reference resonance. If the frequency of resonance in a metal and compound is the same then the resonance in the metal (which undergoes the Knight shift) is always at a *lower* external magnetic field. On the other hand, it is at a *higher frequency* if the external field is held constant. The small field ΔH, which in the metal acts to aid the external field and thus increase the field at the nucleus, will cause an *increase* $\Delta\nu$ in the resonance frequency (cf. Eqn. (1)). The term Knight shift is used to denote either

$$\Delta H = H_r - H_m \text{ or } \Delta\nu = \nu_0 - \nu_r$$

and since, as will be shown later, it is directly proportional to the external field, it is practically always referred to in the form of the *relative* Knight shift $\Delta H/H_r$ or $\Delta\nu/\nu_r$. The two quantities differ by higher order terms in the shift.

Since, when the nucleus occupies its usual place at the centre of an atom, the field at that point, H_0, is not quite equal to H_{ext}, experimentalists find a simple listing of resonance frequency versus external field the most convenient way to express the information they require.* Column 2 of Table 1

TABLE 1

Isotope	*ν_r in Mc for H_{ext} = 10,000 G*	*per cent $\Delta H/H$*	*Reference compound* (a)	*Literature reference*	*Width $\delta\nu$ in kc/s* (d)	*Spin*	*Natural isotopic abundance per cent*
Li^6	6·265	0·0263	LiCl	21,178		1	7·4
Li^7	16·547	0·0261	LiCl	21	10·3(77°K)	3/2	92·6
Be^9	5·983	0·000	$BeCl_2$	19, 20	3·5(f)	3/2	100·0
Na^{23}	11·262	0·112	NaOH	21	2·7(77°K)	3/2	100·0
Mg^{25}	2·606	0·111	$MgCl_2$	6	~ 2(f)	5/2	10·1
Al^{27}	11·094	0·161	$AlCl_3$	21	9·4	5/2	100·0
Si^{29}	8·460	0·018(c)	SiO_2(s)	22		1/2	4·7
K^{39}	1·987	0·265	$KCHO_2$	214, 174	$\lesssim$ 0·7	3/2	93·08
K^{41}	1·092	(0·265)				3/2	6·9
Ti^{47}	2·400					5/2	7·75
Ti^{49}	2·401					7/2	5·51
V^{51}	11·193	0·56	$VOCl_3$	23	12·7	7/2	99·75
Cu^{63}	11·285	0·232	CuCl(s)	19	7·2	3/2	69·09
Cu^{65}	12·090	0·235	CuBr(s)	21	6·5	3/2	30·91
Ga^{69}	10·218	0·449(b)	$GaCl_3$	21	0·34	3/2	60·0

* Most of the difference between H_0 and H_{ext} for non-metals is brought about by the orbital electrons which produce a small field opposing the external field, and by excited paramagnetic configurations which cause internal fields that aid the external field. The former (diamagnetic) effect has been considered by LAMB,[18] the latter by RAMSEY;[7] both are designated as magnetic shielding[3] and contribute to the chemical shifts mentioned previously.

VOL. 9 1961

Isotope	ν_0 in Mc for H_{ext} = 10,000 G	$\Delta H/H$ per cent	Reference compound (a)	Literature reference	Width $\delta\nu$ in kc/s (d)	Spin	Natural isotopic abundance per cent
Ga^{71}	12·984	0·449(b)	$GaCl_3$	21	0·42	3/2	40·0
Se^{77}	8·131			22		1/2	7·50
Rb^{85}	4·111	0·650	RbOH	21	0·21	5/2	72·2
Rb^{87}	13·932	0·653	RbOH	21	0·75	3/2	27·8
Nb^{93}	10·407	0·85	Nb_2O_5	19, 24	8·6	9/2	100·0
Mo^{95}	2·774	0·584	K_2MoO_4	6, 171	0·22	5/2	15·78
Mo^{97}	2·833	0·584	K_2MoO_4	6, 171	0·25	5/2	9·60
Rh^{103}	1·344	(0·3)	(g)	19, 25		1/2	100·0
Pd^{105}	1·74					5/2	22·6
Ag^{107}	1·722	0·522	$AgNO_3$	26		1/2	51·35
Ag^{109}	1·981	0·522	$AgNO_3$	26, 27	0·115	1/2	48·65
Cd^{111}	9·028	0·415(e)	$CdCl_2$	28, 29	1·1	1/2	12·86
Cd^{113}	9·444	0·415(e)	$CdCl_2$	28, 29	1·1	1/2	12·34
In^{113}	9·310	0·786(h)	$In_2(SO_4)_3$	168	$\approx$ 2·1	9/2	4·16
In^{115}	9·329	0·786(h)	$In_2(SO_4)_3$	168, 214	2·1	9/2	95·84
Sn^{117}	15·77	0·725(e)	$SnCl_2$	6, 30	$\sim$ 3·0	1/2	7·67
Sn^{119}	15·87	0·725(e)	SnCl	6, 30	$\sim$ 3·0	1/2	8·68
Sb^{121}	10·19					5/2	57·25
Sb^{123}	5·518					7/2	42·75
Cs^{133}	5·585	1·49	CsCl	21	0·52	7/2	100·0
Ba^{135}	4·230	0·403	$BaCl_2$	28	1·0	3/2	6·56
Ba^{137}	4·732	0·403	$BaCl_2$	28	1·0	3/2	11·25
La^{139}	6·014	0·63(j)	$La(NO_3)_3$	175	7·8	7/2	99·91
Ta^{181}	5·095	$1·1_4$	$KTaO_3$	169	$\lesssim$ 15	7/2	100·0
W^{183}	1·790	1·06	WF_6(g)	217, 25	$\lesssim$ 0·08	1/2	14·28
Re^{185}	9·586					5/2	37·07
Re^{187}	9·684					5/2	62·93
Os^{189}	3·307	(2·4)		19, 31		3/2	16·1
Ir^{191}	0·81	(2·0)		19		3/2	38·5
Ir^{193}	0·86	(2·0)		19		3/2	61·5
Pt^{195}	9·153	− 3·52	H_2PtCl_6	32	2·4	1/2	33·7
Au^{197}	0·691	(4·0)		19		3/2	100·0
Hg^{199}	7·612	2·46(e)	$Hg(NO_3)_2$	33, 19	3·2	1/2	16·92
Hg^{201}	3·08					3/2	13·22
Tl^{203}	24·33	1·56(e)	$Tl(C_2H_3O_2)$	34	>60	1/2	29·52
Tl^{205}	24·57	1·56(e)	$Tl(C_2H_3O_2)$	34	33	1/2	70·48
Pb^{207}	8·899	1·47	$PbSO_4$(s)	35	2·3	1/2	20·8
Bi^{209}	6·842	1·41(i)	$Bi(NO_3)_2$	170, 172	2·9	9/2	100·0
Sc^{45}	10·343	0.24(j)	$Sc(NO_3)_3$	175	16·6	7/2	100·0
Mn^{55}	10·555	−0.13	$KMnO_4$	176	13·6(k)	5/2	100·0
Y^{89}	2·086	0.337	YCl_3	214		5/2	100·0

Shifts enclosed in parentheses are estimated.
(a) in aqueous solution unless otherwise stated.
(b) Knight shift for liquid metal, pure quadrupole resonance in solid[36].

(c) a chemical shift, silicon has no Knight shift.
(d) in the metal at room temperature unless noted.
(e) the Knight shift is anisotropic.
(f) Beryllium is split by first-order quadrupole interaction, magnesium by second order, the width given applies to the central line.
(g) The frequency given in Column 2 refers to the metal.
(h) Knight shift for liquid indium at 170°C., pure quadrupole resonance in solid[173].
(i) Knight shift for liquid bismuth.
(j) Markedly temperature dependent, value given pertains to room temperature.
(k) Value refers to β-Mn, is temperature and field dependent. α-Mn was observed also.
(s) solid.

is such a compilation, giving the resonance frequency (in Mc/s) of the isotope in a compound in an external field of 10,000 G. The values are, of course, approximately $10^4 \times \gamma/2\pi$, i.e. $(\gamma/2\pi)_{Li_7} = 1654{\cdot}7\ G^{-1}\ sec^{-1}$. Only those elements are listed which occur as metals and for which the Knight shift is known or reasonably likely to be measured. The reference compound listed in Column 4 is that used in the measurement of the Knight shift given in Column 3. Chemical shifts among compounds which might be used for the measurements usually amount to no more than a few per cent of the Knight shift for the lighter elements. It is difficult to make a more general statement concerning the chemical shifts because they depend upon the electron configuration of the particular molecule or ion used for comparison. In Column 5 the literature reference for the tabulated Knight shift is cited. Columns 6, 7 and 8 are included in order to provide the reader with sufficient information to aid him in deciding the applicability of nuclear resonance to a particular problem. In this regard the following comments may be helpful. The absence of an isotope from Column 1 means that its absorption has not been observed in the metal. Nuclei with spin greater than one-half may be difficult to detect if they do not occupy positions of cubic lattice symmetry (See Section III-D). For nuclei occupying sites of cubic symmetry we may say, roughly, that the resonance amplitude J' for an isotope is relatively greater, the greater its gyromagnetic ratio, spin, and abundance, and the narrower its absorption.

By considering in detail a small number of interactions which take place between the nuclear moments and their surroundings in metals, it is possible to interpret the data of resonance experiments on metals (expressed as positions, widths, intensities, shapes, T_1, and T_2) in terms of their electronic structure and the atomic configurations present in them on a local scale, within a 5 to 10 Å radius. Conversely, a metal can be partially characterized by its resonance absorption and, more important, changes in structure which it undergoes during alloying, working, etc., can be followed on an atomic scale.

Nuclear magnetic dipole moments interact with the magnetic fields of other nuclei and with the magnetic dipole moments of electrons in the solid. Examples of some specific magnetic interactions to be considered are (*a*) the

VOL. 9 1961

nuclear dipole–electron dipole contact or s-type hyperfine interaction which produces the isotropic Knight shift and, indirectly, an exchange coupling among nuclear spins. (*b*) the nuclear dipole–electron dipole interaction at a distance which can be regarded as an ordinary interaction between point magnets and may cause an anisotropy in the Knight shift if the electron charge distribution has lower than cubic symmetry. (*c*) the direct nuclear dipole–nuclear dipole interaction which describes the effect of the magnetic field of one nucleus on another. The last is often a major source of line width. The exchange coupling mentioned under (*a*) above can also take place between a paramagnetic ion and surrounding nuclei. If the charge density of unpaired electrons is imagined as describing a spatial distribution of electronic magnetization the electron–nuclear interactions are readily visualized. In addition to the magnetic interactions, nuclear electric quadrupole moments interact which electric gradients in the solid which originate in various charge configurations of lower than cubic symmetry.

It appears that for a study of conduction electron distribution and the conduction band in metals, magnetic dipole interactions present the greatest possibilities. Quadrupole interactions, on the other hand, offer the best chance of observing internal strain or slight deviations from perfect lattice symmetry. The causes of internal strains may be vacancies, interstitials, dislocations, or impurities, either substitutional or interstitial. The natural separation of the two major areas of application of resonance in metals according to the type of nuclear moment involved somewhat determines the pattern of the subsequent presentation.

B. *Resonance Position in Metals and Alloys*

The first observation of nuclear resonance in a metal was made by POUND [37] who correctly identified some spurious resonances which he detected as those of the Cu^{63} and Cu^{65} in the copper wire of the coil of his *r–f* spectrometer. Knight, a short time later, showed that the resonance in copper metal was at a different (higher) frequency from that in a non-metal (CuCl) in the same magnetic field and went on to show that this shift was a property of several metals. [38] The effect was promptly explained [39] as being the result of the magnetic field at the nucleus produced by unpaired conduction electron spins. Estimates of the resonance frequency shifts, based on this proposal, were in reasonable agreement with observation so that further search for their explanation gave way to considerations of refinements of the theory. A thorough review article by KNIGHT [19] discusses the shift measurements and their interpretation, especially in pure metals, in some detail. Work on alloys has been somewhat slower in appearing because of the greater difficulties encountered in preparing them in proper form and in interpreting the resulting data.

1. *Knight Shift in Pure Metals*

After the initial measurements of KNIGHT [38] on lithium, sodium, aluminium,

copper and gallium, other workers began to investigate the shift in other metals, and under diverse circumstances of temperature, pressure and alloying. Knight had established that the magnitude of the shift $\Delta\nu$ was directly proportional to the external field strength, and also that the shifts for different isotopes of the same element were identical within the accuracy of the experiments. That accuracy proves to have been sufficient because these two statements have been corroborated on more than a score of other metals since that time. The constancy of the relative Knight shift $\Delta\nu/\nu_r$, and the fact that $\Delta\nu/\nu_r$ is the same for different isotopes of the same element are identifying characteristics which also aided in its explanation. The fact that different isotopes of an element usually possess different nuclear magnetic moments and yet that any one of these isotopes, when used to measure $\Delta\nu/\nu_r$, will give the same value, proved that the measured shift was a property not of the nuclei but solely of the metal in which the nuclei reside.

VOL. 9 1961

The theory mentioned above [39] takes cognizance of the fact that electrons and nuclear dipole moments interact to cause the hyperfine structure common in optical spectra. This interaction was known to be particularly strong for unpaired s-electrons. It was thus reasoned that if one estimated the unpaired electron spin density at the nucleus in the metal and multiplied the ordinary expression for the hyperfine interaction by it, the result would approximate the additional energy of each nucleus in the field.

This point of view leads directly to the expression

$$\frac{\nu_0 - \nu_r}{\nu_r} = \frac{\Delta\nu}{\nu_r} = \frac{8\pi}{3}\chi_p V_0 \langle |\psi(0)|^2 \rangle_F \quad . \quad . \quad . \quad . \quad . \quad (2)$$

where ν_0 and ν_r are, as before, the metal and reference compound resonance frequencies, χ_p is the electron spin paramagnetism in cgs volume units, V_0 is the atomic volume and $\psi(0)$ is the value at the nucleus of the wave function normalized over V_0 for an electron of the Fermi energy E_F. The average of the square of the function $\psi(0)$ is taken for all electronic states on the Fermi surface. $\langle |\psi(0)|^2 \rangle_F$, generally abbreviated P_F, is thus the average probability density at the nucleus for all electronic states on the Fermi surface. All of the essential features of the observed shifts in pure metals are expressed by Eqn. (2); on inspecting it we note that (*a*) the resonance in the metal is always at a higher frequency than in the compounds, (*b*) the shift is proportional to ν_r (or, of course, H_r), (*c*) the factors entering the expression are largely independent of temperature, (*d*) P_F and so $(\Delta\nu/\nu_r)$ gets larger for heavy elements, and (*e*) for metals with low *s*-electron concentration, the shift can be expected to be small. That P_F increases with atomic number is inferred from knowledge of the hyperfine structure constants of the elements. For example, in the monovalent metals, the electron density at the nucleus, P_F, exceeds the value for a uniform density distribution, V_0^{-1}, by a factor which is about 35 for lithium and increases to about 3200 for cesium. [40] These factors correspond to the amount by which the magnetization *at the nuclei* exceeds the bulk conduction electron spin magnetization given by $\chi_p H_m$.

Several other useful forms of this equation appear in the literature. One of the most common variations occurs through a substitution for $\langle|\psi(0)|^2\rangle_F$, a quantity which would be exceedingly difficult to calculate in final form from first principles, but which can be separated into two calculations each of which is conceptually important. If it is first recalled that the hyperfine structure constant for s-electrons[41] is given by $A = (16\pi/3)\,\beta\gamma\hbar|\psi_a(0)|^2$, it is apparent that if we have a *measured* value of A, and can *derive* a renormalization factor $\xi = (P_F/P_A) = \langle|\psi(0)|^2\rangle_F/|\psi_a(0)|^2$, expressing the change in the electron density at the nucleus upon going from the free atom to the top of the band in the metal, then the necessity of calculating $|\psi_a(0)|^2$ *ab initio* is obviated. β is the Bohr magneton, and $|\psi_a(0)|^2$ is the probability density of the valence electron at the nucleus in the free atom; the other symbols are as previously defined. The value of ξ is usually close to one. Since a calculation of $|\psi_a(0)|^2$ is quite difficult (especially for heavy atoms) and is not crucially important to metal theory, its elimination is desirable. Equation (2) can now be written

$$\frac{\Delta\nu}{\nu_r} = \frac{A}{2\beta\gamma\hbar}\,\chi_p V_0\,\frac{\langle|\psi(0)|^2\rangle_F}{|\psi_a(0)|^2} \quad . \quad . \quad . \quad . \quad . \quad . \quad (3)$$

The wave functions appearing represent the step in changing from the free atom to the metal.

Alternatively, χ_p can be replaced in Eqn. (2). This weak paramagnetic susceptibility, arising from a partial alignment of the electron spins in the external magnetic field has been calculated by PAULI[42] for free electrons neglecting interactions between electrons. Important refinements have been made in the theory by PINES.[59] The Pauli result is

$$\chi_p = \beta^2\,N(E_F) \quad . \quad . \quad . \quad . \quad . \quad . \quad . \quad . \quad (4)$$

where, $N(E_F)$ is the density of one-electron states per unit volume and energy at the Fermi surface and χ_p is the susceptibility per unit volume. Equations (2) and (3) become

$$\frac{\Delta\nu}{\nu_r} = \frac{8\pi}{3}\,\beta^2 V_0\,N(E_F)\,\langle|\psi(0)|^2\rangle_F \quad . \quad . \quad . \quad . \quad . \quad (5)$$

and

$$\frac{\Delta\nu}{\nu_r} = AV_0\,N(E_F)\,\frac{\beta}{2\gamma\hbar}\,\frac{\langle|\psi(0)|^2\rangle_F}{|\psi_a(0)|^2} \quad . \quad . \quad . \quad . \quad . \quad (6)$$

Applications of the various expressions for the Knight shift present an almost unparalleled opportunity to check the theoretical values of χ_p and $\langle|\psi(0)|^2\rangle_F$. Very few ways of measuring electron density exist so that although this is only a point determination, it is a significant achievement.

In theoretical estimates of the Knight shift, early workers[44, 39] computed the wave functions, but had to use indirect methods to derive χ_p since it is only one of the three[45, 46] known contributing factors to the measured bulk magnetic susceptibility. In 1954, χ_p of lithium was measured directly using

electron spin resonance,[47] and the result was used[48] to calculate the ratio P_F/P_A. More recently, similar work on sodium has been carried out.[49, 50] The results in each case were gratifying; close agreement existed between the calculated and "measured" values of P_F/P_A, not only increasing our confidence in the correctness of the electron wave functions for the metals, but also providing an estimate of the relative amounts of s and p functions contributing to the total wave function at the Fermi surface. Only the alkali metals and beryllium[51, 52] have proven suitable for electron spin resonance determinations of χ_p; fortunately, however, it is precisely on these metals that electron theory is most often tested.

If an "experimental" value of P_F is desired for metals for which χ_p cannot be directly measured, it becomes necessary to use the relationship (4) to introduce $N(E_F)$ which can be estimated from the measured electronic specific heat, C_e. The relation between C_e and $N(E_F)$, first derived by SOMMERFELD,[53] is

$$(C_e/T) = \pi^2 k^2 N(E_F)/3. \quad . \quad . \quad . \quad . \quad . \quad . \quad (7)$$

T is the absolute temperature, k the Boltzmann constant, C_e and $N(E_F)$ are referred to unit volume of metal. A good summary of electronic specific heat in metals is contained in Ref. 54. It is also possible[19] to derive a value of χ_p from the measured bulk susceptibility. The errors involved in this process may be so great as to vitiate the usefulness of the result and it is only employed as a last resort in estimating χ_p.

From the form of Eqn. (2), it is clear that it can be used equally well to determine χ_p if a reliable value for P_F can be obtained. After the foregoing discussion, there may appear to be a circular argument involved here; this is only true to the extent that we are actually concerned with a product of two quantities, the relative accuracy of which varies from metal to metal. Since χ_p cannot be measured directly except as mentioned above, this alternative way of evaluating it may be of interest when suitable wave functions become available.

2. *Temperature and Volume Dependence of the Resonance Position*

Because theoretical calculations of P_F and χ_p usually depend explicitly on the physical dimensions of the unit atomic cell in a metal it is possible to calculate their dependence on volume with a minimum of additional effort. It is of great interest to compare the results of such calculations with measurements of the temperature and volume dependence of the Knight shift. Even if the calculations are not completely successful in predicting χ_p or P_F in an absolute sense, it is satisfying to know whether they are able to predict changes of the correct sign and magnitude for these quantities as a function of the lattice parameter of the metal.

Early experimental work of this type[55, 56, 57a] measured the Knight shift as a function of temperature at constant (atmospheric) pressure. The radio frequency coil containing the sample of metal was placed in a cryostat,[58]

VOL. 9 1961

and very near it, outside of the cryostat, another identical coil and sample. The difference in applied magnetic field which was necessary to cause first one resonance and then the other to occur was measured, the radio frequency remaining constant. This measurement is, of course, equivalent to determining the frequency difference of the respective resonances in a fixed magnetic field. Measurements of lithium, sodium, rubidium, cesium and gallium were reported. The maximum change in the Knight shift of a solid metal occurred in the case of cesium (Cs^{133} resonance) for which it was about 5 or 6 per cent of the total shift for that metal over the temperature range 78°K to 300°K. An abrupt change of about 3 per cent of the shift also occurred upon traversing the melting point. The temperature dependence of the shifts of these elements was found to be generally linear (a bump in that of rubidium at 254°K remains unexplained even now), and progressively larger for elements with higher atomic number. For cesium and gallium, the shift decreased with increasing temperature; for the others, it increased or was constant.[56] At the time these experiments were completed, there was no information concerning the influence that temperature alone would have on the Knight shift if volume changes accompanying temperature variations could be arrested. In fact, the volume expansion upon heating is such an obvious and large effect that it was assumed, reasonably enough, that the entire temperature dependence of the Knight shift could be explained on the basis of the volume changes in χ_p and P_F. It was correctly reasoned that $V_0\chi_p$ should increase as the metal expands and, therefore, that, at least for cesium and gallium, P_F must decrease appreciably with increasing temperature. This is in accord with intuition, a decrease in electron charge density is expected to accompany an increased volume per electron simply because of renormalization.

It was not until the appearance of work on the pressure dependence of the Knight shift[57, 58] that a clear demonstration of an explicit temperature dependence of the Knight shift could be given. This explicit temperature dependence, the change in the Knight shift with temperature at constant volume, turns out to be comparable in magnitude to the change brought about by volume changes due to temperature, at least for the alkali metals. The experimental arrangement for this work was of necessity quite elaborate, since in lithium, for example, the change in position of the absorption line centre amounted to only about 27 c/s out of 10 Mc/s in going from atmospheric pressure to 10,000 atm. The temperature was held constant (18°C) during the measurements and the external field was fixed to within 3 parts in 10^7. The change in resonance frequency as a function of pressure at constant temperature can be converted directly, using the known compressibilities of the metals, to the change as a function of volume at constant temperature. The latter quantity was of paramount importance for comparison with the theoretical results, which had meanwhile become available in dependable form for both χ_p and P_F. Using the theoretical values of χ_p,[59] the volume dependence of P_F was derived from experiment. This was compared with the theoretical results[50, 60] for P_F over the range of volume corresponding to

the 10,000 atm pressure change, and very good agreement with experiment was obtained for sodium and rubidium. Cesium shows a much stronger volume dependence than is predicted. In order to complete this picture of the changes which take place in χ_p and P_F when a metal is heated, we must explain the one remaining fact which emerged from the studies, i.e. the explicit temperature dependence of the Knight shift. There are valid arguments, based on a comparison of the characteristic time of lattice vibrations with the time it takes for an electron spin to accommodate itself to such fluctuations, for asserting that no temperature dependence of χ_p (at constant bulk volume) is possible. It must then be P_F which changes. The mechanism suggested[58] to explain this is the following. Lattice vibrations are thought of as thermal strain, or rapid changes in the volume occupied by an atom in the lattice. Thus P_F is a time varying function, the instantaneous value of which can be written $P_F(V_0) + (\partial P_F/\partial V)_{V_0}\Delta V + \frac{1}{2}(\partial^2 P_F/\partial V^2)_{V_0}(\Delta V)^2 + \ldots$ where V_0 is the equilibrium atomic volume at temperature T and $\Delta V = V(t) - V_0$. Here $V(t)$ is the instantaneous atomic volume at time t. From this series we see that in first order $P_F = P_F(V_0)$ because $\overline{\Delta V} = 0$, the bar denoting a time average. However, $\overline{(\Delta V)^2}$ is, of course, always positive, so the time average of P_F can in fact be a function of temperature at constant volume. Experimental values[58] of $(\partial^2 P_F/\partial V^2)_{V_0}$ are positive for sodium, rubidium and cesium and large enough to explain the observed temperature dependence of the Knight shift. Even the zero-point vibrations will cause P_F to be slightly different than the ordinarily computed static lattice value. An additional consequence of this zero-point effect has been pointed out by BLOEMBERGEN:[61] the low temperature Knight shifts of Li^6 and Li^7 may be slightly different because of the difference in the vibration amplitudes of these two isotopes. This would constitute a marked exception to the usual situation in which the Knight shift is independent of isotope, and was observed[178].

One of the factors which made possible this highly precise work on the alkali metals was the narrowness of their resonance lines at room temperature or slightly above. In a measurement of line position an accuracy of greater than about one-tenth of the line width is difficult to attain. In the case of these metals, the observed width at room temperature is small due to the effect self-diffusion in the metal, a point which will receive more attention later.

The smooth variation of the Knight shift as a function of temperature can be expected to hold throughout the range over which the metal is solid unless a phase boundary is crossed, or, for superconductors, if the superconducting transition temperature is traversed. Both of these changes will, in general, have a marked effect on the electronic properties of the metal. Mention has already been made of the abrupt change in shift which usually occurs when the metal melts. Because of the relative simplicity of resonance measurements at low temperature, it may be more convenient to determine a phase change by using the Knight shift than X-rays, but the result would not be completely

unambiguous. An abrupt change in the Knight shift certainly denotes a discontinuous change in the spin susceptibility or in the wave functions, indicating that the volume per electron, the electron–electron interactions, or the structure of the metal has been altered. Unfortunately, there is also the possibility, however slight, that the product $\chi_p V_0 P_F$ might have the same value for two different phases. The only two solid phases of a pure metal which have been observed to date are those of the two forms of tin.[30] In this case, of course, the grey form is not only of a different lattice structure, but of quite a different electronic structure, which causes it to be semiconductor. The grey form has a minute Knight shift,[179] and the resonance of Sn^{117} in white tin is found to occur at a frequency about 0·77 per cent higher than it does in grey tin. Resonance studies of phase changes in pure metals offer some potential usefulness, but since it has already been demonstrated that the various phases of an alloy can usually be distinguished by the resonance line positions of a constituent the latter field appears to offer much wider possibilities for the application of resonance to phase changes. It will be discussed in detail in a later section.

Resonance methods have also been used to investigate superconductivity. Since the Knight shift and the spin-lattice relaxation time T_1 are determined by the density of states of the electrons near the Fermi level of both spin directions, the presence of a superconducting energy gap can certainly be expected to produce drastic changes in both quantities. Conversely, the Knight shift and spin-lattice relaxation time can be used to investigate the presence of such a gap. The relative Knight shift in mercury[33] was found to decrease from a value of 2·5 per cent for the normal metal to 1·6 per cent for the superconducting metal in low magnetic fields (750–2300 G.) and to an even lower value[62] at higher fields. The data are rather meagre and some disagreement may exist in these two results so that no definite conclusions can yet be drawn from them. A survey of experimental evidence for an energy gap model which includes a discussion of these experiments appears in Ref. 63. On the basis of the BARDEEN, COOPER, SCHRIEFFER theory[64] a decrease to zero of the Knight shift in the superconductor was anticipated;[65] however, modifications have been suggested by HEINE and PIPPARD[68a] and others[209] which would explain a finite Knight shift at $T = 0°K$.

The difficulties encountered in performing these shift experiments on superconducting material cannot be overemphasized; in fact, upon first consideration the venture appears impossible. The magnetic induction B is known to vanish inside of a superconductor (Meissner effect) so that neither the static nor radio frequency magnetic field can penetrate the superconducting metal and interact with the spin system in the required manner. Also, as is well known, large magnetic fields destroy superconductivity, causing the metal to become "normal" below its superconducting transition temperature in zero magnetic field. Both of these arguments, however, must be reexamined if one chooses to discuss not bulk metal but particles whose size is comparable to thenducting penetration depth, which is of the superco

order of 5×10^{-6} cm. It is then found that the experiments are theoretically possible, but require a dense colloidal sample of particles less than 500 Å in diameter; the smaller the particle size the better. The preparation of the samples is thus formidable and, since the particles obtained are usually not of uniform size but have a distribution of sizes, the interpretation of absorption data to arrive at the Knight shift is exceptionally involved.[33]

An experimental determination of T_1 in superconducting aluminium reported by HEBEL and SLICHTER[66] when considered in conjunction with data on ultrasonic absorption,[67] confirms the basic feature of the new theory of superconductivity,[64] i.e. that electrons of opposite spin and momentum are correlated. Through clever experimental design the actual resonance measurements[66] were carried out on metal in the normal state. Relaxation of the spin system was allowed to occur with the metal in the superconducting state by decreasing the external magnetic field. This field cycling method considerably reduced the troublesome aspects of the magnetic resonance investigation of superconductors.

VOL. 9 1961

An isolated case exists in which the resonance in a pure metal occurs at a lower frequency than it does in the aqueous solution of the compound used for comparison.[32] It is thought that the reason for this exceptional behaviour, which was observed for Pt^{195}, is more likely to relate to the properties of the reference compound than the metal, and may be the result of a very large chemical shift. If this is true[215] we are justified in proceeding as if the metal is behaving normally. Its Knight shift is merely not accessible by the usual technique, but must be obtained indirectly through its relationship with the spin-lattice relaxation time T_1. An expression connecting these two quantities was published by KORRINGA[68] and is generally known as the Korringa relation,

$$T_1 \left(\frac{\Delta H}{H_r}\right)^2 = \frac{\hbar}{\pi k T} \left(\frac{\beta}{\gamma \hbar}\right)^2, \quad . \quad . \quad . \quad . \quad . \quad . \quad . \quad (8)$$

the derivation of which is outlined in Appendix B, accompanied by a discussion of its general applicability. It is apparent that if we know the gyromagnetic ratio γ, the absolute temperature T of the metal during the observation of its resonance, and its relaxation time T_1, then $(\Delta H/H_r)$ can be calculated, the other quantities being physical constants defined previously. By this method, $\Delta H/H_r$ for Pt^{195} was estimated to be 1·8 per cent. The position of the resonance in the metal depends quite strongly on temperature from 78°K to about 340°K, the range over which it has been investigated. To explain this change which amounts to about one third of the total estimated shift, it was suggested that a rapid change in the occupation of states was depleting the s-band at low temperature. The electrons going into the d-band could presumably augment the bulk susceptibility[69] in the manner observed.

The few studies discussed above may serve to demonstrate the usefulness of nuclear magnetic resonance in an investigation of the electron spin susceptibility χ_p, the density of states $N(E_F)$, or the conduction electron proba-

bility density at the nucleus for those electrons at the Fermi surface, $P_F = \langle|\psi(0)|^2\rangle_F$. The temperature dependence of the Knight shift of other metals has been measured [175] and further work, especially on superconductors, will undoubtedly be forthcoming. Experiments of the latter type which utilize multiple thin films of metal [70, 71] and thus avoid the use of very small particles are being attempted. [62] The simplification in geometry combined with the uniformity of sample thickness should greatly simplify the interpretation of the data.

The Knight shift is not significantly influenced by internal strains or by non-paramagnetic impurities present to the extent of a few tenths of a per cent. This has been demonstrated by observations made on filed and annealed particles [30] and by measuring the change in the Knight shift as a function of solute concentration in more concentrated solid solutions; [72, 90] both of these topics will receive further attention in later paragraphs. It should be emphasized that the interaction of nuclear dipoles with conduction electrons *via* the hyperfine interaction mechanism, i.e. the isotropic Knight shift, is with one exception the only source of a shift in the resonance position of a powdered pure metal except the very much smaller and not separately identifiable one due to changes in the atom cores or bonding. The latter are the type giving rise to the chemical shifts, which are the source of uncertainty in measuring the Knight shift. The width, amplitude and shape of a resonance in metal are most often determined by several simultaneous contributions due to various nuclear interactions, and in interpreting the data, these must be separated and identified. The resonance position usually has no such ambiguity, provided the powdered metal sample is used. Other interactions which might conceivably be responsible for a change in the position of a resonance depend upon crystal lattice orientation relative to the external magnetic field and result in no net shift when account is taken of the isotropic distribution of orientations existing in a powder. There may, of course, be a change in line width or shape due to these other interactions, one of which is the electron dipole–nuclear dipole interaction at a distance, giving rise to an anisotropy in the Knight shift of some metals.

3. *The Anisotropic Knight Shift in Pure Metals*

It has been demonstrated [30] that the effects of anisotropy in the distribution of the electron charge density cause characteristic changes in the shape of the nuclear resonance observed using the customary powdered metal samples. Actually, each crystallite in the agglomerate would, if its resonance could be viewed alone, show a symmetric resonance the position of which would depend on the orientation of the crystal axes with respect to the external magnetic field. The resonance would move within a small frequency region as the crystallite orientation is changed, the extreme positions of the line corresponding to alignment of the symmetry axis of the lattice parallel to or perpendicular to the external field. In experiments on metal powders, essentially all orientations are represented and absorption of

energy takes place over the whole range of frequencies, producing a line which looks like the one in Fig. 2a.

The cause of this orientation-dependent shift is the energy of the nuclear dipole in the field of unpaired electron spins *outside* the nucleus in the metal. This mechanism strongly resembles a classical interaction between bar magnets with one of these magnets (the electron) thought of as being smeared out or moving rapidly around the other. The total Knight shift is the sum of the fields at the nucleus, ΔH_{is}, the isotropic s part discussed above, and ΔH_{anis}, the orientation-dependent part produced by the anisotropy in the charge distribution described by the non-s wave functions. ΔH_{anis} has been calculated [30] and for an axially symmetric charge distribution is given by

$$\Delta H_{\text{anis}} = \beta^2 V_0 N(E_F) q_F (3\cos^2\theta - 1) H_0. \quad . \quad . \quad . \quad (9)$$

q_F is a measure of the anisotropy in charge distribution and is related to the conduction electron wave function by $q_F = \langle \int \psi^* (3z^2 - r^2) r^{-5} \psi \mathrm{d}V \rangle_F$, where the axis of symmetry is the Z axis, the integral is over the unit atomic cell, and the average is over the Fermi surface; q_F is a positive number if the charge density is greatest in the direction of the Z axis. ΔH_{anis} is directly proportional to the external magnetic field H_0. The angle θ lies between the symmetry axis and the external field direction; other notation is as used in the discussion of the isotropic Knight shift. The orientations $\theta = 0$ and $\theta = \pi/2$ define the limits of ΔH_{anis}. If $\theta = 0$, the crystal symmetry axis (usually a hexagonal or tetragonal axis) is parallel to the external field and the total additional field at the nucleus due to the conduction electrons is

$$\Delta H_{\parallel} = \Delta H_{\text{is}} + 2\beta^2 V_0 N(E_F) q_F H_0.$$

For $\theta = \pi/2$

$$\Delta H_{\perp} = \Delta H_{\text{is}} - \beta^2 V_0 N(E_F) q_F H_0,$$

and for any arbitrary angle, the field is

$$\Delta H = \Delta H_{\parallel} \cos^2\theta + \Delta H_{\perp} \sin^2\theta.$$

For a positive q_F, $\Delta H_{\parallel}$ is greater than $\Delta H_{\perp}$ and, therefore, the resonance frequency is *higher* for crystals oriented with $\theta = 0$; $\Delta H_{\parallel}$ thus corresponds to the higher frequency ν_2 in Fig. 2a; similarly, $\Delta H_{\perp}$ and ν_1 correspond. For negative q_F, these relationships reverse, but the peak in the line always denotes $\Delta H_{\perp}$. ΔH averages to ΔH_{is} for a polycrystalline material; as a result there is *no* net shift in the line due to this additional interaction, only the field dependent broadening and asymmetry described above. The relative isotropic Knight shift $\Delta H_{\text{is}}/H_r$ is measured from a point two-thirds of the way from $\Delta H_{\parallel}$ to $\Delta H_{\perp}$. Unless it is stated otherwise, the *isotropic* Knight shift is meant in all references to the Knight shift.

Although q_F can be derived from experiment using an approximation for χ_p or $N(E_F)$ it is not yet possible to compute a good theoretical q_F for comparison. The ratio $(\Delta H_{\parallel} - \Delta H_{\perp})/\Delta H_{\text{is}}$ does not contain $V_0 N(E_F)$, so this ratio can be independently subjected to comparison with theory. MASUDA [29]

VOL. 9 1961

has attempted a quantitative interpretation of the data for cadmium based upon the assumptions that the wave function in the metal could be approximated by atomic *s*- and *p*-functions, and that $V_0N(E_F)$ for a free electron model could be used. These allowed him to derive ξ, which in this approximation is simply the amount of *s*-character in the metal; also, by difference, he derived the proportion of *p*-character, and the anisotropy in the *p*-character. Considering the approximations made it is probably fair to say that the amount *p*-character in metallic cadmium lies between 60 and 90 per cent.

If an electron charge distribution of lower than axial symmetry is involved in nuclear resonance measurements, it is possible to observe an even more complicated line shape which has been calculated,[30] but not yet observed in metals. Also it should be pointed out that an anisotropy in the Pauli spin paramagnetism could produce the same effect as that attributed to the electron distribution in the paragraphs above. This would be an anisotropy in the *s*-part of the shift and would still indicate a sizable amount of non-*s* wave function.

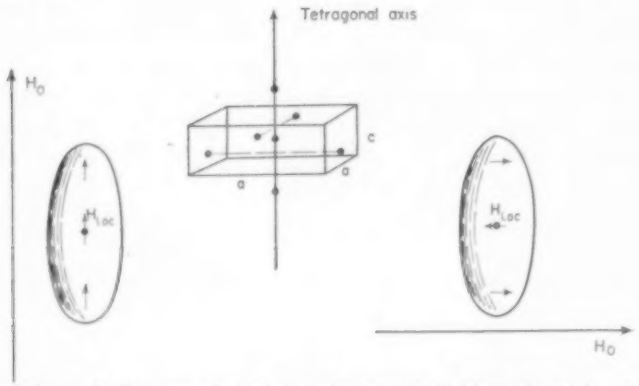

FIG. 4. Schematic diagram of the internal magnetic field produced in white tin when the external field is parallel (*left*), or perpendicular to the tetragonal axis. The anisotropic distribution of conduction electrons with unpaired spin causes the local field at a tin nucleus to depend on lattice orientation relative to H_0.

Anisotropy has been observed in the resonances of tin,[30] cadmium [28, 29] mercury,[33] and to a lesser degree, in thallium;[34] the first two of these have a positive q_F, their electron charge is more dense in the direction of the *c* axis than at right angles to it, a situation depicted in Fig. 4 for the case of tin. The schematic density ellipsoids are symmetric about the tetragonal axis. For mercury and thallium, the electron density is greater in directions perpendicular to the axis of symmetry, i.e. q_F is negative.

4. *Quadrupole Perturbations of the Nuclear Resonance in Pure Metals*

It is primarily to emphasize the true origin of certain width, shape, and amplitude observations that the topic of quadrupole perturbations is classified under resonance "position". The electric quadrupole interaction energies to be considered are sufficiently small, relative to the magnetic splitting $h\nu_0$,

to be treated as slight perturbations of the magnetic energy levels. The situation for powder samples (except in the case of second order quadrupole perturbations) resembles that of the anisotropic Knight shift; that is, if we could examine single crystals experimentally, we would find that the resonance position is dependent upon the orientation of the crystal axes relative to the direction of external magnetic field but the centre of gravity of the powder pattern is unshifted. Again, understanding the properties of the single crystal resonance is prerequisite to the proper understanding of the powder patterns obtained in experiments on metals. Since for nuclei with spin greater than one half, the quadrupole interaction may be very large and result in extremely large changes in the resonance shape, the anisotropic Knight shift and quadrupole effects are seldom observed simultaneously. A distortion of the electron density sufficient to bring about a noticeable anisotropy of the Knight shift ordinarily would cause drastic quadrupole effects. The metals for which anisotropic shifts have been recognized all have $I = 1/2$ and, therefore, $Q = 0$.

VOL. 9 1961

4a. *First-Order Quadrupole Effects in Pure Metals or Ordered Lattices*

In the absence of an electric quadrupole interaction, the $2I + 1$ magnetic energy levels are equally spaced, and the corresponding $2I$ absorptions are superposed. The effect of a quadrupole interaction is to shift the magnetic levels unequally and split the resonance line into its $2I$ components which, according to first order perturbation theory, now fall at frequencies [73]

$$\nu_{m \to m-1} = \nu_0 + (2m - 1)(3\cos^2\theta - 1)\frac{3e^2qQ}{8I(2I-1)h}, \quad . \quad (10)$$

as shown in Fig. 5. This equation applies to the common situation of a nucleus

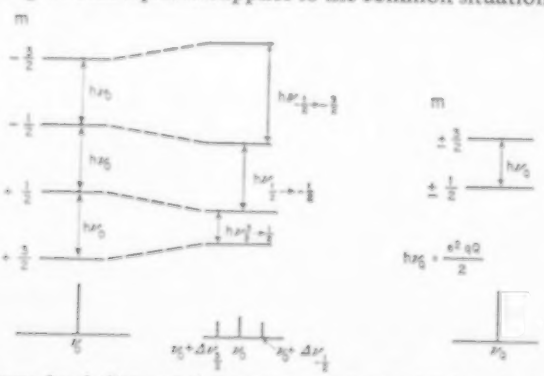

FIG. 5. Energy level diagram for a nucleus of spin 3/2 in a magnetic field, showing the change in level spacing brought about by first order quadrupole perturbation of the magnetic levels by an axial electric field. Pure quadrupole resonance is portrayed on the right.

of quadrupole moment Q in an inhomogeneous electric field of cylindrical (axial) symmetry; $\nu_{m \to m-1}$ is the frequency of the transition between the m and $m - 1$ magnetic levels, θ is the angle between the axis of symmetry

of the electric field and the direction of the external magnetic field and ν_0 is the unperturbed resonance frequency defined by Eqn. (1). In a general treatment of quadrupole effects in crystalline solids,[74] necessary conditions for the existence of an axial field are considered and it is shown that any axis of threefold or higher symmetry will qualify. Most pure metals are included in this category which covers tetragonal, rhombohedral, hexagonal and cubic crystal structures. The electric gradient, eq in (10), is a scalar quantity representing the magnitude of the second derivative of the electrostatic potential at the nucleus due to all charges outside of the nucleus. The derivative is taken with respect to distance in the direction of the symmetry axis. Its value is given directly by

$$eq = \sum_j e_j (3 \cos^2 \phi_j - 1) r_j^{-3}, \quad . \quad . \quad . \quad . \quad (11)$$

where ϕ_j is the angle between the radius vector $\bar{r}_j$ and the symmetry axis, and $\bar{r}_j$ connects the centroid of the nuclear charge with the charge e_j. The sum extends over all charges external to the nucleus concerned, and since this includes all conduction electrons, core electrons, and other nuclear charges, it is usually quite difficult to evaluate. It is very important to note, however, that *at points of cubic or tetrahedral symmetry, the electric field gradient must always vanish, and there will be no quadrupole splitting*. This statement is most easily derived by means of symmetry arguments applied to the potential field in the lattice.[74]

Returning to (10), it is seen that for $m = 1/2$, the frequency of the transition is unchanged, while for $m \neq 1/2$ there is a shift $\Delta\nu_m = \nu_{m \to m-1} - \nu_0$ away from the unperturbed position. In a single crystal, the absorption of nuclei of odd half-integral spin then occurs as a *central* ($m = 1/2 \to -1/2$) line together with $2I - 1$, so-called *satellite* lines[73] symmetrically disposed about the central component in pairs which correspond to the $m \to m - 1$ and $-(m-1) \to -m$ transitions. The splitting $\Delta\nu_m$ is independent of external field strength, and the relative intensity of the satellite corresponding to the $m \to m - 1$ transition is given to a good approximation by $(I + m) \times (I - m + 1)$ (compare Eqn. A1, Appendix A). The relative intensities prove to be quite important in the interpretation of some experiments and are as follows: for nuclei of $I = 3/2$, the three resulting lines have intensity ratio 3 : 4 : 3, for $I = 5/2$ we have five lines and the ratio 5 : 8 : 9 : 8 : 5, and for $I = 7/2$ we have 7 : 12 : 15 : 16 : 15 : 12 : 7.

In a polycrystalline aggregate, such as the metal powder on which most experimental work is done, the individual satellite components are not seen, but only composite structures made up of the satellite lines corresponding to all values of θ. These composite structures are usually referred to as satellites also; their *integrated* intensities have the above ratios. The absorption curve for nuclei of $I = 3/2$ in a powdered sample[75, 72, 76] is shown in Fig. 6 together with an experimental recording of the Be^9 resonance. Since the intensity is spread out over the region $-1 < (3 \cos^2 \theta - 1) < 2$, the

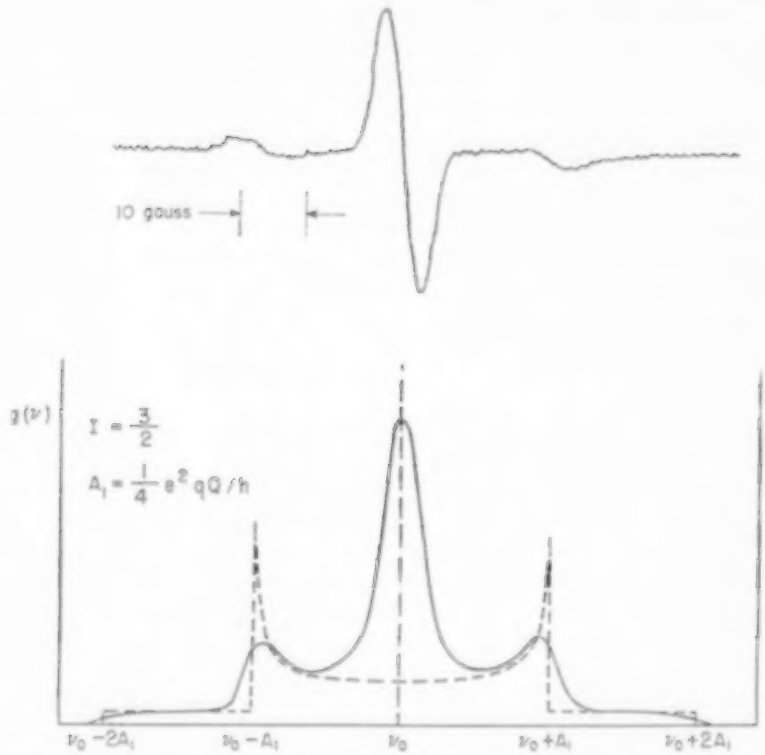

FIG. 6. First-order quadrupole splitting. *Bottom*: The broken line describes the theoretical magnetic resonance absorption of nuclei of spin 3/2 in axially symmetric electric fields of gradient eq, calculated for a powder specimen with isotropic orientation distribution. The full line includes symmetric broadening; an example is the Be^9 resonance in pure beryllium metal (*top*). In an instance in which A_1 is larger and/or inhomogeneous the satellites are not observed.
Be^9 absorption, metal
$H_0 \simeq 11{,}900$ G.; room temperature
2·5 G. peak-to-peak modulation

satellite peaks at $\pm e^2qQ/4h$ are not pronounced in the experimental absorption derivative. For Be^9, the value of the quadrupole moment was felt to be more in doubt than the calculated electric gradient in the lattice; accordingly, from the value $e^2qQ/h = 48$ kc/s given by KNIGHT,[20] and a value of $eq = 2{\cdot}3 \times 10^{13}$ statvolts/cm², calculated in some detail for beryllium by POMERANTZ,[77] a value of $Q(Be^9) = 0{\cdot}029 \cdot 10^{-24}$ cm² was derived.

In spite of the fact that an independent measurement of Q is not available to check the appropriateness of the calculation, the argument of Pomerantz will be outlined because of the insight it offers concerning a possible source of the electric gradient at the nuclei in a metal. The most important observation is that the conduction electrons are spread almost uniformly through the metal; they are, therefore, spherically distributed about any one lattice

point and contribute nothing to the electric gradient. The important contribution to eq is just that of $+2$ ions arranged on the beryllium lattice. The sum (11) was computed for the nearest 1400 lattice sites (by machine) and used as a first approximation to eq. Two corrections were then applied. The first was a shielding factor[78] to account for the fact that the core electrons tend to shield the beryllium nuclei from external electric fields by distorting appropriately; this decreased the gradient to 0·815 of the above computed value. Second, the actual conduction electron distribution was computed and used to revise the estimate of charge on each lattice site. It was found that inside of a sphere close to the nucleus, and containing most of the rapidly varying part of the wave function, there was actually a slightly lower electron density than the average in the metal. This is equivalent to a small positive increment of charge at the beryllium nuclei, tending to increase eq by a factor of 1·08 so that $eq = (0{\cdot}815) \times (1{\cdot}08) \times$ (bare-ion lattice sum). From the size of the corrections it is apparent that the dominant factor in producing the gradient is the Be^{+2} cores, and that the reason for this is that the calculated electron density at the outer part of the atomic sphere is very close to the average density in the metal, leaving very little to concentrate near the nucleus where it would produce screening.

4b. *Second-Order Effects in Pure Metals or Ordered Lattices*

For large field gradients, the first order splitting discussed above may be so great that the correspondingly broad satellite lines of the powder pattern escape detection entirely, leaving only the central $m = 1/2 \rightarrow -1/2$ transition. If the perturbation calculation which leads to (10) is carried to a higher approximation by the use of second order perturbation theory,[73, 79, 74] it is found that for large enough field gradients even the central line is shifted. Of course, second order corrections to $\Delta\nu_m$ are obtained too, but in view of the fact that the satellites in the powder are not observable if eq is very large, these corrections need not be considered here. The position of the central line in a single crystal with axial symmetry is:

$$\nu_{\frac{1}{2}\rightarrow-\frac{1}{2}} = \nu_0 + (A_2/h)(1 - 9\cos^2\theta)(1 - \cos^2\theta) \quad . \quad . \quad (12)$$

where ν_0 is again the frequency of the unperturbed absorption in the metal,

$$A_2 = \frac{9}{64}\,\frac{2I+3}{4I^2(2I-1)}\,\frac{e^4q^2Q^2}{h\nu_0}$$

and the other symbols retain the meaning given for (10). The powder pattern resulting from a random distribution of crystallite orientations is shown in Fig. 7 and with it the recorded absorption derivative of Mg^{25} in metallic magnesium obtained experimentally.[6] Applying the arguments used for beryllium to this resonance, for which $e^2qQ/h \approx 230$ kc/s and eq is estimated to be $2{\cdot}2 \times 10^{13}$ statvolts/cm^2, we find $Q \approx 0{\cdot}14 \times 10^{-24}$ cm^2. This is a credible value[180] and lends additional support to the model based on the "bare-ion" description of the metal. In obtaining eq, the bare-ion value for

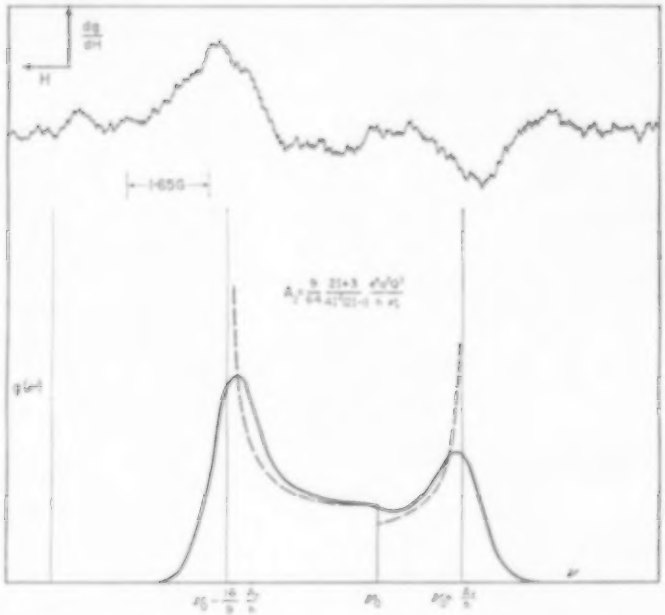

FIG. 7. Second-order quadrupole splitting of the central ($m = 1/2 \rightarrow -1/2$) transition. *Bottom*: The dashed curve shows the theoretical absorption line shape in a powdered sample of axially symmetric crystals. The full curve indicates the effect of dipolar broadening. The width of the Mg^{25} resonance (*top*) in the sample of metal used is partially due to inhomogeneities in the gradients *eq* due to lattice imperfections. The width between outermost derivative peaks is inversely proportional to external field.
Mg^{25} absorption, metal
$H_0 \simeq 7650$ G.; room temperature
1·9 G. modulation

magnesium was computed[80] using Eqn. (11) and summing over about 1300 sites. An antishielding factor of 5 (estimated[78]) was then applied. An effective charge of $+2e$ on each site was assumed. The use of the model is admittedly open to question and further refinement in the calculations should be preceded by an examination of the assumptions upon which the model is based (cf. the discussion of pure quadrupole resonance below).

4c. *Summary of Quadrupole Perturbations in Ordered Structures*

The first order quadrupole splitting in an axially symmetric crystal is characterized by its symmetry about ν_0 and by the fact that the splitting is independent of the external magnetic field strength. The centre of gravity of the individual satellites does not change since $(1 - 3\cos^2\theta)$ averaged over all angles is zero. The second order splitting is inversely proportional to the external field strength since ν_0 appears in the denominator of A_2; the powder pattern is *not* symmetrical about ν_0, and its centre of gravity *does* shift[30] to

VOL. 9 1961

a frequency $(8/15)A_2h^{-1}$ lower than ν_0. Further consideration of quadrupole effects on the magnetic resonance will be deferred to a discussion of absorption intensity, where the influence of imperfections will be reviewed. An analysis of quadrupole perturbation effects which includes crystal types of lower than axial symmetry can be found in the comprehensive review article by COHEN and REIF.[74]

5. *Pure Quadrupole Resonance*

The electric splittings noted above persist even in the absence of the external magnetic field and can cause a resonant absorption of magnetic r–f energy.[73, 81] This absorption, known as the pure quadrupole resonance, is a direct result of the interaction between the nuclear electric quadrupole moment and the electric field gradient at the nuclei in the lattice. It had been observed only in non-metals until recently when the pure quadrupole resonances of Ga^{69} and Ga^{71} in solid gallium were reported.[36] This was followed by a thorough study[77] of the origin of the electric field gradient and its temperature dependence. The pressure dependence has also been investigated.[82] The temperature dependence of the resonance frequency was explained by thermal expansion of the lattice and the averaging of field gradients by the lattice vibrations. In this analysis, the electric gradient resulting from +3 charges arranged on the gallium lattice was found to account for the observed resonance frequency within about 20 per cent[181]. Thus, it appears that again the gradients can be adequately accounted for by assuming them to originate outside of the atomic spheres of the resonant nuclei rather than being a result of the electronic configurations within those spheres. We tend to take this argument on faith because of its previous apparent success in explaining the beryllium and magnesium experiments; however, both beryllium and magnesium have 12 neighbours almost equidistant in the solid state, and outer electron configurations of $2s^2$ and $3s^2$ in the atomic state. In gallium there is but one nearest neighbour with three other pairs of atoms somewhat farther away. An electron anisotropy equivalent to only about 20 per cent of the atomic $4p$ orbital would be required to account for the entire observed quadrupole energy;[83] thus it does not seem unreasonable to believe that at least some of the observed effect is produced by an anisotropy of electron density around the gallium nuclei. Although this source of gradient may be less important in beryllium and magnesium it is undoubtedly present. The existence of such anisotropy in the conduction electron density of other metals is indicated by the presence of the anisotropic Knight shift.

In liquid gallium the ordinary nuclear magnetic resonance is observed.[38, 21, 77] In superconducting gallium, the quadrupole resonance is observed at the same frequency as it is in the normal state. Incidentally, pure quadrupole resonance offers an experimental advantage over magnetic resonance in investigating the superconducting state; no large external magnetic field needs to be applied to the sample, and the interpretation of data is much

simplified. In the case of magnetic resonance, the polarizing field H_0 in the metal, and thus the resonance frequency, are functions of the distance from the surface of the metal particles. Although the depth of penetration of the *r–f* field must still be considered, the pure quadrupole line will be sharp if no internal strains cause the gradient to be inhomogeneous, i.e. to vary from site to site. Using saturation measurements at different temperatures, it has been possible to estimate both the *r–f* penetration depth in the superconducting state and the relaxation time T_1.[84]

6. *The Knight Shift in Alloys*

The application of nuclear magnetic resonance to alloys was, from the first, appealing. It promised to divulge information of interest to all workers in the field of alloy theory. A glance at Eqn. (4) or (5) gave rise to a considerable amount of enthusiastic conjecture about the use of these equations to follow the change in $N(E_F)$ resulting from the alloying process and thus to gain insight into the classic observations of Hume-Rothery and the proposed interpretation of them, on the basis of Brillouin zone theory, by H. JONES.[85] It now appears that these initial ideas over simplified the interpretation of the data that was expected; nevertheless, optimism was and is warranted. For some alloy systems, it has been possible to observe the Knight shift as a function of alloy composition and to interpret the findings in terms of current alloy theories. The interpretation of the experiments is by no means straightforward, nor is the theory complete, but the pattern of behaviour of nuclear resonance in alloys is emerging. Enough alloys have been studied to establish examples of representative situations upon which to base a general discussion of the phenomenon.

When a resonance line of an element in an alloy is observed, there are usually simultaneous changes in all of the parameters of the line. To derive the maximum knowledge of the state of the metal requires the use of all of them. In order to preserve a logical sequence of subject matter, the change in the Knight shift with alloying will be considered at this point in spite of the fact that many of the elementary interactions necessary to explain the complete observed resonance behaviour have not yet been introduced or thoroughly characterized in the present paper. This is not a serious matter in some cases because in alloys, as in pure metals, there are practically no sources of a bodily shift of the line centre other than the Knight shift. On the other hand, we must take some care to specify the location of the atoms whose nuclei are contributing to the observed absorption line in each case, and be cognizant of the possibility that some other interaction may have removed the contribution of certain groups of atoms entirely. In this case, the interpretation of the change in Knight shift applies only to the contributing group, while little or nothing can be said regarding the Knight shift of those whose absorption is not observed. These introductory remarks of caution will be amplified in later considerations of quadrupole effects in alloys.

Concerning the Knight shift in alloys, two general statements can be made

VOL. 9 1961

at the outset: (*a*) within any single-phase region, the position of an absorption changes smoothly with composition, and (*b*) the resonance of any one isotope is split, in a multiphase region, into multiple absorption lines. An X-ray analogy here is almost complete. Throughout single-phase regions, the X-ray diffraction pattern changes line-spacing continuously; in two-phase regions, provided a sufficient quantity of each phase is present and that the lines can be resolved, two individual patterns can be identified. The provisions for separate identification are much the same for nuclear resonance; an appreciable proportion of each phase must be present, and the absorption lines should not overlap excessively. The latter condition is perhaps more difficult to satisfy for nuclear resonance because there is not an extensive pattern with which to work, but only a single resonance absorption peak. The interpretation of the data obtained from investigation of a two-phase alloy can, of course, be aided by separate observations of the pure phases involved.

The possibility exists of observing the resonance of each of the constituent nuclei in a multicomponent system; for each of the constituents, the remarks of the previous paragraph apply. The problem of retaining sufficient amplitude of absorption to perform experiments in alloys is great, however, and only under special circumstances can elements of small concentration be detected. The majority of experiments on alloys reported to date have been on binary systems, but no new fundamental interactions are introduced by additional constituents; consequently, the behaviour of a line in a binary alloy will be taken as illustrative for alloys of a larger number of constituents. This does not mean that the resonances of all of the constituents will necessarily behave similarly, but that the ternary (or higher) alloy can be understood in terms of phenomena demonstrable in binary studies. The increased information made available by observing the various (2 or more) constituents in a single-phase region has not yet been used to full advantage, but the possibility of investigating the wave functions of different elements under quite similar boundary conditions is appealing.

The shift of a *solute* (subscript *b*) in a solvent (subscript *a*) in dilute solid solution can sometimes be roughly predicted [19] by assuming that the Knight shift for a *b* atom in the *a* lattice is primarily determined by the electronic properties of *a*. The Knight shift can be written, in analogy with Eqn. (3)

$$\left(\frac{\Delta\nu}{\nu_r}\right)_{b \text{ in } a} = (A_b/2\beta\gamma_b\hbar)\,(\chi_p V_0)_a \xi_a . \quad . \quad . \quad . \quad . \quad (13)$$

The hyperfine interaction constant of *b* is used to obtain P_A for the *b* atom. This approximation appears to be reasonably good if the lattice structure and valence of the solute and solvent are similar, or if the same solute is used as a "probe" in different solvents of similar valence and structure. Accordingly, useful forms of this equation can be obtained by dividing both sides by $(\Delta\nu/\nu_r)_{\text{pure } b}$ or by dividing both sides by, for example, $(\Delta\nu/\nu_r)_{b \text{ in } c}$; in both cases the factor which includes the hyperfine interaction constant A_b divides out.

Regarding the qualitative behaviour of a nuclear resonance within a single-phase region, the position of the absorption line is usually not a rapid function of composition; the Knight shift usually changes less than 20 per cent of itself. With special reference to terminal solid solutions, this means that the Knight shift of the solvent species in the alloy remains within about 20 per cent of its value for the pure solvent. The Knight shift of the solute in the primary solid solution may, of course, be quite different from the Knight shift of the pure solute metal in accordance with (13) above, but still its variation over the solid solution range is usually no greater than 20 per cent of itself.

Initial experiments[86, 30, 19] on solid solutions indicated that the Knight shift of the solvent did not change with composition. This could easily be explained[87] using the argument that the disturbances in electron density caused by alloying are highly localized by the well-known shielding process[88, 89] which takes place around impurity atoms. It was thus supposed that the Knight shift would be largely unaffected by alloying. Subsequent experiments on silver alloys[72, 90] demonstrated that changes in the Knight shift occur for nuclei at much greater distances from the solute than could be explained on the basis of the screened charge model. Those nuclei do not contribute to the observed copper absorption in primary solid solutions of copper, on which most of the early work was performed, because of quadrupole effects (Section III-D).

Silver has a nuclear spin I of 1/2 and forms rather extensive solid solutions with many elements. Although its nuclear moment is small and its absorption correspondingly weak, its wealth of background in metal physics is a great asset in interpreting results of the resonance measurements. More work has been done in trying to understand the nature of primary solid solutions of the noble metals than any other group in the periodic table, and descriptions of their electronic structure are relatively well developed. For primary alloys of silver with cadmium, indium, tin or antimony, in concentrations of up to 2 per cent, an increased absorption on the high field (low Knight shift) side of the pure silver resonance was observed.[90] In the specific case of a 0·6 atomic per cent tin alloy, a small bump appeared on the side of the essentially unshifted silver resonance. (See Fig. 2b). The shifted components of the absorption are associated with the silver nuclei in the neighbourhood of a solute atom, and clearly demonstrate the fact that the Knight shift varies from point to point in the lattice of an alloy. Since the Knight shifts of the various nuclei are proportional to the external field strength, differences among them will be more pronounced in high magnetic fields, and the best quantitative data can be obtained by working at the highest available field strength consistent with the requisite field homogeneity. The silver atoms neighbouring solutes could have some anisotropic contributions to their Knight shift which would be unidentifiable in this case, but may be important.

On passing to more concentrated solutions, we find that in silver the Knight shift continues to decrease as the solute concentration is increased,

VOL. 9 1961

the decrease being, to a good approximation, directly proportional to Z, the excess charge on the solute, for alloys of the same atomic concentration of solute. The change is linear (within experimental error) with concentration throughout the primary solid solution range after the condition is reached that all silver atoms are likely to have neighbour solutes, and the fluctuations in microscopic concentration are essentially symmetrically distributed around the bulk composition c_0.

It was pointed out by BROOKS [91] that the long-range oscillations of electronic charge density around an impurity, for which Friedel had already given general formulae, [89] fall off more slowly than the exponential decrease around the "screened" charge and may oscillate about the bulk value before leveling off. The wave length of these oscillations varies with $\boldsymbol{k}$, but since the Knight shift depends not on $|\psi(0)|^2$ averaged over all values of $\boldsymbol{k}$, but rather on $|\psi(0)|^2$ averaged over values of $\boldsymbol{k}_F$ corresponding to the momentum at the Fermi level only, it can pick up these oscillations. The complete analysis requires the evaluation of the wave function for the periodic crystalline potential perturbed by the impurity; Friedel and co-workers [92, 93] approximated this with a calculation for free electrons scattered from spherical impurities. They computed the relative change $(\Delta\rho/\rho)$ of $\rho(r)$, the electron charge density per unit energy and volume at the Fermi level at a distance r from an impurity atom. $(\Delta\rho/\rho)$ is an oscillatory function of r taking on both positive and negative values; for large values of r the oscillations decrease in amplitude as $1/r^2$. To evaluate the Knight shift in solid solutions the assumption was made that each solute atom acts independently in causing these fluctuations in charge density. An average value of $\Delta\rho/\rho$ was then obtained for a random solid solution of specified concentration by summing over all neighbours of all silver atoms. This average is equal to the average relative change in the Knight shift at that concentration. The computed shift is linear with concentration and in quantitative agreement with experiment. The analysis does not, of course, undertake the description of the factors $V_0\chi_p$ and P_F which are often of interest individually.

A decreasing solvent Knight shift, in a system for which $N(E_F)$ is increasing with solute concentration, implies a decrease in P_F with increasingly energetic electrons; this decrease is associated with a change from s- to p-character of the states at the Fermi surface. If information on $N(E)$ is available, this allows a determination of the functional dependence of P_F on k_F, the momentum of a Fermi electron. A clearer picture of this dependence is gained by the use of a suggestion made by Knight, [19] that ξ be separated into two parts which he called b and $\bar{s}_k$, where $\xi = b\bar{s}_k$, and $b = |\psi_0(0)|^2/|\psi_a(0)|^2$, while $\bar{s}_k = \langle|\psi(0)|^2\rangle_F/|\psi_0(0)|^2$. The constant b effectively renormalizes the wave function of the free atom to a new value appropriate to the metal lattice for electrons at the bottom of the conduction band, $k = 0$. The function $\bar{s}_k$ has the value one, for $k = 0$, and usually decreases with increasing k. The way in which $\bar{s}_k$ changes with k in the vicinity of k_F can be determined if the density of states curve is established.

As an example, let us assume a parabolic band for which the product $\chi_p V_0$, the spin susceptibility per atom, is proportional to $a^2 n^{1/3}$, where a is the alloy lattice parameter and $n = p + cZ$ is the number of electrons per atom in the alloy. The solvent and solute have, respectively, p and $p + Z$ valence electrons per atom. The relative change of $\chi_p V_0$ as a function of solute concentration, c, is found to be

$$\frac{\mathrm{d} \ln \chi_p V_0}{\mathrm{d}c} = \frac{2\mathrm{d}a}{a\mathrm{d}c} + \frac{Z}{3(p + cZ)} \quad . \quad . \quad . \quad . \quad . \quad (14)$$

Since

$$\frac{\mathrm{d} \ln (\Delta\nu/\nu)}{\mathrm{d}c} = \frac{\mathrm{d} \ln \chi_p V_0}{\mathrm{d}c} + \frac{\mathrm{d} \ln P_F}{\mathrm{d}c} \quad . \quad . \quad . \quad . \quad . \quad (15)$$

we have

$$\frac{\mathrm{d} \ln P_F}{\mathrm{d}c} = \frac{\mathrm{d} \ln (\Delta\nu/\nu)}{\mathrm{d}c} - \frac{2}{a}\frac{\mathrm{d}a}{\mathrm{d}c} - \frac{Z}{3(p + cZ)} \quad . \quad . \quad . \quad (15a)$$

relating the relative rates of change with composition of the measured Knight shift and P_F for a parabolic band; the argument is only expected to be useful for non-dilute solutions where the solute potentials are overlapping. The rigid band approximation[104] is assumed. DRAIN,[72] in analysing his data on silver–cadmium alloys, suggested a different approach in which it was assumed that the shape of the electronic wave function is the same in each atomic cell as it is in the corresponding pure metal. It is interesting to note that there has been no evidence of a rapid drop in the Knight shift near a phase boundary as might be expected on the basis of Jones' picture of alloy phase changes. Also the measurements of Knight shift *versus* concentration in single-phase regions have shown no peak, or other zone boundary effects which would accompany a sharp break in the $N(E)$ curve. COHEN and HEINE,[94] in reviewing the electronic properties of the noble metals and their α-phase alloys, suggest that this is because the wave functions on the zone faces are p-like and do not contribute to the Knight shift.

Because of the random composition fluctuations in a solid solution, the Knight shifts of those solvent nuclei with greater or smaller numbers of solute atoms nearby experience shifts which may differ substantially from the shift characteristic of the most probable nearby composition. The result of these deviations is an increase in the width of an absorption of nuclei in solid solution, attributable directly to the microscopic inhomogeneities. When we discuss the Knight shift of an element in an alloy, it is understood that this is a simplification applicable to the most probable composition, but that the line is actually a composite structure. Its width can be calculated[93] for any particular solute distribution if the electron density around the solute atoms is known. For a phenomenological consideration of the problem, it is expedient to assume that we can assign a unique Knight shift to a particular composition and that microscopic fluctuations in composition contribute to the observed line width.

In a two-phase region, the resonance characteristic of the active nuclei in each phase will appear[30, 72] with an integrated intensity proportional to the

number of active nuclei in that phase. All results on two-phase alloys indicate that the position of the absorption lines does not change with composition within the two-phase region, in agreement with present concepts of alloy properties. Within the two-phase region, considerations are so similar to those applying to X-rays that they need not be discussed in detail here. For instance, if the solid solubility of b in a changes as a function of temperature, one could predict that, in principle, the resonance position and amplitude of a would change with temperature. An extreme case of this might occur in a system with a miscibility gap, such as aluminium–zinc has in the vicinity of 40 atomic per cent zinc.

A quantitative interpretation of the resonance position for intermetallic phases suffers from the same drawbacks that were stressed in the case of primary solid solutions, i.e. while the results can generally be interpreted consistently with band theory, the density of states or the wave functions cannot be obtained from nuclear resonance shifts without making independent measurements or simplying assumptions about one of these quantities. Nevertheless, there are many interesting features of the resonance in these phases which do not depend on a quantitative understanding of the Knight shift. There are, for example, gross changes in the Knight shift at the compositions of some intermediate phases. The cadmium resonance in the γ-phase of the silver–cadmium system [72] has a shift of 0·28 per cent relative to the cadmium resonance in an aqueous solution of $CdCl_2$. This is to be compared with shifts of about 0·55 per cent and 0·44 per cent for the α and β phases, respectively, and with 0·46 per cent for the ϵ phase on the other side of γ. A density of states for the γ phase which is much lower than that of the other phases of this system is indicated, in agreement with the suggestion [85] that the corresponding zone is almost completely full.

In an ordered alloy, the Knight shifts of like nuclei differ if the nuclei are in non-equivalent sites. Each unique site involves the same electronic configuration and the lines are not excessively broadened, in contrast to the situation described for random solid solutions. The relative abundance of the various types of non-equivalent sites is given directly by the integrated intensities of the absorption lines. In this way, nuclear resonance can sometimes be used to augment the information obtained through X-ray diffraction especially in the case where the scattering factors of the constituents may be similar, or the lattice structure sufficiently complex that the X-ray analysis is excessively involved. The above behaviour can be expected for nuclei having a spin 1/2, for nuclei with small quadrupole moments, or for nuclei in atomic sites of complete cubic symmetry. However, for nuclei with large quadrupole moments, the situation will be drastically changed. An analysis of the resonance based on quadrupole interactions (see the previous section) would probably be in order since electric gradients peculiar to the different non-equivalent sites would then split the resonance.

The Knight shift in liquid alloys has been investigated for some mercury–thallium, [30] sodium–potassium and sodium–rubidium [95] alloys. The shifts

have been found to change smoothly with composition in each case and show no composition-inhomogenity broadening of the type described in solid alloys as a major source of line width. The nuclei diffuse rapidly and an average value of $\chi_p V_0 P_F$, taken over all configurations around the active nuclei, is obtained. This diffusion averaging can, in fact, take place below the melting point and should become important at about the same temperature as that at which the line narrowing occurs which is caused by the averaging of static dipolar fields (to be considered in a later section). It was possible to observe the resonances of both atomic species in the liquid state of the sodium–rubidium alloys. The Knight shift of the sodium in a sodium–rubidium liquid alloy decreases as more sodium is added or, in other words, increases as the rubidium concentration increases. Extrapolating the Knight shift of sodium to infinite dilution in rubidium its value is found to be about 1·6 times that of pure sodium. The rubidium shift also is highest in pure rubidium and decreases as sodium is added. Both of these results can be explained largely on the basis of the relationship expressed by Eqn. (13). The form

$$\frac{(\Delta\nu/\nu_r)_{\mathrm{Na\ in\ Rb}}}{(\Delta\nu/\nu_r)_{\mathrm{Na}}} = \frac{(\chi_p V_0 \xi)_{\mathrm{Rb}}}{(\chi_p V_0 \xi)_{\mathrm{Na}}}$$

applies to the shift of sodium in rubidium at infinite dilution. Using Table V in Knight's review[19] (or Table VI in Pines' article[59]) the ratio on the right is found to be about 1·9. The interpretation of these experiments has been considered by BLANDIN and DANIEL.[93] A direct measurement of the electron spin susceptibility of the sodium–rubidium alloy would be of considerable interest in this case.

Although there have as yet been no experiments on liquid alloys which are known to be highly ordered in the solid state (intermetallic compounds), it is quite likely that incipient ordering (or clustering) in the liquid could be studied by resonance techniques. The ordering would appear as a positive or negative deviation from regularity in the shift at the composition of most complete order and should, of course, be more pronounced as the temperature of the liquid approaches the melting point of the solid.

The foregoing discussion of the Knight shift in alloys has been concerned with the introduction of non-transition elements as solutes. Interesting examples of the effects of transition element additions can also be found. We distinguish between the transition element in solid solution which has (*a*) an unfilled *d* (or, more generally, inner) shell, and a resultant magnetic moment of the order of one Bohr magneton, and (*b*) a filled *d* shell. Nuclear resonance can be used to help discriminate between these two alternatives in the event that the electronic configuration of a transition metal atom in solid solution is in question. Furthermore, if solute ions having magnetic moments are present it is possible to gain a semi-quantitative description of the distribution of the polarization of the electrons in the conduction band. Experiments on copper rich copper–manganese alloys[96] proved that this system

represents an example of case (*a*) above. The position of the centre of the resonance changed very little[97] while the width changed drastically with manganese concentration. The width was also found to be proportional to H_m/T where H_m is the applied magnetic field and T the temperature. Preliminary considerations[96] had suggested that a very large shift in the resonance position might result in such an alloy because the unpaired *d*-electrons on the manganese ions would orient the *s*-electrons in the conduction band by means of an *s–d* exchange interaction of the type proposed by FROHLICH and NABARRO[98] and ZENER.[99] This uniform polarization of the electron spins would, on interaction with the nuclear moments give rise to an extra large Knight shift and no appreciable line broadening, i.e. the proportion of unbalanced electron spins in the conduction band would be increased substantially over the value for pure copper and would be constant throughout the metal. The absence of any marked change in the Knight shift and the large increase in width were, therefore, in direct conflict with expectation. Subsequent calculations[100] have explained this observation as resulting from the fact that the conduction electrons are polarized near the impurity manganese ions only. Conduction electrons not in the immediate neighbourhood of a manganese ion experience no change in their polarization and cause only the ordinary Knight shift to occur. Since these experiments were conducted on dilute alloys the excess polarization was absent at many of the copper sites and the line centre appeared largely unaffected. With higher manganese concentrations, the resonance could not be observed due to its very great line width. The magnetic fields of the paramagnetic ions placed randomly throughout the lattice and the polarization mentioned above were responsible for this width which will be considered more thoroughly in a later section. The localization of the *polarization* of conduction electrons in the vicinity of the paramagnetic ion is distinct from the localization of *charge* discussed previously in this section. The copper–manganese data quite clearly indicates both the presence of the magnetic moments on the manganese ions, and the localized character of the spin polarization.

An example of case (*b*) above is nickel in copper. There is no change in either the width or the position[97] of the Cu^{63} resonance in alloys containing up to 10 per cent nickel which could not equally well occur in the case of a non-transition element solute. The intensity is a strong function of composition as a result of quadrupole effects to be discussed in detail in Section III-D. More concentrated solutions of nickel in copper (around 30 per cent nickel) exhibit a Cu^{63} absorption with an excess width[101] which is probably caused by regions of high nickel concentration. These regions would result from normal concentration inhomogeneities in the random solid solution, and might be expected to show strong paramagnetism.

In summary, the resonance results in dilute alloys with either non-transition or transition element solutes demonstrate the fact that disturbances in charge density and/or spin polarization are restricted to the neighbourhood of the impurity centre. The detailed analysis of Knight shift data invariably requires

the simultaneous use of the results of other experimental techniques, such as magnetic susceptibility, electronic specific heat, or electron spin resonance. The factors determining the Knight shift are complex in nature, and changes in each of these factors on alloying are due to a combination of interdependent processes such as charge transfer, local distortion of charge distribution, introduction of excess charge into the lattice, and the ever present screening. For this reason, ambiguities in interpretation arise just as they do for other well-known experimental techniques; resonance does, of course, take its place among them as an independent measurement, the results of which must be predictable by any correct electron theory of alloys. One aspect of the absorption in an alloy which is capable of unambiguous interpretation does not depend on a complete understanding of the magnitude of the Knight shift. It is the excess width caused by the effect of composition fluctuations on the isotropic and anisotropic shifts. The width contributed in this manner can be expected to approach zero in the completely ordered state and, in general, this means a drastic decrease in the line width upon ordering. Several other contributions to the width will remain, even with the alloy in the ordered state, and these will also have changed with ordering, but the spatial inhomogeniety of the Knight shift is always an important source and often the dominant source of width in disordered alloys. It can be identified by its linear dependence on H_0; almost all other broadening is independent of external field strength. Ordering then can be fruitfully investigated (using nuclei of spin 1/2 or nuclei with spin greater than 1/2 in microscopically cubic surroundings) whether or not the Knight shift can be satisfactorily interpreted.

A few investigations of solids exhibiting long-range order have been reported. The resonances have been observed, for example, in intermetallic compounds (valence compounds) of the alkali metal-heavy metal variety [30, 102] (such as NaTl, LiTl), in the compounds frequently used as semiconductors such as InSb or GaAs [103] and in compounds of the W_3O (β-tungsten) structure. [104] These materials show practically no solid solubility for either constituent and do not exist in the disordered state. The Knight shift will, of course, be zero in any substance having a very low conduction electron density. In the case of NaTl a rather large negative shift ($\nu_0 < \nu_r$) has been observed [30] for the thallium relative to Tl^+ in an aqueous solution of the acetate, and for Nb_3Sn, and V_3Ga the tin and gallium resonances were negatively shifted. [104] These are possibly chemical shifts, but they emphasize the point that the nuclear absorption in some well ordered alloys may, in addition to being relatively narrow, have a position quite different from the expected. The compounds having the β-tungsten structure are known to have high superconducting transition temperatures and it is hoped that their electronic structure will be elucidated by this type of measurement.

C. *Width and Shape of Resonance Absorption*

After considering the position of a nuclear resonance in a metal, attention is generally focused on its width and shape, the next two most readily measur-

VOL. 9 1961

able parameters. Examples of broadening caused by composition fluctuation in an alloy, and the anisotropic Knight shift have already arisen in connection with the line position. Both derive from interactions of electron spins with nuclear spins; the quadrupole splitting or the contributions now to be considered are equally significant in the analysis of resonance absorption.

The quantities $\delta\nu$ and $g(\nu)$ introduced in Section II are largely determined by local atomic configurations; accordingly, they reflect diffusion, segregation, order, and possibly precipitation and lattice distortion on a microscopic scale. In interpreting resonance data involved in the study of these processes and expressed as width or shape, one generally asks which of the acknowledged [105, 76] imperfections could be responsible for these data; or conversely, in designing an experiment, one might ask which parameters would be most informative for a particular type of investigation. (For example, diffusion studies imply the measurement of line width.) In order to answer such questions several other nuclear interactions must be introduced, one or more of which contribute to the width of every resonance absorption.

1. *Dipolar Broadening*

The static nuclear magnetic dipole broadening, also referred to as spin–spin, dipole–dipole, or dipolar broadening is caused simply by the local magnetic fields in the lattice generated by the other nuclei of the spin system. For a perfect lattice, this represents the absolute minimum width and one which must be subtracted out before the electronic contributions can be considered. Fortunately, a rigorous expression derived by VAN VLECK [106] can be used to calculate the theoretical second moment of a resonance absorption broadened in this fashion. All that is needed to compute this figure is a knowledge of the nuclear composition (abundance and gyromagnetic ratio of the nuclei present) and of the crystal structure. The formula of Van Vleck specialized to the case of a polycrystalline powder is:

$$\overline{\Delta H^2} = \frac{3}{5} I(I+1)\gamma^2\hbar^2 \sum_f r_{0f}^{-6} + \frac{4}{15}\hbar^2 \sum_j I_j(I_j+1)\gamma_j^2 r_{0j}^{-6}. \quad (16)$$

This is the mean square local field experienced by those nuclei of gyromagnetic ratio γ and nuclear spin I in a lattice made up of other identical nuclei r_{0f} away and other different nuclei (characterized by γ_j, I_j) r_{0j} away from a lattice point; that is, the summation over f includes only identical nuclei, that over j includes all different nuclei. Equation (16) expresses the contribution of one of several interactions occurring among nuclear dipoles or nuclear dipoles and electron spins. The second moments of all of these contributions can be summed to derive the total second moment, which should, if all of the broadening mechanisms have been included, agree with the experimentally determined second moment. The latter is given by $\int_0^\infty (H - H_0)^2 g(H)\,\mathrm{d}H$ and $\int_0^\infty g(H)\,\mathrm{d}H = 1$, where H_0 is the centre of gravity

of the absorption curve g(H). For the common case of a pure metal with two isotopes of abundances p_1 and p_2, to obtain $\overline{(\Delta H^2)}_1$, for the resonance of isotope 1, the first term is weighted by p_1, the second by p_2 and the sums taken over all lattice sites, giving

$$\overline{(\Delta H^2)}_1 = \left[\frac{3}{5} I_1 (I_1 + 1) \gamma_1^2 \hbar^2 p_1 + \frac{4}{15} I_2 (I_2 + 1) \gamma_2^2 \hbar^2 p_2\right] \sum_j r_{0j}^{-6}. \quad (16a)$$

Some useful lattice sums are given in Ref. 21.

Figure 8 portrays the physical situation schematically; the nuclear spin A

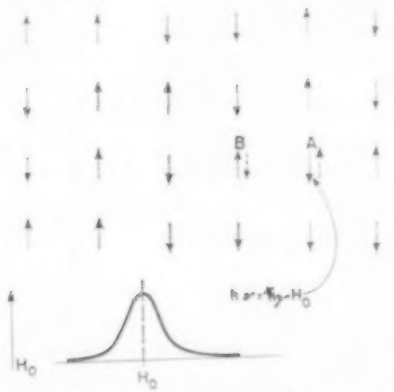

FIG. 8. A lattice of nuclear dipoles in a magnetic field H_0. Neighbouring nuclei cause static local magnetic fields which differ from site-to-site spreading out the resonance absorption around H_0. Also the precession of nucleus A causes an oscillatory field of frequency ν_0 which tends to flip identical nucleus B causing additional broadening.

is in the field of all other surrounding spins. The magnitude of the field at A imposed by the spin B is μ_B/r^3, where r is their separation. Both the static field contribution due to the component of μ_B parallel to H_0, and the oscillating contribution due to the precession of μ_B about H_0 have the same order of magnitude. If the gyromagnetic ratio of B is the same as A, the oscillatory field at A will be at just the proper frequency to induce a transition of A and a mutual flipping of spins will occur, as previously discussed in connection with spin diffusion. This process limits the life time of a spin in a particular state and broadens an absorption line approximately as much as the static fields. Both processes are included by Eqn. (16) and are discussed in detail by BLOEMBERGEN *et al.*[11]

For a *Gaussian* line shape, the line width $\delta\nu$ is related to $\overline{\Delta H^2}$ by the expression $\delta\nu = 2 \cdot (\gamma/2\pi)\,[\overline{\Delta H^2}]^{\frac{1}{2}} = 1/\pi T_2''$ in accordance with the discussion in Section II and Appendix B. A few values calculated from Eqn. (16) are presented in Column 5 of Table 2 and may be compared with the measured $\delta\nu$ listed in Column 6 of Table 1. Comparison of the theoretical and experimental second moments (Table 2, Columns 2 and 3) for pure annealed

VOL. 9 1961

TABLE 2

Isotope	$\overline{\Delta H^2}$, (G^2)		$2(\overline{\Delta H^2})^{\frac{1}{2}}$	$(\gamma/\pi)(\overline{\Delta H^2})^{\frac{1}{2}}$	*Reference*
	Equation (16)	*Experimental*			
Li^7	4·3	4·1	4·2 G	7·0 Kc/s	21
Na^{23}	0·63	0·67	1·6	1·8	21
Al^{27}	7·6	9·0	5·5	6·1	107
Cu^{63}	5·6	5·8	4·7	5·3	21
Nb^{93}	16·2	36(e)	8·05	8·4	24
Ag^{109}	0·0127	0·084(e)	0·226	0·045	27
Cd^{113}	0·05	0·36(e)	0·45	0·43	28, 29
Tl^{205}	0·89	97	1·9	4·7	34

(e) Estimated by using $(\delta H/2)^2$ which is exactly $\overline{\Delta H^2}$ for a Gaussian line of width δH between maximum and minimum slopes.

metals up to atomic number of around 100 shows that dipolar broadening is the major contribution to the line width for these elements. Lattice strain or even minor alloying (less than 10 per cent solute) will not alter the dipolar width by more than 10 to 20 per cent at the most. This fact is of assistance in locating the resonance of pure metals experimentally since the detection techniques normally used (see Section IV) require a field modulation which approximates the line width if maximum sensitivity is to be obtained. For alloys, other contributions to the width are so important that the dipolar width serves only to indicate a lower limit. In applying (16) to ordered alloys, close attention must be given the choice of the appropriate internuclear distances r_{0f} and r_{0f} for the two (or more) atomic species involved as well as the isotopic distribution of nuclei on the ordered lattice. In some instances it may be possible to use the dipolar width to decide between correct lattice structures if the X-ray data are insufficient.

2. *Motional Narrowing*

If the room temperature widths had been listed in every case in Table 1, marked exceptions to the agreement of theory and experiment would have been noted for lithium and sodium. For each of these the line width at room temperature is far less than the value computed from (16). This introduces a topic of more than usual interest with regard to metals, namely, the application of resonance techniques to the study of diffusion. It has been stressed that the broadening of the absorption line depends upon the time-independent interaction between nuclei. The contributions of all of the nuclei in all of the (random) spin configurations are summed to give the observed dipolar broadened line. If, however, through atomic migration the nuclei move about rapidly, these local fields will tend to average to zero at each site. The correlation time τ_c during which an interaction between spins may proceed before being interrupted by a lattice jump decreases as the temperature is increased. The lattice jump disturbs both the static and oscillatory components of local

field and its effect becomes pronounced when this jump occurs in a time equal to or less than T_2'', the characteristic time associated with both of these processes, defined in discussing (16) above.

Ever since the initial comprehensive work of BLOEMBERGEN, PURCELL and POUND,[108, 11] the importance of lattice motion to the understanding of nuclear resonance phenomenon has been realized. Their classic paper on nuclear relaxation developed the complete framework of the theory of relaxation times resulting from the interactions between nuclei and fluctuating local fields. Expressions which describe the motional narrowing of an absorption are derived from considerations of the time dependence of the internal fields in the solid or liquid. For the mutual spin flipping process mentioned above to take place it is necessary that the oscillatory field at nucleus A be correlated with the precession of A until the A and B spins exchange their energy; this occurs in a time T_2'' by definition for the rigid lattice. Suppose now that nucleus B jumps to another site before the spin exchange occurs, thus interrupting the process and thereby decreasing the duration of correlated motion. When this occurs the spin–spin relaxation process by mutual flipping becomes much less effective, the spin–spin relaxation time becomes longer, and the line width $\delta\nu \approx 1/\pi T_2'$, decreases. The narrowing occurs when $\tau_c \approx T_2'' = \gamma[\overline{\Delta H^2}]^{\frac{1}{2}}$. The symbol T_2' has been used here as a modification of T_2'' appropriate to the case of lattice motion. Since τ_c is related to the diffusion coefficient, $D = D_0 \exp(-E_D/RT)$, by $\tau_c = r^2/12D$, where r is the nearest neighbour distance, an opportunity exists to measure D over a limited temperature range by the measurement of line width versus temperature. D_0 is the usual pre-exponential frequency factor, E_D the activation energy for diffusion customarily given in calories per mole, R the gas constant, and T the absolute temperature. Extensive measurements of line narrowing in solids have been made. Unfortunately, however, the narrowing of an absorption line is quite often accompanied by a change in its *shape*. Although the shapes of the *narrowed* lines are always essentially Lorentzian, the shapes characteristic of the rigid lattice for various metals differ widely. The single parameter $\delta\nu$ is inadequate to fully describe this complex phenomenon which is always referred to simply as line narrowing. If the rigid lattice line shape is Gaussian the narrowing process is closely described by the expression[109]

$$\left(\frac{1}{T_2'}\right)^2 = \left(\frac{1}{T_2''}\right)^2 \frac{2}{\pi} \arctan \frac{\pi\tau_c\, a^{\frac{1}{2}}}{T_2'} \qquad . \quad . \quad . \quad . \quad (17)$$

where $\pi a^{\frac{1}{2}} = \pi/(8 \ln 2)^{\frac{1}{2}} \cong 1{\cdot}34$. This equation differs slightly from that originally given by BLOEMBERGEN, PURCELL and POUND[11] in which the factor 1·34 given here is replaced by 2. Of far more importance, however, is the fact that while neither expression claims to describe *precisely* the relationship existing between τ_c and $(1/T_2')$ for a real solid, both are exceedingly helpful in understanding the motional narrowing of dipolar broadened lines. For use in interpreting width data we insert $1/\pi\delta\nu$ for T_2' giving

VOL.
9
1961

$$(\delta\nu)^2 = (\delta\nu_0)^2 \frac{2}{\pi} \arctan (4{\cdot}2\ \tau_c \delta\nu). \quad . \quad . \quad . \quad . \quad (17a)$$

Figure 9 shows the $\delta\nu$ *vs.* T data for Na^{23} in sodium metal.[55] The full line is a plot of $\delta\nu$ *vs.* T from Eqn. (17a) using the figures $D_0 = 0{\cdot}242$ cm²/sec, $E_D = 10{\cdot}45$ kcal, obtained by radioactive tracer measurements,[110] and $r = 3{\cdot}71 \cdot 10^{-8}$ cm. The dashed line is parallel to the full line and contains a correction for modulation broadening and field inhomogeneity. An important feature of (17), which is apparent in Fig. 9, is that the transition from the

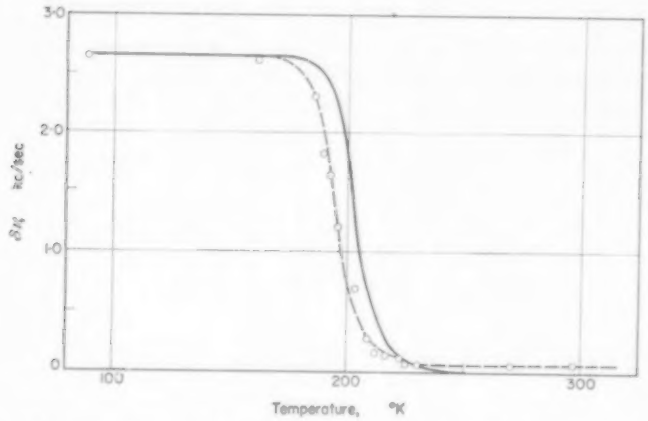

FIG. 9. Absorption line width $\delta\nu$ of Na^{23} in metallic sodium as a function of temperature from Ref. (55) showing the diffusion narrowing of the resonance line which occurs when the jump frequency is approximately equal to or greater than the line width. The full curve was calculated using D_0 and E_D from tracer measurements.

rigid lattice width, $\delta\nu_0$, to the region ($\tau_c\delta\nu \ll 1$) in which $\delta\nu$ is proportional to τ_c is relatively sharp. This represents an inherent disadvantage in deriving D from line width alone because the range over which data can be obtained is so limited compared to the range over which T_2' can be measured by other methods to be discussed below. On the other hand, the abruptness of the transition was significant in suggesting a relationship advanced by SPOKAS and SLICHTER[111] in which a "narrowing temperature" plays an important part. Their analysis emphasizes data taken in the high temperature region within which the narrowed line shape is essentially Lorentzian.

Using essentially Eqn. (17a) to interpret the data, investigations were carried out for lithium,[21] sodium,[55] aluminium[112] and cadmium[113] metals, and for hydrogen in palladium[114, 115] and tantalum.[116] For lithium and sodium the results were quantitatively correct but included an error of about ten per cent for E_D; they were of the wrong order of magnitude for D_0. For aluminium, which has a low-temperature line of rather unusual shape (see Fig. 1) and a second moment somewhat larger than predicted by (16), the E_D value obtained was thought to be seriously in error,[112] as well as D_0.

These experiments nevertheless demonstrated that line narrowing measurements were capable of producing semi-quantitative values for the activation energy and D_0. A reinterpretation[111] of the line narrowing data[112] on aluminium subsequently showed that it was in quantitative agreement with the diffusion constants obtained by more reliable techniques.

It is possible to obtain an estimate of the dependence of D upon composition by comparing the $\delta\nu$ *vs.* T data for a single constituent in a series of alloys. This has been carried out for lithium–magnesium solid solutions containing up to 18 atomic per cent magnesium.[117] The narrowing of the lithium absorption was found to occur at successively higher temperatures as the magnesium concentration was increased, no change in E_D was apparent from an analysis of the data. The primary effect of the magnesium appeared to be a decrease in D_0. This result may not be unexpected, but it would surely have taken longer to establish, even semiquantitatively, by other methods. The need to wait for a reasonable mass transfer to take place is absent for resonance observations which continuously detect the motional effects occurring throughout the sample on a microscopic scale. Since the information desired in this application of line narrowing is relative, the interpretation of the data is less involved than it is for an absolute measurement of D.

Diffusion constants can be determined by another resonance technique more difficult to apply but vastly superior in accuracy to line-width measurements. Instead of estimating T_2' from $\delta\nu$, direct measurements of the quantities T_2 and T_1 (spin-lattice relaxation time) are made from which T_2' can be derived. Work of this type on the alkali metals (reviewed in Ref. 118), and on aluminium[111] has elucidated the relaxation mechanism involved and shown that diffusion constants can be obtained which are in complete agreement with the results of tracer methods. These measurements were accomplished with a pulsed radio frequency technique[119, 120] a description of which can be found in the excellent review article by PAKE.[14] This technique is particularly suitable in the range of relaxation times between 10^{-4} seconds and one second encountered in many metals. The measurements of HOLCOMB and NORBERG[120] on lithium, sodium and rubidium were made over a temperature range from -65 to 250°C over which T_2' changed by a factor of about 10^3. The experimentally observable line-narrowing is largely complete in this temperature range, and the data are interpreted not using (17), but its high-temperature counterpart (modified for $\tau_c/T_2' \to 0$) in which T_2' is inversely proportional to D. Since the measurements extend over three decades on a log plot, highly accurate values for D_0 and E_D can be obtained.

3. *Spin-Lattice Relaxation Time Broadening*

The line width studies of GUTOWSKY[21] showed that the motional narrowing observed for sodium and lithium does not occur for cesium and rubidium, and, therefore, the dominant source of the width must be other than stationary neighbouring dipoles. It turns out that for these metals the spin-lattice

VOL. 9 1961

relaxation time T_1 is sufficiently short[120] that it determines the line width in the metal. This statement follows from the relation $\delta\nu \approx (1/T_2') + (1/2T_1)$ discussed in Appendix B. In the present context, it is pertinent to stress only that T_1 is a contributor to the line width and that it may be the dominant contribution, but seldom is. T_1 in metals is primarily determined by the conduction electrons[68] and must be measured directly, as it has been for copper,[121, 107, 122] aluminium,[107, 122, 123, 111] and the alkali metals,[120, 123] unless it manifests itself strongly in the line width. In the latter case it appears as a temperature-dependent contribution of Lorentzian shape and with a width directly proportional to the absolute temperature. Since the contribution of the conduction electrons, $1/2T_1$, causes $\delta\nu$ to *increase* with temperature, it is easily distinguished from most other sources, and since $1/T_2'$ *decreases* exponentially with temperature, the situation eventually occurs that all line widths in the high-temperature limit are determined by T_1, which is then equal to T_2.[120] The Korringa relation, Eqn. (8), shows that T_1T is inversely proportional to $(\gamma\Delta H/H)^2$ and since $(\Delta H/H)$ is largest for the heavy elements, T_1 can be expected to be an important source of line width for heavy elements having a relatively small isotopic abundance of nuclei with a large gyromagnetic ratio, the other isotopes having $I = 0$. The abundance enters because the prescribed conditions will also give a large width due to dipolar broadening (or spin exchange between unlike neighbours, to be considered below) unless the spins are, so to speak, dilute. Direct measurements of T_1 are used for comparison with the measured Knight shift results to study the deviations from the Korringa relation and, thus, eventually may assist in the development of a more complete understanding of the electronic structure of metals, including correlation and exchange effects.[59]

Lattice motion also contributes to the observed T_1 values in the alkali metals.[120, 118] Knowing the extent of this contribution, additional values of τ_c and D can be obtained by the theory of BLOEMBERGEN *et al.*[11] or by a refined theory due to TORREY.[124] The latter is a random walk diffusion theory which takes into account the discreteness of the actual lattice and gives somewhat better agreement with experiment.[120] The values of τ_c and D derived in this manner agree with those derived from the T_2' data, but are of lower accuracy.

4. *Electron-Coupled Interactions Between Nuclear Spins*

For elements with masses greater than about 100, experiment has shown that the observed line widths exceed the values predicted by (16) alone by substantial amounts. Furthermore, these line widths are largely independent of external magnetic field strength and sample temperature, ruling out shift anisotropies and relaxation time effects as their major cause. The conduction electrons, which provide a contact from one nucleus to the next, are responsible for this behaviour. The nuclear magnetic moments are coupled to each other because each of them in turn interacts, via the hyperfine interaction responsible for the Knight shift, with the conduction electrons. The

process, usually called *nuclear spin exchange* or *indirect exchange coupling* has been considered in detail only for silver[27] and thallium[34] but undoubtedly is a major source of broadening for most of the heavy elements because of their large hyperfine interactions. Returning to Fig. 8, the nuclear exchange process is visualized as follows. An electron passing through the lattice interacts with spin A and tends to be polarized by it; this electron subsequently interacts with spin B, effectively coupling the two spins together in the sense that the orientation of A partially determines the energy of B. In contrast to the ordinary dipolar interaction discussed previously, conduction electrons (or other non-localized electrons) are essential to this indirect exchange process.

The details of nuclear exchange are of interest in metal physics because the computation of the interaction involves the use of the conduction electron wave functions. Second order perturbation theory has been used to derive the form and magnitude of the interaction.[27, 34] It was found to be of the same type as an electron exchange interaction which had been studied by Van Vleck and included in his general paper on dipolar broadening[106] referred to above. In that paper it had been shown that exchange processes between like nuclei contributed nothing to the second moment of the absorption being observed, but that exchange between unlike nuclei resulted in an additional contribution,

$$\overline{\Delta H_x^2} = \frac{1}{3}(\gamma\hbar)^{-2} I'(I'+1) \sum_{j'} A_{ij'}^2(r_{ij'}), \quad . \quad . \quad . \quad (18)$$

where the primes denote a nuclear species whose resonance is not being observed. The sum includes all such nuclei in the lattice. Similar contributions will arise from each different variety of nucleus (having spin) present; for pure metals it is common to have only one other isotope. In (18), γ is the gyromagnetic ratio of the species whose resonance is being observed. The exchange interaction parameter $A_{ij'}(r_{ij'})$ between resonant species i and non-resonant species j' is the quantity involving the hyperfine interaction in the metal; it is, therefore, $A_{ij'}$ which must be determined experimentally if information about the conduction electron wave functions is to be obtained. Considering the complexity of the computation leading to the theoretical expression for $A_{ij'}$, it is very doubtful that any useful information will be forthcoming from studies of exchange broadening; nevertheless its qualitative influence must be understood in order to infer the line widths to be expected in the heavy metals and in alloys containing heavy metals. A brief discussion of $A_{ij'}$ and its measurement may clarify this statement. During the derivation of $A_{ij'}$, a complicated weighted average of hyperfine interactions must be obtained. It is necessary to carry out a double integration over (*a*) all occupied states in the band and (*b*) all unoccupied intermediate states into which the electrons are virtually scattered by the interactions of their spins with the nuclear spins. In order to proceed with the derivation, it is necessary, therefore, to make assumptions concerning (*a*) the shape of the $E(k)$ curve and

VOL. 9 1961

(*b*) the "effective" value of the hyperfine interaction in the metal. This effective value is unfortunately not directly comparable to the "renormalized" hyperfine interaction constant $A\xi$ which enters the expression for the Knight shift, since the latter involves only $\langle|\psi(0)|^2\rangle_F$ (c.f. Eqn. (2) and associated discussion), while the present effective value includes an average of $|\psi(0)|^2$ over the entire band structure. In addition to this, since the quantity finally obtained is only an integral value it cannot be expected to provide any details of the band structure. The expression derived by RUDERMAN and KITTEL [27] for the exchange interaction parameter is:

$$A_{ij'}(r_{ij'}) = \frac{V_0^2\, m^*\, \xi_i\, \nu_a(i)\, \xi_{j'}\, \nu_a(j')}{2\pi\,(2I_i+1)\,(2I_{j'}+1)} \left(\frac{1}{r_{ij'}}\right)^4 \times$$

$$[2k_F r_{ij'} \cos(2k_F r_{ij'}) - \sin(2k_F r_{ij'})] \quad . \quad . \quad (19)$$

where V_0 is the atomic volume; m^* is the effective electron mass, ν_a is the observed atomic hyperfine structure splitting, and $r_{ij'}$ is the internuclear distance separating the interacting nuclei i and j'. If ν_a is expressed in $\sec^{-1}$ and cgs units are used throughout, the result will be in ergs. Substitution of the appropriate values for silver, using m^* equal to the free electron mass, and $\xi_i = \xi_{j'} = 1$ gives $A_{ij'}$ for the nearest neighbours ($r_{ij'} = 2{\cdot}88 \times 10^{-8}$ cm) of about $2{\cdot}6 \times 10^{-25}$ ergs which corresponds to a frequency $A/h \simeq 40$ c/s.

If (18) is specialized to near neighbours in a lattice having a co-ordination number of 12, we find

$$\overline{\Delta H_x^2} = \tfrac{1}{8}(\gamma\hbar)^{-2}\, I'(I'+1)\, 12f\, A_{ij'}^2 \text{ (near)} \quad . \quad . \quad . \quad (18a)$$

where f is the fraction of sites occupied by the non-resonant (primed) species. For silver $f \simeq 1/2$ and (18a) gives 50 c/s for $(\gamma/\pi)[\overline{\Delta H_x^2}]^{\frac{1}{2}}$, the width contributed by this mechanism. This is in excellent agreement with experiment, and although such good agreement is probably accidental, the exchange interaction is seen to be capable of completely accounting for the line width in excess of the contributions previously considered.

In the case of thallium also, the calculated $A_{ij'}$ is in reasonable agreement with the observed value; however, as f approaches zero (and $\overline{\Delta H_x^2}$ approaches zero) there is still a large width contribution in excess of dipolar. The experiments revealing this effect were carried out on isotopically enriched metal so that f could be varied and the dependence of width on f studied. In this case, f is synonymous with isotopic abundance since the thallium was composed entirely of Tl^{203} and Tl^{205} both of which have nuclear moments. This investigation disclosed a pseudo-dipolar interaction brought about by that part of the conduction electron wave function which has non-*s* character. The interaction in this case proceeds via the classical dipolar interaction between nuclear and electron spins which gave rise to the anisotropic Knight shift. The electrons couple two nuclei in such a manner that the form of the nuclear interaction is exactly as if the nuclei were free dipoles interacting at a distance. The magnitude B_{ij} of the interaction depends upon the evaluation of integrals

of non-s wave functions over the band structure [34] and will not be discussed here. This contribution to the line width is indistinguishable from the ordinary dipolar contribution in its behaviour but should only be expected to contribute substantially if the proportion of p-character in the wave function is large, perhaps equal to or greater than the proportion of s-character, in heavy metals. The second moment of a line including the ordinary and pseudo-dipolar interaction between like and unlike nuclei of abundance $(1-f)$ and f, specialized to nearest neighbours in a lattice of co-ordination number 12 is

$$\overline{\Delta H_{fd}^2} = \frac{36}{5}\frac{I(I+1)}{(\gamma\hbar)^2}(1-f)(B+\gamma^2\hbar^2 r^{-3})^2 + \frac{16}{5}\frac{I'(I'+1)}{(\gamma\hbar)^2}f(B+\gamma\gamma'\hbar^2 r^{-3})^2 \quad (20)$$

where the unprimed nuclei are those for which the second moment is given, and where the interaction constant between any two neighbouring nuclei is called B. This interaction is of the same order of magnitude in cubic as in non-cubic crystals. In thallium it produces a width about 5 times the ordinary dipolar contribution. This is considered to be evidence for a large amount of p-character in the wave functions near the Fermi surface of thallium.

The exchange and/or pseudo-dipolar broadening become of comparable magnitude to the ordinary dipolar width when the atomic number is around 80 to 100 and are probably the major source of width for most heavy elements. A possible sharpening of the resonance line [27] in a metal consisting entirely of one isotope may often be masked by the pseudo-dipolar interaction. An important feature of both of these electron-coupled interactions is their dependence on distance through the lattice, both have (modulated) inverse cube dependence and thus operate over a relatively long range through the metal. The same dependence of electron polarization on distance was found by YOSIDA [100] in considering the nuclear resonance of copper–manganese alloys mentioned earlier.

The effect of the exchange coupling process on relaxation time has been included in a general treatment of relaxation processes by REDFIELD. [125]

In random solution alloys, nuclear spin exchange will increase the line width unless the solute has a smaller hyperfine interaction than the solvent. Even then the effect on the width of the resonance of an isotopically pure solvent may be pronounced. It has been generally observed [102, 30] that the line width in alloys of heavy metals is very much larger than the dipolar width; however, without additional data on the field dependence of this width, the composition fluctuation broadening cannot be separated from the spin exchange contribution. Since the latter will also usually be increased by composition fluctuations, a quantitative analysis of the width would be exceedingly difficult. It is worth noting that ordering changes the picture drastically, since it introduces the possibility of quantitative treatment by eliminating composition fluctuations and by providing an opportunity to design experiments partially eliminating exchange effects. At least the exchange interactions for like geometrical configurations of different atomic species can be compared. Studies of this nature have been carried out by

VOL. 9 1961

SHULMAN *et al.*[103] Their investigations were actually concerned with semiconducting compounds of the III-V variety but the concepts employed by them are applications of the foregoing considerations to an ordered structure. They found that the line widths in InSb, GaSb, InAs and GaAs are dominated by the exchange mechanism, and demonstrate the possibility of using this type of analysis to obtain information about the excited electronic states in these compounds.

5. *Electron-Coupled Interactions Between Nuclear Spins and Ion Cores*

KNIGHT and KITTEL[126] have discussed the implications of a coupling of the nuclear spin with the 3*d* shells in pure transition elements. If an antiferromagnetic array of the spins should exist, then very large internal magnetic fields would be generated, and the nuclear magnetic energy levels would undergo a splitting of about 10^5 G. The absence of such a splitting in vanadium, niobium and molybdenum is interpreted as showing[126] that either (*a*) the 3*d* bonding is completely co-valent or (*b*) any coherent antiferromagnetic array exists for a very short time only. (A short correlation time for the interaction would be produced by a rapidly changing spin orientation.)

The nuclear resonance experiments on copper–manganese alloys[96, 97] revealed a low-temperature (liquid helium) copper line width greatly in excess of the value determined by dipolar interaction among nuclear spins and between the manganese ions (acting as dipoles) and the nuclear spins. In this case, the coupling of the ion cores with nuclear spins[100] is responsible for the excess width.[127] The conduction electrons moving through the crystal interact with the manganese ion cores via an exchange coupling, and with the copper nuclei via the hyperfine interaction. The indirect coupling also accounts for the temperature and field dependence of the line width in the very dilute (0·029 atomic per cent manganese) alloy. An estimate of the exchange coupling energy of conduction electrons with the manganese ion cores was obtained from this work. Also, it added to the evidence that manganese dissolves in copper as Mn^{++} as other studies[128] have indicated. At room temperature, the copper line width in the dilute alloy is not increased appreciably over its value in pure copper because the net manganese magnetization is small.

D. *Intensity of Resonance Absorption and Discussion of Quadrupole Interactions in Imperfect Crystals*

The application of nuclear resonance techniques to metals rarely requires either the measurement of absolute absorption intensity (power absorbed per nucleus) or the comparison of the power absorbed by each of two different nuclear species. Comparisons of this type can be made using Eqn. A4 (Appendix A) and the fact that in the absence of saturation the total rate of power absorption by the nuclear spin system is proportional to $H_1^2 \int_0^\infty \nu\chi'' \mathrm{d}\nu$.

The theoretical signal-to-noise ratio of an absorption may be computed using an expression given by Pound in the appendix of Ref. 11 and in Ref. 4.

In practically all studies of metals it is the change of the absorption intensity of one isotope as a function of temperature, composition, or state of strain which is of interest. For these the definition of intensity given in Section II is adequate since only relative values are sought. Because the total area under the absorption curve must remain constant, a noticeable change in the apparent intensity observed within a narrow region $\nu_0 \pm \Delta\nu$, centred at the resonance, signifies a partial redistribution of the absorption. For this to take place a radical difference in the environments at some lattice sites is required. The absorption of the nuclei at these sites may then fall outside of $\nu_0 \pm \Delta\nu$. This precise condition has been observed in several metals and alloys, the nuclei of which undergo quadrupole interaction with defects in the lattice. The phenomenon was observed first in ionic crystals[129, 130] and has subsequently been studied in some detail.[74] The situation can be viewed qualitatively as follows. The defects are visualized as causing inhomogeneous electric fields over a short range, at most a few lattice parameters. It is thus possible for all nuclei in regions of the metal which are not near the defects to escape interaction with them entirely. The absorption of this latter group of nuclei remains near ν_0 and accounts for the observed line intensity. If the effective volume which is to be associated with a particular defect is known, then intensity measurements can determine the number of this type present alone; if the effective volume per defect is not known, then it may be determined by measuring the intensity as a function of the number of defects introduced experimentally. The result of carrying out this procedure for several different defects (e.g. solute species) is a series of relative effective volumes. The refinement of these ideas to include the actual position dependence of interaction energy for nuclei around a defect, and to include the effects of overlap of the defect volumes constitutes the subject of *nuclear quadrupole effects in imperfect crystals*. These effects in powdered samples are invariably associated with the intensity of the nuclear resonance.

1. *Quadrupole Broadening of the Magnetic Resonance*

The background for this topic has been introduced through the subject of quadrupole effects in crystals of pure metal (Section III-B4). It is only necessary to recall (*a*) that nuclei in situations of perfect *cubic* symmetry undergo *no* quadrupole perturbation and (*b*) that nuclei in (homogeneous, axially symmetric) field gradients may give rise to resonance lines of the shapes shown in Figs. 6 and 7. These observations, coupled with the fact that defects in cubic crystals cause large *inhomogeneous* and probably non-axial field gradients, have been used to interpret the resonance results on worked and/or alloyed cubic metals. The methods employed are also applicable to any non-cubic metal whose paramagnetic or pure quadrupole resonance is observable when the material is in the pure strain-free state. In the latter

VOL. 9 1961

case, there will already be an electric gradient eq at each lattice site, and imperfections will cause a change Δeq.

A sharp distinction usually is made between first- and second-order quadrupole effects. *First-order* effects are concerned with the behaviour of the satellite lines as they are described by first-order perturbation theory. The satellites are displaced, according to Fig. 6 and Eqn. (10), in direct proportion to the electric gradient eq experienced by the nuclei. Small gradients will cause no observable effect; the satellite peaks fall well inside of the ordinary dipolar broadening of the resonance. This is the situation for cubic metals, even under slight strain. For larger gradients a small range of eq exists over which a definite excess quadrupolar contribution to the line width would be identified if q were homogeneous. Beyond this the satellites are not observed and the unsplit central line alone will contribute to the intensity until much larger gradients are considered and the central line is perturbed. This splitting of the central ($m = 1/2 \longrightarrow -1/2$) transition is termed *second order* because second-order perturbation theory is used in its description. The fact that there is a large difference in the magnitude of the field gradient required to bring about first- and second-order broadening is crucial, both to the identification and interpretation of the intensity data.

In the discussion to follow, it seems advisable to consider the electric gradients *per se* rather than the more familiar strain, which may cause the gradients. Justification is lacking for the assumption that the gradient is proportional to the strain if the classical concepts of strain [131] as developed over a considerable period of time are retained. As pointed out by BLOEMBERGEN, [76] one can imagine the gradients as arising from both the interaction of an external point charge with the ion core and from a direct ion-core deformation due to the proximity of other cores. We might also include a localization effect which would be present even if the charge-induced core distortion and direct ion-core interaction are absent. Consideration of the experimental data, in part 5 below, has shown, however, that the ordinary shielded charge model of an impurity is not capable of generating the gradient required to explain the quadrupole effects in metals and that the gradients around point defects with excess charge appear to be proportional to $1/r^3$. Also, in copper, [177] experiment indicates that the gradient is proportional to the excess charge Z of the solute except in the case of impurity atoms with zero excess charge or with ionic radii equal to or greater than that of copper. The change in gradient due to the presence of an imperfection will be written

$$\Delta eq = 17\, e\lambda\epsilon(Z)/a_0^3, \quad . \quad . \quad . \quad . \quad . \quad . \quad . \quad (21)$$

where a strain function $\epsilon(Z)$ has been written to indicate the combined effects of size and valence, λ is a dimensionless constant relating gradient to $\epsilon(Z)$, and a_0 is the lattice constant. The individual mention of size and valence is somewhat artificial since at any appreciable distance (e.g. 2 atomic diameters) away from an imperfection it is probably not pertinent to inquire whether the gradient is due to *valence* or *size*. The lattice confuses these concepts so

that valence, meaning charge, brings about lattice displacements. In any case, the behaviour of the absorption line is determined entirely by the charge configurations in the lattice regardless of the relationship these may bear to lattice displacement.

In the vicinity of a point imperfection, $\epsilon(Z)$ will have the value $\epsilon_0(Z)/r^3$ where $\epsilon_0(Z)$ is the "strength" of the centre. No satisfactory expression for this constant has been developed which properly describes the effects of arbitrary solute species; consequently, the effective size of an imperfection, according to resonance measurements, is taken simply to mean the volume within which the change in gradient assumes a value equal to or greater than a critical value $(\Delta eq)_c$. The ratio of these volumes equals the ratio of the $\epsilon_0(Z)$ for various point imperfections. Only the product $\lambda\epsilon_0(Z)$ can be estimated from experiment, and in the actual case of a dilute gold in copper alloy λ must be assumed to be about 200 if $\epsilon_0(Z)$ is given the value derived from X-ray lattice parameter versus composition data[132] and $\epsilon(Z)$ is taken to be the magnitude of the principal shear strain around a gold atom[131].

Dislocations can be treated approximately[133, 76] by inserting b/r for $\epsilon(Z)$, where b is the Burgers vector and r is the distance from the dislocation. In this case, there are no impurity-atom effects involved, and no functional dependence on Z can exist. A test of the proportionality of gradient and strain might best be conceived using dislocations; their strain fields are so extensive, however, that considerable overlap and cancellation of strain undoubtedly occur. The very great body of knowledge which is being accumulated describing in some detail the dislocation arrays brought about by controlled strain-anneal methods may permit further advances in this direction. The gradients at nuclei around dislocations are caused by distortion of the outer closed electronic shells (the core) and also, presumably, by the redistribution of conduction electrons in the strained lattice.[134] It appears that due to the various charge effects involved in $\epsilon_0(Z)/r^3$ its magnitude is considerably larger than the ordinary critical shear strain, but that for dislocations the use of b/r and a λ of the order of 1 is probably reasonable.

2a. *First-Order Quadrupole Effects*

It is possible for virtually every nucleus to experience a gradient large enough to broaden the satellites beyond observability and yet not sufficiently large to split the central line perceptibly. When this occurs, the intensity falls to that contributed by the central line alone; the satellite absorption is spread quite uniformly over a large region around ν_0 and is not detected by the usual experimental methods. An intuitive understanding of this can be obtained from Fig. 6 if the satellites are imagined smeared out so that one might easily mistake the flat part of the absorption on either side of the central line for the true base line of the total absorption. In work on alloys this "mistake" is unavoidable and probably simplifies the interpretation of the data substantially. The intensity of the central line alone constitutes 4/10

VOL. 9 1961

of the total (including satellites) if $I = 3/2$; 9/35 of the total if $I = 5/2$; 4/21 if $I = 7/2$, and 5/33 if $I = 9/2$. These figures are obtained from the intensity ratios given for the various transitions in the paragraph following Eqn. (11). The total relative intensity can usually be obtained by experiment on the pure, well annealed cubic metal. If heavy cold-work or moderate (5 atomic per cent) impurity concentrations cause an approximate decrease from unit intensity to the central line contribution alone, it is probable that the satellites have been eliminated and first-order effects identified. The satellite intensity can then be studied as a function of the concentration of imperfections knowing that the central line will be essentially unperturbed. Upper and lower limits can be placed on the gradients involved, and a plot of satellite intensity *versus* defect concentration can be used to obtain the relative defect volume. Satellite intensity is just the observed relative intensity $(J\delta\nu^2)/(J_0\delta\nu_0^2)$ (see Section II-B) less the contribution of the central line. J_0 and $\delta\nu_0$ refer to the unperturbed resonance of the pure strain-free metal. Illustrations of first-order phenomena are the effects of dislocations in eliminating the satellites in cold-worked copper and in impure aluminium. These will be discussed in more detail further on.

An approximate lower limit for the gradient necessary to eliminate the satellite lines can be obtained from (10) in the light of Fig. 6. To avoid any sizeable satellite contribution to the measured intensity $J\delta\nu^2$, it is reasonable to demand that the *peaks* of the satellite structure (Fig. 6, for $I = 3/2$) fall outside of a region $\nu_0 \pm \delta\nu$, that is, one full line width or more from the line centre. Large values of the derivatives of the satellites are confined to the regions of these peaks, which occur at $\nu_0 \pm e^2qQ/4h$ for $I = 3/2$. For higher spin, the *innermost* ($m = 3/2 \longrightarrow 1/2$; $-1/2 \longrightarrow -3/2$) of the $2I$ satellites falls at $\nu_0 \pm 3e^2qQ/4I(2I-1)h$ and since all other satellites fall outside of this, it is sufficient to demand that $[3e^2qQ/4I(2I-1)h] \geqslant \delta\nu$. Then for all nuclei at which $q \geqslant [4I(2I-1)h\delta\nu/3e^2Q]$ there will be practically no contribution to $J\delta\nu^2$. If it is determined from the experimental work that the central line is *unperturbed* similar reasoning will lead to an upper limit for q;

$$q \leqslant \frac{h}{e^2Q}\left\{\nu_0\delta\nu\,\frac{128I^2(2I-1)}{25\,(2I+3)}\right\}^{\frac{1}{2}}. \qquad . \quad . \quad . \quad . \quad (22)$$

Larger q values would cause noticeable broadening and asymmetry in the absorption. Equation (22) was calculated on the assumption that the distance between the peaks in Fig. 7 must be less than $\delta\nu/2$, half of the unperturbed line width. The upper and lower limits of q differ by a factor approximating $(\nu_0/\delta\nu)^{\frac{1}{2}}$, commonly about 10 or 20. If q is proportional to r^{-3} around a point defect which causes no splitting of the central line, nuclei from the nearest neighbours to those about three times farther away can be significantly broadened in first order. The satellites from successive cylindrical shells around a dislocation will be so closely spaced that the foregoing statements concerning q will be of no real assistance in understanding their structure.

2b. *Second-order Quadrupole Effects*

Second-order perturbation theory describes the manner in which the $m = 1/2 \longrightarrow -1/2$ transition is distorted or diminished. First-order broadening is ordinarily complete and satellite contributions are absent from the observed intensity. A lower limit can be placed on the gradient by assuming that the peaks of the central line, Fig. 7, must be split at least $5\delta\nu$ for their derivatives to escape detection. The magnitude of q must exceed

$$q_c = \left\{ \nu_0 \delta\nu \frac{256\, I^2(2I-1)}{5 \quad 2I+3} \right\}^{\frac{1}{2}} \frac{h}{e^2 Q}, \qquad \ldots \quad (23)$$

for this to happen. The width $5\delta\nu$ was chosen arbitrarily; it must be based on the signal-to-noise ratio in practice. With the vanishing of the central line, no sharp resonance remains near ν_0 and the intensity falls to zero. The gradients required for this marked second-order broadening are about 30 to 60 times larger than those required for satellite disappearance.

3. *Discussion of Experimental Work*

In discussing specific quadrupole effects in imperfect crystals, one can probably do little better than to classify the effects according to the imperfections causing them as BLOEMBERGEN has done.[76] It is essential, however, to recognize that it would be unwise to set out to study the dislocations (for example) in a metal without preliminary data concerning the influence of cold-work on the resonance absorption of that particular metal. In this regard, nuclear resonance has as yet no "typical" examples of quadrupole effects, but merely illustrations of effects as manifested in a few metals which have been explored.

Experimental results on copper[30, 97] and aluminium[125] illustrate the quadrupole effects to be expected in cold-worked metals and solid solutions with random defects. Some of these experiments have been reviewed and discussed at some length[76, 74] but will be included here because they are of value as examples of possible further applications of nuclear resonance to metals. The quadrupole moment of Al^{27} is $0{\cdot}156 \times 10^{-24}$ cm^2 and its spin is 5/2; for copper there are two isotopes with nearly equal quadrupole moments, but with isotopic abundances differing by a factor of two. The behaviour of both resonances is the same and the discussion will be confined to the more abundant Cu^{63} for which $Q = -0{\cdot}157 \times 10^{-24}$ cm^2 and $I = 3/2$. The fact that the signs of the quadrupole moments differ for the aluminium and copper is of no assistance in the interpretation of the experiments since the satellite splittings are always symmetric about ν_0 due to the form of their dependence on m, the magnetic quantum number [Eqn. (10)], and because only Q^2 is involved in the central line splitting.

3a. *Quadrupole Effects in Cold-worked Metal*

Heavily cold-worked (filed) pure copper was found[30] to have a resonance intensity of about 40 to 50 per cent of that measured for well-annealed copper,

VOL. 9 1961

and incomplete anneals gave measured intensities falling between those exhibited by the cold-worked and well-annealed states. This behaviour is the result of first-order quadrupole broadening and must be associated with the gradients produced by the strain fields around dislocations. The intensity of the central line alone should be 4/10, the discrepancy with the observed 0·4 to 0·5 being accounted for by admitting that the cold-worked sample was probably not "perfectly" cold-worked, and that the annealed sample was not a powder of perfect crystals. This explanation is supported by a measurement on filings which had been partially dissolved in acid, thus removing the outer material. Their intensity was found to be about 20 per cent higher than the as-filed metal indicating that the centres of the filings were not as thoroughly distorted as the outside layers. To use these data for quantitative dislocation-density determinations requires either the knowledge of the distribution of electric gradients around the dislocation or a controlled experiment in which the resonance intensity is essentially calibrated using either an independent method (e.g. X-ray), or a carefully developed dislocation array in sheet material. It is probable that filings would be unsuitable for detailed work of this nature. The distribution of dislocations can be studied by nuclear resonance, and, likewise, large local concentrations in the dislocation density accompanied by strain-free regions may give misleading results if uniform or random distributions are assumed. For randomly distributed dislocations, as may be found in a worked, unrelieved specimen, a second moment method may be useful. WATKINS [133, 76] developed a formula relating dislocation density to the second moment of the satellite contribution for a random distribution of dislocations in an ionic (NaCl) lattice. It has been used [102, 76] to derive crude estimates of the dislocation density in cold-worked copper based on the experiments described above. The values obtained were consistent with those derived from other methods.

Dislocations are not retained in pure (99·99) aluminium filings in sufficient numbers to cause significant first-order broadening. A small quantity (0·64 atomic per cent) of magnesium in the lattice locks the dislocations, however, causing the large drop in intensity seen in Fig. 10. Effects in complete analogy with the copper are then obtained, [135] the only difference being that the intensity for the annealed material is now fixed by the impurity content, and the lower intensity limit in the worked alloy is about 9/35, characteristic of a metal with $I = 5/2$. This work demonstrates the possibility of studying the temperature dependence of dislocation break-away and of deriving an activation energy for dislocation motion under conditions of no externally applied stress. Because of the relatively long range (r^{-1}) strain fields around dislocations, it is important to use a statistical approach to their effect on resonance absorption. The concept of a critical radius or volume per imperfection is inadequate.

3b. *Quadrupole Effects in Alloys*

The quadrupole effects of foreign atoms in solid solution are striking.

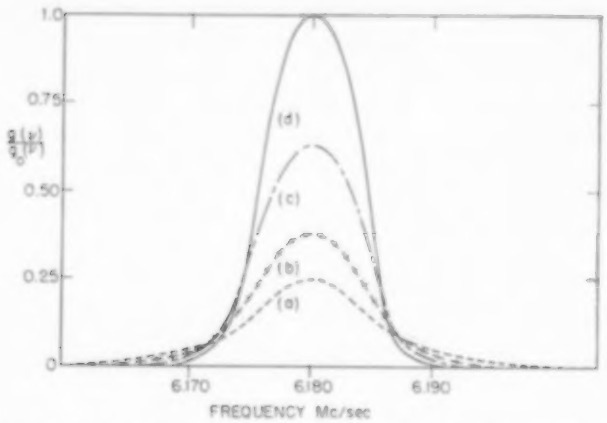

FIG. 10. Absorption of Al^{27} in Al–0·64 atomic per cent Mg showing the effect of magnesium in locking the dislocations. Resonance of alloy: (*a*) as filed at room temperature, (*b*) after filing and 87 hr at 250°C, (*c*) after filing and 2 hr at 480°C. Curve (*d*) is pure aluminium, as filed at room temperature. The magnesium, which alone reduces the intensity to 0·6, binds enough dislocations to obliterate the satellite contribution to the intensity.

A few per cent of the impurity (solute) will often cause more than a 90 per cent drop in the intensity of the absorption. Any copper or aluminium alloy will serve as an example of this, with similar behaviour expected for other metals having nuclei of spin greater than 1/2 and a sufficiently large quadrupole moment. It is particularly interesting to compare copper with aluminium because their lattice structure and quadrupole moments are the same. The marked difference in the experimental results to be discussed is entirely a result of the difference in their electronic structure.

The observed relative intensity of the Cu^{63} absorption in some primary solid solutions of copper [177] is shown in Fig. 11. The data were obtained at a frequency, ν_0, of 4 Mc/s. The intensity for pure copper corresponds to only the full central line ($m = 1/2 \longrightarrow -1/2$) intensity, and all measurements were conducted on the cold-worked alloys so that only the central transition could be observed. This is purely a second-order quadrupole effect. The width and shape of the Cu^{63} resonance change very little during the decrease in amplitude. The relative intensity plotted in Fig. 11 has been corrected for the change in composition so that it is a true measure of the proportion of Cu^{63} nuclei absorbing energy at ν_0.

The decrease in intensity has been interpreted [30] in such a way as to make the "effective defect size" especially simple to visualize. We assume that the electric gradient is very large near a solute atom so that the resonance of any solvent Cu^{63} close to a solute atom will be unobservable. The solvent atoms at greater distance from the solute have their central transitions effectively unperturbed. Any copper atom which has no solute within the critical radius r_c will clearly contribute its full share to the observed intensity. The probability

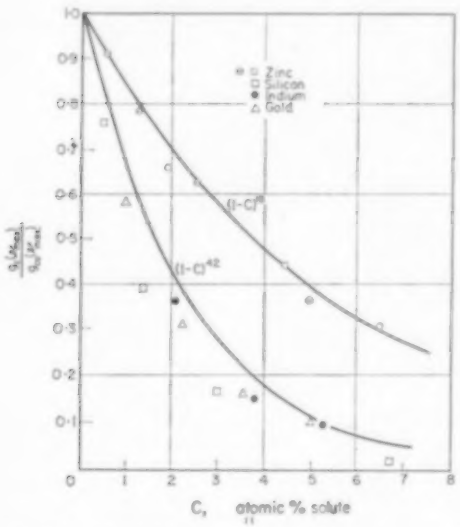

FIG. 11. Intensity of central components of Cu^{63} in primary solid solutions of copper as a function of solute concentration. Measurements were made at 4 Mc/sec using the nuclear induction technique except in the case of the crossed circles which represent data obtained at 6·3 Mc/sec using the nuclear absorption method.[20] The accuracy of the intensity measurements is about ± 10 per cent. Two calculated curves are included for qualitative comparison with the data.

that a copper atom has no solute atoms on any of its n neighbouring lattice sites within r_c is easily determined for a random solid solution. If the relative solute concentration is c, then each lattice site has a probability $1 - c$ of being occupied by a copper atom. The probability of n sites being occupied by copper is just $(1 - c)^n$. Therefore, the proportion of copper nuclei whose absorption should be observable is just $(1 - c)^n$, and if the line shape does not change appreciably, $J\delta\nu^2/J_0\delta\nu_0^2$ should be proportional to $(1 - c)^n$. According to the discussion of intensity in Section II-B, if $\delta\nu = \delta\nu_0$ the relative intensity can equally well be expressed simply as J/J_0, or as $J\delta\nu/J_0\delta\nu_0 = g(\nu_{max})/g_0(\nu_{max})$. The latter form, frequently seen in the literature, actually denotes the relative amplitudes of the peaks of the absorption curves; it will be abbreviated g/g_0. A double log plot of intensity *vs.* composition is used to determine n, that is

$$\log_{10}(g/g_0) = n \log_{10}(1 - c) \approx -nc/2{\cdot}303 \quad . \quad . \quad . \quad (24)$$

using an approximation to the natural logarithm for small c. The data of Fig. 11, replotted in this manner, are shown in Fig. 12. The scatter in the measured intensity is around ± 10 per cent, but the essential correctness of the relationship (24) is seen to be confirmed. In addition, it appears that for zinc, indium, silicon and other B subgroup[177] solutes in copper, n is approximately proportional to the excess solute valence Z (see Table 3). This is to

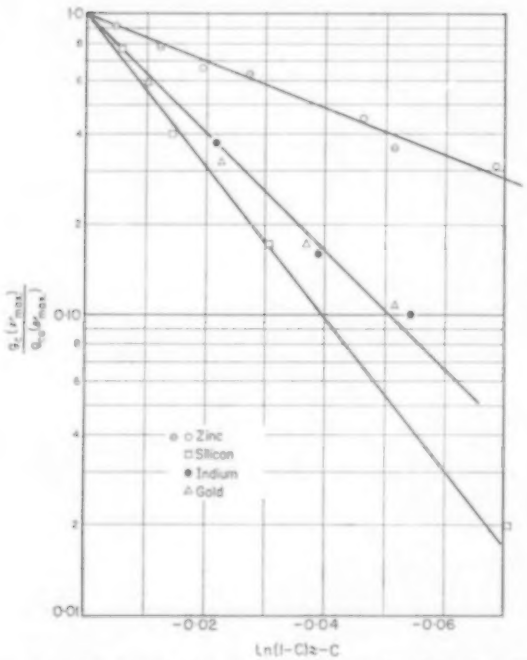

FIG. 12. Copper alloy intensity data of Fig. 11 on a log–log plot. The slopes of the lines give the n values in Table 3.

be expected if q is proportional to Z/r^3 because in a continuum, n would be equal to $(4/3)\pi r_c^3 d_a$ which is proportional to $(4/3)\pi d_a Z/q_c$ where d_a is the number of atoms per cm^3, r_c is the critical radius in cm, and q_c is a constant estimated in (23). Deviations from this proportionality may occur because in a face-centred cubic lattice the numbers of atoms which lie within spheres centred on a lattice site assume certain integral values, n_{fcc}, which are also listed in Table 3.

TABLE 3

Solute	*Z*	*n*	n_{fcc}	*Shell*	*Ionic radii**	$\frac{1}{a}\frac{da}{dx}$†	*Atomic diameter*‡
Zn	1	18	18	2	0·74 Å	0·055	2·67
In	2	46	42	3	0·81	0·259	3·14
Si	3	58	54	4	0·41	0·015	2·75
Au	0	46	42	3	1·37	0·148	2·88

* Values are due to L. PAULING, Ref. 165.
† Relative change in lattice parameter per atomic fraction solute.[130, 132]
‡ Goldschmidt diameter[166] for co-ordination number 12, in Ångström units; for copper it is 2·55.

Since ν_0 enters the expression for the critical q, the experimental values of n depend on ν_0. Their *ratios* would be independent of ν_0 except for any "shell

effects" introduced by the discreteness of the lattice; this can be partially overcome by repeating the intensity measurements at various frequencies. Since it is the ratios which determine the relative defect sizes, the absolute values of n are not of primary interest.

Recently CHAPMAN and SEYMOUR [97] reported an investigation of copper–nickel alloys (containing up to 9·2 atomic per cent nickel) in which they plotted J/J_0 and found $n = 18$ when the experiment was performed at 7 Mc/s, and 28 when repeated at 3 Mc/s. It would be difficult to estimate a value of n at 4 Mc/s from their result because of the complex way in which n may vary with ν_0. The significant feature is that n for nickel is rather near that for zinc, in further support of the observation that n is roughly proportional to the excess solute valence which in this case should be taken as (-1). For comparison with Table 3 we note that for nickel [137] $(1/a)(da/dx) = -0{\cdot}030$. The Cu^{63} absorption line shape in these copper–nickel alloys was calculated [97] by summing the contributions of a set of curves of the shape shown in Fig. 7. The appropriate A_2 for each member of this set was determined by assuming q proportional to r^{-3}, and the contribution of each member was weighted by the probability of a lattice configuration in which one nickel atom was a distance r from a copper atom. Configurations in which two nickel atoms were important were neglected so that Eqn. (12), which is valid only for electric fields of axial symmetry, could be used to calculate the individual contributions. Good agreement with the experimentally observed absorption curve was obtained by setting $q = 1{\cdot}7_5 \times 10^{23}$ cm^{-3} at the position of the second nearest neighbour.

In spite of the lack of understanding of the exact origin of the electric gradients in the lattice there are many interesting features of the work on copper alloys which are well established qualitatively and worthy of note. The remarkable thing is that there is so little correlation with the lattice parameter data, which is generally taken to be a direct measure of the strain around a centre of dilatation. It is only in the case of gold that the ionic radius exceeds that of copper, and the effect of ion core repulsion and electron localization must be the dominating factors causing the gradient. The ionic radii of all other solutes investigated are less than that of copper (0·96 Å). It appears that the quadrupole effects in copper can be compared with the "valency" effects discussed by RAYNOR [138] for copper alloys, with the exception that the constant C, introduced by him to take into account the difference between solutes of the same valence but different periods in the periodic table, is missing from the resonance study. The fractional change in the lattice parameter per atomic fraction solute for silicon, germanium, and tin in copper is in the approximate ratio 1 : 6 : 19, and yet all produce approximately the same electric field gradient at the same distance from the solute, implying that the localized valence effect overlooks a major factor in determining the lattice parameter of a solid solution. In view of the r^{-3} dependence of q this is rather surprising. (See note added in proof.)

There are obvious differences between X-ray and resonance experiments

involving quadrupole effects. First, the resonance observations apply only to material which is free of solute, thus they neglect solute–solute interactions which clearly play a large part in X-ray results. Also, resonance is unaffected by pure dilatation of the lattice. Hydrostatic strain will produce no gradients at the lattice sites of a cubic metal. Uniform lattice dilatation could be brought about by an (hypothetical) increase in the electron-to-atom ratio in the pure metal. If the electron-to-atom ratio in the pure metal regions being observed by resonance were changing, then one could justifiably expect a change in the Knight shift of the observed (residual central) absorption line. The latter is not observed.[19, 30, 177, 97] The electron-to-atom ratio (which begins to have meaning when impurity potentials overlap) and the excess solute charge, play "independent" roles in contributing to the "distortion due to the valency of the solute".[138, 139] Only the excess charge effect has been detected by quadrupole perturbation experiments but the electron-to-atom ratio evidently is significant in the Knight shift experiments on silver alloys discussed previously. Another distinction between the X-ray and resonance methods is the ability of the former to detect *displacement*, while the latter, at best, is able to detect the rate of change of displacement or the rate of change of dilatation. Cumulative lattice misfit should affect X-ray results on atomic displacements, which are interpreted in terms of strain, much more than they affect resonance observations which, of course, have nothing to say about the displacement *or* strain in the portion of the solid solution which is occupied by the solute. It appears that a major factor in accounting for lattice strain around point imperfections must remain the atomic or core effects which have for so long been associated with size. Further detailed comparisons of the resonance results with the findings of other mechanical and electrical experimental techniques applied to primary solid solutions are beyond the scope of the present article; such comparisons can often be made via the parameters in the last three columns of Table 3. Although core effects are largely responsible for lattice distortion, strain *per se* is apparently not as effective in producing electric field gradients as are charge effects. This is to say that a hypothetical atom of smaller ionic radius than the solvent which produces no localization (charge redistribution) or excess charge effects would not be as effective in giving rise to quadrupole broadening as any actual solute atom with its electrical potential difference.

Perhaps it should be added that no work specifically on the first-order quadrupole effects due to impurities in copper has yet appeared. If the r^{-3} dependence of q is correct at large distances, we should expect to find intensity variations corresponding to values of n of about 500 to 1500 for the elements in Table 3. The effects of residual dislocations or other mechanical defects in the annealed material, and of incidental impurities would complicate the interpretation of the data; also, the assumption of a critical radius (even if loosely interpreted) would have to be abandoned and a statistical treatment[74] applied to the results. Roughly the intensity for copper with zinc as solute might be expected to vary as $0{\cdot}6(1-c)^{600} + 0{\cdot}4(1-c)^{15}$.

There seems to be no evidence for the screened Coulomb field[30, 76] as a direct source of the observed gradients in either copper or aluminium. This does not, however, argue against its existence; the gradient derived from it is merely too small, relative to the observed inverse-cube relationship, to exercise any effect on the results.

Impurities in aluminium cause smaller gradients at the aluminium nuclei than they do at the copper nuclei in copper, probably as a direct result of the

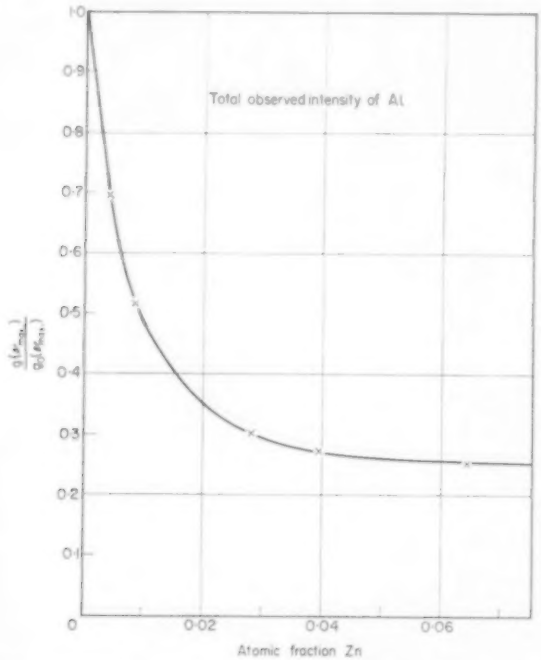

FIG. 13. The intensity of the Al^{27} resonance in filed, annealed, aluminium-zinc alloys at 6·18 Mc/s as a function of zinc concentration. The satellites are rapidly washed out, leaving the unperturbed central transition.

aluminium lattice being rather "open" when compared to the copper lattice of impinging cores. First-order quadrupole effects have been identified in primary solid solutions of aluminium with zinc and magnesium.[135] The investigations were carried out on annealed material to minimize the effects of dislocations. The intensity was found to drop from an initial value of unity for pure aluminium to about one quarter for a few per cent zinc in aluminium, as shown in Fig. 13. Since the full central line intensity is 0·257, the observed intensity was assumed asymptotic to that value and the satellite intensity, $[(g/g_0) - 0{\cdot}257]$, was determined in accordance with the discussion in part 2a above. The logarithm of the *satellite* intensity is plotted as a function of $\ln(1 - c)$ in this case, using arguments similar to those put forth above, but omitting the "all or nothing" character which was associated

with the analysis in copper alloys and adopting a view of n as a relative size parameter. The plots could be fitted by straight lines for which $n = 98$ for zinc, see Fig. 14, and 130 for magnesium with errors of about $\pm$ 10 per cent. The possibility of these absolute values for n being too high has been discussed by COHEN and REIF.[74] In Fig. 14 the satellite intensity relative to the total intensity of the pure metal is plotted; maximum theoretical satellite

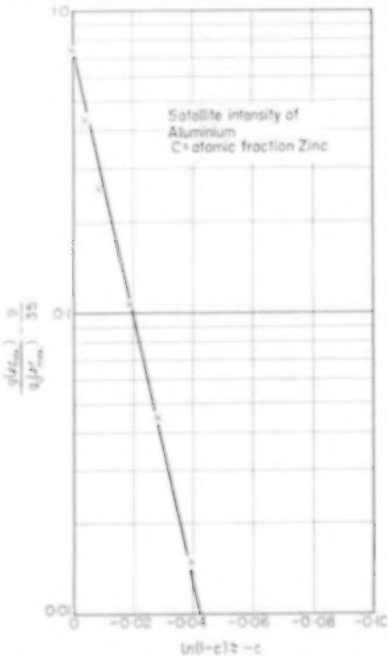

FIG. 14. A log–log plot of the satellite intensity (total minus central line) of Al^{27} in aluminium-zinc alloys as a function of zinc concentration derived from Fig. 13. The slope of the line is 98.

intensity is 0·743. The larger gradients caused by magnesium also gave rise to a small amount of second-order splitting of the nearest neighbour aluminium absorption. The splitting was so slight that instead of disappearing, the central line merely broadened asymmetrically. The change in line shape made the use of $J\delta\nu^2$ invalid as a measure of intensity in the region of large central line contribution.

The success of the model used to interpret these experiments on point defects depends partially on the quantity used as a measure of intensity. $J\delta\nu^2$ tends to neglect background absorption which is spread uniformly over the frequency spectrum in the vicinity of ν_0. The large inhomogeneities in q and the saucer-like shape of the satellites and central lines when split also assist in affording this model a greater degree of validity than might at first seem possible.

Once the presence of strong quadrupole effects has been established for

any particular solvent and solute in a primary solid solution, the intensity can be used as a measure of the composition of the solvent-rich phase. By this means the solid solubility or the extent of a precipitation process can be determined by using appropriate heat-treatment. As long as the composition of interest coincides with the region where the intensity varies rapidly with solute concentration, the method has merit. Since the measurements can be carried out on precisely the same sample material before and after heat-treatment, the relative intensities can be obtained with good accuracy. This type of experiment has been performed on one aluminium–magnesium alloy,[135] but in that case only a small effect due to the second-order splitting of the central line mentioned above was found. The compositions involved did not reach into the range where the satellites contributed significantly to the intensity.

VOL. 9 1961

It has been assumed above that the solid solution being investigated is random. Ordering will, of course, have a profound effect on resonance intensity since the fundamental factor in causing quadrupole perturbation is lattice symmetry. In stoichiometric compounds, if ordering produces cubic symmetry around the nuclei of interest, the intensity will be greater than for random placement of the surrounding atoms. Likewise, if ordering produces a lower symmetry (e.g. tetragonal), the intensity will usually be less than for the random solution. At other compositions, these tendencies may show up as positive or negative deviations from a straight line on a plot of $\ln(g/g_0)$ *vs.* $\ln(1-c)$. Clustering (or coring) will produce positive deviations because part of the lattice is depleted in solute; short-range order should cause negative deviations. An analysis of the intensity change to be expected from the ordering which may exist in alpha brass has been given by BLOEMBERGEN[76] in a more detailed discussion of resonance intensity in partially ordered alloys.

The effects of order are beautifully demonstrated by the resonance of In^{115} in indium antimonide observed by SHULMAN *et al.*[110] Since the radio frequency field was able to penetrate a sizeable single crystal of this semiconductor, the change in the gradient accompanying the application of a static compressive stress could be observed directly. Reversible line broadening was produced by strains within the elastic limit ($< 10^{-4}$) and numerical values were obtained for the "gradient-elastic" constants comprising the tensor relating the electric field gradient to the applied stress. The line broadening was the result of the 8 satellites diverging slightly; In^{115} has a spin of 9/2. Unfortunately, unless acoustic resonance absorption[141] in metals can be observed, the chances of working with single crystals of ordered compounds appear slight. Resonance studies on powdered, well-ordered intermetallic compounds will still be quite valuable, however, in providing greater insight into the lattice perfection of these phases.[142]

4. *Miscellaneous Effect of Quadrupole Interactions*

Quadrupole interactions are responsible for some minor changes in line

width and relaxation time which can best be discussed here. When the spacing of the nuclear energy levels in the magnetic field change, there is also a change in the dipolar line width. The static (second) term in Eqn. (16) remains the same, but the first term is altered because oscillating fields due to the quadrupole-perturbed neighbours may no longer cause mutual spin flipping. The requisite modifications of (16) have been discussed by BLOEMBERGEN[76] and COHEN and REIF[74] on the basis of calculations made by KAMBE and OLLOM.[143] If the field gradient is highly inhomogeneous and the central line unperturbed, the contribution of the first term in (16) to the second moment is decreased by a factor of 4/5 when $I = 3/2$ and by 257/315 when $I = 5/2$. The situation is complicated when the inhomogeneous gradients do not differ greatly from atom to atom and when powdered samples are concerned. In any event, the dipolar second moment should *not* change by more than 10 to 20 per cent because of quadrupole perturbation.

The spin-lattice relaxation time T_1 is altered by the interaction of the nuclear quadrupole moment with conduction electrons (see Appendix B) and the fluctuating electric fields associated with lattice vibration or atomic migration. The effects have been discussed[76, 74] and are not expected to give rise to prominent effects in the observed steady-state resonance absorption. This is because the relaxation times associated with these interactions are usually considerably longer than those already provided by the magnetic (hyperfine) interaction between the nuclei and conduction electrons. In a few metals the non-*s* part of the conduction electron wave function may possibly be large enough to contribute a significant effect. This has been proposed as an explanation for the relaxation times inferred from the line widths[21] of Ga^{69}, Ga^{71}, Rb^{85}, and Rb^{87}. The relaxation times reported for these pairs of isotopes are not inversely proportional to the squares of their gyromagnetic ratios as they should be, according to Eqn. (B4), if non-*s* magnetic and quadrupole relaxation are absent. Since relaxation time data are still relatively meagre, the topic will not be pursued here. Eventually we may expect these effects to yield some information concerning the character of the wave functions. Bloembergen has given an expression[76] for the time necessary for the recovery of equilibrium after saturation of the central transition in cold-worked copper. The predicted time is quite a bit less than it would be in annealed copper. A steady-state saturation experiment is, however, expected to give the same T_1 for both cold-worked and annealed copper except for a small line width correction of the type discussed in a preceding paragraph. Treatments of the effect which quadrupole interactions may have on the relaxation time during diffusion have also been given,[76, 74] although the processes have not been identified experimentally. In fact, it is interesting to note that in the only case when a suspected quadrupole contribution was critically investigated,[120] it was shown to be completely absent. This occurred during the study of lithium near its melting point.

A quite recent development has been the report[144] of direct quadrupole transitions (at zero applied magnetic field) of aluminium nuclei which are

nearest neighbours of zinc atoms. This work complements perfectly the nuclear magnetic resonance observations, since precisely the same aluminium nuclei are *observed* by one technique as are missing from the intensity measured by the other. Using this new approach the quadrupole interaction energy can be measured directly and more precise estimates made on the dependence of gradient on position in the lattice.

5. *Summary of Quadrupole Effects*

Quadrupole effects are generally much more pronounced than magnetic effects. In fact, imperfections often cause such drastic changes in the resonance that the possibility of using nuclear resonance techniques to observe the density and/or distribution of lattice defects appears to be quite good. The applicability of resonance to the study of order, precipitation, the structure of point defects, the density of dislocations, radiation damage and other topics concerning lattice deformation has been demonstrated. The nuclear spins included in Table 1 can be used as a guide in deciding whether a particular nuclear species has a quadrupole moment ($I \geq 1$). Values of the quadrupole moments are given in Refs. 3, 14, 145, 40; they offer only slight assistance in predicting the outcome of an experiment involving quadrupole interaction because the gradients are usually not known before the experiment is accomplished and no general method of estimating them accurately has been developed. Of course, some assistance can be obtained by inference from the results of the work on copper and aluminium. A few exploratory experiments can rapidly establish an estimate of the interaction energy e^2qQ for any particular solvent and defect.

IV. Miscellaneous Topics and Experimental Methods

A. *Remarks on Experimental Technique*

There are many aspects of nuclear resonance in metals which are peculiar to this field and which set it apart from resonance work in non-conductors. The fundamental differences can be summarized by saying that one must take into account the interactions of nuclei with conduction electrons, a topic which has comprised a major part of this review. Consideration of the depth of penetration of the radio-frequency field into the body of a conductor is equally important to the proper interpretation of the experimental observations. This classical effect can complicate the measurements enormously, and steps are usually taken to eliminate the complication rather than correct for it. Sample preparation is often tedious, but this represents nothing new to metallurgists. Finally, the line shapes in all of the experiments on conductors to date represent the composite effect of all lattice orientations, and from this it is necessary to extract the desired information of absorption intensity *versus* crystal orientation, and to derive from it features of the electronic structure. Further complications can arise from the experimental conditions directly; these are more numerous than in many other techniques and can cause serious systematic errors. The difficulty lies in the fact that

almost always the signal-to-noise ratio is low, even when the theoretical optimum is approached. In striving to increase the useful signal output, one invariably must compromise the experimental conditions which would be theoretically most desirable. The situation is roughly akin to that common in X-ray work when the tolerable dead time of the counter and the slit width are decided upon.

Thorough introductions to the experimental methods and equipment [12, 146] have already been given. Early papers by POUND and KNIGHT,[147] and BLOCH, HANSEN and PACKARD[1] also provide interesting discussions of the absorption and induction techniques, respectively. The very large number of possible detection schemes precludes a comprehensive survey of them here. A few aspects common to nearly all of them will be discussed together with some general remarks on techniques. Assume, in the following, that the frequency of the applied *r–f* field is held constant. The object of steady-state measurements of magnetic resonance is to determine the true dependence of nuclear absorption upon external field. A very common method of attempting this is to modulate the external field sinusoidally so that the resonance absorption will cause a modulation of the radio frequency signal appearing at the receiver. This amplitude-modulated signal is then demodulated. The result is an alternating current, whose frequency is precisely that of the initial modulation, and the amplitude of which is determined by the *slope* of the absorption curve. This voltage is sent to a phase-sensitive detector which is the same as a synchronous rectifier as far as the desired signal is concerned. Undesired noise accompanies the signal, but since its phase is random with time, it is possible partially to average out the noise contributions by suitably filtering the rectified output. This averaging process finally determines the theoretical signal-to-noise ratio, all other things being constant. In practice, it seldom pays to average the noise over times greater than a few minutes since other long-time variations in experimental parameters become significant. If the modulation frequency is too high (relative to $1/T_1$), there is a phase difference between the modulation as applied to the nuclei and the received alternating current signal;[107] this affects the rectified output. If the modulating frequency is greater than the line width, distortion of the output may result;[147, 148] this is more likely to be of concern for the reference resonance than for the metal. If the modulation amplitude is too great, the output will not be proportional to the slope of the absorption curve. Instead, the line will be artificially broadened and δH, the peak-to-peak width of the derivative curve obtained experimentally will exceed its true value; also, the second moment will be exaggerated.[149]

Simultaneously with the above modulation and detection process, the external field is being changed slowly with time, so slowly that it is usually assumed stationary at each consecutive value. If this is not true, serious distortion can arise from several sources; the only difficulty commonly encountered in work with metals arises in attempting to pass through the line in a time which is short compared with the integrating time of the output

VOL.
9
1961

circuit referred to above. The amplitude of the radio-frequency field must not be too large or the resonance will be saturated [11, 107] (Section III-A) and, in an extreme case, under conditions of slow passage through the resonance, it will disappear. "Fast passage" experiments [122] make use of a very rapid change in external field and a large r–f field strength to measure T_1; these experiments require no modulation. In a metallic particle, the degree of saturation may depend on the position of the nuclei inside the particles. This complicates the particle size effects to be discussed presently. To avoid spurious line broadening due to inhomogeneities in the applied magnetic field, these inhomogeneities should be very much less than the natural line width of the resonance. An estimate of these inhomogeneities can be obtained easily by observing the width of an inherently narrow line such as that of the protons in water or lithium in an aqueous lithium chloride solution.

During the course of a series of intensity measurements, it is necessary to be especially careful that exactly the same experimental conditions be reproduced for each sample because corrections are difficult to apply with assurance. Ideally, the "filling factor" which is the fraction of the total radio-frequency magnetic energy that is actually stored in the volume occupied by the sample should be kept constant. In practice, the total volume occupied by the powder is kept constant; in this way, the field geometry at the sample in the radio frequency probe coil is not changed appreciably but, of course, the actual sample material does not really fill the volume. A correction is therefore applied by weighing the sample and computing how much of the volume was occupied by metal. When sample composition is changed, a correction is also applied to account for the change in the number of active nuclei. The resonance intensity is directly proportional to the number of absorbing nuclei in the volume occupied by the sample.

The resonance investigation of alloys is sufficiently new that it has been possible for such studies to yield new information only if all of the previously known metallurgical data are used as background in preparing a sample with a well-defined composition and a known history of thermal and mechanical treatment. The fact that this sample is usually desired in finely divided form has complicated the task considerably for alloys; filings from the bulk alloy are the most satisfactory powders, just as for X-ray work. These may, of course, be rounded or etched by subsequent treatment. Various other techniques of producing powders are described in the literature. [163] The powders should be freed of accidental contamination by ferromagnetic particles by cleaning them with a magnet. The presence of such particles introduces an extra source of width similar to external field inhomogeneity. If the particles form a natural adherent oxide coating, this usually is sufficient to keep them insulated from one another; if they do not, or if it is found that this is not adequate insulation, the particles may be coated in some manner, or immersed in oil or paraffin. For example, silver alloy filings are often coated with thin sulphide layers by treatment with NaS or KS solutions. Mercury alloys liquid at room temperature can be kept divided under

paraffin oil with a small quantity of oleic acid added, and the alkali metals are commonly dispersed in mineral oil. These methods are satisfactory at room temperature and below. For work at elevated temperatures, a protective atmosphere and/or refractory material must surround the metal particles.

B. *Influence of Particle Size on the Resonance Absorption in Conductors*

Ordinary conduction losses in the sample can cause a distortion of the observed resonance absorption that can be described as a mixing of the real χ' and imaginary χ'' parts of the complex nuclear susceptibility χ, mentioned in Appendix A. The effects have been described by BLOEMBERGEN[150] and in somewhat greater detail by CHAPMAN and co-workers.[151] The former author included a treatment of saturation which now should be modified in keeping with the findings of REDFIELD.[107] It does serve, however, as a reminder that saturation curves on metals may be seriously in error if at least one dimension of the sample is not small compared to the classical "skin depth" or "depth of penetration", δ, of the *r–f* field in the metal. Similar considerations entered an analysis of data on hydrogen in palladium wires.[114] The results of investigations on metals of large particle size, provided the *r–f* amplitude is *not* sufficient to cause significant saturation of the nuclear spin system, are as follows. When the change in power absorbed by the sample near resonance is measured, either by using a circuit responding to absorption only[147] or by an appropriately adjusted bridge circuit or nuclear induction apparatus, the quantity actually observed may not be the pure nuclear absorption, but a linear combination of the absorption and dispersion as shown in Fig. 15. The proportion of each function is determined by the skin depth $\delta = 5{\cdot}03 \times 10^{-3}\,(\rho'/\nu')^{\frac{1}{2}}$, where δ is expressed in cm, ρ' is the resistivity in microhm-cm, and ν' the frequency in Mc/s. The work of Chapman *et al.* describes in detail the characteristic asymmetric absorption curves which result from resonance work on metallic samples of size comparable to or greater than the skin depth. Theoretical studies were corroborated by experimental work on aluminium sheet of various thicknesses. Although sheet is certainly the best defined shape on which to perform these experiments, it is clear from their theoretical results that it also produces the most extreme distortion of the resonance curves. Spheres, cylinders, or even the geometrically poorly defined filing should not be as bad in this respect. The asymmetric absorption derivative curves resulting from any of these sample shapes have their zeros shifted and have unequal maximum and minimum values, in addition to a small subsidiary peak which appears to the right of the main peak in Fig. 15. The shift in zero can cause a serious error in the measurement of the Knight shift, and the asymmetry can complicate amplitude studies. The distortion also makes the accurate determination of true line shape very difficult, so that if the line is not known beforehand to be symmetrical, every effort is usually made to use samples of the smallest possible dimensions and avoid the possibility of this complication.

VOL.
9
196

Certain aspects sometimes not stressed in discussions of particle size (incidentally, the effect of particle size is quite similar to that of the "u" and "v" mode mixing encountered in bridge and nuclear induction experiments) are that the inequality in b and a (Fig. 15) and the shift in the zero are inseparable. Also that to a first approximation, for $b/a \geq 0{\cdot}7$, the peak-to-peak amplitude $|b| + |a|$ of the derivative is the same within about 5 per cent for asymmetric and symmetric curves. The fact that the zero shift d is *always* accompanied by the asymmetry about the zero can be a great help in detecting particle size effects; it must be remembered, however, that an innocuous-looking asymmetry may accompany a significant change in the

FIG. 15. An asymmetric Cu^{63} absorption derivative measured using copper spheres of 0·8 mm diameter. The distortion is characteristic of that obtained from large metal particles (thickness comparable to or greater than the skin depth). This resonance was observed at room temperature and at a frequency of 13 Mc/s, for which the diameter-to-skin depth ratio was about 45.

position of the zero. This change is relatively more important in Knight shift measurements as the line width increases because the error in position, for a given particle size and skin depth, is a constant proportion of the line width. For relatively narrow lines and large Knight shifts, the possible errors are decreased appreciably. In any actual metal, knowledge of the true nuclear absorption line shape is prerequisite to the calculation of the spurious shift; such an analysis has been carried out for aluminium.[151] A rough idea of the magnitude of the change, d, (Fig. 15) accompanying a particular asymmetry can be gained from a very brief investigation of the skin effect by MASUDA[29] done in conjunction with his work on cadmium. Assuming the absorption to have a Lorentzian shape, he plots some of the pertinent line parameters in an easily comprehended manner.

The field of electron spin resonance in metals has received no attention in this review beyond the mention of the work of SLICHTER and co-workers[47, 49]

in connection with their direct measurement of χ_p (Section III-B1). Other work on conduction electron resonance[152, 51, 52, 153] has been primarily concerned with the understanding of line shapes and relaxation times. There is one aspect of the subject, however, which may be of considerable interest to workers in the field of nuclear resonance in metals. OVERHAUSER[154] proposed a method for polarizing nuclear spins by keeping the conduction electron spin resonance continuously saturated. From a practical standpoint this encounters some difficulty because the sample of very fine metallic particles must be subjected to a continuous source of considerable microwave power. If this condition is met, however, the nuclear resonance intensity can be enhanced by several orders of magnitude. The nuclear spins assume a degree of polarization equal to that which they would have if their gyromagnetic ratio were that of the electron. Striking verification of Overhauser's theoretical prediction was achieved by CARVER and SLICHTER[155] in lithium. They also observed the effect in sodium but were unable to produce an appreciable saturation of the electron spin resonance. This phenomenon will be of great significance to the study of nuclear resonance in metals if it proves to be applicable to even a few interesting problems. The enhancement of the resonance intensity is accompanied by a disappearance of the Knight shift in direct consequence of the fact that the electron spins no longer provide a net magnetization in the direction of the magnetic field H_0. At saturation all of the electron spins are paired, the Pauli susceptibility is zero, and the Knight shift vanishes. KNIGHT[19] discusses the possibility of using this fact to eliminate the uncertainties (see Section II-C) introduced into the Knight shift measurements by the chemical shifts.

C. *Derivation of Absorption Line Shapes for Polycrystalline Samples*

Several times during the course of this survey, nuclear absorption curves obtained from samples of finely divided metal have been shown. Accompanying theoretical expressions may have given only $\nu(\theta)$, the resonance position as a function of crystal orientation. The procedure[156, 30] for obtaining the "powder pattern" is straightforward. The sample is assumed to be made up of randomly oriented crystallites. The number of nuclei in those crystallites for which the magnetic field makes an angle θ with the crystallographic Z-axis is proportional to $\sin\theta$. The amplitude of absorption between ν and $\nu + \mathrm{d}\nu$, which we shall call $I(\nu)\mathrm{d}\nu$, is thus proportional to $\sin\theta\,\mathrm{d}\theta$. Ordinarily it is found that the number of nuclei absorbing varies markedly over the frequency interval corresponding to the extreme possible orientations; this is obvious in Figs. 2a, 6 and 7, for example, where the absorption is seen to peak at certain frequencies. In sheet samples of metals with anisotropic crystal structure, one should, of course, be cognizant of the possible influence of preferred orientation or rolling texture. The nuclear resonance line shape may differ appreciably from that for an aggregate of randomly oriented powder particles. There is no orientation effect for cubic metals, so one need not be concerned about this phenomenon in sheet specimens of them; there

VOL. 9 1961

may, however, be interest in oriented sheet specimens of dilute alloys of some cubic metals in order to enhance the satellites in experiments on quadrupole effects. The wide availability of computing machines simplifies the rapid calculation of line shapes. No explicit analytical expression for absorption amplitude versus frequency needs to be developed. If frequency as a function of orientation is known, then for an axially symmetric crystal, for example, we can write $I(\nu) \propto f(\theta)\,(\mathrm{d}\nu/\mathrm{d}\theta)^{-1}$, where $f(\theta)$ is $\sin\theta$ for a powdered sample of randomly oriented particles. Since ν and $I(\nu)$ are explicit functions of θ, it is easy to compute them both directly and plot $I(\nu)$ *versus* ν. After obtaining this result, it is a desirable refinement to include the symmetric broadening also in order to provide a direct comparison with $g(\nu)$, the observed line shape. The parameters of $I(\nu)$ must be known in order to derive the correct magnitude of anisotropic Knight shift or quadrupole interaction, for example, from the observed traces. The combined effect of the symmetric and asymmetric broadening can be obtained (see Ref. 97 for an example) by an integration process similar to that used in a slightly different context to derive the combined shape function for two symmetric curves.[21]

Approximate relationships for estimating the total line width produced by two or more separate sources of width can be obtained by noting that a Gaussian distribution of Gaussian components (all of which have the same width) is another Gaussian the width of which is equal to the square root of the sum of the squares of the widths of the composing curves. On the other hand, two Lorentzian curves similarly combine to give a curve whose width is the arithmetic sum of the two initial widths. The second moments of magnetic dipolar interactions add to give the second moment of the composite line.[106] The conditions under which it is possible in practice to measure the second moment accurately are restricted to cases in which the resonance is not so broad that a large proportion of the second moment is contributed by the wings (distant parts) of the absorption curve. These contributions are difficult to evaluate because signal-to-noise ratio for them can be very low.

D. *Summary and Comments*

Nuclear resonance has provided an additional vantage point from which to consider metals. The addition of a new investigative tool to any field is twofold. It stimulates the work necessary to the complete understanding of the new information it yields and, equally important, it supplies an incentive to reconsider the results of older techniques.

Nuclear resonance studies have already improved our understanding of the electronic structure of the alkali metals. They have also given vivid evidence of the local disturbances in the electron density and polarization around imperfections. The method has been applied to the investigation of atomic diffusion, lattice distortion, superconductivity and the study of phase diagrams. Since the nuclear properties rather than the electronic properties of the metal primarily determine whether the nuclear resonance can be

observed in any specific metal, the use of nuclear resonance will always be restricted to special situations, however, within this limitation it has unique and valuable information to offer.

APPENDIX A

This appendix is meant to supplement the discussion given in Section III-A, and to serve as a convenient source of reference for some standard expressions which occur in the basic formulation of resonance absorption theory. Its brevity is a consequence of the general availability of many good introductions [14, 4, 12, 11, 157] to the phenomenon of nuclear resonance. The articles of PAKE [14, 157] are especially recommended as a general introduction although those of POUND [4] and BLOEMBERGEN, PURCELL and POUND [11] stress the approach used below. ANDREW's book [12] includes references to all common experimental techniques.

The transition probability for a nucleus of moment μ and spin I, placed in a strong magnetic field H_0 and a weak monochromatic oscillating magnetic field, $2H_1 \cos 2\pi\nu t$ perpendicular to H_0 is

$$W_{m \to m-1} = \tfrac{1}{4} \gamma^2 H_1^2 \, g(\nu) \, (I + m) \, (I - m + 1) \quad . \quad . \quad \text{(A1)}$$

where m is magnetic quantum number of the initial state, $\gamma = 2\pi\mu/Ih$, h is Planck's constant, and the nucleus is assumed to be one of N_0 other identical nuclei in one cubic centimetre of the metal. Interactions between nuclei will have the effect of broadening the $2I + 1$ energy levels giving rise to an absorption of finite width which is expressed by the shape function $g(\nu)$.

Due to the fact that the populations of the various $2I + 1$ levels are governed by the Boltzmann factor, the equilibrium population N_m of level m exceeds that of the next higher energy level $(m - 1)$ by

$$N_m - N_{m-1} = N_m \frac{\mu H_0}{IkT} \cong \frac{N_0}{(2I + 1)} \frac{\mu H_0}{IkT} = \frac{N_0}{(2I + 1)} \frac{h\nu}{kT} \quad . \quad \text{(A2)}$$

Here the nuclei are in thermal contact with the metal at temperature T°K, $\nu = (\gamma/2\pi)H_0$, and k is the Boltzmann constant. This difference is essential to the existence of resonance absorption because the transition probabilities for induced emission and absorption are the same, and it is only due to the excess number of nuclei in the lower energy state that a net absorption of energy is possible.

As a result of the transition $m \to m - 1$, the net rate at which energy is absorbed per unit volume of sample is

$$P_{a,\, m \to m-1} = \gamma^2 H_1^2 \, N_0 \, (h\nu)^2 \, g(\nu) \, (I + m) \, (I - m + 1)/4 \, (2I + 1) \, kT.$$

One may define an effective Q for this sample in analogy with that of a tuned circuit, as the ratio of 4π times the average energy stored in the sample

to the energy absorbed by it per cycle. The average magnetic density stored in the sample is $H_1^2/4\pi$ giving an inverse Q for the transition of

$$(1/Q)_{m\to m-1} = \gamma^2 \hbar^2 N_0 \nu g(\nu) (I + m) (I - m + 1)/4 (2I + 1) kT.$$

In the absence of electric and higher magnetic multipole interactions, ν is the same for all transitions $m \to m - 1$ and the total inverse Q is

$$(1/Q)_{\text{tot}} = \sum_{m=I}^{-I+1} (1/Q)_{m\to m-1} = \gamma^2 \hbar^2 N_0 \nu g(\nu) I (I + 1)/6 kT. \quad \text{(A3)}$$

The quantity is simply related to the imaginary part of the nuclear magnetic susceptibility χ'' by

$$\chi'' = (1/4\pi Q)_{\text{tot}} = (\pi/2) \chi_0 \nu g(\nu) \quad . \quad . \quad . \quad . \quad \text{(A4)}$$

where $\chi_0 = N_0 \gamma^2 \hbar^2 I (I + 1)/3 kT$ is the static susceptibility of the spin system. The amplitude of the resonance absorption is inversely proportional to the absolute temperature.

In developing his theory of nuclear induction, BLOCH[17] derived the same quantity by another method based on an analysis of the forces on the resultant magnetization of all the nuclear spins when they are placed in the polarizing field H_0 and subjected to a radio-frequency magnetic field as described above. He obtained an expression for the total nuclear magnetic susceptibility $\chi = \chi' + i\chi''$, either component of which can be detected by properly adjusted nuclear induction or bridge equipment. χ'' produces a magnetization which is out of phase with the radio-frequency field inducing the transitions and can thus be shown to be entirely responsible for the absorption of energy by the nuclear spin system. The real component of the susceptibility, χ', is responsible for the component of the nuclear magnetization in phase with the radio-frequency field, and describes the dispersion accompanying the absorption. In the nuclear induction method, these components of magnetization are observed directly by the voltage they induce into a receiving coil which is placed with its axis perpendicular to the plane containing H_0 and the driving field H_1. The functions χ' and χ'' are related by the Kronig–Kramers relations which allow χ' to be calculated from χ'' or *vice-versa*,[158] provided the radio-frequency power is low enough to avoid saturation of the nuclear spin system. The saturation case has been considered by REDFIELD.[107]

These two different approaches to steady-state resonance provide some insight into the processes responsible for the observed macroscopic phenomenon which can be described merely as a susceptibility change in the sample. The analyses and development of electronic circuits used to detect nuclear resonance need be concerned only with the detection of this change as a function of frequency.

Bloch pointed out that if an intense *r–f pulse*, shorter in duration than T_2 is applied to a spin system at equilibrium in H_0, then the macroscopic magnetic moment acquires a non-equilibrium orientation. Immediately

following the pulse the macroscopic moment precesses freely about the applied field H_0, and a transient nuclear induction signal can be observed as a voltage in a pickup coil surrounding the sample. HAHN[13] describes and analyses a related effect called "spin echo" in which spontaneous nuclear induction signals appear after the application of *more than one r–f* pulse. These signals are caused by the constructive interference of precessing macroscopic moment vectors and are used to measure the time during which the nuclei continue to precess in phase with each other. HOLCOMB and NORBERG[120] made extensive application of this technique to the measurement of relaxation times in alkali metals (Section III-C2).

VOL.
9
196

APPENDIX B

The theory of spin lattice relaxation time T_1 in metals has been discussed by HEITLER and TELLER,[159] BLOEMBERGEN,[121] KORRINGA,[68] REDFIELD,[107, 125] OVERHAUSER,[160] PINES,[59] and others.[161] Heitler and Teller first suggested that at low temperatures the conduction electrons bring about the primary energy contact of the nuclear spin system with the lattice; they derived an order of magnitude expression for the time T_1 based on their model.

The dominant relaxation process in metals is one in which the electrons in a metal are pictured as moving about through the lattice and sometimes colliding with the nuclear spins; during this process, both a nucleus and an electron undergo transitions such that their total spin is conserved; that is, their spins flip simultaneously, the nucleus losing energy and the electron gaining it. (Thus the nuclear spin system transfers energy to the electrons; the latter are in excellent contact with the thermal vibrations of the lattice.) Only electrons which are able to take up the difference in energy of these two spin flips $(\gamma_{el} - \gamma)\hbar H_0$, where γ_{el} is the gyromagnetic ratio of the electron, can take part in this process. This they do by changing their translational energy a corresponding amount, a process possible only for those electrons near the surface of the Fermi distribution because of the very small amount of energy involved. The probability of the process is expected to be proportional to kT. Apparently GORTER[68] suggested that a simple relationship should exist between the Knight shift and T_1 because both originate largely in the same nuclear spin–electron spin interaction, the hyperfine interaction. KORRINGA[68] set out to demonstrate this relationship using Bloch wave functions for the electrons, by deriving first the relaxation time and then the energy change which gives rise to the Knight shift. Both of these are given by Korringa in terms of the density of states, the wave functions of the electrons, and the hyperfine interaction constant. His complete expression for the relaxation time includes relaxation effects of non-s electrons, but does not

include electron correlation or exchange, discussions of which may be found in his paper, and in articles by PINES[59] and BLOEMBERGEN.[167] The isotropic Knight shift takes place only *via* the *s*-electrons and, therefore, only the term in the relaxation time arising from these electrons can be related directly to the isotropic Knight shift. We write, following Korringa,

$$\frac{1}{T_1} = \frac{\pi kT}{\hbar}\left[\frac{16\pi}{3}\beta\gamma\hbar V_0 N(E_F)\langle|\psi(0)|^2\rangle_F\right] + [\text{non-}s\text{ magnetic contribution}] \quad . \quad . \quad . \quad \text{(B1)}$$

and then since the relative isotropic Knight shift may be written

$$\frac{\Delta H}{H_r} = \frac{16\pi}{3}\beta^2\langle|\psi(0)|^2\rangle_F V_0\, N(E_F), \quad . \quad . \quad . \quad \text{(B2)}$$

Eqn. (B1) becomes

$$\frac{1}{T_1} = \frac{\pi kT}{\hbar}\left[\frac{\gamma\hbar}{\beta}\frac{\Delta H}{H_r}\right]^2 + [\text{non-}s\text{ contribution}] \quad . \quad . \quad . \quad \text{(B3)}$$

The nomenclature here corresponds to that used in the text. The presence of the second term on the right means that the Korringa relation

$$\frac{1}{T_1} = \frac{\pi kT}{\hbar}\left[\frac{\gamma\hbar}{\beta}\frac{\Delta H}{H_r}\right]^2 = \frac{T}{4{\cdot}765}\left[\frac{\gamma}{2\pi}\frac{\Delta H}{H_r}\right]^2 \quad . \quad . \quad . \quad \text{(B4)}$$

between the Knight shift and the relaxation time is only approximately valid, even for nuclei of spin $\frac{1}{2}$. If the resonance under discussion is of a nucleus of spin $I \geqslant 1$, still another contribution to the relaxation must be considered.[30] This is caused by the interaction between the nuclear quadrupole moment and the gradient of the electric field due to the conduction electrons; that is, for $I \geqslant 1$ we must write

$$\frac{1}{T_1} = \frac{\pi kT}{\hbar}\left[\frac{\gamma\hbar}{\beta}\frac{\Delta H}{H_r}\right]^2 + [\text{non-}s] + [\text{quadrupole contribution}]. \quad \text{(B5)}$$

All three of the terms on the right were included in a calculation by MITCHELL[162] who also used Bloch wave functions. For multivalent metals, where the wave functions are expected to have a large *p*-component, the non-*s* and/or quadrupole terms may measurably decrease the relaxation time calculated using only the contact *s*-part of the hyperfine interaction. Since the hyperfine interaction for an *s*-state is much larger than for non-*s*, and since the quadrupole contribution is generally small, the Korringa relation will be a good approximation even if the wave function at the Fermi level is largely (more than 50 per cent) non-*s*. From the form of Eqn. (B5), it is clear that provided the first term is not much increased by correlation and exchange, the true relaxation time can only be *less* than that due to the contact hyperfine interaction alone, given by the first term; alternate relaxation paths always shorten the relaxation time. Errors in the Korringa relation (B4) due to these paths should always be such as to give too large a relative Knight

shift when the measured T_1 is inserted. This has not always been found to be the case in practice.[120, 59, 111]

If T_1 contributes to the width of a resonance, it is because the lifetime of the nucleus in a given state is limited through interaction with the lattice. The line width contribution is approximately $1/T_1$, and the total line width is a sum of the spin–spin (T_2') and spin–lattice (T_1) contributions

$$\frac{1}{T_2} = \frac{1}{T_2'} + \frac{1}{2T_1} \quad \ldots\ldots\ldots \quad \text{(B6)}$$

where the actual relaxation times must be used if the relation is to hold. In practice the relaxation times are often associated with line widths, so that when special line shapes are associated with T_1 and T_2' broadening, and the whole Eqn. (B6) is made consistent with the definition $T_2 = (1/2)\, g(\nu_{max})$, numerical factors of the order of unity appear as coefficients of $1/T_2'$ and $1/2T_1$. The important point in the present discussion is that the inverse relaxation times are additive and, thus, line widths contributions are additive to a good approximation. A further introduction to the topic can be obtained by consulting Refs. 11 and 120. Often one or the other term in (B6) dominates, so that $T_2 \approx T_1$ or $T_2 \approx T_2'$. (T_2' approaches $2T_1$ as an upper limit, so T_2 never can exceed T_1.) T_2 is related to the line width $\delta\nu$ of a Gaussian curve by $T_2 = 1/\sqrt{(2\pi)}\delta\nu$. If dipolar broadening is the primary cause of this width, then usually $T_2'' = \sqrt{(\pi/2)}T_2$, where T_2'' is defined as $1/\gamma[\overline{\Delta H^2}]^{\frac{1}{2}}$ [see Eqn. (16)]. Here T_2'', the rigid lattice value, has been substituted for T_2'. The latter takes into account the modification of T_2'' due to lattice motion.

T_2 is related to the line width $\delta\nu$ of a Lorentzian by $T_2 = 1/\sqrt{(3)}\pi\delta\nu$. If lifetime broadening is the dominant source of this width, then the width may be used directly to measure T_1 since it is equal to the observed T_2.

Note Added In Proof

Since the article was written, several significant advances have been made. These will so extend the usefulness and understanding of nuclear magnetic resonance studies of metals that their inclusion at this time seems justified. Fortunately some of these developments are discussed at greater length in a review article by A. G. Redfield which will appear in a forthcoming volume containing the papers presented at the 1959 American Society for Metals Seminar in Chicago, Illinois.

The observation of nuclear magnetic resonance in ferromagnetic metals by Gossard and Portis[182] initiated a field of investigation quite divergent from the main stream of contemporary resonance work. An extraordinarily strong resonance was detected in a sample of finely divided face-centred cubic cobalt metal. In zero applied field and room temperature the resonance frequency was 213·1 Mc/s corresponding to a field of 213·4 kilogauss at the sites of the Co^{59} nuclei. The astonishing amplitude of the resonance (about

VOL. 9 1961

5×10^5 times more intense than computed for dipole transitions in the applied *r–f* field) comes about because the bulk of the absorption arises from nuclei in the domain walls where the applied *r–f* field is enhanced through wall motion by a factor of about 10^3 in zero external field[183]. This enhancement is decreased by the application of an external magnetic field, and will, of course, be peculiar to multidomain ferromagnetic particles. Investigation of the temperature[184, 185] and volume[186] dependence of the resonance frequency followed promptly. The former confirmed the applicability of spin wave theory to cobalt, the latter is more difficult to interpret. The zero (external) field nuclear resonance of Fe^{57} in iron was subsequently observed[187, 188] at a frequency of 45·6 Mc/s corresponding to an effective nuclear field of about 330·5 kilogauss. This field has been shown to be *opposed* to the magnetization in a ferromagnetic domain[189] (i.e. its direction is opposite to that of a large external field), and must arise through the contact interaction of the nuclei with *core–s* electrons which have undergone exchange polarization with the 3*d* electrons[190]. This core polarization occurs to some extent in all metals[191] (a fact not recognized at the time the text, especially Section IIIB, was written), and is likely to be the cause of the negative Knight shift[32] of Pt referred to in Section III–B2, and of the negative Knight shift of Mn[176]. Exchange polarization[212] comes about because of the tendency of electrons with parallel spins to avoid each other. In the presence of polarized 3*d* electrons, for example, the *s* wave functions for spin up electrons differ from those for spin down, resulting in a non-zero value for the quantities $|\psi_{ns\uparrow}(0)|^2 - |\psi_{ns\downarrow}(0)|^2$ which determine the effective field at the nucleus via the contact interaction. In the case of Pt^{195} if we adopt this view of the cause of its negative shift, rather than that expressed in the text, and assume that the estimated Knight shift of 1·8 per cent is caused by the conduction *s* electrons, then the core *s–5d* interaction must be responsible for an opposing field of at *least* 5·2 per cent at room temperature and 6·0 per cent at 78°K. This assumes no enhancement of the type reported in the next paragraph. The present profusion of possible shift mechanisms suggests in the interest of clarity we consider reserving the name "Knight shift" to describe that portion of the observed shift $\Delta\nu$ (or ΔH) which can be ascribed to the interaction of the nucleus with the conduction *s* electrons. Unfilled *d* shells and/or bands appear to accompany departures (positive or negative) from the "classical" Knight shift. Their negative contribution might reasonably be called core-induced hyperfine shift, or some such. The foregoing suggestion retains some of the spirit of the original expression[39] relating Knight shift directly to spin susceptibility. Alternatively the Korringa relation might be taken as the primary definition of the Knight shift. We note that at least for many transition metals the distinction between negative and positive shifts is one of degree not kind.

The Knight shifts of scandium and lanthanum[175] when compared with those of vanadium and niobium seem inordinately large. Another indication of this enhancement is found in the relaxation time measurements which

BUTTERWORTH[192] has made on vanadium. He finds a large discrepancy between the measured shift and that computed from the measured relaxation time T_1 using the Korringa relation (Equation 8, Section III–B2). The latter predicts a shift of about the size that Blumberg *et al.*[175] would also find reasonable; however, it is about 2·5 times smaller than that observed experimentally. Apparently the polarization of the charge at the nucleus is being increased by a factor of about 2·5. Butterworth's arguments probably best describe the situation since the Korringa relation should be valid except when there is direct interaction between *conduction* electrons. A resonance survey of the Al^{27} absorption in the rare earth (X) intermetallic compounds XAl_2[193] has given evidence for an exchange interaction between localized *f* electrons and the conduction electrons.

A broad, systematic investigation of the V^{51} resonance in vanadium intermetallic compounds V_3X of the β-wolfram structure[195, 194] revealed a subtle, yet striking correlation between the *temperature dependence* of the vanadium Knight shift, and the superconducting transition temperature T_c of the compound. (Here X was As, Au, Co, Ga, Ge, Ir, Pt, Sb or Si). For example the shifts of V_3Si and V_3Ga have temperature coefficients five times greater than those of other compounds investigated, and also have markedly higher T_c. Arguments involving the characteristics of various interactions discussed in the body of this article led to the association of the temperature-dependent effects in these superconductors with the *s* electrons. The observed correlation exists well above the superconducting region, and is the more interesting because it links T_c with local atomic properties.

Sugawara has made a lengthy study[196] of the temperature dependence (1·4 to 85°K.) and field dependence of the position, width, and T_1 of the Cu^{63} resonance in copper alloys containing very small (<0·2 atomic per cent) concentrations of the iron group metals Ti, Cr, Mn, Fe, Co and Ni. Alloys containing 4·15 at. % Zn and 0·35 at. % Sn were studied for comparison. Of the former group, Cr, Mn, and Fe caused very pronounced increases in the line width with increasing field and decreasing temperature. These width contributions were of the type observed by Owen *et al.*[96], discussed in section III–C5, and Van der Lugt *et al.*[213]. In addition, however, Sugawara noted a shift in the point of zero absorption derivative, in the direction of increased Knight shift, for these three alloys at the lowest temperatures. Blandin and Friedel[197] considered the theory of spin exchange polarization of the conduction electron charge density around transition metal impurities with *non*-bound *d* electrons in copper (more specifically, in "ordinary" metals like the noble metals and Al). They found that these "*virtual*" 3*d* bound states (discussed previously in other connections[198]) can be responsible for a localized magnetization which exceeds the value obtained by Yoshida[100] (using *s–d* exchange only) by roughly a factor of ten. This can bring about complete agreement between theory and experiment in the case of Cu–Mn alloys (cf. Section III–C5) and probably can also explain the observations on Cu–Cr and Cu–Fe. Previously the observed line

VOL. 9 1961

widths could be understood only by taking a value for the *s–d* exchange coupling constant from [127] 2 to [97] 6 times the free atom value.

The discussion in Section III–D1 and –D3b concerning the electric field gradients in metals unfortunately reflects the incomplete understanding which prevailed at that time with regard to the origin of the gradients. The experimental evidence strongly implied a Z/r^3 dependence of the gradient eq upon the excess charge Z of the solute, and distance r from it. A lack of theoretical support for that behaviour led to the vague $\epsilon(Z)$ concept presented in III–D1 as an extension of earlier strain arguments [135, 76]. Additional experimental and theoretical work now provide a clear picture of the origin of these gradients. Experiments by Averbuch *et al.* [199] combined the results of X-ray measurements of mean square lattice strain with the results of nuclear resonance measurements of mean square gradients in lightly cold-worked pure copper. A relationship between the gradients and the averaged components of the deformation tensor of the form $\overline{(\partial^2 V/\partial Z^2)^2} = \alpha^2 \Lambda \overline{(\Delta L/L)^2}$ can be derived, where Λ is a calculable constant, and α is to be determined experimentally. The components of the deformation tensor were assumed to be independent random variables. The contribution of *first* order quadrupole broadening to the second moment of the copper absorption was used to measure $eq = (\partial^2 V/\partial Z^2)$. A maximum of 90 per cent of the nuclei were involved according to an absorption area comparison between the worked and subsequently annealed powder. Presumably the other nuclei were in positions of higher gradient so the value for α may be even somewhat low. The proportionality constant $\alpha \simeq 15 \times 10^{13}$ e.s.u. obtained was then used, together with generally accepted values for the strain in the vicinity of solute atoms, to derive the gradients which would be caused by this mechanism. The values found were much too low to explain the gradients around zinc [30] or any other solute in copper. The experiment thus offered convincing evidence that the lattice strains thought to exist near solute atoms are *not* capable of producing the observed gradients. Simultaneously, a comprehensive study of the resonance of copper in copper-base solid solutions containing the B subgroup elements [177] demonstrated conclusively the close proportionality of q to Z/r^3, and indicated no marked correlation between q and solute size. The latter observation bore out the deductions of Averbuch. The positive conclusion could thus be drawn that the electric field gradients surrounding solute atoms *are* primarily the result of "valence effects," i.e. a charge redistribution, which is *not*, however, of the exponentially screened Coulomb variety. Kohn and Vosko [201] showed that gradients of the required magnitude arise from the redistribution of the conduction electron charge density near solute atoms. The displaced charge overlaps the neighboring nuclei in this case, and the complete definition $eq = (\partial^2 V/\partial Z^2) - (1/3)\nabla^2 V$ is used to compute q. An essential feature of their theory is that at large distances r from a solute atom the electron density behaves approximately as $\cos(2k_F r + \phi)/r^3$, where k_F is the Fermi wave number, and ϕ is a phase. The gradients appearing at the nuclei are significantly enhanced [201] because

of the high charge density near the center of the atom. This effect is more pronounced for the heavier atoms, but even for copper the gradients which would derive from the free electron model (plane waves) are enhanced by a factor of about 25 when the lattice potential is introduced. In the light of the foregoing argument, $\epsilon(Z)$ in Eqn. 21, Section III–D1 may, as a first approximation, be replaced by 0·0236 $Z\, a_0^3 \cos(2k_F r_n + \phi)/r^3_n$. Here r_n is the distance from a solute to the nucleus at the nth lattice site, and λ should be regarded as a numerical factor, characteristic of the matrix, which includes the amplification factor mentioned above. The latter depends primarily upon the wave functions of the solvent. These oscillations in the *total* conduction electron density arise in the same manner as those mentioned in connection with silver alloys in Section III–B6, however, the latter are oscillations in the charge density ρ_F of only those electrons on the Fermi surface. A calculation of the change in relative Knight shift $\Delta K = \Delta(\Delta H/H) = \Delta\rho_F$ does not require the use of Bloch functions, whereas evaluation of the gradients requires a fairly accurate knowledge of the distribution of total charge, especially near the nucleus. These long-range oscillations graphically reflect the *kinetic* aspect of conduction electrons, the moving, colliding, scattering side of their behavior. The range of the oscillations observed is a direct reflection of the sharpness of the Fermi surface.

Advantage has been taken of diffusion narrowing (Section III–C2) in *alloys* to detect rather small changes in the position of the absorption peaks of the constituents. With dipolar broadening, inhomogenous Knight shift, and other sources of line width averaged out it is possible to do position measurements to an accuracy which would otherwise be unattainable. Of course, the properties measured pertain to the elevated temperature state of the metal. This technique has been applied to a study of the Li^7 Knight shift, and motional narrowing, in lithium–magnesium alloys (to 10 atomic per cent magnesium [202]) and to primary solid solutions of aluminium containing zinc and magnesium [203]. In the latter instance the intensity and position of the Al^{27} resonance were investigated as a function of solute concentration, temperature, and applied magnetic field to obtain both Knight shift and quadrupole interaction data. The investigation of the Na^{23} and Rb^{87} absorptions in Na–K and Na–Rb alloys [95] mentioned in Section III-B6 included both the diffusion narrowed solid and liquid regions. An interpretation of the Knight shift *vs.* composition data in terms of scattered waves [93] was attempted for the liquid alloys. The result did not agree quantitatively with experiment although the charge accumulation assumed to occur in the solute "cell" was varied arbitrarily. Daniel's [204] results should be viewed critically in the light of *all* of the data [95]. The strict validity of the theoretical approach used in these calculations is questionable in the case of solid solutions with solute concentrations exceeding about five per cent, and especially so in concentrated *liquid* alloys. For liquid alloys one might reverse the argument and take any agreement with the Friedel theory [93]

VOL.
9
1961

as indicative of a rather well-defined Fermi surface in liquid alloys. The amplitude of the oscillations under discussion is actually proportional to an additional factor $e^{-(\Delta k)r}$ where Δk is the width of the Fermi surface. In solid pure metals at temperatures far below their Fermi temperature $T_F = E_F/k \approx 5 \times 10^4$ °K (k being the Boltzman constant and E_F the Fermi energy for the system) this factor is thought to be negligible. Until now all calculations of the change in Knight shift with alloying caused by the long range oscillations have neglected the effects of multiple scattering, variations in Fermi level and possible changes in the shape of $N(E_F)$ with alloying. These can not be minor effects for concentrated alloys and a simple picture such as that expressed in Section III-B6 may be helpful.

Rimai and Bloembergen[95] also give a theoretical estimate of the relative change in Knight shift for the solute b in dilute solution in a. After removing the braces in their Eqn. 6 the first term is just $(K_{b \text{ in } a}/K_b)$. They use an experimental solute renormalization to approximate the wave function of b in a in the absence of polarization, otherwise their expression employs the same approximation that Daniel[200] used in justifying Knight's rule (Eqn. 13 of Section III-B6) for estimating $K_{b \text{ in } a}$. Here K_b and K_a are the relative Knight shifts of pure b and pure a respectively. Bloembergen also points out that the Korringa relation (Section III-B2) applied to alloys, implies that the conduction electron–nucleus contact interaction contribution to the spin-lattice relaxation time T_1 of constituent x should vary according to $\overline{(T_{1e})_x^{-1}} = (T_{1e})_{x0}^{-1}(\overline{K_x^2}/K_{x0}^2) = (T_{1e})_{x0}^{-1}[(1 + K_{x0}^{-1}\overline{\Delta K_x})^2 + \overline{\delta K_x^2}K_{x0}^{-2}]$. Subscripts $x0$ refer to pure metal x, $\overline{\Delta K_x} = \overline{K_x} - K_{x0}$ is the change in the relative shift (position)of x upon alloying and $\overline{\delta K_x^2}$ is the contact contribution to the second moment of the alloy line about its mean, $\overline{K_x}$. $\overline{\delta K_x^2}$ is brought about by the variation in Knight shift from nucleus to nucleus. In order to satisfactorily account for the observed line widths in Rb rich Na–Rb alloys very long range interactions were suggested. These depend sensitively on the shape of the Fermi surface and can be expected to occur whenever it has rather sharply peaked irregularities. The investigation provides a good example of the general approach used in the determination of phase diagrams, by means of nuclear magnetic resonance. The precision of the method depends largely on the rate of change of Knight shift with composition since one must look either for the "break" in slope in traversing the phase boundary (as with similarly conceived X-ray determinations) or, in a two phase region, one must be able to determine accurately the compositions of the two phases in equilibrium from previously gathered K_x *vs.* c data. Without the latter the integrated intensities are of no use in determining the amounts of each phase present.

Other interesting developments include:

a. A study of the copper resonances in β-brass as a function of composition and heat treatment[205] revealing the degree of lattice perfection attained; b. the observation of the position dependent Knight shifts of nuclei in the region of rapidly changing electronic structure near the surface of extremely

fine particles of metallic tin[206]; c. a comparison of the electronic structures of the liquid and solid states of several metals on the basis of resonance observations in the two states[172]; d. a method of determining activation volume for diffusion by measuring the line width as a function of pressure in the temperature range in which motional narrowing occurs[216]; e. work elucidating spin-lattice relaxation in metals[205], and persuing the application of resonance to the study of superconductors, as summarized by Redfield[209, 210].

Knight shifts published since the body of the article was completed nevertheless appear with Table 1.

REFERENCES

(1) BLOCH, F., HANSEN, W. W. and PACKARD, M.; *Phys. Rev.* 70 (1946) 474.
(2) PURCELL, E. M., TORREY, H. C. and POUND, R. V.; *Phys. Rev.* 69 (1946) 37.
(3) RAMSEY, N. F.; *Nuclear Moments*, John Wiley, New York, 1953.
(4) POUND, R. V.; *Progress in Nuclear Physics*, ed. O. R. Frisch, Pergamon Press, London, 1952, p. 21.
(5) REDFIELD, A. G.; *Rev. Sci. Instrum.* 27 (1956) 230.
(6) ROWLAND, T. J.; not previously published.
(7) RAMSEY, N. F.; *Phys. Rev.* 78 (1950) 699; 86 (1952) 243.
(8) ORGEL, L. E.; *Mol. Phys.* 1 (1958) 322.
(9) DICKINSON, W. C.; *Phys. Rev.* 81 (1951) 717.
(10) PURCELL, E. M.; *Science* 118 (1953) 431.
(11) BLOEMBERGEN, N., PURCELL, E. M. and POUND, R. V.; *Phys. Rev.* 73 (1948) 679.
(12) ANDREW, E. R.; *Nuclear Magnetic Resonance*, Cambridge University Press, 1955.
(13) HAHN, E. L.; *Phys. Rev.* 80 (1950) 580.
(14) PAKE, G. E.; *Solid State Physics*, Vol. 2, ed. Seitz and Turnbull, Academic Press, New York, 1956, p. 1.
(15) BLOEMBERGEN, N.; *Physica* 15 (1949) 386.
(16) BLOEMBERGEN, N., PURCELL, E. M. and POUND, R. V.; *Nature, Lond.* 160 (1947) 475.
(17) BLOCH, F.; *Phys. Rev.* 70 (1946) 460.
(18) LAMB, W. E.; *Phys. Rev.* 60 (1941) 817.
(19) KNIGHT, W. D.; *Solid State Physics*, Vol. 2, ed. Seitz and Turnbull, Academic Press, New York, 1956, p. 93.
(20) KNIGHT, W. D.; *Phys. Rev.* 92 (1953) 539.
(21) GUTOWSKY, H. S. and MCGARVEY, B. R.; *J Chem. Phys.* 20 (1952) 1472.
(22) WEAVER, H. E., JR.; *Phys. Rev.* 89 (1953) 923.
(23) WALCHLI, H. E. and MORGAN, H. W.; *Phys. Rev.* 87 (1952) 541.
(24) KNIGHT, W. D.; *Phys. Rev.* 85 (1952) 762.
(25) SOGO, P. B. and JEFFRIES, C. D.; *Phys. Rev.* 98 (1955) 1316.
(26) SOGO, P. B. and JEFFRIES, C. D.; *Phys. Rev.* 93 (1954) 174.
(27) RUDERMAN, M. A. and KITTEL, C.; *Phys. Rev.* 96 (1954) 99.
(28) ROWLAND, T. J.; *Phys. Rev.* 103 (1956) 1670.
(29) MASUDA, Y.; *J. Phys. Soc. Jap.* 12 (1957) 523.
(30) BLOEMBERGEN, N. and ROWLAND, T. J.; *Acta Met.* 1 (1953) 731.

(51) LOELIGER, H. R. and SARLES, L. R.; *Phys. Rev.* 95 (1954) 291.
(52) ROWLAND, T. J.; *J. Phys. Chem. Solids* 7 (1958) 95.
(53) REIF, F.; *Phys. Rev.* 102 (1956) 1417; 106 (1957) 208.
(54) BLOEMBERGEN, N. and ROWLAND, T. J.; *Phys. Rev.* 97 (1955) 1679.
(55) PIETTE, L. H. and WEAVER, H. E.; *J. Chem. Phys.* 28 (1958) 735.
(56) KNIGHT, W. D., HEWITT, R. R. and POMERANTZ, M.; *Phys. Rev.* 104 (1956) 271.
(57) POUND, R. V.; *Phys. Rev.* 73 (1948) 1112.
(58) KNIGHT, W. D.; *Phys. Rev.* 76 (1949) 1259.
(59) TOWNES, C. H., HERRING, C. and KNIGHT, W. D.; *Phys. Rev.* 77 (1950) 852.
(60) KOPFERMANN, H.; *Nuclear Moments*, Academic Press, New York, 1958, p. 123ff. were used to estimate P_F.
(61) FERMI, E.; *Z. Phys.* 60 (1930) 320.
(62) PAULI, W.; *Z. Phys.* 41 (1927) 81.
(63) POULIS, N. J.; *Physica* 16 (1950) 373.
(64) KOHN, W. and BLOEMBERGEN, N.; *Phys. Rev.* 80 (1950) 913; 82 (1951) 283.
(65) LANDAU, L.; *Z. Phys.* 64 (1930) 629.
(66) MEYERS, W. R.; *Rev. Mod. Phys.* 24 (1952) 15, 178.
(67) SCHUMACHER, R. T., CARVER, T. R. and SLICHTER, C. P.; *Phys. Rev.* 95 (1954) 1089.
(68) KOHN, W.; *Phys. Rev.* 96 (1954) 590.
(69) SCHUMACHER, R. T. and SLICHTER, C. P.; *Phys. Rev.* 101 (1956) 58, and (211).
(70) KJELDASS, T., JR. and KOHN, W.; *Phys. Rev.* 101 (1956) 66.
(71) FEHER, G. and KIP, A. F.; *Phys. Rev.* 95 (1954) 1343.
(72) FEHER, G. and KIP, A. F.; *Phys. Rev.* 98 (1955) 337.
(73) SOMMERFELD, A.; *Z. Phys.* 47 (1928) 1.
(74) GORTER, G. J., ed.; *Progress in Low Temperature Physics*, Chapter II, Interscience, New York, 1955.
(75) GUTOWSKY, H. S.; *Phys. Rev.* 83 (1951) 1073.
(76) MCGARVEY, B. R. and GUTOWSKY, H. S.; *J. Chem. Phys.* 21 (1953) 2114.
(77) BENEDEK, G. B., BLOEMBERGEN, N. and KUSHIDA, T.; *Bull. Amer. Phys. Soc.*, Ser. II, 1 (1956) 124.
(77a) KNIGHT, W. D.; *Phys. Rev.* 96 (1954) 861.
(78) BENEDEK, G. B. and KUSHIDA, T.; *J. Phys. Chem. Solids* 5 (1958) 241.
(79) PINES, D.; *Solid State Physics* 1 (1955) 367, see especially part on Knight shift, p. 420ff. A correction of equation (9.14) is given by BENEDEK (Reference 58).
(80) Unpublished calculations of H. Brooks, the results of which appear in Reference 58.
(81) BLOEMBERGEN, N.; private communication, and Ref. 167.
(82) KNIGHT, W. D., ANDROES, G. M. and HAMMOND, R. H.; *Phys. Rev.* 104 (1956) 852, See also Ref. 206.
(83) BIONDI, M. A., FORRESTER, A. T., GARFUNKEL, M. P. and SATTERTHWAITE, C. B.; *Rev. Mod. Phys.* 30 (1958) 1109.
(84) BARDEEN, J., COOPER, L. N. and SCHRIEFFER, J. R.; *Phys. Rev.* 108 (1957) 1175.
(85) YOSIDA, K.; *Phys. Rev.* 110 (1958) 769.
(99) HEBEL, L. C. and SLICHTER, C. P.; *Phys. Rev.* 107 (1957) 901; *ibid.* 113(1959) 1504.
(88a) HEINE, V. and PIPPARD, A. B.; *Phil. Mag.* 3 (1958) 1046, and REDFIELD. (209)
(87) MORSE, R. W. and BOHM, H. V.; *Phys. Rev.* 108 (1957) 1094.
(88) KORRINGA, J.; *Physica* 16 (1950) 601.
(89) HOARE, F. E. and MATTHEWS, J. C.; *Proc. Roy. Soc.* A212 (1952) 137.
(70) OLSEN, L. O., SMITH, C. S. and CRITTENDEN, E. C.; *J. Appl. Phys.* 16 (1945) 425.
(71) LOCK, J. M.; *Proc. Roy. Soc.* A208 (1951) 391.
(72) DRAIN, L. E.; *Phil. Mag.* 4 (1959) 484.
(73) POUND, R. V.; *Phys. Rev.* 79 (1950) 685.

[74] COHEN, M. and REIF, F.; *Solid State Physics*, Vol. 5, ed. Seitz and Turnbull, Academic Press, New York, 1957, p. 321.
[75] FELD, B. and LAMB, W. E.; *Phys. Rev.* 67 (1945) 15.
[76] BLOEMBERGEN, N.; *Defects in Crystalline Solids, Bristol Conference* 1954, Physical Society, London, 1955, p. 1.
[77] POMERANTZ, M.; *Thesis*, University of California, 1958 (unpublished), see [207].
[78] DAS, M. P. and BERSOHN, R.; *Phys. Rev.* 102 (1956) 733. This paper also contains references to the series of papers by Sternheimer in which shielding is discussed.
[79] VOLKOFF, G. M.; *Canad. J. Phys.* 31 (1953) 820.
[80] This computation was carried out by Dr. J. Ford in 1958.
[81] DAS, T. P. and HAHN, E. L.; *Nuclear Quadrupole Resonance Spectroscopy*, Academic Press, New York, 1958.
[82] KUSHIDA, T. and BENEDEK, G. B.; *Bull. Amer. Phys. Soc.*, Ser. II, 3 (1958) 167.
[83] TOWNES, C. H. and SCHAWLOW, A. L.; *Microwave Spectroscopy*, McGraw-Hill, New York, 1955. Table 9-8.
[84] HAMMOND, R. H. and KNIGHT, W. D.; *Phys. Ref.* 120 (1960) 762.
[85] MOTT, N. F. and JONES, H.; *Properties of Metals and Alloys*, Oxford University Press, 1936.
[86] TEETERS, D. R. and KNIGHT, W. D.; *Phys. Rev.* 96 (1954) 861.
[87] FRIEDEL, J.; *J. phys. radium* 16 (1955) 444.
[88] MOTT, N. F.; *Progress in Metal Physics*, New York: Interscience Publishers, 1952, Vol. 3, p. 98.
[89] FRIEDEL, J.; *Phil. Mag.* 43 (1952) 153; *Advanc. Phys.* 3 (1954) 446.
[90] ROWLAND, T. J.; to be published.
[91] Private communication to N. BLOEMBERGEN, reference 76, p. 6.
[92] BLANDIN, A., DANIEL, E. and FRIEDEL, J.; *Phil. Mag.* 4 (1959) 180.
[93] BLANDIN, A. and DANIEL, E.; *J. Phys. Chem. Solids*; 10 (1959) 126.
[94] COHEN, M. H. and HEINE, V.; *Advanc. Phys.* 7 (1958) 395.
[95] RIMAI, L. and BLOEMBERGEN, N.; *J. Phys. Chem. Solids* 13 (1960) 257.
[96] OWEN, J., BROWNE, M., KNIGHT, W. D. and KITTEL, C.; *Phys. Rev.* 102 (1956) 1501.
[97] CHAPMAN, A. C. and SEYMOUR, E. F. W.; *Proc. Phys. Soc.* 72 (1958) 797.
[98] FROHLICH, F. and NABARRO, F. R. N.; *Proc. Roy. Soc.* (London) A175 (1940) 382.
[99] ZENER, C.; *Phys. Rev.* 87 (1951) 440.
[100] YOSIDA, K.; *Phys. Rev.* 106 (1957) 893.
[101] WEINBERG, D. and BLOEMBERGEN, N.; *J. Phys. Chem. Solids* 15 (1960) 240.
[102] ROWLAND, T. J.; "Nuclear Magnetic Resonance in Metals and Alloys", *Thesis*, Harvard University, 1954 (unpublished).
[103] SHULMAN, R. G., MAYS, J. M. and MCCALL, D. W.; *Phys. Rev.* 100 (1955) 692; SHULMAN, R. G., WYLUDA, B. J. and HROSTOWSKI, H. J.; *Phys. Rev.* 109 (1958) 808.
[104] SHULMAN, R. G., WYLUDA, B. J. and MATTHIAS, B. T.; *Phys. Rev. Letters* 1 (1958) 278.
[105] SEITZ, F.; *Imperfections in Nearly Perfect Crystals*, ed. Shockley, New York: John Wiley, 1952.
[106] VAN VLECK, J. H.; *Phys. Rev.* 74 (1948) 1168.
[107] REDFIELD, A. G.; *Phys. Rev.* 98 (1955) 1787.
[108] BLOEMBERGEN, N.; *Nuclear Magnetic Relaxation*, Martinus Nijhoff, The Hague, 1948.
[109] KUBO, R. and TOMITA, K.; *J. Phys. Soc. Jap.* 9 (1954) 888. Note that their T_2' is defined in terms of a half width at half power.
[110] NACHTRIEB, N. H., CATALANO, E. and WEIL, J. A.; *J. Chem. Phys.* 20 (1952) 1185.
[111] SPOKAS, J. J. and SLICHTER, C. P.; *Phys. Rev.* 113 (1959) 1462.
[112] SEYMOUR, E. F. W.; *Proc. Phys. Soc. Lond.* A66 (1953) 85.

VOL.
9
1961

(113) MASUDA, Y.; *J. Phys. Soc. Jap.* 13 (1958) 597.
(114) NORBERG, R. E.; *Phys. Rev.* 86 (1952) 745.
(115) NORBERG, R. E.; *Thesis*, University of Illinois (1951) (unpublished).
(116) GARSTENS, M. A.; *Phys. Rev.* 79 (1950) 397; 81 (1951) 288.
(117) SUKENIK, H. J.; private communication through W. D. Knight.
(118) SLICHTER, C. P.; *Defects in Crystalline Solids, Bristol Conference* 1954, Physical Society, London, 1955, p. 52.
(119) NORBERG, R. E. and SLICHTER, C. P.; *Phys. Rev.* 83 (1951) 1074.
(120) HOLCOMB, D. F. and NORBERG, R. E.; *Phys. Rev.* 98 (1955) 1074.
(121) BLOEMBERGEN, N.; *Physica* 15 (1949) 588.
(122) REDFIELD, A. G.; *Phys. Rev.* 101 (1956) 67.
(123) ANDERSON, A. G. and REDFIELD, A. G.; *Proceedings of the International Conference on Low Temperature Physics*, Madison, Wisconsin, August 1957.
(124) TORREY, H. C.; *Phys. Rev.* 92 (1953) 962; 96 (1954) 690.
(125) REDFIELD, A. G.; *IBM Journal* 1 (1957) 19.
(126) KNIGHT, W. D. and KITTEL, C.; *Phys. Rev.* 86 (1952) 573.
(127) BEHRINGER, R. E.; *J. Chem. Phys. Solids* 2 (1957) 209.
(128) OWEN, J., BROWNE, M., ARP, V. and KIP, A. F.; *J. Chem. Phys. Solids* 2 (1957) 58.
(129) WATKINS, G. D. and POUND, R. V.; *Phys. Rev.* 89 (1953) 658.
(130) POUND, R. V.; *J. Phys. Chem.* 57 (1953) 743.
(131) ESHELBY, J. D.; *Solid State Physics*, Vol. 3, ed. Seitz and Turnbull, Academic Press, New York, 1956, p. 79.
(132) BARRETT, C. S.; *Structure of Metals and Alloys*, McGraw-Hill, New York, 1952, p. 221.
(133) WATKINS, G. D.; *Thesis*, Harvard University, 1952 (unpublished).
(134) COTTRELL, A. H., HUNTER, S. C. and NABARRO, F. R. N.; *Phil. Mag.* 44 (1953) 1064.
(135) ROWLAND, T. J.; *Acta Met.* 3 (1955) 74.
(136) OWEN, E. A.; *J. Inst. Metals* 73 (1947) 471.
(137) COLES, B. R.; *J. Inst. Metals* 84 (1956) 346.
(138) RAYNOR, G. V.; *Trans. Faraday Soc.* 45 (1949) 698.
(139) HUME-ROTHERY, W. and RAYNOR, G. V.; *The Structure of Metals and Alloys*, The Institute of Metals, London, 1954, p. 162.
(140) SHULMAN, R. G., WYLUDA, B. J. and ANDERSON, P. W.; *Phys. Rev.* 107 (1957) 953.
(141) MENES, M. and BOLEF, D. I.; *Phys. Rev.* 109 (1958) 218.
(142) RHODERICK, E. H.; *Phil. Mag.* 3 (1958) 545; COHEN, M., *loc. cit.*, p. 564.
(143) KAMBE, K. and OLLOM, J. F.; *J. Phys. Soc. Jap.* 11 (1956) 50.
(144) ANDERSON, A. G.; *Phys. Rev.* 115 (1959) 863.
(145) BLIN-STOYLE, R. J.; *Theories of Nuclear Moments*, Oxford University Press, London, 1957; also *Rev. Mod. Phys.* 28 (1956) 75.
(146) GRIVET, P. ed.; *La Resonance Paramagnetique Nucleaire*, Centre National de la Recherche Scientifique, Paris, 1955.
(147) POUND, R. V. and KNIGHT, W. D.; *Rev. Sci. Inst.* 21 (1950) 219.
(148) BURGESS, J. H. and BROWN, R. M.; *Rev. Sci. Inst.* 23 (1952) 334.
(149) ANDREW, E. R.; *Phys. Rev.* 91 (1953) 425; HALBACH, K. *ibid.* 119 (1960) 1230
(150) BLOEMBERGEN, N.; *J. Appl. Phys.* 23 (1952) 1383.
(151) CHAPMAN, A. C., RHODES, P. and SEYMOUR, E. F. W.; *Proc. Phys. Soc.* B70 (1947) 345.
(152) GRISWOLD, T. W., KIP, A. and KITTEL, C.; *Phys. Rev.* 88 (1952) 951.
(153) LEVY, R. A.; *Phys. Rev.* 102 (1956) 31.
(154) OVERHAUSER, A. W.; *Phys. Rev.* 92 (1953) 411; the "Overhauser effect" is reviewed in Reference 14.
(155) CARVER, T. R. and SLICHTER, C. P.; *Phys. Rev.* 92 (1953) 212; 102 (1956) 975.

(156) PAKE, G. E.; *J. Chem. Phys.* 16 (1948) 327.
(157) PAKE, G. E.; *Am. J. Phys.* 18 (1950) 438, 473.
(158) PAKE, G. E. and PURCELL, E. M.; *Phys. Rev.* 74 (1948) 1184.
(159) HEITLER, W. and TELLER, E.; *Proc. Roy. Soc.* A155 (1936) 629.
(160) OVERHAUSER, A. W.; *Phys. Rev.* 89 (1953) 689.
(161) PINES, D. and SLICHTER, C. P.; *Phys. Rev.* 100 (1955) 1014.
(162) MITCHELL, A. H.; *J. Chem. Phys.* 26 (1957) 1714.
(163) SEYBOLT, A. U. and BURKE, J. E.; *Procedures in Experimental Metallurgy*, John Wiley, New York, 1953, Chapter 10.
(164) JONES, H.; *Proc. Roy. Soc.* A144 (1934) 255.
(165) PAULING, L.; *J. Am. Chem. Soc.* 49 (1927) 765.
(166) Reference 139, p. 87ff.
(167) BLOEMBERGEN, N.; *Can. J. Phys.* 34 (1956) 1299.
(168) FLYNN, C. P. and SEYMOUR, E. F. W.; *Proc. Phys. Soc.* 76 (1960) 301
(169) BENNETT, L. H. and BUDNICK, J. I.; *J Phys. Chem. Solids* 16 (1960) 37.
(170) FLYNN, C. P. and SEYMOUR, E. F. W.; *Proc. Phys. Soc.* 73 (1959) 945.
(170) AKSENOV, S. I.; *Soviet Phys.* JETP 8 (1959) 207.
(172) KNIGHT, W. D., BERGER, A. G. and HEINE, V.; *Ann. Phys.* 8 (1959) 173.
(173) HEWITT, R. R. and KNIGHT, W. D.; *Phys. Rev. Letters* 3 (1959) 18.
(174) GAGER, W. B. and MILFORD, F. J.; *Phys. Rev.* 121 (1961) 716.
(175) BLUMBERG, W. E., EISINGER, J., JACCARINO, V., and MATTHIAS, B. T.; *Phys. Rev. Letters* 5 (1960) 52.
(176) JACCARINO, V., PETER, M. and WERNICK, J. H.; *Phys. Rev. Letters* 5 (1960) 53.
(177) ROWLAND, T. J.; *Phys. Rev.* 119 (1960) 900.
(178) KLEIN, M. P. and ABELL, D. F.; *Bull. Am. Phys. Soc.* 5 (1960) 74.
(179) BLUMBERG, W. E. and EISINGER, J.; *Phys. Rev.* 120 (1960) 1965.
(180) LURIO, A.; *Bull. Am. Phys. Soc.* 4 (1959) 419.
(181) W. D. Knight has considerately informed the author that this statement is incorrect. A subsequent recalculation by M. Pomerantz gave only "about 2·5 Mc/s for the ions against about 11 Mc/s experimental. This lends more support to the idea that covalent bonds contribute appreciably."
(182) GOSSARD, A. C. and PORTIS, A. M.; *Phys. Rev. Letters* 3 (1959) 164.
(183) PORTIS, A. M. and GOSSARD, A. C.; *J. Appl. Phys.* 31 (1960) 205S.
(184) JACCARINO, V.; *Bull. Am. Phys. Soc.* 4 (1959) 461.
(185) KOI, Y., TSUJIMURA, A. and YUKIMOTO, Y.; *J. Phys. Soc. Japan* 15 (1960) 1342.
(186) JONES, R. V. and KAMINOW, I. P.; *Bull. Am. Phys. Soc.* 5 (1960) 175.
(187) GOSSARD, A. C., PORTIS, A. M., and SANDLE, W. J.; *J. Phys. Chem. Solids*, to be published.
(188) ROBERT, C. and WINTER, J–M.; *Compt. rend.* 250 (1960) 3831.
(189) HANNA, S. S., HEBERLE, J., PERLOW, G. J., PRESTON, R. S., and VINCENT, D. H.; *Phys. Rev. Letters* 4 (1960) 513.
(190) GOODINGS, D. A., and HEINE, V.; *Phys. Rev. Letters* 5 (1960) 370.
(191) COHEN, M. H., GOODINGS, D. A. and HEINE, V.; *Proc. Phys. Soc.* 73 (1959) 811.
(192) BUTTERWORTH, J.; *Phys. Rev. Letters* 5 (1960) 305.
(193) JACCARINO, V., MATTHIAS, B. T., PETER, M., SUHL, H. and WERNICK, J. H.; *Phys. Rev. Letters* 5 (1960) 251.
(194) CLOGSTON, A. M. and JACCARINO, V.; *Phys. Rev.*, to be published
(195) BLUMBERG, W. E., EISINGER, J., JACCARINO, V. and MATTHIAS, B. T.; *Phys. Rev. Letters* 5 (1960) 149.
(196) SUGAWARA, T.; *J. Phys. Soc. Japan* 14 (1959) 643, also see Ref. 101.
(197) BLANDIN, A. and FRIEDEL, J.; *J. phys. radium* 20 (1959) 160.
(198) FRIEDEL, J.; *Can. J. Phys.* 34 (1956) 1190.
(199) AVERBUCH, P., DEBERGEVIN, F. and MÜLLER-WARMUTH, W.; *Compt. rend.* 249 (1959) 2315. Also see Falkner, E. A.; Phil. Mag. 5 (1960) 843.

VOL.
9
196

[200] DANIEL, E.; *J. Phys. Chem. Solids* 10 (1959) 174.
[201] KOHN, W. and VOSKO, S. H.; *Phys. Rev.* 119 (1960) 912.
[202] HUGHES, D. G.; *Phil. Mag.* 5 (1960) 467.
[203] WEBB, M. B.; *J. Phys. Chem. Solids*, to be published.
[204] DANIEL, E.; *J. Phys. Chem. Solids* 13 (1960) 353.
[205] WEST, G. W.; *Phil. Mag.* 5 (1960) 899.
[206] ANDROES, G. M. and KNIGHT, W. D.; *Phys. Rev.* 121 (1961) 779.
[207] POMERANTZ, M. and DAS, T. P.; *Phys. Rev.* 119 (1960) 70; LURIO, A. and BLACHMAN, A. G.; *Bull. Am. Phys. Soc.* 5 (1960) 344.
[208] ANDERSON, A. G. and REDFIELD, A. G.; *Phys. Rev.* 116 (1959) 583.
[209] REDFIELD, A. G.; *Nuclear Magnetic Resonance in Metals* to be published in a forthcoming volume of the ASM Seminar series.
[210] MASUDA, Y. and REDFIELD, A.; *Bull. Am. Phys. Soc.* 5 (1960) 176.
[211] SCHUMACHER, R. T. and VEHSE, W. E.; *Bull. Am. Phys. Soc.* 5 (1960) 296.
[212] HEINE, V.; *Phys.Rev.* 107 (1957) 1002.
[213] VAN DER LUGT, W., POULIS, N. J. and HASS, W. P. A.; *Physica* 25 (1959) 97.
[214] JONES, W. H., Jr., GRAHAM, T. P. and BARNES, R. G.; *Acta Met.* 8 (1960) 663.
[215] See the NOTE ADDED IN PROOF; this presumably remains a valid use of the Korringa relation however.
[216] BARNES, R. G., ENGARDT, R. D. and HULTSCH, R. A.; *Phys. Rev. Letters* 2 (1959) 202.
[217] KLEIN, M. P.; using his measured $\nu(W^{183})/\nu(F^{19})$ together with $\nu(W^{183})/\nu(D)$ from Ref. 25; private communication.

VOL
9
196

PROGRESS IN MATERIALS SCIENCE VOLUME 9
(INCORPORATING PROGRESS IN METAL PHYSICS)
GENERAL EDITOR: BRUCE CHALMERS

VOL.
9
1961

The Effect of Temperature and Alloying Additions on the Deformation of Metal Crystals

by
R. W. K. HONEYCOMBE
Department of Metallurgy, University of Sheffield, England

PERGAMON PRESS
OXFORD · LONDON · NEW YORK · PARIS

D

PERGAMON PRESS LTD.
Headington Hill Hall, Oxford
4 & 5 *Fitzroy Square, London, W.1*

PERGAMON PRESS INC.
122 *East 55th Street, New York* 22, *N.Y.*
Statler Center 640, 900 *Wilshire Boulevard,*
Los Angeles, California

PERGAMON PRESS S.A.R.L.
24 *Rue des Écoles, Paris V^e^*

PERGAMON PRESS G.m.b.H.
Kaiserstrasse 75, *Frankfurt-am-Main*

VOL
9
196

Copyright
©
1961
PERGAMON PRESS LTD.

Library of Congress Card Number 49—50107

Set in Times New Roman 10/12pt. and
made and printed in Great Britain at Page Bros. (Norwich) Ltd.

PROGRESS IN MATERIALS SCIENCE

(INCORPORATING PROGRESS IN METAL PHYSICS)

PUBLISHER'S NOTE

THE twelve years that have elapsed since the publication of the first volume of PROGRESS IN METAL PHYSICS has seen a great increase in the rate of publication of papers in this, as in most other fields of science, and realization that the physics of metals is an important part of, but not the whole of, the science of materials, a field of considerable practical and theoretical importance.

It is becoming extremely difficult, if it is not already impossible, for most scientists to keep up-to-date in their own and closely related fields by reading all the relevant original papers; one approach to the solution of this problem is the provision of adequate up-to-date critical review articles. For these reasons the Editor and the Publisher of PROGRESS IN METAL PHYSICS have decided to broaden the subject matter to include the whole of the field of the Science of Materials, and, in order to ensure maximum availability, to publish each article as a separate entity; thus, an individual subscriber need no longer purchase a whole volume in order to obtain some of the articles. This new procedure will make it possible to publish each article within five months of its receipt by the Editor.

VOL.
9
1961

VOL
9
196

THE EFFECT OF TEMPERATURE AND ALLOYING ADDITIONS ON THE DEFORMATION OF METAL CRYSTALS

Contents

		Page
1.	Introduction	95
2.	The Critical Resolved Shear Stress for Glide	96
3.	The Effect of Temperature on the Critical Shear Stress	97
	3.1 Face-centred cubic metals	97
	3.2 Close-packed hexagonal metals	99
	3.3 Body-centred cubic metals	100
4.	Effect of Elements in Solid Solution on the Critical Shear Stress	101
	4.1 Face-centred cubic metals	101
	4.2 Close-packed hexagonal metals	104
5.	Effect of Temperature on τ_0 for Alloy Crystals	105
6.	Interpretation of Experimental Results on the Critical Shear Stress	106
	6.1 Pure metals	106
	6.2 Solid solution alloys	108
7.	The Temperature Dependence of Stress–Strain Curves of Metal Crystals	
	7.1 Face-centred cubic metals	111
	7.1.1 Aluminium	114
	7.1.2 Lead	114
	7.1.3 Copper	114
	7.1.4 Nickel	115
	7.2 Hexagonal metals	116
	7.2.1 Magnesium	116
	7.2.2 Zinc	118
	7.2.3 Cadmium	118
	7.2.4 Titanium, Rhenium	119
8.	Variation of Slip Markings with Temperature	119
	8.1 Face-centred cubic metals	119
	8.2 Hexagonal metals	120
	8.3 Body-centred cubic metals	121
9.	Theoretical Interpretation of Stress–Strain Curves	121
10.	Effect of Alloying on the Stress–Strain Curve	123
11.	The Deformation of Two-phase Alloy Crystals	125
	References	
	Bibliography	127

VOL.
9
1961

THE EFFECT OF TEMPERATURE AND ALLOYING ADDITIONS ON THE DEFORMATION OF METAL CRYSTALS

R. W. K. Honeycombe

OL.
9
961

1. Introduction

In the last decade much progress has been made in understanding the plastic deformation of metals in terms of dislocation movement and interactions. Dislocation theory has now developed to the stage where the behaviour of different groups of metals can be compared, and detailed reasons advanced for differences in behaviour within one group, e.g. face-centred cubic metals. A recent survey by Seeger [1] deals very fully with the deformation of face-centred cubic and close-packed hexagonal metals, bringing out clearly the important role of stacking faults which must be taken into account in examining the behaviour of individual metals.

From time to time in this series, reviews of the current state of dislocation theories have been given, and experimental results on the plastic deformation of crystals of various metals described.* In recent years increasing attention has been paid to the temperature dependence of deformation behaviour of single crystals, and it now seems that the time is ripe for a survey of the results. At a time when the behaviour of pure metal crystals is being rapidly organized into a coherent picture, more interest is being shown in the effects of alloying elements on deformation. Experiments with increasingly pure metals have underlined the significant role of small traces of chance impurities, while the effects of deliberate alloying additions on the deformation behaviour of metal crystals are now being more widely studied.

The emphasis in this review will be on the relevant experimental results of the last decade but earlier work will be referred to when necessary to complete the picture. An effort will be made to relate these results to current theoretical concepts where possible. In the first part of the review, the influence of temperature and alloying elements on the stress to initiate plastic flow will be summarized, then subsequently the effect of these variables on the stress–strain curves will be outlined.

* The most recent survey is by Clarebrough and Hargreaves in *Progress in Metal Physics*, Volume 8.

2. The Critical Resolved Shear Stress for Glide (τ_0)

The law of constant critical shear stress was put forward by Schmid [2] many years ago on the basis of work with hexagonal metal crystals, when it was thought that the critical resolved shear stress τ_0 was orientation independent. Opinion is now divided on this subject partly because of the difficulties inherent in the accurate measurement of τ_0. Firstly, it is often very difficult to determine when plastic flow commences, and secondly τ_0 is very structure sensitive being markedly affected by small traces of impurities, or dislocation arrays introduced during handling of the crystals. In the case of the familiar hexagonal metals it seems likely that τ_0 is constant when basal glide is

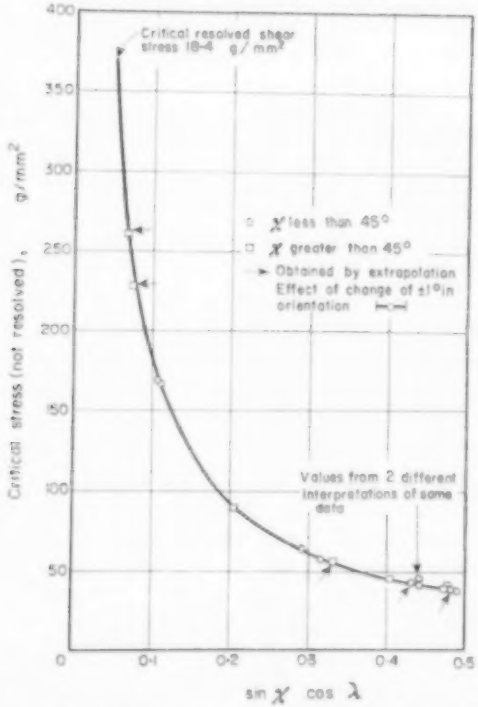

Fig. 1. Critical resolved shear stress of zinc at room temperature. The curve represents the variation of critical stress with orientation taking $\tau_0 = 18{\cdot}4$ g/mm.² (Jillson[66]).

predominant. For example, Jillson [66] deformed extremely pure zinc (99·999 per cent +) crystals at room temperature and found highly consistent values for τ_0 averaging 18·4 g/mm.² The close agreement of the experimental results with the theoretical curve is shown in Fig. 1. In some recent work on nickel crystals, Haasen [3] expresses the opinion that τ_0 at a given temperature is independent of orientation although some experimental scatter is observed. On the other hand, Andrade and Aboav, [4] and Diehl [5]

investigating single crystals of copper found that τ_0 was lower for orientations towards the centre of the stereographic triangle. It is unlikely that this problem will be easily resolved at present because of inevitable variations in the quality and surface condition of crystals, and in the testing techniques.

3. The Effect of Temperature on the Critical Shear Stress

Two approaches have been made to the experimental determination of the temperature dependence of the flow stress necessary to cause plastic deformation. Firstly, the resolved shear stress for the onset of slip can be determined for a number of differently oriented crystals over a wide temperature range. Secondly, the one crystal has been tested at different temperatures by deforming it first at one temperature, altering the temperature and determining the new flow-stress. This method is very suitable for finding the temperature dependence of the flow stress after substantial deformation;* its extrapolation to small strains is possible but not always justified.

3.1 *Face-centred Cubic Metals*

Andrade and Henderson[8] investigated the deformation of gold, silver and nickel crystals over a large temperature range and measured τ_0 (Table 1) taking as their value the point at which the slope of the shear stress–shear strain curve first rapidly diminishes. Some results for silver were anomalous because of the suspected presence of an oxide film in tests at elevated temperatures, but the values at 93°K, 193°K and 290°K are probably reliable.

TABLE 1

Temperature Dependence of τ_0 for Gold and Silver Single Crystals[8]

Temperature °K	τ_0 g/mm²	
	Au 10 *p.p.m. impurity*	Ag 10 *p.p.m. impurity*
93	59	55
193	48	52
290	50	37·5
603	37·5	—
687	27·5	—

The sensitivity of τ_0 to small traces of impurity is shown in the comparison of Andrade and Henderson's results for nickel with those of Haasen.[3]

Garstone and Honeycombe[9] have determined τ_0 for pure copper (99·98 per cent) over the temperature range 78°K–290°K (Fig. 2) for which it varied from 105 g/mm² to 50 g/mm.² Andrade and Aboav,[4] on the other hand, found no systematic variation over the range 78°K to 620°K, which may be a result of non-metallic impurities as their τ_0 at room tempera-

* For this reason, results obtained by this method are dealt with in Section 7.

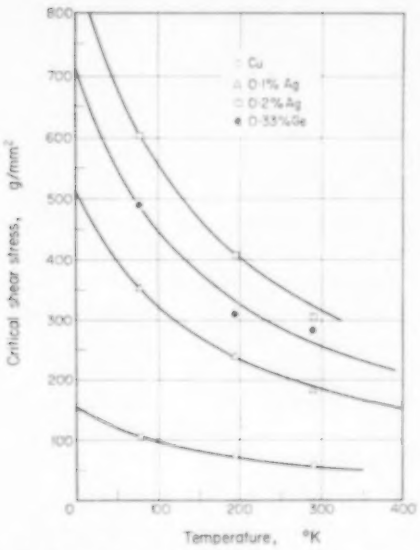

FIG. 2. Temperature dependence of τ_0 for copper and copper alloy crystals. (GARSTONE and HONEYCOMBE[91]).

TABLE 2

Dependence of τ_0 of nickel crystals on temperature and purity

Temperature	τ_0 g/mm²	
	Andrade and Henderson[9] (99·9 per cent Ni)	*Haasen*[23] (99·98 per cent Ni)
20°K	—	900–1100
180–195°K	1360	750– 850
290–300°K	1040	330– 750
508°K	970	—

ture was approximately 100 g/mm² compared with 50 g/mm² determined by Garstone and Honeycombe. The latter authors have found that very high values of τ_0 ($\sim$ 200–300 g/mm²) can be obtained if oxygen (and possibly sulphur) contaminate the metal. The results of DIEHL[5] on 99·98 per cent copper at room temperature which gave values of τ_0 of 86–120 g/mm² also suggest that some contamination has occurred. Aluminium crystals have been extensively studied, but little attention has been paid to the careful determination of the temperature dependence of τ_0. ROSI and MATHEWSON[23] working with aluminium crystals of 99·996 per cent purity over the range 77°K to 353°K, found a marked dependence of τ_0 on temperature, particularly below 200°K. Their results are summarized in Fig. 3. These authors also give the temperature dependence of the elastic modulus E and SEEGER[25] has shown

that if τ_0/E is plotted against temperature, the ratio is constant above 200°K.

ROSI[47] has determined τ_0 at room temperature for silver crystals of 99·99, 99·97 and 99·93 per cent purity and found it to be an average of 48 g/mm², 73 g/mm² and 131 g/mm² for the three purities, confirming the large effect which is known also to occur in copper.

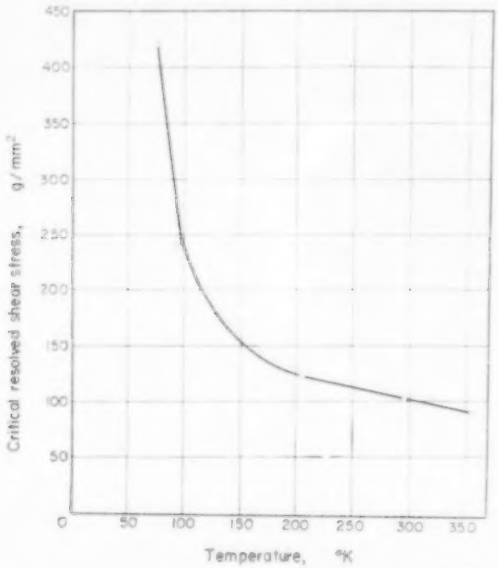

FIG. 3. Temperature dependence of τ_0 of aluminium crystals (99·996 per cent). (ROSI and MATHEWSON[23]).

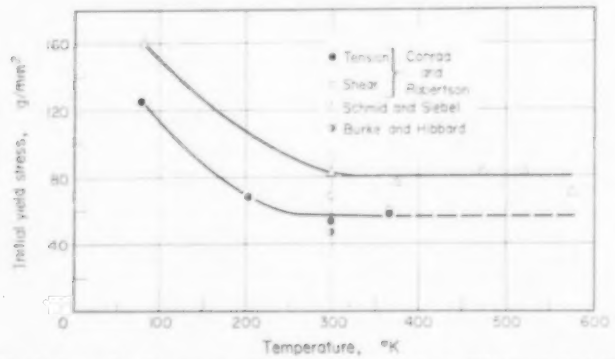

FIG. 4. Variation of τ_0 for magnesium with temperature. (CONRAD and ROBERTSON[10]).

3.2 *Close-packed Hexagonal Metals*

Data on the temperature dependence of τ_0 of the close-packed hexagonal metals was obtained originally by SCHMID and BOAS[2] in the period 1925–1931, and in many cases modern data with crystals of higher purity is not

available. This early information showed that τ_0 varies by a factor of 2–3 up to about 350°K then there is little change at higher temperatures Recent work on pure magnesium crystals by CONRAD and ROBERTSON[10] shows that the same trend occurs, but the level of the whole curve is lowered. Fig. 4 compares these results with the earlier results of SCHMID and SIEBEL.[11] It is interesting to note that at room temperature the latter authors found τ_0 to lie in the range 57–127 g/mm² whereas Conrad and Robertson found τ_0 between 40 and 65 g/mm.²

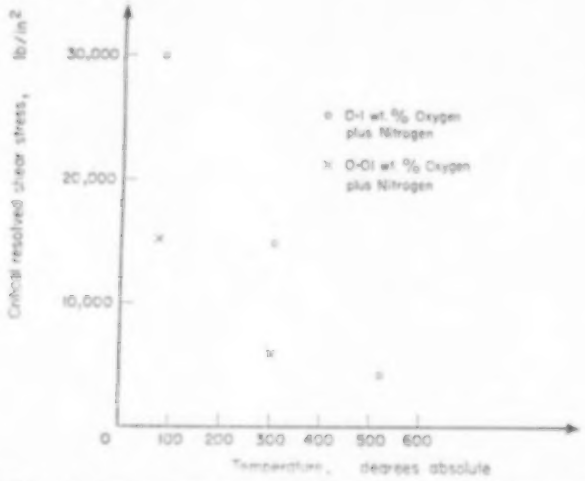

FIG. 5. Effect of temperature on τ_0 of titanium crystals. (CHURCHMAN and SMITH[70]).

The critical shear stress of titanium crystals varies markedly in the range 100°K to 500°K (Fig. 5) according to CHURCHMAN and SMITH.[70] The behaviour is very sensitive to the interstitial impurities oxygen and nitrogen.

LEE and BRICK[50] have given some values for τ_0 for beryllium crystals in the temperature range 298–773°K but as τ_0 at 773°K is given as higher than the 298°K value (~ 3000 g/mm²) it can be concluded that contamination has taken place at the elevated temperature.

Recent data on the temperature dependence of τ_0 for zinc is scanty but work by GILMAN[12] has confirmed that τ_0 is practically constant over the temperature range 455–680°K.

3.3 *Body-centred Cubic Metals*

There are few results on the resolved shear stress for glide of body-centred cubic crystals, and much of the published data is complicated by the presence of a sharp yield point due to interstitial impurity atoms. VOGEL and BRICK[67] have investigated single crystals of ingot iron over the temperature range 203°K to 463°K, and shown that τ_0 determined both in tension and compression falls from 14,000 g/mm² at 203°K to 4200 g/mm² at room temperature. There is only a slight change between room temperature and 463°K at

which temperature τ_0 is approximately 2800 g/mm.² ALLEN, HOPKINS and MCLENNAN[15] have tested crystals of purer iron (99·96 per cent) over the temperature range 77°K to 373°K. Their results are shown in Fig. 6. COX, HORNE and MEHL[93] have examined single crystals of decarburized mild steel and their results for the critical resolved shear stress show a similar temperature dependence. It should be emphasized, however, that there is need for such information on iron and other body-centred cubic metals using crystals prepared from zone-purified material where locking of dislocations by interstitial atoms would be at a minimum.

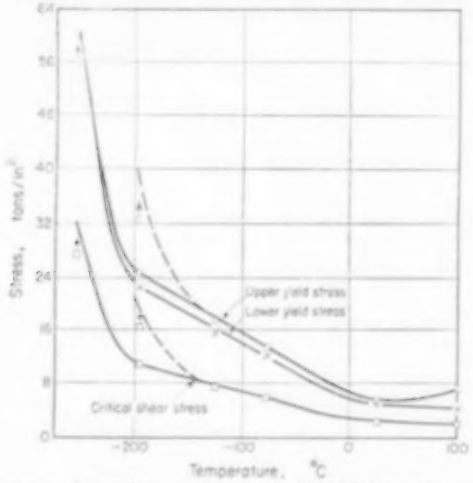

FIG. 6. Temperature dependence of τ_0 and the yield stresses of iron crystals 99·96 per cent purity. Dashed curve represents orientations near [001]. (ALLEN *et al.*[15]).

MADDIN and CHEN[68] have investigated single crystals of molybdenum at room temperature and in the range 1570°K–2770°K. The yield stress falls from 5 kg/mm² at room temperature to 1·5 kg/mm² at 1570°K then to 0·3 kg/mm² at 2770°K.

4. EFFECT OF ELEMENTS IN SOLID SOLUTION ON THE CRITICAL SHEAR STRESS

4.1 *Face-centred Cubic Metals*

The effect of alloying elements can be complicated by the existence in some alloys of a sharp yield point. Whilst the interstitial solid solutions such as carbon in iron produce pronounced yield points because of the strong interaction between the carbon atoms and the dislocations, the weaker interactions of dislocations with atoms in substitutional solid solution can also produce yield points. In many cases the upper yield point probably represents the true critical shear stress for the particular alloy crystal. The absence of an upper yield point may arise from non-axiality of loading causing a stress concentration which leads to too low a value for the flow stress, or from the use of too "soft" a tensile machine.

LINDE and co-workers[16, 17] have studied the effect of small concentrations of silicon, manganese, nickel, germanium, indium, tin, antimony and gold on τ_0 for copper measured at room temperature. Up to 1 or 2 atomic per cent of alloying element, τ_0 was found to vary almost linearly with the concentration confirming the earlier work of VON GÖLER and SACHS[18] for dilute copper–zinc alloys. The slope of the τ_0-composition curve was found to be related to the change in lattice parameter thus

$$\frac{d\tau_0}{dc} = K\theta^n \quad . \quad . \quad . \quad . \quad . \quad . \quad . \quad . \quad . \quad (1)$$

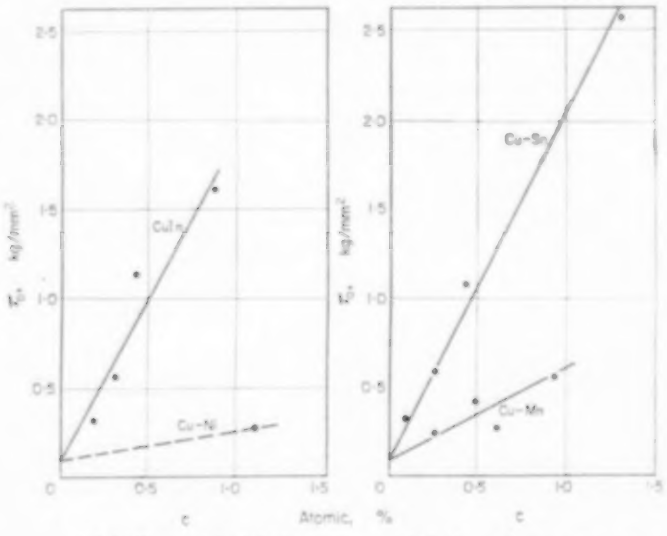

(a) indium and nickel (b) tin and manganese

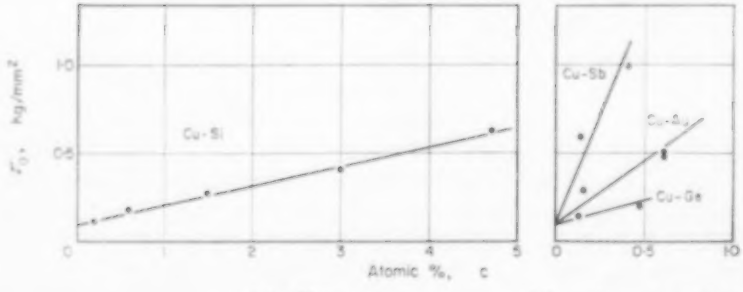

(c) silicon (d) antimony, gold and germanium.

FIG. 7. Effect of various solute metals on τ_0 of copper. (LINDE and EDWARDSON[17]). Concentration expressed in atomic per cent.

where τ_0 = critical resolved shear stress

c = atomic concentration

$\theta = \frac{1}{a} \cdot \frac{da}{dc}$ where a = lattice parameter

$n \sim 2$ from experiment.

Figure 7 shows some of the results; there is a marked variation from one system to another. The smallest effect is achieved by silicon which has an atomic size close to that of copper, whereas antimony, indium and tin which have substantially larger atoms than copper have a relatively big effect on τ_0. If we ignore the data on one copper–nickel alloy, and plot log $d\tau_0/dc$ against

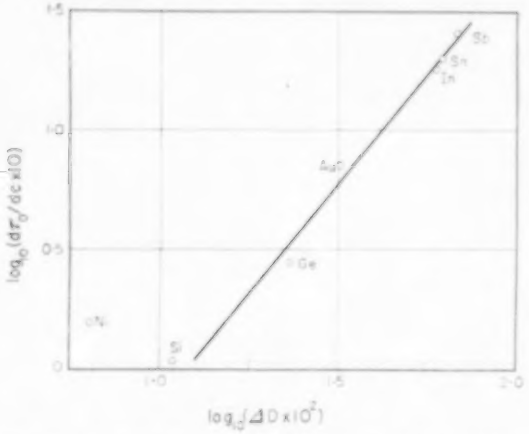

FIG. 8. Log of change in τ_0 with concentration of solute against log of the difference in atomic diameters. (Data of LINDE and EDWARDSON[17]).

log of the difference in Goldschmidt's atomic diameter between solvent and solute (ΔD), the points lie fairly well on a straight line (Fig. 8) the slope of which is approximately 2. So $\frac{1}{a} \cdot \frac{da}{dc}$ in Eqn. (1) could be replaced by ΔD.

GARSTONE and HONEYCOMBE[9] also found a linear relationship between τ_0 and atomic concentration for dilute copper–gold and copper–silver alloy crystals. Results for copper–silver crystals at three different temperatures are shown in Fig. 2. Values for $d\tau_0/dc$ measured at room temperature for copper–gold, –silver, –germanium alloys when plotted on a log scale against log ΔD fell approximately on a straight line.

The linear relationship between τ_0 and atomic concentration only holds for quite dilute alloys and is already inaccurate at atomic concentrations of 1 per cent. This had been shown originally for copper–zinc alloys by VON GÖLER and SACHS[18] while OSSWALD[19] investigating copper–nickel alloy crystals obtained a smooth curve for the plot of τ_0 against concentration with a maximum at 60 atomic per cent nickel. Similarly, SACHS and WEERTS[20] obtained a linear relationship for dilute gold–silver alloy crystals, but a

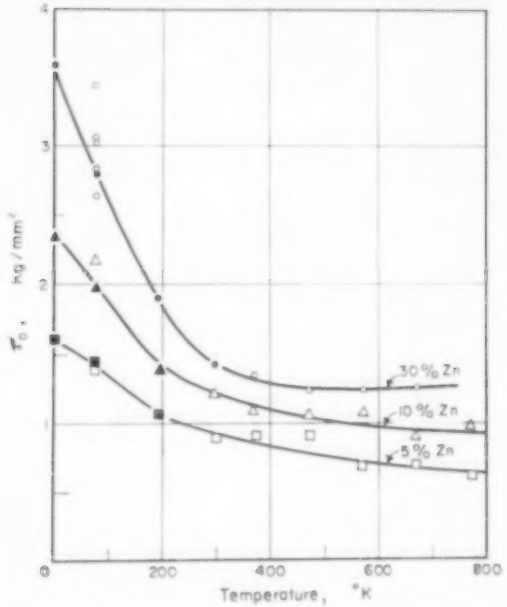

FIG. 9. Dependence of τ_0 for brass crystals on concentration and temperature (taken from JAMESON and SHERRILL,[21] SUZUKI[22]).

curve with a maximum at 50 atomic per cent was obtained for the whole range of compositions.

More recently, JAMESON and SHERRILL,[21] and H. SUZUKI and collaborators[22] have investigated the dependence of τ_0 on zinc concentration and temperature in α-brasses (Fig. 9). At higher concentrations τ_0 does not vary linearly with concentration; furthermore the effect of the solute is much more pronounced at low temperatures over the whole composition range investigated.

SUZUKI and collaborators[22] have also studied copper–nickel crystals over the complete system, and confirmed the earlier work of Osswald that a maximum in τ_0 occurs between 50 and 60 per cent nickel.

4.2 *Close-packed Hexagonal Metals*

Of the close-packed hexagonal alloy crystals only magnesium-base have received much attention. In a recent investigation LEVINE, SHEELY and NASH[24] have determined the effect of small concentrations of aluminium, cadmium, indium, thallium and zinc on τ_0 for magnesium. The results are summarized in Fig. 10, from which it can be seen that zinc has the greatest strengthening effect and indium the least. The strengthening was again shown to be dependent on the distortion produced in the structure measured by the change in lattice parameter, and when $d\tau_0/dc$ was plotted against $(1/a)(da/dc)$

a straight line relationship was obtained for zinc, aluminium and cadmium alloys. However, those solutes which caused little lattice distortion (indium, thallium) did not fall on the line, as Linde and co-workers found for nickel and silicon, which produce only small lattice parameter changes in copper. Despite the small lattice parameter change, thallium is more effective in hardening magnesium than is cadmium (Fig. 10), so it seems clear that an analysis based solely on lattice distortions is not completely justified.

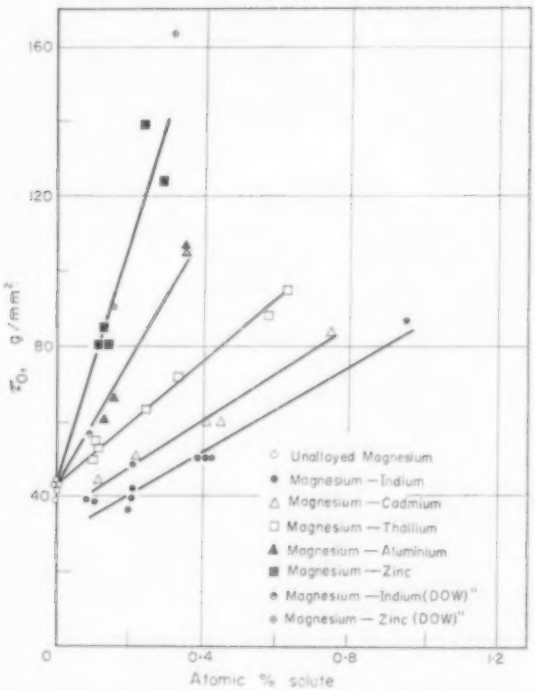

FIG. 10. Effect of solute concentration on τ_0 for magnesium alloy crystals. (LEVINE, SHEELY and NASH[24]).

5. EFFECT OF TEMPERATURE ON τ_0 FOR ALLOY CRYSTALS

There is reliable evidence for several alloy systems that τ_0 is strongly temperature-dependent in the presence of solute atoms. For example, in Fig. 2 results for τ_0 are plotted for copper and dilute copper–silver and copper–germanium crystals over the range 80–300°K.[9] Similarly, JAMESON and SHERRILL[21] and SUZUKI and co-workers[22] have shown that the temperature dependence of τ_0 is greater the higher the zinc content of α-brass crystals (Fig. 9). This is more clearly shown by JAMESON and SHERRILL[21] by plotting the ratio of τ_0 at a given temperature to that at room temperature against zinc content or lattice parameter (Fig. 11) for four different temperatures. However, it should be pointed out that the value of the ratio of unity

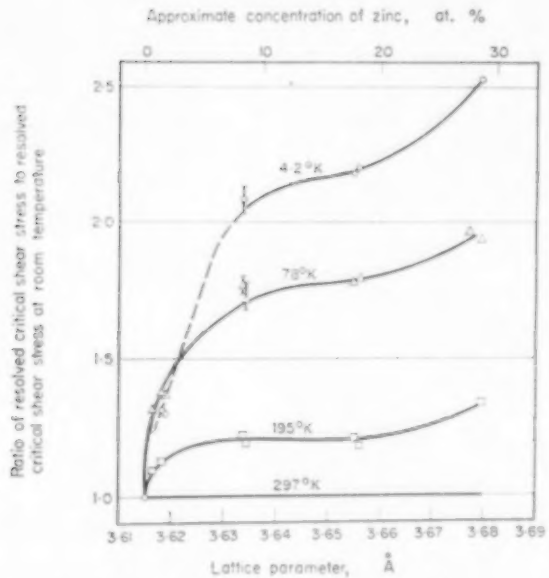

FIG. 11. The ratio of τ_0 for brass crystals at each of three lower temperatures to that at room temperature plotted as a function of zinc concentration. (JAMESON and SHERRILL[21]).

for 0 per cent zinc (based on previous work) is incorrect, for example, at 78°K the work of GARSTONE and HONEYCOMBE[9] on copper crystals indicates that the ratio should be approximately 1·7. This implies that the brass crystals have a stronger temperature dependence of τ_0 only at the higher zinc contents.

The critical shear stress of copper–nickel alloys has also been investigated over a wide range of temperature[22] but if the ratio of τ_0 at temperature T to τ_0 at room temperature is plotted against alloy content, only the higher alloyed crystals show big differences from the pure metals.

6. INTERPRETATION OF EXPERIMENTAL RESULTS ON THE CRITICAL SHEAR STRESS

6.1 *Pure Metals*

The recent experimental results are best viewed against the background of the theory of the temperature dependence of the flow stress τ as developed by SEEGER[6] and FRIEDEL.[7] The flow stress* is determined by two contributions, one (τ_G) from the internal stress fields of dislocations with the same Burgers vector as the first dislocations to move when the stress is applied;

* The critical shear stress τ_0 can be defined as the flow stress of a previously undeformed crystal. The flow stress τ can be applied to any stage of the stress–strain curve.

the fluctuation of the internal stress is over about 10^{-4} cm the estimated spacing of dislocations and is temperature independent. The other contribution (τ_S) arises from the interaction of the first moving dislocations with the "dislocation forest" which comprises dislocations cutting through the operative slip planes. This is both temperature- and strain rate-dependent. Seeger gives the following approximate expression in which the second contribution is absent at high temperatures

$$\tau(T) = \tau_G + \frac{U_0 - kT \log (NAbv_0/\dot{\epsilon})}{v}$$

$$\text{when } T \leqslant T_0 = \frac{U_0}{k \log \left(\frac{NAbv_0}{\dot{\epsilon}}\right)}$$

$$= \tau_G + \tau_S \quad . \quad . \quad . \quad . \quad . \quad . \quad . \quad . \quad . \quad . \quad . \quad (2)$$

$$\tau(T) = \tau_G \text{ when } T \geqslant T_0$$

where U_0 = activation energy for cutting through dislocations
T = absolute temperature
N = density of dislocations in forest
A = constant
b = strength of dislocation
v = activation volume
$\dot{\epsilon}$ = strain rate.

The elastic constants vary with temperature and cause a small temperature dependence but if τ/G where G = shear modulus, is plotted against temperature, then τ/G is temperature independent above T_0 when τ_G is the sole component of τ_0.

As Seeger points out, this approach is satisfactory for metals in which the dislocations do not readily extend to form stacking faults, i.e. the hexagonal metals magnesium, zinc, cadmium and cubic metals such as aluminium which possess high stacking fault energy. In these cases only a single activation energy, that for the formation of jogs in dislocations need be invoked. However, with metals of low stacking fault energy, there are likely to be additional rate-determining processes in certain temperature ranges, e.g. formation of vacancies by jogs in screw dislocations.

Recent results on magnesium and zinc support the view that in these hexagonal metals, τ_0 is largely temperature independent above room temperature. Similarly cubic metals with high stacking fault energy typified by aluminium show the same trend particularly if the temperature dependence of the elastic modulus is taken into account. At the higher temperatures the jogs formed when the dislocations on the slip plane cut through the forest are able to move readily with the rest of the dislocation line, whereas at lower temperatures a higher stress is needed for detectable plastic flow to occur.

The data for cubic metals of low stacking fault energy is less extensive and more difficult to interpret. The extension of the dislocations due to stacking

fault formation leads to difficulties when dislocations attempt to cut across each other. There is some conflict in the experimental results, but it is likely that τ_0 for copper increases by about 100 per cent between room temperature and 80°K, and even when the ratio τ_0/E is calculated where E is the modulus of elasticity for a given temperature, the same trend occurs. On the other hand, ADAMS and COTTRELL[14] found for copper crystals deformed in stage I of the tensile curve, that this ratio only changed over the range 180–250°K. There is thus a need for a wider exploration of the effect of temperature on τ_0 for metals with low stacking fault energy.

6.2 *Solid Solution Alloys*

Turning to the effect of solute atoms on τ_0 there appear to be four ways in which the high values for τ_0 in alloy crystals can be explained.

1. MOTT and NABARRO[50, 90] hardening due to the interaction of dislocation lines with the stress fields of isolated solute atoms.
2. COTTRELL[26] locking due to the elastic interactions between solute atom atmospheres and dislocations.
3. SUZUKI[27] intereactions produced when the stacking faults formed by dissociation of dislocations contain concentrations of solute atoms which differ from the average for the crystal.
4. Short range order hardening (FISHER[28]) which could arise as a result of the energy change when short range order present in the undeformed crystal is destroyed by initial dislocation movement.

Mott and Nabarro considered the interaction of a dislocation line with internal stress fields of various wave lengths arising from dispersion of particles in a metal, however the relevant case is that where the stress field is small (from individual solute atoms) compared with the limiting radius of curvature of the dislocation line. The wave length $\_\Lambda\_$ is defined thus

$$\_\Lambda\_ = ac^{-\frac{1}{2}}$$

where a is the inter-atomic spacing
c is concentration of solute.
Their original calculation for the flow stress gave

$$\tau_0 = G\theta^2 c \quad . \quad . \quad . \quad . \quad . \quad . \quad . \quad . \quad . \quad (3)$$

where G is the shear modulus, which is in part agreement with some of the results of LINDE and co-workers[17] and also GARSTONE and HONEYCOMBE.[9] A later modification of the calculation by MOTT[50] gave

$$\tau_0 = 2{\cdot}5\, G\theta^{\frac{1}{2}} c \quad . \quad . \quad . \quad . \quad . \quad . \quad . \quad . \quad (4)$$

which COTTRELL[26] has shown predicts a greater solution hardening than observed by a factor 10. To account for the discrepancy he suggests that the length of dislocation which moves simultaneously may be longer than assumed in the theory. Also the hardening observed at room temperature

VOL. 9 1961

may well be less than calculated because of thermal fluctuations assisting the dislocation to free itself from solute atoms. The experimental results have shown a marked dependence of τ_0 on temperature below 273°K. Furthermore the results on τ_0 for magnesium alloy crystals suggest that the valency of the solute relative to that of the solvent is a significant factor in addition to the well-established size factor effect.

An attempt to distinguish between the Cottrell and Suzuki mechanisms can be made if the temperature dependence is examined. The Cottrell effect would be expected to be a maximum at the lowest temperatures, but on raising the temperature thermal fluctuations would assist the applied stress in forcing the dislocations away from their atmospheres. A recent estimate by COTTRELL[73] for iron containing carbon indicates that the yield stress σ should vary as the cube root of the temperature.

$$\sigma = \sigma_0 - C(T)^{\frac{1}{3}} \quad . \quad . \quad . \quad . \quad . \quad . \quad . \quad . \quad (5)$$

where C = constant, σ_0 = shear stress at 0°K, T = absolute temperature. Cottrell predicts that the steep rise of σ towards σ_0 as 0°K is approached, will not occur as the energy barrier at these temperatures may well be overcome by the quantum-mechanical tunnel effect without the need for thermal energy. COTTRELL[73] has calculated an expression for the activation energy $U(\sigma/\sigma_0)$ for the break away of a dislocation from its atmosphere:

$$U(\sigma/\sigma_0) = 0{\cdot}9\left(1 - \frac{\sigma}{\sigma_0}\right)^3 \quad . \quad . \quad . \quad . \quad . \quad . \quad (6)$$

and applied it to the results of CLARK and WOOD[74] on delayed yield in iron. The agreement of the theory with the experimental results was good indicating that the estimate of the activation energy was fairly accurate.

On the other hand, the locking due to Suzuki interaction is much weaker at low temperatures; SUZUKI[29] suggests that it is about one-tenth as effective as Cottrell locking. However, at high temperatures the Suzuki locking is little affected whereas the Cottrell locking is no longer important. Suzuki gives the following relationship for the dependence of the critical shear stress on solute concentration and temperature calculated on the basis of the interaction of solute atoms with stacking faults.

$$\tau_0 = \frac{2h}{vb} Hc_0(1 - c_0)\frac{1 - e^{-H/RT}}{1 - c_0(1 - e^{-H/RT}} \quad . \quad . \quad . \quad (7)$$

where τ_0 = maximum locking stress, c_0 = average concentration of solute, b = Burgers vector, v = molecular volume, H is proportional to $\gamma_a - \gamma_b$ where these are the stacking fault energies in metals a and b, h = half the width of the stacking fault.

Using this relationship SUZUKI[29] has calculated the contribution to τ_0 of the Suzuki or chemical interaction at 600, 800 and 1000°K for copper–nickel crystals over a wide range of composition. The fairly good agreement with experimental points suggests that at these elevated temperatures Suzuki

locking is the prime factor. Suzuki has likewise calculated the curve of τ_0 against composition at 0°K assuming that the Cottrell effect is predominant, and again there is reasonable agreement with values of τ_0 obtained by extrapolation from higher temperatures.

It is possible that short-range order contributes to hardening at elevated temperatures in alloys with a high concentration of solutes. Suzuki has derived the relationship

$$\tau_0 = \frac{2}{9}\sqrt{\frac{2}{3}} \cdot \frac{W^2}{cRT} c^2 (1-c)^2 \quad . \quad . \quad . \quad . \quad . \quad (8)$$

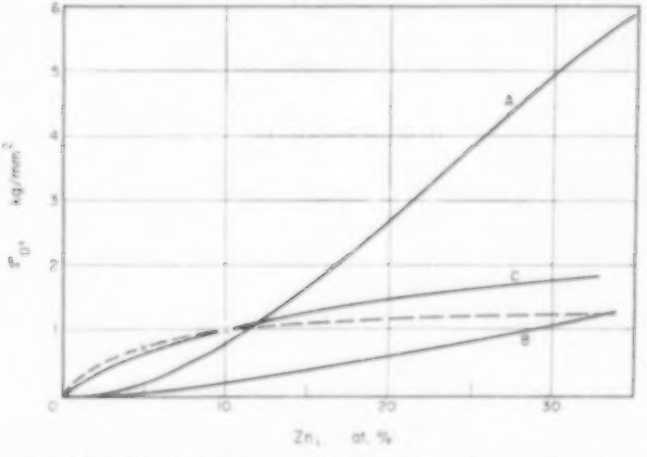

FIG. 12. Critical shear stress of copper–zinc alloys at 600°K.
Curves A and B. Two calculations of short-range order hardening.
Curve C. Calculated hardening due to chemical interaction.
Dashed curve. Observed values (SUZUKI[20]).

where c = concentration of solute in stacking fault,
$W = ZN\,[\chi_{AB} - (\chi_{AA} + \chi_{BB})/2]$,
Z is the number of nearest neighbours,
N is Avogadro's number,
χ_{AB}, χ_{AA} and χ_{BB} are the potential energies of the respective atomic pairs,

from which he has calculated the dependence of τ_0 on composition of α-brass at 600°K making two different assumptions for the short-range order hardening, Fig. 12 (A) and (B). It is clear from Fig. 12 that curve *C* using the Suzuki interaction most closely fits the experimentally determined curve (dashed line).*

There are some difficulties in the way of accepting Cottrell locking as the predominant low-temperature hardening mechanism. Firstly, a sharp yield point is not usually developed in substitutional solid solution crystals until

* Flinn[97] has recently made a similar analysis to assess the relative contributions.

VOL. 9 1961

the solute concentration is quite high ($\sim$ 1 atomic per cent) and at this stage τ_0 has already been increased by several hundred per cent. Secondly, SEEGER [1] has pointed out that although the temperature dependence of τ_0 is marked, it is not very different from that of pure metals and alloys. He therefore considers that locking effects are not important, and puts forward the view that the main initial hardening in alloy crystals arises from higher dislocation densities. TILLER [30] recently has shown that during the growth of alloy crystals from the melt, solute segregation structures which always form, must have dislocations at their boundaries. In the light of these results it is difficult to see how the dislocation populations in alloy crystals can be made comparable to those in pure metal crystals when melt methods are employed. There is no detailed information on the dislocation population of alloy crystals grown by the strain anneal method.

7. The Temperature Dependence of Stress–Strain Curves of Metal Crystals

Until recently it seemed that the shear stress–shear strain curves of metal crystals fell into two main groups, particularly if measured at room temperature. On one hand the cubic metals such as copper, nickel, silver showed marked strain hardening and only moderate shear strains, whereas the hexagonal metals, magnesium zinc and cadmium together with tetragonal tin showed low strain hardening combined in certain orientations at least, with very high shear strains. While some measure of understanding of strain hardening has derived from this generalization it should not be regarded uncritically. For one reason, no data on high melting hexagonal metals was included and for another, the distinction becomes much less pronounced when temperatures much lower than room temperature are chosen for comparison.

7.1 *Face-centred Cubic Metals*

During the last ten years much work has been done on the orientation and temperature dependence of the stress–strain curves of cubic metal crystals of high purity, in particular aluminium, but also copper, nickel, silver and gold.* It is now possible to generalize about the shape of the stress–strain curves along the lines indicated by DIEHL, MADER and SEEGER [1, 33] and FRIEDEL. [7, 48] Fig. 13 is a schematic representation of the temperature dependence of the stress–strain curves of cubic metal crystals. At high temperatures the curves are approximately parabolic while at intermediate temperatures (room temperature for Cu), the initiation of plastic deformation is followed by a linear range of low hardening, the "easy glide" range, so-called by ANDRADE and HENDERSON [8] who studied the phenomenon in very pure gold and silver crystals. Seeger refers to this as stage I while stage II

* This work has now been very adequately described in the article on work hardening of metals by CLAREBROUGH and HARGREAVES in *Progress in Metal Physics*, Volume 8.

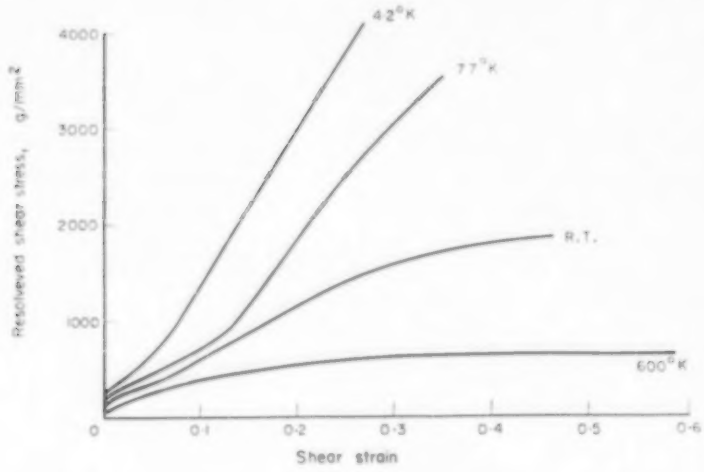

FIG. 13. Temperature dependence of stress–strain curves of face-centred cubic metal crystals. Schematic, approximating to the behaviour of copper.

follows as another approximately linear range in which the rate of strain hardening is much higher. Stage II merges into stage III a region of decreasing strain hardening. At certain temperatures and with some orientations the distinction between stages II and III is blurred giving a parabolic curve. At low temperatures (77°K for copper) the stage I is longer and stage III may disappear completely. At 4·2°K the curve is mainly linear and stage II predominates.

ANDRADE and HENDERSON[8] showed that stage I in crystals of silver and gold increased with decreasing temperature. MASING and RAFFELSEIFER[31] observed stage I in pure aluminium crystals deformed at room temperature, but it was much shorter than in silver and gold; the extent of this stage was also very orientation-dependent. LÜCKE and LANGE[32] confirmed this for 99·99 per cent aluminium, but showed that stage I was absent at room temperature in aluminium of lower purity (99·6 per cent). Added to this, GARSTONE, HONEYCOMBE and GREETHAM[9] showed that copper crystals in the size range from $\frac{1}{4}$ to $\frac{3}{8}$ in. and grown from the same seed showed different degrees of stage I hardening, the extent increasing with decreasing diameter of crystals. SUZUKI, IKEDA and TAKEUCHI[35] also found a size effect with copper crystals varying in diameter from 0·6 mm to 10 mm. It is thus clear that in face-centred cubic metal crystals the extent of stage I linear hardening is dependent on

1. the metal,
2. purity of the metal,
3. orientation of the crystal,
4. temperature of the deformation,
5. size of crystal.

VOL. 9 1961

For the purposes of this review 3 and 5 are largely irrelevant but it is necessary to bear them in mind when comparing results from different workers for the size of the crystals and their orientations may vary within wide limits. Below are summarized results on several face-centred cubic metals which have been studied in recent years.

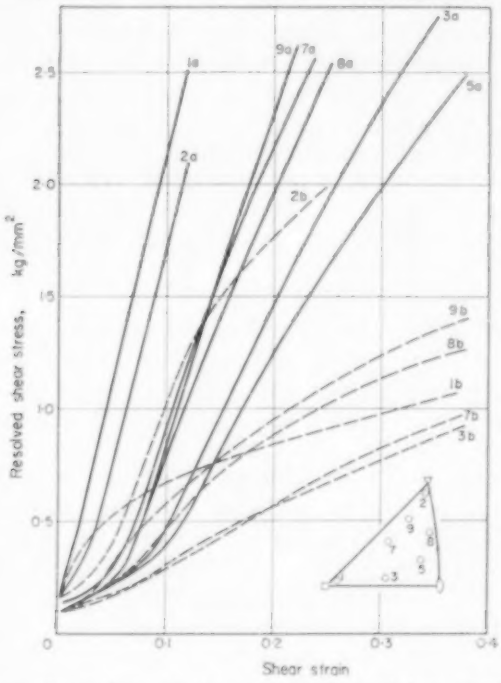

FIG. 14. Shear stress–shear strain curves of aluminium crystals at room temperature and 77°K. ---- Room temperature —— 77°K (STAUBWASSER[38]).

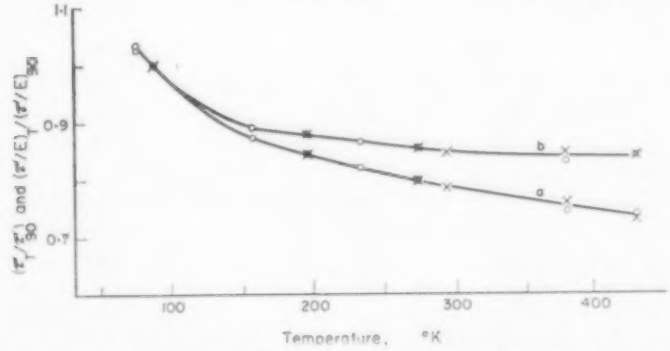

FIG. 15. Reversible changes of flow stress of aluminium crystals with temperature. (a) before and (b) after correction for change of elastic constant with temperature.
τ_T = flow stress at temperature T. (COTTRELL and STOKES[13]).

7.1.1 *Aluminium*

It seems clear from the experiments of LÜCKE and LANGE[32] that only a small region of easy glide develops in crystals of some orientations at room temperature in 99·99 per cent Al. More recent work,[9, 13] particularly experiments with identically oriented crystals, has shown that the easy glide range is more extensive at 77°K, comparable to copper at room temperature, and all three stages of the deformation are present. KOEHLER and co-workers,[36, 37] have extended experiments to 4·2°K where they found that only stage I and stage II were present, the majority of the stress–strain curve being linear with a steep slope (stage II).

STAUBWASSER[38] has compared the behaviour of aluminium crystals of identical orientation at room temperature and at 77°K, and has shown that in the former case stage II is weakly developed except for crystals of symmetrical orientations (Fig. 14). Seeger has pointed out that this behaviour is characteristic of metals which have a high stacking fault energy when extended dislocations are not readily formed.

COTTRELL and STOKES[13] have studied the temperature dependence of the flow stress of aluminium crystals at different stages of the stress–strain curve, the stress being first measured at a higher temperature then at a lower one. They found that after the early stages of deformation, the ratio of the flow stress at T°K to that at 90°K was almost independent of the amount of deformation. When the ratio was plotted against T there was a steady fall with increasing temperature (Fig. 15) but when corrections were made for the change in elastic constants with temperature, the curves showed a negligible gradient above 300°K. These observations have been confirmed recently in similar experiments by BASINSKI.[55]

When aluminium crystals were first strained at a lower temperature then at a higher one, Cottrell and Stokes found that a yield phenomenon was obtained which revealed instability in the low temperature dislocation distribution. This phenomenon of work softening is explained in terms of the release of dislocation pile-ups by thermally activated cross-slip.

7.1.2 *Lead*

Lead is the only other f.c.c. metal supposedly of high stacking fault energy,* of which single crystals have been deformed at different temperatures. FELTHAM and MEAKIN[39] have deformed lead single crystals at 77°, 194° and 295°K. Easy glide was not observed at any temperature but this may have been a consequence of the testing conditions. At room temperature as in aluminium, only stage III was observed while at 194°K and 77°K small regions of linear hardening corresponding to stage II were evident.

7.1.3 *Copper*

ROSI[47] and GARSTONE, HONEYCOMBE and GREETHAM[9] have shown that

* The frequency of annealing twins suggests that lead has a much lower stacking fault energy than aluminium. THORNTON and HIRSCH[40] have recently found experimental values for a number of metals which confirm this view.

VOL. 9 1961

in copper crystals deformed at room temperature there is a much longer stage I than for aluminium crystals of comparable size. DIEHL[5, 33] and co-workers have shown that this stage increases in length though not in slope when the temperature is lowered to 88°K. BLEWITT, COLTMAN and REDMAN[34] have given stress–strain curves for identically oriented crystals at 300°, 200°, 78° and 4·2°K which show clearly that stage II (linear hardening) does not change its slope very much as the temperature falls. ANDRADE and ABOAV[4] have studied the deformation of identically oriented crystals over a wide temperature range from 87° to 1173°K and found, as in their earlier experiments on gold and silver that the easy glide range decreases with increasing temperature being practically absent above 573°K. The orientation of the crystal axis in this case was initially fairly close to [110]. The slope of the easy glide range was found to be insensitive to temperature in the range 93 to 293°K, while the slope of stage II was almost constant over the range 93 to 623°K. Both FRIEDEL[7] and SEEGER[1] have pointed out that the ratio of the work hardening coefficient in this range to the shear modulus is almost independent of the temperature and also of the applied stress. On the other hand, the point at which the transition to stage III occurs is markedly temperature-dependent.

ADAMS and COTTRELL[14] measuring the reversible change in flow stress of copper crystals over the temperature range 90°K to 473°K, found as in the case of aluminium that above a certain temperature (250°K) the flow stress ratio corrected for the temperature dependence of the elastic constants was almost independent of temperature. This behaviour was confirmed by MAKIN,[79] but recently BASINSKI[55] found that the corrected flow stress decreased steadily with temperature in the same range. He obtained similar results with silver crystals over the range 4°K to 375°K.

7.1.4 *Nickel*

HAASEN[3] has recently examined the deformation of 99·98 per cent Ni crystals between 4·2°K and 300°K, and confirmed the same general features of the stress–strain curves which were found with copper. The extent of easy glide increased markedly with decreasing temperature, but this tendency did not exist in crystals of 99·4 per cent purity. The slope of the easy glide range decreased only slightly with decreasing temperature.

Nickel crystals showed a well-developed stage II at room temperature which became more extensive as the temperature was lowered to 20°K. The slope of stage II (work hardening coefficient) was not strongly dependent on temperature, nevertheless the dependence was greater than that observed by BLEWITT and co-workers,[34] and ANDRADE and ABOAV[4] for copper. The transition from stage II to stage III occurred at a higher stress the lower the temperature. Fig. 16 shows the results both for nickel and for copper.

Haasen also carried out measurements of flow stress at two different temperatures by the Cottrell and Stokes method after various amounts of plastic deformation to determine the temperature dependence of a given

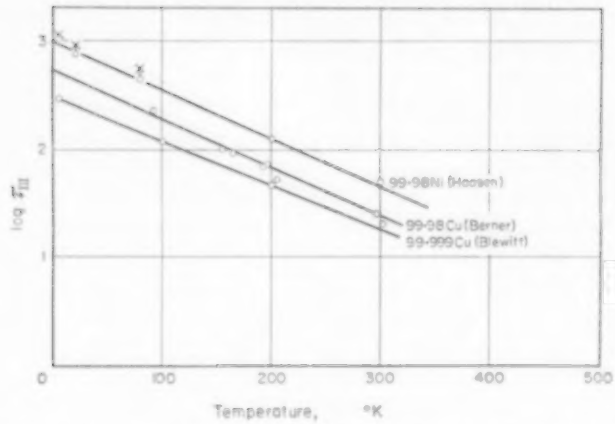

FIG. 16. Dependence on temperature of the stress τ_{III} for the transition from stage 2 to stage 3 hardening. Data on nickel and copper crystals (HAASEN[3]).

cold-worked state. He plotted $\tau_1-\tau_2$ against τ_2 where $\tau_1-\tau_2$ is the measured change in flow stress and τ_2 is the flow stress at the higher temperature. A linear relation was found for various temperature ranges, but deviations from the curve occurred at low strains in the easy glide range.

7.2 *Close-packed Hexagonal Metals*

The stress–strain curves of hexagonal metal crystals of high stacking fault energy (magnesium, zinc, and cadmium) appear to be practically linear to moderate strains and over a wide temperature range. There is not a marked dependence on orientation except for crystals with symmetrical orientations such that the critical shear stress is the same in two of the basal slip systems. It follows that one strain hardening coefficient suffices to describe the behaviour of crystals at a given temperature.

However, at large strains marked deviation from linearity occur, and the rate of strain hardening increases substantially. This has been particularly observed at room temperature (in zinc), but is also found at lower temperatures and in other metals. There has been less work done on titanium and rhenium, but this already indicates that these metals are closer to f.c.c. metals in their strain hardening behaviour.

7.2.1 *Magnesium*

CONRAD and ROBERTSON[10] have studied the temperature dependence of the flow stress and strain hardening coefficients of magnesium crystals using two methods. Firstly, the temperature was maintained constant while the crystals were incrementally loaded, some in tension and others in pure shear, and secondly, the method of Cottrell and Stokes was used. The range 78°K to 364°K was investigated. Typical stress strain curves are shown in Fig. 17 for 78°K, 203°K and 364°K; although the curves are nearly linear, deviations

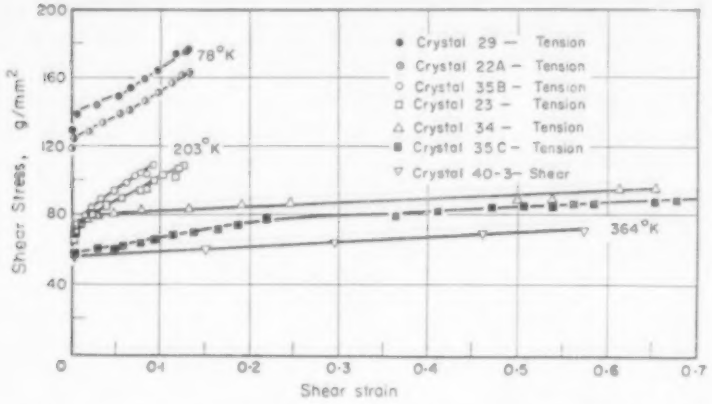

FIG. 17. Shear stress–shear strain curves of magnesium crystals at 78°, 203° and 364°K. (CONRAD and ROBERTSON[10]).

are apparent after relatively small strains, particularly at 78°K. In Fig. 18 the slope of these curves is plotted against temperature to show the marked increase in work hardening coefficient in the range 300–200°K. Conrad and Robertson associated the decrease above 200°K with recovery, the coefficient being constant in the absence of recovery. It was found also that the strain hardening coefficient was independent of the strain history of the specimen. The earlier results of SCHMID and SIEBEL[11] followed the same general trend; the difference in magnitude of the coefficient at low temperatures can probably be attributed to the less pure magnesium used.

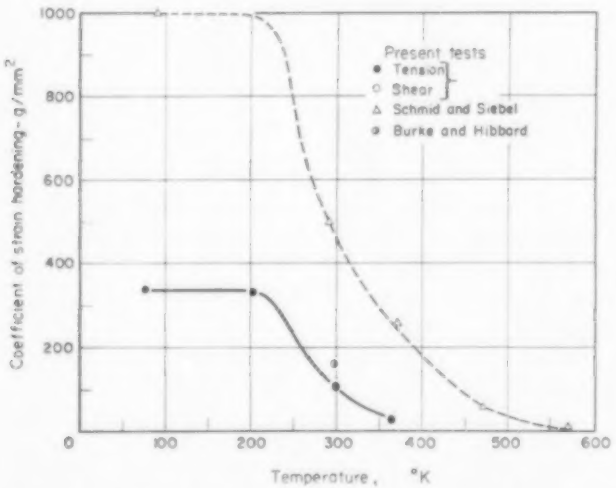

FIG. 18. Coefficient of strain hardening of magnesium crystals determined from Fig. 17 as a function of temperature. (CONRAD and ROBERTSON[10]).

7.2.2 *Zinc*

Experiments by LÜCKE, MASING and SCHRÖDER[52] with zinc crystals of 99·995 per cent purity indicated that while the stress–strain curves were approximately linear at 90°K, at 294°K crystals of most orientations developed a stage II hardening after 100 per cent glide strain comparable to that in aluminium crystals (Fig. 19). At 90°K about 50 per cent glide strain was the maximum before fracture occurs; however, the curves already showed appreciable deviations from straight lines. The work hardening coefficient

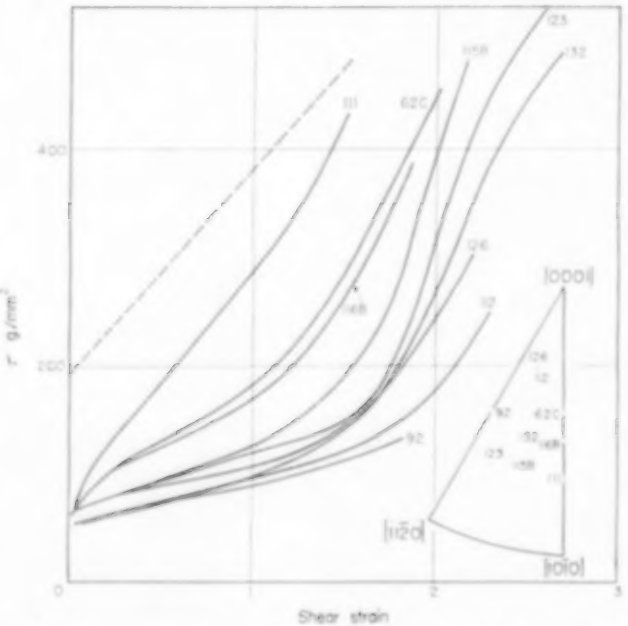

FIG. 19. Shear stress–shear strain curves of zinc crystals deformed at 294°K. ---- average curve for less fine metal. (LÜCKE, MASING and SCHRÖDER[52]).

was found to be much higher than at room temperature. DERUYTERRE and GREENOUGH[53] found similar deviations below 50 per cent shear strain in zinc crystals deformed at 77°K and 196°K and furthermore they observed that the rate of work hardening at 196°K was greater than at 77°K, an anomaly also found in the earlier results of FAHRENHORST and SCHMID[54] but not explained. It is interesting to note that in this work, despite the anomaly, the strain hardening coefficient dropped markedly in the range 200–300°K (cf. magnesium).

7.2.3 *Cadmium*

The early work of BOAS and SCHMID[69] remains the most complete on the effect of temperature on the shear stress–shear strain curves of cadmium single crystals. The results reinforce the above remarks on the behaviour of

zinc. Firstly, even at room temperature, the stress strain curves are no longer linear at high strains (above 200 per cent glide strain) and secondly, there is a marked degree of strain hardening at 87°K and lower which is unlikely to be explained simply in terms of basal glide. The substantially lower glide strains at these temperatures support this viewpoint.

7.2.4 *Titanium, Rhenium*

Whereas in zinc, cadmium and magnesium, basal glide is predominant, at least at room temperature, in the higher melting hexagonal metals it is not; moreover, a high degree of work hardening is often obtained. At room temperature pure titanium (oxygen and nitrogen $\sim$ 0·01 wt per cent) deforms on $\{10\bar{1}0\}$ planes and shows marked work hardening. On the other hand, CHURCHMAN and SMITH[70] have found that less pure crystals (0·1 wt per cent oxygen and nitrogen) yield at much higher stresses but exhibit little work hardening. At 90°K crystals of both purities exhibited a yield hump but little subsequent work hardening. ROSI[77] working with 99·77 per cent metal at room temperature found a τ_0 of 4900 g/mm² and a work hardening coefficient of 25,900 g/mm² which is much higher than those for zinc or cadmium.

Rhenium crystals exhibit particularly severe work hardening both at room temperature and at 90°K according to CHURCHMAN and JEFFREY[62] who find that the behaviour is not particularly orientation-dependent.

8. VARIATION OF SLIP MARKINGS WITH TEMPERATURE

8.1 *Face-centred Cubic Metals*

Prior to 1951 it was thought that the initial plastic deformation in face-centred cubic metal crystals was localized on widely spaced slip bands. However, BROWN and HONEYCOMBE[41] and WILSDORF and KUHLMANN-WILSDORF[42] showed that carefully prepared metal crystals (copper, aluminium) exhibited very closely spaced fine slip, micro slip or elementary structure, at the beginning of plastic deformation. As a result of the electron microscopic investigations of SEEGER[63] and co-workers, and MADER,[44] it is now thought that fine slip is characteristic of the easy glide range (stage I). The slip lines at this stage are quite long, possibly greater than 1 mm. and the step heights between 50 and 100 Å. Observations on aluminium, copper and on nickel support this viewpoint, although it should be pointed out that fine slip is observed between coarse slip bands, on aluminium crystals deformed slowly at elevated temperatures, when easy glide is absent.

In stage II, more distinct slip lines appear with varying heights but no cross slip is observed. It is only in stage III that well-defined coarse slip bands appear which are comprised of clusters of slip lines. These bands are very much shorter and exhibit at their ends well-defined cross-slip. It follows that slip markings at different temperatures are more likely to be rationalized if they are related to equivalent regions of the stress–strain curves. For example, copper crystals at room temperature show clearly the transition between the three stages. The slip lines in stages II and III are illustrated in Figs. 20a

and 20b for deformed copper. In aluminium at room temperature the distinction is much less well defined as the three stages tend to merge with each other. As the temperature is lowered, the slip bands become finer and when stage III is eliminated they no longer occur. For example, NOGGLE and KOEHLER [37, 45] found slip bands in aluminium crystals deformed at room temperature where 80 per cent of the deformation occurred on them, but at 78°K only fine slip lines were observed at strains up to 0·5. At this temperature slip bands developed only at the later stages. At 4°K the stress–strain curves exhibited only stages I and II, and all the deformation was by fine slip (Fig. 21).

FELTHAM and MEAKIN [39] did not observe slip bands optically in lead crystals until the stage II hardening was passed: however, slip bands with some evidence of cross slip were detected at 77°K. At room temperature slip band formation was pronounced and there was ample evidence of cross slip associated with the bands.

At very low temperatures ($\leqslant$ 77°K) the deformation of crystals of copper, [34] nickel, [3] silver and gold, [46] is complicated by the onset of discontinuous slip and twinning. Discontinuous slip which is observed at 4°K is a burst phenomenon in which localized deformation occurs by rapid formation of a large number of closely-spaced slip lines comprising a coarse band. The deformation may be triggered off by the release of heat when the first band forms; this is only slowly dissipated because of the low thermal conductivity of the metal at 4°K (BASINSKI [45]). These bursts of slip usually are revealed by slight serrations in the load-elongation curves.

Deformation twinning on the other hand is encountered at higher temperatures; SUZUKI and BARRETT [46] have found twins in favourably oriented crystals of silver at 273°K. Gold, gold–silver alloys [46] (Fig. 22a) and copper [34] form deformation twins at 77°K while nickel [3] also deforms to some extent by twinning if the temperature is lowered to 20°K (Fig. 22b).

8.2 *Hexagonal Metals*

In recent years it has become increasing evident that non-basal slip plays an important part in the deformation of hexagonal metals including the more familiar zinc, cadmium and magnesium. The early work of SCHMID and WASSERMAN [56] showed that above 498°K pyramidal slip on the system $\{10\bar{1}1\}$ $[11\bar{2}0]$ could occur in magnesium crystals. BAKARIAN and MATHEWSON [57] confirmed these results and found that τ_0 for pyramidal slip at 603°K was 400 g/mm² compared with 66 g/mm² for basal slip, indicating that non-basal slip would occur only in crystals which were very unfavourably oriented for basal slip. However, BURKE and HIBBARD [58] detected pyramidal slip at 298°K when the stress axis was 6° from the basal plane, and moreover τ_0 for pyramidal slip (52 g/mm²) was only slightly greater than τ_0 for basal slip (46 g/mm²). Recently REED-HILL and ROBERTSON [59] using crystals oriented to suppress basal slip (tension axis // basal plane and $[10\bar{1}0]$ direction) have confirmed non-basal slip at 298°K and 77°K but have

OL.
9
961

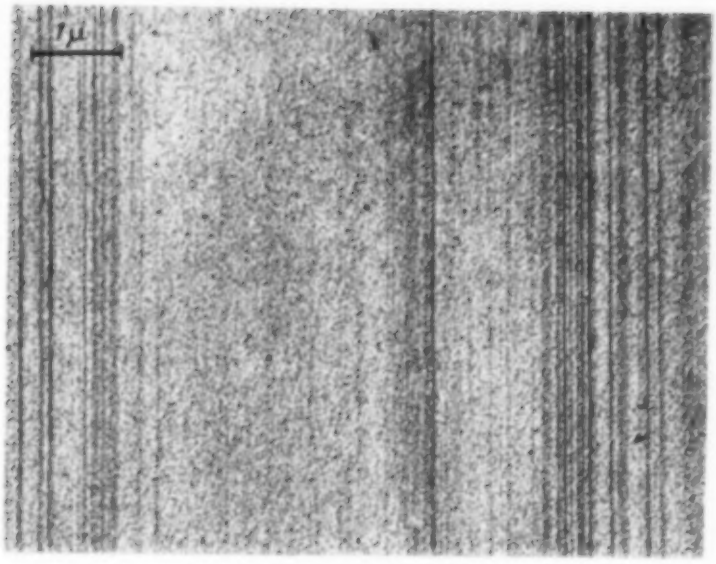

(*a*) middle of stage II.

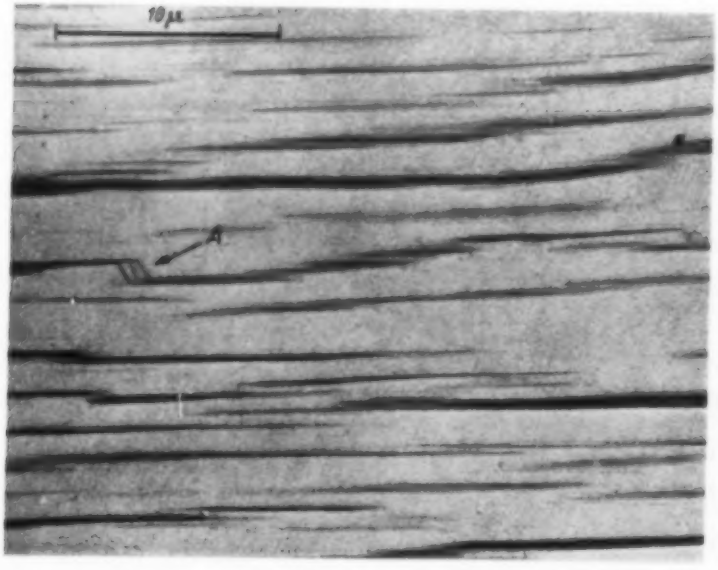

(*b*) middle of stage III.

FIG. 20. Electron micrographs of copper crystals deformed at room temperature. (MADER[44]).

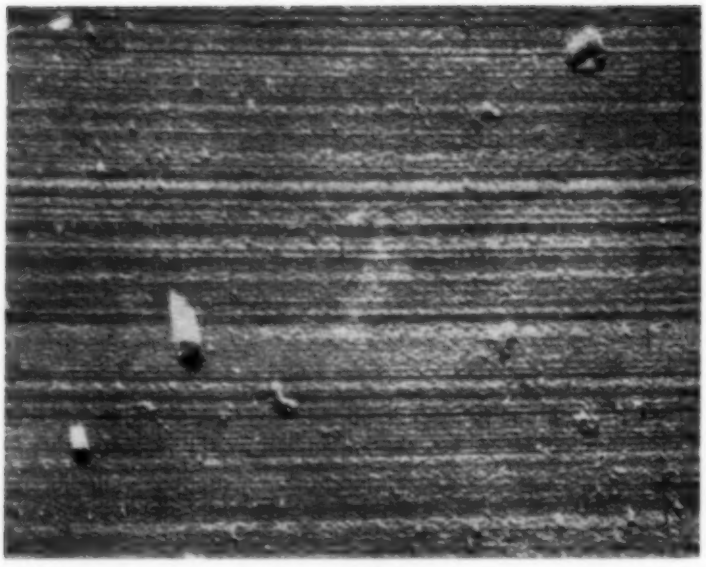

FIG. 21. Electron micrograph of an aluminium crystal deformed to 0·5 shear strain at 4 K. Near end of stage II.
× 27,000. (NOGGLE and KOEHLER[55]).

VOL.
9
1961

OL.
9
961

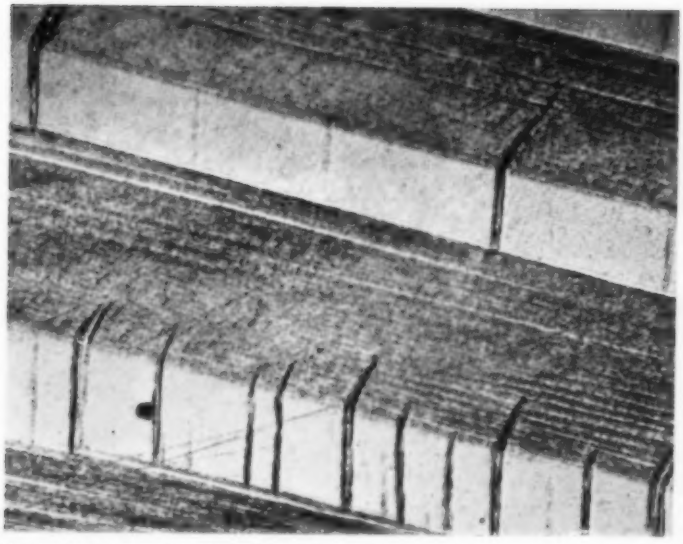

(*a*) silver—10 per cent gold deformed at 77° K × 330
(SUZUKI and BARRETT[36]).

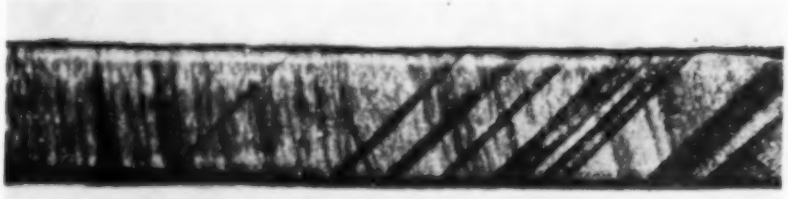

(*b*) nickel deformed 54 per cent at 20° K, polished and etched. × 10
(HAASEN[31]).

FIG. 22. Deformation twinning in face-centred cubic metals.

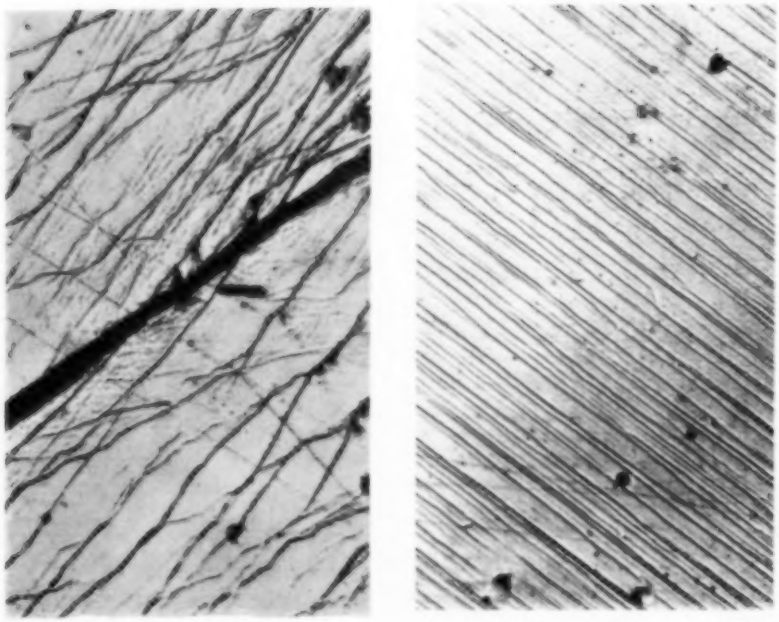

(*a*) $\{10\bar{1}0\}$ slip at 573 K. × 170 (*b*) basal slip at 298 K. × 200

FIG. 23. Slip bands in beryllium.
(LEE and BRICK[91]).

VOL.
9
1961

identified it as prismatic $\{10\bar{1}0\}$ $[11\bar{2}0]$. They have, however, found pyramidal slip $\{10\bar{1}1\}$ at 423°K and 559°K.

BELL and CAHN[60] in the course of a study of twinning in zinc crystals with the basal plane almost parallel to the tension axis, observed non-basal slip at room temperature which was identified as pyramidal $\{11\bar{2}2\}$ $[1\bar{1}23]$. They found that τ_0 for this system was between 1050 and 1600 g/mm², many times that for basal glide ($\sim$ 35 g/mm²) so that basal slip predominates at room temperature. GILMAN[61] also recently observed $\{11\bar{2}2\}$ slip at room temperature as a result of compression parallel to the basal plane.

In the hexagonal metals of higher melting points, non-basal slip is frequently predominant as the smaller axial ratios cause closer packing on non-basal planes. In rhenium,[62] titanium,[63, 72] zirconium,[64] the dominant system is $\{10\bar{1}0\}$ $[11\bar{2}0]$ and is associated with the occurrence of marked work hardening. There is, of course, the opportunity for slip on more than one $\{10\bar{1}0\}$ plane. Beryllium also shows slip on this system but according to TUER and KAUFMANN,[65] basal slip is predominant at room temperature. LEE and BRICK[94] found during compression tests of beryllium crystals at room temperature that non-basal slip only occurred extensively when the basal plane was unfavourably oriented. The non-basal slip was on $\{10\bar{1}0\}$ planes and was usually very wavy (Fig. 23a). The basal slip was usually straight and in well defined bands, with ample evidence of local cross slip (Fig. 23b).

8.3 *Body-centred Cubic Metals*

Both ALLEN *et al.*[15] and COX *et al.*[93] have studied the temperature dependence of the slip systems in α-iron crystals in the range 373°K to 20°K. The latter authors found that the glide elipse could occupy any position in the [111] zone but that lowering of the temperature tended to favour {110} slip. Allen *et al.* found that the three operative systems were $(\bar{1}01)$ [111], $(\bar{3}12)$ [111] and $(\bar{2}11)$ [111], and that the critical shear stresses on each were very similar. The operative slip system was determined more by the orientation of the crystal than by the temperature of testing.

9. THEORETICAL INTERPRETATION OF STRESS–STRAIN CURVES

The present theoretical interpretation of the flow-stress $\tau(T)$ in terms of two components (Eqn. (2)) τ_G and τ_S has already been described, and reference has been made to experiments on the reversible change of flow stress with temperature. τ_G for a given dislocation density depends only on the modulus thus (SEEGER[1])

$$\tau_G = \alpha b \,.\, G \,.\, \sqrt{N} \quad . \quad . \quad . \quad . \quad . \quad . \quad . \quad (9)$$

where G = shear modulus, N = dislocation density, b = Burgers vector, α = constant, and so once a correction is made for the temperature dependence of G, τ_G should be temperature-independent. τ_S is temperature-dependent because cutting through the forest of dislocations involves the

formation of jogs which requires an activation energy U_0 (Eqn. (2)). At very low temperatures the τ_s contribution will be large, probably more than τ_G at 0°K.

The experiments of COTTRELL and STOKES,[13] ADAMS and COTTRELL[14] and HAASEN[3] have shown that for aluminium, copper and nickel, the flow stress ratio, throughout most of the stress–strain curve, is in fact temperature-independent above a certain temperature, when changes in the elastic constants are taken into account.

During the easy glide range, slip is essentially on one set of planes so the number of Lomer-Cottrell locks will be small and the rate of work hardening is low. The τ_G contribution is about half and the temperature-dependence is that of τ_S, and approximates to the temperature-dependence of the critical shear stress τ_0, as defined in Eqn. (2). In the easy glide range the ratio $\tau_S/\tau_G \sim 1$ but rapidly decreases to a value of about 0·5 in stage II. THORNTON[96] has found that values of U_0 determined from logarithmic creep tests on copper crystals in stage I do not vary much. The main change in τ_S/τ_G seems to be due to τ_G which changes continuously with increasing strain.

CONRAD[51] has done incremental loading creep tests on copper crystals and also tensile tests at 90°K and 170°K during which changes in strain rate were made. He found that the strain rate could be expressed thus.

$$\dot{\epsilon} = C \exp B(\tau - \tau_G) \quad . \quad . \quad . \quad . \quad . \quad . \quad (10)$$

where C and B are constants.

However, B is practically independent of temperature instead of being proportional to $1/\tau$ as required by the theory. Conrad concludes that the cutting through the forest cannot be the rate-controlling mechanism in stage I (and stage II), and puts forward an alternative mechanism involving the formation of "thermal kinks" in dislocations lying in close-packed directions.

The temperature dependence of the flow stress in stages II and III is much less than in stage I, so while in stage I $\tau_G \cong \tau_S$, in the latter stages of the stress–strain curve it must be concluded that $\tau_G \gg \tau_S$. However, one would expect that if τ_G increases more rapidly than τ_S in stage II then in strain rate experiments the ratio $\Delta\tau/\tau$ would decrease rapidly with increasing strain. Recent work by BASINSKI[55] shows that this ratio is constant and also that both the flow stress and strain rate sensitivity continue to increase down to 4°K. The conclusion is that τ_G and τ_S must be proportional to each other, so Basinski considers that they arise from the same source, namely, the dislocation forest. It is pointed out that there must be appreciable elastic interaction between intersecting dislocations on {111} planes which must be overcome before thermal agitation will help them to cut across each other. THORNTON and HIRSCH[40] have recently expressed a similar view on the basis of combined measurements of logarithmic creep and flow stress of a large number of close-packed cubic and hexagonal metals.

Stage 3 is initiated when thermally activated cross slip is sufficiently

VOL. 9 1961

extensive. Metals of high stacking fault energy such as aluminium more readily undergo cross-slip, so stage 3 will be obvious at lower temperatures and stresses than in copper crystals where the dissociation of the dislocations to form stacking faults renders cross slip more difficult.

10. Effect of Alloying on the Stress–Strain Curve

It is now well established that alloying elements in solid solution increase substantially the easy glide region. Garstone and Honeycombe [9] have shown

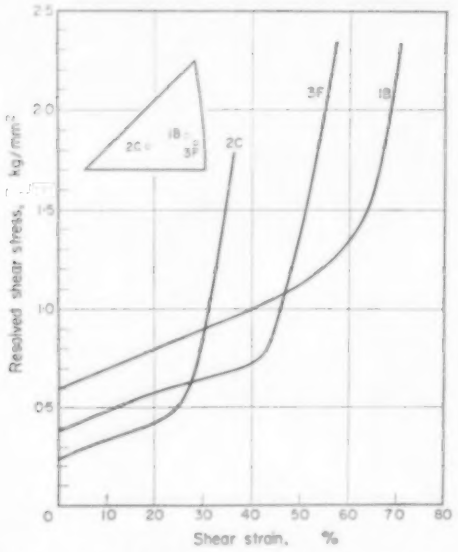

Fig. 24. Shear stress–shear strain curves of copper–silver crystals at 290°K.
2C. 0·13 at per cent Ag. 3F. 0·27 at per cent Ag.
1B. 0·5 at per cent Ag. (Garstone and Honeycombe[9]).

the effect of small concentrations of silver and gold on the easy glide range of copper crystals of comparable orientations (Fig. 24). They showed that while the length of stage 1 increases, the slope or coefficient of hardening remains practically unaltered.

Jaoul and Bricot [75] have found that additions of silicon (0·2 wt per cent) and copper (1 wt per cent) increase the easy glide range in aluminium. Greetham [76] has tested crystals containing ½ and 1 wt per cent silver, and 4·5 wt per cent copper in the solid solution condition, and found longer easy glide ranges than in pure aluminium crystals. Haeszner and Schrieber [83] have also observed that small concentrations of silver (up to 0·5 at. per cent) increase the length of stage 1 hardening.

Turning to alloys of higher concentration, α-brass crystals have received much attention, but it is doubtful whether their behaviour can be considered

to be typical of alloy crystals. MADDIN, MATHEWSON and HIBBARD[80] confirmed the much earlier work of VON GÖLER and SACHS[19] that 70/30 brass crystals exhibited a long stage 1 (20–30 per cent shear strain) with practically no hardening, followed by substantial hardening when secondary slip commenced. A further examination of α-brass crystals by PIERCY, CAHN and COTTRELL[81] confirmed this lack of strain hardening until secondary slip was observed, but showed that in stage 1 slip propagated by a type of Lüders

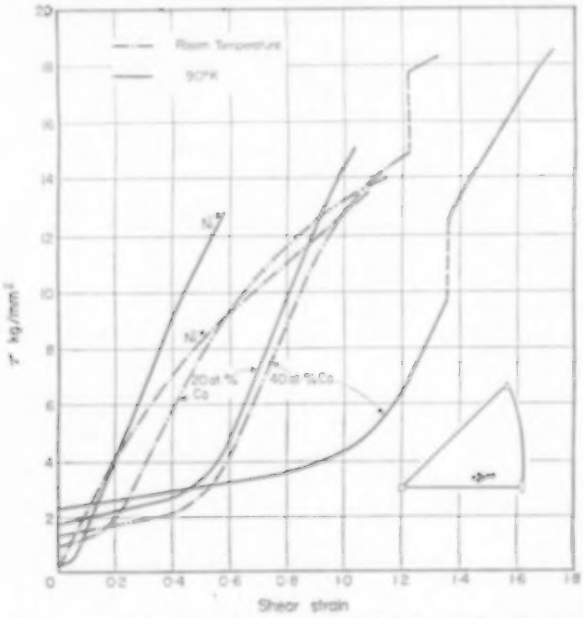

FIG. 25. Shear stress–shear strain curves of nickel–cobalt alloy crystals deformed at room temperature and at 90°K.
(MEISSNER[77]).

band from one end of the specimen. It is thus clear that the behaviour of α-brass crystals is intimately associated with a yield elongation; this region should not be directly related to the easy glide stage in other crystals.

The early work of OSSWALD[19] on copper–nickel crystals and SACHS and WEERTS[20] on gold–silver crystals over the complete solid solution range gave some indications of stage 1 hardening. However, this is more clearly brought out in the recent work of Meissner[77] on nickel–cobalt crystals over a wide composition range (Fig. 25). With a crystal containing 40 at. per cent cobalt, an easy glide range of 100 per cent shear strain was obtained at 90°K compared with only several per cent for the pure metals. In all of the alloys a fairly constant slope was observed for stage 1 indicating an appreciable but constant degree of strain hardening. Similar behaviour was observed by SACHS and WEERTS[20] with disordered crystals of Cu_3Au but not with the

ordered crystals; recent work by ARDLEY[82] has shown that for the early stages of deformation the ordered alloy crystals do not strain harden. Nevertheless, this behaviour cannot be regarded as typical, because of the effect arising from the destruction of order by movement of the initial dislocations.

SEEGER[78] has taken the behaviour of α-brass as typical of alloys with high solubility, and characterizes them by increasing easy glide and decreasing coefficient of work hardening. He distinguishes another class with limited solid solubility which has a work hardening coefficient for stage I comparable to that of the pure metal. However, it does not appear that α-brass exhibits behaviour typical of extensive solid solutions; for example, the behaviour of nickel–cobalt crystals is more akin to that of the more dilute aluminium and copper alloy crystals. Thus the normal behaviour of alloy crystals in stage I is not absence of strain hardening, but on the contrary, the coefficient of hardening is comparable to that in pure metals and the mechanism of hardening should be similar.

11. THE DEFORMATION OF TWO-PHASE ALLOY CRYSTALS

The formal dislocation theory of precipitation hardening due to MOTT and NABARRO is well established;[50, 90] one aspect of this theory has already been referred to in connection with solution hardening. The formation of precipitate particles represents a change in the wave length of the internal stresses which is dependent on the state of dispersion. However, the detailed mechanisms of the interaction of dislocations with zones and precipitates are still not fully determined. Most work on alloy crystals has been concentrated on stable solid solutions and it is only recently the mechanical properties of crystals containing zones or fine precipitates have been studied in detail.

In an early investigation, KARNOP and SACHS[85] studied the behaviour of crystals of an aluminium-5 wt per cent copper alloy in an aged and an over-aged conditions, and observed marked differences in the behaviour during deformation although no metallographic observations were made. CARLSEN and HONEYCOMBE[60] examined identically oriented crystals of an aluminium 3·5 per cent copper alloy in the air-cooled, aged to peak hardness and over-aged conditions. They found that the super-saturated solid solution exhibited easy glide and behaved like a pure metal, whereas aged and over-aged crystals showed no easy glide but marked parabolic hardening which was not very temperature-sensitive.

GREETHAM[70] has examined more closely the behaviour of aluminium-4·5 per cent copper crystals in several heat-treated conditions. Typical stress–strain curves for crystals of very similar orientations deformed at 77°K are shown in Fig. 26. Very big differences in the flow stress are apparent. The easy glide range is very pronounced in the solution-treated crystal, and is still evident in crystals aged 2 days at 130°C which contain G.P. I zones, although the absence of strain hardening is probably associated with a yield

phenomenon arising from the cutting through of zones by dislocation lines. The appearance of slip in the two types of crystal deformed at 77°K is similar. Fig. 27 shows a typical micrograph. As in the earlier work, the fully aged crystals showed marked parabolic hardening which was relatively insensitive to temperature in the range 77°K to room temperature. In this condition dislocations probably loop around the particles in the way first put forward by OROWAN[88] and developed by FISHER, HART and PRY.[87] The residual

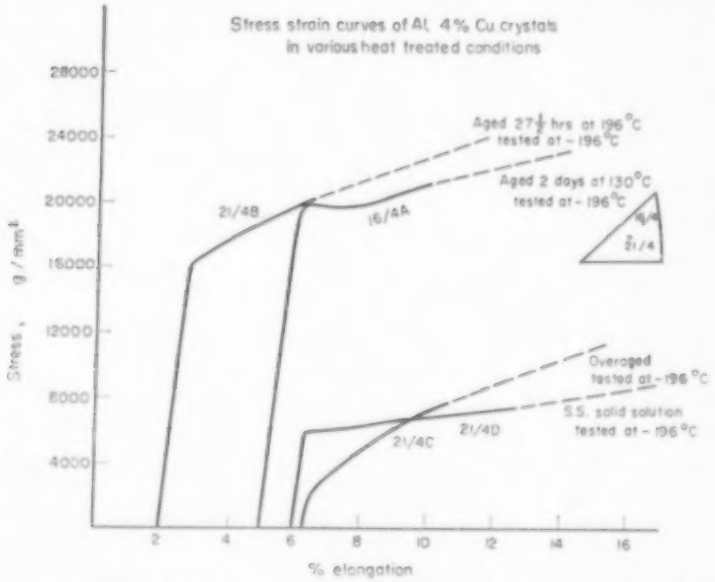

FIG. 26. Stress–strain curves of similarly oriented aluminium–4·5 per cent copper crystals in various heat-treated conditions. Deformed at 77°K. GREETHAM[76]).

dislocation rings act as obstacles for subsequent dislocations, leading to substantial strain hardening. Distinct slip bands are rarely shown in the optimum aged condition (Fig. 28) except in the region of fracture.[92] In over-aged crystals small regions of secondary slip are frequently associated with the large precipitate particles (Fig. 29), which could account for the high rate of work hardening observed.

KELLY and CHIOU[89] have investigated the effect of temperature on the flow stress of aluminium–4 per cent copper crystals aged at 125°C to produce G.P. 1 zones. They found that the critical resolved shear stress was fairly constant between 370°K and 150°K but rose substantially at 77°K (Fig. 30). These authors measured the reversible change of flow stress when the temperature was altered during deformation; and found that when corrections for changes in elastic constants were made, it was approximately constant above 150°K, a result similar to that obtained with pure aluminium. Analysis of their results on the Seeger model lead to a dislocation density for the

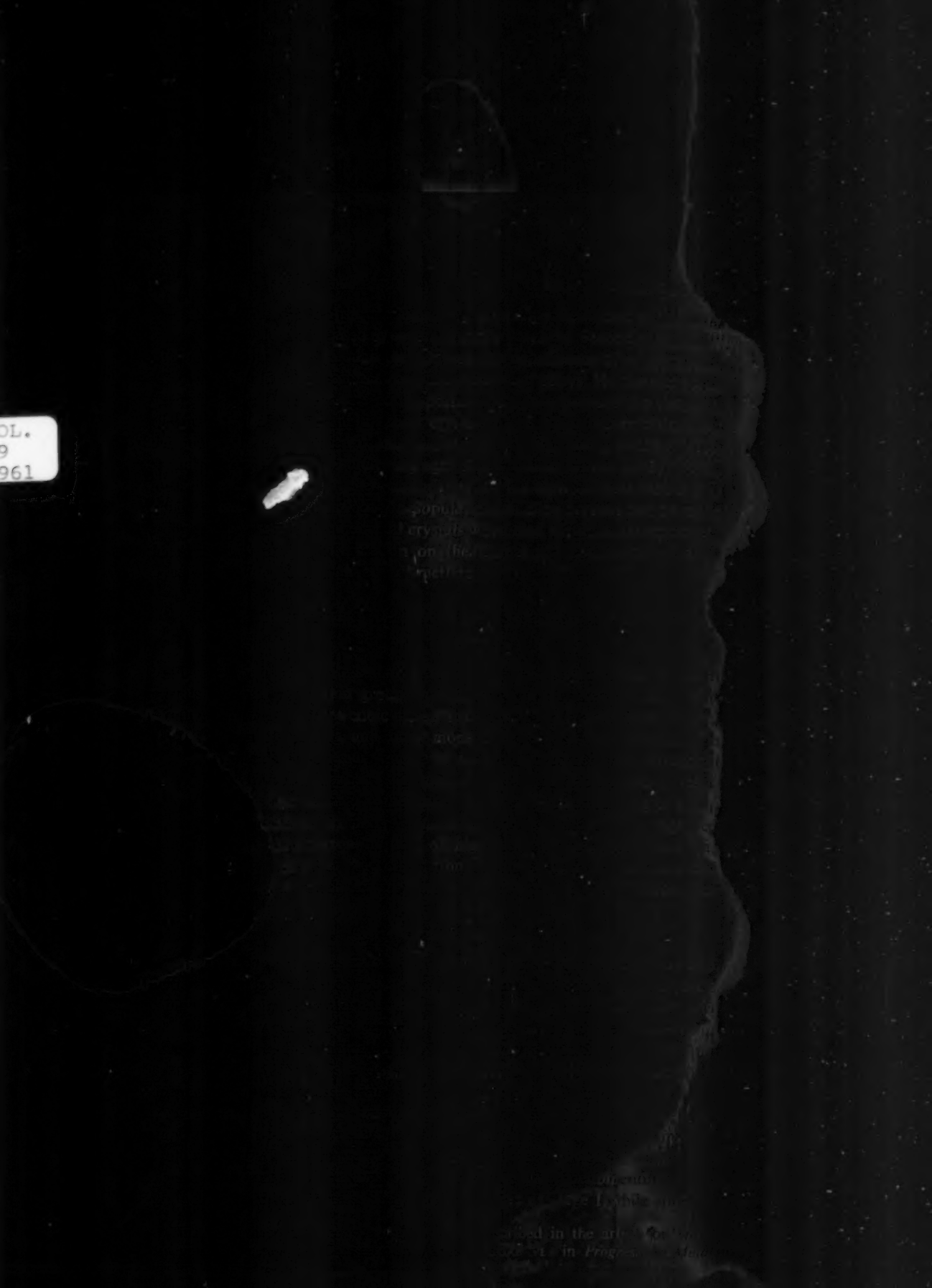
OL.
9
961

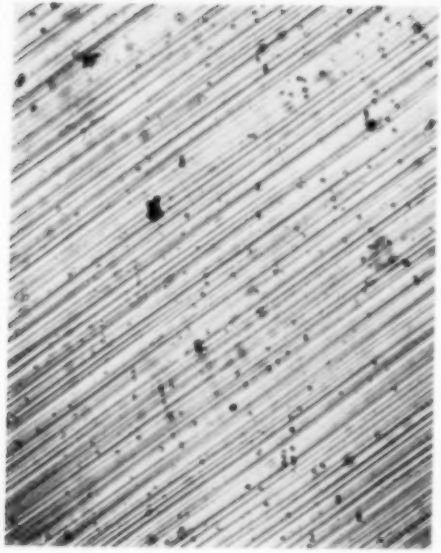

FIG. 27. Slip in aluminium–4·5 per
then deformed to 4% shea
(GRE

FIG. 28. Aluminium–4·5 per cent c
deformed to 11% shear strain at

FIG. 29. Aluminium–4·5 per cent co
to 28% shear strain a
(GRE

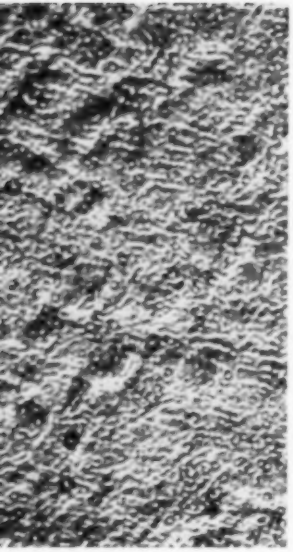

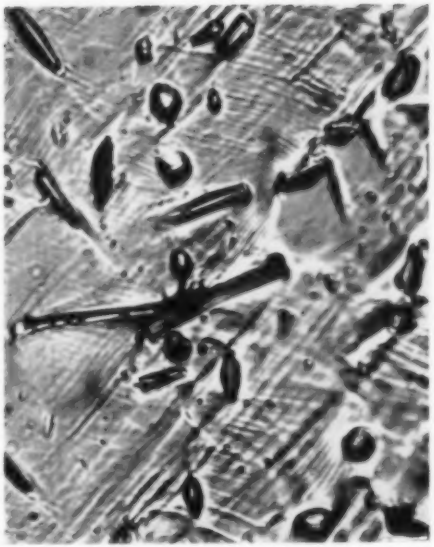

per cent copper crystal, aged 2 days at 130°C
, shear strain at 77°K. × 100
(GREETHAM[76]).

ent copper crystal aged 27½ hr at 190°C, then
ain at 77°K (GREETHAM[76]). × 100

nt copper crystal, furnace cooled then deformed
rain at 77°K. × 900
(GREETHAM[76]).

VOL.
9
1961

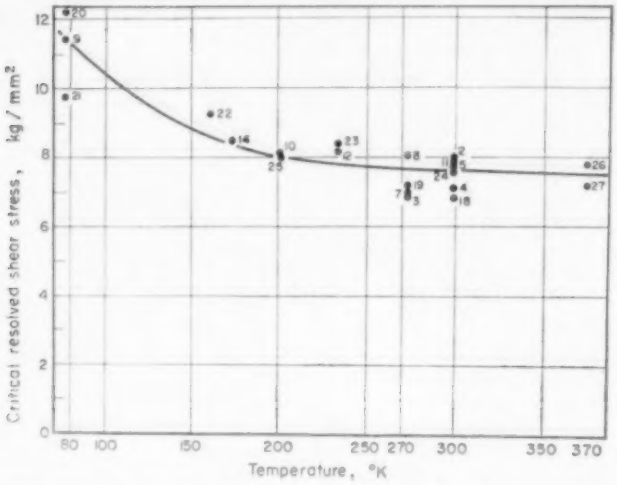

FIG. 30. Temperature dependence of τ_0, for aluminium–copper crystals containing G.P. zones (KELLY and CHIOU[89]).

forest of $10^{10} - 10^{12}$ lines/cm² to account for the high value of τ_S compared with that for pure aluminium. As there is no indication that such high dislocation densities exist, Kelly and Chiou accept the zone hardening concept of MOTT and NABARRO[90] and suggest that at the higher temperatures the zones are avoided by cross slip of screw dislocations in the way put forward by HIRSCH[91] for over-aged alloys. Greetham's results support the view that at 77°K the dislocations cut through the G.P. zones whereas at room temperature a different deformation mechanism occurs. The process at room temperature is however complicated by the occurrence of strain age-hardening.

Electron microscopy of thin metal films is likely to provide in the near future direct information on the question of the interaction of dislocations with zones and precipitates, and already one study of dislocations in quenched aluminium-4 per cent copper alloy films has been published.[95]

I am indebted to Dr. B. A. Bilby and Dr. W. J. M. Tegart who read the manuscript and made many helpful comments.

REFERENCES

[1] SEEGER, A.; *Dislocations and Mechanical Properties of Crystals*, p. 243–329 (Lake Placid Conference), John Wiley, 1957.
[2] SCHMID, E. and BOAS, W.; *Kristallplastizität*, Springer, 1936, (English translation published by F. A. Hughes, 1950).
[3] HAASEN, P.; *Phil. Mag.* 3 (1958) 384.
[4] ANDRADE, E. N. DA C. and ABOAV, D. A.; *Proc. Roy. Soc.* A240 (1957) 304.

(6) DIEHL, J.; *Z.f. Metallkunde* 47 (1956) 331.
(7) SEEGER, A.; *Z. Naturf.* 9A (1954) 758, 856, 870.
(7) FRIEDEL, J.; *Phil. Mag.* 46 (1955) 1169.
(8) ANDRADE, E. N. DA C. and HENDERSON, C.; *Phil. Trans.* 244 (1951–52) 177.
(9) GARSTONE, J. and HONEYCOMBE, R. W. K.; *Dislocations and Mechanical Properties of Crystals*, 391–405, John Wiley, 1957.
(10) CONRAD, H. and ROBERTSON, W. D.; *Trans. Amer. Inst. Min. (Metall.) Engrs.* 209 (1957) 503.
(11) SCHMID, E. and SIEBEL, G.; *Z. Electrochem.* 37 (1931) 447.
(12) GILMAN, J. J.; *Trans. Amer. Inst. Mech. Engrs.* 206 (1956) 1326.
(13) COTTRELL, A. H. and STOKES, R. J.; *Proc. Roy. Soc.* A233 (1956) 17.
(14) ADAMS, M. A. and COTTRELL, A. H.; *Phil. Mag.* 46 (2) (1955) 1187.
(15) ALLEN, N. P., HOPKINS, B. E. and MCLENNAN, J. E.; *Proc. Roy. Soc.* A234 (1956) 221.
(16) LINDE, J. O., LINDELL, B. O. and STADE, C. H.; *Ark. Fys.* 2 (11) (1950) 89.
(17) LINDE, J. O. and EDWARDSON, STURE; *Ark. Fys.* 8 (51) (1954) 511.
(18) VON GÖLER, F. and SACHS, G.; *Z. Physik* 55 (1929) 581.
(19) OSSWALD, E.; *Z. Physik* 83 (1933) 55.
(20) SACHS, G. and WEERTS, J.; *Z. Physik* 62 (1930) 473.
(21) JAMESON, R. E. and SHERRILL, F. A.; *Acta Met.* 4 (1956) 197.
(22) SUZUKI, H. (IKEDA, S. and TAKEUCHI, S.); *Dislocations and Mechanical Properties of Crystals*, p. 384, John Wiley, 1957.
(23) ROSI, F. D. and MATHEWSON, C. H.; *Trans. Amer. Inst. Mech. Engrs.* 188 (1950) 1159.
(24) LEVINE, E. D., SHEELY, W. F. and NASH, R. R.; *Trans. Met. Soc. Amer. Inst. Mech. Engrs.* 215 (1959) 521.
(25) SEEGER, A.; *Z. Naturforsch.* 9A (1954) 876.
(26) COTTRELL, A. H.; *Dislocations and Plastic Flow*, Oxford University Press, 1953.
(27) SUZUKI, H.; *Sci. Rep. Res. Inst. Tohoku Univ.* A4 (1952) 455.
(28) FISHER, J. C.; *Acta Met.* 2 (1954) 9.
(29) SUZUKI, H.; *Dislocations and Mechanical Properties of Crystals*, 361, John Wiley, 1957.
(30) TILLER, W. A.; *J. Appl. Phys.* 29 (1958) 611.
(31) MASING, G. and RAFFELSIEFER, J.; *Z. Metallkunde* 41 (1950) 65.
(32) LUCKE, K. and LANGE, H.; *Z. Metallkunde* 43 (1952) 55.
(33) DIEHL, J., MADER, S. and SEEGER, A.; *Z. Metallkunde* 46 (1956) 650.
(34) BLEWITT, T. H., COLTMAN, R. R. and REDMAN, J. K.; Report of a Conference on Defects in Crystalline Solids. Physical Society, 369, London, 1955.
(35) SUZUKI, H., IKEDA, S. and TAKEUCHI, S.; *J. Phys. Soc. Japan* 11 (1956) 382.
(36) SOSIN, A. and KOEHLER, J. S.; *Phys. Rev.* 101 (1956) 972.
(37) NOGGLE, T. S. and KOEHLER, J. S.; *J. Appl. Phys.* 28 (1957) 53.
(38) STAUDWASSER, W.; Thesis, University of Göttingen, 1954.
(39) FELTHAM, P. and MEAKIN, J. D.; *Acta Met.* 5 (1957) 555.
(40) THORNTON, P. R. and HIRSCH, P. B.; *Phil. Mag.* 3 (1958) 738.
(41) BROWN, A. F. and HONEYCOMBE, R. W. K.; *Phil. Mag.* 42 (1957) 1146.
(42) WILSDORF, H. and KUHLMANN-WILSDORF, D.; *Naturwissenschaften* 38 (1951) 502.
(43) SEEGER, A., DIEHL, J., MADER, S. and REBSTOCK, R.; *Phil. Mag.* 2 (1957) 323.
(44) MADER, S.; *Z. Physik.* 149 (1957) 73.
(45) NOGGLE, T. S. and KOEHLER, J. S.; *Dislocations and Mechanical Properties of Crystals*, p. 208, John Wiley, 1957.
(46) SUZUKI, H. and BARRETT, C. S.; *Acta Met.* 6 (1958) 156.
(47) ROSI, F. D.; *Trans. Amer. Inst. Min. (Metall.) Engrs.* 200 (1954) 1009.
(48) FRIEDEL, J.; *Proc. Roy. Soc.* A242 (1957) 147.

VOL.
9
1961

(49) BASINSKI, Z. S.; *Proc. Roy. Soc.* A240 (1957) 229.
(50) MOTT, N. F.; *Imperfections in Nearly Perfect Crystals*, ed. W. Shockley, John Wiley, 1952.
(51) CONRAD, H.; *Acta Met.* 6 (1958) 339.
(52) LÜCKE, K., MASING, G. and SCHRÖDER, K.; *Z. Metallkunde* 46 (1955) 792.
(53) DERUYTTERE, A. and GREENOUGH, G. B.; *J. Inst. Metals* 84 (1956) 337.
(54) FAHRENHORST, W. and SCHMID, E.; *Z. Physik* 64 (1930) 845.
(55) BASINSKI, Z. S.; *Phil. Mag.* 4 (1959) 393.
(56) SCHMID, E. and WASSERMAN, G.; *Handbuch der physikalische und technische mechanik* 4 (2) (1931) 319.
(57) BAKARIAN, P. W. and MATHEWSON, C. H.; *Trans. Amer. Inst. Min.* (*Metall.*) *Engrs.* 152 (1943) 226.
(58) BURKE, E. C. and HIBBARD, W. R.; *Trans. Amer. Inst. Min.* (*Metall.*) *Engrs.* 194 (1952) 295.
(59) REED-HILL, R. E. and ROBERTSON, W. D.; *Trans. Amer. Inst. Min.* (*Metall.*) *Engrs.* 209 (1957) 496.
(60) BELL, R. L. and CAHN, R. W.; *Proc. Roy. Soc.* A239 (1957) 494.
(61) GILMAN, J. J.; *Trans. Amer. Inst. Min.* (*Metall.*) *Engrs.* 203 (1955) 206; 206 (1956) 998.
(62) CHURCHMAN, A. T. and JEFFERY, H.; unpublished work.
(63) ROSI, F. D., DUBE, C. A. and ALEXANDER, B. H.; *Trans. Amer. Inst. Min.* (*Metall.*) *Engrs.* 197 (1953) 257.
(64) LUSTMAN, B. and KERZE, F.; *The Metallurgy of Zirconium*, McGraw-Hill, 1955.
(65) TUER, G. L. and KAUFMANN, A. R.; *The Metal Beryllium*, Amer. Soc. Metals, p. 372, 1955.
(66) JILLSON, D. C.; *Trans. Amer. Inst. Min.* (*Metall.*) *Engrs.* 188 (1950) 1129.
(67) VOGEL, F. L. and BRICK, R. M.; *Trans. Amer. Inst. Min.* (*Metall.*) *Engrs.* 197 (1953) 700.
(68) MADDIN, R. and CHEN, N. K.; *Trans. Amer. Inst. Min.* (*Metall.*) *Engrs.* 200 (1950) 280; CHEN, N. K. and MADDIN, R.; *Trans. Amer. Inst. Min.* (*Metall.*) *Engrs.* 191 (1951) 937.
(69) BOAS, W. and SCHMID, E.; *Z. Physik* 61 (1930) 767.
(70) CHURCHMAN, A. T. and SMITH, E.; Private communication.
(71) ROSI, F. D.; *Trans. Amer. Inst. Min.* (*Metall.*) *Engrs.* 200 (1954) 58.
(72) CHURCHMAN, A. T.; *Proc. Roy. Soc.* A226 (1954) 216.
(73) COTTRELL, A. H.; *J. Chart. Mech. Engnrs.*, 448, November 1957.
(74) CLARK, D. S. and WOOD, D. S.; *Proc. Amer. Soc. Test. Mat.* 49 (1949) 717.
(75) JAOUL, B. and BRICOT, I.; *Rev. Met.* 52 (1955) 629.
(76) GREETHAM, G.; Ph.D. thesis, University of Sheffield, 1959.
(77) MEISSNER, J.; *Z. Metallk.* 50 (1959) 207.
(78) SEEGER, A.; *Handbuch der Physik*, Vol. 7, No. 2, Kristallphysik 2, Springer, 1958.
(79) MAKIN, M. J.; *Phil. Mag.* 3 (1958) 309.
(80) MADDIN, R., MATHEWSON, C. H. and HIBBARD, W. R.; *Trans. Amer. Inst. Min.* (*Metall.*) *Engrs.* 185 (1949) 527.
(81) PIERCEY, G. R., CAHN, R. W. and COTTRELL, A. H.; *Acta Met.* 3 (1955) 331.
(82) ARDLEY, G. W.; *Acta Met.* 3 (1955) 525.
(83) HAESZNER, F. and SCHRIEBER, D.; *Z. Metallk.* 48 (1957) 263.
(84) SACHS, G. and WEERTS, J.; *Z. Physik* 67 (1931) 507.
(85) KARNOP, R. and SACHS, G.; *Z. Physik* 49 (1928) 480.
(86) CARLSEN, K. M. and HONEYCOMBE, R. W. K.; *J. Inst. Metals* 83 (1955) 449.
(87) FISHER, J. E., HART, E. W. and PRY, R. H.; *Acta Met.* 1 (1953) 336.
(88) OROWAN, E.; Institute of Metals, Symposium on Internal Stresses in Metals and Alloys, 451, 1948, 1.

[89] KELLY, A. and CHIOU, C.; *Acta Met.* 6 (1958) 565.
[90] MOTT, N. F. and NABARRO, F. R. N.; Report on Conference on Strength of Solids, Physical Society, London, 1948, 1.
[91] HIRSCH, P. B.; *J. Inst. Metals* 86 (1957) 13.
[92] BEEVERS, C. J. and HONEYCOMBE, R. W. K.; *Proceedings of Conference on Fracture*, Swampscott, U.S.A., 1959.
[93] COX, J. J., HORNE, G. T. and MEHL, R. F.; *Trans. Amer. Soc. Metals* 49 (1957) 118.
[94] LEE, H. T. and BRICK, R. M.; *Trans. Amer. Soc. Metals* 48 (1956) 1003.
[95] THOMAS, G. and WHELAN, M. J.; *Phil. Mag.* 4 (1959) 511.
[96] THORNTON, P. R.; Ph.D. Thesis, University of Cambridge, 1958.
[97] FLINN, P. A.; *Acta Met.* 6 (1958) 631.

VOL.
9
1961

CONTENTS OF PREVIOUS VOLUMES IN THE PROGRESS OF METAL PHYSICS SERIES

OL.
9
961

VOLUME 1

Progress in the Theory of Alloys G. V. RAYNOR
Theory of Dislocations A. H. COTTRELL
Crystal Boundaries R. KING and B. CHALMERS
Age Hardening of Metals G. C. SMITH
Hardening Response of Steels E. H. BUCKNALL and W. STEVEN
Preferred Orientation in Non-Ferrous Metals T. Ll. RICHARDS
Diffusion of Metals in Metals A. D. LE CLAIRE

VOLUME 2

Order-Disorder Changes in Alloys H. LIPSON
Rate Process in Physical Metallurgy I. I. BETCHERMAN
Anisotropy in Metals W. BOAS and J. K. MACKENZIE
Developments in Magnesium Alloys H. G. WARRINGTON
Internal Strains and Recrystallization R. W. CAHN
Researches on the Polygonization of Metals A. GUINIER and J. TENNEVIN
Polygonization in Strongly Deformed Metals C. CRUSSARD, F. AUBERTIN, B. JAOUL and G. WYON

VOLUME 3

Crystallography of Transformations J. S. BOWLES and C. S. BARRETT
Properties of Metals at Low Temperatures D. K. C. MacDONALD
Recent Advances in the Electron Theory of Metals N. F. MOTT
Twinning R. CLARK and G. B. CRAIG
Ferromagnetism URSULA M. MARTIUS
Quantitative X-ray Diffraction Observations on Strained Metal Aggregates G. B. GREENHOUGH
Recrystallization and Grain Growth J. E. BURKE and D. TURNBULL
Structure of Crystal Boundaries B. CHALMERS

VOLUME 4

Internal Friction in Metals A. S. NOWICK
The Mechanism of Oxidation of Metals and Alloys at High Temperatures KARL HAUFFE
Gases in Metals C. R. CUPP
The Theory of Sintering G. A. GEACH
Theory of Dislocations A. H. COTTRELL
Diffusion in Metals A. LE CLAIRE
Nucleation J. H. HOLLOMON and D. TURNBULL

VOLUME 5

The Fracture of Metals N. J. PETCH
Geometrical Aspects of the Plastic Deformation of Metal Single Crystals R. MADDIN and N. K. CHEN
The Structure of Liquid Metals B. R. T. FROST
Report of Precipitation H. K. HARDY and T. J. HEAL
Solidification of Metals URSULA M. MARTIUS

VOLUME 6

The Effect of Hydrostatic Pressure on the Electrical Resistivity of Metals A. W. LAWSON
The Filamentary Growth of Metals H. K. HARDY
The Austenite : Pearlite Reaction R. F. MEHL and W. C. HAGEL
Recent Advances in Knowledge Concerning the Process of Creep in Metals A. H. SULLY
The Mechanism of Evaporation O. KNACKE and I. N. STRANSKI
Mosaic Structure P. B. HIRSCH

VOL.
9
1961

VOLUME 7

Equilibrium, Diffusion and Imperfections in Semiconductors J. N. HOBSTETTER
The Physical Metallurgy of Titanium Alloys R. I. JAFFEE
Thermodynamics and Kinetics of Martensitic Transformations LARRY KAUFMAN and MORRIS COHEN
The Stored Energy of Cold Work A. L. TITCHENER and M. B. BEVER
The Properties of Metals at Low Temperatures H. M. ROSENBERG

VOLUME 8

Work Hardening of Metals L. M. CLAREBROUGH and M. E. HARGREAVES
Grain Boundaries in Metals F. WEINBERG
X-ray Studies of Deformed Metals B. E. WARREN
Substructures in Crystals Grown from the Melt C. ELBAUM
Defects in Pure Metals W. M. LOMER

PROGRESS IN MATERIALS SCIENCE VOLUME 9
(INCORPORATING PROGRESS IN METAL PHYSICS)
GENERAL EDITOR: BRUCE CHALMERS

Effects of Environment on Mechanical Properties of Metals

by
IRVIN R. KRAMER
Martin Company, Baltimore, Maryland.
and
LOUIS J. DEMER
University of Arizona, Tucson, Arizona

PERGAMON PRESS
OXFORD · LONDON · NEW YORK · PARIS

PERGAMON PRESS LTD.
Headington Hill Hall, Oxford
4 & 5 *Fitzroy Square, London, W.*1

PERGAMON PRESS INC.
122 *East* 55*th Street, New York* 22, *N.Y.*
Statler Center 640, 900 *Wilshire Boulevard,*
Los Angeles, California

PERGAMON PRESS S.A.R.L.
24 *Rue des Écoles, Paris V*e

PERGAMON PRESS G.m.b.H.
Kaiserstrasse 75, *Frankfurt-am-Main*

VOL.
9
1961

Copyright
©
1961
PERGAMON PRESS LTD.

Library of Congress Card Number 49—50107

Set in Times New Roman 10/12pt. and
made and printed in Great Britain at Page Bros. (Norwich) Ltd.

PROGRESS IN MATERIALS SCIENCE

(INCORPORATING PROGRESS IN METAL PHYSICS)

PUBLISHER'S NOTE

THE twelve years that have elapsed since the publication of the first volume of PROGRESS IN METAL PHYSICS has seen a great increase in the rate of publication of papers in this, as in most other fields of science, and realization that the physics of metals is an important part of, but not the whole of, the science of materials, a field of considerable practical and theoretical importance.

It is becoming extremely difficult, if it is not already impossible, for most scientists to keep up-to-date in their own and closely related fields by reading all the relevant original papers; one approach to the solution of this problem is the provision of adequate up-to-date critical review articles. For these reasons the Editor and the Publisher of PROGRESS IN METAL PHYSICS have decided to broaden the subject matter to include the whole of the field of the Science of Materials, and, in order to ensure maximum availability, to publish each article as a separate entity; thus, an individual subscriber need no longer purchase a whole volume in order to obtain some of the articles. This new procedure will make it possible to publish each article within five months of its receipt by the Editor.

VOL.
9
1961

EFFECTS OF ENVIRONMENT ON MECHANICAL PROPERTIES OF METALS

Contents

I. General Introduction 133

II. Oxide and Metal Films 134
Background in dislocation theory 134
Effect on critical resolved shear stress 136
Critical stress for twinning in metal crystals 144
Effect on shape of the stress–strain curve 145
Strain rate effects on the shape of the stress–strain curve 150
Microscopic deformation characteristics 151
Surface effects on fracture 154
Creep effects 157
Internal friction and abnormal after-effects 161
General ductility and strength 163
Effects on fatigue properties 164

III. Surface-active Agents and Electrolytes 165
Theoretical background 165
Effects of surface-active agents 170
Effects of electrolytes 173
Investigations of mechanisms of the weakening effect 180
Effects on polycrystalline metals 190

IV. Discussion 192

Acknowledgement 196
References 196

VOL.
9
1961

EFFECTS OF ENVIRONMENT ON MECHANICAL PROPERTIES OF METALS

Irvin R. Kramer and Louis J. Demer

OL.
9
961

I. General Introduction

Scientific interest in the effects of surface films on the mechanical properties of metals was promoted by the discovery of Roscoe[1] in 1934 that solid, thin films of oxide exert a profound effect on the mechanical properties of cadmium crystals, generally increasing their strength. Many experimental studies conducted since that time have provided numerous additional instances of similar effects which, under certain conditions, are exerted by extremely thin films on the mechanical properties of metals in general. The investigations have been concerned principally with the effects on their plastic properties.

There have been few attempts at presenting reviews of the general phenomena observed in this field of surface effects dealing with the mechanical properties. A report by Glen[2] which, unfortunately, was never published, is possibly the only attempt thus far to present an inclusive, critical review of this wide field of surface effects. A less inclusive review by Andrade[3] treated substantially the same effects. However, both of these are outdated and neither touched upon effects noted in connection with the fatigue and corrosion-fatigue properties of materials. Other papers such as those by Gilman[4] and Weiner and Gensamer[5] have included brief reviews of specific parts of the field dealing with the effects of metal films on certain mechanical properties of crystals, and a publication by Lichtman, Rehbinder and Karpenko[6] dealt generally with the effects of surface-active media on the mechanical behavior of solids.

This article presents a review of the current situation concerning various surface effects on metals. Included are experimental observations of the effects on the tensile, bending, creep, fatigue and the abnormal elastic after-effects, internal friction and damping behavior of metals. Not discussed in the following are effects resulting from the technological hardening processes involving surface alloying additions, nor the effects of purposefully introducing surface internal stresses. Results of these processes have been dealt with separately and extensively in the technical literature. Other effects which are also of considerable importance on mechanical properties, but of which mention will be omitted here because of space limitations, are the

effects of size and shape of the specimen, effects of surface finish, effects of surface bombardment by nonpenetrating particle radiation, and surface effects in the wear behavior of metals.

Discussed in the following sections are effects on the mechanical properties of metals due to thin metal films, oxide and similar films, and the effects of surface adsorption from solutions containing surfactants and electrolytes. It has been observed that most of these effects are considerably larger for single crystals than for polycrystalline aggregates with respect to most of the mechanical properties. The emphasis has been on single crystal studies with the objective of gaining better understanding of the fundamental deformation mechanisms. However, even with polycrystalline metals these effects are often found to exert considerable influence on certain of the mechanical properties and, therefore, may be of considerable practical importance.

VOL.
9
196

II. Oxide and Metal Films

Background in Dislocation Theory

Consideration of the theory of dislocations as it has developed over the past quarter of a century now leads to certain expected behaviors and effects of solid surface films on the mechanical properties of metallic crystals. It is now reasonably clear that such a film might be expected to exert effects on the initiation of plastic flow, on the rate of work hardening and the shape of the whole stress–strain curve, and also on the fracture characteristics. It is true that the majority of these concepts have arisen subsequent to experimental findings over the years. Nonetheless, it seems appropriate for purposes of presentation to discuss some of the ideas underlying the mechanism of the phenomena concerned with the mechanical effects of solid surface films before examining the results of the experimental studies.

Dislocation theory suggests that a thin surface film may exert an important effect on the initiation of slip in crystals if this is due primarily to surface sources. It has been explained by Fisher [7] that a surface Frank-Read source can result from a dislocation segment that is pinned at one end, with the other end terminating at the surface of the crystal. Such a surface source can be considered as pinned to a point outside the crystal resulting in an effective length of twice its actual length. Thus the critical stress for generating such a half loop at such a surface source is $\tau_s/G \approx b/2L_s$ where L_s is the distance from the pinned point to the surface, G is the shear modulus, and b is the magnitude of the Burgers vector. The initial stress to activate a Frank-Read dislocation source within a crystal is $\tau_i/G \approx b/L_i$ where L_i is the distance between pinning points. Thus, assuming statistically similar distributions for L_s and L_i for the crystal, it is indicated that the stress required to generate dislocation loops at the average surface source should be about half that for generating loops at the average interior source.

The above reasoning supports the idea that surface sources can play an important role in the deformation of metal single crystals. This possibility

exists since only moderate strengthening of the surface of a metal crystal should then produce equal strengthening of the entire crystal if surface Frank-Read sources are responsible for flow. In this case, then, a thin surface film should raise the actual critical resolved shear stress of a crystal by a factor having a maximum value of about two.

Dislocation theory further indicates that a dislocation approaching a free surface of a crystal experiences an attractive force tending to draw it from the crystal. An explanation of this behavior, given by COTTRELL,[8] is that the work required to move the dislocation through the lattice is lessened due to the absence of the periodic structure on the outside of the crystal surface, thereby reducing the strain energy of the dislocation stress field ahead of the dislocation approaching the surface. The resultant condition may be represented by the presence of a dislocation of opposite sign existing on the opposite side of the boundary an equal distance away from the boundary. Thus, the force of attraction increases as the crystal dislocation gets nearer to the surface.

No surface of a reactive metal specimen, however, is completely free from all surface contamination, especially if the metal is in air. In practically all cases a thin oxide film is formed on the surface. When such a thin surface film is present on the surface of a metal crystal, it can be expected to exert an effect on a dislocation approaching the surface. There are, in this case, two discontinuities in the crystal structure: (1) between the metal crystal and the surface film, and (2) between the film and the surrounding medium. The crystal structure of an oxide or similar film, or of an applied metal film, may be expected to differ from that of the base crystal in its type of atomic structure and certainly in the atomic spacing, thus creating a degree of atomic misfit. Furthermore, the elastic properties of the film and the base crystal would ordinarily be dissimilar.

There are three situations possible when a dislocation approaches a film-covered surface in a real crystal: (1) it experiences some attraction, but smaller than that if the surface were entirely clean, (2) the surface exerts little effect, or (3) the dislocation experiences a degree of repulsion, the strength of which is dependent upon the relative structural characteristic and elastic properties of the film and the substrate crystal. The latter case would result in an increase in the stress required for initiation of slip.

A current view of fracture in metals postulates that the stress concentration due to pile-ups of dislocations results in sufficiently high stresses to initiate a crack. Any factors which affect the dislocation distribution throughout a metal crystal may be expected to have an effect on the fracture characteristics. The presence of a thin film on the surface may exert a retarding effect on the progress of dislocations through the film and cause dislocation pile-ups. The resulting stress concentrations would promote cracking and the onset of fracture at a far smaller strain than in the absence of such a film.

Although the various ideas presented above have been only lightly treated, it may be well to consider their implications in reviewing the results of some

of the experimental investigations performed. This may promote an understanding of the effects of thin solid surface films on the mechanical behavior of metals. The various studies in this field have employed a number of different experimental tests and techniques, but in all of these the aim was to obtain further information on effects obtained either on the initiation, the progress, or the termination of plastic flow. The general division of experimental work to be reviewed has been made in accordance with this classification.

Effect on Critical Resolved Shear Stress

ROSCOE[1] in 1934, using cadmium wire single crystals, found that the conditions at the surface exercised a surprisingly large effect on the critical resolved shear stress of the crystals. He reported[9] that an oxide film less than 20 atoms thick on cadmium crystals caused an increase of approximately 50 per cent. An increase in the thickness of the oxide film to approximately 1200 atoms increased the initial stress for slip by a factor of nearly 100 per cent. He also found that the effect for a particular thickness of surface film decreased with increase in specimen thickness. He noted no dependence of the effect on crystal orientation. Removing the oxide film on a crystal by brushing the surface with a dilute acid reduced the critical shear stress to the normal value.

Roscoe considered that the observed strengthening effects could not be due to any strength of the oxide film, firstly, because of the thinness of the film and, secondly, because of an observed increase in flow stress as deformation proceeded. A decrease in flow stress would have occurred on rupture of the oxide film if its tensile strength were a determining factor. It was suggested that the observed effects indicated initiation of slip at the surface of a crystal and proceeding inward. He suggested that the added strength had its origin in the healing of submicroscopic cracks by the film analogous to the behavior of rock salt, as shown by JOFFÉ,[10] in its behavior under water.

A number of other investigators also examined the effect of oxide coatings on the critical shear stress for slip in crystals. COTTRELL and GIBBONS[11] in confirmation of Roscoe's results reported that the presence of a thin oxide film on cadmium crystals free from nitrogen increased the critical shear stress from 12 to 30 g/mm². HARPER and COTTRELL[12] on investigating the effects of various surface treatments on the plastic properties of zinc crystals also confirmed Roscoe's strengthening effect. They reported that electrolytically polished specimens had critical shear stresses of about 33 g/mm² whereas specimens etched in HCl and steamed for 1 hr had values up to 65 g/mm².

A significant point to consider with respect to these findings is that the amount of increase in critical shear stress reported as due to a particular surface condition is rather severely dependent on the particular definition of critical shear stress employed. This has been taken variously as the stress at the first recognizable departure from elastic behavior (which is very

VOL. 9 1961

dependent on strain measuring sensitivity), the intersection of the extensions of the elastic and initial plastic portions of the stress–strain curve, or the stress at an arbitrary value of strain (which might vary from 0.05 per cent to 0.5 per cent strain).

The actual mechanism of strengthening imposed by a surface film should determine whether the stress for the initiation of slip is markedly increased or whether the stress for continuation of slip is greatly affected. An early investigation of this point was made by HARPER and COTTRELL[12] who examined the very early stages of plastic flow in detail for two sets of zinc single crystal specimens: (*a*) electrolytically polished, and (*b*) lightly etched to produce a thin surface film (through the attack of dilute HCl). Flow stress measurements were made at extensions of 0.05, 0.1, 0.5 and 1 per cent. The results showed that at a rate of strain of about 10^{-2} per sec, the critical shear stresses for the two groups of specimens started at about the same value and that the greater strength of the etched specimens did not appear until some plastic deformation had occurred. When this experiment was repeated at a lower strain rate, 10^{-5} per sec, the difference between the polished and etched specimens was no longer detectable. It was concluded that the greater strength of the etched specimens was a dynamical effect connected with the amount and rate of plastic flow, rather than with the stress required to start flow.

Experiments concerning the effect of oxide films on the critical stress have been performed on metals other than those having a hexagonal crystal structure. TAKAMURA[13] compared the stress–strain curves for aluminum crystals with different thicknesses of oxide films. In addition to measuring strain, the amount of macroscopic twisting about the tension axis during the course of plastic extension was observed in an apparatus which permitted such twisting to occur. Similar twisting in single crystal rods has also been observed by PAXTON and COTTRELL.[14] Results of tests on two crystals of aluminum are shown in Fig. 1. The oxide coating thickness was reported as 100 Å and 500 Å for crystals *A* and *B*, respectively. Critical resolved shear stress values of 76 and 174 g/mm² were reported by Takamura for the tests as indicated by the arrows in the figure.

In Takamura's tests it was found that the crystal twisting occurred during the plastic extension and gave a very sensitive indication of slip. In the specimen with the thicker anodic film, slip bands could not be detected microscopically up to the yielding stress, but the twisting was observed to have begun at a much lower stress. He considered this as strong evidence that submicroscopic fine slip had already occurred far below the yielding stress, but that the dislocations approaching the surface had been held up by the presence of a surface film. In this view, the yield point is interpreted as the stress at which the surface film can no longer withstand the pressure of piled-up dislocations.

FLEISCHER and CHALMERS[15] in studying size effects in the deformation of aluminum also drew some conclusions concerning the effects of an oxide film. From computations made on their results, they obtained an effective

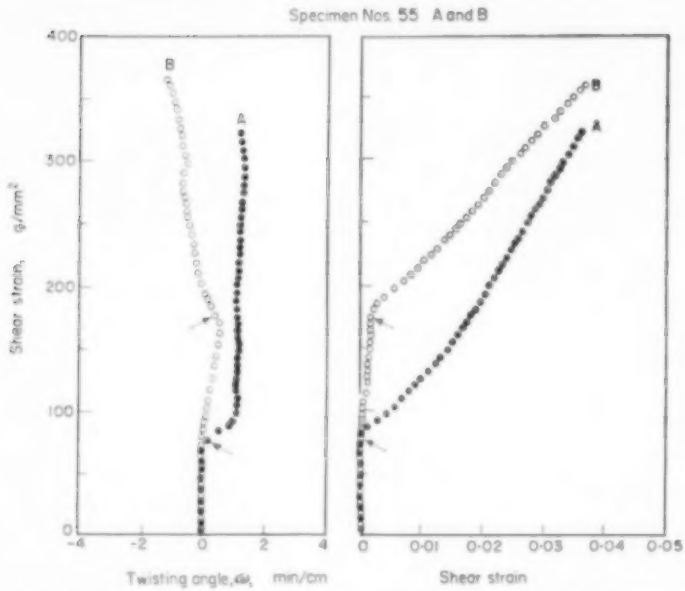

FIG. 1. Correlation between stress–strain curves and stress-twisting curves at the early stages of deformation. TAKAMURA.[13]

shear strength of a thin oxide film approximately equal to the theoretical value for a perfect solid. They attributed the origin of the high stress at the oxide to either the piling up of dislocations from the interior of the crystal or the suppression of surface sources. According to HEAD,[16] to oppose the motion of dislocations, the oxide should have a larger shear modulus than the bulk material. This could explain why the size effect on the yield stress is large for aluminum and cadmium, as reported by ROSCOE[9] and MAKIN and ANDRADE,[17] but not for copper as reported by SUZUKI *et al.*[18]

ANDRADE and HENDERSON[19] noted that the surface contamination of silver single crystals which takes place by exposure to air at room temperature raises the critical shear stress to a small degree but has more effect on the hardening after considerably greater strain has occurred.

Effects on the critical shear stress due to the deposition of various metal films on metal crystals have been reported by a number of investigators. Among these, LIPSETT and KING[20] found that thin gold films increased the stress at which plastic deformation started in cadmium single crystals by about 25 per cent of the critical shear stress of uncoated crystals. They found no variation with film thickness ranging from 1500 to 24,000 Å and no significant increase in the effect of the film when straining at four times the normal testing rate, that is, at 0.25 mm/min. A curve of their results is shown in Fig. 2. χ_0 and λ_0 refer to the initial angles between the specimen axis and the slip plane and slip direction, respectively.

VOL. 9 1961

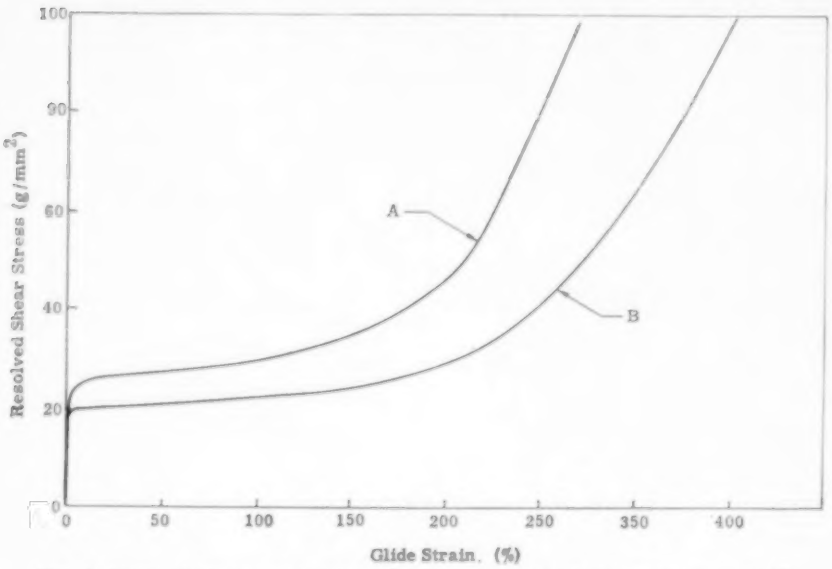

FIG. 2. Stress–strain curves for sections of a crystal of cadmium with $\chi_0 = 14.5°$ and $\lambda_0 = 15°$. A, as-grown and annealed sections. B, sections with gold film 12,000 Å thick. LIPSETT and KING.[20]

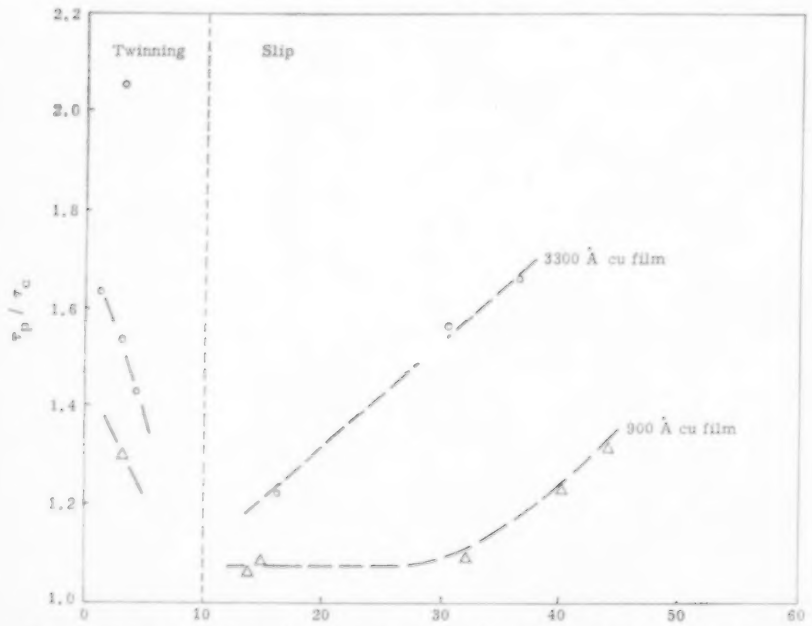

FIG. 3. Orientation dependence of the effect of a copper plate on the critical shear stress of zinc crystals. τ_p is the critical shear stress of the plated crystal; τ_c is the critical shear stress of the clean crystal. GILMAN and READ.[21]

GILMAN and READ[21] earlier found that plated copper films raised the tensile stress–strain curves of zinc, tin and lead crystals by an amount too large to be explained by the strength of the copper alone. The difference between the stress–strain curves was greater at moderate (10 per cent) strains than at small strains. Similar results were obtained for copper, nickel, gold and zinc plates ranging in thickness from 700 to 6000 Å. The magnitude of the copper plate effect on the critical shear stress for a given thickness varied

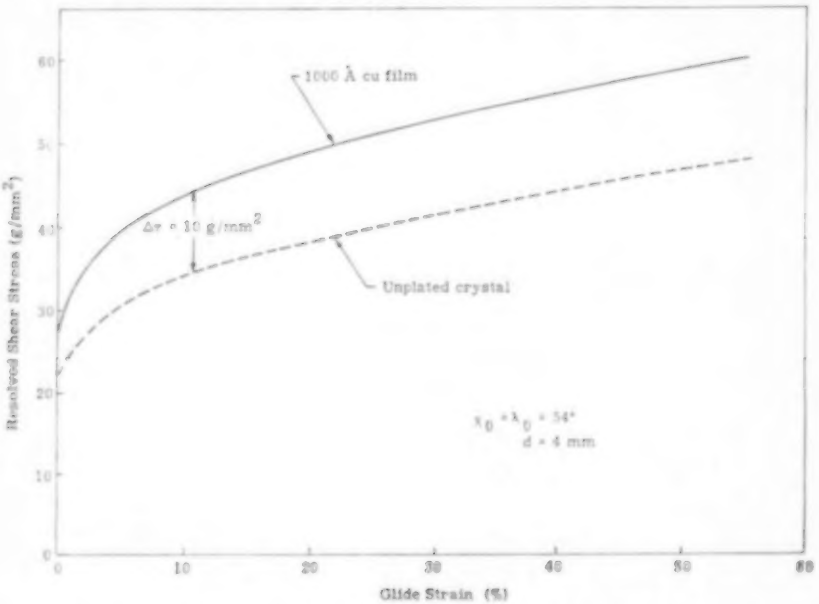

FIG. 4. Comparison of stress–strain curves for zinc crystal with copper surface film and crystal with etched surface. GILMAN.[4]

with orientation as indicated in Fig. 3. Effects to be mentioned later were also noted in this work on the critical stress for twinning as seen in the figure.

GILMAN[4] later presented data comparing the stress–strain curves for a zinc crystal with a copper surface film and a crystal with its surface etched with hydrochloric acid to clean it, and indicated somewhat different results. From curves such as those shown in Fig. 4, Gilman observed that the copper had little or no effect on the initial yield stress of the plated crystal but that the initial strain hardening rate was higher for this crystal than for the clean one. He concluded that the fact that the critical yield stress of crystals is not appreciably affected by surface films shows that the films do not support the entire load.

GARSTONE, HONEYCOMBE and GREETHAM[22] found an effect caused by an electro-deposited metal film much thicker than that employed by Gilman. They reported that a copper crystal plated with 10,000 Å of nickel did not

VOL. 9 1961

show an effect, but with the addition of a further 10,000 Å of chromium, a marked increase in the critical shear stress and elimination of Stage I of the stress–strain curve occurred as shown in Fig. 5. The thickness of the film in this case was appreciably greater than those previously discussed.

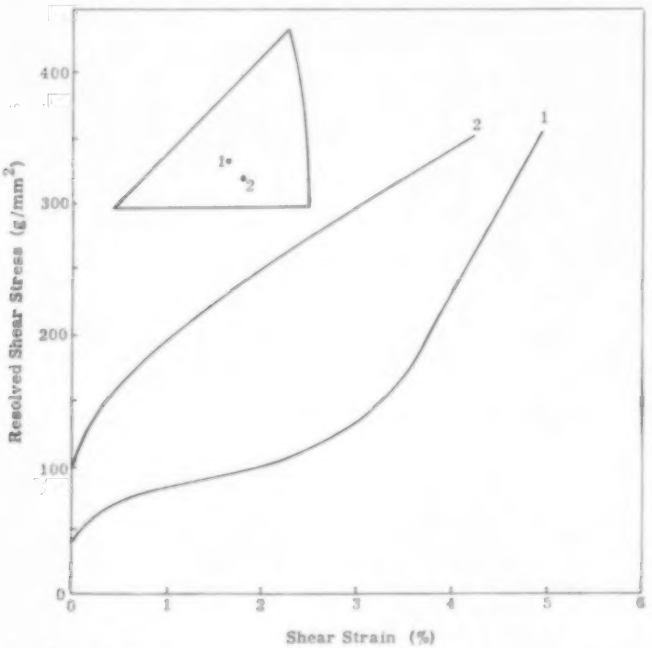

FIG. 5. Effect of surface coatings on the easy-glide range in two similarly oriented copper crystals: (1) unplated, (2) nickel-chromium plated. GARSTONE, HONEYCOMBE and GREETHAM.[22]

Recently, there have been two additional investigations in which important effects on the critical shear stress due to the presence of metal surface films have been observed. As contrasted with the previous studies, the specimens were heated to cause appreciable diffusion between the film and the substrate metal prior to actual testing so that there existed an alloy layer at or very near the surface.

ROSI[23] used copper crystals which had been plated with 4×10^{-4} cm of silver and obtained a surface alloy layer by a diffusion treatment. Metallographic examination revealed a surface alloy depth of 3×10^{-2} cm, which represented a very small fraction of the crystal diameter (approx $\frac{3}{8}$ in.). His data showed that the critical shear stress for the onset of plastic flow was not affected by the presence of the silver plate, but was greatly increased (by approximately 50 per cent) by the diffusion of the silver plate into the copper crystal to form a Cu-Ag alloy surface. The initial observation confirms that of GARSTONE, HONEYCOMBE and GREETHAM.[22] The second observation of

Rosi supports his suggestion that the onset of plastic flow in metal crystals is closely associated with dislocations at the crystal surface and not with those associated with internal surfaces such as low-angle boundaries. A sample of his results, Fig. 6, suggested to Rosi that the increase in critical stress on

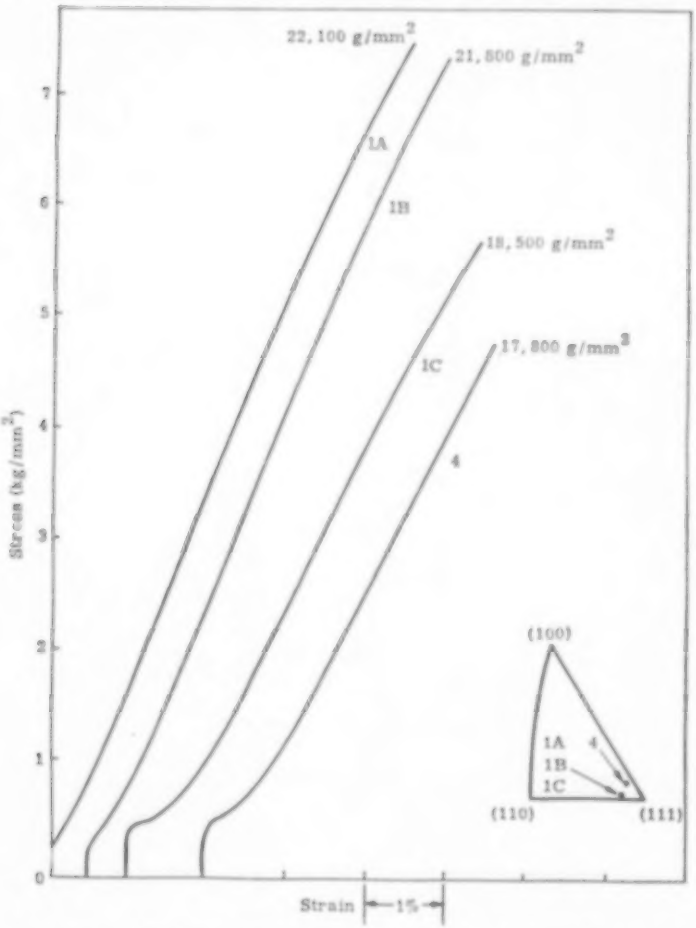

FIG. 6. Stress–strain curves for copper crystals with different surface conditions; 1A-nitric acid etch, 1B—4 × 10^{-4} cm silver plate, 1C—copper alloy surface; crystal No. 4 is a Cu–0.5 per cent Ag alloy. ROSI.[33]

surface alloying is most likely due to the Cottrell anchoring of the surface dislocations by the diffused silver atoms.

Curve 4 of Fig. 6 shows that a Cu–0.5 per cent Ag alloy crystal grown under identical conditions and with similar orientation to the copper crystals gives a rise in critical shear stress similar to the crystal with the diffused silver surface layer.

ADAMS[24] has provided further indication of the importance of surface sources. Tensile tests were made on copper crystals containing various concentrations of zinc in the surface layer. Crystals containing small amounts of zinc, after a small prestrain and an anneal at 200°C, showed a yield point, while in crystals of higher surface zinc content, the yield point was absent. Previous deformation affected the yielding behavior of both lightly and heavily zincified specimens. It is known that pure copper shows no yield point and an increase in zinc content increases the critical resolved shear stress. According to Adams, as the zinc content of the surface layer is increased, the stress necessary to activate the surface dislocation sources is also increased. When the zinc content reaches a value so that the stress necessary to activate the dislocation sources in the interior of the crystal is less than that to operate the surface sources, the yield point disappears. Therefore, no yield point should be found in heavily zincified crystals, that is, those in which the zinc content is sufficient to raise the strength of the surface by more than a factor of 2; in this case, the action of the surface sources should be suppressed by alloy hardening.

Critical shear stress measurements made by ADAMS[24] showed that a lightly zincified surface strengthens a copper crystal more effectively than a heavily zincified surface. Some average values of his results are given in Table 1. Some scatter is present in Adams' results but the general trend

TABLE 1

Showing effects on the critical resolved shear stress of copper crystals caused by various percentages of zinc in the surface alloy layer. ADAMS.[24]

Critical resolved shear stress (g/mm^2)	*Normal surface zinc content* (*per cent*)
56·5	0
75	1/3
101	1
149	8
136	12

indicates that the critical shear stress increases rapidly with zinc content. It is increased from 50–60 g/mm² for pure copper up to an average value of 100 g/mm² for a 1 per cent surface zinc alloy. It is then raised further only to about 150 g/mm² when the surface zinc content is increased to 8 per cent.

ADAMS[24] explained that for crystals in which surface sources are operating, the strengthening is direct. The zinc in the surface layer interferes with the process of generating dislocation loops from the surface alloy. When interior surface sources are active, the strengthening imposed by zinc in the surface layer is indirect, that is, the alloying surface does not interfere with the

process of generation of dislocation loops, but merely impedes the egress of dislocation loops once they have been generated. In this role, the alloyed surface is not a very effective strengthener. The surface layer may hold up the first loop, but others will pile up behind it, raising the stress on the first loop by a factor equal to the number of dislocations in the pile-up, according to COTTRELL,[8] and the strengthening effect of the surface is overcome by the cooperative action of these loops. Therefore, if surface sources are effectively twice as long as interior ones, the critical shear stress of copper should rise rapidly to twice its original value and then increase only slowly with further increases in the zinc content.

Removal of the surface layer from a lightly zincified crystal causes a large decrease in strength and a disappearance of the yield point. Further, zincified crystals should have the same critical shear stress as homogeneous alpha brass crystals of the same composition as those of the alloyed surface layer. Reasonable agreement was also found by Adams in such a comparison.

VOL. 9 1961

Critical Stress for Twinning in Metal Crystals

There have also been observations made that twinning is influenced by a surface film in both zinc and cadmium crystals. For example, GILMAN[25] found that an electro-deposited polycrystalline film of copper approximately 4000–5000 Å thick, on a previously cleaned (by dipping for 5 min in 10 per cent HCl) zinc crystal markedly increased the critical stress required to cause twinning in crystals so oriented that the initial deformation by slip would be negligible. Increases in the tensile stress for twinning ranged from approximately 40–100 per cent. Gilman pointed out that the effect did not seem to be caused simply by the mechanical strength of the copper since the loading would have caused a stress in the film of about 1500 kg/cm², whereas the tensile strength of pure copper is usually in the range of about 23 kg/mm², and the yield point is much lower. It appears that the effect is caused by an interaction between the zinc and the copper film. Gilman suggested the possible application of the dislocation theory of twinning by COTTRELL and BILBY.[26]

KING[27] reported results similar to the above on the effect of surface condition on the twinning behavior of cadmium crystals. In this case, however, the surface film was an oxide or a hydroxide. An increase was observed in the twin stress ratio, that is, the ratio of the stress necessary to cause twinning in an oxidized specimen to that necessary for twinning in an untreated length of the same crystal. Crystal orientations were limited to those which were not deformed by slip to any measurable extent before twinning occurred. The twin stress ratio increased with time of oxidation approaching a limit of about 30 per cent. With an electrolytically deposited hydroxide layer, the twin stress ratio was increased by up to 50 per cent. Removal of the surface layer in each case reduced the twin stress to the initial value.

Results of a more extensive investigation of the effects of a copper film on the twinning behavior of zinc crystals are given by GILMAN and READ.[21]

A plot of some of these data may be seen on the left portion of Fig. 3, showing the effect of orientation on the ratio of the critical stress for twinning in plated and clean crystals. The further observation was made that the copper plate affects the appearance of the twin bands in zinc crystals. The twin bands are wider, on the average, in the clean section of the crystal than in the plated portion. Gilman and Read observed that the difference in width of the twin bands may reflect a direct effect of the copper film on the growth of twins. Alternately, the film may have affected only the nucleation of the bands, and the thickness difference arose because most of the twins in the plated portion of the crystal formed at a higher stress than those in the cleaned portion of the specimen.

Effect on Shape of the Stress–Strain Curve

It was noted by ANDRADE and HENDERSON[19] that an oxide coating on a silver crystal, although increasing the critical shear stress to some extent, has a much more marked effect on the hardening after some tens of per cent of glide has occurred. In one pronounced case, the effect of a very thin film of oxide on the strain hardening of a crystal was so great that at 20 per cent glide strain, a crystal was 10 times stronger than a clean crystal. The length of Stage I of the stress–strain curve was also reduced.

GILMAN and READ[21] observed that the difference between the shear stress of the clean and copper-plated portions of a zinc crystal was usually less at the critical shear stress than after 10 per cent elongation. Results of their tests on two sets of crystals are shown in Fig. 7. It is seen that the initial strain-hardening rate was higher for the plated crystal than for the clean one in Fig. 7a. The hardening rate of the plated crystal dropped at larger strains and the two stress–strain curves then became approximately parallel for a considerable range of strain. GILMAN[4] has presented analyses to show that under ordinary plating conditions, thin films are not much stronger than bulk material. Supposing that the mechanical strength of the film alone is considered to have caused the differences, Gilman shows that to explain the difference in strength between the two crystals, the film would have to support a stress of about 20 times that of the normal yield stress in copper. He checked the strength of plated polycrystalline films and found that they are not much stronger than the bulk material. The explanations of the strengthening by the film then is evidently an interaction between the film and the crystal as ROSCOE[1] had earlier pointed out.

The mode of this interaction as described by GILMAN[4] could be the holding up of the dislocations at the film, causing pile-ups of groups of dislocations. This results in an internal back stress on the dislocation sources which cancels out some of the effect of the applied stress. The applied stress must increase with strain at a higher than normal rate until the blocked dislocations can break through the surface film—at which time a steady state exists with dislocations breaking through as rapidly as they approach the surface from the interior. This would result in normal strain hardening at a

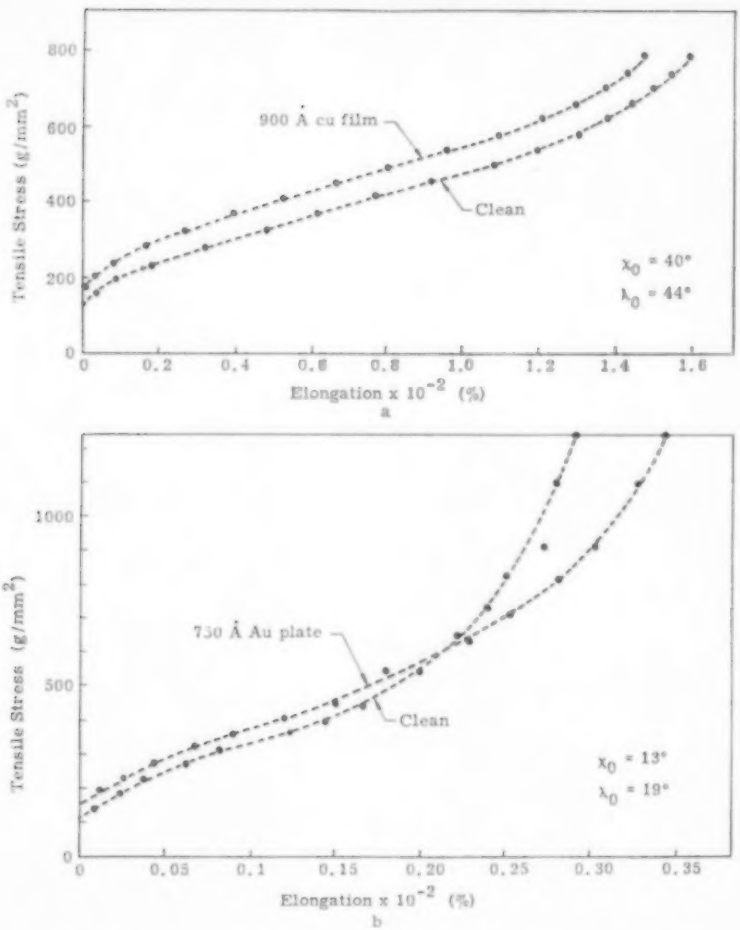

FIG. 7. Tensile stress–strain curves of zinc crystals. GILMAN and READ.[21]

higher stress level than for a clean crystal. In GILMAN and READ's[21] tests, the copper surface film showed good adherence after elongations of 20 per cent apparently having deformed in ductile fashion without rupture.

An effect of orientation on the shape of the stress–strain curve is shown by a comparison of Figs. 7a and 7b. With the orientation shown in Fig. 7b, the crystals initially deformed by slipping, but as their basal planes rotated toward low values of χ, they began to deform by twinning. This occurred first in the clean sections of the crystal and resulted in rapid strain hardening resulting in the crossing of the two curves.

Data from another set of copper-coated zinc crystals, as reported by GILMAN[4] are shown in Fig. 8. In this case, the strain-hardening rate of the

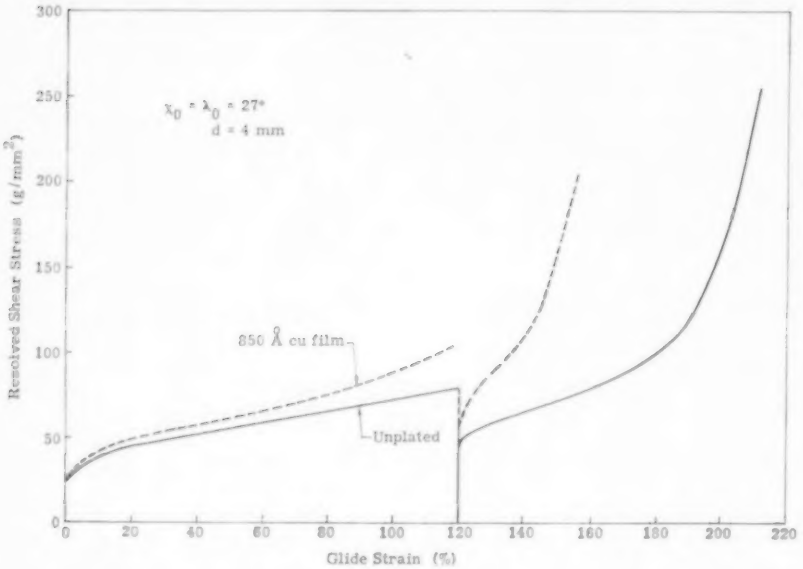

FIG. 8. Stress–strain curves for zinc crystal with copper surface film and crystal with etched surface. At 120 per cent glide strain, the load was removed and both crystals were allowed to recover for 24 hours at room temperature before they were reloaded. GILMAN.[4]

plated zinc crystal increased more rapidly with strain than did the strain hardening rate for the clean crystal.

LIPSETT and KING,[20] investigating effects of gold films on cadmium crystals, noted several effects on the stress–strain curves. They also found that the influence of the film upon the stress–strain curve was dependent upon the orientation of the crystal. A stress–strain curve for one set of their crystals is presented in Fig. 2. Note that the curve for the coated specimen rises early to a value above that of the uncoated specimen and continues at about the same height above that curve until a rapid increase in work hardening begins at 200 per cent glide. This was typical of crystals for which χ_0 was around 15°. In crystals with higher values of χ_0 and for films of approximately 12,000 Å in thickness, after the initial large differences in the curves for the coated and uncoated crystals, the two curves approached each other with increasing glide.

Sample curves from TAKAMURA's[13] study of the effect of anodic surface films on the plastic deformation of aluminum crystals were shown previously in Fig. 1. He found that the stress–strain curves were usually raised throughout their entirety by surface films as shown in that figure. Occasionally, however, it was observed that crystals whose axes were near the [001]–[111] boundary of the stereographic triangle yielded stress–strain curves which

crossed at certain values of strain. At larger strains, the curve for a thicker-coated crystal fell below that for one with a thinner coating, Fig. 9.

It was also noted that the stress–strain curve of a specimen with a thicker anodic film did not show the Stage I region as clearly as did a companion with thinner surface film. Takamura attributed the crossing of the stress–strain curves in Fig. 9 to the difference between the two specimens in the

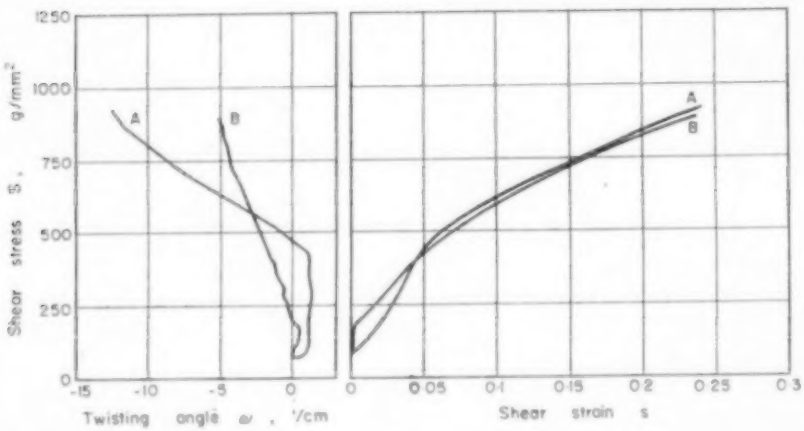

FIG. 9. Stress–strain curves and stress–twisting curves for aluminum crystals with anodic coatings 100 Å (A) and 500 Å (B) in thickness. TAKAMURA.[13]

development of the inhomogeneities such as kink bands, and especially, "bands of secondary slip"[25] which cause the intense work hardening; a surface film suppresses the development of these inhomogeneities.

In another experiment employing a face-centered cubic metal, GARSTONE, HONEYCOMBE and GREETHAM[22] found that the plated crystal of copper resulted in elimination of the Stage I region as compared with an unplated one, Fig. 5. Curves for the two crystals, however, approached each other as the shear strain increased beyond some 3 per cent.

ROSI[23] made a comparison of copper crystals having a surface layer of silver with copper crystals cleaned by etching, Fig. 6. This shows that the silver-plated surface had no effect on either the strain hardening coefficient nor the gross shape of the stress–strain curve whereas a copper–silver alloy surface obtained by diffusion, produced not only a significant decrease in the shear hardening coefficient, but also a region of easy glide. This occurred in spite of the fact that this orientation usually produces multiple glide at the very onset of plastic flow.

From another set of crystals so oriented as to ensure a region of easy glide see Fig. 10, the silver plate alone caused a slight decrease in the extent of easy glide, but did not affect the shear hardening in the later stages of flow.

VOL.
9
1961

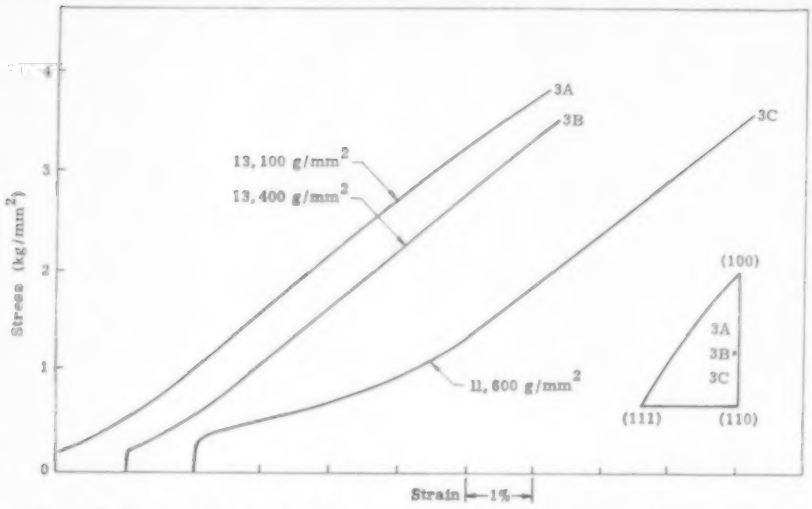

FIG. 10. Stress–strain curves for copper crystals of identical orientation with different surface conditions: 3A—nitric acid etch, 3B—4×10^{-4} cm silver plate, 3C—copper–silver alloy surface. ROSI.[23]

With surface alloying, Curve 3C, the region of easy glide was extended to higher values of strain and the shear hardening associated with both easy glide and the region of higher hardening was decreased. Rosi concluded that the effect of surface alloying on the plastic properties of metal crystals was similar to that for bulk alloying in that the critical shear stress for flow and the amount of easy glide increases and the shear hardening for the entire stress–strain curve decreases.

By superposition of the curves from crystals of the same orientation in the results of ADAMS,[21] and eliminating the yield points resulting from intermediate annealing treatments at low temperatures, the effects of various amounts of zinc in the surface layers of copper crystals on the shape of the stress–strain curve may be observed. Figure 11 is a summary replot of some of Adams' data showing comparison of the curves for companion crystals of three different orientations selected for different amounts of easy glide. These disclose the effect, in each case, of increasing the surface zinc content from 1 to 8 per cent. An increase in the zinc content, in addition to raising the critical shear stress for flow, increases the easy glide portion of the curve, where such exists, but does not have a great effect on the rate of work hardening after this stage. The latter effect, however, depends to an extent on the orientation considered for comparison.

ROSI[30] studied the effect of impurity content in solid solution on the gross shape of the shear stress–shear strain diagram. His results disclosed that the less pure the material, the greater will be the extent of Stage I, although, as he pointed out, this conclusion appears initially to be contradictory to the results of LÜCKE and LANGE[31] and ANDRADE and

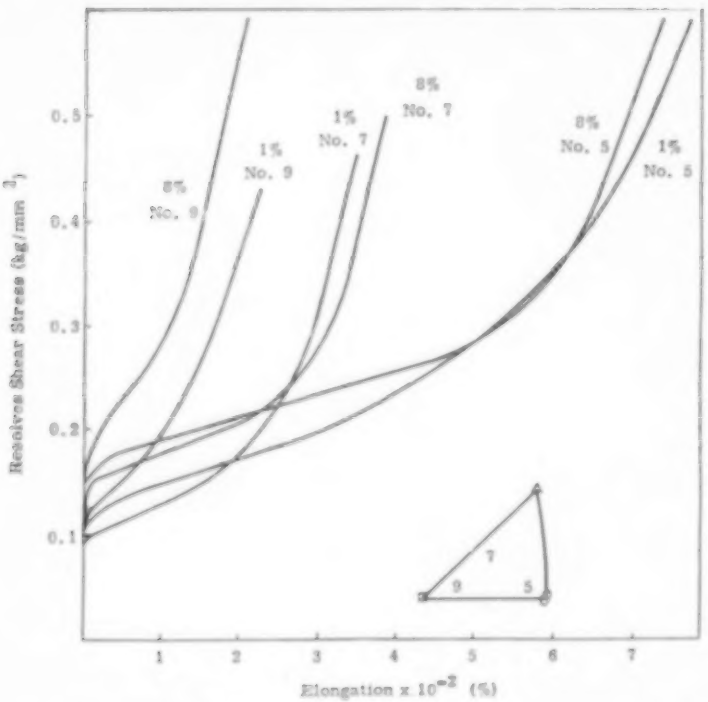

FIG. 11. Comparison of the stress–strain curves for pairs of copper crystals of the same orientation but with different surface zinc contents. Replotted from results of ADAMS.[24]

HENDERSON[19] who failed to observe a Stage I region in commercially pure aluminum and nickel. However, the impurities in these materials, particularly in the case of the aluminum, were of such a nature to suggest that they did not all go into solution. The presence of insoluble impurities, according to Rosi, especially in regions near dislocations corresponding to mosaic and lineage boundaries, can be expected to stop moving dislocations, thereby lowering the mean value of slip distance. This would result in an increased work hardening rate immediately following the onset of plastic flow which could account for the absence of a Stage I region in commercial purity materials containing precipitants. An increase in the first stage of the flow curve with impurity content, however, is accompanied by a higher yield point, which probably is caused by the anchoring of dislocation sources by impurity atoms in a manner proposed by COTTRELL[3] or SUZUKI.[28]

Strain Rate Effects on the Shape of the Stress–Strain Curve

The influence of strain rate as an important variable on the effect of surface films was referred to by GILMAN.[4] He examined the effect of strain rate using copper films about 600 Å thick on zinc crystals. When the strain rate

was changed from 3×10^{-5} to 3×10^{-4} per sec, the stress at 0.05 per cent elongation increased by 1.5 per cent for a crystal cleaned by etching as compared with 9.5 per cent for a copper-plated crystal. On the other hand, LIPSETT and KING [20] did not find any significant increase in the effect of a gold film on cadmium crystals by increasing the rate of extension by four times. Presentation of further evidence concerning this effect of strain rate on coated crystals is desirable.

Microscopic Deformation Characteristics

In some of the surface effect studies employing tension tests, observations of the effects caused by the films on the deformation characteristics have been made. These observations are important in the clues they offer in explaining the mechanism of the effects of surface films.

GILMAN [4] employed X-ray examination of the copper-plated and unplated portions of zinc crystals deformed in tension. Comparison was made of rocking curves from an X-ray spectrometer using copper radiation. The plated crystals gave indications of surface deformation that was more severe than for the clean crystals. It was found further that more distortion occurred near the surface of the plated crystal than in its interior. The local surface distortions due to the film denote a local concentration of dislocations caused when slip is impeded in leaving a crystal. Gilman points out further that the fact that the distortions are plastic as well as elastic accounts for the effect of a film on the strain hardening rate.

TAKAMURA, [13] examining the effect of oxide on aluminum single crystals, found metallographic effects attributable to the surface film. As noted earlier, he found that the surface film suppresses the development of kink bands and bands of secondary slip. He found that the surface film also suppresses fine slip, an observation also made by BROWN and HONEYCOMBE. [19] Furthermore, abnormal slip markings often appeared on aluminum single crystals coated with anodic films of more than 300 Å. These effects were explained by assuming that dislocations pile up beneath the surface film.

Examination of cadmium crystals at various stages during tensile deformation and after final removal from the testing apparatus was made by LIPSETT and KING [20] in searching for any differences between gold-coated and uncoated specimens. Inspection of a partially coated crystal after 9 per cent extension showed an appreciable density of slip bands relatively uniformly distributed along the length in the uncoated region. The gold sputtered portion had only a few isolated slip bands. A further important observation is as follows. The slip steps on the surface where edge dislocations broke through the film were clean, sharp and bright on both coated and uncoated specimens and no differences could be observed, point A in Fig. 12. At the sides of the crystal where screw dislocations would break through, as at point B, differences were obtained between the coated and uncoated portions. In an uncoated crystal slip lines disappear at points corresponding to B since no slip step is formed. In coated crystals, however, the evidence of

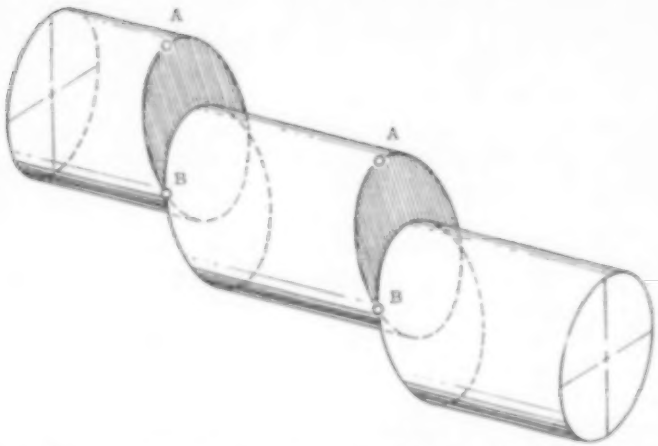

FIG. 12. Diagram illustrating translational slip in a cadmium crystal. The gold films were easily broken at point A, and flaking off commenced at point B. LIPSETT and KING.[20]

the existence of slip lines was very marked. At relatively small extensions, the surface showed corrugations parallel to the slip direction. With further extension there was an increase in roughness of the corrugations until the film or at least an appreciable part of it lost adherence and flaked off. Thus the film is not highly resistant to shear forces lying in its plane. Edge dislocations pass more readily through the film than do screw dislocations: the film tears away from the crystal rather than allow the passage of screw dislocations whereas passage of the edge dislocations does not cause similar loss of adherence to the crystal. Lipsett and King suggested that these observations may explain other effects observed, for example, by GILMAN and READ,[21] that the mechanical behavior of a crystal depends on the shape of the cross section and of the orientation of the glide direction in that cross section.

CHALMERS and DAVIS[23] deformed by about 0.5 per cent an aluminum crystal oriented for easy glide, and examined it by the Schultz technique. After annealing, the high resolution Laue spot was broken into parallel bands separated from each other. This suggested the formation of arrays of edge dislocations, all of the same sign in the region examined. According to these investigators, the sign of the dislocations was such that their motion was away from the surface during the plastic deformation on tension. This gives support to the idea that the dislocations that move during the early stages of plastic deformation of single crystals originate at Frank-Read sources of which one end is free to move on the surface of the crystal.

A very careful investigation of the deformation of surface films on solid substrates has been made by BRAME and EVANS.[34] To obtain a more fundamental understanding of the inhibition mechanism of surface films, their

experiments were performed on this single crystal film prepared by vacuum evaporation onto single crystal substrates so that the film and substrate lattices were in parallel orientation. In this manner, the boundary misfit between the two lattices can be accommodated by a two-dimensional network of dislocations with a spacing determined by the degree of misfit. Their objective was to examine the parameters which determine the ease of propagation of dislocations through the boundary. Thus, a number of face-centered cubic films were oriented on silver single crystals and deformed in tension. The films were examined by transmission electron microscopy after stripping from the silver substrate. Subsidiary experiments were also carried out with polycrystalline films on single crystal silver substrates, oriented films and polycrystalline palladium substrates, and also single crystal films attached to noncrystallographic substrates to determine the film behavior under various conditions.

Conclusions reached by Brame and Evans are too lengthy to be included in detail here. However, the experimental evidence they obtained is consistent with the assumption that the metal film behavior is determined by its reaction to dislocations arising from sources activated in the interior of the substrate. These produce dislocation loops on the active slip planes and the mechanical response of the film depends upon the ability of these dislocations to pass into and through the film. Factors determined as affecting the ease of passage of dislocations into the film were found to include: (*a*) alloying between the substrate and the film, (*b*) the structure of the film itself, (*c*) the difference in elastic moduli of the substrate and the thin film, and (*d*) the degree of misfit between the substrate and the film.

A polycrystalline film on a single crystal substrate was found by BRAME and EVANS[34] to cause great difficulty in the transference of a dislocation because of the randomness of orientation of slip planes in the film. It therefore accommodates the imposed strain by cracking in the directions of the slip traces in the underlying crystal. HEAD[16] analyzed the image forces arising when a screw dislocation in a substrate approaches a surface to which is attached a thin film of different elastic modulus. He found that if the elastic modulus of the film is greater than that of the substrate, a dislocation approaching the surface experiences first an attraction up to a critical distance and thereafter a repulsion from the surface. The critical distance depends on the relative elastic moduli and film thickness. Although Head's analysis concerned screw dislocations, he considered that the same conditions hold for an edge. Brame and Evans found that the ratio of the shear moduli does have some effect on the passage of dislocations from the substrate into the film. The main influence, however, in determining the transfer of dislocations from the substrate to an oriented film was the difference in lattice parameter between them. Accommodating networks of dislocations forming at the interface act as a sharp barrier to the passage of dislocations in an active slip plane because the barrier dislocations lie in the same plane. The effect increases with the number of dislocations passing

from the substrate into the film. The rate of increase of such a hindering process would be directly related to the degree of misfit of the two lattices.

Surface Effects on Fracture

A few studies have been made of the effects of surface factors on the fracture of metal crystals. GILMAN[35] made the observation that a thin (approximately 3000 Å) electrodeposited layer of copper on zinc single crystals makes them much more brittle at room temperature. A single observation showed that the plating reduced the stress for fracture.

GREENOUGH and RYDER[36] attempted to alleviate the lack of systematic experimentation by determining the effect of surface films on the stress necessary to cause cleavage fracture for single crystals under widely varying conditions. The effect of an electrodeposited layer of copper on the tensile stress necessary to cause cleavage in zinc single crystals of various orientations at − 196° C was studied. There is some scatter in their experimental results, summarized in Fig. 13, but they indicate that for crystals of orientations between $20° < \chi_0 < 70°$, the cleavage stress is approximately twice that for unplated crystals. It was also observed that the plastic deformation before fracture was much less in the electroplated crystals than in the unplated ones. The scatter precluded valid conclusions in regard to the effects at high angles of χ_0. The cause of the observed increase in fracture stress was attributed to the anchoring of the free ends of Frank-Read dislocation sources at the surface of the zinc crystals by the electrodeposited layer.

The normal fracture stress of zinc crystals oriented with $\chi_0 = 3°$ and tested in tension at room temperature was found by WEINER and GENSAMER[37] to be increased some 40 per cent upon applying a surface film of copper, gold, zinc oxide, tin, or zinc thicker than about 500 Å. Above this value the increase was independent of film thickness. It was also independent of the type of surface coating. Furthermore, the total percentage elongation was increased twofold, the primary mode of deformation being twinning accompanied by parent basal slip both before and after twinning as well as basal slip within the twins. Metallographic examination revealed more twins in the coated crystals and a more uniform distribution of them.

WEINER and GENSAMER[37] also found that the fracture stress of coated crystals with $\chi_0 = 83°$ was about 50 per cent less than the value observed for clean-surfaced crystals. This is in accord with the results of GREENOUGH and RYDER.[36] The presence of existing twins produced by precompression caused the fracture stress of both clean and coated crystals to be increased. These results, as well as observations on prestrain and recovery, and experiments on film removal, were explained by a dislocation-pile-up-at-a-barrier model in which twins play an important role by modifying the dislocation path and acting as barriers.

In an extension of the above work, the aim of a study by WEINER[38] was to investigate the effects of solid environments on the flow and fracture behavior of zinc crystals of the same orientations over a wide temperature

VOL. 9 1961

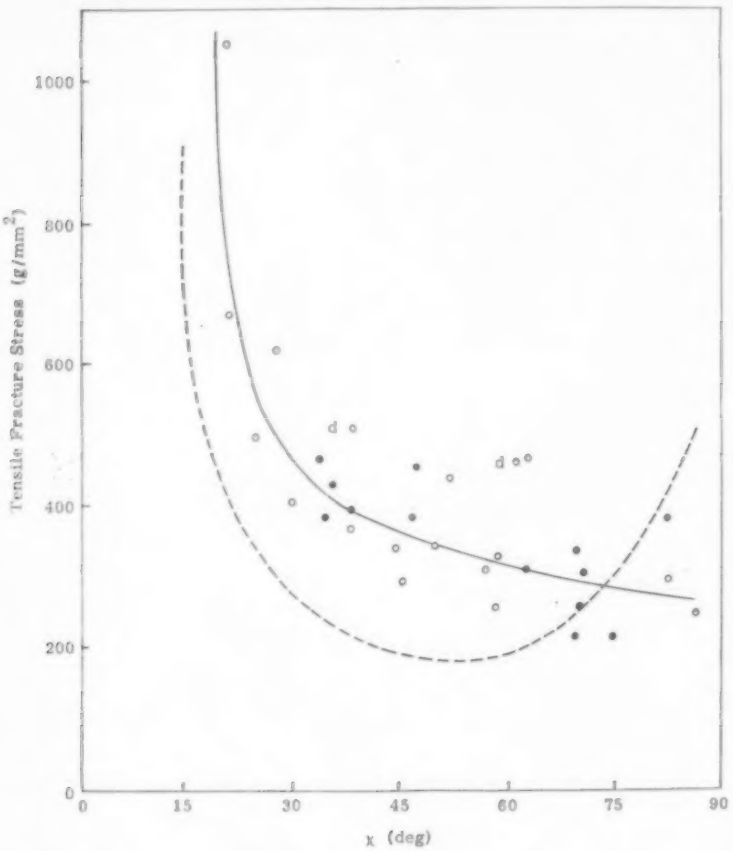

FIG. 13. Tensile fracture stress of copper-plated zinc single crystals. GREENOUGH and RYDER.[36]

○ Points for crystal used in earlier experiments
● Points for new crystals
—— Best curve through the points
- - - Curve for unplated zinc crystals

range. Uniform, adherent, copper surface films were electrodeposited on the surface of clean zinc crystals. Their thicknesses, determined by weight observations, were between 2000 and 4000 Å. Tensile tests were made at a strain rate of 5×10^{-3} per sec and over a temperature range from $-196°$ C to $+100°$ C. It was found that for single crystals oriented at $\chi_0 = 3°$, a surface film raised both the cleavage and yield strengths. The increase in the former was greater than that in the latter. The brittle temperature for both

clean and coated crystals occurred at between 60 to 70° C. This was associated with the onset of large amounts of slip subsequent to the completion of a constant amount of twinning.

A ductile-to-brittle transition temperature is often interpreted as the point

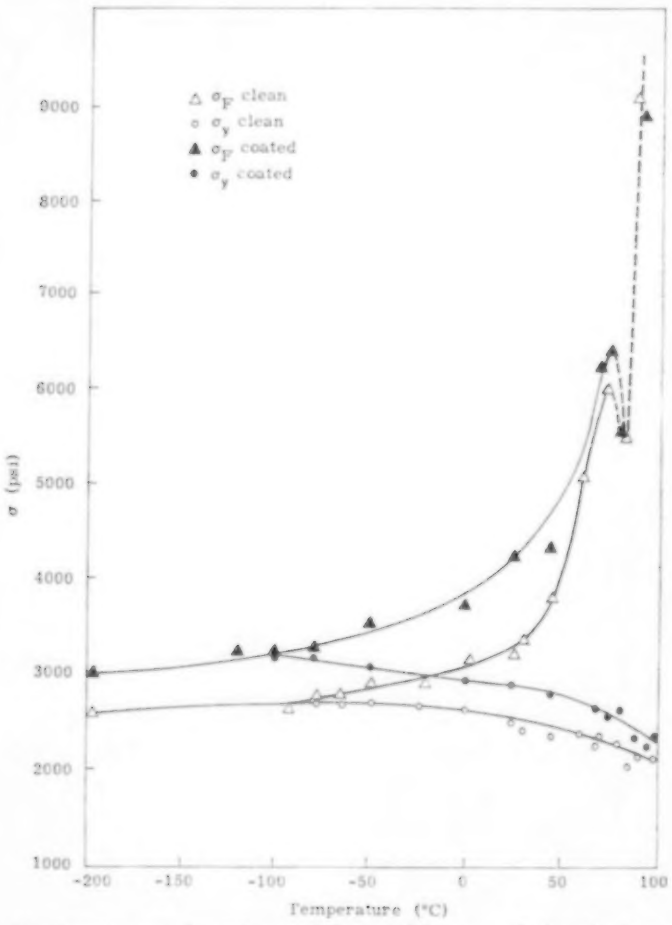

FIG. 14. Temperature dependence of flow and fracture of zinc single crystals for $\chi_0 = 3°$. WEINER.[38]

of intersection of the curves showing stress for flow and fracture as a function of temperature. In this case, however, this intersection did not coincide with the brittle temperature. The intersection temperatures were found to be − 80° and − 100° C, as shown in Fig. 14, for clean and coated crystals, respectively. Weiner found them to be associated with the onset of the temperature dependence of twinning. The fracture stress was temperature independent below the intersection temperature, while above it became

VOL. 9 1961

markedly dependent, increasing with increasing temperature. Twinning was found to play a vital role in the cleavage of both clean and coated crystals oriented at $\chi_0 = 3°$. The fracture stress correlated with the resolved mean maximum distance between twins. It was determined that the smaller the deformation by twinning, the greater the resolved mean maximum distance between twins and the lower the fracture stress.

For crystals oriented $\chi_0 = 83°$, WEINER[38] observed that a surface film

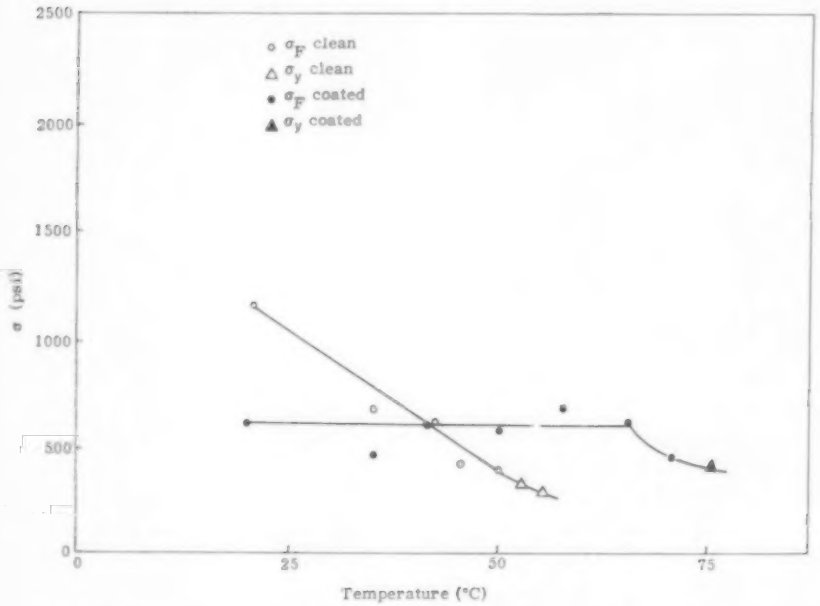

FIG. 15. Temperature dependence of flow and fracture of zinc single crystals with $\chi_0 = 83°$. WEINER.[38]

acts as a barrier to dislocations and decreases the fracture stress making it independent of temperature as shown in Fig. 15. In this case the brittle temperature coincides with the intersection of the flow and fracture curves. Figure 15 shows that a surface film raises this temperature 20° C from 50 to 70° C.

WEINER[38] also investigated a wide variety of gaseous and liquid environments on the brittle fracture of zinc crystals with the basal plane close to the tension axis ($\chi_0 = 3°$). He noted that these environments increased the cleavage strength of those initially clean single crystals only if the environment acts to form an adherent surface film more than 200 to 300 Å thick.

Creep Effects

The importance of surface condition on the creep behavior of metal single crystals was early demonstrated by ANDRADE and RANDALL[39] by

surrounding a creeping cadmium crystal with certain electrolytes which increased the creep rate presumably by removal of an oxide coating hindering the creep. Although it certainly is an arbitrary separation, discussion of this type of behavior will be withheld until Section III of this review. Although the studies now discussed were preceded chronologically by several others involving the effect of electrolytes, here will be treated only the investigations concerned with the effects of oxide and metallic films on the creep behavior of metals.

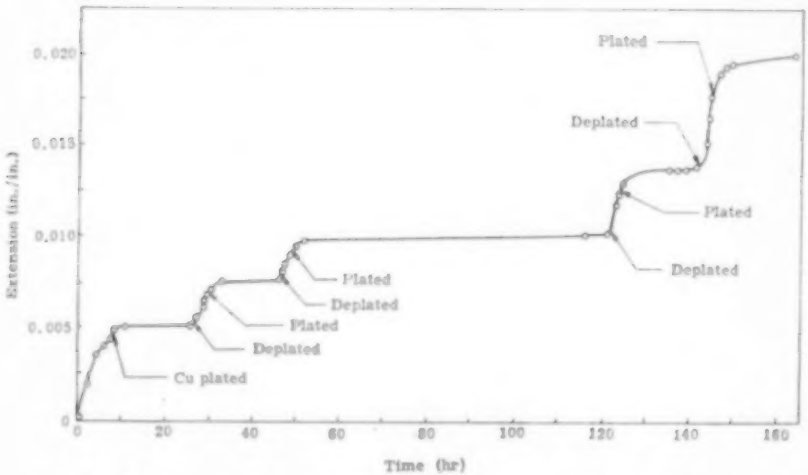

FIG. 16. Change in creep rate of a zinc single crystal produced by a thin copper plate. PICKUS and PARKER.[40]

One of the first experiments concerned with the effect of such surface films on creep is that of PICKUS and PARKER[40] who studied the effect on the secondary creep rates for zinc and "A" nickel. Both single crystal and polycrystalline zinc were studied. In the case of the single crystals, in a number of crystal orientations, the creep rate was sharply decreased by the presence of a thin copper layer. When the copper was removed, the creep rate increased to the value obtained for the unplated specimens. Figure 16 gives an example of the type of results obtained. The temperature dependence of creep for polycrystalline and single crystal zinc was also determined with and without copper in the surface layer with the results shown in Fig. 17 in which creep rate is designated as $\dot{e}$ and a and b are constants.

Numerous tests on the polycrystalline specimens showed conclusively that the presence of a thin layer of copper had no effect on the creep behavior of polycrystalline zinc. In all the tests that were performed, diffusion between zinc and copper occurred. The surface layer, therefore, consisted of a Cu–Zn alloy. However, a study by SWEETLAND and PARKER[41] of the effect of an oxide coating on the creep of 2S aluminum and commercial drawn copper

indicated that the presence of an oxide surface layer on these materials increases the creep strength of these polycrystalline metals.

The question arose as to whether the effect of the copper on the creep of zinc single crystals was analogous to increasing the diameter of the zinc specimen by an equivalent thickness of zinc. Pickus and Parker from stress

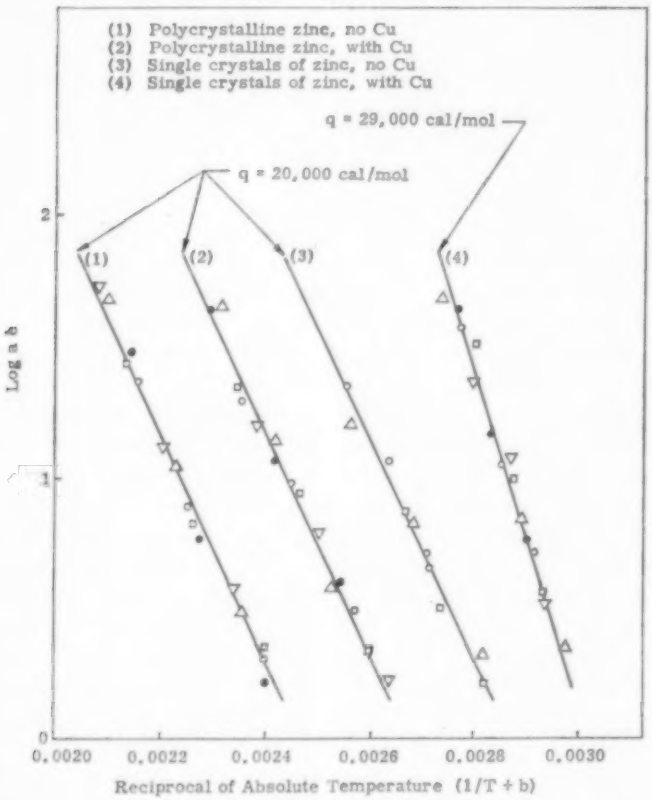

FIG. 17. Composite plot of data from 18 tests designed to establish the temperature dependence of oxide free polycrystalline and single crystal zinc both with and without copper on the surface. PICKUS and PARKER.[40]

considerations indicated that this is unlikely. Furthermore, for this to be the case, no difference in the temperature dependence would be expected between plated and unplated crystals. METZGER[42] in discussion of the above offered some calculations to show that for one test, the surface layer may be supporting 3 per cent of the applied stress. This, of course, is not large enough to explain the sevenfold decrease in creep rate shown by the data, but there may be some effect due to this cause.

GILMAN and READ[21] found that the creep properties as well as the tensile properties of zinc, tin and lead monocrystals are affected by evaporated and

electrodeposited films of copper, gold, zinc and silver. Evaporated films of copper and silver about 2000 Å thick reduced the creep rates of zinc crystals. They found that the effect was small immediately on applying the films, but that it increased for several days thereafter. Copper films plated onto zinc crystals during the creep tests reduced the creep rates of zinc crystals depending on the film thickness. This effect could be accounted for in the creep tests by assuming that the effect of the copper plate was just to support part of the load.

A quantitative study on the influence of the surface composition on the creep of zinc single crystals under constant loads has been carried out by COFFIN and WEIMAN.[43] From creep curves obtained on clean and oxide-coated single crystals of zinc, they showed that a continuous layer of oxide strengthens the crystal only at low loads and that the presence of cracks in this layer allows the metal to creep at its normal rate. They interpreted these facts as support for the theory that the oxide film acts to relieve the metal of part of the load. However, an alternative interpretation may be given in terms of an easy egress of dislocations through the cracked film.

METZGER and READ[44] attempted to discriminate between the possible mechanisms of the strengthening effect of a surface film on metals by some quantitative studies of the creep behavior of cadmium with special attention to film thickness, dynamical effects, and comparison of films of different properties. Films employed were of hydroxide and synthetic plastics, Formvar, and Vulcalock. The creep test was chosen for its sensitivity and creep rates of the order of 0.01/hr were employed with strains of about 0.01. Data obtained and theoretical considerations suggested to these investigators that neither the pinning of surface-dislocation sources nor the elastic repulsion of dislocations by the hydroxide film, nor the macroscopic stresses associated with the hydroxide film is the primary factor involved in the strengthening effects observed. They stated that a naive mechanical model accounted for all the major features of the data, notwithstanding that the effects were not linear with thickness and independent of orientation and of strain rate as such an explanation would imply. The mechanical model assumes that the shear-stress relaxation across the active slip planes in the metal transfers the load to the film until it deforms and slip can proceed. The authors postulated a dislocation-film interaction mechanism phenomenologically equivalent to the naive mechanical model at low strain rates which was consistent with the relatively small dynamical effects obtained in a few tests on the thickest (600 Å) hydroxide films.

In most of the studies cited above the work was performed with single crystals or polycrystalline samples of high purity metals or single alloys. Effects have also been noted using more complex alloys having solid surface films. For example, significant improvements in the creep characteristics of 80–20 Ni–Cr alloys at 1975° F resulting from the application of a ceramic coating were reported by CUTHILL and HARRISON.[45] Another study of the creep behavior of ceramic-coated Ni–Cr alloys, by CUTHILL, RICHMOND

and TIGHE[46] was made using different temperature and stress conditions. CeO_2 containing frits applied to sheet metal specimens reduced the creep rate by as much as 50 per cent at 600 psi and 1975° F, but with a stress of 2200 psi at 1800° F, the enamel coatings had a deleterious effect.

Internal Friction and Abnormal After-Effects

More unusual effects of solid surface films than those discussed above have also been observed. SHAPIRO and READ[47] made internal friction measurements by the composite quartz oscillator method on cadmium single crystals with and without oxide films formed by immersion in cadmium nitrate solution. Their results indicated that the oxide film caused a much more rapid rise in internal friction with increase in vibration amplitude, particularly in the range of amplitude in which an increase in internal friction is produced by the measurement. Upon removal of the film and recovery of the crystal, the internal friction behavior returned to that observed prior to oxidation. It was pointed out by Shapiro and Read that this result made it impossible to ascribe the effect of oxide films on plastic properties to an inhibiting effect on dislocation formation at the specimen surface.

BARRETT[48] first demonstrated an abnormal after-effect in metals. It is well known that a metal wire that has been subjected to plastic flow in torsion generally untwists at a rate such that equal strains occur in equal intervals of log time. Barrett showed that this behavior was true with single crystal and polycrystalline wires of iron and of zinc, both when coated with oxide films and when freshly cleaned of oxide. But the normal after-effect following plastic twisting of these wires was shown to be replaced by an abnormal after-effect (twisting instead of untwisting) which occurred as a transient when an etchant was suddenly applied to an oxide-coated wire that had been twisted. Typical behavior obtained is that shown in Fig. 18 for single crystals of zinc.

Similar results were obtained for polycrystalline zinc wires and for polycrystalline, decarburized mild steel wires. The transient reversal of the after-effect noted had been predicted on the basis that adherent oxide films on metals act as barriers to the movement of dislocations. Upon twisting a wire, dislocations pile up beneath the oxide-metal interface. When an acid is applied, these escape through the surface. An after-effect in the normal direction but with a reduced rate follows the transient effect and may also be accounted for by the escape of dislocations which had previously been piled up beneath the surface. Following this initial work, other studies were made which demonstrated the generality of the effect and provided a more intensive consideration of factors affecting the general phenomenon of abnormal elastic after-effect.

BARRETT[49] demonstrated an abnormal twisting when the film was removed by etching in torsion tests on polycrystalline cadmium wires with anodic or other oxide films, similar to the effects previously observed with the iron and zinc wires. In this study the sensitivity of the test was sufficient

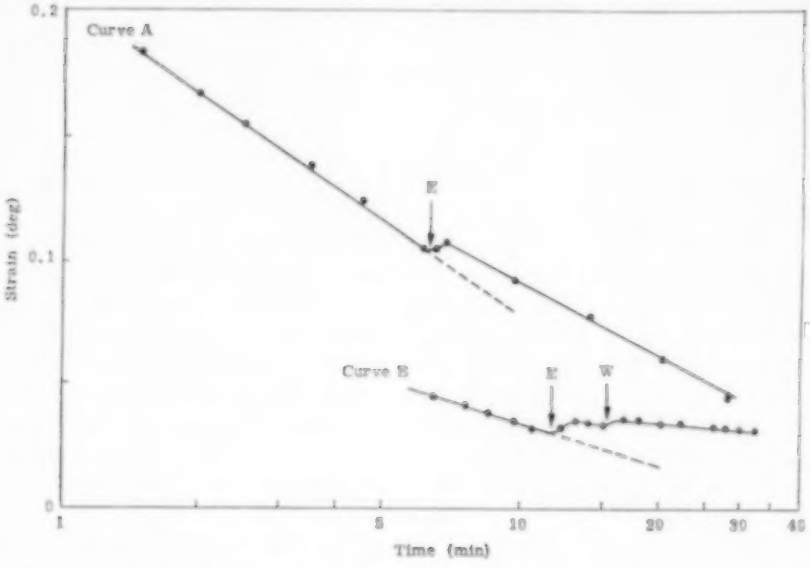

FIG. 18. Torsional after-effect curves for single crystals of zinc. Water was replaced by etchant at points indicated by *E*, and this was continued to the end of the test in curve *A*, but was replaced by water at *W* in curve *B*. BARRETT.[48]

to detect the films formed in air at room temperature in fractions of an hour. These oxide films retained their influence after the wire had been subjected to moderate plastic deformation. Prior cold work increased the rate of untwisting in the normal after-effect; the transient abnormal effect was slower when the etchant was more dilute. Control tests indicated that thermal transients were not involved in the phenomenon.

EDELSON and ROBERTSON[50] also studied the effect of a surface oxide film on the torsional relaxation of polycrystalline cadmium wires investigating such physical parameters as metallurgical history of the metal, film conditions and time factors. They showed the abnormal after-effect to be a reproducible effect directly dependent on the presence and elastic properties of a surface film. They offered two explanations—one in terms of a two-component mechanical model, and an equivalent explanation in terms of the dislocation barrier theory.

Further evidence in support of the dislocation barrier explanation of the abnormal elastic after-effect was offered by CHEN.[51] He reported observation of the formation of slip bands directly under the microscope by removal of an oxide layer on a previously stressed single crystal of high purity aluminum.

Another type of abnormal after-effect in twisted metal wires was observed by COCHARDT[52] upon heating. Annealed, polycrystalline wires of aluminum, copper, silver and nichrome were twisted in a helium atmosphere through an angle corresponding to a surface shear strain of 2 per cent. The wires

were then released and a normal after-effect observed for 20 min at room temperature. Then the wires were suddenly heated electrically to various temperatures from 300 to 700° C and the observations continued. All wires untwisted at room temperature in the initial tests. Aluminum continued to untwist, but at an accelerated rate, at the higher temperatures. Silver and copper began to retwist at the higher temperatures, with the greater effect in silver. Nichrome retwisted by a relatively large amount at the higher temperatures and then began to untwist again.

Cochardt explained these phenomena in a manner similar to that offered for the previous behaviors, that dislocations pile up under the oxide layer near the surface as a result of the plastic deformation. Heating the metal reduces the stress required for the dislocations to break through the oxide layer. When such a break-through occurs, the wire will twist further as in the case with copper and silver. Cochardt suggested that this does not occur in aluminum probably because of a much stronger oxide layer. No explanation was offered for the more complex behavior of the nichrome.

OL.
9
961

General Ductility and Strength

A few investigations dealing with effects of surface films on the general ductility and plastic deformation and strength of metals and alloys will be mentioned. LOGAN[53] evaluated effects of chromium plating on SAE 4130 steel from results of tensile impact, bending and crushing tests. It was found that the chromium plating materially reduced the percentage of elongation, true stress at beginning of fracture and ratio of original cross-sectional area to area at beginning of fracture. Values of these properties decreased with increased plating thickness. Another study by KENNEDY[54] examined the effect of cadmium plating on the behavior of SAE 4340 steel in the presence of stress concentrations at elevated temperatures.

A general review of the effects of chromium plating on the strength of steel is given by MORISSET[55] with regard to the structure of chromium deposits and the effects of the deposition process on mechanical properties of the underlying steel. Such observations are too lengthy to be included here.

Results of a general survey of the effects of brittle skins in general on otherwise ductile metals was made by FORM and BALDWIN[56] for oxidized high-purity iodide titanium, nitrided AISI 303 stainless steel, hydrogen-embrittled tough-pitch copper, chromium-plated copper, carburized SAE 1020 steel, and induction-hardened SAE 4340 steel. The results suggested that a brittle skin on an otherwise ductile material is essentially equivalent to the introduction of a "potential" notch into the metal. Supporting points of evidence for this view are: (*a*) the skin of each of the surface-embrittled metals under study cracked early in the tension test, thus introducing a circumferential notch into the specimen although the extension of the initially formed crack into the core was delayed until a late stage of the test, and (*b*) the ductility behavior of a metal under the influence of a varying case depth followed practically the same pattern as that of the same metal

(without a brittle skin) under the influence of varying notch depth. This similarity was true for both notch sensitive and notch insensitive metals.

It was pointed out by Form and Baldwin that the above simple interpretation of the effect of a brittle surface layer on a ductile core in terms of the notch tensile behavior of the base material is affected by other considerations. For example, some electroplates may be brittle enough to crack early in the tension test. Others have no adherence whatsoever and flake off before introducing a surface notch into the core. Further, residual stresses induced by the surface embrittling procedure may place a different stress state around the nose of a crack induced by stretching a surface-embrittled metal than that which exists at the base of a machined notch. Thus, the effects obtained may be very dependent on the type and properties of coating or surface treatment.

VOL.
9
1961

Effects on Fatigue Properties

Probably no other phase of fatigue studies can contribute more directly to an understanding of the fatigue mechanism and to the prevention of fatigue failures than those associated with the study of surface conditions. In recent years renewed efforts have been turned towards deformation studies and crack initiation and propagation investigations. Many interesting facts are being uncovered in regard to the fatigue process in metals. Comparatively little attention, however, has been given to the effect of surface films on the fatigue properties of materials except for a limited number of studies performed chiefly from the applied point of view. In general, the effect of an oxide or metal film can be to increase the fatigue strength or life in the upper region of the stress-cycle fatigue curve if the coating is stronger or harder than the base metal but not too brittle. Excessive brittleness may cause premature cracking in the coating and accompanying stress concentrations, thus accelerating fracture.

The fatigue strengths of aluminum alloys under the influence of anodic films have been studied by several groups.[57, 58, 59, 60] A hard anodic coating was found to reduce the fatigue strength of one alloy by more than 50 per cent, whereas chromic acid anodizing increased the endurance and strength. In the bending fatigue behavior, it was found[61] that an anodic (HAE) coating caused a significant reduction in fatigue strength of an aluminum alloy.

A study on ingot iron[62] showed that ceramic coatings improved the fatigue strength and fatigue life at stresses above the endurance limit. Another study[63] was made on ceramic-coated stainless steel. The effect of an inorganic coating on the fatigue properties of lead alloys has also been investigated.[64]

A very common treatment involving surface conditioning is electroplating. The most popular of these processes are chromium plating on steel and aluminum, and anodizing of aluminum; less popular are tin and zinc coatings on steel. Several investigators[65, 66, 67, 68, 69] have studied the effect of chromium plating on the fatigue properties of steels. It appears that the resulting effects are dependent on a number of factors including rate of deposition, thickness

of layer, and heat treatment after plating. Generally, a chromium plating reduces the fatigue limit; the ratio of fatigue limit to tensile strength decreases with increased hardness of the steel; the plating should be thin; and it should be heat-treated after the deposition. A prime factor for consideration is the intensity and character of the residual stress in the coating.

Cadmium plating on steel, as it affects the fatigue strength, has not received much attention, but a limited amount of work [70, 71, 72, 73] indicates that the process results in no serious reduction in the fatigue limit. Hot galvanizing appears to seriously affect the fatigue limit of steel, while electrodeposited zinc results in no ill effects.

There is little information concerning chromium plating of aluminum. BEERWALD [74] reported tests on rotating beam specimens of pickled and heavily chromium-plated Dural in which the fatigue strength was reduced 15 per cent owing to the pickling and was restored by the 0.08-mm chromium plating. In another study [75] static and fatigue tests were made on nickel-plated and chromium-plated aircraft materials. A reduction in fatigue strength in air was observed in all cases with the exception of the bright nickel coating.

The cladding of aluminum reduces the fatigue life of the core material, since the outer shell is usually of a lower strength material than the core. Though the cladding is only a small portion of the total sheet thickness, its effect on the fatigue life of the core is quite pronounced as observed by BRICK and PHILLIPS [76] who found a reduction of about 35 per cent due to the cladding. Similar results have been observed by others. [77, 78, 79, 80]

Recently, SUZUKI [81] investigated strain figures appearing on the surface of copper electrodeposits subjected to fatigue. Copper alloys were used as the underlying material and the major concern was with the strain figures formed due to flecking, the disposition of the flecks, and the magnitude of the critical maximum shear strain. Apparently, however, the effect of the plating on the fatigue strength was not determined.

The volume of literature on the effects of liquid metal environments and corrosion-fatigue in general is enormous and no attempt will be made to review it here. Russian scientists have been among the foremost investigators in this field.

From the brief review of the solid surface film effects on the fatigue of metals, it appears that very little basic work has been done especially concerning the effects of oxide and metallic films. The whole subject of surface film effects on fatigue properties appears to be worthy of considerable study because of its extreme practical importance as well as fundamental interest.

III. Surface-Active Agents and Electrolytes

Theoretical Background

The chemistry and physics of surfaces play an important role in the consideration of the effects of surface-active agents and electrolytes on the

mechanical behavior of materials. This subject is, however, too vast to be covered adequately here and only a few of the important aspects will be treated.

Since a surface contracts spontaneously, there is free energy associated with it and work must be done to extend the surface. In the solution of problems involving surfaces, almost invariably, a hypothetical tension is substituted for the free energy. This tension is assumed to act in all directions parallel to the surface and it is equal to the free surface energy. Such a surface tension has the same dimensions as surface energy (mass/time^2). The work done in extending by 1 cm^2, a surface which is pulling with a tension of γ dynes per cm will be γ ergs per cm^2 and is equal to the free surface energy. GIBBS[82] was careful to point out the distinction between surface tension γ and surface stress for a solid. The surface stress is a measure of the work required to deform a surface, while γ measures the work required to create a new surface. Whether these two quantities differ numerically depends upon the statistical mechanics of the distribution of atoms or molecules at the surface.[83] In general, the surface stress and surface tension γ are the same for liquids and different for solids. OROWAN[84] has given a simple argument to show that for a homopolar crystal the surface stress may easily be compressive rather than tensile, while LENNARD-JONES and DENT[85] have made calculations which show a tensile surface for ionic crystals of the rock-salt type. SHUTTLEWORTH,[86] after making more refined calculations for rare gas crystals and alkali halides, considered that although the sign of the surface stress is uncertain there was no question that it is greatly different from the surface energy. These points regarding the difference between surface stress and surface tension are important in that many of the investigations concerned with surface phenomena in solids consider the two to be equal. The subject is made more complicated when dislocations or piled-up groups of dislocations at the surface are considered. In this case, the surface stresses are localized within atomic dimensions of the surface and are combined with a quasi-surface distribution of stress due to the dislocations which will extend to a depth beneath the surface for at least as great as the mean distance between dislocations. For piled-up groups, the effect will extend further into the crystal.

Adsorption is the concentration of one constituent of a solution or of a gaseous mixture at a surface. Positive adsorption of a constituent is an increase in concentration at a surface; a decrease in concentration is negative adsorption. GIBBS[82] defined adsorption or "surface excess" for a solution as the amount by which the total quantity of a component in an actual system exceeds that in an idealized system. In an actual system (Fig. 19a), the horizontal dotted lines represent approximately the limits of the transitional region between a phase A and a phase B. A normal to the surface is rotated so as to enclose a volume of cross-section A perpendicular to the surface. The volume is defined by drawing surfaces P_AQ_A and P_BQ_B parallel to the physical surface at a point in the bulk phase where the composition of the

VOL. 9 1961

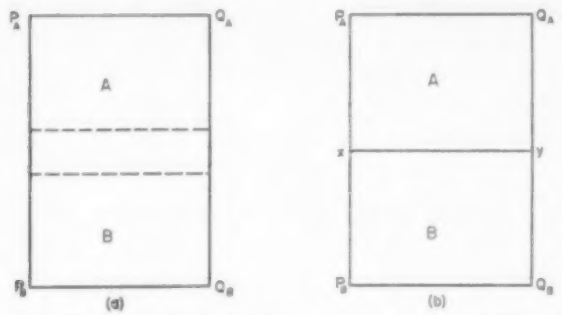

FIG. 19. Gibbs' method of defining "surface excess." GIBBS.[82]

matter in each phase is the same as that of the interior. There will be a definite amount of each component contained in this volume. For the idealized system (Fig. 19b), the phases are separated by a mathematical plane XY, parallel to the physical surface; the composition of both phases remains absolutely constant up to the dividing surface.

The amount of each component in the idealized system depends upon the position of the surface XY.

By considering the thermodynamic properties of the above system, Gibbs derived the relationship:

$$d\gamma = SdT - \Gamma_1 d\mu_1 - \Gamma_2 d\mu_2 \ldots - \Gamma_i d\mu_i, \quad . \quad . \quad . \quad (1)$$

where S is the entropy, Γ_i the surface excess of component i and μ_i the chemical potential.

For a system of two components, i.e., solvent and one solute at constant temperature:

$$d\gamma = -\Gamma_1 d\mu_1 - \Gamma_2 d\mu_2. \quad . \quad . \quad . \quad . \quad . \quad . \quad . \quad (2)$$

If the surface XY is fixed so that the surface excess of component 1 vanishes,

$$d\gamma = -\Gamma_2 d\mu_2. \quad . \quad . \quad . \quad . \quad . \quad . \quad . \quad . \quad (3)$$

The following expression may be written for solutions where the activity coefficient of component 2 is f_2 and its mole fraction N_2:

$$d\gamma = -RT\,\Gamma_2 d\ln f_2 N_2. \quad . \quad . \quad . \quad . \quad . \quad . \quad . \quad (4)$$

Where

$$\mu_i = \mu_i^\circ + RT \ln f_i N_i, \quad . \quad . \quad . \quad . \quad . \quad . \quad . \quad (5)$$

Equation (4) can be rewritten

$$\Gamma_2 = -\frac{f_2 N_2}{RT} \frac{\partial\gamma}{\partial(f_2 N_2)} \quad . \quad . \quad . \quad . \quad . \quad . \quad . \quad (6)$$

For dilute and ideal solutions where C_2 is proportional to the mole fraction and $f_2 = 1$,

$$\Gamma_2 = -\frac{C_2}{RT} \frac{\partial\gamma}{\partial C_2} \quad . \quad . \quad . \quad . \quad . \quad . \quad . \quad . \quad (7)$$

The ability of a liquid to wet a surface may be measured by the contact angle θ (Fig. 20). When $\theta = 0$, a solid is said to be completely wet, and incompletely wet if there is a finite contact angle. By convention, the angle is measured through the liquid. The relationship between contact angle and surface tension has been shown by SUMNER[87] to be:

$$\gamma_{SV} - \gamma_{SL} = \gamma_{LV} \cos\theta, \quad . \quad . \quad . \quad . \quad . \quad . \quad . \quad (8)$$

where S, V, L refer to the solid, vapor and liquid phases. DUPRE[88] showed

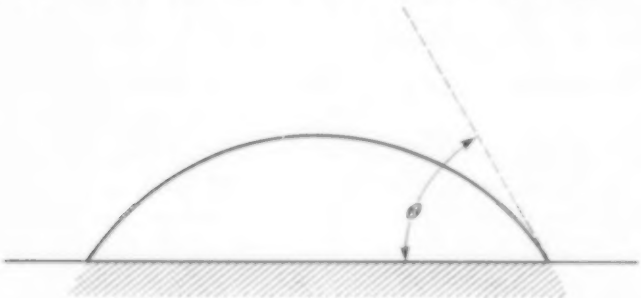

FIG. 20. Method of defining contact angle.

that W_A, the reversible work of adhesion of liquid and solid is related to the free surface energy terms:

$$W_A = \gamma_{S^\circ} + \gamma_{LV} - \gamma_{SL}, \quad . \quad . \quad . \quad . \quad . \quad . \quad . \quad (9)$$

where γ_{S° is the free surface energy at the solid–vacuum interface. The reversible work of cohesion of the liquid W_C is:

$$W_C = 2\,\gamma_{LV} \quad . \quad . \quad . \quad . \quad . \quad . \quad . \quad . \quad (10)$$

Combining Eqs. (8) and (9)

$$W_A = (\gamma_{S^\circ} - \gamma_{SV}) + \gamma_{LV}\,(1 + \cos\theta) \quad . \quad . \quad . \quad . \quad (11)$$

$\gamma_{S^\circ} - \gamma_{SV}$ is the free energy decrease on immersion of the solid in the saturated vapor of the liquid.

COOPER and NUTTALL[89] derived the conditions for the spreading of a liquid "b" on a solid (or liquid) body "a":

For spreading $\quad S > 0$

For nonspreading $\quad S \leqslant 0$

where: $\quad S = \gamma_a - (\gamma_b + \gamma_{ab}). \quad . \quad . \quad . \quad . \quad . \quad . \quad . \quad (12)$

Also $\quad S = W_A - W_C, \quad . \quad . \quad . \quad . \quad . \quad . \quad . \quad . \quad (13)$

or $S = \partial F/\partial\sigma$ where F is the free energy of the system and σ the surface area.

Combining Eqs. (9), (10) and (13),

$$S = -\frac{\partial F}{\partial \sigma} = \gamma_{S^\circ} - \gamma_{SL} - \gamma_{LV}. \quad . \quad . \quad . \quad . \quad . \quad (14)$$

VOL. 9 1961

The penetration of liquids into fine cracks or capillaries has been used by various investigators to explain the effects of surface-active agents. The treatment of the subject is based upon the difference in pressure ΔP across the meniscus into a tube of radius r and advancing contact angle θ_A.

$$\Delta P = \frac{2\gamma \cos\theta}{r} \quad . \quad . \quad . \quad . \quad . \quad . \quad . \quad . \quad (15)$$

When the material is completely wet, $\cos\theta = 1$ and

$$\Delta P_{max} = \frac{2\gamma}{r} \quad . \quad . \quad . \quad . \quad . \quad . \quad . \quad . \quad (16)$$

For small capillary tubes or microcracks, the ΔP value may be very high.

When a metal is immersed in a medium containing organic molecules which have a polar group, the molecule first becomes attached to the metal through dipole-image forces and any chemical combination with the surface atoms of the adsorbing metal must develop afterwards. DUBRISAY[90] and PRUTTON *et al.*[91] demonstrated that fatty acids react with many metals to form salts only after the metal oxide has been formed. TINGLE[92] has shown that traces of water also must be present for the formation of the metal salt. However, HILTON-SMITH and co-workers[93, 94, 95] have recently demonstrated that clean, dry, oxide-free metals can react with fatty acids at ordinary temperature to form soap films when the metal surface has been freshly scraped or cut. This mechanical activation of the surface decreases rapidly with time and will not occur with an old surface. These investigators associated the reaction with the KRAMER[96, 97] effect. This phenomenon involves a property of freshly exposed metal surfaces whereby electrons are made available at room temperature at a work function considerably below that associated with an aged surface. Kramer has shown that these electrons may be detected by use of a modified Geiger point counter tube. The energy of such an electron is estimated to be somewhere below four electron volts. This amount of energy is sufficient in the case of the reaction of stearic acid and copper to form copper stearate. The free energy for this reaction is 46.86 Kcal/mole and since each electron volt is equivalent to 23 Kcal/mole, it is enough to satisfy the free energy requirement of the reaction.

The rate of formation of metal soaps on the surface of the metal is not necessarily rapid so that in many cases a complete monolayer is not formed. DOBY and MAHNCKE[98] have shown that at ordinary temperatures, only one-fourth of the molecules in an adsorbed monolayer of stearic acid on copper are chemically combined with the surface. However, Hilton-Smith and co-workers have shown that n-nonadecanoic acid deposited from solutions of cyclohexane reacted with freshly cut surfaces of specimens of copper, lead, aluminum and magnesium to form a complete monolayer. ZISMAN *et al.*[99] has demonstrated that in many cases mixed films of the solvent and the fatty acid soap are formed if the time of immersion of the specimen is short. A 20-hour immersion was necessary to form a complete mono-layer of docosylamine ($C_{22}H_{45}NH_2$) from a hexadecane solution.

Effects of Surface-Active Agents

Surface films or electrical double layers have long been known to change the surface energy of liquids and solid bodies. It was considered possible therefore for such layers to affect the mechanical properties of solids. These effects on single and polycrystalline metals and on nonmetals have been studied largely by Rehbinder and co-workers in Russia. The term "Rehbinder Effect" here refers to the change in the mechanical properties of solids

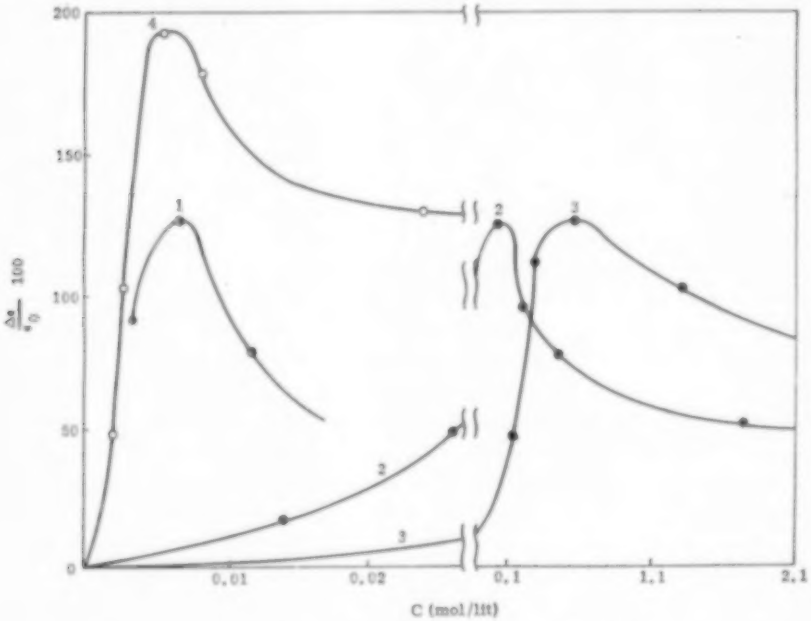

FIG. 21. Adsorption effect of various surface-active agents on the creep behavior of tin single crystals. Solvent—octane. LICHTMAN *et al.* [6]

1—stearic acid
2—caprylic acid
3—propionic acid
4—oleic acid

(whether oxide-coated or not) on immersion in solution of certain polar substances (referred to as surface-active agents of "surfactants") such as oleic acid or cetyl alcohol.

Rehbinder first found an effect of such surface-active substances in 1928 in connection with the pendulum hardness of minerals. Subsequently, it was looked for and found in connection with the flow of metals and reported by REHBINDER [100] and REHBINDER and WENSTROM. [101] They observed that the flow of lead, tin and copper sheets under constant load was much faster if small amounts of surfactants (cetyl alcohol, N-valeric, N-heptoic, stearic, oleic, palmitic and cerotic acids) were present in the hydrocarbon (paraffin) bath in which the metal was immersed. As with nonmetals, the weakening effect was a function of concentration of the active agent and the length of

the active molecule. The relationship which was found[101, 102, 103] between the change in mechanical properties and the concentration of solution is of particular interest. Figure 21 shows the effect on the creep behavior of tin single crystals; Table 1 gives the results on the yield strength. The data show that the yield strength first decreases with increasing concentration of the solution and then increases. The creep rate follows the same weakening effect as a function of concentration.

TABLE 2

Effect of Oleic Acid–Vaseline oil solution on the mechanical deformation of single crystals of tin

Dia = 0.76 – 0.96 mm. $41° < \chi_0 < 48°$ $\dot{\varepsilon} = 4.8$ per cent min^{-1}

Mechanical Properties	*Oleic Acid Concentration in Vaseline Oil (per cent)*				
	0	0.1	0.2	0.5	1
Yield point, g/mm^2	250	210	145	180	200
Work-hardening coefficient	0.54	0.42	0.11	0.21	0.24
Width of slip bands, in μ	52	38	36	8.5	9.5

The maximum (Cm) in the curve of the change in yield strength or creep rate, as related to the concentration of polar molecules, is believed by these investigators to occur when a monomolecular layer is formed. The concentration (Cm) decreases with increasing molecular weight of the organic homologues by a factor of 1.3 to 1.4 for each $-CH_2$ link. The nature of the solvent was also reported to be important. A relationship was observed between the weakening effect in creep and yield strength and the orientation of the crystal. The maximum effect was at $\chi_0 = 45°$.

LICHTMAN *et al.*,[104] in his work on tin and lead single crystals, demonstrated that both temperature and strain rate considerably influenced the activity of the surface-active agents on the flow characteristics (Fig. 22). In these experiments the decrease in rupture stress was taken as a measure of the adsorption effect. At 20°C, the maximum effect occurred at a strain rate of about 250 per cent per min. When the temperature was increased to 100°C, the curve was displaced and the maximum occurred at 1000 per cent per min. The type of surface-active agent used did not seem to change the deformation rate at which the maximum effect occurred. Oleic acid, palmitic acid and cetylalcohol solution produced the same strain rate maximum for lead crystals. For tin single crystals at 20°C, the maximum effect was obtained at a strain rate of 5 per cent per min; at 100°C, it occurred at 500 per cent per min. The above effects are believed by the investigators to show evidence that physical adsorption is important. While oleic and palmitic acids react with lead to form chemical compounds (lead oleate and lead palmitate), it is stated that cetylalcohol does not. The decrease in the adsorption effect was

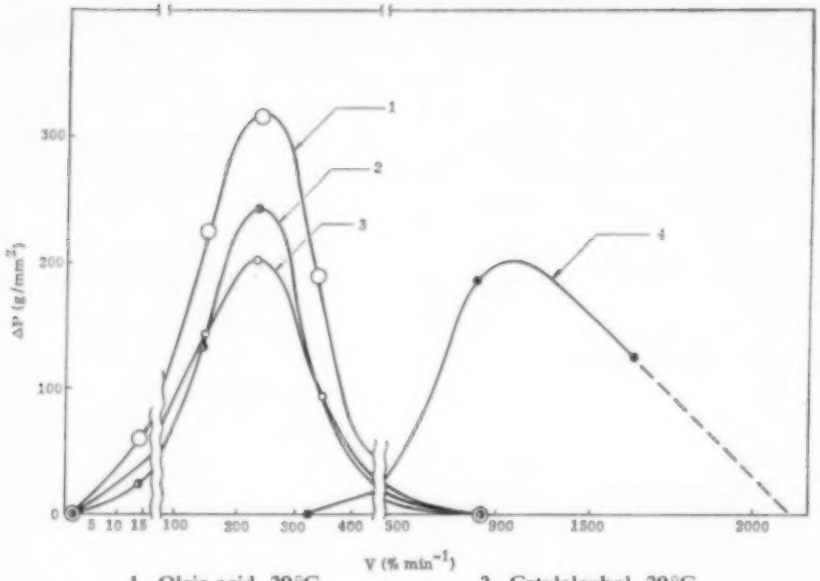

1. Oleic acid, 20°C
2. Palmitic acid, 20°C
3. Cetylalcohol, 20°C
4. Oleic acid, 100°C

FIG. 22. Effect of adsorption on the decrease of rupture stress ΔP, as a function of strain rate and temperature. LICHTMAN *et al.*[104]

explained by a change in the type of adsorption. It was supposed that at the higher temperature, chemi-adsorption took place and decreased the mobility of the adsorbed molecules so that fewer molecules were able to enter the microcracks which were postulated to exist on the surface.

The effect of adsorbed surfactants on the size of the slip bands of deformed single crystals of tin, lead and aluminum was studied by the associates of Rehbinder. MASLENNIKOV,[105] using cinematography (64 frames per second), found that in the presence of a surface-active medium, a very fine uniform structure of slip bands 3 to 4 microns wide was developed, whereas in air the slip bands were about 50-microns wide. From an electron microscope study of oxide replicas obtained on single crystals of aluminum deformed 75 per cent in paraffin oil, Maslennikov reported that at a magnification of 14,000 to 16,000 the width of the slip bands did not exceed 1000 Å, although the width varied considerably. Certain bands were evidently less than 200 Å wide. When the specimen was deformed in a bath containing a surface-active agent, systematic shear along one octahedral system of glide planes was absent. He assumed from these observations that during the early stages of plastic deformation in the surface-active media, several slip systems were operative. Microcracks varying in width from 200 to 1000 Å also were reported.

Other tests were performed[105] on single crystals of zinc and tin, and it was observed that the yield strength was the same for specimens tested in air and

VOL. 9 1961

in a nonpolar paraffin oil. When 0.2 per cent of oleic acid was added to the oil, the strength was halved. Similarly, the rate of flow in a creep test could be increased five to ten times by the addition of oleic acid. These effects were accompanied by an increase in the number of glide lamellae and a decrease in their width as reported for the tensile tests. It was claimed further that while the load was applied, the electrical conductivity of the specimen at a given strain rate was less in the crystals deformed in oleic acid solutions, and that when the load was removed, the conductivity increased toward its normal value. This was taken to show the healing of the microcracks.

Several attempts were made later in other laboratories to repeat and explain Rehbinder's results on single crystals. KEMSLEY [106] sought the effect on the yield stress and electrical conductivity of tin single crystals and found no effect. This result was explained by REHBINDER and LICHTMAN [107] as due to Kemsley's very slow rate of stressing and also due to the use of impure paraffin oil. Other investigators also failed to confirm the electrical conductivity effect, although the yield stress observations were noted.

Concerning the effects of a surface-active medium on the deformation and associated changes in the electrical resistance of metallic crystals, it was shown [108] in tests on zinc and tin monocrystals extended rapidly in air or in a 0.2 per cent solution of oleic acid in petrolatum, that although the percentage elongation in the surface-active solution was about twice that in air for all orientations of the crystal, yet at a given strain of the monocrystals their electrical resistance was independent of the medium in which the deformation occurred. This suggests that the original controversial resistivity observations of Rehbinder may not have been taken for the same percentage elongation when comparing results in air and in the active medium.

Effects of Electrolytes

Effects of immersion in aqueous solutions containing electrolytes, with or without changes in the applied potential, on the mechanical properties have been studied by several groups of investigators. REHBINDER and WENSTROM [109] first reported an effect on both the indentation hardness and tensile properties of metals in various electrolytes. These authors have shown that in conducting materials such as pyrite, graphite, thallium, zinc, lead and tellurium the hardness (H) varied as a function of the potential drop ϕ at the solid interface. The resulting curves of the variation of hardness (Fig. 23) or tensile stress for a given strain with the applied potential were similar to the electrocapillary curve for a mercury-electrolyte interface. The maximum values for these mechanical properties occurred at the maximum value for the electrocapillary effect which corresponds to the potential when the surface is uncharged (not at zero potential). The hardness was measured by using the amplitude damping of an oscillating pendulum similar to that of the Herbert's pendulum tester.

Electrocapillary effects may be measured by an apparatus shown schematically in Fig. 24. A long tube (A) containing mercury, drawn out into a

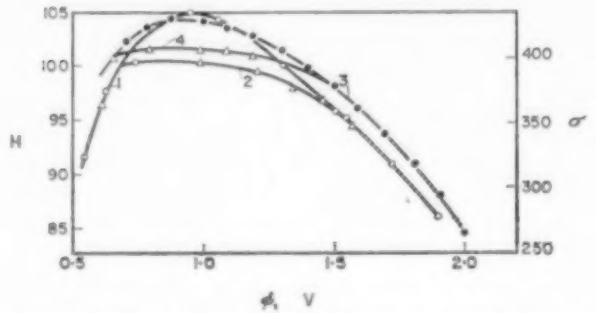

FIG. 23. The variation of hardness and surface tension of thallium as affected by the potential drop ϕ. REHBINDER.[109]
1—Hardness in 1N Na_2SO_4.
2—Hardness in 1N Na_2SO_4 + isoamylalcohol 0.185 mole/1.
3—Surface tension σ for thallium amalgam (41.5 per cent Tl) in 1N H_2SO_4.
4—Same + isoamylalcohol 0.175 mole/1.

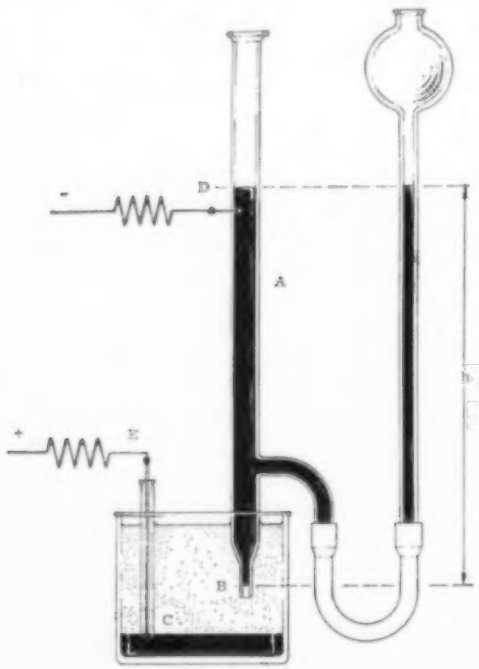

FIG. 24. Electrocapillary apparatus.

capillary (B), is immersed in an aqueous solution. As a result of the interfacial tension, the surface of separation appears in the capillary tube. The difference in level between the upper and lower surfaces of the mercury is a

measure of the interfacial tension. When a potential is applied between the mercury layer (C) and the mercury column at (D), a change in the interfacial tension occurs. This can be measured by determining the alteration in the height of the mercury column required to bring the surface in the capillary tube back to its original position. If initially the mercury has a positive potential with respect to the solution and gradually is made more negative, it is found that the surface tension first increases until a maximum is reached and then decreases.

The thermodynamic equation for electrocapillary effect first deduced by LIPPMAN[110] can be written:

$$\left|\frac{\partial\sigma}{\partial\phi}\right|_s = -e_s, \quad . \quad . \quad . \quad . \quad . \quad . \quad . \quad . \quad (17)$$

where e_s is the charge density at the interface and σ is the surface free energy.

As Fig. 25 illustrates, the hardness $H(\phi)$ curve has the usual parabolic

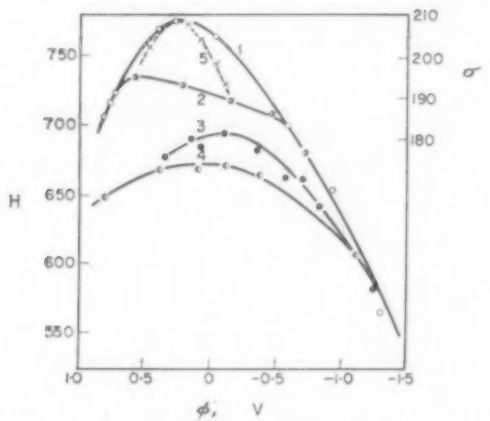

FIG. 25. Hardness H and surface tension σ of tellurium plotted against potential drop ϕ:

1—H in 1N Na_2SO_4.
2—Same + isoamylalcohol 0.185 mole/l.
3—Same + thiocarbomide 0.5 mole/l.
4—Same + pyrogallol 1 mole/l.
5—Molten tellurium in a melt of KCl + LiCl at 550°C. See LICHTMAN.[6]

shape of the electrocapillary curve $\sigma(\phi)$ and the maximum hardness corresponds to the uncharged surface $-\partial\sigma/\partial\phi = e_s = 0$. The addition of surface-active materials to aqueous solutions of sodium sulphate lowers the maximum hardness. Using 1N Na_2SO_4 and NaCl, the effect of polarization on the hardness of tellurium was investigated (Fig. 25). The position of the maximum hardness corresponds to that of the maximum surface tension for molten tellurium. The addition of isoamylalcohol lowers the hardness of tellurium and displaces the maxium towards the anodic region.

The investigation of the electrocapillary effect was extended to the study

of the creep behavior of metal single crystals.[111] Lead and tin single crystals were subjected to a cathodic polarization treatment ($\phi = 3.5$V) to reduce the oxide before extension in the creep apparatus. The reformation of the oxide was prevented by using an acid medium of pH = 2.8. The crystals were tested in aqueous solutions of 0.1N Na_2SO_4 and in 0.1N Na_2SO_4 to which sodium hexadecyl-bensolsulphonate ($C_{16}H_{33}C_6H_4SO_3Na$) had been added. The data (Figs. 26 and 27) reported in terms of strain (ϵ) after five hours

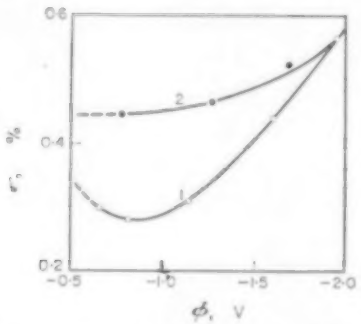

FIG. 26. Electrocapillary curves of the adsorption-assisted creep deformation of lead single crystals. Tests conducted in aqueous solutions of: 1—0.1N Na_2SO_4; 2—0.2N Na_2SO_4 + 0.07 mole/l $C_{16}H_{33}C_6H_4SO_3Na$. WENSTROM.[111]

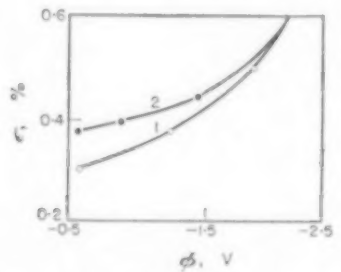

FIG. 27. Electrocapillary curves of the adsorption-assisted creep deformation of tin single crystals. Tests conducted in aqueous solution of: 1—0.1N Na_2SO_4 + 0.01N H_2SO_4; 2—same + 3.30 mole/l C_3H_7OH. WENSTROM.[111]

follow the electrocapillary curves of hardness with a minimum instead of a maximum when $\epsilon_s = 0$. Only the cathodic part of the curve was investigated for metals because of the formation of oxides in the anodic region. Sodium hexadecyl-bensolsulphonate additions accelerated the strain rate and its effect is most marked at the minimum. As the polarization increases, independent of sign of the charge, the effect of the organic additive diminishes and becomes zero at a voltage of −1.8 for tin and −2 volts for lead. In the interpretation of their results, Rehbinder and Wenstrom place emphasis on the effects of adsorption on microcrack formation and not on the removal of the oxide layer as did other investigators. Rehbinder and Wenstrom point

VOL. 9 1961

out that in their experiments, the single crystals were deformed under conditions of prolonged cathodic polarization which excludes the possibility of surface oxide films. Typical electrocapillary curves can not be obtained in the presence of oxide films. Their effects agree with those of PFUTZENREUTER and MASING[112] on gold and platinum. At the same time, it is claimed that the presence and thickness of oxide films considerably influence the value of the adsorption effect.[113]

The effect of electrolytes on the mechanical properties of metals has also been studied by Andrade and his co-workers and others. ANDRADE and

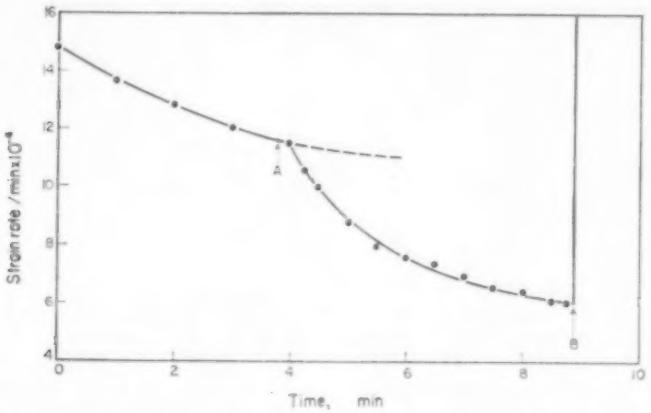

FIG. 28. Effect of formation of a film on the creep behavior of cadmium single crystal. PHILLIPS and THOMPSON.[116]

RANDALL[39, 107] first noticed that immersion of cadmium single crystals in cadmium nitrate gave an initial increase in the rate of creep which, however, quickly stopped; twice the stress was then needed to give further flow. With zinc nitrate, immediate hardening occurred. It was also found that the creep rate of cadmium single crystals increased by a factor of 20 when immersed in a plating solution. Polycrystalline wires showed none of these effects. In a later publication, ANDRADE[107] reported that the accelerating effect of electrolytes on the creep behavior occurred only on specimens with an initial oxide film. Other studies[114, 115] of the effect of electrolytes on zinc crystals indicated that the effects were caused by removal of an oxide film and, in the case of the nitrate ion, by removal of a hydroxide film.

The effect of the formation of a film on the creep behavior of a clean crystal of cadmium and its subsequent removal is shown in Fig. 28 from the investigation of PHILLIPS and THOMPSON.[116] In these experiments, crystals were first extended in distilled water up to point *A* where 0.5N $Cd(NO_3)_2$ was added. The strain rate began to decrease a short time after the addition of the cadmium nitrate and continued to decrease until at point *B*, 2 per cent H_2SO_4 was substituted for the nitrate. At that point the creep rate immediately began to increase. On the other hand, when the crystal had been previously

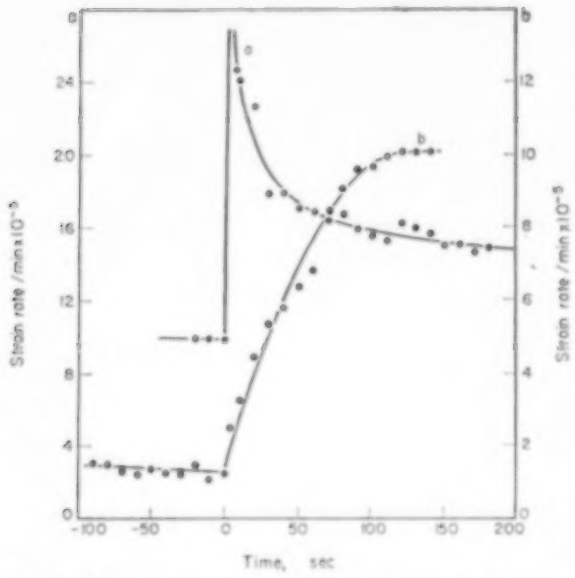

FIG. 29. Effect of cadmium nitrate on the creep behavior of a cadmium single crystal with an initial hydroxide film. PHILLIPS and THOMPSON.[116]

given an anodic treatment to form a *thick* hydroxide film, the application of cadmium nitrate (0.5N) caused an increase in the creep rate (Fig. 29). Curve *b* shows the effect obtained when a 0.5N $Cd(NO_3)_2$ solution was applied (at $t = 0$) to a cadmium crystal which had been previously coated electrolytically with a hydroxide film. The strain rate rose by a factor of 6.3 in 120 sec and subsequent weighing showed that the film thickness had been reduced. When at the end of 147 sec, 2 per cent sulphuric acid was added, the creep rate fell rapidly (Curve *a*).

During the course of their investigation, PHILLIPS and THOMPSON[116] observed that when a *thin* film of hydroxide on cadmium single crystals was removed rapidly by the application of sulphuric acid, a sudden extension occurred at the instant of removal. The removal of the film appeared to be similar in its effect upon creep rate to a sudden small increase in load. Hydrated oxide films were allowed to form on cadmium crystals by immersing them in water containing air. The crystals were subjected to a constant load creep test in water until the creep rate ceased to fall rapidly. They were then exposed alternately to distilled water and to 2 per cent sulphuric acid. At each change from water to acid, a transient extension occurred but none was observed on the reverse interchange. In Fig. 30, the changes from acid to water are marked by single ordinates and those from water to acid by double ordinates.

PFUTZENREUTER and MASING[112] studied, in a manner similar to the Rehbinder work, the effects of an applied potential on the creep behavior

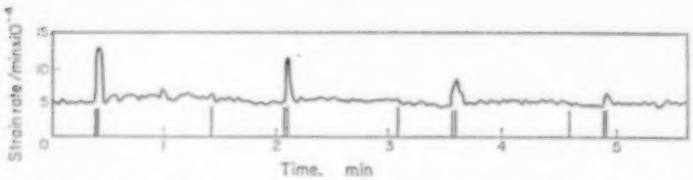

FIG. 30. Transient extensions caused by the addition of sulphuric acid during a creep test. PHILLIPS and THOMPSON.[110]

of various metals. They found that when specimens of lead, zinc, silver, gold and platinum (of many single crystals each extending throughout the cross section) were undergoing creep, the addition of an electrolyte changed the creep rate. When a potential was applied between the specimen and the solution, the resulting data for steady creep rate plotted as a function of the applied potential were similar to that of the electrocapillary effect.

ANDRADE and RANDALL[118] were able to show that the electrolyte alone, without an applied potential, had a marked effect on the mechanical behavior of single crystals. Although the results were variable with respect to the magnitude of the effect, both cadmium and zinc crystals, when exposed to a sulphate solution of the metal, exhibited marked changes in creep behavior. The ratio R of the flow rate when the specimen was immersed in the electrolyte to the rate before immersion was as large as 9.6; in some cases R varied between 2 and 3.5. In this work, the load was increased in small steps until a slow rate of flow was produced; afterwards, the electrolyte was introduced when a definite pre-strain was attained. The effect of the pre-strain (Table 3) seems to be constant for values greater than 10 per cent. It was

TABLE 3

Effect of pre-glide P on the average values of R

Pre-glide per cent	0–9	10–24	25–49	50–80
Average R	1.4	3.3	3.4	3.4
Number of tests	8	10	16	4

reported that nitric acid (1 : 500) and (1 : 50) gave R values of 1.6 and 7, respectively. Saturated solutions of cadmium cyanide, cadmium iodide, and water used as a control had no effect on the creep behavior of cadmium single crystals.

The creep behavior of cadmium crystals in cadmium nitrate differs in some important aspects from those crystals in cadmium sulphate. Even though the creep rate of the crystals in the nitrate bath began to increase immediately upon coming in contact with cadmium nitrate, as it did in the sulphate solution, within five minutes the flow almost completely stopped (Fig. 31). The effect of zinc nitrate on the creep rate of cadmium (Fig. 32) was found to be such that the initial increase in rate was absent; instead

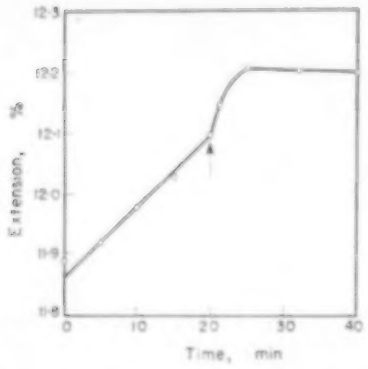

FIG. 31. Flow of cadmium crystal ($\phi_0 = 32°$) exposed to cadmium nitrate solution. Contact of the electrolyte produces an initial increase in rate, but after five minutes, flow has practically ceased. ANDRADE and RANDALL.[115]

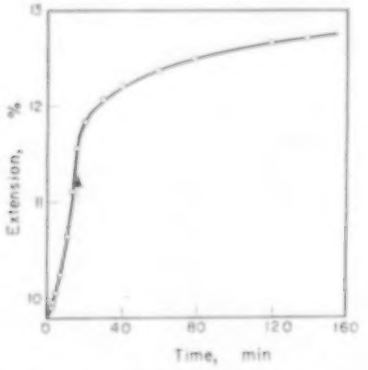

FIG. 32. Flow of cadmium crystal ($\phi_0 = 48°$) exposed to zinc nitrate solution. There is no initial increase in rate: the rate decreases continuously from the moment of contact. ANDRADE and RANDALL.[115]

there is a continuous rate decrease. Apparently, the cadmium ions act on the surface oxide film of a cadmium crystal so as to diminish its effect; however, the zinc ions do not.[115] The nitrate ion builds up an oxide or hydroxide layer on the surface which inhibits flow and raises the critical shear stress.

Investigations of Mechanisms of the Weakening Effect

One of the major questions which arose during the early stage of the research work on the effects of electrolytes and surface-active agents was concerned with the mechanism causing the decrease in the strength properties. Since it is known that the presence of a film, formed either by chemical reaction or by plating, increased the strength of single crystals, it was believed by some that

VOL. 9 1961

the decrease was due to the removal of such films. A general answer to this question is difficult to obtain since, with the exception of gold, metals generally have an air-formed oxide film. This inability to obtain film-free specimens makes it difficult to determine whether the strength characteristics of a metal in an electrolyte or surface-active medium are those of a metal with a surface layer which does not impede the motion of dislocations or whether other effects are also important. There can be no doubt that the removal of the surface film alone will reduce the strength of crystals.

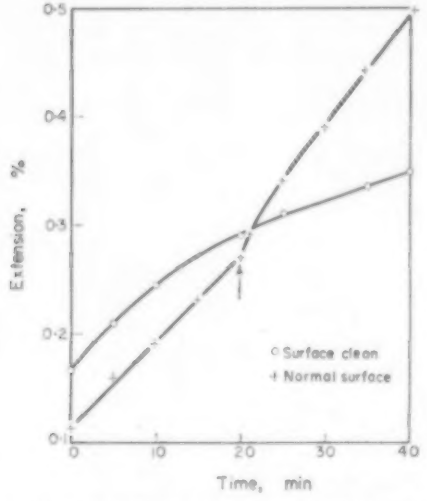

FIG. 33. Behavior of surface-clean and normal cadmium crystal ($\phi_0 = 22°$) contrasted. ANDRADE and RANDALL.[115]

In an attempt to provide data on this question, cadmium single crystals[115] were cleaned by heating in vacuo (pressure $\sim 10^{-4}$ mm Hg).[117] This treatment causes the surface of the crystal to be covered with pits. When subjected to a creep test, the rate ratio for specimens which had not been cleaned in vacuum was 1.5 when cadmium sulphate was used as the electrolyte. There was no change in the creep rate with the cleaned specimens. These data are reported in Fig. 33 where the arrow designates the time when the electrolyte was introduced to the testing cell. It is important to observe that the creep rate for the crystals designated as having a normal surface is considerably greater than that for the cleaned crystals after the introduction of the cadmium sulphate. If the cleaned specimens really had clean surfaces, free from all traces of films, the two curves would be expected to have the same strain rate in some region unless there is an additional effect caused by the action of the electrolyte. Unfortunately, the tests were conducted for a period of only 20 min and it is not known whether the creep rates for the specimens would change for a longer period of testing.

HARPER and COTTRELL,[12] in their study of the effect of surface conditions

on the deformation characteristics of zinc single crystals tested in a medium containing an electrolyte or a surface-active agent, arrived at the conclusion that the role of polar molecules was to remove the strengthening effect of the oxide coating. Five crystals which had been heavily oxidized in steam and subjected to a constant resolved shear stress of 70 g/mm^{-2} for 37 min were immersed in a dilute hydrochloric acid bath. The rate of flow immediately increased followed by a fast transient flow (Fig. 34). In a similar experiment

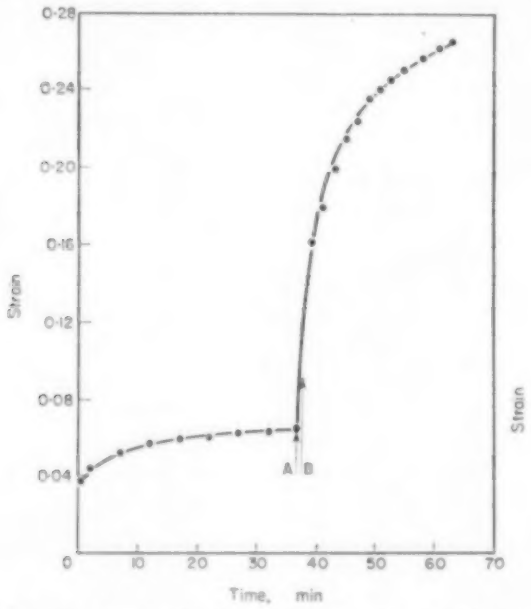

FIG. 34. Creep curve of an oxidized crystal. Hydrochloric acid was applied at A and removed at B. HARPER and COTTRELL.[12]

with specimens which had been electropolished and stressed to 39 g/mm^{-2}, after 40 min under load, a perceptible but small decrease in creep rate was observed upon immersion in the hydrochloric acid (Fig. 35). A creep specimen which had been etched in hydrochloric acid, washed, dried and stressed to 42 g/mm^{-2} did not exhibit any change in creep rate when the hydrochloric acid was introduced after 30 min of test.

Contrary to the results obtained by Rehbinder and his co-workers, Harper and Cottrell reported that the creep behavior of zinc crystals was affected by the addition of oleic acid to paraffin oil only when the specimen had an oxidized surface. Figure 36 shows the creep curve of a zinc specimen under a stress of 63.5 g/mm^{-2}. At point *A*, paraffin oil was introduced and, within 5 min after immersion the flow rate increased. At point *B*, when the paraffin was replaced by a solution of paraffin oil and oleic acid (0.2 per cent), a further increase occurred. Paraffin by itself produced an effect only in

VOL. 9 1961

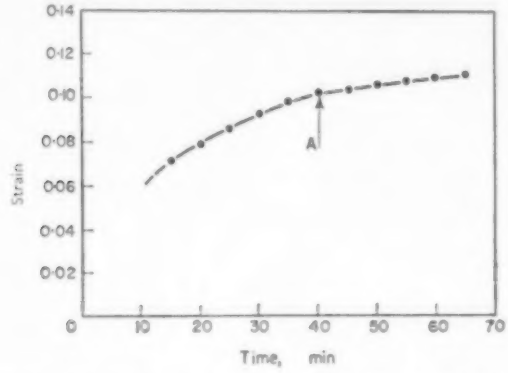

FIG. 35. Creep curve of a polished crystal. Hydrochloric acid was applied at A. HARPER and COTTRELL.[12]

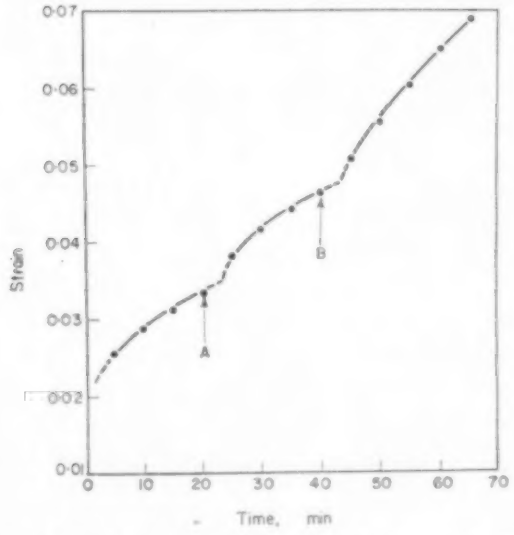

FIG. 36. Creep curves of an oxidized crystal. Paraffin was applied at A and oleic acid solution at B. HARPER and COTTRELL.[12]

heavily oxidized specimens, and with lightly oxidized ones, it was necessary that oleic acid be present. The creep rate of heavily oxidized zinc crystals also was found to increase upon immersion in kerosene and ethyl alcohol, whereas polished or etched specimens showed no response to these agents. The fact that there was an immediate response to kerosene and alcohol and a time lag in the response in paraffin oil suggested to Harper and Cottrell that the effect was concerned with the penetration of the surface film by the surface-active agent. In a set of experiments, kerosene in various proportions was added to paraffin oil and a linear relation was reported between kinematic

viscosity and the time of response to the medium (Fig. 37). Although this correlation at first appears to be valid, the activity of the paraffin oil and kerosene suggests that polar molecules were present in these materials. Further additions of an impure kerosene, for example, would increase the concentration of polar molecules and cause the reaction to proceed faster.

KLINKENBERG, LUCKE and MASING [118] confirmed the results of Rehbinder *et al.* Using tin and gold single crystals which had been cleaned by electrolytically

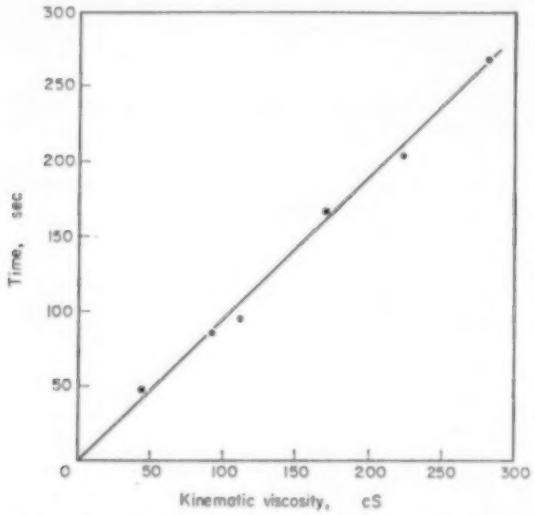

FIG. 37. Variation of time of response with viscosity of medium. HARPER and COTTRELL.[12]

polishing, a large increase in the creep rate was observed when the specimens were tested in a 1 per cent oleic acid–paraffin oil solution (Fig. 38). Similar results were found for cadmium single crystals. These results tend to confirm the viewpoint that the increase in the creep rate or a decrease in the tensile flow curve by a surface-active agent is not confined to specimens which have an oxide coating. For most metals, an oxide film forms immediately upon exposure to air; in an electrolytic polishing bath, the specimen is anodic and it can be argued that an oxide film may be present. These points cannot be raised for gold, however, for it is known that oxides do not form under ordinary conditions. In comparison with tests in paraffin oil, KLINKENBERG *et al.* [118] demonstrated that the creep rate of polycrystalline gold is increased when specimens were tested in 0.2 per cent oleic acid. Although the experimental results obtained with gold specimens definitely eliminated the necessity for assuming that a surface-active agent affects the plastic flow characteristics when an oxide film is present, it does not rule out the effects of oxygen or water or any other condensable species.

In a further attempt to clarify the controversy regarding the effects of

VOL. 9 1961

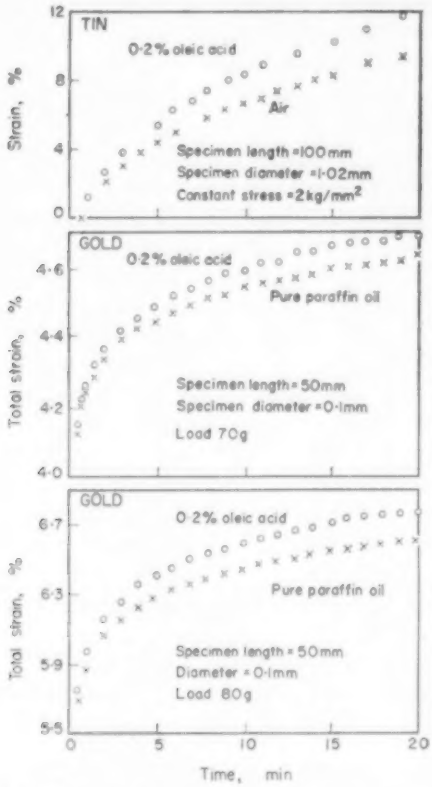

FIG. 38. Rehbinder effect on polycrystalline tin at constant stress and polycrystalline gold at constant load. KLINKENBERG, LUCKE and MASING.[118]

surface-active agents when an oxide layer is not present on the surface of metal single crystals, ROZHANSKII and REHBINDER[119] investigated the effects in a thorough manner. They tested both oxide-coated and clean tin specimens *in vacuo* and in rarefied vapors of various polar and nonpolar substances. Their results showed that while a large effect existed for oxide-coated crystals (creep was up to 100 times faster in ethyl alcohol at the optimum pressure than *in vacuo*), no great effect occurred on clean crystals unless they were very short. They suggested that stress concentrations greatly assist the effect and that these occur at the ends of a clean specimen or at the cracks in the oxide film. They discount the explanation of Andrade, and Harper and Cottrell, that the effect of the surface-active substance is to annul the hardening effect of the oxide film, not only because of the existence of a small effect on clean crystals, but also because the strength reduction by the surface-active substance is much greater than the strengthening produced by the oxide film.

In a more recent study, KRAMER[120] found strong evidence that the weakening effect of surface-active agents is associated with chemical adsorption. This point of view is directly contrary to those of the Russian investigators who, in a recent publication,[6] claim that the effect is due to physical adsorption. For example, it is cited that cetyl alcohol does not chemiadsorb on lead, but a decrease in the yield strength is found when these crystals are tested in such solutions. In Kramer's investigation, a number of single crystals of aluminum, copper, zinc and lead were deformed one per cent after first being chemically or electrolytically polished. The specimens were immediately placed in high-purity solvents containing the surface-active agents in concentrations which have been shown to affect the mechanical behavior of the metal specimens. In all cases, including lead in cetyl alcohol, the metal salt of the organic surface-active agent was found to be in the solution (Table 4). The presence of the metal soaps could only have been due to the solution of the products of reaction of the surface-active agent and the metal specimen. KRAMER[120] also showed that when aluminum single crystals were pulled in tension in a solution of paraffin oil and stearic acid, the extent and slope of Stages I and II were affected, but not the critical resolved shear stress. The extent of Stages I and II increased and their slopes decreased as the concentration of stearic acid increased up to 0.002 mole/l. Further addition of stearic acid caused a decrease in the extent and an increase in the slope. When aluminium stearate was added to the solution containing 0.002 mole/l, the extent and slope of Stages I and II was the same as those of crystals pulled in pure paraffin oil. According to Kramer, the adsorption follows the normally accepted process in that the polar molecules

VOL. 9 1961

TABLE 4

Formation of metal soaps
(specimens deformed 1 per cent and immersed for 24 hr)

No.	*Solution*	*Metal*	*Results*
1	0.1 Caprylic acid in benzene	Cu	Present
2	0.05N Caprylic acid in hexadecane	Cu	Present
3	Saturated sol. of stearic acid in benzene	Cu	Absent
4	0.01N Stearic acid in benzene	Cu	Present
5	0.006N Oleic acid in paraffin oil	Cu	Present
6	0.25N Caprylic acid in hexadecane	Zn	Present
7	0.1N Caprylic acid in paraffin oil	Zn	Present
8	0.006N Oleic acid in paraffin oil	Zn	Present
9	0.75N Capryl alcohol in hexadecane	Al	Present
10	1.0N Capryl alcohol in hexadecane	Al	Present
11	0.5N Capryl alcohol in paraffin oil	Al	Present
12	0.1N Caprylic acid in benzene	Al	Present
13	0.01N Stearic acid in benzene	Al	Present
14	0.005N Stearic acid in paraffin oil	Al	Present
15	0.006N Oleic acid in paraffin oil	Al	Present
16	0.003N Cetyl alcohol in paraffin oil	Pb	Present

are first physically adsorbed. However, in the presence of water or oxygen or, as recently found by HILTON-SMITH,[94, 95] when plastic strain is produced, chemical reaction can take place to form metal soaps. The metal soap thus formed will not remain on the surface for there will be a dynamic equilibrium and, at any given time, a fraction of the soap molecules leave the surface by dissolving in the solution while other molecules are adsorbed. The net effect is a removal of metal from the surface and, as a consequence, a decrease in the number of dislocations in the piled-up groups at the surface. The solution of metal soap may also be interpreted as a decrease in surface energy since the bond of strength between neighboring atoms must also have been reduced. The decrease in the number of dislocations at the surface will decrease the interaction between dislocation groups, will tend to decrease the formation of Lomer-Cottrell locks and thus decrease the work-hardening coefficient. Since the plastic flow characteristics are determined by the ease with which dislocations leave the crystal, the removal of dislocations by chemical action will decrease the flow stress and increase the creep rate. The effect of a surface-active agent is then not different materially from that of removing the surface by electrolytically polishing.[121] The effectiveness of a surface-active agent will depend upon the rate of solution of the soap formed and will be determined by the concentration of the solution, the solvent, the length and type of organic molecule, the type of polar group and the energy of adsorption.

With chemical adsorption and subsequent solution of the metal soap as a basic explanation of the weakening effect of surface-active agents, it is possible to explain the shape of the curve in Fig. 21, as well as the other phenomena reported. At low concentrations of the surface-active agents, the rate at which the polar molecules reach the metal surface is low but the rate of solution of the metal soap can be high. The amount of metal removed and, therefore, the number of dislocations removed from a piled-up group is correspondingly low. As the concentration is increased, the rate of adsorption of the polar molecules is increased and the number of metal soap molecules that pass into solution is increased. However, at some value of the concentration, the rate of solution of the soap will decrease because the solution is becoming saturated with respect to the soap molecules. This point will correspond to the maximum of the curve. In brief, on the rising portion of the curve of Fig. 21, the weakening effect is limited by the rate of adsorption which will increase with increasing concentration. On the falling portion of the curve, the weakening effect is limited by the rate of desorption of the metal soap. The rate of desorption in this case will decrease with increasing concentration of the polar molecules. For a given solvent and a given metal, in general, the solubility of the metal soap will decrease with the chain length of the organic acid. (The solubility is, of course, modified by the presence of double and triple bonds, side branched groups, etc.). Thus, it is expected, as shown in Fig. 21, that the maximum in the curve moves to lower concentrations as the chain length of the surface-active agent increases. In addition to the weakening effect due to the removal of metal from the surface there

should be a tendency to strengthen the crystal because of the presence of strongly adsorbed metal soap compounds. The net effect then would be due to the difference between the two competing mechanisms. At very high concentrations approaching saturation, an overall strengthening of the crystal results.

In another study by KRAMER and DEMER,[121] the effect of the surface on

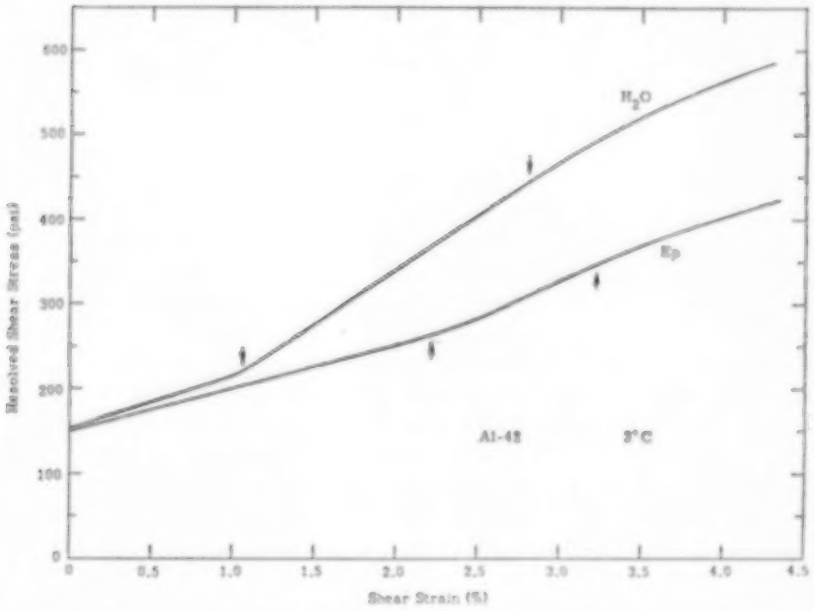

FIG. 39. Stress–strain curve for aluminum strained at 3°C at a rate of 10^{-5} sec^{-1}. H_2O—pulled in water, E.P.—pulled in electropolishing bath. KRAMER and DEMER.[121]

the characteristic stages (I, II and III) of the tensile stress–strain curve was investigated by pulling aluminum single crystals in an electrolytic bath to remove the surface during the deformation. The tests were conducted at 3°C using a current density of 1.3 A/in.^{2} which removed the metal at a rate of 0.0003 in./min per surface. At a strain rate of 10^{-5} sec^{-1}, the extent of Stage I and Stage II increased and their slopes decreased when compared to the deformation characteristics of specimens tested in water at the same temperature and strain rate. The stress at which Stage III began also was decreased (Fig. 39). These changes in the deformation behavior were affected by the strain rate and the rate of metal removal. At a strain rate of 10^{-4} sec^{-1}, using a current density of 1.3 A/in.^{2}, the deformation characteristics were changed, but to a lesser extent. A dislocation pop-out phenomenon was also observed. During the deformation process when the current density was increased, the

specimen elongated suddenly. A typical load-deformation curve shown in Fig. 40 was obtained at a strain rate of 10^{-5} sec^{-1} with an initial current of 2 A. During the early portion of Stage III, the current was allowed to decrease to 1.5 A and then suddenly brought back to 2 A. At this point a sudden decrease in the load occurred due to the rapid elongation of the specimen. As the test was continued at the 2 A level, the slope of the load-deformation curve began to decrease slowly. When the current was decreased to 0.5 A, the slope of the work-hardening curve again began to increase. A change in

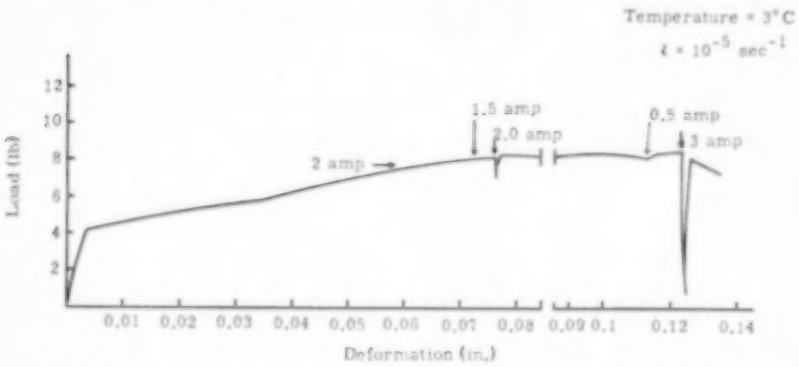

FIG. 40. Discontinuities in load deformation curve of aluminum single crystal caused by changes in electrolytic cell current. KRAMER and DEMER.[121]

the current to 3 A caused a large drop in load to occur and after recovery of the load the slope of the curve decreased rapidly. In no case was a discontinuity found when the current was changed from a high value to a low value.

The authors[121] interpreted the "pop-out" phenomenon as evidence of piled-up dislocation groups at the surface. When the current is increased in the electrolytic cell, the rate of removal of the metal ions is increased or, thermodynamically, the free energy of the surface at the dislocation sites is decreased. The stress due to the pile-up of dislocations is then sufficient to allow them to escape more easily. In another set of experiments, Kramer[120] showed evidence that in the Stage I region a large fraction of the dislocations were held up at the surface. Single crystals of aluminum were strained within the Stage I region, the load was relaxed and 0.040 inch was removed from the cross section by electrolytical polishing. Upon a re-application of the load, the critical resolved shear stress and the extent of stage I became the same as that of the virgin specimen.

KRAMER,[120] using the above experimental observations, proposed that the current theories of work-hardening must be modified to take into account the large effects exerted by the surface on the plastic flow characteristics. He has suggested that at the surface of a crystal, piled-up groups of dislocations on the primary and secondary slip systems can interact and greatly influence the slope and extent of Stages I and II of the stress–strain curve.

Effects on Polycrystalline Metals

Surface-active agents and electrolytes appear to affect the mechanical properties of polycrystalline metals as well as those of single crystals. Most of the research work in this field seems to have been done by REHBINDER and his associates.[6]

ZAKOSHCHIKOVA[122] reported that polycrystalline copper strips (0.04 mm) showed a marked elastic after-effect and hysteresis after stressing in tension to 7–12 kg/mm² and unloading at the same rate. REHBINDER and WENSTROM[123] studied the creep behavior of strips of foil of tin, lead and copper specimens in pure vaseline oil and in kerosene containing various surface-active agents. Valeric acid, heptylic acid, cetyl alcohol and stearic acid markedly decreased the elongation to rupture. The time to rupture was reduced roughly 50 per cent and a minimum in the curve of rupture life versus concentration was found similar to that obtained for single crystals. Grain size was also reported to have an important effect; as the grain size increased the creep rate increased.

Surface-active agents in solution in a nonpolar solvent decreased the fatigue strength of steel[124] when tested in a rotating bending machine. The presence of 0.2 per cent oleic acid in Vaseline oil decreased the fatigue life over 50 per cent (Table 4). However, when the metal was shot-peened or nitrided, there was practically no effect of the surface-active agent.

TABLE 5

Number of cycles to failure (in millions) as a function of the medium

Medium	*Specimens*			
	I	II	III	Average
Vaseline oil (air)	1.64	1.73	1.60	1.66
Vaseline oil + 0.2 per cent oleic acid	0.62	0.59	0.90	0.70

SATO[125, 126] in his study of the effect of various media reported that the breaking strength of steel was decreased as the surface tension of the solution increased and then began to increase with further increase in the surface tension. He also reported that the elastic modulus decreased by as much as 20 per cent. BENEDICKS[127] has reported that adsorption of liquids affects the mechanical strength and volume of solids including metals; thus water reduces the strength of glass 23 per cent and of tempered steel 22 per cent, while petrol increases the strength of steel 27 per cent. Both silica and platinum wires increased in length after immersion in water, returning to their original length on drying. For quartz, the increase of length in different liquids increased with the surface tension of the liquid. This phenomenon, which Benedicks called "liquostriction," may possibly be connected with and provide a method of measuring the interfacial surface energy of the solid in the liquid.

VOL. 9 1961

Perhaps closely related to activity of organic films and electrolytes are the effects produced by testing metals in vacuum or special atmosphere. When exposed to ordinary atmospheres all materials are quickly covered with an oily layer often mixed with water. This layer, which is adsorbed from the fatty oils and water vapor in the air, contains large percentages of polar molecules and unsaturated hydrocarbons. It is suggested that these films may act in a manner similar to that of surface-active agents in a solvent or to that of an electrolyte if the film contains soluble electrolytes. Unfortunately, very little research work has been carried out to study the effects of reduced pressures on the mechanical behavior of metals.

GOUGH and SOPWITH[128] determined the S–N fatigue curve of various metals using a push-pull Haigh machine designed to accommodate specimens at a pressure of 10^{-3} mm Hg. The endurance limit of lead was more than doubled while that of copper and brass was increased 13 per cent and 26 per cent, respectively. The reduction of strength was found to be associated with the presence of oxygen and water vapor. Neither gas was very effective alone.[129, 130] WADSWORTH[131] found that the fatigue life of copper, aluminum and gold was increased by factors of 20, 10 and 1 when the pressure was reduced from atmospheric to 10^{-5} mm Hg. Water vapor reduced the life of aluminum but not copper. Oxygen reduced the fatigue life of copper and aluminum but the presence of water vapor did not affect the results. The fatigue behavior of gold specimens did not seem to change as a result of changes in the composition of the atmosphere. The effect of the gases on aluminum appeared to be associated with an increase in the rate of propagation of cracks; the time for the initiation of the cracks was the same whether the specimens were tested in vacuum or in air.

Fatigue behavior and surface deformation differences between lead fatigued in air and in a partial vacuum was studied recently by SNOWDEN and GREENWOOD.[132] The fatigue life of high-purity lead in a vacuum of 5×10^{-3} mm Hg was found to be appreciably greater than in air. Specimens fatigued in air failed along grain boundaries with little surface deformation, whereas, in vacuo, they developed sets of furrows in the maximum shear–stress direction and failed along certain of these furrows. The presence of fatigue cracks in the surface of air-treated specimens appears to relieve the surface stress which consequently reduces the surface deformation.

In a study by SHAHINIAN[133] of the environment on creep-rupture properties of some commercial alloys, including low alloy steels and various super alloys, it was found that rupture life and creep resistance were greater in air than in other atmospheres, oxygen, nitrogen, helium and vacuum. The alloys of relatively low ductility were more susceptible to the effects of atmosphere in the notched than in the unnotched condition. An alloy which was notch strengthened in one atmosphere might be weakened in another.

Creep-rupture tests were also made in vacuum and in air on an 80 Ni–20 Cr alloy and nichrome V by SHAHINIAN and ACHTER.[134] It was found that the alloy was stronger in air than in a vacuum at high temperatures and

low strain rates, but that the reverse was true at low temperatures and high strain rates. In long time tests at high temperature, a marked strengthening accompanied by an increase in ductility occurred. The mechanism of the atmosphere effect was suggested as involving competition of the strengthening effect of oxidation with the weakening effect of decrease in surface energy by adsorption of gas which reduces the work required to propagate a crack.

Calculations presented by ACHTER and FOX[135] show that adsorption in a vacuum is probably at least two orders of magnitude too slow to saturate the freshly formed surfaces as the crack is propagated even in tests of long duration. In shorter tests, the required saturation time is further reduced which accounts for the larger differences in strength in air and in vacuum.

Nickel tubes tested at 1500°F[136] have been found to possess higher stress rupture properties in air than in argon. Further information concerned with the effect of environment and testing atmospheres on the behavior of steels and various alloys over a range of temperatures is given in a recent publication.[137]

PICKUS and PARKER[138] found the creep rate of nickel was lower in air than in hydrogen or nitrogen. The creep rate of aluminum and copper was observed to be lower in air than in helium.[139] FORESTIER and CLAUSS[140] found that the fracture stress of fine wires, pulled in a variety of gases, is lower than in vacuum. They explained their observations by "condensation" of the gases on the surface. Recently, ACHTER[141] reported some results on nickel when tested in nitrogen, vacuum (10^{-5} mm Hg) and in air at 1200 and 1500°F. The stress-to-rupture time of specimens in nitrogen was shorter than in air or vacuum. The rupture life became shorter with increasing purity of the nitrogen. At 10,000 psi and 1200°F, specimens lasted 102 hr in vacuum, 78 hr in air and 30 hr in nitrogen. Since nickel nitride is unstable at 1200°F, Achter proposes that the decrease in rupture life is due to the absence of the strengthening influence of oxygen, and the surface adsorption of nitrogen causes early failure by promoting crack propagation. The number of cracks in the specimens tested in nitrogen was more numerous than those in specimens tested in the other two environments.

IV. DISCUSSION

There are a number of conditions that may exist on the surface of a metal specimen which may affect the mechanical behavior. Large effects have been reported on the modification of the tensile plastic flow characteristics, creep behavior, fatigue strength and the internal friction and hysteresis behavior. These effects have been found for both single and polycrystalline materials ranging from high-purity metals to complex alloys. In general, the presence of a solid film tends to increase the yield stress and increase the work-hardening rate. Often, on single crystals, the Stage I and, at times, Stage II regions are completely suppressed. The creep rate is lowered by the presence of solid films on single crystals; however, on polycrystalline materials,

the effects are uncertain. Polycrystalline metals tested in an atmosphere which can cause the specimen to oxidize are generally stronger in creep than those tested in "inert" atmospheres. However, the changes due to the surface effects may be obscured by strengthening due to internal oxidation which may occur during the test procedure. The fatigue strength of metals is generally increased by the presence of a solid film provided the film does not crack. However, the fatigue strength is also usually increased when the specimens are tested in a vacuum or an "inert" atmosphere.

Surface-active agents, in general, tend to decrease the strength properties of both single and polycrystalline materials. There may be some question concerning the decrease of the initial yield stress, but the evidence for decrease in the plastic flow curve is quite strong. The creep and fatigue strengths of single and polycrystalline metals are decreased, sometimes very markedly. Some question still exists whether a surface-active agent is effective on a metal having a clean surface.

Electrolytes also have a pronounced effect on the mechanical properties of metals. Practically all the work reported in this field has been concerned with the creep behavior. The effect of the electrolyte is variable and seems to depend upon the type of film formed by the products of the reaction between the metal and the electrolytes, and whether an oxide is present on the surface. In some cases the creep strength is lowered and in others it is increased. General methods for predicting the effect of the electrolyte cannot be given at this time, but it appears that the greater the reactivity of the metal throughout the entire period of the test, the lower is the creep strength. Apparently when the products of reaction form adherent films which block the egress of dislocations from the surface of the specimen, the creep strength is enhanced.

The various mechanisms which have been offered for the effects of oxide and metal films are as follows:

(1) Penetration of oxide into surface cracks.
(2) Load carrying capacity of the film.
(3) Locking of surface dislocation sources.
(4) Blocking of dislocations at the surface, resulting in pile-ups.

Little support is now given to the suggestion of the healing up of surface cracks in metals by an oxide film, principally because there is no evidence to support this point of view. The concept of the ability of the film to offer mechanical support for a portion of the applied load has been suggested by a number of investigators. The "naive" mechanical model, where shear–stress relaxation across the active slip plane in the metal transfers the load to the film until it deforms and slip can proceed, predicts that the crystal with a surface film requires, for flow, an increment of applied shear stress [42] equal to:

$$\Delta\tau = \frac{4hS_f}{d} \quad . \quad . \quad . \quad . \quad . \quad . \quad . \quad . \quad (18)$$

where S_f is the unit shear resistance of the film, h its thickness, and d the specimen diameter. This equation requires the effect to be linear with thickness and independent of strain rate and to be a negligible fraction of the flow stress unless the film is very much stronger than the crystal. This explanation[44] appears to satisfy the phenomenological observations in certain studies and over a limited range of coating thickness, but an interpretation using a dislocation model offers a more satisfactory explanation when effects of all test variables are considered.

The locking of surface dislocation sources should exert a primary influence only on the critical resolved shear stress for flow. The blocking at the surface of dislocations from internal sources may also affect the critical resolved shear stress. Furthermore, the latter process may exert an influence throughout the whole plastic range. The same experimental observation—an increase in critical resolved shear stress—has been explained by both of these mechanisms, each having its own advocates. Unfortunately, major difficulty arises in designing an experiment which unequivocably distinguishes between the two. It would appear that any experiment intended to make such a distinction must be concerned primarily with the very initial deviation of the stress–strain curve from elastic behavior, rather than with effects observed at large plastic strains.

From the experiments conducted thus far, the change in yield stress can be explained equally as well on the basis of the locking of surface dislocation sources as by the blocking of internally produced dislocations by the surface film.

For the observations made on the effects of surface films on the brittle fracture of crystals, an explanation[44] has been offered in terms of dislocation pile-up against barriers. At low values of χ_0 in hexagonal crystals, the surface film affects the twinning characteristics in such a manner as to decrease the distance between twins and, consequently, the distance between dislocation sources and barriers, thus resulting in an increase in fracture stress. For high angles of χ_0, less twinning occurs and the surface film acts as a more effective barrier than in the case of clean crystals, resulting in larger dislocation pile-ups and, therefore, a decrease in fracture stress.

Several theories have been proposed to explain the "weakening" effect of surface-active agents. REHBINDER and his co-workers[6] assume that the process is associated with the existence of microcracks on the surface. According to their theory, the surface-active agents are physically adsorbed and are able to migrate into the root of the crack. A large pressure is said to be created according to the equation developed for capillary pressure,

$$\Delta P = \frac{2\,\gamma\,\cos\,\theta}{r} \quad . \quad . \quad . \quad . \quad . \quad . \quad . \quad (15)$$

When the radius (r) is small, the pressure may become very large. The validity of this explanation appears questionable upon consideration of the following facts. It has been shown[142] that high-purity liquids which have a low surface

VOL.
9
1961

tension will always wet ($\theta = 0$) a high energy surface of a solid. The presence of an adsorbed layer will increase the contact angle θ. The surface tension will also be decreased by the presence of an adsorbed layer. Thus in the above equation ΔP should be decreased by the presence of a surface-active agent and not increased. Further, the maximum ΔP should occur when a pure solvent is employed for in this case, cos θ is equal to one.

An explanation of the weakening effect of surface-active agents has also been given in terms of the removal of an oxide layer which would, if present, tend to increase the strength. However, the research investigations on gold (which does not have an oxide layer) have shown that active agents decrease the creep strength. This seems definitely to rule out this hypothesis.

MASING [112, 118] attributed the weakening effect to a decrease in the surface energy. According to this point of view,

$$\frac{V_2}{V_1} = \exp\left(-\frac{\Delta\gamma\Delta A}{kT}\right) \quad . \quad . \quad . \quad . \quad . \quad . \quad . \quad (19)$$

where V_1 and V_2 are the strain rates in an inert medium and in a medium containing a surface-active agent or electrolyte, respectively. ΔA is the increase in surface area and $\Delta\gamma$ is the change in surface energy. It is not possible at this time to evaluate the validity of this equation for the change in surface tension of the solid when immersed in a liquid surface-active agent is not known.

KRAMER [120] showed that metal soaps are found in the solutions containing surface-active agents in which metals have been immersed. He suggests that the weakening effect is associated with a chemical adsorption process in which the rate of removal of the metal by the solution of the metal salt is the controlling feature. In this manner, metal ions are removed at the dislocation pile-up sites. This allows the dislocations to leave the crystal more easily. Thermodynamically, this is equivalent to a decrease in the surface energy or bond strength of the metal ions at the dislocation site.

In many of the investigations reported in the literature, the results are difficult to interpret properly because of the failure to account for many of the important factors which may affect surface reactions. In investigations concerned with surface-active agents, it is necessary to use solvents of the highest purity possible—free from all traces of polar molecules. High-purity compounds of the polar molecules are also required if the specific effects of a given chemical species is desired. The exact method of preparation of the surface must also be considered. As was pointed out earlier, metal soaps will not form under ordinary conditions when the surface has not been allowed to come into contact with oxygen and/or water molecules. The failure to take this into account may explain the difference in the results obtained by the various investigators. There are other apparent subtleties which exert an effect of considerable proportion. In some of the investigations, for example, a treatment used to obtain "clean" surfaces was the same one used by others to obtain an oxide film on the specimen.

Acknowledgement—The authors wish to acknowledge the support and encouragement of The Martin Company during the preparation of the manuscript. The partial support of some of the research work done by the authors was support by the U. S. Air Forces under Contract AF33(616)-6220.

REFERENCES

(1) Roscoe, R.; *Nature, Lond.* 133 (1934) 912.
(2) Glen, J. W.; Atomic Energy Research Establishment, Report M/TN 22, Harwell, England (1953), p. 31.
(3) Andrade, E. N. da C.; *Inst. of Metals Monograph and Report Series No.* 13, London, England (1953) pp. 133–143.
(4) Gilman, J. J.; A.S.T.M. STP No. 171, Phila., Pa. (1955) 3–13.
(5) Weiner, L. C. and Gensamer, M.; *J. Inst. Metals* 85 (1956–57) 441–448.
(6) Lichtman, V. I., Rehbinder, P. A. and Karpenko, G. V.; "Effect of a Surface-Active Medium on the Deformation of Metals," Her Majesty's Stationery Office, London (1958).
(7) Fisher, J. C.; Discussion *Trans. Amer. Inst. Min.* (*Metall.*) *Engrs.* 194 (1954) 531.
(8) Cottrell, A. H.; *Dislocations and Plastic Flow in Crystals*, Oxford (1953).
(9) Roscoe, R.; *Phil. Mag.* 21 ser. 7 (1936), p. 399.
(10) Joffé, A. F.; *Physics of Crystals* (1928) McGraw-Hill, N.Y.
(11) Cottrell, A. H. and Gibbons, D. F.; *Nature, Lond.* 162 (1948) 488.
(12) Harper, S. and Cottrell, A. H.; *Proc. Phys. Soc.* B63 (1950) 331–345.
(13) Takamura, J.; *Mem. Fac. Eng. Kyoto Univ.* 18 (3) (1956) 255–279.
(14) Paxton, H. W. and Cottrell, A. H.; *Acta Met.* 2 (1954) 3.
(15) Fleischer, R. L. and Chalmers, B.; *Trans. Met. Soc. Amer. Inst. Min.* (*Metall.*) *Engrs.* 212 (2) (1958) 265–274.
(16) Head, A. K.; *Proc. Phil. Mag.* 44 (1953) 92.
(17) Makin, M. J. and Andrade, E. N. da C.; see Ref. (3).
(18) Suzuki, H., Ikeda, S. and Takeuchi, S.; *J. Phys. Soc. Japan* 11 (1956) 382.
(19) Andrade, E. N. da C. and Henderson, C.; *Phil. Trans. Roy. Soc.* A244 (1951) 177–203.
(20) Lipsett, F. R. and King, R.; *Proc. Phys. Soc.* (B) 70 (6) (1957) 608–620.
(21) Gilman, J. J. and Read, T. A.; *Trans. Amer. Inst. Min.* (*Metall.*) *Engrs.* 194 (1952) 875–883.
(22) Garstone, J., Honeycombe, R. W. K. and Greetham, G.; *Acta Met.* 5 (1956) 485–494.
(23) Rosi, F. D.; *Acta Met.* 5 (1957) 348–350.
(24) Adams, M. A.; *Acta Met.* 6 (1958) 327–338.
(25) Gilman, J. J.; *Nature, Lond.* 169 (1952) 149–150.
(26) Cottrell, A. H. and Bilby, B. A.; *Phil. Mag.* 42 (1951) 573.
(27) King, R.; *Nature, Lond.* 169 (1952) 543–544.
(28) Honeycombe, R. W. K.; *J. Inst. Metals* 80 (1951) 49.
(29) Brown, A. F. and Honeycombe, R. W. K.; *Phil. Mag.* 42 ser. 7 (1951) 1146–1149.
(30) Rosi, F. D.; *Trans. A.I.M.E.* 200 (1954) 1009–1020.
(31) Lücke, K. and Lange, H.; *Z. Metallk.* 43 (1952) 55.
(32) Suzuki, H.; Science Reports of the Research Institute, Tohoku University, Japan, A4, No. 5 (1952) 455.

VOL.
9
1961

(33) CHALMERS, B. and DAVIS, R. S.; *Conf. Dislocations Mech. Properties Crystals*, 1956, Lake Placid, John Wiley (1957) 232–233.
(34) BRAME, D. R. and EVANS, T.; *Phil. Mag.* (viii) (33) 3 (1958) 971–986.
(35) GILMAN, J. J.; *Trans. Amer. Inst. Min.* (*Metall.*) *Engrs.* 191 (1951) 1148–1149.
(36) GREENOUGH, G. B. and RYDER, D. A.; *J. Inst. Metals* 84 (1956) 467–470.
(37) WEINER, L. C. and GENSAMER, M.; *J. Inst. Metals* 85 (1956–57) 441–448.
(38) WEINER, L. C.; *Trans. Met. Soc. Amer. Inst. Min.* (*Metall.*) *Engrs.* 212 (1958) 342–343.
(39) ANDRADE, E. N. DA C. and RANDALL, R. F. Y.; *Nature, Lond.* 162 (1948) 890–891.
(40) PICKUS, M. R. and PARKER, E. R.; *Trans. Amer. Inst. Min.* (*Metall.*) *Engrs.* 191 (1951) 792.
(41) SWEETLAND, E. D. and PARKER, E. R.; *J. Appl. Mech.* 20 (1953) 30–32.
(42) METZGER, M.; Discussion *Trans. Amer. Inst. Min.* (*Metall.*) *Engrs.* 194 (1952) 532.
(43) COFFIN, F. D. and WEIMAN, A. L.; *J. Appl. Phys.* 24 (3) (1953) 282–289.
(44) METZGER, M. and READ, T. A.; *Trans. Met. Soc. Amer. Inst. Min.* (*Metall.*) *Engrs.* (2) 212 (1958) 236–243.
(45) CUTHILL, J. R. and HARRISON, W. N.; U.S. O.T.S., P.B. 121493 (1956) p. 53
(46) CUTHILL, J. R., RICHMOND, J. C. and TIGHE, N. J.; *Indust. Heating* 24 (3) (1957) 582, 584, 586, 588.
(47) SHAPIRO, S. and READ, T. A.; *Phys. Rev.* 82 (2) (1951) 341.
(48) BARRETT, C. S.; *Acta Met.* 1 (1953) 2–7.
(49) BARRETT, C. S.; *Trans. Amer. Inst. Min.* (*Metall.*) *Engrs.* 197 (1953) 1652–1654.
(50) EDELSON, B. I. and ROBERTSON, W. D.; *Acta Met.* 2 (1953) 583–590.
(51) CHEN, N. K.; Discussion *Trans. Amer. Inst. Min.* (*Metall.*) *Engrs.* 197 (1953) 1661.
(52) COCHARDT, A. W.; *Acta Met.* 3 (1955) 607–608.
(53) LOGAN, H. L.; *J. Res. Nat. Bur. Stand.* 46 (1951) 472–479.
(54) KENNEDY, E. M., JR.; W.A.D.C. TR-58-108 (Pt. 1) (1957) p. 40
(55) MORISSET, P.; *Chrome Dur* (1957) 28–39.
(56) FORM, G. W. and BALDWIN, W. M., JR.; *Proc. A.S.T.M.* 56 (1956) 645–661.
(57) STICKLEY, G. W. and HOWELL, F. M.; *Proc. A.S.T.M.* 50 (1950) 735.
(58) SAVAGE, E. G., SAMPSON, E. G. and CURRAN, J. K.; R.A.E. TN MET 200 (1954).
(59) SHREIDER, A. V., BIOLOBZHESKII, A. V., ZOGRITSENKA, Z. I. and SEREBRENNIKAN, B. V.; *Metallovedenie i. Obrabotka Metallov* (4) (1956) 14–20.
(60) NIKISHOV, A. S., KURGANOV, G. V. and YARZHEMSKAYA, N. I.; *Metallovedenie i. Obrabotka Metallov* (12) (1957) 66–68.
(61) BENNETT, J. A.; *Proc. A.S.T.M.* 55 (1955) 1015–1020.
(62) PLANKENHORN, W. J.; *Amer. Ceramic Soc.* 37 (1954) 281–288.
(63) WOMELDORPH, W. J., PLANKENHORN, W. J. and BENNETT, D. G.; A. F. Tech. Rep. 6092 (October 1950).
(64) FERGUSON, L. and BOUTON, G. M.; *Symp. on Stress-Corrosion Cracking of Metals, A.I.M.E.-A.S.T.M.* (1945).
(65) HOGAN, H. L.; *J. Res. Nat. Bur. Stand.* 43 (1949).
(66) CABBLE, G. M., JR.; *Bull. of Va. Poly. Inst. Engrg. Expmt. Sta.* Ser. 82, XLVI (1) (1952).
(67) WILLIAMS, C. and HAMMOND, R. A. F.; *Metal Industry* 86 (May 27, 1955) 435.
(68) WILLIAMS, C. and HAMMOND, R. A. F.; *Inst. Metal Finishing, Trans.* 34 (1956–57) 317–353.
(69) BORISOV, V. S. and NAUMOV, F. N.; *Metallovedenie i. Obrabotka Metallov* (12) (1956) 50–56.
(70) HARVEY, W. E.; *Metals and Alloys* 3 (1932) 69–72.
(71) DOLAN, T. J. and BENNINGER, H. H.; *Proc. A.S.T.M.* 40 (1940) 658–659.

[72] SOPWITH, D. G. and GOUGH, H. J.; *J. Iron Steel Inst.* 135 (1937) 315–339.
[73] ZAPPFE, C. A. and HASLEM, M. E.; *Trans. Amer. Soc. Metals* 39 (1947) 241–258.
[74] BEERWALD, A.; *Metall. Abstract* 10 (7) (1943).
[75] PAIGE, H., JAMES, J. H. and WILLIAMS, F. S.; *Product Engineering* 24 (12) (1953) 162–167.
[76] BRICK, R. M. and PHILLIPS, A.; *Trans. Amer. Soc. Metals* 29 (June 1941).
[77] RUSSELL, H. W., JACKSON, L. R., GROVER, H. J. and BEAVER, W. W.; N.A.C.A. TN 1485 (February 1948).
[78] SMITH, F. C., BRUEGGEMAN, W. C. and HARWELL, R. H.; N.A.C.A. Tech. Note 2231 (December 1956).
[79] SEBISTY, J. J. and EDWARDS, J. O.; *Inst. Metals, J.* 84 (1956) 291–297.
[80] HUNTER, M. S. and FRICKE, W. G., JR.; *Proc. A.S.T.M.* 54 (1954) 717–736.
[81] SUZUKI, M.; *J. Inst. Metals* 85 (1956–57) 206–208.
[82] GIBBS, J. W.; *On the Equilibrium of Heterogeneous Substances.* Collected Works (1928) 315.
[83] HERRING, C.; *Structure and Properties of Solid Surfaces*, Gomer and Smith; University of Chicago Press (1953) 5.
[84] OROWAN, E.; *Z. Phys.* 79 (1932) 573.
[85] LENNARD-JONES, J. E. and DENT, B. M.; *Proc. Roy. Soc.* (1928) A121, 247.
[86] SHUTTLEWORTH, R.; *Proc. Phys. Soc.* A63, (1950), 444.
[87] SUMNER, C. G.; *Symposium on Detergency*, Chem. Publ. Co., N.Y. (1937) 15.
[88] DUPRE, A.; *Theorie Mechanique de la Chalem* P369 Paris: Gauthier-Villars (1869).
[89] COOPER, W. A. and NUTTALL, W. H.; *J. Agric. Sci.* 7 (1915) 219.
[90] DUBRISSAY, R.; *C.R. Acad. Sci., Paris* (1940) 210, 533.
[91] PRUTTON, C. F. *et al.*; *Industr. Engng. Chem.* 37 (1945) 90.
[92] TINGLE, E. D.; *Trans. Faraday* 46 (1950) 98.
[93] SMITH, H. A. and ALLEN, K. A.; *J. Phys. Chem.* 58 (1954) 449.
[94] SMITH, H. A. and FORT, T.; *J. Phys. Chem.* 62 (1958) 519.
[95] SMITH, H. A. and MCGILL, R. M.; *J. Phys. Chem.* 61 (1957) 1025.
[96] KRAMER, J.; *Z. Physik* 125 (1949) 739.
[97] KRAMER, J.; *Z. Physik* 128 (1950) 538.
[98] DOBRY, A. and MAHNCKE, H. A.; *Nature, Lond.* 174 (1954) 507.
[99] LEVINE, O. and ZISMAN, W. A.; *J. Phys. Chem.* 61 (1957) 1188.
[100] REHBINDER, P. A.; *Byull. Akad. Nauk, URSS*, Classe, Sci. Mat. Nat. Ser. Chem. (1936) 639–704.
[101] REHBINDER, P. A. and WENSTROM, E. K.; *Byull. Akad. Nauk, URSS*, Classe Sci. Mat. Nat. Ser. Phy. (1937) 531–548.
[102] LICHTMAN, V. I., REHBINDER, P. A. and KARPENKO, G. V.; *Dokl. Akad. Nauk, URSS* (1954).
[103] AUBMANN, A. B. and WENSTROM, E. K.; *Dokl. Akad. Nauk, URSS* (1956) 2.
[104] LICHTMAN, V. I., REHBINDER, P. A. and YANOVA, L. P.; *Dokl. Akad. Nauk, SSSR* (8) (1947) 56.
[105] REHBINDER, P. A., LICHTMAN, V. I. and MASLENNIKOV; *Comptes Rendue Dokl. Akad. Nauk, URSS* 32 (1941).
[106] KEMSLEY, D. S.; *Nature, Lond.* 163 (1949) 381.
[107] ANDRADE, E.; *Nature, Lond.* 164 (1949) 538.
[108] ROZHANSKII, V. N., GORYUNOV, YU. V., and DEKARTOVA; *Zh. Fiz. Khim.* 31 (1957) 882–886.
[109] REHBINDER, P. A. and WENSTROM, E. K.; *Z. Fich.* (1) 19 (1945). *Acta Physioochim URSS* 11 (144) 417 *Dokl. Akad. Nauk, SSSR* (2) 68 (1949).
[110] LIPPMANN, G.; *Ann. Chim. Phys.* (5) 5 (1875) 494.
[111] WENSTROM, E. K. and REHBINDER, P. A.; *ZhFICH* (12) 26 (1952).
[112] PFUTZENREUTER, A. and MASING, G.; *Z. Metallkunder* 42 (1951) 361.

VOL.
9
1961

[113] ROZHANSKII, V. N. and REHBINDER, P. A.; *Dokl. Akad. Nauk, SSSR* (1) 91 (1953).
[114] MENTER, J. W. and HALL, E. O.; *Nature, Lond.* 165 (1950) 611.
[115] ANDRADE, E. and RANDALL, R. F. G.; *Proc. Phys. Soc. Lond.* (B) 65 (1952) 445.
[116] PHILLIPS, D. J. and THOMPSON, N.; *Proc. Phys. Soc., Lond.* (B) (1950) 839.
[117] ANDRADE, E., RANDALL, R. and MAKIN, M.; *Proc. Phys. Soc. Lond.* 63 (1950) 990.
[118] KLINKENBERGER, V. W., LÜCKE, K. and MASING, G.; *Z. Metallkunder* 195B 44, 362.
[119] ROZHANSKII, V. N. and REHBINDER, P. A.; *Dokl. Akad. Nauk, SSRR* 91 (1953) 129–131.
[120] KRAMER, I. R.; Private Communication. (1959)
[121] KRAMER, I. R. and DEMER, L. J.; Private Communication. (1958)
[122] LICHTMAN, V. I. and ZAKOSCHCHIKOVA; *Dokl. Akad. Nauk, SSSR* (4) (1949) 66.
[123] REHBINDER, P. A. and WENSTROM, E. K.; *Zv. Omen Akad. Nauk, SSSR S* (4–5) (1937) 531.
[124] KOROVSKII, Sh. YA.; *Dokl. Akad. Nauk., SSSR* (8) (1948) 59.
[125] SATO, M.; *Ark. Fys.* 10 (1956) 37.
[126] SATO, M.; *Ark. Fys.* 10 (1956) 45.
[127] BENEDICKS, C.; *Rev. de Metallurgie* 46 (1949) 291.
[128] GOUGH, H. J. and SOPWITH, D. G.; *J. Inst. Metals* 49 (1932) 93.
[129] GOUGH, H. J. and SOPWITH, D. G.; *J. Inst. Metals* 56 (1935) 55.
[130] GOUGH, H. J. and SOPWITH, D. G.; *J. Inst. Metals* 72 (1946) 415.
[131] WADSWORTH, N. J.; *Proceeding of the Symposium on Internal Stresses and Fatigue in Metals.* Elsevier Publishing Co. (1959) 382.
[132] SNOWDEN, K. O. and GREENWOOD, J. NEILL; *Trans. Met. Soc., Amer. Inst. Min. (Metall.) Engrs.* (5) 212 (1958) 626–627.
[133] SHAHANIAN, P.; *Trans. Amer. Soc. Metals* 48 (1956) 952–967.
[134] SHAHANIAN, P. and ACHTER, M. P.; *Trans. Amer. Soc. Metals* Preprint No. 1, 69 (1957) p. 11
[135] ACHTER, M. R. and FOX, H. W.; *Trans. Met. Soc. Amer. Inst. Min. (Metall.) Engrs.* 215 (1959) 295–296.
[136] MCHENRY, H. T. and PROBST, H. B.; N.A.C.A. Tech. Note 3987 (1958) p. 23
[137] *High Temperature Materials*, John Wiley, New York, 1959.
[138] PICKUS, M. R. and PARKER, E. R.; Special Technical Publication No. 108, ASTM (1951) 26.
[139] SWEETLAND, E. D. and PARKER, E. R.; *J. Appl. Mech.* (January 1953), also ASM 75 (1953) 30.
[140] FORESTIER, H. and CLAUSS, A.; *Revue de Metallurgie* 52 (1955) 961.
[141] ACHTER, M. R.; Private Communication, March 1960.
[142] FOX, H. W., HARE, E. F. and ZISMAN, W. A.; *J. Phys. Chem.* 1097 (1955) 59.

CONTENTS OF PREVIOUS VOLUMES IN THE PROGRESS IN METAL PHYSICS SERIES

VOL.
9
1961

VOLUME 1

Progress in the Theory of Alloys G. V. RAYNOR
Theory of Dislocations A. H. COTTRELL
Crystal Boundaries R. KING and B. CHALMERS
Age Hardening of Metals G. C. SMITH
Hardening Response of Steels E. H. BUCKNALL and W. STEVEN
Preferred Orientation in Non-Ferrous Metals T. LI. RICHARDS
Diffusion of Metals in Metals A. D. LE CLAIRE

VOLUME 2

Order-Disorder Changes in Alloys H. LIPSON
Rate Process in Physical Metallurgy I. I. BETCHERMAN
Anisotropy in Metals W. BOAS and J. K. MACKENZIE
Developments in Magnesium Alloys H. G. WARRINGTON
Internal Strains and Recrystallization R. W. CAHN
Researches on the Polygonization of Metals A. GUINIER and J. TENNEVIN
Polygonization in Strongly Deformed Metals C. CRUSSARD, F. AUBERTIN, B. JAOUL and G. WYON

VOLUME 3

Crystallography of Transformations J. S. BOWLES and C. S. BARRETT
Properties of Metals at Low Temperatures D. K. C. MacDONALD
Recent Advances in the Electron Theory of Metals N. F. MOTT
Twinning R. CLARK and G. B. CRAIG
Feromagnetism URSULA M. MARTIUS
Quantitative X-ray Diffraction Observations on Strained Metal Aggregates G. B. GREENHOUGH
Recrystallization and Grain Growth J. E. BURKE and D. TURNBULL
Structure of Crystal Boundaries B. CHALMERS

VOLUME 4

Internal Friction in Metals A. S. NOWICK
The Mechanism of Oxidation of Metals and Alloys at High Temperatures KARL HAUFFE
Gases in Metals C. R. CUPP
The Theory of Sintering G. A. GEACH
Theory of Dislocations A. H. COTTRELL
Diffusion in Metals A. LE CLAIRE
Nucleation J. H. HOLLOMON and D. TURNBULL

VOLUME 5

The Fracture of Metals N. J. PETCH
Geometrical Aspects of the Plastic Deformation of Metal Single Crystals R. MADDIN and N. K. CHEN
The Structure of Liquid Metals B. R. T. FROST
Report of Precipitation H. K. HARDY and T. J. HEAL
Solidification of Metals URSULA M. MARTIUS

VOLUME 6

The Effect of Hydrostatic Pressure on the Electrical Resistivity of Metals A. W. LAWSON
The Filamentary Growth of Metals H. K. HARDY
The Austenite : Pearlite Reaction R. F. MEHL and W. C. HAGEL
Recent Advances in Knowledge Concerning the Process of Creep in Metals A. H. SULLY
The Mechanism of Evaporation O. KNACKE and I. N. STRANSKI
Mosaic Structure P. B. HIRSCH

VOLUME 7

Equilibrium, Diffusion and Imperfections in Semiconductors J. N. HOBSTETTER
The Physical Metallurgy of Titanium Alloys R. I. JAFFEE
Thermodynamics and Kinetics of Martensitic Transformations LARRY KAUFMAN and MORRIS COHEN
The Stored Energy of Cold Work A. L. TITCHENER and M. B. BEVER
The Properties of Metals at Low Temperatures H. M. ROSENBERG

VOLUME 8

Work Hardening of Metals L. M. CLAREBROUGH and M. E. HARGREAVES
Grain Boundaries in Metals F. WEINBERG
X-ray Studies of Deformed Metals B. E. WARREN
Substructures in Crystals Grown from the Melt C. ELBAUM
Defects in Pure Metals W. M. LOMER

VOL.
9
1961

PROGRESS IN MATERIALS SCIENCE VOLUME 9
(INCORPORATING PROGRESS IN METAL PHYSICS)
GENERAL EDITOR: BRUCE V. CHALMERS

The Hydrogen Embrittlement of Metals

by

P. COTTERILL
Metallurgy Department, Battersea College of Technology, London

PERGAMON PRESS
OXFORD · LONDON · NEW YORK · PARIS

PERGAMON PRESS LTD.
Headington Hill Hall, Oxford
4 & 5 *Fitzroy Square, London, W.*1

PERGAMON PRESS INC.
122 *East* 55*th Street, New York* 22, *N.Y.*
Statler Center 640, 900 *Wilshire Boulevard,*
Los Angeles, California

PERGAMON PRESS S.A.R.L.
24 *Rue des Écoles, Paris V*e

PERGAMON PRESS G.m.b.H.
Kaiserstrasse 75, *Frankfurt-am-Main*

VOL.
9
1961

Copyright
©
1961
PERGAMON PRESS LTD.

Library of Congress Card Number 49—50107

Set in Times New Roman 10 on 12 pt. and
made and printed in Great Britain at Page Bros. (Norwich) Ltd.

PROGRESS IN MATERIALS SCIENCE

(INCORPORATING PROGRESS IN METAL PHYSICS)

PUBLISHER'S NOTE

THE twelve years that have elapsed since the publication of the first volume of PROGRESS IN METAL PHYSICS has seen a great increase in the rate of publication of papers in this, as in most other fields of science, and realization that the physics of metals is an important part of, but not the whole of, the science of materials, a field of considerable practical and theoretical importance.

It is becoming extremely difficult, if it is not already impossible, for most scientists to keep up-to-date in their own and closely related fields by reading all the relevant original papers; one approach to the solution of this problem is the provision of adequate up-to-date critical review articles. For these reasons the Editor and the Publisher of PROGRESS IN METAL PHYSICS have decided to broaden the subject matter to include the whole of the field of the Science of Materials, and, in order to ensure maximum availability, to publish each article as a separate entity; thus, an individual subscriber need no longer purchase a whole volume in order to obtain some of the articles. This new procedure will make it possible to publish each article within five months of its receipt by the Editor.

VOL.
9
1961

THE HYDROGEN EMBRITTLEMENT OF METALS

CONTENTS

1. Introduction 205

2. Hydrogen-Metal Relationships 206
2.1 General 206
2.2 Adsorption 208
2.2.1 Physical adsorption 208
2.2.2 Chemi-sorption 210
2.3 Solution 212
2.3.1 Endothermic occlusion 212
2.3.2 Exothermic occlusion 213
2.3.3 The location of hydrogen in solid-solution 214
2.4 The units used in the measurement of sorption phenomena 215
2.5 Diffusion 217
2.6 Summary 218

3. Brittle Fracture and the Ductile-to-Brittle Transition Temperature in Metals 219
3.1 General aspects of fracture in metals 219
3.2 The Griffith theory of fracture 219
3.3 Applications of the Griffith theory 221
3.4 The nature of the "Griffith-cracks" in metals 221
3.4.1 Intergranular fracture 222
3.4.2 Brittle fracture by cracking within the grains 222
3.5 The propagation of cleavage cracks 224
3.6 The ductile-to-brittle transition 225
3.6.1 Characteristics of the transition 225
3.6.2 General dislocation theory of the transition 226
3.6.3 Recent work on the ductile-to-brittle transition temperature 228

4. The Hydrogen Embrittlement of Steel 230
4.1 The solubility of hydrogen in iron 230
4.2 The characteristics of hydrogen embrittlement in steel 231
4.3 The mechanism of hydrogen embrittlement in steel 232
4.3.1 Early theories 232
4.3.2 The Planar pressure theory 232
4.3.3 Other theories based on brittle fracture mechanisms of the Griffith type 233
4.3.4 Theories based on the interaction of hydrogen and dislocations 235
4.3.5 A recent theory based on the effect of hydrogen in interstitial solution 236

5. The Hydrogen Embrittlement of Titanium and Its Alloys 241
5.1 The titanium–hydrogen system 241
5.2 The hydrogen embrittlement of alpha-titanium 244

5.2.1 High purity titanium 244
5.2.2 Commercial purity titanium 246
5.2.3 Alpha-stabilized alloys 247
5.2.4 Summary of the effect of hydrogen on alpha-titanium 248
5.2.5 The precipitation of the hydride phase in alpha-titanium 249
5.3 The hydrogen embrittlement of alpha–beta titanium alloys 250
5.3.1 The characteristics of hydrogen embrittlement in alpha–beta titanium alloys 250
5.3.2 The mechanism of hydrogen embrittlement in alpha–beta titanium alloys 255
5.3.3 A comparison of the hydrogen embrittlement of alpha–beta titanium with that of steel 257
5.4 The effect of hydrogen on the mechanical properties of beta–titanium alloys 259

6. The Hydrogen Embrittlement of Alpha-Zirconium 259
6.1 The zirconium–hydrogen system 259
6.2 The characteristics of the hydrogen embrittlement of alpha-zirconium 262
6.3 The mechanism of hydrogen embrittlement in alpha-zirconium 264

7. The Hydrogen Embrittlement of Alpha-Uranium 267
7.1 The uranium–hydrogen system 267
7.2 The effect of metal purity on the solubility of hydrogen in alpha-uranium 270
7.3 The characteristics of the hydrogen embrittlement of alpha-uranium 272
7.4 The mechanism of hydrogen embrittlement in alpha-uranium 274

8. The Hydrogen Embrittlement of the Body-Centred-Cubic Metals 276
8.1 General introduction 276
8.2 The metal–hydrogen systems for these metals 276
8.2.1 Group VA (vanadium, niobium and tantalum) 276
8.2.2 Group VI A (chromium, molybdenum and tungsten) 277
8.3 The characteristics of hydrogen embrittlement in these metals 278
8.4 The mechanism of hydrogen embrittlement in b.c.c. metals 280
8.4.1 Vanadium, niobium, tantalum, molybdenum, tungsten and steel 280
8.4.2 Beta-titanium and beta-zirconium (alloys) 283

9. The Development of a General Theory of Hydrogen Embrittlement in Metals 284
9.1 General introduction 284
9.2 Hydrogen-metal relationships and the mechanism of brittle fracture in metals 284
9.3 The mechanisms of hydrogen embrittlement in individual cases 286
9.3.1 Alpha-titanium and alpha-zirconium 286
9.3.2 Alpha–beta titanium alloys 288
9.3.3 The hydrogen embrittlement of alpha-uranium 288
9.3.4 The body-centred-cubic metals, including steel 289
9.3.5 The effect of hydrogen on the mechanical properties of the close-packed metals 290
9.4 A general theory of hydrogen embrittlement in metals 292

VOL. 9 1961

10. General Summary and Conclusions 296

11. Acknowledgements 297

12. References 297

OL.
961

VOL.
9
1961

THE HYDROGEN EMBRITTLEMENT OF METALS

*P. Cotterill**

SYNOPSIS

THIS paper represents a comprehensive survey of the literature with regard to the subject of hydrogen embrittlement in metals. There is a review of the current knowledge of hydrogen–metal relationships in which it is shown that the behaviour of any element, with respect to hydrogen, depends upon its position in the periodic table. The current theories of the nature of brittle fracture, and of the ductile-to-brittle transition in metals are then reviewed in terms of the origin and propagation of brittle fractures on the application of an external stress.

These reviews are then followed by a detailed critical analysis of the characteristics and mechanisms of hydrogen embrittlement in the body-centred-cubic metals (including steel), titanium and its alloys, alpha-zirconium and alpha-uranium. In each case these effects are discussed in terms of the present knowledge of the appropriate metal–hydrogen system and the theory of brittle fracture in metals. The conclusions from each of these individual reviews are then combined in the proposal of a general theory of the hydrogen embrittlement of metals which not only incorporates the essential features of each case of hydrogen embrittlement, but also suggests an explanation for the absence of similar effects in other metals.

INTRODUCTION

The first observation of the effect of hydrogen on the mechanical properties of metals was reported, in 1926, by PFEIL,[1] who found that the presence of hydrogen in steel caused a considerable loss of ductility at room-temperature under normal tensile conditions. The hydrogen embrittlement of steel is now a well-known—if not well understood—phenomenon. However, steel is not the only metal to be embrittled by hydrogen; recent work has shown that the mechanical properties of titanium,[2] zirconium,[3] uranium[4] and vanadium[5, 6] are also seriously affected by the presence of hydrogen. The

* The author is a lecturer in the metallurgy department of the Battersea College of Advanced Technology, London. This paper was written during the course of his secondment to the Metals Division of the Atomic Weapons Research Establishment, Aldermaston, Berkshire, from the Atomic Energy Division of the General Electric Company, Ltd.

purpose of this review is therefore to discuss the present state of the knowledge of these various cases of hydrogen embrittlement and to develop a general theory of hydrogen embrittlement which accounts for the characteristics of each of these individual cases and which also accounts for the absence of similar effects in other metals.

Obviously the effect of hydrogen on the mechanical properties of any given metal will depend upon the hydrogen–metal system in question, and, in particular, on such factors as the solubility of hydrogen and the formation of a hydride phase. Consequently the first chapter of the paper presents a review of the more general aspects of hydrogen–metal relationships. Furthermore, since the effect of hydrogen is to cause brittle fracture to occur under conditions for which the hydrogen-free metal fails in a ductile manner, the mechanisms of the various hydrogen embrittlement effects are closely associated with the nature of brittle fracture. Hence, the second chapter is devoted to a brief review of the relevant aspects of this subject.

VOL.
9
1961

The remaining chapters of the review give a comprehensive account of the various aspects of the hydrogen embrittlement effects in each of the metals mentioned earlier. They can therefore be regarded as being complete in themselves with respect to any one metal. The form of these chapters is to present a review of the metal–hydrogen system in question, followed by an account of the characteristics of the embrittlement effect. The chapter is then completed by a critical review of the mechanisms which have been put forward to explain this effect. Finally, there is a brief general summary of the pertinent points from each of these reviews, which is then incorporated into a general theory of the nature of hydrogen embrittlement in metals.

This review is essentially a critical review of the literature, and as such it is not concerned with the presentation of any results of original (and otherwise unpublished) research on the subject.

2. Hydrogen–Metal Relationships

2.1 *General*

The subject of gases in metals has recently been reviewed by Cupp[7] and Rylski.[2] Most papers on the subject refer to Smithells' monograph,[8] which was the first of a succession of books [8–11] and reviews [12–17] dealing with various aspects of this topic. Smithells[8] recognizes that three main processes can occur when a gas is in contact with a metal. Firstly, the gas may condense on to the metal surface forming a layer, the thickness of which is of the order of one or two molecules: this is known as adsorption. Secondly, the gas may enter into solution within the interior of the metal: this process is referred to as absorption, or as occlusion. Thirdly the occluded gas may then diffuse through the interior of the metal. In many cases the gas may be present in both the adsorbed and the absorbed states. The term sorption is often used to refer to this duplex condition.

Smithells also suggests that chemical, or activated, adsorption on the

metal surface, with a heat of adsorption which is sufficient to dissociate the molecules of the gas into atoms, must precede the entry of the gas into the metal. Sieverts' law (which states that the solubility of a gas, in a metal, at constant temperature, is proportional to the square root of the gas pressure) excludes the possibility of molecular diffusion and requires the gas to be present in an atomic form.

FAST[12] has analysed the process of gas permeation through metals into five steps, thus:

(1) The dissociation of the gas molecules in the layer adsorbed on the metal surface.

(2) The transfer of the gas from the adsorbed layer to true solution within the metal.

(3) The diffusion of the gas through the metal.

(4) The transfer of gas from solution to the adsorbed layer on the exit side of the metal.

(5) The re-combination of the gas atoms, to the molecular form, on the exit side of the metal.

On the basis of experimental results, Fast concluded that any one of these five steps could be the controlling factor in the overall permeation of the metal to the gas. He suggests that the tendency for gases to diffuse through metals is associated with their ability to combine with the metals. This statement is valid when applied to hydrogen, oxygen and nitrogen, but it does not apply to the more reactive halogens, the diffusion rate of which is very low.

RHINES[15] modified Fast's hypothesis by expressing the belief that diffusion is appreciable in those metals in which the solubility of the gas is high.

Smithells' explanation of the solubility of gases in metals depends upon statistical mechanics. He regards the metal as containing a series of "holes" of low potential energy, distributed throughout the lattice. The precise distribution of these holes depends on the particular lattice structure of the metal. Atomic gas is said to be absorbed in these low energy regions: the gas then diffuses, by movement of the atoms from one hole to another, when sufficient activation energy has been acquired.

There are four possible types of interaction which can occur when a metal is in contact with hydrogen, thus:

(1) Hydrogen reacts to form salt-like hydrides with the alkali and alkaline-earth metals. These primary hydrides, which are ionic and generally crystalline, are analagous to the corresponding halides.

(2) The metals of groups IVB, VB and VIB form covalent hydrides which are gaseous at room-temperature. These compounds are analogous to the hydrocarbons, a typical example being arsine.

(3) Many metals form true solid-solutions with hydrogen, as indicated by the facts that (*a*) the hydrogen solubility varies as the square-root of the pressure (Sieverts' law) and (*b*) the solubility increases as the temperature increases. These metals are known as endothermic occluders. Typical of

this group are: chromium, iron, cobalt, nickel, copper, silver, platinum, magnesium, molybdenum, and aluminium.

(4) Hydrogen forms what DUSHMANN [16] refers to as "pseudo-hydrides" with metals of groups IVA and VA together with the "rare earths" and the "actinides". In this case the amount of gas absorbed by the metal decreases as the temperature increases. Hence, this type of metal is referred to as an exothermic occluder.

The occurrence of these four types of reactions, throughout the various elements of the periodic table, is summarized in Fig. 1. However, the remainder of this review is restricted to the latter two classes.

2.2 *Adsorption*

2.2.1 *Physical Adsorption*

The first process to occur when hydrogen is in contact with a metal of the type described in sections (3) and (4) above is the adsorption of a layer of the gas on to the surface of the metal. Experimental results show that there is a definite relationship between the amount of hydrogen which is adsorbed by a unit surface area of a metal and the pressure, at any given temperature. Adsorption phenomena can be represented in a number of ways, thus:

(1) a plot of the amount of gas adsorbed versus the pressure, at constant temperature, is known as an adsorption isotherm.

(2) a plot of the variation of equilibrium pressure with temperature, for a given quantity of adsorbed gas, is called an isotere. This type of plot is directly analagous to vapour pressure curves for liquids, and

(3) a plot of the variation of the amount of gas adsorbed with temperature, at constant pressure, is referred to as an isobar.

The most popular form of presentation is by means of the adsorption isotherm, and a typical example (that for the adsorption of hydrogen on tungsten [17]) is shown in Fig. 2. Many equations have been suggested in order to represent the adsorption isotherm mathematically. The most popular of these is that given by LANGMUIR, [18] the derivation of which is discussed in detail by DUSHMANN. [16] The bonding characteristics of the atoms which form the surface layer of a metal are unsaturated due to the assymetrical conditions of their geometry. Consequently, when gas molecules impinge against a metal surface they tend to condense there, being held there by the unsaturated field of force of the surface atoms. In discussing this effect, LANGMUIR [18] suggests that the range of the surface forces which are responsible for adsorption is of the order of 10^{-8} cm. That is, the range of these forces is usually less than the diameter of most gas molecules. Hence, in the case of true adsorption, the adsorbed layer will not be more than one molecule deep, for as soon as the surface becomes covered by a single layer the surface forces are chemically saturated.

In the above case of simple molecular adsorption LANGMUIR [18] has shown

VOL. 9 1961

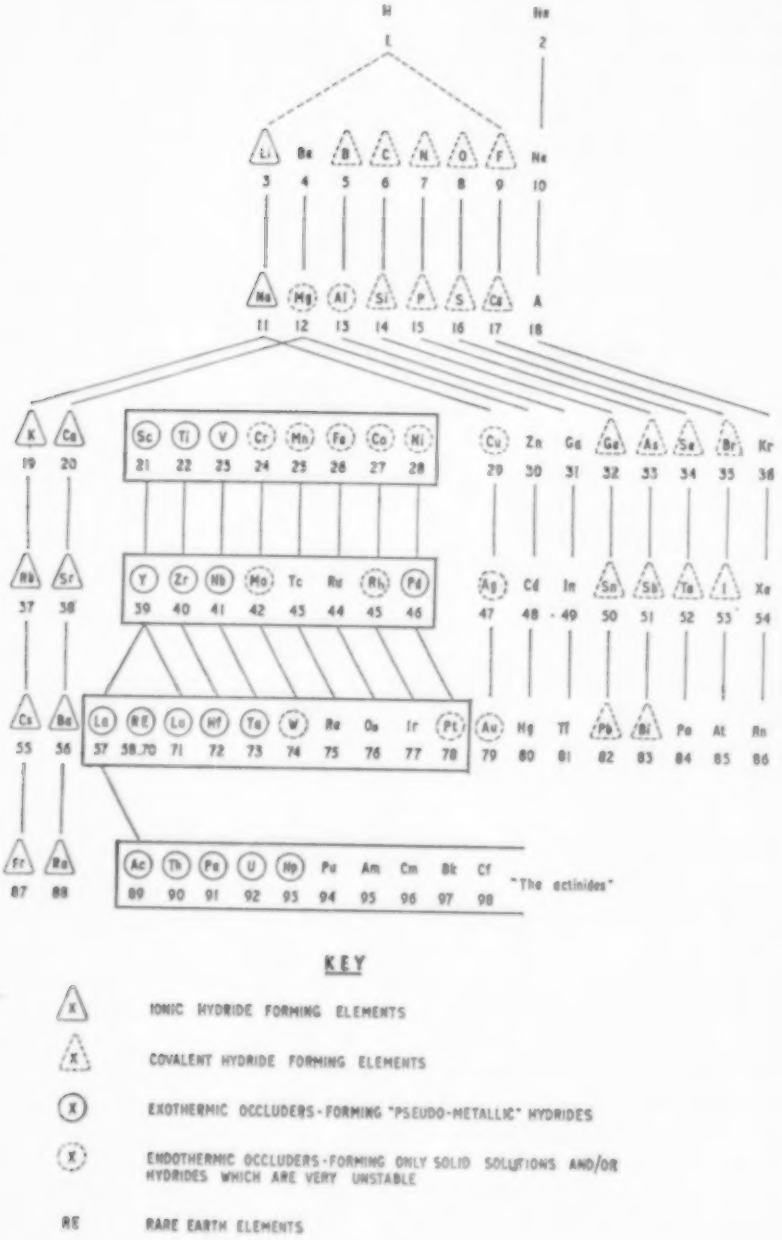
H
He
1
2
Li Be B C N O F Ne
3 4 5 6 7 8 9 10
Na Mg Al Si P S Cl A
11 12 13 14 15 16 17 18
K Ca Sc Ti V Cr Mn Fe Co Ni Cu Zn Ga Ge As Se Br Kr
19 20 21 22 23 24 25 26 27 28 29 30 31 32 33 34 35 36
Rb Sr Y Zr Nb Mo Tc Ru Rh Pd Ag Cd In Sn Sb Te I Xe
37 38 39 40 41 42 43 44 45 46 47 48 49 50 51 52 53 54
Cs Ba La RE Lu Hf Ta W Re Os Ir Pt Au Hg Tl Pb Bi Po At Rn
55 56 57 58-70 71 72 73 74 75 76 77 78 79 80 81 82 83 84 85 86
Fr Ra Ac Th Pa U Np Pu Am Cm Bk Cf "The actinides"
87 88 89 90 91 92 93 94 95 96 97 98
KEY
IONIC HYDRIDE FORMING ELEMENTS
COVALENT HYDRIDE FORMING ELEMENTS
EXOTHERMIC OCCLUDERS - FORMING "PSEUDO-METALLIC" HYDRIDES
ENDOTHERMIC OCCLUDERS - FORMING ONLY SOLID SOLUTIONS AND/OR HYDRIDES WHICH ARE VERY UNSTABLE
RE
RARE EARTH ELEMENTS

FIG. 1. Schematic representation of the reaction types for each element with hydrogen.

that the quantity of gas adsorbed onto a unit area of a surface is a hyperbolic function of the gas pressure. This equation, which is popularly referred to as "Langmuir's isotherm", has also been derived thermodynamically by VOLMER,[20] and by the use of statistical mechanics by FOWLER[21] and by LAIDLER, GLASSTONE and EYRING.[22]

The "Langmuir isotherm", discussed above, can be shown to fit many cases of adsorption in which the gas is adsorbed in the molecular state: for example argon or carbon dioxide. However, LANGMUIR,[18], suggests that in many cases, particularly those of the diatomic gases, there is evidence that the adsorption forces act on the individual atoms of the gas rather than on the molecules. Consider then the case of the adsorption of a diatomic gas, such as hydrogen, on the surface of a metal. The steady-state adsorption film on the surface is the net result of two opposing factors; (*a*) the condensation of hydrogen on to the surface in order to saturate the bonding characteristics of the metal surface, and (*b*) the evaporation of the gas from the surface in equilibrium with the external pressure.

Starting with a bare surface, if a small amount of hydrogen is adsorbed the adjacent atoms will frequently be the atoms which condensed together when a molecule was adsorbed. However, the surface will rapidly become covered by a layer of hydrogen, the atoms of which (according to LANGMUIR [17, 18]) are held individually. Hence the condensing molecules will rapidly lose their identity as the surface becomes covered by an adsorption film. It is therefore a matter of statistical chance whether an evaporating molecule contains two atoms which condensed as a molecule, or whether such a molecule will contain a pair of atoms, from adjacent adsorption sites, which were part of two different molecules during the condensation process. However, in order that a molecule is adsorbed it is necessary that two adjacent adsorption sites are vacant. If θ is the fraction of the surface which is covered by adsorbed atoms, and $(1 - \theta)$ is the fraction which is bare, it follows that the chance that two adjacent sites shall be vacant is $(1 - \theta)^2$. The rate of condensation is thus proportional to $(1 - \theta)^2$. Similarly, evaporation occurs only when adsorbed atoms are in adjacent spaces, and the chance that this will occur is θ^2. The rate of evaporation is thus proportional to θ^2. Finally, the kinetic theory of gases shows that the pressure of a gas is proportional to the number of molecules present. Hence, in the case of the diatomic gases discussed above, LANGMUIR[18] modified his equation for the adsorption isotherm to involve the square root of the pressure. In particular at low pressures, where the adsorbed layer is incomplete, the total amount of gas adsorbed is proportional to the square-root of the pressure.

This type of adsorption is usually referred to as "physical adsorption", for which the amount of gas adsorbed on to the surface of a metal decreases as the temperature increases—see Fig. 2.

2.2.2 *Chemi-sorption*

In some cases the temperature dependence of adsorption is more complex

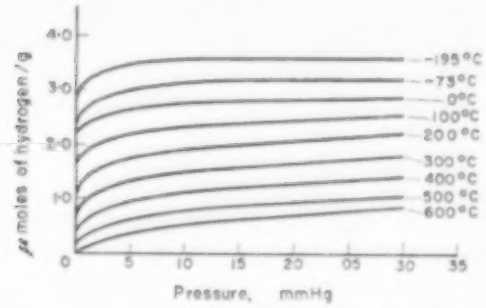

FIG. 2. Isotherms for the adsorption of hydrogen on tungsten powder; after FRANKENBURG.[17]

than would be imagined from the hydrogen–tungsten curves referred to above. It has frequently been found that as the temperature increases the adsorption falls to a minimum value and then increases as the temperature increases further: having then achieved a maximum value the amount of gas adsorbed falls once more. BENTON and WHITE[23] have found that this type of effect occurs during the sorption of hydrogen by nickel powder—see Fig. 3. In this case equilibrium can be attained almost at once at — 180°C, but a time of the order of 1 to 2 hr is needed at — 100°C, when the amount of hydrogen adsorbed is increased by a factor of about three times.

There are many other cases in which the physical adsorption occurring at low temperatures is replaced by a greater amount of adsorption which occurs more slowly at high temperatures. TAYLOR[24] has called this second stage "activated adsorption" or "chemi-sorption", since the energy involved is of a similar order to that involved in chemical reactions. This type of reaction has not been found for the sorption of the inert gases, for nitrogen on copper or for hydrogen on gold and silver.[16] SMITHELLS[8] states that ". . . this type

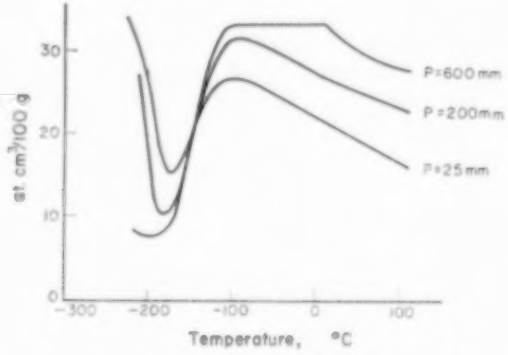

FIG. 3. Isobars for the adsorption of hydrogen on nickel powder at three different pressures; after BENTON and WHITE.[23]

of adsorption depends on a chemical attraction between the metal surface and the gas, and is most strongly marked in such systems as oxygen–silver and hydrogen–nickel. . . . Although it cannot actually be chemical combination, since no new phase is formed, it is probably a necessary preliminary to chemical action which may occur at still higher temperatures. In the cases just mentioned, for example, definite compounds, argentous oxide, nickel hydride etc., between gas and metal are known."

According to SMITHELLS[8] physical adsorption is reversible with respect to pressure and temperature: whereas chemi-sorption is not fully reversible, particularly with respect to temperature. If the equilibrium value is found by admitting gas to a material at temperature T_1, and the system is then heated to a higher temperature (T_2 say) then on cooling to T_1 the equilibrium value will be higher than the original value at this temperature. The gas adsorbed as the result of "thermal activation" of this type cannot be removed at the lower temperature, but only at high temperatures.

An excellent example of activated adsorption is afforded by Kingdom and Langmuir's work on the effect of adsorbed oxygen on the thermionic emission of tungsten filaments.[25] At low temperatures and pressures oxygen is adsorbed on to tungsten causing the emission to decrease by a factor of the order of 10^5 compared to that of pure tungsten. In order to remove this adsorbed layer, and thereby fully restore the thermionic emission, it is necessary to heat the filament to a temperature of at least 1700°C in vacuum. The authors[25] say that an oxygen film will not evaporate from tungsten in less than a year at about 1200°C; furthermore, such an adsorbed layer of oxygen will not react with hydrogen at this temperature. This can therefore be taken as striking evidence that the adsorbed film is in a condition which is very different from that of gaseous oxygen.

2.3 *Solution*

2.3.1 *Endothermic Occlusion*

Solution is an endothermic process.[13] Hence, in the case of those metals in which only a simple solution of hydrogen occurs (the so-called endothermic occluders), the solubility increases as the temperature increases. Both the dissociation of hydrogen during surface adsorption, and the fact that hydrogen enters into solid solution in the atomic form, lead to the experimentally observed fact that the solubility of hydrogen is proportional to the square-root of the hydrogen pressure, at constant temperature. This latter relationship is referred to as Sievert's law.

Thus the solubility of hydrogen in endothermic occluders can be expressed[16] as a function of temperature and pressure by an equation of the form:

$$S = S_0\sqrt{P}\exp(-Q/2RT) \quad . \quad . \quad . \quad . \quad . \quad (1)$$

where S = the solubility of hydrogen; S_0 = a constant. P = the pressure

of hydrogen; Q = the heat of solution, in calories per gram-mole of hydrogen. R = the gas constant and T = the temperature in degrees Absolute.

The factor 2 in the denominator of the exponential term takes into account the fact that hydrogen enters into solution in the atomic form.

This equation can be expressed logarithmically as follows:

$$\log S = \log S_0 + 0{\cdot}5 \log P - \frac{Q}{CT} \quad . \quad . \quad . \quad . \quad . \quad (2)$$

(where C is constant).

Hence the value of the heat of solution can be derived from a linear plot of log S against $^1/T$.

2.3.2 *Exothermic Occlusion*

In the case of the endothermic occluders mentioned above, the only reaction with hydrogen is the formation of a simple solid-solution, the extent of which varies according to the pressure of the gas and the temperature. However, in the case of the exothermic occluders the behaviour is complicated by the formation of pseudo-metallic hydrides. In these latter cases it is important to distinguish between the solubility of hydrogen and the total amount of hydrogen which is absorbed by the metal. Since one of the major characteristics of the exothermic occluders is the formation of a hydride it is possible to represent the equilibrium conditions of this type of metal–hydrogen system by a phase diagram analagous to the phase diagrams which are used to represent normal metallic alloy systems. These can then be used to depict the difference between the two above-mentioned quantities, as followers.

As the hydrogen content of a metal of this type is increased from zero the initial hydrogen addition will go into solid-solution within the metal, thereby leaving the metal in a single-phase condition (as occurs in the case of the endothermic occluders). However, particles of the hydride phase will eventually begin to be formed within the metal. The solubility of hydrogen should therefore be taken as that composition at which the specimen leaves the single-phase region of the pseudo-equilibrium diagram and becomes a two-phase alloy. This definition of solubility is therefore directly equivalent to that normally applied to the solid-solutions of metallic alloy systems. However, the hydrogen content of the specimen can be increased beyond this solubility limit by the formation of the hydride-phase. Thus the total amount of hydrogen which is absorbed by an exothermic occluding metal depends upon the kinetics of hydride formation and will always exceed the solubility, as it is defined above. Ideally hydrogen should be absorbed until all the metal has been converted to the hydride of the maximum hydrogen content.

The precise form of the pseudo-diagram depends on the characteristics of the metal in question (e.g. allotropy, etc.) and on the kinetics of hydride formation. Generally speaking, the solubility of hydrogen (as defined above) increases as the temperature increases, since solution is an endo-thermic

process. However, the total amount of hydrogen absorbed decreases as the temperature increases, due to the exothermic nature of hydride formation.

In the cases of true solution the concentration of hydrogen is proportional to the square-root of the hydrogen-pressure (Sieverts' law); but considerations of the phase rule show that the equilibrium pressure of hydrogen remains constant within a two-phase region of the phase diagram.

2.3.3 *The Location of Hydrogen in Solid-Solution*

The nature of the surface adsorption of hydrogen (as outlined in Section 2.2.1), and the fact that the concentration of hydrogen in solid-solution varies as the square-root of the pressure, suggest that hydrogen dissolves in metals in the atomic form.[13] The diameter of a hydrogen atom is usually taken as being of the order of 1 Å. Hence, by the usual geometrical model, of the packing of spheres, which is normally used to depict the structure of metal lattices, hydrogen is generally regarded as being present in interstitial solution within metals,[8] since the smallest metal atom diameter is approximately 2·25 Å.

However, SMITH,[9] in a monograph which deals exclusively with hydrogen in metals, has proposed an alternative theory, which is dominated by a rift hypothesis. All the experimental effects of hydrogen–metal relationships are explained in terms of lattice defects; the basic concept being that only metals which contain lattice intervals which have been enlarged beyond their normal size are capable of dissolving hydrogen or permitting its diffusion. The theory can be summarized as follows:

(1) Endothermic occlusion occurs in expanded regions of the metal lattice, without involving interstitial solution.

(2) Exothermic occlusion is assisted by occlusion through strain-opened regions and does involve interstitial solution, with a consequent distortion of the lattice. Solubilities of this type are much larger than those of endothermic occlusion.

The strain-opened regions, required by this theory, are formed by a continuous network of "rifts" within the metal lattice. Such regions can be enlarged (according to Smith) in order to allow occlusion by either (*a*) further mechanical straining, (*b*) thermal expansion or (*c*) the occlusion process itself. Smith suggests that when a metal is deformed the interatomic forces are distorted, stress gradients are produced, and the forces acting on ions and electrons are disturbed. A strain-induced "rift" is therefore considered to be a region of great ionizing power. Hence, Smith suggests that hydrogen is present as protons not as atoms. Since a strained state is needed, on this type of mechanism, for either type of occlusion, endothermic occlusion in the rifts is said to precede entry into the lattice in the case of the exothermic occluders. The rift walls, which bound the regions of ionization, are said to constitute a barrier which is passed in endothermic occluders by external pressure, and in exothermic occluders by an exothermic process.

VOL.
9
196

Smith questions the existence of true interstitial solid-solutions in the "endothermic metal hydrogen systems" and his treatment of the subject is completely dominated by this "rift" hypothesis. It is important to notice that this hypothesis is entirely qualitative, and is challenged by several workers. For example, RANSLEY[27] has written: "Indeed, it is not unfair to say that in a good many instances the author (i.e. Smith) has strained the facts very severely in an attempt to make them conform to this theory, when a simple explanation based on lattice solution and diffusion would appear to be perfectly adequate."

As was suggested in the previous section there seems to be a considerable amount of confusion, in the literature, between the terminal solubility and the total amount of hydrogen absorbed by the exothermic occluders. Undoubtedly this latter quantity behaves in an exothermic manner as the result of the formation of the hydride which it represents. However, there seems to be little evidence that the single-phase solubility of hydrogen in the exothermic occluders behaves any differently than the solubility in the endothermic occluders; except that in the former case the solubility limit is always greater than in the latter, under any given set of conditions.

The particular details of those metal–hydrogen systems which are of interest from the point of view of hydrogen embrittlement are discussed in the appropriate chapter.

2.4 *The units used in the measurement of sorption phenomena*

The amount of gas involved in the various sorption phenomena, with metals, can be quoted in a variety of ways, the most popular being as follows:

(1) a = the volume, in cubic centimetres, of gas at 0°C and 760 mm Hg pressure, absorbed on to 1 cm² of metal surface.

(2) V_0 = the volume, in cubic centimetres, of gas at 0°C and 760 mm Hg, per g of metal.

(3) S_0 = the volume in cubic centimetres, of gas, at 0°C and 760 mm Hg, per 100 g of metal.

(4) r = the volume, in cubic centimetres, of gas, at 0°C and 760 mm Hg, per cubic centimetre of metal (this is often referred to as r "relative — volumes").

(5) x = the weight of gas involved in sorption phenomena in terms of x "parts per million", by weight. (This is often quoted as x mg per 1000 g).

(6) w = the concentration of gas, in a metal, expressed in terms of percentage by weight.

(7) A = the concentration of gas, in a metal, expressed in terms of atomic percentage.

Since adsorption is a surface-controlled process, rather than a volume process, the first unit, a, is particularly suited to the expression of adsorption results, whilst the others are all suitable for the expression of absorption data, such as solubility limits, gas contents and, in the case of the exothermic

occluders, the amount of hydrogen absorbed during hydride formation. The actual measurements of sorption phenomena are usually done by observing the pressure changes, on absorption or de-gassing, in an apparatus having a known volume. It is then a matter of simple arithmetic to convert these pressure changes into the volume of the gas at 0°C and 760°C; hence the first three units (a, V_0 and S_0) are those in most popular use. The relationships between the various units, for the particular case of hydrogen in metals, are given below:

$$(a)\ S_0 = 100\ V_0 \quad . \quad . \quad . \quad . \quad . \quad . \quad . \quad . \quad . \quad . \quad . \quad . \quad . \quad . \quad . \quad (3)$$

$$(b)\ r = \rho V_0 = 10^{-2}\ \rho\ S_0 \quad . \quad . \quad . \quad . \quad . \quad . \quad . \quad . \quad . \quad . \quad . \quad . \quad . \quad . \quad (4)$$

$$(c)\ x = 0{\cdot}00009 \times V_0 \times 10^6 = 90\ V_0 = 0{\cdot}9\ S_0 \quad . \quad . \quad . \quad . \quad . \quad . \quad . \quad . \quad . \quad . \quad . \quad . \quad . \quad . \quad (5)$$

$$(d)\ w = x \times 10^{-4} = 9 \times V_0 \times 10^{-3} = 9 \times S_0 \times 10^{-5} \quad . \quad . \quad . \quad . \quad . \quad . \quad . \quad . \quad . \quad . \quad . \quad . \quad . \quad . \quad (6)$$

$$(e)\ A = \frac{100}{1 + \frac{G}{M}\left(\frac{100}{w} - 1\right)} \quad . \quad . \quad . \quad . \quad . \quad . \quad . \quad . \quad . \quad . \quad . \quad . \quad . \quad . \quad (7)$$

and

$$(f)\ w = \frac{100}{1 + \frac{M}{G}\left(\frac{100}{A} - 1\right)} \quad . \quad . \quad . \quad . \quad . \quad . \quad . \quad . \quad . \quad . \quad . \quad . \quad . \quad . \quad (8)$$

where ρ = the density of the metal, in gm per cm^3,
M = the atomic weight of the metal,
and G = the atomic weight of the gas.

In the case of low concentrations (of the order $w = 0{\cdot}1$) such as are normally involved in hydrogen solubilities, the conversion from atomic per cent to weight per cent, and vice versa, can be simplified as follows:

$$\text{for low values of } w,\ A = Mw/G \quad . \quad . \quad . \quad . \quad . \quad . \quad . \quad . \quad . \quad . \quad . \quad . \quad . \quad . \quad (9)$$

Or specifically in the case of low hydrogen concentrations we have

$$A = Mw = M\ .\ x\ .\ 10^{-4} \quad . \quad . \quad . \quad . \quad . \quad . \quad . \quad . \quad . \quad . \quad . \quad . \quad . \quad . \quad (10)$$

The choice of which unit should be used, in any particular case, depends to a large extent on the particular circumstances and object of the case. For example it would appear that the first unit mentioned above (a, the volume of gas adsorbed by a unit surface area) represents the most useful means of expressing adsorption data. In the case of the gas which is absorbed into a metal (whether in solution or in hydride formation) the three volume units (V_0, S_0 and r) give a physical picture of the amount of gas involved, whilst the latter three (x, w and A) give values which can be compared with normal analytical data. Any of the above-mentioned units may be used, as a matter of convenience, for the comparison of absorption data etc., in any one metal under a variety of conditions (temperature, pressure etc.): consequently the choice of unit used often depends upon factors of the type mentioned above. However, solubility limits and the effect of hydrogen on the physical and mechanical properties of metals depend, to a very large extent, on the relative

concentration of hydrogen atoms within the metal. Hence the only means of directly comparing the behaviour of hydrogen within two different metals is by the expression of the hydrogen content in terms of the atomic percentage of hydrogen in the various metals.

Hence, in the course of the ensuing discussions the hydrogen contents involved will be quoted in terms of the atomic percentage of hydrogen, and the relative weights of hydrogen and the metal—either as the percentage by weight or, as x parts per million by weight. Conversion to any other system of units can be achieved by reference to the appropriate conversion factors, listed above. The importance of the use of atomic percentages, for comparison purposes, can be seen from the following example. A hydrogen content of 5 cm^3 per g of metal would represent a concentration of the order of 0·4 atomic per cent in beryllium whereas the same figure would represent a concentration of approximately 10·7 atomic per cent in uranium.

2.5 *Diffusion*

The relative dimensions of hydrogen atoms and the lattice constants of the metals affords a ready explanation of the ease with which hydrogen diffuses through most metals. The concept of interstitial solution suggests that the rate of diffusion will be greater as the size of metal atom increases. The various possibilities are that hydrogen atoms may diffuse through (a) the interstices of the lattice structure, (b) grain-boundaries of poly-crystalline specimens or (c) structural imperfections within grains. Controversy about the case which applies to any given metal is understandable in the light of FAST's[12] experimental work on the rate-controlling factors in the permeation of metals by gases.

SMITHELLS[8] takes the view that interstitial diffusion is the predominant factor, whilst the grain-boundaries and lattice imperfections are of secondary importance. This has been verified, in the case of iron, by a series of experiments involving the use of single crystal specimens.[2] In this case the diffusion characteristics are identical to those of polycrystalline specimens under the same conditions. However, the theory of interstitial solution and diffusion is by no means clear. SPEISER, SPRETNAK and TAYLOR[28] have pointed out that geometrical considerations alone do not provide a complete explanation, since some metals (e.g. zinc, and cadmium etc.), do not seem to yield interstitial solutions although their interstitial "holes" are larger than those occurring in some transition metals (e.g. iron).

SMITHELLS and RANSLEY[29] suggest that, in the general case of gases in metals, activated adsorption, with the dissociation of the gas molecule, is a necessary preliminary to the diffusion of the gas through a metal. They suggest that purely physical adsorption with relatively weak bonding between the metal and the "gas" will not result in diffusion: but rather that diffusion results from the formation of a series of unstable metal-gas atom pairs, the gas atom being handed on from one metal atom to another throughout the lattice. In support of their ideas they quote the experiments of SEITH[30, 31]

on the diffusion of various elements in lead. Here it was shown that the diffusion rate increased as the difference between the outer electron shell of the solute atom and that of the solvent atoms increased. SMITHELLS and RANSLEY [29] suggest that this is evidence for their belief that the distortion of the lattice resulting from the chemical affinity of the solute atom and the solvent metal is an essential factor in the diffusion process. As stated earlier, RHINES [15] has modified the ideas concerning diffusion by suggesting that diffusion is most appreciable in those metals in which the solubility of the diffusing gas is high.

Diffusion rates increase rapidly with temperature, in accordance with the exponential law which governs all rate processes. In most cases the diffusion rate of hydrogen is proportional to the square root of the hydrogen pressure, at constant temperature. As in the cases of adsorption and solution this latter effect is due to the fact that hydrogen is dissociated on entering into surface reactions with metals, and in particular it is dissolved in the atomic form.

VOL. 9 1961

2.6 *Summary*

It would therefore appear that in order to obtain a homogeneous solution of hydrogen in a metal three different processes are involved, (*a*) surface adsorption, (*b*) solution in the region immediately below the surface and (*c*) diffusion of the hydrogen through the metal in order to homogenize the hydrogen distribution throughout the specimen. As FAST [12] has pointed out, the overall speed of this process will be controlled by the speed of the slowest of the above-mentioned processes. Although the mechanism of diffusion of gases in metals is by no means clear it would appear that most people consider that those factors which are needed for chemi-sorption to occur (principally an appreciable bond strength between the metal and gas atoms) are also needed in order to attain high solubilities and diffusion rates.

In discussing the inter-relation of adsorption and solution, LAIDLER [32] has shown, by a mathematical treatment, that at low pressures the attainment of a complete adsorption film is the rate controlling process whereas at high pressures this condition is relatively easy to achieve and the rate controlling process is the rate of diffusion of hydrogen within the metal.

The elements at the extreme ends of the periodic table (Fig. 1) form hydrides, the bonding in which is entirely chemical in nature. In the case of these compound-forming elements the stability of the hydrides decrease as the atomic weight of the metallic element increases. [33]

The extreme difficulties involved in obtaining solubility data from one investigation to another (e.g. impurity variations, etc.), make a similar comparison of the solubility limits of the occluding metals qualitative rather than quantitative. However, a brief examination of the relevant data suggests that the solubility of hydrogen tends to decrease as the atomic number of the solvent increases, in any one group: for example chromium, molybdenum, and tungsten, of group VIA; or titanium, zirconium and hafnium of group

IVA. The solubility of hydrogen in the exothermic occluders is greater than that in the endothermic occluders. Hence, examination of Fig. 1 shows that (with the notable exception of palladium) the solubility of hydrogen decreases as the position of the solvent moves across the periodic table from left to right.

Some metals do not absorb hydrogen, despite the fact that their structure contains relatively large interstices. This may be due to some restriction on the maximum size of an interstitial "hole" which can contain a hydrogen atom under equilibrium conditions. HUME-ROTHERY and RAYNOR[34] have shown that if the atomic radius of the atom is of the order of 0·41 times that of the solvent the solute atom will fit exactly into the octohedral interstice of a close-packed lattice. They suggest that if the solute atoms are too small to fulfil the above critical value, and so become a loose fit in these interstices, the resulting structure would be thermodynamically unstable, and, hence, it would not be formed.

However, it is also possible that the solubility of hydrogen in metals is influenced by chemical factors, as is postulated for chemi-sorption, and, in some cases, for diffusion. This is suggested by the fact that the endothermic occluders (with solubilities of the order of less than 0·1 atomic per cent) all lie mid-way between the exothermic occluders (hydride formers,—with solid-solubilities of the order of 2 to 10 atomic per cent hydrogen) and those elements which do not absorb hydrogen, in the periodic table.

It would therefore appear that the hydrogen–metal relationships, for those metals which do not form conventional "chemical" hydrides, are a complex function of several factors the most important of which are probably the sizes and chemical affinities (for hydrogen) of the metal atoms.

3. BRITTLE FRACTURE AND THE DUCTILE-TO-BRITTLE TRANSITION TEMPERATURE IN METALS

3.1 *General Aspects of Fracture in Metals*

The fracture of metals can occur by any one of a number of phenomenologically different mechanisms.[35] Single crystals may fracture by cleavage or by shear processes associated with either slip or twinning. In the case of polycrystalline metals these same fracture modes apply, but they are modified by the presence of grain boundaries. Metals of moderate, or high, ductility first of all undergo plastic deformation, which is then followed by "necking". The specimen then fractures, the fracture starting near to the centre of the "neck". In this case a significant increase in strain is needed to propagate the fracture, which passes irregularly *through* the grains. At low temperatures those metals which fracture by cleavage as single crystals may also cleave in the polycrystalline state. Finally, polycrystalline metals may also fail by *inter*crystalline fracture.

3.2 *The Griffith Theory of Fracture*

The basic problem in fracture is to find some factor that will account for

the "order of magnitude" difference between the observed and the theoretical breaking strength of solids. The first major attempt to solve this problem was given by GRIFFITH,[36] who postulated the presence, within the specimen, of micro-cracks at which the stress concentration is of sufficient magnitude that the theoretical strength can be exceeded locally from quite a low applied stress.

Griffith considered the case of a flat plate, of uniform thickness, containing a crack of elliptical cross-section and width equal to $2c$, such that this crack extends right through the plate.[35] The stresses and strains around such a crack, when it is subjected to a tensile stress (σ) perpendicular to the plane of the crack (the other principal stresses lie in this plane), have been used by INGLIS,[37] to calculate the strain energy due to the presence of the crack. Since crack propagation creates a relief of strain energy this expression is negative. For plane stresses this strain energy is equal to $(-\pi c^2\sigma^2/E)$ per unit thickness, where E equals Young's modulus.

The corresponding surface energy associated with such a crack is given by $4cS$, where S is the surface tension of the material.

Such a crack will spread, under the influence of a tensile stress, only when the decrease in strain energy of the material is greater than the increase in the surface energy due to the formation of the newly exposed crack surface.

Hence the equilibrium size of the "Griffith crack" is given by:

$$\frac{d}{dc}\left(4cS - \frac{\pi c^2\sigma^2}{E}\right) = 0 \quad . \quad . \quad . \quad . \quad . \quad . \quad . \quad (11)$$

therefore

$$4S - \frac{2\pi\sigma^2 c}{E} = 0 \quad . \quad . \quad . \quad . \quad . \quad . \quad . \quad (12)$$

Hence

$$\sigma = \sqrt{\left(\frac{2ES}{c}\right)} \quad . \quad . \quad . \quad . \quad . \quad . \quad . \quad . \quad . \quad (13)$$

Since the crack can spread when this stress is exceeded, Eqn. (13) gives the fracture stress in the presence of such a crack.

Since the width of the crack (c) increases as the crack spreads the stress needed to maintain crack propagation decreases, hence[36, 37] the smallest tensile stress (σ_g) needed to propagate an elliptical crack in a thick plate of material having Poisson's ratio equal to v is given by:

$$\sigma_g = \sqrt{\left[\frac{2ES}{(1-v^2)\pi c}\right]} \quad . \quad . \quad . \quad . \quad . \quad . \quad . \quad (14)$$

SACK[38] has applied this type of analysis to a very flat oblate ellipsoidal crack (penny shaped) in a thick plate. The fracture stress, in this case, is given by:

$$\sigma_g = \sqrt{\left[\frac{ES}{(1-v^2)\,2.\,c}\right]} \quad . \quad . \quad . \quad . \quad . \quad . \quad . \quad (15)$$

It can be seen that this differs from Griffith's value for elliptical cracks by

VOL. 9 1961

a numerical factor only. ELLIOTT[39] has presented a detailed treatment of this type of cracking in terms of an atomic model. The results of this analysis again differ from those of Griffith only by a simple numerical factor. Thus there is general agreement on the form of the expression that gives the strength of a body containing a microcrack, when that body behaves elastically up to its fracture.

3.3 *Applications of the Griffith Theory*

Griffith verified his theory by a series of experiments on the tensile testing of glass containing micro-cracks. He also obtained fracture-strengths approaching the theoretical value in very thin glass fibres which were crack-free. However, it is important to note that this experimental verification was confined to amorphous elastic materials and not extended to include metals. The viscous nature of glass is such that plastic deformation is non-existent at room temperature, and consequently localized stress concentrations cannot be relieved except by a fracture of the Griffith type.

OROWAN[40] has shown that, although the Griffith concept is a necessary and sufficient criterion for the tensile fracture of perfectly brittle (elastic) solids, a modification has to be made when it is applied to brittle fracture in metals. X-ray back reflection photographs[41] show that a thin layer at the surface of apparently brittle fractures, in low-carbon steel, contains significant plastic deformation. The plastic work in this layer ($P = 2 \times 10^6$ ergs/cm^2) is considerably greater than the surface energy of the newly-developed crack ($S = 10^3$ ergs/cm^2). Orowan therefore suggests that the "Griffith equation" should be modified to account for this plastic deformation. Thus:

$$\sigma_f \simeq \sqrt{\left(\frac{2EP}{\pi c}\right)} \quad . \quad . \quad . \quad . \quad . \quad . \quad . \quad (16)$$

The only difference between this condition and Griffith's original condition (for perfectly elastic solids) is the substitution of the plastic deformation energy (P), for the surface tension energy (S). Orowan states that after a cleavage crack has arisen it may propagate quite rapidly, provided that the condition of Eqn. (16) is satisfied: i.e. provided that the release of elastic strain energy around the crack is sufficient to increase the kinetic energy of the moving crack.

The Griffith crack condition cannot be applied to the case of ductile fracture of metals since in this case the deformation is essentially plastic, whereas the Griffith principle applies only to cases where plastic deformation is either absent or confined to a thin layer on the crack walls so that the bulk of the specimen remains perfectly elastic.

3.4 *The Nature of the "Griffith Cracks" in Metals*

The theories mentioned above are concerned with the propagation of micro-cracks under the influence of an applied stress. They assume that such

cracks exist, under the conditions of the test, and consequently they make no attempt to explain the form which the cracks take. However, present-day knowledge of the structure of metals, and in particular the nature of lattice imperfections, has enabled several workers to postulate mechanisms whereby the micro-cracks required by Griffith's theory of fracture are formed and propagated during the deformation of a metal.[42–44] There are two types of brittle fracture, intergranular and cleavage. The origin of the fracture-cracks, for each of these cases, is discussed below.

3.4.1 *Intergranular fracture*

ZENER[42] and CHANG and GRANT[43] have postulated mechanisms for the creation of intergranular cracks based on the stresses present at grain boundaries. It is important to differentiate between the overall deformation of a specimen and the highly localized deformation of certain microscopic regions. The deformation which a specimen suffers is not homogeneous in any one grain, but since, in isotropic materials, neighbouring grains deform at similar rates the specimen deformation appears to be uniform over areas which are large when compared to the grain-size.

ZENER[42] suggests that the rate of shear strain across a grain boundary is proportional to the shear stress across the boundary, but that there is no relative movement of the grain corners; i.e. the grain corners act as a "locking" device which restricts the relative movement of adjacent grains. The stress system is then such that the grain corners become sites of intense stress concentration. This effect increases until the theoretical fracture strength is reached and a crack is formed at the intersection of three neighbouring grains. Zener calculates that if the grain diameter is 0·1 mm the stress at such an intersection is of the order of 1000 times that applied to the specimen.

In order to achieve continuity of strains and hence ductility, throughout a specimen, deformation by grain boundary sliding must also be accommodated by deformation within the grains, and a strain in one grain must be transmitted across the boundary to the neighbouring grains. CHANG and GRANT[43] postulate that if this does not occur, then a brittle intergranular fracture is created by one of two possible mechanisms. Firstly, grain-boundary sliding leads to the creation of a three dimensional stress system at the intersection of grain-corners; the relative movement of the boundaries may then lead to crack formation—see Fig. 4. Secondly, in the absence of grain-boundary sliding, if one grain deforms more than its neighbour, and this additional deformation is not transmitted across the boundary between the two grains, tensile or bending stresses are created across the boundary. An intergranular crack may then be formed in an attempt to relieve this stress system, in the absence of grain boundary movement.

3.4.2 *Brittle fracture by cracking within the grains*

ZENER[42] has explained the nucleation of micro-cracks, within a grain, in terms of dislocation theory. The deformation, in any one grain, is very

VOL. 9 1961

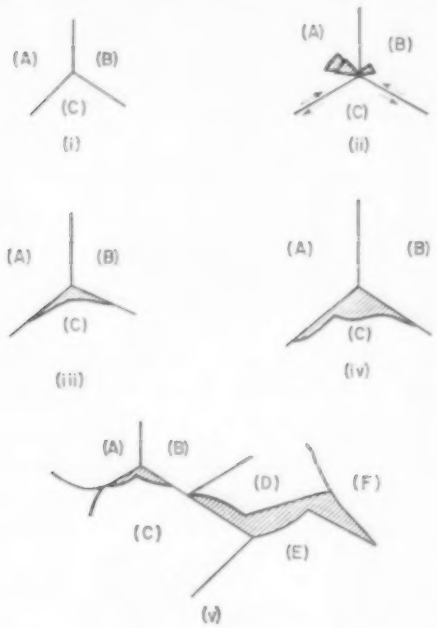

FIG. 4. The sequence of initiation and growth of an inter-crystalline crack proposed by CHANG and GRANT.[43]

heterogeneous and is confined to the slip-bands of the grain. When a moving slip-band is stopped by an obstruction, the shear stress in the slip-band continues to be relaxed; hence, a stress concentration is created at the junction of the slip-band and the obstruction. This can lead to one of two possible consequences. If the obstruction is a grain-boundary it is possible for a slip-band to be initiated in the neighbouring grain. However, this stress concentration may lead to a separation of the atoms in this region, particularly if the obstruction is a hard precipitate platlet. Hence, this latter possibility leads to the formation of a micro-crack which can then propagate by the Griffith–Orowan mechanism.

A slip-band consists of a linear array of dislocations, the dislocation density being greatest at the ends of the slip-band where the strain is greatest. As the applied stress increases, the end of the slip-band will become "locked" by obstructions such as grain-boundaries. A further increase in the applied stress will cause an increase in the dislocation density at the end of the slip-band, until finally a crack is initiated by the amalgamation of several dislocations of the same sign (see Fig. 5).

STROH[44, 45] has calculated the stresses around a piled up group of dislocations, and has formulated the conditions under which a crack will be opened up on the dislocation model. Using these results, together with a relationship derived by ESHELBY, FRANK and NOBARRO,[46] he has shown

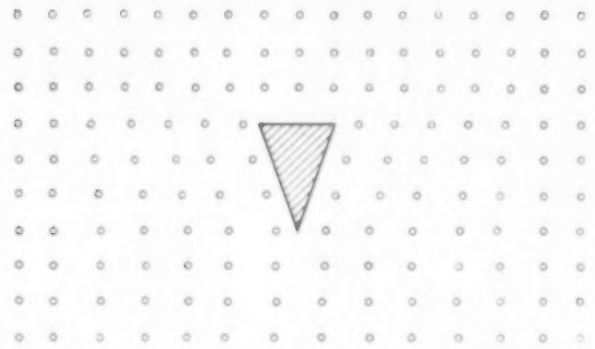

FIG. 5. Schematic representation of a micro-crack nucleus formed by the amalgamation of three positive line dislocations; after ZENER.[42]

VOL.
9
1961

that the cleavage strength should be inversely proportional to the square-root of the grain-size. This proportionality has been verified experimentally by PETCH,[47] for ferrite, and by GREENWOOD and QUARRELL[48] for zinc. The constants of proportionality, calculated from STROH's[44] theory, agree favourably with experimental values. For ferrite the calculated value is $2{\cdot}0 \times 10^8$ compared with the experimental value of $2{\cdot}3 \times 10^8$, and for zinc the values are $1{\cdot}2 \times 10^8$ and $1{\cdot}0 \times 10^8$ respectively.

This model has been used, by Stroh, to account for the variation of the lower yield point, in ferrous metals, with grain-size and temperature, together with its insensitivity to the nature of the specimen. It also gives a value for the absolute yield-point which agrees, in order of magnitude, with the experimentally observed value.

3.5 *The Propagation of Cleavage Cracks*

The cleavage fracture of a polycrystalline aggregate takes place in three stages: (*a*) nucleation of the crack at the atomic level, (*b*) propagation of the crack through the grain in which it is nucleated, and (*c*) the bursting of the crack out of this grain to propagate through the remainder of the aggregate. GILMAN[49] suggests that the controlling factor, in brittle fracture, is crack propagation rather than crack nucleation.

There are several mechanisms whereby a crack may be nucleated, but nevertheless, at the tip of such a crack there is a stress concentration, the principal stresses at which are not equal, so that high shear stresses are present. These should cause *plastic* flow. This plastic flow should then relieve the stress concentration and prevent the crack from propagating. MOTT[50] rationalized this difficulty by suggesting that a finite time may be needed for such plastic flow to occur at the tip of a moving crack. This emphasizes the importance of the crack velocity in determining whether or not a brittle crack can propagate in a solid.

Three factors determine the velocity of a crack in an ideally elastic

medium.[50] The driving force is the elastic energy that is released as the crack moves forward. This is balanced by the surface energy created during the motion of the crack, and by the kinetic energy associated with the rapid lateral displacement of the material on either side of the crack. However, for materials that are not ideally elastic the driving energy of the crack is dissipated by at least two other processes, in addition to the surface energy. One of these is plastic deformation on the crack surface;[40, 41] whilst the other results from the fact that crack surfaces are normally not plane smooth surfaces.[51]

GILMAN[49] elaborates on this theme to show that the controlling factor, in crack propagation, is the velocity of the crack, and not the factors determining its nucleation, and this argument is used to explain the relationship between fracture and grain size.

There will be a sudden change in the energy absorption of a crack as it crosses a grain boundary. If the mis-orientation of the two grains is slight the energy absorption will be due to the change of direction of the crack as it passes to the cleavage plane of the second grain. This will possibly lead to a "stepped" cleavage fracture. On the other hand, if the mis-orientation between the two grains is large the crack may not be able to continue into the second grain. In this case the crack will stop at the boundary, until the stress concentration at this point initiates a crack in the second grain. In either case, this will result in a reduction of the velocity of the crack on crossing a boundary. If the crack velocity is reduced to less than the critical propagation velocity the fracture process will be halted until an increase in the stress–concentration effect initiates a new crack. However, if the new crack velocity is high enough, it will cross into the second grain and continue at the slower velocity.

Thus Gilman proposes that there are two critical crack velocities, in cleavage fracture, (*a*) the velocity needed to propagate a crack through a grain, and (*b*) a higher velocity which will allow it to break out of the grain and fracture the aggregate. This interpretation imposes a critical velocity condition on the Griffith–Orowan energy criterion, but it does not help to explain the source of the micro-cracks.

3.6 *The Ductile-to-Brittle Transition*

3.6.1 *Characteristics of the transition*

Many metals which are ductile at or above room temperature, fail in a brittle manner at lower temperatures. The generally accepted qualitative concept of the ductile-to-brittle transition is that brittle fracture occurs when the yield strength exceeds the brittle fracture strength. This condition can apparently be achieved by decreasing the temperature or increasing the strain rate. Also, a normally ductile metal can be made to fracture in an apparently brittle manner by the introduction of triaxial stresses (e.g. by the introduction of surface notches), where the ratio of normal to shear stresses may be increased to such an extent that the normal stress exceeds the fracture strength

before the shear stress reaches the critical value for plastic flow. This concept does not require any prior plastic deformation, nor does it explain why the observed fracture strength is so much less than the theoretical cohesive strength.

The results of several investigations of the ductile-to-brittle transition, particularly in body-centred-cubic metals show that measurable amounts of non-elastic deformation do precede cleavage fracture even at very low temperatures.[52–57] The amount of pre-yield plastic strain reported is usually of the order of 10^{-6}, but WESSEL[57] claims to have measured as much as 10^{-3} to 10^{-2} (0·1 per cent to 1·0 per cent) in a review of the behaviour of iron, molybdenum, tantalum and niobium. This is by no means negligible, and must therefore be accounted for in any theory of the transition effect.

VOL. 9 1961

3.6.2 *General dislocation theory of the transition*

The increased resistance to initial plastic deformation with decreasing temperature, as illustrated by the pronounced temperature dependence of the yield strength, has probably best been explained as being due to the anchoring of dislocations by impurity atoms, as described by COTTRELL.[58, 59] The original Cottrell concept assumes that stresses, aided by thermal fluctuations, enable small groups of dislocations to break away from anchoring impurity "atmospheres", and that the nucleation of the first dislocation loop is the beginning of pronounced yielding. During the subsequent extension of such a loop, or loops, other dislocations break away from their atmospheres, thereby resulting in rapid yielding. Since thermal fluctuations decrease as the temperature decreases greater external stresses are needed to remove dislocations from the "locking" influence of impurity atoms at low temperatures; hence, the temperature dependence of the yield strength.

To account for the large amounts of pre-yield strain observed by WESSEL[57] it is necessary to assume that many dislocations must be moved through the lattice prior to a sudden yield: for example in steel, at −196°C, the above mechanism would require the movement (and eventual pile-up at grain boundaries and other obstructions) of about 1000 dislocations per grain.

Figure 6 shows an exaggerated schematic representation of the deformation of a tensile specimen, in the region of the yield point, at temperatures above the ductile-to-brittle transition temperature, whilst Fig. 7 depicts the behaviour of a similar specimen below this temperature.[57] On the dislocation model outlined above the difference between ductile fracture and brittle fracture depends on the behaviour of the dislocations after they have broken away from their impurity atmospheres. As the result of the piling up of dislocations at barriers, and the accompanying increase in the general applied stress, high stress concentrations are developed in the region of the pile-up. The abrupt yielding now becomes associated with the relaxation of these local stresses by the activation of new dislocation sources in the adjoining material, and also, to a lesser extent, by the continued propagation of the piled up dislocation groups. The achievement of the necessary critical stress

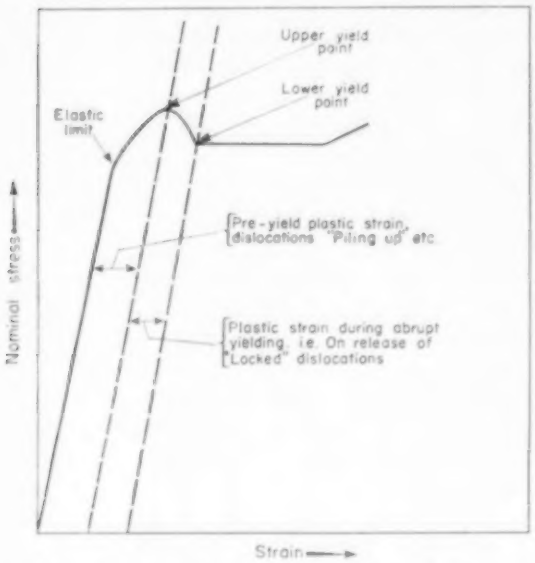
Upper yield point
Lower yield point
Elastic limit
Pre-yield plastic strain, dislocations "Piling up" etc.
Plastic strain during abrupt yielding, i.e. On release of "Locked" dislocations
Nominal stress
Strain

FIG. 6. Factors involved in early stages of plastic flow at temperatures above the transition temperature; after WESSEL.[58]

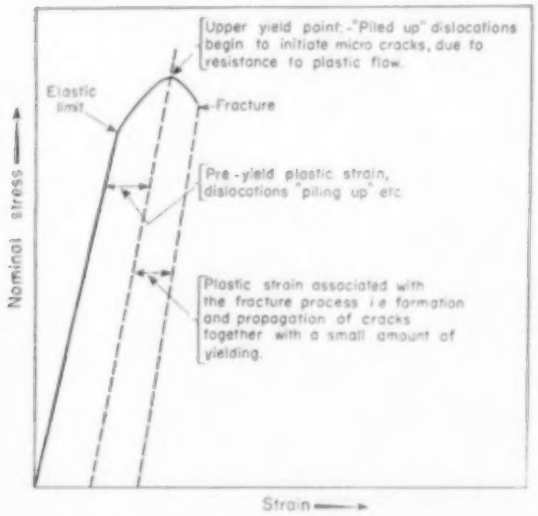
Upper yield point:-"Piled up" dislocations begin to initiate micro cracks, due to resistance to plastic flow.
Elastic limit
Fracture
Pre-yield plastic strain, dislocations "piling up" etc.
Plastic strain associated with the fracture process i.e. formation and propagation of cracks together with a small amount of yielding.
Nominal stress
Strain

FIG. 7. Factors involved in early stages of plastic flow at sub-transition temperatures; after WESSEL.[52]

concentration near the dislocation groups results in the "break-away" of a group from its barrier, which then causes rapid yielding and a drop in the load on the specimen.

At temperatures above the ductile-to-brittle transition there is little or no resistance to plastic deformation. The rapid movement of dislocations at the yield point then leads to extensive deformation of the specimen by activating its various slip systems, thereby giving ductile behaviour. However, the resistance to plastic deformation increases as the temperature decreases; consequently, higher local stresses are needed to enable the dislocations to break away from their barriers, or to activate slip systems. Therefore, as the temperature falls, a temperature will be reached at which the resistance to plastic deformation is so high that the localized stress concentration will exceed the cohesive strength and, hence, lead to brittle fracture (see section 3.3) rather than allow extensive plastic deformation. This temperature is the ductile-to-brittle transition temperature.

VOL. 9 1961

3.6.3 *Recent work on the ductile-to-brittle transition temperature*

There have been two recent reviews which tend to confirm the ideas developed above. The first is a general theory, in which the ductile-to-brittle transition is described in mathematical terms; whilst the second is an account based on experimental evidence. In the first of these two reviews STROH [44] has shown that the stresses around a dislocation pile-up may either initiate a crack—in which case the metal is brittle—or operate a nearby dislocation source—in which case the metal is ductile. At low temperatures the "thermal" liberation of dislocations is shown to be too slow to occur in the time needed for the pile-up to initiate a crack, hence decreasing the temperature favours brittle fracture.*

The probability that a nearby source will not have operated (to cause slip) by the time that the pile-up has grown large enough to initiate a crack is given by the following equation: [44]

$$\text{where } P = \exp - \left\{\frac{r l}{b}\, t_0\right\}^{e^{-(u(\sigma)/kT)}} \qquad \ldots\ldots\ldots\ldots \quad (17)$$

r = an atomic frequency of vibration.
l = the length of the dislocation source.
t_0 = a time of the order of that needed to form the pile-up on the source.
b = the Burgess vector of the crack.

* *Author's Footnote*

Two other theoretical accounts of the nature of the ductile-to-brittle transition have been proposed [140, 141]—independently—since the manuscript of this present paper was written. Each of these describes the effect as being due to the temperature dependence of the forces needed to propagate a dislocation in the lattice structure, rather than to the forces associated with Cottrell-locking or dislocation release. PETCH [140] considers the formation of a dislocation pile-up from dislocations originating on a single crystallographic plane; whereas COTTRELL [141] considers the intersection of dislocations from different planes. PETCH [142] has reported experimental verification of his mechanism in the case of alpha-iron alloys.

$\mu(\sigma)$ = the activation energy for the source to break away from its locking impurity atoms.
k = Boltzmanns constant.
T = Absolute temperature (°K).

Because of the double exponential, P will change abruptly from 1 to 0 as T increases, which is in accordance with the sharp transition from brittleness to ductility.[44] The transition temperature is given by:

$$T = \frac{\mu(\sigma)}{k \,.\, \ln\left(\frac{vl}{b}\frac{t_0}{}\right)} \quad . \quad . \quad . \quad . \quad . \quad . \quad . \quad . \quad (18)$$

Using the results of COTTRELL and BILBY,[58] Stroh then calculated (*a*) that the transition temperature for mild steel should be of the order of 300 °K, and (*b*) that P decreases from 0·9 to 0·1 for a rise in temperature of 40 °C, which may therefore be taken as a measure of the transition range. These results are of the right order, but, in view of the assumptions made in the calculations, there is some uncertainty as to the precise value of the transition temperature.

In the cases of steel, tantalum, niobium and molybdenum, WESSEL[57] has measured the difference between the upper yield point and the limit of proportionality, together with both the amount of plastic strain preceding yielding and the plastic strain which is associated with abrupt yielding. This data appears to confirm the concepts of yielding and fracture developed above.

Each of the above-mentioned properties, measured by Wessel, has a maximum value at the ductile-to-brittle transition temperature. It is suggested that the increase in the difference in stress level between the yield point and the true elastic limit (and hence the stress associated with the pre-yield plastic deformation) results in the formation of a more extensive and denser accumulation of piled up dislocations, with an associated increase in potential energy. Hence, as the temperature decreases to the transition temperature, more pre-yield plastic strain occurs, and, after yielding has taken place, it is reasonable to find that greater amounts of plastic deformation occur.

At temperatures at, or below, the transition temperature cracks are initiated by piled up dislocations and brittle fracture occurs during the subsequent yielding. The increased ability, as the temperature decreases, of a piled-up dislocation group to initiate micro-cracking, and, hence, brittleness results in a decreased amount of pre-yield plastic strain. The development of total fracture during yielding also results in a decrease in the magnitude of the drop in load and the associated plastic strain which occurs during yielding.

It is therefore apparent that the dislocation model outlined in this chapter is consistent with numerical calculations, and also with the experimentally observed behaviour of a series of metals which exhibit a ductile-to-brittle transition temperature.

4. The Hydrogen Embrittlement of Steel

4.1 *The Solubility of Hydrogen in Iron*

As in the case of all the endothermic occluders, the solubility of hydrogen in iron is extremely low. Table 1, below, gives the values of the solubility of hydrogen in iron obtained by Sieverts[60] for the range 400°C to 1650°C at a pressure of one atmosphere. As can be seen from Table 1 the solubility of hydrogen undergoes a sudden increase on passing from the alpha-phase to the gamma-phase (approximately 900°C) and there is a further sudden increase on melting. The practical significance of this behaviour is that comparatively large quantities of hydrogen may be absorbed during fabrication at high temperatures (particularly melting) with the result that steel will become super-saturated with respect to hydrogen, at lower temperatures unless very slow-cooling rates are used.

VOL. 9 1961

TABLE 1

The Solubility of Hydrogen in Iron at a Pressure of One Atmosphere (after Sieverts[60])

Temperature, °C	*Solubility of Hydrogen in Iron*		
	cm^3 *per* 100 g	*p.p.m. by weight*	*Atomic per cent*
400	0·35	0·32	0·002
500	0·75	0·68	0·004
600	1·20	1·08	0·006
700	1·85	1·66	0·009
800	2·45	2·21	0·012
900	4·07	3·66	0·020
1000	5·50	4·95	0·026
1100	6·60	5·94	0·034
1200	7·95	7·16	0·040
1300	9·50	8·55	0·048
1400	11·20	10·08	0·060
1500	12·75	11·48	0·064
1535 (solid)	13·32	12·00	0·067
1535 (liquid)	26·64	24·00	0·134

The solubility of hydrogen in iron has also been investigated by Miss M. Armbruster,[61] at 400°C, 500°C and 600°C. By using a variety of pressures in the range 18·9 mm Hg to 629 mm Hg, at 600°C, she showed that the solubility is proportional to the square-root of the pressure. The solubility data quoted in Table 1 applies to equilibrium conditions at a hydrogen pressure of one atmosphere. It is therefore important to notice that the equilibrium solubility values, under normal fabrication and working conditions, are considerably less than those quoted in Table 1. For example, if the partial pressure of hydrogen is reduced to 1 mm Hg, the solubility of hydrogen at 900°C is reduced from approximately 0·02 atomic per cent to 0·0072 (or from 4 cm^3 per 100 g to approximately 0·15 cm^3 per 100 g).

According to SIEVERTS, ZAPFFE and MORITZ,[62] the solubility of deuterium in iron is lower than that of ordinary hydrogen. The difference in values is of the order of 0·1 to 0·9 cm^3 per 100 g (approximately 0·005 to 0·45 atomic per cent) at a pressure of one atmosphere.

4.2 *The Characteristics of Hydrogen Embrittlement in Steels*

The phenomenon of hydrogen-induced embrittlement in steel has been the subject of a considerable amount of research and comment since Pfeil's original experiments in 1926.[1] A recent bibliography[63] of all the relevant literature, up to 1949 lists 1191 references. It is impossible to give a fully comprehensive review of the subject within the compass of this paper. Hence, all that is attempted is to give a summary of the characteristics of the phenomenon together with a brief review of the various mechanisms which have been proposed to explain this embrittlement effect.

The physical effects of hydrogen on the mechanical properties of iron and steel, are as follows:

(1) Hydrogen has no significant effect on the elastic properties.

(2) The hardness remains unaffected by hydrogen in the range 0·10 cm^3/100 g[64] although the U.T.S. is decreased.[65]

(3) The fracture stress is lowered in proportion to the hydrogen concentration.[65, 66]

(4) Hydrogen can produce a small yield point in pure iron at low temperatures.[67] At normal temperatures the presence of hydrogen can prevent the occurrence of the yield phenomena which are usually found in mild steel.[68]

(5) Both the ductility parameters (elongation and reduction of area) are reduced in proportion to the hydrogen content up to about 5 cm^3 per 100 g (approximately 0·025 atomic per cent). Above this figure the ductility has a constant, low, value.[64, 65]

(6) Hydrogen embrittlement is reduced as the rate of strain is increased,[64] the limiting case being that of the impact test, on which hydrogen has virtually no effect.[65, 69]

(7) The embrittlement effect occurs in the temperature range from $-$ 100°C to $+$ 100°C, the maximum effect being at, or just below, room temperature.

(8) There are no instances, in the literature, of a hydrogen embrittlement during the compression testing of steels. It would appear that tensile stresses are required in order to cause this embrittlement.

(9) The presence of hydrogen in steel changes the fracture type from that of a typically ductile metal to that of a typically brittle material, (usually by cleavage).

(10) The phenomenon of hydrogen embrittlement is dependent upon the treatment to which any given sample has been subjected. Steels are particularly susceptible if they are in either a hardened or a sphereodized condition. Cold-working also increases the likelihood of hydrogen embrittlement.[73]

(11) The presence of hydrogen causes premature brittle fracture, under static loading conditions, in high strength alloy steels. This phenomenon is often referred to as "delayed failure" or "static fatigue".[69, 71, 72]

(12) The presence of hydrogen in steel does not affect the metal in the unstrained state. The removal of hydrogen, from solid steel, prior to straining ensures full ductility. It would appear that hydrogen embrittlement requires the presence of diffusable hydrogen during the course of straining.

(13) If the hydrogen concentration varies throughout a specimen the hydrogen-rich areas will be those which are least ductile, and their premature fracture—during a tensile test—will result in an overall ductility of the specimen which is typical of that of the locally enriched areas, rather than the average hydrogen content.

VOL.
9
1961

4.3 *The Mechanism of Hydrogen Embrittlement in Steel*

4.3.1 *Early theories*

The earliest theories of the mechanism of hydrogen embrittlement assumed that the drop in ductility was due to a strain-hardening effect which was attributed to the formation of iron–hydrogen compounds. However, embrittlement can occur when the hydrogen content is of the order of one atom in 100,000. This, together with the fact that iron does not form a hydride, suggests that the embrittlement effect is not due to any hydrogen-containing compounds.

Later, when the solubility–pressure–temperature relationships had been established, the effect was attributed to the effect of the very high pressure which hydrogen would establish if it was thrown out of solution (e.g. by cooling) and allowed to collect in internal voids within the metal. Some workers have suggested that such pressures are sufficient to strain the surrounding lattice, whilst others suggest that the embrittlement is due to the triaxial nature of the internal stresses containing a gas at such a high pressure.

Decarbonization of the steel by hydrogen, leading to the formation of hydrocarbons, has also been suggested as a source of internal pressure. This type of reaction is very unlikely to occur at the low temperatures which are important here.

4.3.2 *The Planar pressure theory*

ZAPFFE[70] has proposed a mechanism for hydrogen embrittlement which is based on Smith's theory of solution.[9] He believes that the pressure generated by the "gas" which is located in the "rift network" increase as more hydrogen is precipitated. He suggests that there will be a critical pressure at which the metal lattice is sprung apart by the hydrostatic forces of this gas. At this point, and not until, the steel is said to be embrittled. If a stress is then applied to the metal premature fracture follows.

There are several deficiencies in this theory when it is compared with the

experimentally observed facts outlined in section 4.2. These can be summarized as follows:

(1) It is difficult to see how this type of theory could account for the absence of a hydrogen embrittlement effect in compression.

(2) It is very difficult to account for the strain-rate and temperature dependence of the hydrogen embrittlement effect on the basis of this theory.

(3) Finally, no embrittlement would be expected for low hydrogen contents which give sub-critical pressures: however, experimental evidence shows that there is a continuous decrease in the ductility as the hydrogen content increases.

It is therefore concluded that Zapffe's explanation is not a valid representation of the mechanism of hydrogen embrittlement in steel.

4.3.3 *Other theories based on brittle fracture mechanisms of the Griffith type*

Following Zapffe's account of the phenomenon of hydrogen embrittlement, many other theories have been advanced in an attempt to explain this process. Whilst all the factors mentioned in section 4.2 are relevant, there are five characteristics which must be considered in formulating any theories, thus:

(1) The drop in ductility associated with the presence of hydrogen increases progressively as the hydrogen content increases until an optimum value (of the order of 5 cm^3 per 100 g) is reached, at which stage the material is unaffected by further hydrogen additions. This point is illustrated in Fig. 8.

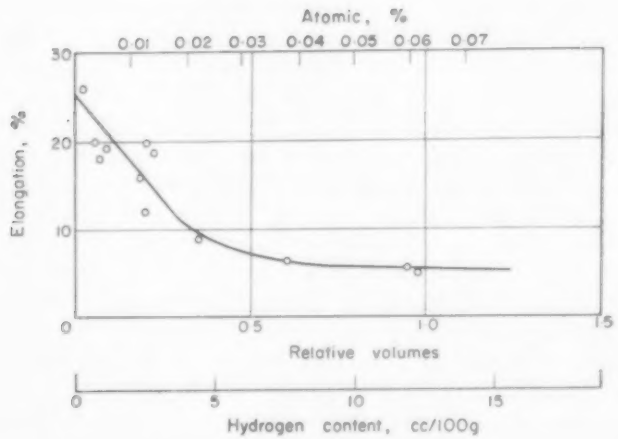

FIG. 8. The variation of elongation with hydrogen content for a normalized mild steel tested at a slow strain-rate at room temperature; after SIMS, MOORE and WILLIAMS.[66]

(2) The fracture of hydrogen-containing steels is essentially a brittle one.

(3) The degree of embrittlement (for a given hydrogen content) decreases as the temperature decreases below room temperature and also as the strain-rate increases. These observations suggest that a diffusion-controlled mechanism is involved.

(4) Embrittlement also decreases as the temperature is increased above room-temperature, and disappears above 100°C. Many people take this as a suggestion that the formation of "gaseous" hydrogen—within the specimen—is an important factor because the equilibrium pressure of any gas, within voids in the metal, will decrease rapidly above temperature of the order of 100°C.

These factors suggest that a mechanism of the GRIFFITH [36] type is involved. The basic mechanism is that brittle materials contain minute cracks which can propagate catastrophically once a critical stress is exceeded. There is a definite relationship between the size of the cracks and the critical stress needed to cause propagation. This is due to the influence of two opposing factors: (*a*) the increase in surface energy due to the increase in the size of the crack and (*b*) the decrease in strain energy within the material surrounding the crack. When these two terms are of such a size that there is a net gain in free energy (due to the formation of an enlarged crack surface) then the crack will propagate rapidly, leading to premature fracture.

PETCH [73] has recently suggested that hydrogen atoms are adsorbed on to the surface of micro-cracks, thereby reducing the surface energy. This would have the effect of reducing the amount of strain-energy required to form a new surface. Hence, the critical stress for crack propagation would be lower in the presence of hydrogen than in a fully degassed steel. This theory has been developed to show a correlation between the hydrogen content and the fracture stress, [74, 73] which is in reasonable agreement with experiment.

An alternative mechanism has been advanced by KAZINCZY. [75] He suggests that the main factor in hydrogen embrittlement is the presence of hydrogen, in the gaseous state, within the micro-cracks which are required by the Griffith model: the main point of his theory being that the adiabetic expansion of this gas, during the growth of a crack, adds an additional term to the expression for the total energy released. Thus the critical stress for crack propagation is lowered, in the presence of hydrogen, because less strain energy is needed to counterbalance the energy required to form a new crack surface. This theory requires a two-stage process thus: (*a*) initially the rate of crack growth will be slow due to the need for diffusion of hydrogen to the crack and then (*b*) when the hydrogen has precipitated within the crack and an equilibrium pressure has been established, the crack will propagate rapidly as the result of the expansion of the gas within the crack. Increasing the initial hydrogen content of the metal will lead to increased pressures within the cracks, and, hence, a lower applied stress will be needed to propagate the crack. The degree of embrittlement will therefore increase as the hydrogen content increases.

VOL. 9 1961

Each of these two theories depends on the diffusion of hydrogen to microcracks within the metal. This would explain the dependence of embrittlement effect on strain-rate and its decrease as the temperature falls below room temperature. However, some other factor must be introduced in order to explain the diminishing embrittlement as the temperature rises above room temperature. The essential difference in the two theories lies in the influence of the hydrogen on the thermodynamics of cracks propagation. Rapid propagation occurs when the energy released by the extension of the crack is greater than the energy needed to create the new surface of the enlarged region of the crack. Each of the above theories suggests that this will occur at a lower applied stress in the presence of hydrogen, than in hydrogen-free material. Petch suggests that hydrogen decreases the energy required to form a new surface, whereas Kazinczy believes that hydrogen increases the energy released during crack propagation.

4.3.4 *Theories based on the interaction of hydrogen and dislocations*

An alternative theory has been proposed by VAUGHAN and DE MORTON,[76, 77] who revert to the idea of a strain-hardening effect. The embrittlement is attributed to the formation of Cottrell-type atmospheres which interfere with the movement of dislocations in the metal lattice; a suggestion which was originally made by BASTIEN and AZOU.[78] The essential difference between this mechanism and the more usual strain-hardening effects in metals is that the hydrogen atmospheres are said to be formed on straining, and they are not present in the unstrained metal. It is suggested that initially the hydrogen is present in interstitial solution but the application of stress causes hydrogen to diffuse to the active slip planes, thereby forming atmospheres which hinder the movement of dislocations and lead to premature fracture.

It has been shown that the presence of hydrogen can suppress the yield-point phenomena which are usually associated with carbon or nitrogen in steel.[68, 79] Vaughan and de Morton suggest that this is due to the formation of hydrogen atmospheres, rather than carbon or nitrogen atmospheres, due to the greater interaction energy of the former. If this is the case then the high diffusion rate of hydrogen is taken to indicate that the strain-induced hydrogen atmospheres can maintain contact with the movement of dislocations, thereby preventing any yield-point effects. However, this last hypothesis is in direct contradiction to the embrittlement effect suggested by the same authors, wherein hydrogen atmospheres hinder dislocation movement.

Recent French work[79] has suggested that hydrogen segregates to the dislocations which are present on the (112) planes of iron. In this investigation specimens of Armco iron were examined by the Laue back-reflection X-ray technique, before and after hydrogenation. It was found that the diffration spots from the (222) planes remained sharply defined in each case, whereas those from the (112) and (123) planes became diffused when the specimen contained hydrogen. The authors[79] suggest that this is due to the distortion of

the lattice as a result of the formation of hydrogen atmospheres around dislocations on the (112) planes. However, the equilibrium formation of such atmospheres would arise from the need to relieve strain-energy in these regions, and it should not, therefore, lead to a distortion of the surrounding lattice. Hence the correct interpretation of these results is by no means clear.

ROGERS[80] has shown that the suppression of the normal yield-point by hydrogen decreases as the temperature decreases. For example, he finds that hydrogenated material shows no yield-point at room temperature, but the yield-point reappears, at about — 12°C. He has also shown that hydrogen, itself, can cause a yield-point effect, but that this only occurs at low temperatures (of the order of — 100°C). This suggests that a hydrogen atmosphere is bound less tightly to dislocations that is one of carbon or nitrogen, which is the reverse of Vaughan and de Morton's hypothesis.[76, 77]

VOL. 9 1961

In this case hydrogen would not displace any significant amount of carbon or nitrogen, from dislocations, but would attach itself to any dislocation loops which may have been freed from the latter by thermal vibrations. This would then lower the energy (and hence, the stress) needed to form a loop of a critical size. At room temperature hydrogen then depresses the yield stress sufficiently to suppress any yield-point phenomena. Lowering the temperature raises the yield stress and causes a discontinuity in the stress–strain curve, and hence, a yield point. Thus the yield-point would increase as the temperature decreases, but would always be less than that of hydrogen-free materials.

This is precisely the behaviour that ROGERS[80] has reported for hydrogen in Armco iron. It is therefore suggested that Roger's hypothesis that the bonding of hydrogen to dislocations is weaker than that of carbon or nitrogen affords a more reasonable explanation of the relevant behaviour than does VAUGHAN and DE MORTON'S[76, 77] suggestion that the reverse is the case. It is therefore unlikely that the hydrogen embrittlement of steel is caused by a strain-hardening mechanism.

4.3.5 *A recent theory based on the effect of hydrogen in interstitial solution*

MORLETT, JOHNSON and TROIANO[81] have recently published the results of a series of experiments which represents a novel approach to the problem of hydrogen embrittlement. They point out that all the previously postulated mechanisms incorporate a lattice containing defects of one sort or another. The precise form of these imperfections varies from author to author (the terms rift, void, Griffith-crack, and dislocation pile-up have all been used) and Morlett, Johnson and Troiano prefer to refer to the lattice imperfections by use of the term "voids" in a general sense. The assumption is that these voids are large when compared with the volume of a unit cell of the lattice. The damaging hydrogen is then assumed to be localized at, or near to, the voids. The need for the heterogeneous distribution of the hydrogen arises from the very low hydrogen contents which can lead to the embrittlement of steel.

It has long been accepted that, as the result of its high diffusion rate,

hydrogen can readily diffuse out of steel at relatively low temperatures.[82] This being the case it is to be expected that the extent of any hydrogen embrittlement should decrease accordingly. MORTLETT and his companions[81] have investigated the effect of ageing on the hydrogen embrittlement of specimens which had previously been subjected to a small amount of plastic deformation, and also on samples in the unstrained condition. The difference in the behaviour of the two classes of specimens reveals a hitherto unreported characteristic of hydrogen embrittlement which requires a considerable modification to the mechanisms which have been discussed so far.

The specimens were hydrogenated by cathodic deposition in an acid solution, and then subjected to cadmium plating. As the result of this treatment the majority of the hydrogen content was distributed at, or near to, the specimen surface. Consequently the hydrogen distribution was homogenized by a short anneal at 300°F (approximately 150°C), the cadmium ensuring that the hydrogen did not diffuse out of the specimen. Having shown that hydrogen does not cause embrittlement at — 196°C, the specimens were given pre-determined amounts of plastic strain at this temperature. Final testing was then carried out at a slow strain rate (to enhance the embrittlement effect) at various times after pre-straining, at a series of temperatures in the range from — 15° to 300°F (approximately — 25° to 150°C).

The results of this type of treatment on the ductility at 150°F (71°C) are shown in Fig. 9. It can be seen that the ductility of the pre-strained specimens

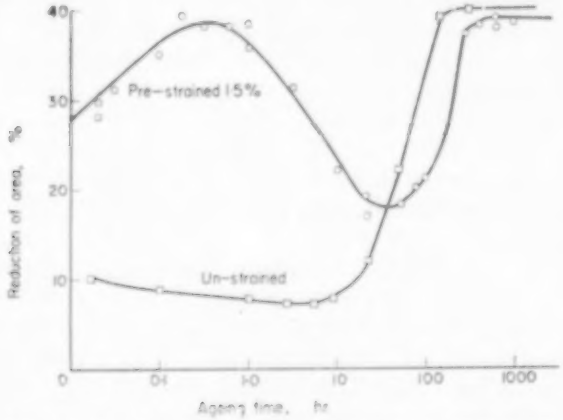

FIG. 9. Reduction of area v. ageing time for steel (SAE–AISI 4340) specimens aged at 65°C (150°F) and tested at a slow strain-rate at room temperature; after JOHNSON, MORLET and TROINO.[81]

first of all rises, as the ageing time increases. This is referred to as Stage 1 of the ageing process. As the ageing time is further increased the ductility then falls to a minimum value (Stage 2); finally, the ductility then increases again (Stage 3). The behaviour of the unstrained specimens contrasts sharply with this, in that, during stages 1 and 2 for the strained specimens, the ductility

of the unstrained specimens falls very slightly before rising in the same way as that for Stage 3 of the strained specimens. These results should be critically examined in the light of the embrittlement mechanisms which have already been discussed.

Prior to straining there is a steady-state distribution between the hydrogen in solution within the lattice and that present in the voids. (N.B. The terms void is used, here, in the most general sense to include any form of lattice imperfection which is large compared to the size of the lattice unit cell). This follows from the interdependence of the solubility of the hydrogen and the pressure of gas in contact with the metal surface (in this case the "surface" of the void). However, straining can be expected to disturb this distribution of the hydrogen by increasing the size of the voids. Since hydrogen is incapable of diffusing at the temperature of straining (— 196°C in this case), the required diffusion must take place during the ageing at higher temperatures.

On Kazinczy's pressure theory[78] the changes in ductility should represent changes in the pressure of hydrogen within the voids. However, due to the increased size of the voids (after pre-straining) it is to be expected that the hydrogen pressure within the voids will be a minimum immediately after straining, but as soon as ageing commences, and hydrogen becomes capable of diffusing to the voids, the pressure within the voids will increase until the new steady-state distribution is achieved. Furthermore, as soon as ageing commences the amount of hydrogen adsorbed on to the void surface will also increase as the result of the additional surface of the void and the increase in pressure which is taking place within the void. Consequently if the mechanism of hydrogen embrittlement is of the form proposed by either Kazinczy or Petch the ductility of the strained specimens should fall progressively, as ageing takes place, until the new steady state distribution is achieved. Obviously this does not happen and it is to be concluded, therefore, that the above-mentioned theories do not fully account for the mechanism of hydrogen embrittlement in steels.

However, MORLETT and his co-workers[81] have suggested a novel mechanism which depends, not only on the presence of hydrogen in the voids, but also on the distribution of the hydrogen which is in solution within the lattice of the metal. They believe that the severity of hydrogen embrittlement depends on the combined effect of hydrogen and stress within the metal. They suggest that, on a micro-scale, the voids may be regarded as internal notches which act as points of stress concentration. When a stress is then applied to the metal a multi-axial stress system is established around each void. In this case at some point near to each void there will be a region at which the stress system is tri-axial in nature. The essence of their hypothesis is that the degree of embrittlement depends, not on the hydrogen within the voids, but rather on the hydrogen concentration within those regions at which the tri-axiality of the stress system is a maximum.

When ageing commences, after straining at low temperatures, the hydrogen

VOL. 9 1961

moves from the lattice into the voids, thereby depleting the void boundary region. However, the hydrogen concentration in the "triaxiality region" is only slightly diminished since this region is a finite distance from the surface of the void. The diffusion process will continue until the new steady-state distribution of hydrogen has been achieved. At this stage the hydrogen concentration within the lattice must be less than in the unstrained condition due to the increased capacity of the voids. It is suggested that the hydrogen concentration at the point of triaxiality undergoes a reversal during the course of this diffusion process, since hydrogen has been shown to concentrate in a highly stressed region of the lattice, thereby creating a concentration gradient which conforms to the stress gradient.[83] This effect is considered to be induced by the stress state and it is not a classical diffusion process. With an equilibrium (steady-state) distribution of hydrogen a high concentration, with a steep gradient, may be formed at the regions of triaxial stressing during the test. However, if the lattice has been depleted of hydrogen, and the equilibrium capacity has not been attained, a significant stress-induced concentration gradient will not be formed, since the hydrogen will be drawn into the void in an attempt to attain the new equilibrium state.

The observed ductility changes can now be correlated with the hydrogen distribution changes during ageing. During Stage 1 the hydrogen concentration in the region of triaxiality decreases due to the influence of diffusion to the void. Hence the ductility increases. The ductility decrease of Stage 2 is caused by the fact that the hydrogen concentration in the triaxiality region is now increasing again. This is due to (*a*) the diffusion of hydrogen to this region during the achievement of a new steady-state distribution and (*b*) (in the later stages) the effect of a stress-induced concentration gradient at this region as the driving force for diffusion to the voids decreases. Thus the ductility can be expected to decrease during Stage 2 until a new steady-state has been reached, or until outgassing effects deplete the lattice of some of its hydrogen. The rise of ductility during Stage 3 in the ageing process for pre-strained specimens, coincides with a similar rise for the specimens which were tested in the unstrained condition. This is therefore attributed to the gross outgassing of the specimens after long times at the ageing temperature.

As the result of discussions of this type MORLETT, JOHNSON and TROIANO[81] suggest that the dependence of hydrogen embrittlement on the existence of minute regions of triaxiality, within the lattice of the specimen, affords a reasonable explanation of the results as they are known to date. The hydrogen precipitated within the voids is non-damaging and of importance only in determining the steady-state hydrogen distribution.

Having shown that the amount of hydrogen embrittlement which a specimen may undergo depends on the amount of plastic deformation which it has received prior to testing. Morlett *et al.* also investigated the influence of the amount of pre-straining and the temperature of ageing on the embrittlement effect. As the amount of prior straining increased the drop in ductility

referred to as Stage 2 decreased and occurred at longer ageing times. This can be attributed to two factors: (*a*) increasing the prior deformation increases the driving force for the diffusion of hydrogen to the voids (which will be larger for higher strains) on ageing, thereby depleting the lattice of hydrogen at the regions of triaxiality and elsewhere to a greater extent and (*b*) the increased importance of outgassing at long ageing times, when the hydrogen content of the lattice is relatively low. The authors also show that when the specimens were subjected to 12 per cent plastic deformation at — 196°C and then aged at 150°F (65·5°C) the resulting ductility–ageing curve is a horizontal line at a ductility which is equal to, or just below, that of un-hydrogenated specimens. This is said to be because at such large amount of pre-strain the lattice is completely denuded of hydrogen in establishing the new steady-state distribution. It is also shown that prior-straining in the elastic range has no effect on the ageing behaviour when compared with that of unstrained specimens. This is because elastic pre-straining will not have any permanent effect on the size of the lattice voids, after the stresses which caused it have been relaxed. These two results afford striking evidence that (*a*) hydrogen embrittlement depends on the hydrogen in solution in the lattice as well as that entrapped in voids, and (*b*) plastic deformation causes a considerable local redistribution of hydrogen which is unaffected by elastic deformation.

VOL.
9
1961

The diffusion-controlled nature of these effects is confirmed by the effect of the ageing temperature on the ductility behaviour. Both Stages 1 and 2 of the ageing process are displaced to longer times as the temperature of ageing is lowered from 150°F (65·5°C) to — 15°F (— 26°C). Morlett and his companions calculate that the activation energy for this diffusion-controlled process is of the order 8500 cal/g, which is in good agreement with published data [84] for the activation energy for diffusion of hydrogen in iron.

The above account deals with effects of pre-straining and ageing which they obtained. In accepting this mechanism it remains to show that it can be used to account for the characteristics of hydrogen embrittlement reviewed in section 4.2. Such an explanation depends on the diffusion of hydrogen during the test.

Since the effect occurs at slow strain-rates ample opportunity exists for the creation of a severe stress-induced concentration gradient, in the region of triaxiality, near to the voids. The size of this concentration gradient depends on three factors: (*a*) the original hydrogen concentration, (*b*) the diffusion rate of hydrogen, and (*c*) the time available for the diffusion of hydrogen. The disappearance of hydrogen embrittlement at low temperatures obviously results from the decreasing diffusion rate as the temperature falls. At high temperatures the ease of diffusion overcomes the establishment of stress-induced segregation of the hydrogen. The increased embrittlement effect which occurs as the strain rate is decreased is attributed to the increased ease of the stress-induced diffusion of hydrogen, to the regions of triaxiality within the lattice, which results from the increased time of stress application

as the strain-rate is reduced. Furthermore, since there will always be a steady-state equilibrium distribution of hydrogen between the lattice and the voids, no matter how low the overall hydrogen content, it is reasonable to expect embrittlement, by the above mechanism, at very low hydrogen contents.

Finally, it has recently been shown[71, 72, 83] that hydrogen causes severe embrittlement in steel under "static fatigue" or "stress rupture" conditions. In this case—which can be likened to an extremely slow tensile test—small micro-cracks have been observed within the specimen a short distance away from the root of a notch on the specimen surface.[83] It is considered that the formation of these micro-cracks occurs as the result of the segregation of hydrogen at points below such notches where the stress system is a triaxial one.

It is therefore suggested that the above mechanism, proposed by MORLETT *et al.*[81] affords the best explanation which has been given to date for the phenomenon of hydrogen-induced embrittlement in steel. However, the precise way in which the concentration of dissolved hydrogen at points of triaxiality causes brittle fracture is as yet unexplained. It should be pointed out that the "voids" which lead to localized triaxial stress systems, and consequently to hydrogen segregation, are themselves the normal imperfections of a metallic lattice. Hence the embrittlement is caused by the segregation of hydrogen in interstitial solution, i.e. by a localized supersaturation of the lattice structure. This suggests that a wholly satisfying account of the phenomenon may have to await the further development of the general theory of fracture in metals. (See also section 8—"The hydrogen embrittlement of the body-centred—cubic metals of groups Va and VIa", and section 9—"The development of a general theory of hydrogen embrittlement in metals").

5. THE HYDROGEN EMBRITTLEMENT OF TITANIUM AND ITS ALLOYS

5.1 *The Titanium–Hydrogen System*

The titanium–hydrogen system has been investigated by a number of workers.[85–93] Titanium, unlike iron, belongs to the exothermic occluding group of metals mentioned in section 2.1 and 2.3.2. The metal–hydrogen relationships of this system are therefore complicated by the formation of a hydride phase, as well as by the allotropic change which occurs in pure titanium.

MCQUILLAN,[85–88] operating at temperatures above 500°C, found three phases in the titanium–hydrogen system; viz, alpha (close-packed hexagonal), beta (body-centred cubic) and gamma (face-centred cubic). The first two are the low and high temperature allotropes of the pure metal, whilst the third corresponds to the hydride found by HÄGG and SHIPKO[90] in their examination at temperatures below 500°C. McQuillan's technique, in the main, was to measure the equilibrium pressure of hydrogen as a function of cotncenration and temperature. His results are summarized in Fig. 10. It follows from

the phase-rule that in single-phase alloys the pressure of hydrogen in equilibrium with the alloy will vary as the hydrogen content varies, whereas in the two-phase regions the pressure will be constant. Hence, the horizontal parts of the pressure-concentration curves (Fig. 10) indicate that for these particular conditions of composition, pressure and temperature, the alloy exists as a two-phase structure.

The hydride phase (referred to by McQuillan as the gamma phase) exists over a composition range and has a structure in which the hydrogen atoms occupy interstitial sites such that, under ideal conditions, they have four

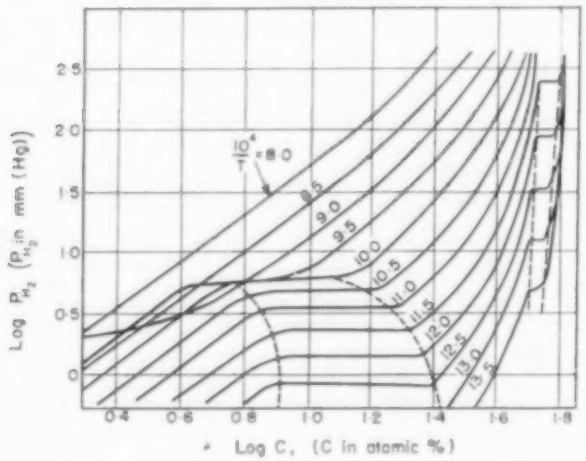

FIG. 10. Isothermal pressure concentration curves for the hydrogen–titanium system; after MCQUILLAN.[88]

titanium neighbours.[34] This phase can be regarded as an interstitial compound which is analagous to the intermediate phases of normal alloy systems. Hence the results of the various investigations can be represented in the form of an equilibrium diagram for the "titanium–hydrogen alloy system". This is the method of presentation used by MCQUILLAN.[85] This system has also been investigated by LENNING, CRAIGHEAD and JAFFEE,[89] using titanium of a higher standard of purity than any of the previous workers. Their results are summarized in the equilibrium diagram shown in Fig. 11.

It is important to notice that this equilibrium diagram refers only to the two-component system of pure (iodide refined) titanium and hydrogen, at a hydrogen pressure of one atmosphere. The diagram would be modified considerably by the presence of a third element, or by any variation of the hydrogen pressure. However, with these reservations in mind, it is apparent that the presence of hydrogen in titanium causes the retention of the beta-phase to quite low temperatures, until finally this phase transforms eutectoidally to form two-phase alloys consisting of alpha-titanium and the hydride (gamma). This latter transformation occurs at about 325°C, and,

VOL. 9 1961

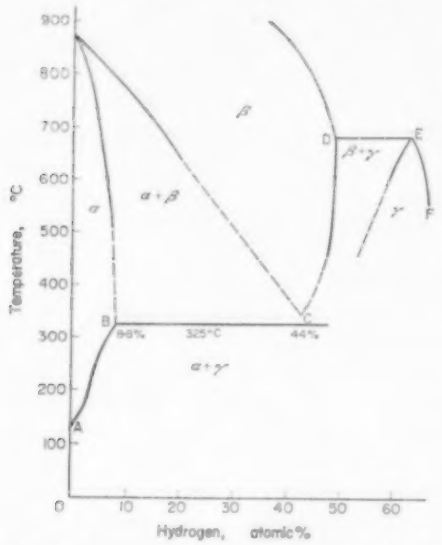

FIG. 11. The titanium-hydrogen equilibrium diagram (for hydrogen at 760 mms (Hg)) based on the work of LENNING;[89] and MCQUILLAN.[85]

according to Lenning *et al.*, the eutectoid composition is of the order of 44 atomic per cent (or approximately 1·5 weight per cent) hydrogen. The solid solubility of hydrogen in pure alpha-titanium rises from 0·1 atomic per cent (approximately 0·002 weight per cent) at room temperature, to about 8 atomic per cent (approximately 0·17 weight per cent) at the eutectoid temperature, above which the beta-phase becomes stable in the presence of hydrogen. The solubility of hydrogen in beta-titanium at this temperature corresponds to the eutectoid composition. Hence, the equilibrium diagram shows that the solubility of hydrogen in the beta-phase is considerably higher than that in alpha-titanium.

This diagram affords a good example of the difference between the solubility and the total amount of hydrogen absorbed by a sample, which was discussed in section 2.3.2.

The solubility of hydrogen in either form of titanium increases as the temperature increases, (ABCD in Fig. 11); whereas the reverse is true of the total amount of hydrogen which can be contained in the gamma-phase, (EF in Fig. 11), since the formation of the hydride phase occurs exothermically.

McQuillan's early work[85] was not conducted on high purity titanium and it is noticeable that the pressure-concentration curves of Fig. 10 are not exactly parallel to the concentration axis in the alpha–beta region. This is contrary to the requirements of the phase rule for two components systems referred to above. Hence, to satisfy these requirements it is to be concluded that any alloy involving commercially pure titanium and hydrogen is to be regarded as a multi-component system.

The solubility of hydrogen in commercially pure titanium differs from that in the refined metal. These differences, which are discussed in the sections dealing with the embrittlement of these classes of metal, are considered to be due to the fact that certain impurities (notably iron) cause small amounts of the beta-phase to be retained at the grain boundaries of the less pure metal, at sub-eutectoidal temperatures.

5.2 *The Hydrogen Embrittlement of Alpha-Titanium*

5.2.1 *High purity titanium*

The solubility of hydrogen in alpha-titanium, and its effects thereon, depend on the purity of the metal. It is therefore important to differentiate between high purity titanium, commercially pure titanium, and alpha-titanium containing deliberate additions of alloying elements. As was mentioned in the previous section the solubility of hydrogen in pure alpha-titanium is of the order of 8 atomic per cent (0·17 weight per cent) at 325°C and 0·1 atomic per cent (0·002 weight per cent) at 125°C.

The effect of hydrogen on the mechanical properties of high purity alpha-titanium is shown in Fig. 12, which is taken from a paper by JAFFEE.[94] From

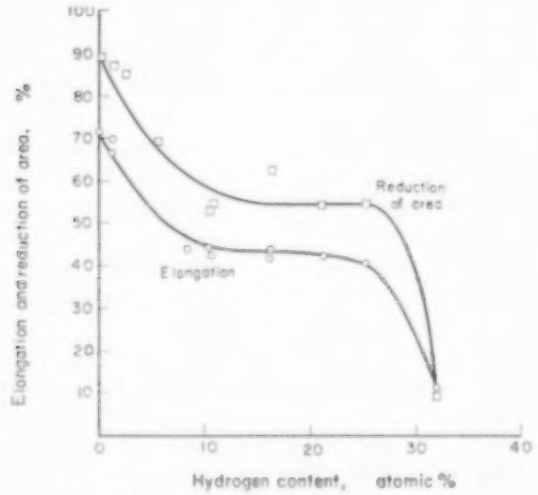

FIG. 12. Normal tensile ductilities of high purity titanium as a function of hydrogen content at room-temperature; after JAFFEE.[94]

this it can be seen that normal tensile properties of high purity titanium are considerably affected by the presence of hydrogen. If the hydrogen content is restricted to less than 1 atomic per cent the tensile ductility is high (circa 70 per cent elongation). Increase in the hydrogen concentration leads to a sharp fall in ductility, although the elongation of specimens containing approximately 10 atomic per cent of hydrogen is still of the order of 40 per

VOL. 9 1961

cent. However, further increases in the hydrogen content above 25 atomic per cent lead to a catastrophic fall in ductility at room temperature.

RYLSKI[2] has written a comprehensive review of the effect of hydrogen on the mechanical properties of titanium and its alloys, in which he shows that the tendency of high purity alpha-titanium to suffer hydrogen embrittlement is increased by (*a*) increasing the strain rate, (*b*) decreasing the temperature of the test and/or (*c*) by the presence of a notch on the surface of the specimen. The most damaging instance of this effect is to be observed on the notched impact strength: as little as 0·25 atomic per cent (0·005 weight per cent) causes a very substantial drop in this property whilst a complete loss of strength occurs at a hydrogen content of 2 atomic per cent (0·042 weight per cent). These results are summarized in Fig. 13. It should be noted that a complete loss of notch impact strength occurs at a hydrogen content which has virtually no effect on the tensile elongation.

Metallographic and X-ray data indicates that an insoluble hydride phase is present in alpha-titanium when the hydrogen content is more than 0·1 atomic per cent (0·002 weight per cent)[95] as is to be expected from Lenning's equilibrium diagram for the hydrogen-titanium system. The presence of this

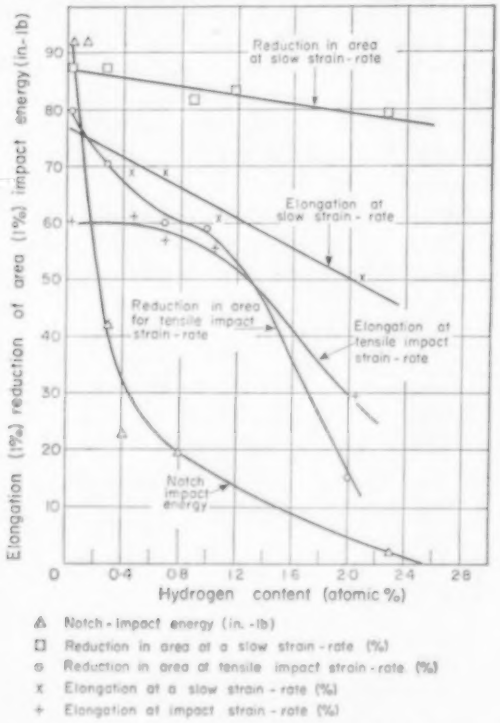
Elongation (1%) reduction of area (1%) impact energy (in.-lb)
Reduction in area at slow strain-rate
Elongation at slow strain-rate
Reduction in area for tensile impact strain-rate
Elongation at tensile impact strain-rate
Notch impact energy
Hydrogen content (atomic %)
Notch-impact energy (in.-lb)
Reduction in area at a slow strain-rate (%)
Reduction in area at tensile impact strain-rate (%)
Elongation at a slow strain-rate (%)
Elongation at impact strain-rate (%)

FIG. 13. The variation of the mechanical properties of pure titanium as a function of hydrogen content and testing speed at room-temperature; after RYLSKI.[2]

plate-like hydride phase is considered to be the basic cause of the hydrogen embrittlement effect in this material. If this hydride is precipitated in a finely dispersed form, by quenching after a solution heat-treatment, the mechanical properties of alloys of this type can be improved. However, ageing at room temperature results in the agglomeration of the hydride to a more massive form with a corresponding deterioration in the impact and tensile properties.

5.2.2 *Commercial purity titanium*

The solubility of hydrogen in the alpha-phase of commercially pure titanium is less than that in high purity (iodide) titanium.[3] At 400°C the figure is of the order of 5·4 to 6·5 atomic per cent (0·12 to 0·15 weight per cent) compared to a figure of more than 8 atomic per cent (0·17 weight per cent) for titanium of the higher purity. The solubility of hydrogen at sub-eutectoid temperatures is difficult to determine due to the presence of retained beta at the grain boundaries. Solution heat-treatments followed either by slow cooling or by quenching do not lead to the precipitation of a hydride phase in alloys containing 0·26 atomic per cent hydrogen (0·0053 weight per cent), a composition at which a hydride would certainly exist in a high purity titanium. These differences between the solubility and form of hydrogen in the two qualities of the metal are due to the presence of beta-retaining elements in the less pure metal since the solubility of hydrogen is much greater in the beta-phase than it is in the alpha-phase.

The detrimental effect of hydrogen on the mechanical properties of commercial purity titanium becomes evident at much lower hydrogen contents than for high purity titanium. Figure 14 shows the tensile properties of commercially pure titanium as a function of its hydrogen content. The normal tensile ductility of this material is reduced from approximately 70 per cent to a value of the order of 10 per cent, by the presence of 12 atomic per cent

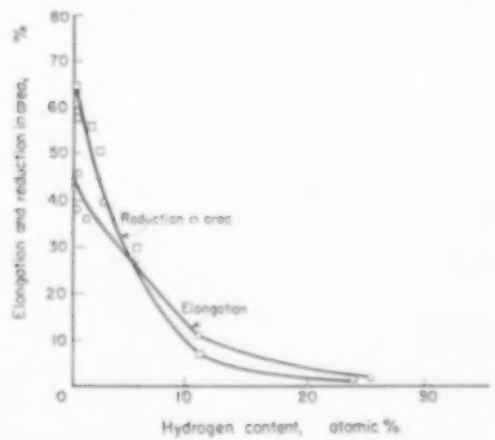

FIG. 14. Normal tensile ductilities of commercially pure titanium as a function of hydrogen content; after LENNING, CRAIGHEAD and JAFFEE.[89]

VOL. 9 1961

hydrogen. The corresponding concentration for high purity titanium is over 30 atomic per cent. Furthermore, there is an almost complete loss of notch impact strength at about 1 atomic per cent hydrogen (0·22 weight per cent), which is approximately half the value for high purity titanium.

Quenching from the all-alpha phase field improves the impact strength of hydrogen-containing commercially pure titanium, but, as in the case of purer metal, the effect is only temporary (see Fig. 15): room temperature

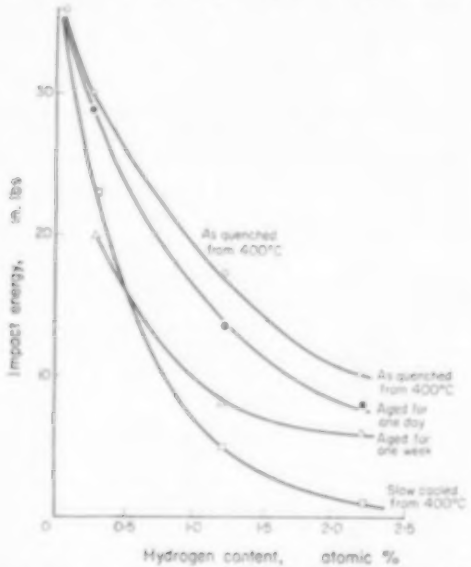

FIG. 15. The room temperature impact strength of commercially pure titanium as a function of hydrogen content after solution heat-treatment followed by room-temperature ageing; after RYLSKI.[2]

ageing leads to a decay in the properties. Furthermore an alloy containing 0·24 atomic per cent (0·005 weight per cent) has been shown to exhibit a considerable loss of notch impact strength,[2] yet no hydride phase could be detected in this alloy. However, RYLSKI[2] suggests that the partition function for hydrogen in the alpha and beta phases is such that nearly all the hydrogen should be in solution in the retained beta phase, thereby explaining the absence of a detectable hydride phase when the hydrogen content of the specimen is above the solubility limit for pure alpha-titanium. It is therefore suggested that, in the commercially pure metal, the presence of particles of the beta-phase having significantly large hydrogen contents may well be a factor in the embrittlement phenomena.

5.2.3 *Alpha-stabilized alloys*

Titanium alloys are generally classified by the characteristics of the alloying elements, depending on whether they enter into solution interstitially or substitutionally. Such elements are then sub-divided into groups

depending on their preference for the alpha or the beta phase. The effect of hydrogen has been investigated in alloys which contain alpha stabilizing elements of both the interstitial and the substitutional types.[2] Nitrogen is representative of the former, whilst aluminium is typical of the latter. The impact properties and the microstructures of alpha-stabilized alloys show that they are susceptible to a hydrogen embrittlement caused by the precipitation of a hydride phase. The resulting low impact strength can be improved by vacuum annealing, as can be seen from the results summarized in Table 2 below.

TABLE 2

The effect of hydrogen on the mechanical properties of alpha-stabilized titanium alloys[2]

Addition to high purity titanium		*Hydrogen content*	*Mechanical properties*				
Nitrogen wt. %	*Aluminium* wt. %		*U.T.S.* (*p.s.i.*)	*Yield point* (*p.s.i.*)	*Elongation* %	*Reduction of Area* %	*Impact Strength* (ft. lb)
0·06	0	0·07 at. % 0·0014 wt. %	82,000	72,000	36	55	24*
		0·63 at. % 0·0135 wt. %	77,000	63,000	30	57	4
0·18	0	0·09 at. % 0·0017 wt. %	114,000	110,000	23	26	16*
		0·6 at. % 0·0125 wt. %	122,000	117,000	25	23	3
0	2·55	0·07 at. % 0·0014 wt. %	93,000	78,000	26	47	41*
		0·6 at. % 0·0125 wt. %	96,000	82,000	23	34	7

* After vacuum annealing for 2 hr at 775°C.

5.2.4 *Summary of the effect of hydrogen on alpha-titanium*

The above discussion has shown that the mechanical properties of alpha-titanium are considerably influenced by the presence of hydrogen within the metal. The degree of the embrittlement caused by a given quantity of hydrogen depends largely on the purity of the metal. The following is a brief summary of the pertinent points.

(1) The solubility of hydrogen in high purity alpha-titanium is of the order of 8 atomic per cent at 325°C and 0·1 atomic per cent at 125°C. The presence of impurities can lead to the retention of the high temperature beta phase at the grain-boundaries of commercially pure titanium. This

VOL. 9 1961

affects the hydrogen concentration since hydrogen is more suitable in beta- than in alpha-titanium.

The solubility of hydrogen in the alpha phase of commercially pure titanium has been given as approximately 6 atomic per cent at 350°C.[2]

(2) Hydrogen causes a deterioration of those properties which are notch and/or strain-rate sensitive. It causes a considerable decrease in the notched impact strength but its embrittling effects diminishes as the strain-rate is decreased; normal tensile properties, therefore, are only affected at relatively high hydrogen concentrations.

(3) The embrittlement of high purity alpha-titanium arises when the hydrogen content exceeds the solubility limit. Under these conditions a plate-like hydride is precipitated from solid solution when the metal is slowly cooled, from the alpha-phase field. The embrittlement can be relieved if the hydride is precipitated in a more finely dispersed form, e.g. by quenching. However, the embrittlement returns on ageing at room temperature as the hydride particles agglomerate.

(4) In impure alpha-titanium the characteristics of hydrogen embrittlement are the same as those found in the pure metal (namely an increased sensitivity with increasing strain-rate). However, the amount of hydrogen needed to cause embrittlement is less than that in the case of the pure metal: in some cases it may even be less than the solubility limit for the material in question. In this case the embrittlement is said to be enhanced by the presence of a brittle beta phase, having a relatively high hydrogen content, at the grain-boundaries of the alpha phase. The presence of this retained-beta phase is caused by the impurities, such as iron, which tend to make the high temperature phase stable at lower temperatures.

5.2.5 *The precipitation of the hydride phase in alpha-titanium*

The hydrogen-induced embrittlement of alpha-titanium is associated with the presence of hard platelets of a hydride phase within the metal.[2] Recently LIUE and STEINBERG[96] have investigated the mode of hydride precipitation in alpha-titanium and they offer an explanation for the drastic effect of hydride particles on the mechanical properties of this metal. Their experiments were conducted on coarse grained material (approximately 1 mm grain diameter), whilst in the case of high purity titanium single crystals were also used. The specimens were hydrogenated in a standard Sieverts type of apparatus and examined by means of the Laue back-reflection X-ray technique.

In single crystals of high-purity titanium, the hydride platelets were found to take the form of narrow line-markings arranged in a definite geometrical pattern with respect to each other (see Fig. 16). These hydride line-markings were easily distinguishable from the Twins which were also present in some of the specimens. In some cases when the hydride precipitates, which made perfect 60° angles with each other, met a twin there was a definite and abrupt change of direction of the markings, whilst in other cases they crossed the

twins without any such change of direction. From this the authors infer that the hydride is precipitated on two habit planes of the alpha-titanium lattice. X-ray examination showed these habit planes to be the (10$\bar{1}$0) and the (10$\bar{1}$1) planes.

The general appearance of the hydride precipitates in coarse-grained alpha-titanium alloys was very similar to that discussed above. The four alloys investigated contained 2 per cent vanadium, 10 per cent zirconium, 3 per cent tantalum, and 3 per cent aluminium, respectively, the habit planes of the hydride platelets being (10$\bar{1}$0) and (10$\bar{1}$1); (10$\bar{1}$1) and (11$\bar{2}$2); (10$\bar{1}$1) (11$\bar{2}$1) and (11$\bar{2}$2); and, (10$\bar{1}$1), (11$\bar{2}$1) and (10$\bar{1}$2); respectively. It should be noted that, although the overall precipitation of hydride occurs on different sets of planes in different alloys, the (10$\bar{1}$1) plane is always included. The authors point out that the (10$\bar{1}$0) and (10$\bar{1}$1) planes figure amongst the principal slip planes at room temperature. Hence it is suggested that embrittlement is caused by the blocking of these two slip planes by hydride platelets.

It should be noted that the precipitation of this hydride is the direct result of the decrease in hydrogen solubility as the temperature is lowered. Hence it is to be expected that the temperature at which this precipitation occurs will increase as the hydrogen content increases. It therefore follows that the embrittlement effect will also extend to increasingly high temperatures as the hydrogen content is increased.

Recent work by BERGER, WILLIAMS and JAFFEE[97] has shown that increasing the aluminium content of alpha-titanium alloys increases the solubility of hydrogen and raises the resistance to hydrogen embrittlement. For example they report that a titanium–aluminium alloy containing 7 weight per cent aluminium did not suffer hydrogen embrittlement at hydrogen contents of the order of four times that which embrittles commercially pure titanium.

5.3 *The Hydrogen Embrittlement of Alpha–Beta Titanium Alloys*

5.3.1 *The characteristics of hydrogen embrittlement in alpha–beta titanium alloys*

Hydrogen is a beta-stabilizing element, and has a marked preference for the beta-phase in alpha–beta alloys. At the eutectoid temperature the partition ratio for hydrogen is of the order of 5 : 1.[2] At room temperature it is probably higher as the result of the considerably reduced solubility in the alpha-phase, as the temperature is lowered below the eutectoid temperature. The hydrogen embrittlement of alpha–beta titanium has been studied by several workers.[94, 98–103] RYLSKI[2] has suggested that alpha–beta titanium alloys containing up to 4·5 atomic per cent (0·1 weight per cent) of hydrogen (which is about 5 times the embrittling concentration) did not contain a hydride phase. However, recent autoradiographic work[104] on alpha–beta alloys with not more than 2·7 atomic per cent (0·06 weight per cent) of hydrogen has shown that hydrogen segregates to the alpha–beta boundaries on thermal ageing. Since a large number of beta-stabilizing elements are used

VOL. 9 1961

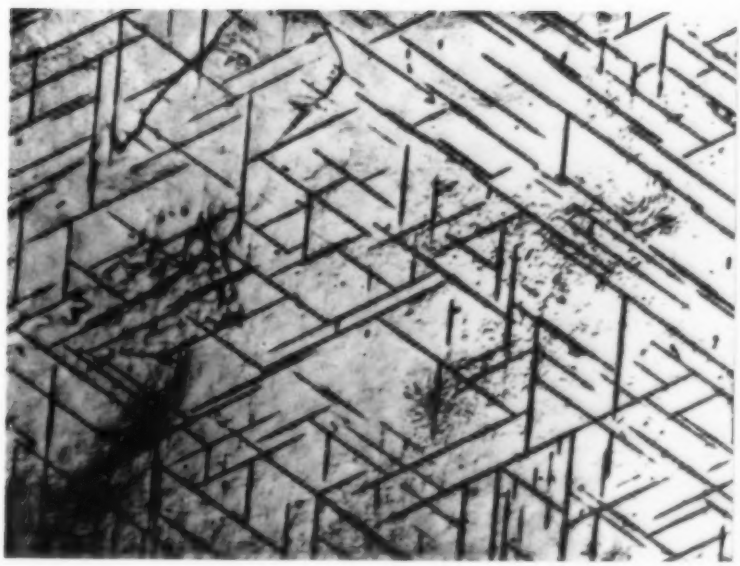

FIG. 16. Hydride platelets in a single crystal of high-purity alpha-titanium; after LIUE and STEINBERG.[96]

VOL.
9
1961

in the production of commercially pure alpha–beta alloys it is not surprising that the numerous hydrogen embrittlement studies should cover a wide composition range of titanium-based alloys. However, the general characteristics of the hydrogen embrittlement effect are very similar for all the various alloys which have been considered. In view of the high solubility of hydrogen in the beta-phase, compared with the alpha-phase, it is not surprising that the hydrogen embrittlement characteristics of alpha–beta alloys differ considerably from those of the single phase alpha-titanium. In these alloys it is the normal tensile properties, rather than the impact properties, which are affected by the presence of hydrogen.

A typical commercially produced alpha–beta alloy is that containing 8 per cent (by weight) of manganese, the hydrogen embrittlement of which is reported by CRAIGHEAD, LENNING and JAFFEE.[99, 101] Figure 17 shows tensile

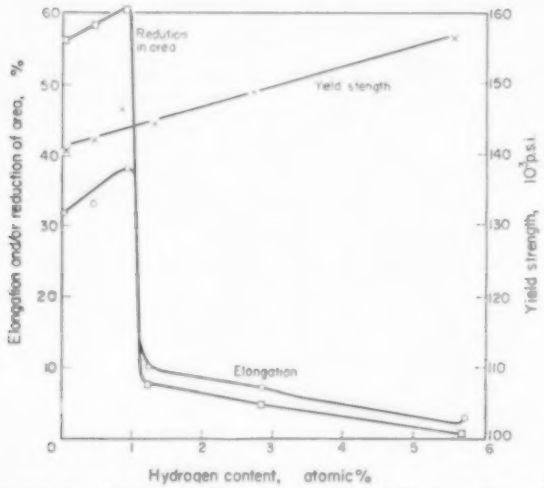

FIG. 17. Normal tensile properties of a commercially pure Ti – 8 Mn alloy as a function of hydrogen content; after CRAIGHEAD, LENNING and JAFFEE.[99]

data obtained from slow strain-rate tests of this alloy at room temperature. It can be seen that the ductility rises very slightly at low hydrogen contents and then falls abruptly as the hydrogen content concentration is increased from 0·86 atomic per cent to 1·28 atomic per cent (0·018 to 0·027 weight per cent respectively).

The notch impact strength is hardly affected by hydrogen contents up to 4·9 atomic per cent (0·110 weight per cent) in the temperature range — 196°C to 100°C, which includes the normal brittle-to-ductile transition range for the unhydrogenated alloy. There is, however, a slight decrease in the notch-impact strength of a manganese–aluminium titanium alloy, as the hydrogen level increases, at 100°C. From this it can be inferred that the presence of hydrogen causes a slight elevation of the impact strength transition temperature. These impact data are summarized in Tables 3 and 4 below.

TABLE 3

Notch impact data for a titanium–8 per cent manganese alloy at various hydrogen contents in the range from − 196°C to 100°C[99]

Hydrogen Content		*Impact energy absorbed* (in. lb.)			
At. %	*wt.* %	*at* − 196°C	*at* − 40°C	*at* 25°C	*at* 100°C
0·07	0·0015	2	6	10·5	18
0·32	0·0066	1	6	12	16·5
0·86	0·0180	2	4·5	9	16
1·28	0·0270	2·5	4	9	20
2·8	0·0600	2·5	4	8·5	17
5·5	0·1200	2	4	7	20

TABLE 4

Notch impact data for a titanium–4 per cent manganese–4 per cent aluminium alloy at various hydrogen contents in the range − 196°C to 100°C[99]

Hydrogen Content		*Impact energy absorbed* (in. lb.)			
At %	*wt.* %	*at* − 196°C	*at* − 40°C	*at* 25°C	*at* 100°C
0·05	0·0011	3	10	16·5	34
0·25	0·0050	6	8	14	24
0·70	0·0150	5	9	8	13
1·0	0·022	6	8	9	12
1·1	0·024	6	5	14	12
2·2	0·050	4	8	10	12
4·4	0·100	4	10	10	13·5
4·9	0·110	4	8	12	14

It is quite evident from the results discussed in the previous paragraph, that the susceptibility of this class of alloys to hydrogen embrittlement increases as the strain-rate decreases, whereas the reverse is the case for alpha-titanium. The strain-rate dependence of the ductility of alpha–beta titanium alloys containing hydrogen has been discussed in most of the investigations mentioned earlier. Samples of the alloy Ti-140A (which contains traces of iron, chromium, molybdenum and carbon) have been tested at strain-rates of the order of 0·02 in/min and 0·10 in/min at room temperature.[103] The results of these tests are shown in Fig. 18. It can be seen that this material suffers embrittlement at the slow strain-rate when the hydrogen content exceeds the critical value of 0·1 atomic per cent (0·020 weight per cent), whereas the ductility is unaffected at the fast strain-rates when the hydrogen content exceeds this amount.

The general conclusion to be drawn from the various publications on this subject is that, under normal tensile testing conditions, the ductility of

VOL. 9 1961

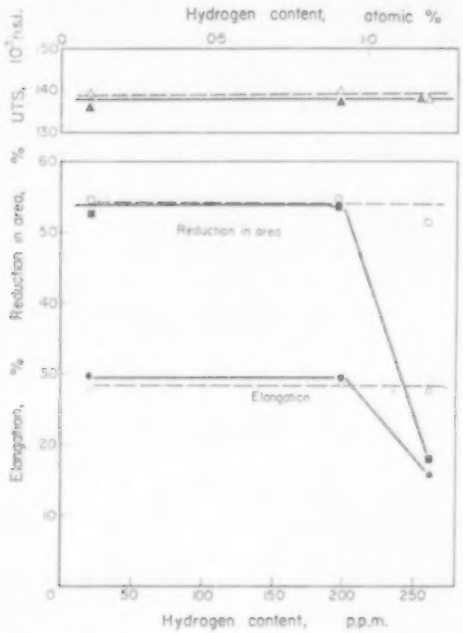

FIG. 18. The effect of hydrogen on the room temperature tensile properties of a Ti-140A alloy at a slow strain-rate (0·02 ins/min-broken curves) and a fast strain-rate 0·10 ins/min-full curve); after RYLSKI.[2]

susceptible specimens decreases linearly as the strain-rate is decreased. The rate of deformation can be reduced below that of a tensile test by means of a sustained loading type of stress-rupture test. Tests of this type, carried out at room temperature on the Ti-140A alloy, show that the reduction of area value is particularly affected.[103] A hydrogen-containing specimen fractured prematurely, in a brittle manner, at a stress level at which hydrogen-free material did not fracture after very prolonged testing.

The extent of the hydrogen embrittlement of these alloys is also dependent on temperature. BURT *et al.*[103] have shown that, in the case of the Ti-140A alloy, the embrittlement effect disappears at about 200°F (approximately 90°C), whilst several other workers have reported that the effect is negligible below — 40°C. In this respect the embrittling characteristics are very similar to those occurring in steel, the optimum conditions for embrittlement being slow strain-rates applied at, or about, room temperature.

The quantity of hydrogen which is required to produce a given amount of embrittlement is, like the extent of the embrittlement effect, also a function of the strain-rate and temperature. As might be expected from the temperature dependence of the embrittlement effect, the amount of hydrogen causing embrittlement is a minimum at room temperature and increases as the temperature is raised or lowered from this value. At all temperatures the

amount of hydrogen required to cause embrittlement increases as the strain-rate is increased. Two examples may be quoted in support of this latter statement; (*a*) in the case of an alloy containing 8 per cent manganese, tested at room temperature, embrittlement can be caused by 1 atomic per cent of hydrogen (0·020 weight per cent) at a fairly slow strain rate, whereas the relevant concentration for a fast tensile strain-rate and for impact tests are 2·7 atomic per cent and 5·3 atomic per cent (0·059 weight per cent and 0·117 weight per cent) respectively, and (*b*) in the case of the Ti-140A alloy tested at room temperature, embrittlement in slow tensile tests requires 1·2 atomic per cent of hydrogen (0·025 weight per cent), whereas 0·85 atomic per cent (0·017 weight per cent) is sufficient to cause premature fracture in very slow stress-rupture tests.[8]

Figure 19 shows the variation in ductility (in this case the reduction of area

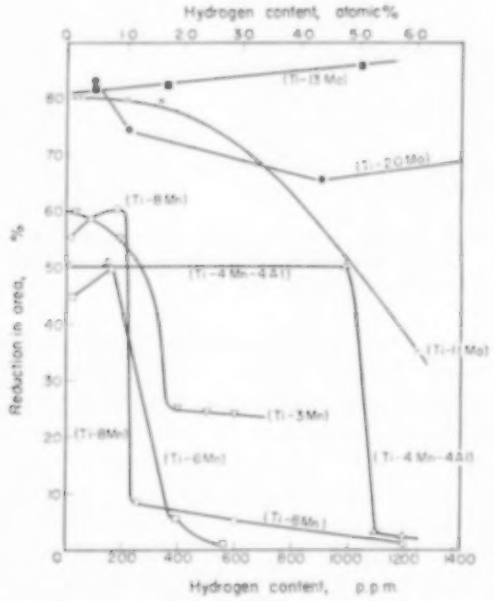

FIG. 19. Effect on hydrogen on the reduction of area of a series of alpha–beta titanium alloys tested at a slow strain-rate at 25°C; (data from CRAIGHEAD, LENNING and JAFFEE,[69] and from RYLSKI.[8])

at fracture) with hydrogen content for a variety of alpha–beta alloys. From this it can be seen that each alloy suffers a very sudden catastrophic loss in ductility when a particular hydrogen content is exceeded, although the critical hydrogen content varies from alloy to alloy.

The high purity 3 per cent and 6 per cent manganese alloys and the commercially pure 8 per cent manganese alloys all show a loss in ductility at about 1 atomic per cent hydrogen (0·02 weight per cent or 200 p.p.m.),

VOL. 9 1961

whereas the titanium — 4 per cent manganese — 4 per cent aluminium alloy does not suffer embrittlement until the hydrogen content exceeds 5 atomic per cent (1000 p.p.m.). This may be taken as an indication that, from the point of view of retaining a high ductility, the hydrogen tolerance of an alpha–beta alloy can be raised by the addition of an alpha-stabilizing element such as aluminium. Comparison of the manganese alloys with those in which the beta-phase is retained by the use of molybdenum shows that the hydrogen tolerance also depends on the choice of the beta stabilizer. It seems that molybdenum is much superior to manganese in this respect.

In view of the catastrophic effect of hydrogen on the ductility of these alloys the main investigations seem to have been directed towards this property, rather than to the effect of hydrogen on other aspects of the stress-strain curve. So far as is known, the variation of fracture stress, with hydrogen content, has not been reported. CRAIGHEAD, LENNING and JAFFEE[99] report that the yield strength and Vickers hardness of the titanium — 8 per cent manganese alloy increase very slightly as the hydrogen content increases, and also that the U.T.S. of a titanium — 4 per cent manganese — 4 per cent aluminium alloy behaves in a similar fashion. BURKE[103] says that the U.T.S. of the Ti-140A alloy is not affected by the hydrogen content within the embrittlement range.

5.3.2 *The mechanism of hydrogen embrittlement in alpha–beta titanium alloys*

The effect of temperature and strain-rate on the susceptibility of alpha–beta titanium alloys to hydrogen embrittlement is very similar to that occurring in steels. It is not surprising, therefore, that the essential features of the mechanism of hydrogen embrittlement in alpha–beta titanium, proposed by BURKE[103] and endorsed by JAFFEE, LENNING and CRAIGHEAD[101] are very similar to the mechanism proposed for steel by MORLET, JOHNSON and TRIANO.[81]

According to Burke, the onset of deformation within the metal causes hydrogen to diffuse from interstitial solution within the beta-phase to certain preferred sites within the specimen. This process leads to what Burke terms "micro-segregation" of hydrogen at places where, under the influence of the applied stress, micro-cracks can be initiated. The propagation of these cracks may then cause a brittle fracture. This segregation of hydrogen, being a diffusion-controlled process, requires time in order to be damaging. Therefore when the strain-rate is fast the rate of deformation is such that the critical concentration is not achieved before the metal has exhibited considerable ductility. However, when the strain-rate is slow a considerable degree of microsegregation may occur, before the material has undergone a large amount of plastic deformation, with the result that the material fractures in a brittle manner.

Decreasing the temperature will decrease the diffusion rate of hydrogen. Consequently, a strain-rate which is sufficiently slow to lead to embrittlement at room temperature (say) will not be sufficiently slow at a much lower

temperature. Therefore the susceptibility to embrittlement decreases as the temperature decreases. Embrittlement at the lower temperature will occur, however, if the hydrogen content is increased. This will have the effect of providing more hydrogen for diffusion, so that the critical amount of micro-segregation may still occur even at the lower diffusion rate. Similarly, at any given temperature, as the strain-rate is increased the amount of hydrogen required to cause embrittlement will be increased. This results from the shorter time available for the stress-induced diffusion (which leads to the critical amount of segregation) to occur.

When testing is conducted at temperatures of the order of 100°C the hydrogen-induced embrittlement disappears. Burke attributes this to either (*a*) the diminishing tendency for segregation at higher temperatures, or to (*b*) the increase in the general ductility of the material at higher temperatures. If the former is the case, then he suggests that the greater thermal vibrations, etc., which occur as the temperature is increased, will cause the distribution of hydrogen to remain sufficiently homogeneous to prevent the critical amount of microsegregation from arising. If the second possibility is the case, then he suggests that this may be because the higher ductility is such that crack initiation and/or propagation cannot take place even in the presence of segregated hydrogen.

VOL. 9 1961

Burke makes no definite mention of the nature of the sites at which his proposed micro-segregation takes place. However, in endorsing this hypothesis, JAFFEE, LENNING and CRAIGHEAD[101] suggest that this segregation, occurs at the alpha–beta interfaces. This seems reasonable, in view of the relatively low solubility of hydrogen in the alpha-phase as compared with the beta-phase. If, as is postulated here, the application of stress causes hydrogen to migrate from its equilibrium position within the beta-phase, the hydrogen will be forced to collect at the alpha–beta boundary, since very little of the migrating hydrogen will be able to dissolve in the alpha-phase at the other side of the boundary as a result of its very low solubility in this phase at room temperature.

It should be pointed out that although this phase boundary segregation, proposed by Jaffee and his co-workers[101] appears to be a logical consequence of the mechanisms suggested by Burke, no supporting metallographic evidence of the existence of such a hydrogen-containing phase was offered in their samples which had suffered this form of embrittlement. However, as was mentioned in the previous section, some recent work, based on the combined use of the electron microscope and autoradiography has revealed a hydrogen-containing phase existing, in small amounts, at the alpha–beta interface of a complex alloy containing 2·7 atomic per cent (0·06 weight per cent) of hydrogen.[104] In the course of this examination it was shown that this hydrogen-containing constituent was produced as the result of thermal ageing. It is therefore conceivable that a similar type of precipitation may occur as the result of strain ageing during the deformation of this type of alloy.

5.3.3 *A comparison of the hydrogen embrittlement of alpha–beta titanium with that of steel*

The variation of the susceptibility of alpha–beta titanium alloys to hydrogen embrittlement, as a function of temperature and strain-rate, is very similar to that occurring during the hydrogen embrittlement of steel. BROWN and BALDWIN[105] have described the latter effect in terms of the slope of the two surfaces that produce the appropriate depression in a three-dimensional plot of ductility versus temperature and strain-rate. One of these surfaces, that describing the low temperature behaviour, can be represented mathematically by the following equations.

$$\left(\frac{\delta\epsilon}{\delta T}\right)_{\dot{\epsilon}} > 0 \text{ and } \left(\frac{\delta\epsilon}{\delta\dot{\epsilon}}\right)_{T} > 0 \quad . \quad . \quad . \quad . \quad . \quad (19)$$

The second surface, that describing the behaviour above room temperature is of the form;

$$\left(\frac{\delta\epsilon}{\delta T}\right)_{\dot{\epsilon}} > 0 \text{ and } \left(\frac{\delta\epsilon}{\delta\dot{\epsilon}}\right)_{T} > 0 \quad . \quad . \quad . \quad . \quad . \quad (20)$$

where ϵ represents the ductility (strain at fracture)
$\dot{\epsilon}$ represents the strain-rate
and T represents the temperature.

RIPLING[100] investigating the effects of hydrogen on ductility has shown that the above equations can also be applied to the susceptibility to hydrogen embrittlement of the Ti-140A alloy. He therefore concludes that ". . . the hydrogen embrittlement (of alpha–beta titanium) seems to result from the same mechanism which produces hydrogen embrittlement in steels." However, there is one point of difference between the characteristics of embrittlement in the two cases.

A survey of the literature concerning the hydrogen embrittlement of steels[63] shows that the ductility is decreased progressively as the hydrogen content is increased from infinitesimal values until a certain upper limit is reached. Above this limit the ductility remains unaffected by any further increases in the hydrogen content. The embrittlement therefore occurs over a wide range of hydrogen concentration starting at the lowest measurable value. This contrasts very sharply with the behaviour of the alpha–beta titanium alloys in which the ductility remains almost constant until the hydrogen content reaches a certain critical value. The full extent of the embrittlement effect then takes place over a very narrow hydrogen concentration range. This contrast in the dependence of the embrittlement effect on the hydrogen content can be seen by comparing Figs. 8 and 13.

In steel the embrittlement is said to be caused by the segregation of hydrogen at points of triaxiality within the lattice structure of the metal.[81] Voids of the type that give rise to these positions of triaxiality are also likely to exist in titanium alloys since they are merely the normal imperfections which are present in any metallic lattice. Nevertheless the embrittlement in alpha–beta titanium alloys is said to be caused by the segregation of hydrogen at

the alpha–beta phase boundaries[99]—a possibility which is supported by autoradiographic evidence.[104] In each case the driving forces are (*a*) the stress-activated diffusion of hydrogen (towards voids in steel, and out of beta-phase solution in the alpha–beta titanium alloys) which decreases as the temperature falls and (*b*) the thermally activated homogenization of hydrogen concentration gradients which counteracts the former effect as the temperature increases. Hence, as RIPLING[100] has pointed out, the equations for ductility, temperature and strain-rate for hydrogen embrittlement in steel can also be applied to alpha–beta titanium alloys. However, the difference between the location of the embrittling segregation of hydrogen, in the two cases, may allow a possible explanation of the different behaviour of the two metals.

VOL.
9
1961

In the case of steel the process depends on the redistribution of hydrogen between the lattice and the imperfections (or voids) of the lattice structure on the application of stress to the metal. There will always be an equilibrium distribution of this type, no matter how low the total hydrogen content, as the result of the thermodynamic interdependence of solubility (in the lattice) and pressure (in this case, in the voids). It may therefore seem reasonable to expect that the diffusion controlled segregation of hydrogen will occur, on stressing, at the lowest possible hydrogen content. Naturally as the hydrogen content is increased the critical conditions will be achieved more readily throughout the specimen. It is therefore not unreasonable, on the mechanism proposed by MORLET, JOHNSON and TRIANO[81] to expect that embrittlement of steel will occur at the lowest measurable hydrogen content, as is the case.

In the case of an alpha–beta titanium alloy, however, the embrittlement is said to be caused by the segregation of hydrogen at the alpha–beta boundaries[99]—presumably as the result of the dislocation blocking effect of a grain-boundary precipitate. It follows that in order to become effective in this way a finite amount of hydrogen segregation will be required at these boundaries, even though the size of the precipitated hydrogen-rich constituent is too small to be observed by normal metallographic techniques. Consequently very low hydrogen contents may not lead to embrittlement, although once the segregation has reached the critical value the drop in ductility will be very rapid, as is the case.

The fact that the critical hydrogen content can be varied by the use of different alpha- and beta-stabilizing elements (see Fig. 19), suggests that the onset of embrittlement depends on the relative amounts of hydrogen dissolved in the two phases of the alloy. In particular the presence of an alpha-stabilizing element, such as aluminium, increases the amount of hydrogen which can be absorbed by the alloy before embrittlement occurs. If the embrittlement is solely due to the precipitation of hydrogen from the beta-phase, the following explanation of this aspect of the hydrogen embrittlement of alpha–beta titanium alloys is suggested. The greater the proportion of alpha-phase in an alloy of a given hydrogen content the smaller will be the quantity of hydrogen which is initially distributed in the beta-phase. Hence,

the total hydrogen content needed to cause embrittlement increases as the proportion of alpha-phase present increases.

Furthermore, suppose that the initial portion of the hydrogen arriving at the alpha–beta boundary can be taken into solution within the alpha-phase. It then follows that, as the hydrogen content of an alloy increases, embrittlement will not occur until the overall hydrogen content is sufficiently high for the beta-precipitated hydrogen to give rise to two effects: firstly, the saturation of the adjacent alpha-phase, and secondly the precipitation (or coherent formation) of a hydrogen-rich constituent at the alpha–beta boundary in a sufficient quantity to cause brittle fracture. Hence, the absorption of migrating hydrogen by the alpha-phase enhances the concentration dependence of embrittlement and also affords a qualitative explanation of the results summarized in Fig. 19. This is particularly so in the case of aluminium-containing alloys since this constituent has been shown to increase the solubility of hydrogen in the alpha-phase.[97] Therefore, if the hydrogen dissolved in alpha-titanium is non-damaging these alloys will be more resistant to the embrittlement effect than those which do not contain aluminium.

In conclusion it should be pointed out that, on the basis of the mechanism discussed above, the variation of ductility of alpha–beta titanium alloys with hydrogen content, for any one alloy, can be explained by the requirements of the grain boundary segregation which is said to lead to embrittlement. However, in order to explain the variation of behaviour from one alloy to another, it is necessary to assume that the hydrogen which is in solution in the alpha-phase does not contribute to the embrittlement phenomena; as is to be expected from the fact that the ductility of alpha-titanium is unaffected by the presence of hydrogen at the slow strain-rates at which embrittlement of alpha–beta titanium occurs.

5.4 *The Effect of Hydrogen on the Mechanical Properties of Beta-Titanium Alloys*

In view of the relatively high solubility of hydrogen in the beta-phase it was expected that any hydrogen embrittlement effects in single phase beta alloys would require a high hydrogen content in order to become effective. However, CRAIGHEAD, LENNING and JAFFEE[99] have shown that the impact and tensile properties of a series of alloys of this type are unaffected by hydrogen in quite high proportions. For example, an all-beta alloy containing 13·1 per cent molybdenum had a ductility of the order of 90 per cent at a hydrogen content of approximately 9 atomic per cent (0·19 weight per cent).

6. THE HYDROGEN EMBRITTLEMENT OF ALPHA-ZIRCONIUM

6.1 *The Zirconium-Hydrogen System*

Zirconium and titanium are metallurgically similar to one another. It is therefore to be expected that the effect of hydrogen on zirconium will be similar to that on titanium. The zirconium–hydrogen system has been

investigated by a number of workers.[105–113] HÄGG's[106] X-ray study suggested the existence of four separate zirconium–hydrogen phases in the composition range 0 to 66 atomic per cent hydrogen. These phases were,

(1) alpha, a solid-solution of hydrogen in zirconium extending to 5 atomic per cent hydrogen;

(2) gamma, another close-packed hexagonal phase, based on Zr_2H, at 28 to 36 atomic per cent hydrogen;

(3) delta, a face-centred cubic phase, based on ZrH, at 47 to 52 atomic per cent hydrogen, and

(4) epsilon, a face-centred tetragonal phase, based on ZrH_2, at 59 to 66 atomic per cent hydrogen.

These phases were separated by the appropriate two-phase regions. Hägg's work was carried out on metal which had been slowly cooled to room temperature in an atmosphere of hydrogen. GULBRANSEN and ANDREW[110] have recently reported a study of this system which was based on X-ray diffraction and equilibrium pressure measurements. Their results suggest that only two hydride phases exist at low temperatures. These are the delta and epsilon phases proposed by HÄGG.[108]

The thermodynamic aspects of this system have received attention from several workers.[109, 112–114] These investigations include the derivation of equations which express the solubility and decomposition pressures of hydrogen in terms of the heat, entropy and free energy, of solution in the various phases. The solubility of hydrogen in both alpha and beta zirconium has been studied by MALLETT and ALBRECHT[112] in the temperature range 700°C to 1000°C at pressures within the range 0·1 to 4·0 μ Hg.

The general impression to be gained from this array of studies is that the zirconium–hydrogen system is very similar to the titanium–hydrogen system, although it is complicated by the formation of at least two different hydrides. Most of the work on the solubility seems to have been concentrated within the temperature range from 300°C to 600°C: a region which is of importance from the point of view of the embrittlement effect of hydrogen (see later sections). The terminal solubility of hydrogen increases as the temperature increases; whereas the total amount of hydrogen absorbed, during hydride formation, decreases as the temperature increases. At low pressures the solubility obeys Sievert's Law.

The experimentally determined values of the terminal solubility of hydrogen in alpha-zirconium differ slightly from one investigation to another. Such discrepancies also exist in the literature on titanium and are probably due either to the effect of varying impurity contents,[108, 113, 114] or to the presence of an oxide or nitride film on the surface of zirconium which inhibits the absorption of hydrogen.[115] If the metal is heated to a sufficiently high temperature for the oxygen or nitrogen to diffuse into the metal hydrogen absorption re-occurs, though to a lesser degree than in the complete absence of these impurities. It is therefore suggested that the dissolved oxygen or

VOL.
9
1961

nitrogen atoms occupy the octohedral interstitial sites, and, in so doing, restrict the entry of hydrogen, to either these, or the tetrahedral interstitial sites. Similar effects have been found to occur in the presence of dissolved carbon. The effect of these elements on both the lattice expansion and the absorption of hydrogen appears to increase in the order oxygen–nitrogen–carbon; which is also the order of increasing atom diameters. Hence, their effect on the hydrogen absorption is likely to be due to the distortion of the zirconium lattice, resulting from their solution in the octohedral sites.

Although the evidence on this point is slight, MARTIN, HALL and REES[108] suggest that hydrogen acts as a beta-retaining element in zirconium, and also that the solubility of hydrogen is higher for the beta-phase than for the alpha-phase, as is the case in titanium.

The terminal solubility of hydrogen in alpha-zirconium, as found by two sets of workers is given in Tables 5 and below.

TABLE 5

The terminal solubility of hydrogen in alpha-zirconium[111]

From a graph of log pressure vs. 1/T			*From a Sievert's Law plot*		
Temperature °C	*Terminal solubility*		*Temperature* °C	*Terminal solubility*	
	At. %	*Wt. %*		*At. %*	*Wt. %*
378	1·48	0·0167	450	2·86	0·0322
410	1·96	0·0220	475	3·43	0·0396
453	2·82	0·0318	500	4·32	0·0496
471	3·3	0·0372	525	5·25	0·0607
			575	6·1	0·0713

TABLE 6

The solubility of hydrogen in alpha-zirconium[3]

Temperature °C	*Solubility of hydrogen*	
	At. %	*Wt. %*
400	2·6	0·028
425	3·5	0·038
450	3·7	0·041
475	4·4	0·048
500	5·2	0·057

SCHWARTZ and MALLETT[3] confined their solubility determinations to the temperature range 400°C to 500°C. However, they extrapolated the straight line obtained by plotting the solubility against the reciprocal of the absolute temperature to lower temperatures. Whilst conceding that such an extrapolation introduces a possible source of error they then estimated that the

equilibrium solubility at room temperature is of the order of 30 to 40 p.p.m. hydrogen: (approximately 0·3 atomic per cent). As will be shown later this value is in reasonably good agreement with the qualitative implications of the hydrogen embrittlement effect in alpha-zirconium.

6.2 *The Characteristics of the Hydrogen Embrittlement of Alpha-Zirconium*

In view of the limited use of zirconium and its alloys, compared with that of titanium, the reported investigations of the effect of hydrogen on the mechanical properties of the former have been confined to commercially pure zirconium and alpha-zirconium alloys containing up to 5 weight per cent of tin. In each case the hydrogen embrittlement is very similar to that occurring in alpha-titanium.

VOL.
9
1961

Measurements of the impact strength of commercially pure alpha-zirconium usually show a ductile to brittle transition at about 200°C. Until recently it had been assumed that this transition was an intrinsic property of the metal. However, it has been shown that the low temperature ductility of this material can be improved considerably if the material is heated to a temperature of 315°C, or higher, and then water-quenched.[3] On re-heating to 315°C and slow cooling to room temperature the impact strengths revert to their previously accepted low values, thereby showing that the process is reversible. In this case the microstructure of the brittle specimens contain needles of a second phase, whilst that of the ductile specimens do not. It was then shown that when hydrogen was added to the zirconium the proportion of this second phase increased. It was therefore concluded that this was a hydride, analogous to that occurring in alpha-titanium (see section 5.2).

Although the investigations of the hydrogen embrittlement of pure alpha-zirconium have been restricted to room temperature MUEHLENKAMP and SCHWARPE[110] have shown that the brittle to ductile transition for the notch-impact testing of any alloy containing 1·6 weight per cent tin increases progressively as the hydrogen content increases. For example, when the hydrogen content is of the order of 10 p.p.m. (approximately 0·09 atomic per cent) the transition temperature is of the order of − 80°C and hence, the metal has appreciable strength at room temperature. However, the notch-impact transition temperature of a similar alloy containing 490 p.p.m. (approximately 4·5 atomic per cent) hydrogen is of the order of 400°C (see Fig. 20). These workers demonstrated the strain-rate dependence of this embrittlement effect by showing that the reduction of area, at the base of a notch, increased as the speed of bending decreased.

As mentioned above, the embrittlement effect is dependent on the thermal history of the specimen—the important factor being the cooling rate in the range 315°C to room temperature. In the course of a metallographic examination of this effect YOUNG and SCHWARTZ[117] used arc-melted bar zirconium specimens which had been subjected to one of three heat-treatments. Firstly all the specimens were degassed at 800°C, after which the specimens which

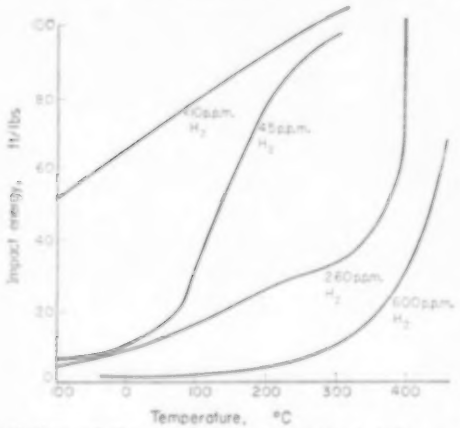

FIG. 20. The variation of the notch-impact ductile-brittle transition temperature of alpha-zirconium with hydrogen content; after MUELENKAMP and SCHWARPE.[116]

were to be used in the degassed condition were annealed at 550°C and then quenched in water. The remainder of the specimens were hydrogenated to approximately 100 p.p.m. (approximately 0·9 atomic per cent) hydrogen. These were then slow cooled to room temperature or quenched from 550°C. After heat-treatment they were subjected either to impact tests (at a strain-rate of 18·1 ft/sec) or to slow tensile tests (at a strain-rate of 0·03 in/min), at room temperature. The results of these tests, which are given in Table 7,

TABLE 7

The effect of heat-treatment and strain-rate on the room-temperature hydrogen embrittlement of alpha-zirconium[117]

Heat-treatment	*Impact test data* (18·1 ft/sec)			*Tensile test data*	
	Elongation (%)	*Reduction of area* (%)	*Breaking energy* (ft lb)	*Elongation* (%)	*Reduction of area* (%)
Degassed and quenched from 550°C to room-temperature	72	40	24·5	80	·57
Hydrogenated and quenched from 550°C to room-temperature	50	30	25		
Hydrogenated and slow cooled from 550°C to room-temperature	31	19	11·5	66	41

below, clearly show the effect of strain-rate and heat-treatment on this phenomenon.

The basic facts which have to be explained by any theory of the mechanism of the embrittlement phenomenon are therefore as follows:

(1) With hydrogen contents of the order of, or above, that normally found in zirconium slow cooling from 315°C causes the precipitation of a second phase, with a drop in ductility and impact strength.

(2) Quenching similar material from 315°C does not lead to either of these effects, unless the hydrogen content is very high.

(3) Removal of hydrogen to less than 10 p.p.m. (0·01 atomic per cent) removes the embrittlement effect, and

(4) The embrittlement effect is most severe under impact conditions and diminishes as the strain-rate is decreased.

VOL. 9 1961

6.3 *The Mechanism of Hydrogen Embrittlement in Alpha-Zirconium*

It is evident, from the above discussion, that the hydrogen-induced embrittlement of alpha-zirconium is concerned with the precipitation of a second phase (presumably a hydride) under certain conditions, within the matrix of the metal. This aspect of the phenomenon has been examined very thoroughly by SCHWARTZ and MALLETT[3] using solubility determinations, optical microscopy and X-rays and electron diffraction techniques. They showed that a specimen containing 30 p.p.m. (approximately 0·27 atomic per cent) hydrogen had the typical single-phase alpha-structure after quenching from 790°C. An adjacent specimen from the same bar contained small needle-like particles of a precipitated phase, within the alpha-grains as a result of being reheated to 315°C and cooled slowly after the alpha-quenching treatment used in the former case. In the case of a specimen containing 500 p.p.m. (approximately 4·5 atomic per cent) hydrogen the precipitation of this phase could not be suppressed by rapid cooling from 790°C.

Initial attempts to detect the second phase of embrittled zirconium by X-ray diffraction methods were inconclusive. However, a "reflection" electron diffraction technique was more successful. The etching characteristics of this material are such that the needles of the precipitate stand out in relief and, hence, the phase can be identified by the use of an electron diffraction beam at a glancing angle to the specimen surface. The diffraction pattern obtained from the precipitate in this way is very similar to that of a face-centred cubic lattice with a cell edge of 4·7 Å. In order to identify this phase the authors also examined a series of samples which had been treated in a way which resulted in a concentration gradient of hydrogen at the specimen surface. The diffraction pattern referred to above was then shown to be identical to that of the hydride phase which occurred adjacent to the pure metal in these samples. This phase is very similar to the tetragonal hydride of minimum hydrogen content in the haffnium-hydrogen system.[118]

The precipitated-phase, in alpha-zirconium, was further identified by the

examination of two specimens having vastly different hydrogen contents. Metallographic evidence had already shown that the proportion of the precipitated phase increased as the hydrogen content increased. The electron diffraction pattern, which was now known to be that of the hydride phase, was obtained from both samples but the intensity of this pattern was very weak for the low-hydrogen specimen and very strong for the high-hydrogen containing specimen.

Solubility determinations,[106–114] suggest that the terminal solubility of hydrogen in alpha-zirconium falls from values of the order of 300 p.p.m. (2·8 atomic per cent) at about 400°C to something of the order of 10 p.p.m. (0·09 atomic per cent) at room temperature. If this is the case it is to be expected that slow-cooling commercially-pure zirconium (which usually contains about 30 to 40 p.p.m., or 0·27 to 0·36 atomic per cent, hydrogen) from 315°C will lead to the rejection of hydrogen from solution and the consequent precipitation of a hydride. The effect of quenching can also be explained in terms of the effect of temperature on hydrogen solubility. In the case of commercially-pure zirconium the hydrogen will all be in solution at about 315°C. Hence, quenching from this temperature will retain a single-phase structure, although precipitation of the excess hydrogen may occur on ageing at room-temperature. In the case of a specimen which has a high hydrogen content, however, the hydrogen content is likely to be so grossly in excess of the room temperature solubility that quenching will not prevent the precipitation of the hydride phase.

It is therefore concluded that the second phase, which is present in the form of needles or platelets, in the embrittled zirconium is a hydride of the type which can be expected to be in equilibrium with the metal at the hydrogen contents and temperatures in question. Furthermore it follows from the above discussion that as the hydrogen content is increased the temperature at which precipitation occurs, on slow cooling, will be raised. Hence it is to be expected that the embrittlement effect will occur up to progressively increasing temperatures as the hydrogen content increases.

The photo-micrographs reported by SCHWARTZ and MALLETT[3] show that the hydride is precipitated in the form of thin plates within the grains of alpha-zirconium. Although no work has been done on the precise mode of precipitation, it is to be expected that, as is the case in alpha-titanium, the embrittlement phenomenon results from the formation of hard hydride plates on certain preferred planes, some of which may normally be slip plares within the zirconium lattice.*

The formation of micro-cracks in hydrogen embrittled alpha-zirconium

* *Author's footnote:* Recent work [143] has shown that the habit-planes for the precipitation of the hydride-phase in alpha-zinconium are $(11\bar{2}2)$, $(10\bar{1}2)$ and $(11\bar{2}1)$. These are also amongst the hydride habit planes in alpha-titanium (see section 5.2.5). The $(10\bar{1}2)$ plane is one of the principal twinning planes, but the major slip planes —(1000) and $(10\bar{1}0)$—are not amongst those mentioned as hydride habit planes in this work.

has been studied by YOUNG and SCHWARTZ[119] by use of the electron microscope. They found that hydrogenated alpha-zirconium showed evidence of profuse twinning, and little slip, after impact (or fast tensile strain-rate) testing but that the reverse was true for specimens which had been subjected to slow strain-rate tensile testing. In nearly all the cases the twins terminated as hydride platelets and fine micro-cracks were frequently found on the opposite side of such a hydride plate: i.e. immediately opposite a twin terminus. In some cases twins approached a hydride plate from both sides, and in these cases small holes were often found at the twin-hydride junction. Very few micro-cracks were found in degassed zirconium, even after impact testing, whilst the number of micro-cracks in hydride-containing material increase as the strain-rate (and number of twins) increased.

The formation of the micro-cracks is clearly concerned with the interruption of twin bands by precipitated hydride platelets. This is represented diagrammatically in Fig. 21(*b*). It was frequently found that the end of a twin

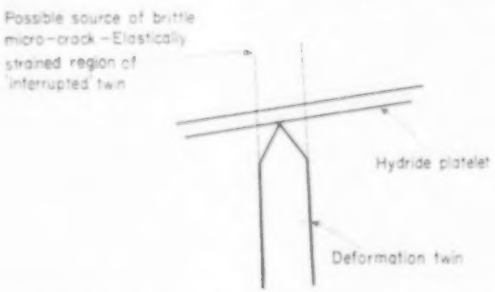
Possible source of brittle micro-crack – Elastically strained region of interrupted twin
Hydride platelet
Deformation twin

FIG. 21b. Diagrammatic representation of the source of a brittle micro-crack in hydrogenated zirconium; after YOUNG and SCHWARTZ.[119]

band became pointed at its junction with a hydride plate. It has, therefore, been suggested that the interrupted region of the twin (the region between the broken lines of Fig. 21(*b*)) is subjected to considerable elastic strain, and that the elastic strain energy then stored in this region can lead to the formation of micro-cracks, or small holes, in this region either by parting at the metal-hydride interface or by fracture within the hydride. YOUNG and SCHWARTZ's results[119] suggest that the former is the case: although the ductility of the metal is such that the micro-cracks are small, and that continuous cracks (leading to brittle fracture) only occur when the material contains a significant number of hydride plates and is subjected to deformation by heavy twinning. Hence it would appear that the strain-rate dependence of the hydrogen embrittlement of alpha-zirconium is related to the formation of micro-cracks in the region of precipitated hydride platelets, within the alpha-zirconium grains, under fast strain-rate conditions.

It should be noted that the amount of information which is available concerning the hydrogen embrittlement of alpha-zirconium is considerably less than that concerning the similar effect in alpha-titanium. The specimens used

VOL. 9 1961

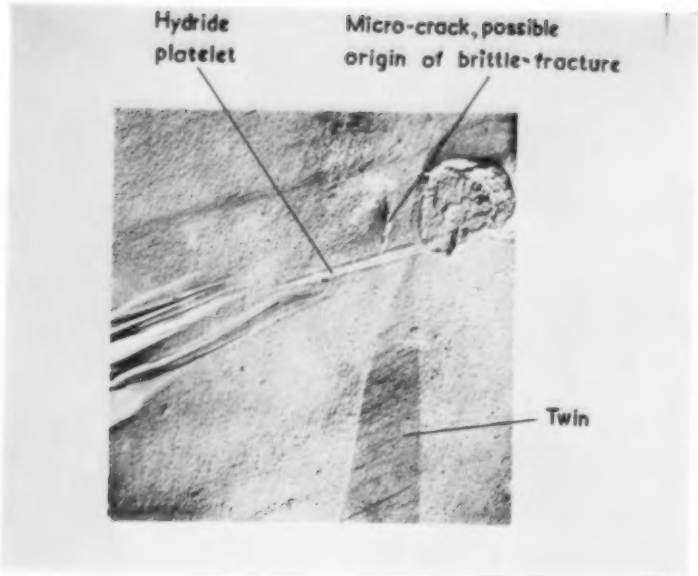

FIG. 21a. A micro-crack formed at the junction of a deformation twin and a hydride platelet in a specimen of hydrogen embrittled commercially-pure alpha-zirconium; after YOUNG and SCHWARTZ[119].

VOL.
9
1961

in the investigations of this latter case have covered a wide range of compositions, including high-purity (iodine-refined) titanium, commercially pure titanium from different sources and solid-solution alpha-titanium alloys; whereas in the former case most of the investigational effort has concerned with the hydrogen embrittlement of solid-solution alloys of alpha-zirconium containing small additions of tin. In each case it has been shown that the embrittlement is due to the precipitation of a stable hydride at hydrogen contents which exceed the equilibrium solid-solubility at the appropriate temperature. In the case of alpha-titanium it has been shown that this hydride is precipitated on specific crystallographic planes, which always include one of the principal slip-planes. In the case of alpha-zirconium the hydride precipitation has been shown to occur within the individual grains, although the particular planes upon which the precipitation occurs have not been identified.

7. The Hydrogen Embrittlement of Alpha-Uranium

7.1 *The Uranium–Hydrogen System*

Uranium—like titanium and zirconium—is a member of the exothermic occluding class of metals, and the uranium–hydrogen system gives an excellent example of the principles discussed in section 2.3.2. The solution of hydrogen in metallic uranium occurs endothermically, whilst the exothermic formation of the hydride occurs by a typically chemical process at the metal-hydride interface. Uranium hydride is an extremely pyrophoric compound, the decomposition of which has been used as a means of producing finely divided uranium powder, of a high standard of purity, for research purposes.[120, 121]

The hydride phase exists over a range of compositions the upper limit of which corresponds to UH_3. Non-stoicheiometric compositions, at hydrogen contents of less than 75 atomic per cent, are usually taken to represent a solid solution of uranium in UH_3. The structure of this hydride is unusual (for the pseudo-metallic hydrides of the exothermic occluders) in that it does not depend on conventional intermetallic bonds, but on a series of "bridge-bonds" in which the hydrogen atoms are situated between the uranium atoms.[122] The unit cell is cubic—of cell edge approximately 6·63 Å—and contains eight uranium atoms. According to Rundle[122] there are two types of uranium atom in the compound—"a" atoms and "c" atoms. Each "a" atom is said to be bonded to 12 "c" atoms by hydrogen "bridge-bonds", the U–H–U distance being approximately 3·70 Å. Each "c" atom is bonded to four "a" atoms through a similar bond and also directly to two other "c" atoms at a U–U distance of 3·31 Å.

The thermodynamics of the formation and dissociation of this hydride have been studied by several groups of workers,[123–127] whilst the solubility of hydrogen in uranium has been investigated by Mattraw,[128] Davies,[129] and Shulman, Anderson and Blakey.[130] These various publications have

been correlated, in a review of the uranium–hydrogen system, by MALLETT and TRZECIAK.[131] MULFORD, ELLINGER and ZACHARAISEN[127] have suggested that there are two allotropic forms of the hydride, the higher temperature allotrope being the one that is usually regarded as being in equilibrium with uranium under normal conditions.

MALLETT and TRZECIAK[131] also measured the sorption of hydrogen on uranium powder in the temperature range 250°C to 500°C at pressures ranging from 22 to 324 μ Hg. They showed that the amount of sorption which takes place depends on the surface area of uranium which is exposed to the hydrogen: a conclusion which is in agreement with the findings of SCHULMAN, ANDERSON and BLAKEY.[130]

It is therefore suggested that in the case of uranium powder a strong surface effect (possibly chemisorption) plays an important part in the sorption of hydrogen. Consequently, measurements of the hydrogen pressure before and after a uranium specimen has been allowed to come to equilibrium with hydrogen do not give a direct measure of solubility data.

There are three allotropic modifications of pure uranium: the alpha–beta (about 660°C), and the beta–gamma transformation at about 770°C. These temperatures have been used by Mallett and Trzeciak in compiling a phase-diagram for the uranium–hydrogen system (see Fig. 22). The hydride phase —which has a range of composition in the region of UH_3—is designated by the symbol ϵ in this diagram in recognition of the fact that the form referred

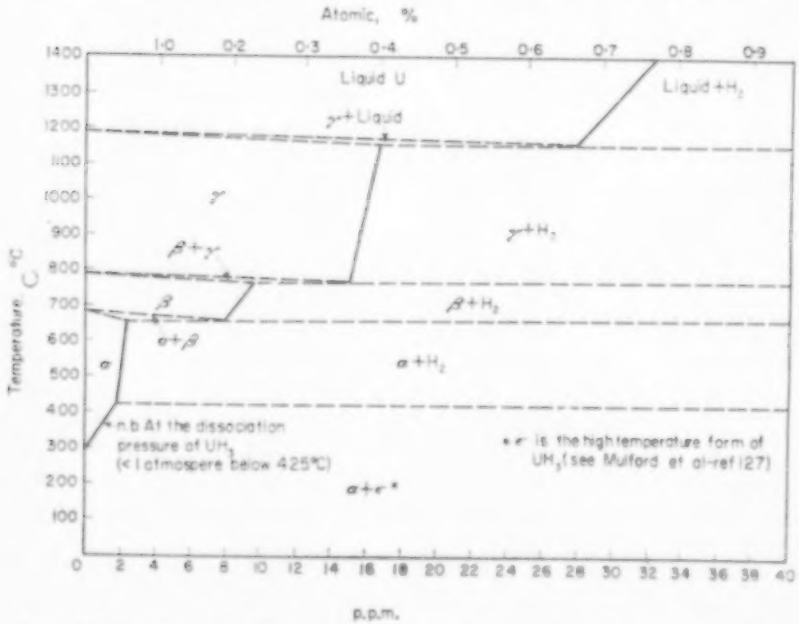

FIG. 22. The uranium–hydrogen system at one atmosphere pressure; after MALLET and TRZECIAK.[131]

VOL. 9 1961

to here is the high temperature allotrope ($\beta - UH_3$) of MULFORD *et al.*[127] No reference is made to the low temperature form ($\alpha - UH_3$) which would be designated by the δ-phase of the uranium–hydrogen system.

Table 8 below gives Mallett and Trzeciak's calculated values for the solubility of hydrogen in uranium, at a hydrogen pressure of one atmosphere, in the temperature range from 100°C to 1400°C.

TABLE 8

The solubility of hydrogen in uranium at one atmosphere pressure[131]

Temperature (°C)	*Solubility* (*p.p.m.*)	(*At. %*)	*Temperature* (°C)	*Solubility* (*p.p.m.*)	(*At. %*)
Alpha-phase			Gamma-phase		
		approx.			
100 *	0·0006	$1{\cdot}4 \times 10^{-5}$			
200 *	0·02	5×10^{-4}	769	14·7	approx. 0·340
300 *	0·2	5×10^{-3}	800	15·0	,, 0·346
400 *	1·1	0·026	900	15·6	,, 0·360
500	1·8	0·043	1000	16·2	,, 0·374
600	2·0	0·047	1100	16·7	,, 0·385
662	2·2	0·052	1129	16·9	,, 0·390
Beta-phase			Liquid-phase		
		approx.			
662	7·8	0·186	1129	28·1	,, 0·650
700	8·5	0·205	1200	29·3	,, 0·677
769	9·7	0·231	1300	31·1	,, 0·709
			1400	32·7	,, 0·755

* These values refer to pressures equal to the dissociation pressure of UH_3 and less than 1 atm.

The relationship between the dissociation pressure of the hydride and the temperature is such that the decomposition pressure is less than one atmosphere at temperatures below 400°C.[131] Hence, the solubilities quoted in Table 8 and used in the phase diagram (Fig. 20) in this range refer to the solubility at the decomposition pressure of the hydride at the appropriate temperature. The results of the various investigations suggest that the solubility of hydrogen obeys Sieverts' Law (thereby denoting that the hydrogen is dissolved in the atomic form). Figure 22 shows that the terminal solubility–temperature relationship (the heavy line of the phase diagram) is an endothermic one.

It is important to realize that this phase-diagram represents a reasonable summary of present data, but it is by no means complete. For example, more data is needed to establish the form of the two-phase solid-solution regions and the extent of the stability of the δ phase. It is not known, at present, whether hydrogen acts as a beta-stabilizer in uranium, as it does in titanium and (probably) in zirconium. However, the diagram is useful in that it summarizes the present status of the uranium–hydrogen system.

7.2 *The Effect of Metal Purity on the Solubility of Hydrogen in Alpha-Uranium*

DAVIES[125] has studied the solubility, diffusion and mechanical effects of hydrogen in uranium. The solubility was measured at pressures varying from 60 mm Hg to 760 mm Hg in the temperature range 400°C to 800°C; the variation of solubility with temperature is shown in Fig. 23. These solubility

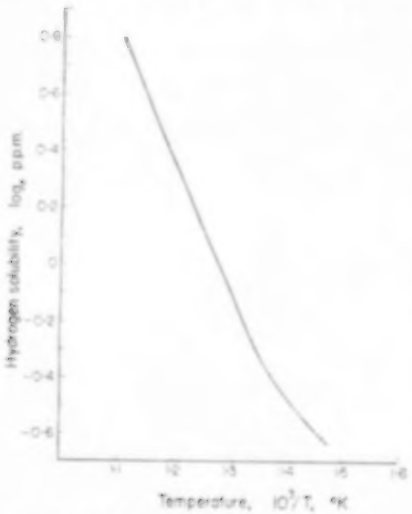

FIG. 23. Variation of the solubility of hydrogen in alpha-uranium with temperature at a pressure of one atmosphere; after DAVIES.[125]

values are of the same order as those calculated by MALLETT and TRZECIAK[132] which are quoted in Table 8 above. DAVIES[125] found that although the solubility followed Sieverts' Law in the beta and gamma phases of commercially pure uranium, this was apparently not the case in the alpha-phase. Figure 24 shows that if the measured solubility is plotted against the square root of the hydrogen pressure, for each of the temperature investigated, the various points lie on a family of straight lines which, when extrapolated to zero pressure, intersect the ordinate above the zero solubility, instead of passing through the origin as would be the case if Sievert's Law was directly applicable.

To eliminate the possibility that this unusual behaviour was caused by experimental error, the solubility of hydrogen, at 600°C, was determined over a range of low pressures by two methods. Firstly, samples of de-gassed uranium were allowed to come to equilibrium with known volumes of hydrogen and the solubility was calculated from the volume of the residual hydrogen. Secondly, samples of uranium were soaked in hydrogen at the desired temperature and pressure, quenched in a stream of helium and then analysed for hydrogen. The results of these determinations, which were in

VOL. 9 1961

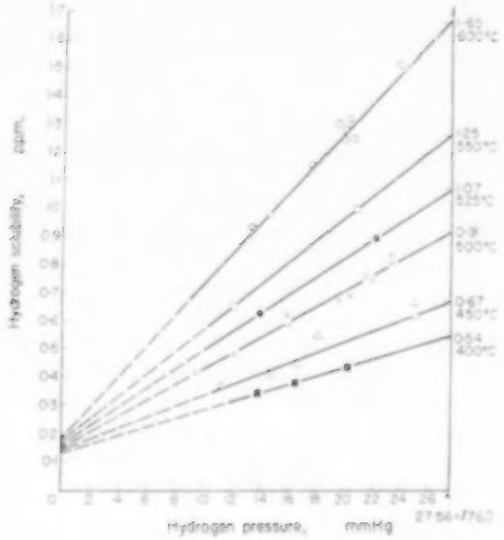

FIG. 24. Variation of the solubility of hydrogen with pressure in alpha-uranium for range 400°C to 600°C; after DAVIES.[129]

reasonable agreement with each other, showed that the solubility of hydrogen, in commercial purity alpha-uranium is directly proportional to the square root of the hydrogen pressure at low pressures (of the order of 1 mm Hg), but that at pressures of the order of 2 mm Hg the slope of a graph of solubility versus the square root of the pressure decreases to approximately that which had been found for the higher pressure determinations.

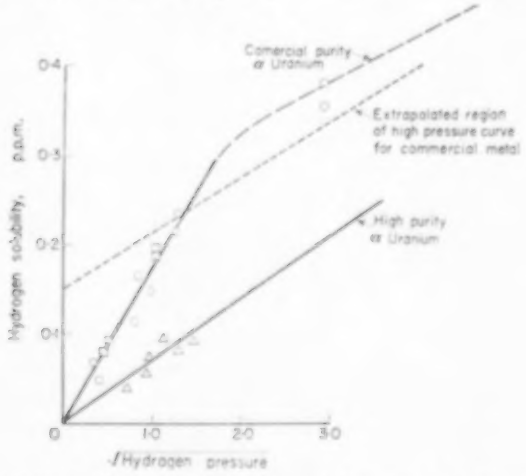
Comercial purity α Uranium
Extrapolated region of high pressure curve for commercial metal
High purity α Uranium
Hydrogen solubility, p.p.m.
√Hydrogen pressure

FIG. 25. Solubility of hydrogen in commercially pure and super-pure alpha-uranium at low pressures at 600°C; after DAVIES.[129]

DAVIES[129] then showed that this behaviour is due to the presence of impurities in the commercially pure material by determining the solubility of hydrogen in a sample of super-pure uranium. In this case the graph of solubility versus the square root of the pressure passes through the origin and has a slope which is similar to that of the commercially pure metal at pressures of 2 mm Hg. The results of these various determinations are showing in Fig. 25.

Davies suggests that there is an impurity in the normal grade metal which causes an abnormally high absorption of hydrogen for the first few millimetres of hydrogen pressure. When this impurity is saturated with hydrogen the solubility curve follows a normal Sievert's Law relationship at a slope which is assumed to be that for pure uranium. This suggests that the impurity which is responsible for this behaviour is present as a separate phase (possibly as a grain-boundary segregate) rather than as a solute within the uranium.

The composition of the two grades of metal are compared in Table 9 below, from which it can be seen that the major impurities of the commercial quality metal which are reduced in the purer sample are iron and carbon, (reduced from 100 p.p.m. to 8 p.p.m., and from 450 p.p.m. to 65 p.p.m. respectively).

VOL. 9 1961

TABLE 9

The composition of the uranium samples used by Davies[129] (expressed as p.p.m. by weight)

Element	Al	B	Be	C	Ca	Co	Cr	Cu
Commercial uranium	20	0·5	<0·1	450	<10	5	7	15
Super-pure uranium	5	0·2	<0·2	65	<10	<10	16	20
Element	Fe	Li	Mg	Mn	Na	Ni	Si	V
Commercial uranium	<100	0·1	0	3	<1	25	50	10
Super-pure uranium	8	0·2	1·2	8	<1	20	25	8

7.3 *The Characteristics of the Hydrogen Embrittlement of Alpha-Uranium*

Recent American work[4, 129] has shown that the mechanical properties of alpha-uranium are impaired by the presence of hydrogen, although the information which is available on this effect is limited when compared with that concerning steel, titanium and zirconium. MARSH, MUHLENKAMP and MANNING[6] have shown that uranium undergoes a brittle-to-ductile transition at about room temperature under normal tensile conditions. They have shown that increasing the hydrogen content from approximately 0·8 p.p.m. to 4·7 p.p.m. (i.e. from approx. 0·02 atomic per cent to approx. 0·11 atomic per cent) raises the transition temperature and hence causes a severe drop in the ductility at room temperature. The pertinent results are given in Table 10 below.

TABLE 10

The effect of hydrogen on the ductile-to-brittle transition of uranium[4]

H_2 *content* 0·8 *p.p.m.* (0·02 *at.* %)			H_2 *content* 4·7 *p.p.m.* (0·11 *at.* %)		
Temperature (°C)	*Elongation* (%)	*Reduction of area* (%)	*Temperature* (°C)	*Elongation* (%)	*Reduction of area* (%)
− 56	10·5	9·2	24	13·5	12·9
10	12·5	11·2	66	28·5	30·5
24	32·5	28·0	100	30·0	41·0
100	39·0	51·0	149	35·5	45·0

Unfortunately the authors did not investigate this effect at hydrogen contents between the values quoted above or the effect of strain-rate. However, following his investigation of the solubility at low hydrogen pressures, DAVIES[129] determined the variation of the embrittlement effect in the temperature range from − 50°C to 100°C for hydrogen contents up to 5 p.p.m. (0·12 atomic per cent), by annealing tensile specimens, at either 600°C or 700°C, in hydrogen at various pressures, and testing at a strain rate of 2·5 per cent per min.

The shape of the stress–strain curve, prior to fracture, was unaffected by the hydrogenation treatment, the general effect of hydrogen being to reduce the elongation at fracture. A considerable proportion of the decrease in ductility takes place after annealing in hydrogen at pressures below 4 mm Hg. The dependence of ductility on the hydrogen content is clearly shown in Fig. 26. The change from ductile to (relatively) brittle behaviour occurs at

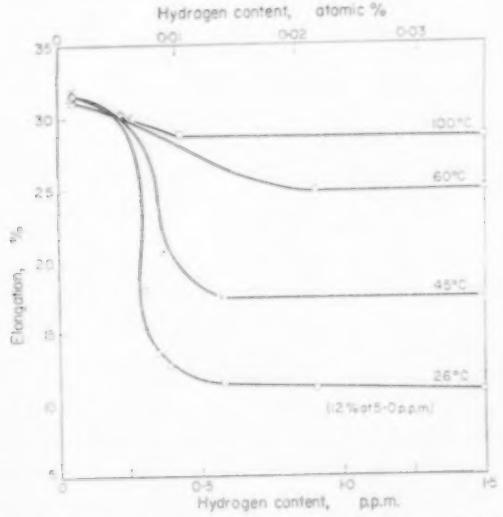

FIG. 26. The effect of hydrogen on the tensile elongation of alpha-uranium at a strain-rate of 2·5% per min; after DAVIES.[129]

hydrogen concentrations of the order of 0·3 p.p.m. (approx. 0·007 atomic per cent). DAVIES[129] also interprets his results in terms of the elevation of the ductile-to-brittle transition temperature by hydrogen. In alpha-annealed hydrogen-free uranium the transition temperature is said to be of the order of -10°C, whilst for the β-annealed uranium the transition temperature is about $+15$°C. In each case the presence of hydrogen raises the transition temperature to approximately 45°C.

Davies found that the ductility of his "as received" metal was very similar to that of the hydrogenated specimens. This is to be expected since he found that the hydrogen content of these specimens was of the order of 2 p.p.m. (approx. 0·0048 atomic per cent) which is a much higher content than that needed to cause embrittlement in his specimens. However, the quantity of hydrogen which is needed to cause embrittlement is not constant, since the hydrogen content of MARSH *et al.*[4] ductile specimens was of the order of 0·8 p.p.m.; a content which is higher than that which caused embrittlement in DAVIES[129] specimens. It is therefore suggested that the quantity of hydrogen leading to embrittlement varies from material to material, and possibly depends on such factors as the metallurgical history and purity of the specimen.

VOL. 9 1961

7.4 *The Mechanism of Hydrogen Embrittlement in Alpha-Uranium*

In discussing the mechanism of the hydrogen embrittlement of alpha-uranium it is important to note (from DAVIES' work[129]) that the embrittlement occurs at very low hydrogen contents and that further increases in the hydrogen content do not cause any decrease in ductility. Furthermore, for material of a given composition the embrittling concentration of hydrogen remains constant as the temperature is raised, although the embrittlement effect which it causes decreases.

It has been suggested[4] that the effect may be due to the precipitation of hard particles of the hydride within the uranium—as is the case for alpha-titanium and alpha-zirconium. However, DAVIES[129] did not find any metallographic evidence of a second phase in his embrittled specimens and it is therefore suggested that some other mechanism may be responsible for the embrittlement of alpha-uranium. This being the case, considerable significance is attached to the variation of hydrogen solubility with pressure and specimen purity (Fig. 25) since the embrittlement effect occurs at much the same hydrogen content as the change in slope of the solubility–pressure curve for the commercially pure metal.

The steep slope of the early part of this curve is taken to indicate that hydrogen is preferentially absorbed by impurities which must therefore be present as segregated constituents—probably at the grain boundaries. The reduced slope for the purified metal, and for the commercially pure metal above 0·3 p.p.m. (hydrogen), is taken to represent the true solubility–pressure relationship for alpha-uranium. In this case two different embrittlement mechanisms may apply. Firstly, the mechanical properties may be unaffected

by the initial dissolution of hydrogen in the impurities, but embrittlement may arise as soon as hydrogen enters into solution within the uranium. In this case one would expect the embrittlement effect to be due to the stress-induced local interstitial segregation of hydrogen similar to that which has been postulated in the hydrogen embrittlement of steel. Secondly, the embrittlement effect may be concerned with the formation of hydrides by impurities situated at the grain-boundaries, when the hydrogen content exceeds a critical value. If this latter mechanism is the case it is to be expected (*a*) that the critical hydrogen content will be low (since the amount of hydride forming impurities present in also low), and (*b*) that no further embrittlement will occur at hydrogen contents above this critical value: both of which criteria apply, according to DAVIES.[129]

The proposed influence of the impurity content on the embrittlement phenomena is to some extent corroborated by the fact that the embrittling concentration of hydrogen differed in the two investigations: i.e. MARSH *et al.*[4] observed the normal ductility at room temperature in specimens containing 0·8 p.p.m. (0·02 atomic per cent) hydrogen, whereas DAVIES[129] found that the embrittlement took place considerably below this concentration; although the hydrogen embrittlement of alpha-titanium varies with the impurity content without being due to such an impurity hydride type of mechanism.

However, there are two factors which suggest that this effect is not due to the diffusion of hydrogen in the uranium lattice (as in the case of steel). Firstly, the embrittling concentration does not vary significantly with temperature which suggests that the process is not controlled by the diffusion of hydrogen or by the precipitation of a uranium hydride phase. Secondly, the effect of hydrogen is to raise the brittle-to-ductile temperature rather than to give rise to a ductile-brittle-ductile fracture sequence, as in steel, which also suggests that the mechanism differs from that in this latter metal.

The similarities between the embrittling hydrogen content and the effect of impurities on the hydrogen solubility–pressure curve suggest that these two effects are related. The preferential solution of hydrogen in some impurity phase (which is so far unidentified) situated at the grain-boundaries of the metal may reasonably be expected to cause embrittlement by increasing the "dislocation-barrier" effect of the grain-boundaries. This would occur if the stress–concentration effect of a dislocation "pile-up" (at such an impurity) was to be increased, in comparison to that of a hydrogen-free sample, so that a brittle-fracture would be initiated before nearby dislocation sources could be brought into operation to cause ductile behaviour.

Hence the effects of such a grain-boundary segregation of a hydrogen-containing phase would be (*a*) to raise the ductile-to-brittle transition temperature of the metal (compared to that of the hydrogen-free metal), and (*b*) to cause an inter-granular brittle fracture: both of which results were observed by each investigation.[4, 129] The effect of temperature on the phenomenon can then be explained by assuming that the relevant impurity

is taken into solution as the temperature is increased, although it is difficult to see why embrittlement should then still occur at the same hydrogen content.

It would therefore appear to be fair to conclude that although the mechanical properties of alpha-uranium are affected by the presence of hydrogen, in quite low concentrations, the precise mechanism by which the embrittlement occurs is by no means clear. The most likely mechanism is that loss of ductility results from the formation of a hydrogen-rich phase, connected in some way with the impurities at the grain-boundaries of the uranium.

8. The Hydrogen Embrittlement of the Body-Centred-Cubic Metals

8.1 *General Introduction*

The requirements of modern industrial techniques (e.g. the aircraft and/or nuclear power industries) have led to the study and development of many metals which were until recently regarded more as metallurgical curiosities than as commercially useful materials. It is not surprising, therefore, that comparatively little is known about the occurrence of hydrogen in the metals, vanadium, niobium, and tantalum. However, recent American[5, 132] and French[133] work has suggested that, along with the body-centred-cubic metals molybdenum and tungsten, they are susceptible to a hydrogen embrittlement effect when tested at slow strain-rates in the region of room temperature. These observations have caused Baldwin[132] to remark that . . . "It appears possible that the hydrogen embrittlement of b.c.c. metals (including molybdenum) follows a stereotyped pattern."

8.2 *The Metal-Hydrogen Systems for these Metals*

8.2.1 *Group VA (vanadium, niobium and tantalum)*

The amount of published information on the metal-hydrogen systems for vanadium, niobium and tantalum is very limited. However, Duschmann[16] classifies them as exothermic occluders, along with titanium and zirconium. Unpublished data on the structure of vanadium hydride (which corresponds to the formula $VH_{0.92}$) suggests, but does not prove, that the hydrogen atoms lie in a simple cubic planar array which is parallel to one set of (100) vanadium atom planes.[5] Although very little is known about the solid-solubility of hydrogen in the metal, Sieverts and his co-workers[134, 135] have shown that the sorption of hydrogen to form this hydride obeys the usual $\sqrt{P}$ law indicating that the hydrogen is dissolved in the atomic form.

Sieverts and Bergner[136] have shown that a tantalum wire heated in vaccuo to 1200°C can absorb hydrogen slowly at temperatures above 500°C. However, if the wire is saturated with hydrogen at higher temperatures, it absorbs much more rapidly at lower temperatures.[16] As in the case of vanadium, the sorption of hydrogen by tantalum obeys the $\sqrt{P}$ law. There are three known phases in the tantalum–hydrogen system. According to Duschmann[16] the body-centred-cubic solid solution of hydrogen in

VOL. 9 1961

tantalum (the α-phase) occurs up to 12 atomic per cent of hydrogen; between 31 and 35 atomic per cent hydrogen the structure is that of a close-packed hexagonal lattice (the β-phase) 1 and between 48 and 52 atomic per cent hydrogen a γ-phase, having a slightly distorted b.c.c. structure, is formed.

Very little is known about the niobium-hydrogen system. The isotherms for 300°C and 400°C do not follow the $\sqrt{P}$ law, although this law applies (approximately) to isotherms at, and above, 500°C.[16, 137] As in the case of tantalum, sorption of hydrogen occurs very rapidly if the metal has been cooled after heating to 1100°C in a good vacuum. According to DUSCHMAN,[16] the maximum amount of hydrogen absorbed (corresponding to the maximum solubility in the hydride) corresponds to approximately 47 atomic per cent, which is said to be the lowest value observed for any of the exothermic occluders.

8.2.2 *Group VI A (chromium, molybdenum and tungsten)*

Chromium, molybdenum and tungsten are all endothermic occluders of hydrogen, consequently the solubility of hydrogen is very low and they do not form any hydrides. The solubility values for hydrogen in chromium and molybdenum quoted by DUSCHMANN[16] are given in Table 11 below, after having been converted from the original units (cm^3/100 g) to parts per million (by weight) and atomic percentages. The original investigations were by MARTIN,[138] for chromium, and by SIEVERTS and BRUNING,[139] for molybdenum.

Although tungsten is classified as an endothermic occluder the nature of the chemi-sorption effect of hydrogen on tungsten surfaces is such that no values have been quoted for the solubility of hydrogen within the metal; although it is to be expected that the solubility should be less than that in molybdenum: (see sections 2.2.2 and 2.5).

TABLE 11

The solubility of hydrogen in chromium and molybdenum (after Duschmann[16])

Temperature	*Chromium*			*Molybdenum*		
°C	cm^3 100 g	*p.p.m.* (*approx.*)	*at. %* (*approx.*)	cm^3 100 g	*p.p.m.* (*approx.*)	*at. %* (*approx.*)
400	—	—	—	0·165	0·15	$0{\cdot}6 \times 10^{-3}$
500	—	—	—	0·175	0·15	$0{\cdot}7 \times 10^{-3}$
600	0·5	0·45	$1{\cdot}1 \times 10^{-3}$	0·185	0·17	$0{\cdot}7 \times 10^{-3}$
700	—	—	—	0·21	0·19	$0{\cdot}8 \times 10^{-3}$
800	1·0	0·90	$2{\cdot}2 \times 10^{-3}$	0·25	0·23	$0{\cdot}9 \times 10^{-3}$
900	2·0	1·8	$4{\cdot}3 \times 10^{-3}$	0·29	0·26	$1{\cdot}1 \times 10^{-3}$
1000	3·0	2·7	$6{\cdot}5 \times 10^{-3}$	0·50	0·45	$1{\cdot}9 \times 10^{-3}$
1100	4·2	3·8	$9{\cdot}1 \times 10^{-3}$	0·62	0·56	$2{\cdot}3 \times 10^{-3}$

8.3 *The Characteristics of Hydrogen Embrittlement in these Metals*

In view of the very limited knowledge of the metallurgy of these metals it is not surprising that little is known about the details of the effect of hydrogen on their mechanical properties. However, ROBERTS and ROGERS[5] have reported that vanadium foils and wires containing hydrogen, either cold-worked or recrystallized, show a ductile-brittle-ductile fracture sequence with temperature. Their specimens were tested at a slow strain-rate at − 196°C, 24°C and 160°C after having been either (*a*) vacuum annealed or (*b*) heat treated to contain approximately 2 atomic per cent of hydrogen. The values of the reduction of area (for wires having an initial diameter of 0·035 in.) are given in Table 12, below.

TABLE 12

The reduction of area of vanadium wire of various hydrogen contents tested at a slow strain-rate in the range − 196°C to + 160°C (after Roberts and Rogers[5])

Material	*Hydrogen Content*		*Reduction of Area (%)*		
	Weight %	*Atomic %*	*at* − 196°C	*at* 24°C	*at* 160°C
Fine Grained Vanadium	0·003 0·042	0·15 2·1	64 33, 29	— 0	— 80
Coarse Grained Vanadium	0·003 0·045	0·15 2·2	60 29	77 8, 6	89, 90 —

Clearly, the hydrogen-containing wires are ductile at 160°C, the fracture in this case being of the typical ductile "cup and cone" type. However, at room temperature they are brittle and the fracture is of the cleavage type; whilst at liquid nitrogen temperatures they are again ductile, although to a lesser extent than at 160°C.

In the case of cold-rolled vanadium foil ROBERTS and ROGERS[5] found that specimens containing 0·1 weight per cent of hydrogen (4·9 atomic per cent) failed at room temperature by a cleavage fracture along the (100) planes of the sheet; which had a very pronounced (100) (110) texture. Hydrogen contents of the order of 0·15 weight per cent (6·9 atomic per cent) caused a brittle fracture to occur in random directions with respect to the rolling direction of the sheet.

BALDWIN[132] has investigated the variation of the ductility of vanadium containing 0·008 weight per cent of hydrogen (i.e. approximately 0·04 atomic per cent) as a function of strain-rate and temperature. His results are shown in Fig. 27, from which it can be seen that the characteristics of the embrittlement effect are very similar to those occurring in hydrogen-containing steel, i.e. an embrittlement effect which increases as the strain-rate decreases and which occurs to the maximum extent at intermediate temperatures.

VOL. 9 1961

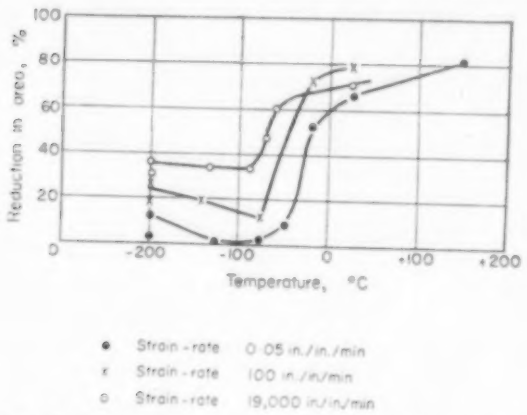

FIG. 27. Effect of temperature and strain-rate on the ductility of vanadium containing 80 p.p.m. (approx. 0·04 atomic %) of hydrogen; after BALDWIN.[132]

BALDWIN[132] also reports that preliminary experiments on tungsten and molybdenum indicate that similar ductility curves can be expected for these metals. He therefore suggests that all body-centred cubic metals may be susceptible to a slow strain-rate hydrogen embrittlement effect. It should be pointed out that according to Baldwin's results the optimum temperature for the hydrogen embrittlement of vanadium appears to be of the order of — 70°C, whereas that of steel is nearer room temperature (see section 4.2). However, this may well be due to a difference of degree rather than to a fundamental difference in the mechanism for the two cases. This is particularly so in view of the fact that the wires and foils tested by ROBERTS and ROGERS[5] showed a considerable embrittlement, due to hydrogen at room temperature.

Baldwin's generalization with regard to the hydrogen embrittlement of b.c.c. metals is strengthened by a recent French report of a slow strain-rate embrittlement effect in tantalum and niobium. CLAUS and FORESTIER[133] have reported that the rupture strength of tantalum wires is considerably reduced by the presence of hydrogen at room temperature. For example, hydrogenation is said to reduce the rupture strength of de-gassed tantalum filaments (of length 4 cm and diameters in the range 0·050 mm to 0·100 mm) by a factor of approximately 6 times. They also report that a similar effect has been found to occur in vanadium and niobium although in these cases no results are given.

This paper represents the only known publication concerning a hydrogen embrittlement in either tantalum or niobium. Unfortunately, therefore, little is known about the variation of this effect with strain-rate and/or temperature under normal tensile conditions in these two metals. However, by comparing the conclusions of BALDWIN's statements[132] concerning vanadium, molybdenum and tungsten with the scanty information contained in CLAUS and FORESTIER's paper[133] dealing with tantalum (and, by inference, with

niobium) it seems reasonable to conclude that each of these body-centred-cubic metals may suffer a slow strain-rate hydrogen embrittlement effect which is of the same kind as that occurring in steel.

8.4 *The Mechanism of Hydrogen Embrittlement in Body-centred-cubic Metals*

8.4.1 *Vanadium, niobium, tantalum, molybdenum, tungsten and steel*

The published evidence, to date, concerning the effect of hydrogen on the mechanical properties of vanadium, niobium, tantalum, molybdenum and tungsten is restricted to the few papers discussed above.[5, 122, 123] There is, therefore, very little direct evidence to suggest any details of the embrittlement mechanism. However, in view of the characteristics discussed above, it seems quite probable that the effect is fundamentally similar to that occurring in steel. Hence, the various points discussed in sections 4.2 and 4.3 should also apply to the metals mentioned above. In particular, it is to be expected that the variation of the ductility of hydrogen-containing samples of any one of the above-mentioned metals, as a function of ageing after plastic deformation, should be the same as that found by MORLET, JOHNSON and TROIANO[81] for steel.

The embrittlement is therefore likely to result from the accumulation of a localized hydrogen concentration at points of triaxiality near lattice imperfections, i.e. by a localized supersaturation of the metal lattice. Although a satisfactory account of the way in which such a super-saturated solution can lead to embrittlement may have to await the further development of a general theory of fracture, it is of interest to examine the factors affecting this hypothesis as they apply to the various body-centred-cubic metals.

In the case of steel, this localized concentration of hydrogen is said to be due to the precipitation of "gaseous" hydrogen from interstitial solution into internal "voids" within the specimens.[81] It should be noted that these "voids" are taken (by MORLET *et al.*[81]) to be any lattice imperfections which are large compared to the size of a lattice unit cell. This then poses the question as to what is the nature of the site at which this localized concentration occurs.

In discussing the effect of hydrogen on the yield point of armco-iron ROGERS[80] has shown that a "Cottrell-atmosphere" of hydrogen would be less tightly bound to a dislocation than would one of carbon or nitrogen. In this case hydrogen cannot be expected to displace any significant amounts of carbon and/or nitrogen from their normal position around dislocations, but rather it should only attach itself to a very few dislocation loops if they have been freed from the latter by thermal vibrations or similar effects. Since the number of "free" dislocations will be very low indeed it therefore becomes apparent that the localized concentration of hydrogen referred to above must occur (at any rate in iron and steel) as a relatively high concentration of hydrogen atoms in conventional interstitial solution within a locally

VOL. 9 1961

perfect metal lattice. It is therefore relevant to consider the effect of such a solution on the stress-state within a specimen.

As HUME-ROTHERY and RAYNOR have pointed out[34] geometrical considerations of the body-centred-cubic structure show that, in spite of its more open structure, this type of lattice cannot contain such large spheres in its interstices as can be accommodated in a close-packed array (face-centred-cubic or close-packed hexagonal) built up from atoms of the same size. This is because in a close-packed lattice the octohedral hole is capable of containing the largest interstitial sphere, whereas in the body-centred-cubic arrangement this hole is extremely distorted in shape, and consequently can only contain a sphere the radius of which is not greater than 0·154 times that of the solvent atoms. The symmetrical holes in the body-centred-cubic structure are of the tetrahedral type and their size is such that they can only accommodate spheres having a radius which is not more than 0·291 times that of the solvent atoms—which is smaller than the size of a sphere which can be contained in the octohedral hole of a close-packed lattice: (0·41 times the metal atom diameter).[34]

Table 13, below, lists the closest distance of approach (as given by HUME-ROTHERY and RAYNOR[34]) for each of the metals which crystallize with a body-centred-cubic structure. These values can be taken as the atom diameters for this structure and the sizes of the tetrahedral interstices (0·291 × the atom diameter) have been calculated on this basis, for each of these metals.

TABLE 13

The hydrogen occlusion behaviour and the size of the tetrahedral interstice for each of the body-centred-cubic metals (after Hume-Rothery and Raynor[34])

Metal	*Chemical group*		*Atomic diameter* (kX *units*)	*Diameter of tetrahedral sphere* (kX *units*)	*Type of occlusion behaviour with hydrogen*
β- Titanium	IV	A	2·86*	0·83*	Hydride-forming exothermic occluders
β- Zirconium	IV	A	3·13†	0·91†	
Vanadium	V	A	2·63	0·76	
Niobium	V	A	2·85	0·83	
Tantalum	V	A	2·85	0·83	
Chromium	VI	A	2·49	0·73	Endothermic occluders, *not* hydride formers
Molybdenum	VI	A	2·72	0·79	
α- Tungsten	VI	A	2·74	0·80	
α- Iron	VIII	A	2·48	0·72	

* At 900°C; † at 867°C.

The diameter of a hydrogen atom is usually taken to be of the order of 1·05 kX units, which is considerably larger than that of the largest sphere

which can be fitted into the tetrahedral interstices of any of the body-centred-cubic metals mentioned above (see Table 13). This therefore suggests that the localized concentration of hydrogen atoms, in the tetrahedral holes of an otherwise locally perfect body-centred-cubic lattice will cause considerable internal strain in this region. Furthermore, on the basis of the mechanism proposed by MORLET *et al.*[81] to explain the hydrogen embrittlement of steel, it is suggested that these regions of interstitial super-saturation with respect to hydrogen—occur at points where the internal stress achieves maximum triaxiality during a tensile test. Hence, it is conceivable that a brittle (cleavage) fracture may be initiated as the result of a very localized concentration of strain energy *within the* lattice of these metals. Such a region would be near to, but not in contact with, the normal lattice imperfections which occur in all metal crystals. It is important to note that the strain energy concentration referred to above is the additive result of two factors: namely (*a*) the "mis-fit" between a hydrogen atom and the surrounding metal atoms and (*b*) the triaxiality of the stress-system at this point.

VOL. 9 1961

It is to be expected that this hetereogeneous distribution of hydrogen will not arise until the metal has been subjected to plastic deformation, since in an unstrained specimen there will be a steady-state distribution of hydrogen between that in solution in the lattice and that in the "gaseous" form within internal "voids". On straining, the "voids" will be enlarged, and hence the pressure within them will decrease, thereby disturbing the distribution of hydrogen between the lattice and the "voids". Consequently, hydrogen will diffuse towards the "voids" and in so doing will also be attracted to the positions of triaxiality near to these internal defects.[81, 83] The stress-distribution will then be such as to cause hydrogen to segregate at these points of triaxiality[83] and the resultant intensification of the strain-energy in these regions will lead to the initiation of a brittle fracture at these points.

The above description of the sequence of events leading to the brittle fracture of a hydrogen-containing body-centred-cubic metal is based entirely on Morlet, Troiano and Johnson's mechanism for the hydrogen embrittlement of steel.[81] It is entirely consistent with all the factors discussed, for that metal, in sections 4.2 and 4.3. If it is true to say that the body-centred-cubic metals mentioned above (V, Nb, Ta, Mo and W) suffer a fundamentally similar form of embrittlement then the same sequence of events must apply in their case also. In the case of vanadium, hydrogen-containing samples fracture by cleavage along the (100) planes. It is therefore perhaps significant that the tetrahedral interstices, which are said to contain the embrittling hydrogen atoms, occur in sets of four which are parallel to the cube faces of the body-centred-cubic lattice.[34]

The metals vanadium, niobium and tantalum are all hydride-forming exothermic occluders, whereas molybdenum, tungsten and iron are all endothermic occluders which do not therefore form any hydride phases (see Fig. 1, section 2 and Table 13 above). The significance of this difference with respect to the occlusion behaviour lies in the fact that the embrittlement of

the latter metals cannot be associated with the formation of a hydride phase. Hence, if the hydrogen embrittlement of all the above metals occurs by fundamentally the same mechanism, it equally cannot be concerned with the formation of hydride phases in the former metals. The conclusion to be drawn from this analysis is therefore that the minimum hydrogen content which is likely to be required to cause embrittlement in the metals vanadium, niobium and tantalum must be less than the limit of solid solubility for each case—within which composition range the metals in question are likely to behave in the manner as the endothermic occluders (see section 2.3). This deduction is consistent with BALDWIN's results,[133] since he found that the hydrogen embrittlement of vanadium can occur at hydrogen contents of the order of 80 p.p.m. (approx. 0·04 atomic per cent)—a value which is very likely to be less than the solid solubility of hydrogen in a member of the exothermic occluding group of metals.

The conclusion to be drawn from the above theory, as applied to the body-centred-cubic metals in general, is therefore that although the embrittlement results indirectly from the migration of hydrogen to expanding "voids" within the metal (during the course of plastic deformation) it is the hydrogen which remains in interstitial solution which actually causes the initiation of the brittle fracture.

8.4.2 *Beta-titanium and beta-zirconium (alloys)*

Any theory which attempts to postulate that the hydrogen embrittlement of body-centred-cubic metals occurs by a single mechanism, which is fundamental to this type of structure must be shown to be applicable to all such metals. The theory developed above has been shown to be applicable to the hydrogen embrittlement effects in steel, vanadium, niobium, tantalum, molybdenum and tungsten as they are known at present. As far as is known no work has been done on the effects of hydrogen on the mechanical properties of chromium. This metal occurs in the same chemical group as molybdenum and tungsten, and is metallurgically similar to these metals. Hence, in view of (*a*) the brittleness of chromium and (*b*) Baldwin's evidence for molybdenum and tungsten,[132] it is to be expected that a similar effect may be found to occur in chromium.

However, there is at least one body-centred-cubic metal which does not appear to be subjected to such an effect. This anomalous material is the molybdenum stabilized β-phase of titanium, for which CRAIGHEAD, LENNING and JAFFEE[99] have shown that in the case of an alloy containing 13·1 per cent molybdenum the reduction in area is as high as 90 per cent at a hydrogen content of 9 atomic per cent (0·19 weight per cent)—see Fig. 18, section 2.4. The reason for this anomalous behaviour is difficult to explain in terms of the general mechanism proposed above. Although it is perhaps not without significance that hydrogen is considerably more soluble in the β-phase of pure titanium than in any of the metals mentioned above (see section 5.1). The tensile tests on the molybdenum–titanium alloys were carried out at a

slow strain-rate at room temperature, which are the optimum conditions for the hydrogen embrittlement of the other body-centred-cubic metals. According to the data presented in Table 13 (above) the tetrahedral interstices in the β-phase of pure titanium (at 900°C) are no larger than those occurring in niobium and tantalum at room temperature. Hence it is suggested that the lattice parameters of the beta-titanium alloys referred to above are not likely to be sufficiently different from those of pure-titanium to account for the lack of embrittlement (in this case) on grounds of "size-factor" alone.

According to DUSCHMANN[16] the body-centred-cubic phase of tantalum can dissolve up to 12 atomic per cent of hydrogen into solid solution, whereas the geometrically similar β-phase of titanium has a limit of solid solubility (of hydrogen) which exceeds 44 atomic per cent.[89] It is therefore apparent that the limit of solid-solubility of hydrogen in these two metals is governed by some other factor(s) (presumably chemical) in addition to those of crystallographic geometry. It may very well be, therefore, that these factors are also responsible for the absence of a hydrogen embrittlement effect in beta-titanium, since the high solubility of hydrogen under equilibrium conditions in this case, suggests that stress-induced localized concentration of hydrogen in interstitial solution will not lead to local straining, and consequent brittle fracture, as has been postulated as the mechanism of hydrogen embrittlement in other body-centred-cubic metals. In this case it is probably significant that the hydrogen embrittlement effect occurs most markedly in those metals (such as iron) which lie towards the centre of the periodic table, and for which the limit of solid solubility of hydrogen (and also the general chemical affinity for hydrogen) is smallest.

VOL. 9 1961

9. THE DEVELOPMENT OF A GENERAL THEORY OF HYDROGEN EMBRITTLEMENT IN METALS

9.1 *General Introduction*

The development of a general theory of the hydrogen embrittlement of metals requires that the resultant hypothesis should satisfy three conditions. Firstly, it must incorporate an explanation for the characteristics of each of the individual embrittlement effects which have been observed in various metals; secondly, it must be of sufficient general application to account for the absence of hydrogen embrittlement where such effects do not occur; and thirdly, it must also be compatible with the general aspects of (*a*) hydrogen-metal relationships, and (*b*) brittle fracture mechanisms, as they are each known at present.

The objects of this chapter are therefore to show that the mechanisms which have been proposed, by various workers, for each of the hydrogen embrittlement effects discussed previously are compatible with modern theories of the initiation of brittle fractures in metals and following this, to formulate a general theory of hydrogen embrittlement which fulfils the conditions listed above.

9.2 *Hydrogen–Metal Relationships and the Mechanisms of Brittle Fracture in Metals*

The nature of the inter-action between a metal and hydrogen depends principally on the chemical characteristics of the metal. The alkali and alkaline earth metals form malt-like hydrides, those in groups IVB, VB and VIB form co-valent hydrides, whilst those in groups IIB and IIIB do not react with hydrogen in any way.[16, 33] These metals are therefore of no interest from the point of view of a general survey of the problems of hydrogen embrittlement.

However, the remainder of the elements can be divided into two classes with regard to their behaviour with hydrogen. Firstly, the metals of groups IB, VIA, VIIA and VIII absorb hydrogen endothermically to form very dilute solid-solutions, the hydrogen content of which increases as the temperature and/or pressure increases. Secondly the metals of groups IIIA (except boron and aluminium) IVA and VA absorb hydrogen exothermically in order to form "Pseudo-metallic" hydrides.[16] In these cases it is necessary to draw a distinction between the solution of hydrogen into the metal, which occurs endothermically (as in the previous class of metals), and the formation of this hydride phase, which occurs exothermically in a manner analogous to a chemical reaction. In view of their behaviour with hydrogen, metals in the former class are referred to as "endothermic occluders", whilst the latter are referred to as "exothermic occluders" (see Fig. 1—section 2).

The diameter of the hydrogen atom (approximately 1·05 kX units) is less than a half that of the smallest metal atom (beryllium). Hence, hydrogen is generally regarded as being present, within metals, in interstitial solid-solution. SMITH[9] has recently written a monograph in which he questions the existence of a true solid-solution of hydrogen in metals, and postulates that hydrogen is present within "rifts", or lattice defects, within the interior of a metal. However, there is a considerable amount of opposition to this hypothesis, which is entirely qualitative. In many cases, the various aspects of hydrogen–metal phenomena can best be explained by a more simple hypothesis of lattice solution and diffusion.[27] The results of the present review would suggest that this is particularly so in the case of hydrogen embrittlement phenomena.

In general the deformation of metals occurs by means of the movement of dislocations along certain preferred directions (the "slip directions") within the individual crystals of the metal. Under these conditions the moving dislocations tend to accumulate—or "pile-up"—at barriers (such as grain-boundaries or hard precipitate particles) situated at the ends of slip-planes. It is then easy to visualize that such a "dislocation pile-up" will lead to the formation of an embryo micro-crack and/or intensive local stress concentration at such a barrier.

At high temperatures the general resistance of a metal to plastic deformation is low, and it is therefore relatively easy for such dislocation—containing slip systems to propagate. Under these conditions the effect of

these local stress concentrations is to initiate the propagation of another set of dislocations (slip systems) in the neighbouring material. This process may continue until the metal has been subjected to quite a large amount of plastic deformation; thereby resulting in considerable ductility.

However, the resistance to plastic deformation increases as the temperature decreases; i.e. the stress required to activate a neighbouring dislocation source (and to cause slip once the dislocations have been formed) increases as the temperature falls. Consequently, at low temperatures, the local stress concentration, which results from the "pile-up" of dislocations at the ends of slip planes, can lead to the formation, and propagation, of a micro-crack within the specimen before the neighbouring dislocation sources have been activated. Hence the metal fractures in a brittle manner after having sustained only a very small amount of plastic deformation.

VOL. 9 1961

Therefore, there will be some temperature at which the resistance to plastic deformation is so high that the localized stress concentration will just exceed the cohesive strength, before propagating nearby slip systems. Above this temperature the specimen will be ductile, since slip will occur before the formation of micro-cracks; whilst below it the reverse will be the case, and brittle fracture will occur. This, then is the ductile-to-brittle transition temperature.

Brittle fracture can be one of two types; (*a*) that which propagates around the grain-boundaries of a poly-crystalline specimen (intergranular fracture), or (*b*) that which propagates across a particular type of plane within a crystal (transgranular or cleavage, fracture). However, in either case, the fracture originates from the initiation of a micro-crack which has been formed by the concentration of internal stresses (usually at a piled-up group of dislocations) within the specimen. Hence, any change in the metallurgical condition of a specimen which increases the stress concentration within a specimen is likely to raise the ductile-to-brittle transition temperature by enhancing the formation and propagation of a micro-crack prior to the propagation of additional slip systems.

A typical example of this type of effect is the influence of a notch on the surface of a specimen. Such a notch creates a triaxial stress-system within the neighbouring material and causes a severe local stress concentration at the base of the notch, with the result that the critical stress required for the formation of a (brittle) micro-crack can be achieved at much lower applied stresses than in the absence of such a notch; whereas the unnotched material may exhibit ductile behaviour since the cohesive strength may not be exceeded before various slip systems have been brought into operation.

In each case, the various characteristics of hydrogen embrittlement have therefore to be explained in terms of the influence of the situation and effects of the dissolved hydrogen on the ability of the metal to withstand plastic deformation.

9.3 *The Mechanisms of Hydrogen Embrittlement in Individual Cases*

9.3.1 *Alpha-titanium and alpha-zirconium*

One of the simplest ways in which the change from ductility to brittleness

of a specimen can be affected by changes in its metallurgical condition is the occurrence of hard platelets of a second (precipitated) phase. In such cases, the sharp edges of a precipitated particle act as points of intensive internal stress-concentration and, hence, initiate a micro-crack leading to brittle fracture, at comparatively low applied stresses. Furthermore, precipitates of this type will obviously act as effective barriers to the propagation of dislocations, thereby causing a considerable number of dislocation "pile-ups" (with the resultant stress concentration and micro-crack formation) which would not occur in the absence of the second phase.

The hydrogen embrittlement of alpha-titanium and alpha-zirconium occurs as the result of the precipitation of a hydride phase of this type. In each case the solid-solubility of hydrogen in the alpha-phase increases very rapidly with increase in temperature; for example, in alpha-titanium the equilibrium solubility of hydrogen is of the order of 0·1 atomic per cent whereas at 300°C it is of the order of 8 atomic per cent,[89] whilst for alpha-zirconium the solubilities are of the order of 0·3 atomic per cent and 1 atomic per cent respectively.[111] In each case, the commercially pure metal usually contains significant quantities of a hydride precipitate.

In the case of alpha-titanium, it has been shown that this hydride is precipitated in the form of very narrow platelets along certain habit planes of the titanium crystal.[96] In the examination of four different alpha-titanium alloys, together with a sample of high-purity titanium, these precipitation planes have always been found to contain the $(10\bar{1}1)$ plane—which is one of the principal slip-planes of this metal. Furthermore, in both alpha-zirconium[11] and alpha-titanium,[96] the use of electron-microscopy has shown that, after fast strain-rate tensile testing, there was little evidence of any slip in the hydride-containing specimens; moreover, in many cases, twins terminated at these precipitate platelets, and, some cases, micro-cracks were seen at the twin-hydride interface.

It is likely that rapid strain-rates (e.g. impact testing and/or very fast tensile testing) enhance the possibility of brittle fracture in specimens in which the applied stresses are amplified by surface markings such as notches. It therefore appears to be quite certain that the hydrogen embrittlement effect in alpha-titanium and alpha-zirconium—which increases as the strain-rate increases,—is caused by the presence of a precipitated hydride phase, since specimens which do not contain this second phase exhibit considerable ductility under the same conditions.

The influence of temperature on the hydrogen embrittlement of alpha-titanium and alpha-zirconium arises, indirectly, as the result of the variation of the solubility of hydrogen with temperature. As the temperature is raised the solubility of hydrogen increases; hence, it is to be expected that the temperature at which the precipitation of the hydride phase occurs will increase as the hydrogen content increases. It therefore follows that the embrittlement effect will extend to increasingly higher temperatures as the hydrogen content is increased.

9.3.2 *Alpha–beta titanium alloys*

The effect of hydrogen on the mechanical properties of the alpha–beta titanium alloys contrasts with that in alpha-titanium. Severe embrittlement occurs at slow strain-rates in the region of room temperature. The extent of this embrittlement decreases as the strain-rate increases, or as the temperature is either raised or lowered from the region of room temperature. In all cases, there is a very sudden and catastrophic drop in tensile ductility at a critical hydrogen content, the value of which depends upon the temperature, the strain-rate and the composition of the alloy in question.

The mechanism of this effect has been described as being due to the stress-induced diffusion of hydrogen from solution within the beta-phase (in which hydrogen is extremely soluble) to cause segregation at the alpha–beta phase boundaries.[101] It is important, in this respect, to note that recent work based on the combined use of the electron microscope and autoradiography has shown that a hydrogen-containing phase exists in small amounts, at the alpha–beta boundaries of a complex alloy, containing 2·7 atomic per cent of hydrogen.[100] In the course of this examination it was shown that this hydrogen-containing constituent was produced as the result of thermal ageing. It is therefore conceivable that a similar type of hydrogen segregation may occur as the result of strain-ageing during the deformation of this type of alloy.

The facts that the extent of the embrittlement decreases as the strain-rate increases (thereby reducing the time available for the stress-induced diffusion of hydrogen) and as the temperature decreases (below room temperature) are taken to suggest that the effect is controlled by a diffusion process. The decrease of the embrittlement effect as the temperature *increases* above room temperature has been said to be due to the increased ease of the thermal homogenization of any stress-induced hydrogen distribution.[101]

The initiation of a brittle-fracture, in this case, probably arises from the increased "dislocation blocking" effect of the alpha–beta grain boundaries as the result of the presence of this diffusion-controlled hydrogen-rich constituent. It is important, in this respect, to note that the brittle fracture of such a hydrogen-containing alloy is of the *inter*-granular type, as would be expected on the basis of the above mechanism. Finally such a mechanism requires the accumulation of a critical amount of the hydrogen-containing phase before an intergranular (brittle) fracture can be initiated at the expense of the propagation of ductility-giving dislocation sources in nearby material. This mechanism therefore explains why a critical hydrogen content has to be exceeded before the embrittlement occurs, and also why further increases in the hydrogen content do not lead to further losses of ductility.

9.3.3 *The hydrogen embrittlement of alpha-uranium*

Uranium—like titanium and zirconium—is a member of the hydride-forming "exothermic occluding" group of metals. However, unlike the cases of alpha-titanium and alpha-zirconium, the hydrogen embrittlement of alpha-uranium is not caused by the visible precipitation of a hydride phase.

VOL. 9 1961

The amount of information which is available regarding the effect of hydrogen on the mechanical properties of alpha-uranium is very limited, and it is not possible, therefore, to decide upon the embrittlement mechanism with any certainty.

It is significant that the embrittlement occurs suddenly (and completely) at a hydrogen concentration which coincides with that of a rapid change in the slope of the hydrogen pressure–solubility curve.[129] This latter change of slope has been postulated as being due to the preferential absorption of hydrogen in the impurities which are present in commercially pure metal, followed by a more gradual solution in the uranium itself. In this case, the embrittlement effect is most likely to be due to the preferential solution of hydrogen in the impurity constituents (which are presumably situated at the grain-boundaries) which may lead to the formation of an embrittling phase. Hence, the initiation of fracture, in alpha-uranium may well arise from the same general cause as that in alpha–beta titanium; i.e. the "dislocation blocking" effect of a hydrogen-rich phase at the grain boundaries. Again the fracture is of the intergranular type.

However, the factors leading to the formation of this embrittling phase differ in the two cases. In alpha-uranium, the phase is formed as the result of the preferential solution of hydrogen in impurities. It is therefore to be expected that this phase is present *before* the application of an external stress. Indeed, the characteristics of the effect in this case, whilst fully compatible with the mechanism proposed above, show quite clearly that it is not controlled by the stress-induced diffusion of hydrogen during the test. However, the embrittlement still occurs at a critical hydrogen content, as is to be expected from the formation of a grain-boundary embrittling phase.

9.3.4 *The body-centred-cubic metals, including steel*

In the case of the body-centred-cubic metals hydrogen embrittlement has been found to be a maximum during the course of slow strain-rate tensile tests at room temperature. The difference in ductility between specimens which contain hydrogen and those which are hydrogen-free decreases as the temperature is raised or lowered beyond room temperature. It is considered that, prior to the deformation of such metals, some of their hydrogen content is present as "gaseous" hydrogen within microscopic imperfections in the metal structure. This "gaseous" hydrogen is then considered to be in a state of thermodynamic equilibrium with the remainder of the hydrogen content which is present in interstitial solution within the metal lattice.

As the result of plastic straining the imperfections are enlarged and hydrogen then diffuses towards them in order to produce a second equilibrium distribution. However, such imperfections act as sources of internal stress concentration within the metal and, hence, give rise to positions within the lattice at which the stress system is triaxial. It is considered that, as the result of the stress-distribution which is created at these regions of triaxiality, hydrogen is attracted to such regions during the course of its diffusion within

the metal.[83] Brittle fracture is said to ensue from this concentration of hydrogen within these triaxial regions.[81]

It has been shown that in the case of steel hydrogen is not attracted to dislocations as strongly as are carbon or nitrogen,[80] and it is therefore postulated that these triaxially stressed regions of hydrogen concentration must occur in locally perfect regions of the b.c.c. lattice. If this embrittlement mechanism is to be used to explain the hydrogen embrittlement effect in all the body-centred-cubic metals (which shows similar temperature and strain-rate characteristics in each case) then it is to be expected that similar concentrations will arise in all cases. Geometrical considerations of the b.c.c. structure have been used to show that such a supersaturation of interstitial solution of hydrogen—if formed—could lead to a considerable amount of local straining in all the body-centred-cubic metals considered. It is therefore very probable that such an effect may lead to a cleavage fracture—which is the type which is usually found in these cases of hydrogen embrittlement.

Obviously the formation of such regions of local super-saturation requires the diffusion of hydrogen to occur. The fact that such diffusion only takes place after the lattice imperfections have been enlarged by plastic deformation (since the interstitial hydrogen distribution will be homogenous in an unstrained metal) is used to explain the decreased extent of the embrittlement as the strain-rate is increased or the temperature lowered below room temperature. The fact that the embrittlement effect also decreases as the temperature is *raised above* room temperature is explained by postulating that the increased case of diffusion (at elevated temperatures) prevents the formation of the highly heterogeneous hydrogen distribution which is said to be needed to cause the embrittlement.

However, the lack of such an embrittlement effect in single-phase beta-titanium alloys is anomalous to this mechanism, since the size of the interstitial site in beta-titanium is of the same order as that in tantalum and niobium,—both of which exhibit this type of embrittlement effect. The fact that hydrogen is soluble in beta-titanium to the order of 44 atomic per cent suggests that the formation of an extensive interstitial solution in this metal is governed by some other factor(s), (presumably chemical) in addition to those of crystallographic geometry. However, it is possible that this high solubility of hydrogen in beta-titanium is responsible for the absence of a hydrogen embrittlement effect on this case, since it is the difficulty of the formation of a local concentration of interstitially dissolved hydrogen (without causing high internal strains) which is said to be responsible for the embrittlement of the other body-centred-cubic metals. (For example, the solubility of hydrogen in iron is of the order of 0·1 atomic per cent, whereas that in beta-titanium is of the order of 44 atomic per cent.

9.3.5 *The effect of hydrogen on the mechanical properties of the close-packed metals*

It has been suggested above that the presence of hydrogen in body-centred-

VOL. 9 1961

cubic metals can cause brittle fracture, under conditions for which the hydrogen-free metal fails in a ductile manner (by the generation of high internal strain-energies, at certain points within the metal lattice) as the result of the stress-induced diffusion of hydrogen to lattice defects and nearby positions of triaxial stressing. This has been explained in terms of the geometrical properties of the body-centred-cubic lattice, and, in particular by the fact that the hydrogen atom is much larger than the interstitial sites which are available for its solution in such a lattice. It is therefore relevant to consider the effects of the size of the hydrogen on the internal stress within the regions which surround its interstitial solution in the close-packed metallic lattices.

HUME-ROTHERY and RAYNOR [34] have shown that from the point of view of the size of their interstitial sites the close-packed-hexagonal lattice and the face-centred-cubic lattice can be considered to be geometrically equivalent to each other. In each case the largest interstitial site is that which is surrounded by six metals atoms forming the corners of an octohedron. If the lattice is regarded as being built up of close-packed spheres, of radius "r" then the octohedral hole will just contain a sphere of 0·41 r. These lattices also contain a set of interstices which are surrounded by four metal atoms arranged tetrahedrally. These are capable of containing spheres of radius 0·225 r. On the other hand, the geometry of the body-centred-cubic lattice is such that the octohedral interstices are very distorted in shape. This has the effect that the largest sphere which can be fitted into the body-centred-cubic lattice is one having a radius of 0·291 r, which would occupy the tetrahedral interstices. [34] Thus, despite its more open nature, the body-centred-cubic structure cannot contain such large interstitial spheres as can a close-packed structure, built up from atoms of the same size. It is considered that this difference in crystal geometry can be used to account for the difference in the behaviour of the mechanical properties of the two types of metals in the presence of dissolved hydrogen.

In the close-packed metals, the octohedral interstice exceeds 1·00 kX units in diameter (except in the case of beryllium—for which the octohedral diameter is 0·92 kX units). Hence, from the point of view of atomic "size-factors" hydrogen is capable of fitting into the octohedral interstices of the close-packed-metal lattices without causing the severe strains which are thought to be responsible for the embrittlement effect in body-centred-cubic metals. Consequently, one would not expect to find a slow strain-rate hydrogen embrittlement effect (of the kind which occurs in steel, etc.) in any of the metals which crystallize with either close-packed-hexagonal or face-centred-cubic structures (with the possible exception of beryllium).

The fact that the only hydrogen embrittlement effects which have been reported in the literature, as occurring in close-packed-metals, are those which are caused by the precipitation of a hydride phase in alpha-titanium and alpha-zirconium can be taken as evidence to support this hypothesis. The octohedral interstices of these metals have diameters which are of the order of

1·2 and 1·3 kX units respectively, whilst the tetrahedral interstices have diameters of the order of 0·66 kX units and 0·72 kX units respectively. It therefore follows that considerable amounts of interstitial solution of hydrogen could be tolerated, without the creation of internal stresses, in the lattice, if the hydrogen occupied the octohedral interstices. Hence, local concentrations of hydrogen in *octohedral* interstitial solution will not result in an embrittlement effect of the type which is proposed for the case of the body-centred-cubic metals, even though stress-induced diffusion of hydrogen towards the "voids" may produce such a heterogeneous hydrogen distribution.

It has been suggested that hydrogen occupies the tetrahedral, rather than the octohedral, sites in alpha-zirconium;[2] however, the evidence for this is not conclusive. It is important to note that these interstices are smaller than those in steel, in which the formation of such a solution—under the action of an applied stress—is said to give rise to the well-known embrittlement effect. If then, the mechanism proposed by MORLET *et al.*[81] for steel represents a true account of the phenomenon in that case, there would appear to be no reason why a similar effect should not occur in alpha-zirconium if the solution occurs solely in the tetrahedral sites.

VOL. 9 1961

However, no such effect has been found in the latter metal. This fact would be explained if any stress-induced local concentration of hydrogen was able to occur in the larger octohedral interstices, rather than the smaller tetrahedral sites, since this would then lead to little lattice strain and would not give the conditions required for brittle fracture. Brittle failure would then only be initiated when the solubility limit was exceeded, and hydride precipitation had occurred, as discussed previously.

9.4 *A General Theory of Hydrogen Embrittlement in Metals*

Modern theories of the mechanism of brittle fracture in metals are based on the formation and propagation of micro-cracks within the metal. These micro-cracks are said to be formed as the result of the general resistance to plastic (ductile) deformation of metals at the temperatures in question, whilst their propagation occurs when the release of elastic strain energy in the region surrounding the crack is sufficient to overcome the absorption of energy by the formation of a new surface (i.e. that of the sides of the crack) and also to increase the kinetic energy of the moving crack.[40]

It has been shown, above, that each of the mechanisms which have been proposed for the hydrogen embrittlement effects which have been observed to date is individually compatible with the conditions required for the formation of a micro-crack, and its propagation as a brittle fracture. It is to be noted that, although the detailed features of the characteristics and mechanisms of these effects differ in several cases, there are two features which are common to the characteristics of hydrogen embrittlement in all cases. These are, firstly, that the embrittlement effects always occur at temperatures which are just above those of the ductile-to-brittle transition for the corresponding hydrogen-free material, and, secondly, that the extent of the

embrittlement effect (i.e. the loss of ductility when compared to a hydrogen-free specimen under the same conditions) decreases as the temperature increases.

These two factors suggest a relationship between the effects of hydrogen and the dislocation theory of the brittle-to-ductile transition temperature in metals (see section 3.6 and 9.2), from which it is possible to formulate a general theory of hydrogen embrittlement in metals, which results from the development of the mechanism proposed by Morlet, Johnson and Troiano for the hydrogen embrittlement in steel.[81] It has been shown that, at a temperature which is just above that of its ductile-to-brittle transition, the deformation of a metal occurs by means of the propagation of a series of dislocations along the various slip systems which are available, thereby resulting in considerable ductility.

Consider now the case of a metal which contains a finite amount of hydrogen in solution and which is about to be subjected to a tensile deformation. Prior to the application of an external stress, to such a metal, there will be a steady-state equilibrium between the hydrogen which is present in interstitial solution and that which is present as "gaseous" hydrogen within the "voids" which are to be found in the metal. (N.B. Following MORLET *et al.*[81] a "void" is defined as any lattice imperfection which is large in comparison to the size of a lattice unit cell).

At the onset of *plastic* deformation the size of these "voids" will be increased. Hence the hydrogen pressure within them will decrease below that of the steady-state distribution which prevailed prior to straining. Hydrogen will then diffuse towards the "voids" in order to achieve a new distribution. However, the nature of these "voids" will be such as to lead to the formation of a triaxial stress-system at some nearby point *within the metal lattice*. It has been shown that, under these conditions, hydrogen will diffuse, not only towards the voids, but also towards these points of triaxiality; thereby causing the creation of a hydrogen concentration gradient which conforms to the induced stress-gradient.[83]

The essential feature of the present theory is that this stress-induced redistribution of hydrogen causes the formation of small regions of high hydrogen concentration at points of extreme triaxiality within the metal lattice. The consequences of this redistribution of hydrogen then depend upon the geometrical characteristics of the metal structure. In the case of the body-centred-cubic metals, it has been shown that the formation of such an *interstitial* solution would lead to a considerable amount of local strain. It is therefore suggested that this internal strain, together with the triaxiality of the stress system at such a point, leads to the initiation of a (brittle) microcrack, within the metal crystal. This in turn leads to the premature failure of the metal by means of the propagation of a (brittle) cleavage fracture.

Such a mechanism explains the features of the hydrogen embrittlement phenomena of the body-centred-cubic metals as they are known at present, including the fact that the fracture in these cases is usually of the cleavage

type. If it represents a true account of the sequence of events in such cases, it can also be shown to account for the absence of such an effect in the close-packed-metals if it is assumed that the localized hydrogen concentration occurs in the octohedral interstices of these metals. This latter assumption seems reasonable in view of the fact that the internal energy of such a system would be considerably reduced, by the formation of an *octohedral* solution (due to the absence of any lattice deformation energy) as compared with that which would arise if the postulated concentration of hydrogen was to occur in the smaller tetrahedral interstices.

It can therefore be concluded that the postulated nature of the hydrogen embrittlement effect in the body-centred-cubic metals precludes the occurrence of a similar effect in the close-packed-metals. However, the mechanical properties of the latter metals can be expected to be severely affected by the occurrence of a second (hydrogen-rich) phase, as the result of its effect upon the movement of dislocations within the slip-systems of the metal. It is suggested that the hydrogen embrittlement of alpha-titanium, alpha-zirconium, alpha-beta titanium alloys and alpha-uranium, although differing considerably in detail, are all fundamentally of this latter type.

In the cases of alpha-titanium and alpha-zirconium the embrittlement arises from the presence of a hydride phase at hydrogen contents which exceed the equilibrium solid–solubility value. In the case of alpha-beta titanium alloys, the embrittlement arises from the stress-induced diffusion of hydrogen to form a non-equilibrium hydrogen-rich phase at the alpha-beta grain boundaries, whilst in the case of alpha-uranium the embrittlement arises from the equilibrium formation of an impurity–hydrogen phase (presumably at the grain-boundaries) during the absorption of hydrogen.

It is conceded that this hypothesis does *not* account for the absence of such an effect in the body-centred-cubic beta-titanium alloys. However, it is considered that the unidentified factors which are responsible for the high solubility of hydrogen in beta-titanium are also responsible for the lack of a hydrogen embrittlement effect in this metal, since it is the difficulty of the formation of a local concentration of interstitially dissolved hydrogen which is said to be responsible for the embrittlement of the body-centred-cubic metals.

It is therefore suggested that the presence of hydrogen within a metal will lead to an embrittlement effect if its solution and diffusion characteristics are such as to increase the possibility of the "piling-up" of dislocations, to form micro-cracks (and so initiate brittle fracture), at the expense of the general ability of the material to withstand plastic deformation. This embrittling condition can arise in one of two ways; firstly, as the result of an increase in the internal strain of a metallic lattice following the formation of a tightly-packed interstitial solution of hydrogen, and, secondly, as the result of the presence of particles of a hydrogen-rich phase which can act as barriers to the movement of dislocations, thereby causing a local stress-concentration and the initiation of a brittle fracture.

VOL. 9 1961

The general applicability of these two forms of hydrogen embrittlement is shown by a comparison of the behaviour of (say) alpha-titanium (group IVA) with that of vanadium (group VA). Each of these metals belongs to the exothermic occluding class, and they both, therefore, form pseudo-metallic hydrides the precipitation of which is likely to cause severe embrittlement. In the case of alpha-titanium, the crystal lattice is of the close-packed-hexagonal type, with the result that the interstitial solution of hydrogen does not cause severe internal straining—even if the hydrogen distribution is not homogenous. Hence, hydrogen-induced embrittlement does not occur (in alpha-titanium, etc.) until the hydrogen content is sufficiently high as to cause the precipitation of a separate hydride phase.

However, in the case of vanadium (a body-centred-cubic metal) the formation of local concentrations of hydrogen, in interstitial solution within the vanadium lattice, leads to severe internal strains as a result of the mis-fit between the size of the hydrogen atom and the interstice which it occupies. Hence, in this case (vanadium, etc.) hydrogen embrittlement occurs as the result of straining within the lattice, at hydrogen contents which are much lower than that needed to cause the precipitation of a hydride phase. The characteristics of this effect are therefore similar to those of the hydrogen embrittlement of the body-centred-cubic endothermic occluders.

Finally, it has been noted that hydrogen embrittlement always occurs at temperatures which are just above that of the ductile-to-brittle transition for hydrogen-free metal. Clearly, at temperatures below this value, the metal will be brittle whatever its hydrogen content, whereas as the temperature rises above this value it will become increasingly difficult to form, and propagate, brittle micro-cracks before plastic deformation occurs in adjacent regions. On the basis of the hypothesis developed above, the general effect of the presence of hydrogen is to produce an additional source of micro-cracks which can lead to the propagation of a brittle fracture. Hence, it is to be expected that this will be most readily noticeable at temperatures which are just above that of the ductile-to-brittle transition for the hydrogen-free metal.

The present hypothesis, therefore, represents an extension of Morlet, Johnson and Troiano's theory of the mechanism of hydrogen embrittlement of steel[81] to cover the wider range of metals, as a whole, rather than as a series of specific instances. It has been developed to explain not only those hydrogen embrittlement effects which have been found to occur in various metals but also the absence of such effects in many of the close-packed metals. It can be summarized, very briefly, in the following statement:

"Hydrogen embrittlement occurs under those conditions of composition, temperature, and strain-rate, for which the presence of hydrogen leads to the formation and propagation of (brittle) micro-cracks, when such cracks would *not* be formed in the absence of hydrogen; when these conditions do not apply the presence of hydrogen does *not* lead to embrittlement".

10. General Summary and Conclusions

In the cases of these metals which absorb hydrogen without suffering a loss of their metallic characteristics, (the so-called (*a*) "endothermic occluders" and (*b*) "exothermic occluders"), hydrogen is assumed to be present, in the metal, in one of two possible forms. Firstly, in the case of the endothermic occluders hydrogen is assumed to be present in normal interstitial solid-solution within the metal. This solution also occurs in the exothermic occluders when the hydrogen content is below the limit of the solid–solubility. Secondly, in the case of the exothermic occluders, hydrogen in excess of the limit of solid–solubility is present in the form of a "pseudo-metallic" hydride. However, the dependence of the solubility on the hydrogen pressure leads to the conclusion that the nature of the solid-solution, in either type of occluder, is such that there is a thermodynamic equilibrium between the hydrogen which is present, in interstitial solution and that which is present, as "gaseous" hydrogen, within the micro-porosities which occur in normal metals.

VOL.
9
1961

The hydrogen embrittlement of both the body-centred-cubic metals (excluding beta-titanium alloys and possibly beta-zirconium alloys) and alpha–beta titanium alloys occurs to maximum extent at, or about, room temperature. In each case the extent of the embrittlement decreases as the strain-rate is increased or as the temperature is raised, or lowered, from room temperature. In each case the embrittlement effect is due to the stress-induced diffusion of hydrogen to "preferred sites" within the lattice of these metals. In the case of the b.c.c. metals segregation is considered to occur in interstitial solution within the lattice, whilst in alpha–beta titanium alloys the segregation occurs at the alpha–beta phase boundaries.

The hydrogen embrittlement of alpha-zirconium and alpha-titanium occurs at fast strain-rates as a direct elevation of the ductile-to-brittle transition, by the presence of a hydride-phase, at hydrogen contents which are above that of the equilibrium solid-solubility at any given temperature. In the case of alpha-uranium, the embrittling effect of hydrogen has not been investigated as fully as in the metals mentioned above. However, the embrittlement, in this case, is said to result from the preferential solution of hydrogen in the impurities which are present in the metal of commercial purity.

General considerations of the current theories of the ductile-to-brittle transition effect in metals, together with a detailed survey of each of the individual cases mentioned above, have led to the formulation of a general theory of hydrogen embrittlement. This has been shown to account both for the characteristics of the individual cases of hydrogen embrittlement and also for the absence of such effects in many of the close-packed metals.

Briefly, it is considered that hydrogen embrittlement arises as the result of the formation of micro-cracks—leading to brittle fracture—in hydrogen-containing metals. This micro-crack formation can arise in one of two ways:

firstly, as the result of severe internal strains caused by the stress-induced formation of a local concentration of hydrogen in interstitial solution, (for the b.c.c. metals), or secondly, as the result of the embrittling effect of hydrogen-rich constituents within the grains (alpha-titanium or alpha-zirconium) or at grain-boundaries of metals (alpha–beta titanium alloys or alpha-uranium). The absence of an effect of the first type in the close-packed metals is considered to be due to the occurrences, in these metals, of octohedral interstices which are capable of accommodating hydrogen atoms without resulting in a distortion of their lattices.

11. Acknowledgements

The author wishes to express his grateful thanks to Mr. G. C. Ellis and Dr. B. C. Woodfine for their permission to undertake this survey of the literature, and for their continued interest in it: to Dr. A. J. Martin and Mr. R. E. Goosey for their many helpful discussions of the various problems involved in this subject, and to the staff of the library, A.W.R.E., whose assistance has made the compilation of a literature survey of this length possible.

12. References

(1) Pfeil, L. B.; *Proc. Roy. Soc.* A 112 (1926) 182.
(2) Rylski, O. Z.; Dept. of Mines and Technical Surveys, Mines Branch, Ottawa, Canada. PM.203 (CAN).
(3) Schwartz, C. M. and Mallett, M. W.; *Trans. Amer. Soc. Metals* 46 (1954) 640–654.
(4) Marsh, L. L., Muhlenkamp, G. T. and Manning, G. K.; U.S.A.E.C. Report No. B.M.I 980, unclassified.
(5) Roberts, B. W. and Rogers, M. C.; *J. Metals* 8 (10) (1956) 1213–1215.
(6) Roberts, B. W., Sears, G. W. and Zemany, P. D.; *Trans. Met. Soc. Amer. Inst. Mech. Engrs.* 212(i), pp. 71–73.
(7) Cupp, C. R.; *Progress in Metal Physics*, Vol. 4, Pergamon Press (1954) 105–167.
(8) Smithells, C. J.; *Gases and Metals*, John Wiley (New York) and Chapman and Hall (London), 1937.
(9) Smith, D. P.; *Hydrogen in Metals*, University of Chicago Press, 1948.
(10) Barrer, R. M.; *Diffusion in and through solids*, Cambridge University Press, 1941.
(11) Eastwood, L. W.; *Gases in Light Alloys*, John Wiley (New York) 1946.
(12) Fast, J. D.; *Phillips Technical Review* 6 (1941) 365; 7 (1942) 72.
(13) Smithells, C. J.; *Roy. Soc. Arts.* 86 (1938) (4472), p. 36, (4473), p. 951, (4474), p. 971.
(14) Smithells, C. J.; *Metal treatment* 1 (1935) 165.
(15) Rhines, N. F.; *Trans. Amer. Soc. Metals* 43A (1951) 174.
(16) Dushman, S.; *Scientific foundations of vacuum technique*, John Wiley (New York), 1950.
) Frankenburg, W. G.; *J. Amer. Chem. Soc.* 66 (1944) 1827.

[18] LANGMUIR, I.; *J. Amer. Chem. Soc.* 40 (1918) 1361.
[19] LANGMUIR, I.; *J. Chem. Soc.* 511 (1940). The 17th Faraday Lecture.
[20] VOLMER, M.; *Z. Physik. Chem.* 115 (1925) 235.
[21] FOWLER, R. H.; *Proc. Camb. Phil. Soc.* 31 (1935) 260, 32 (1936) 144.
[22] LAIDLER, K. J., GLADSTONE, S. and EYRING, H.; *J. Chem. Phys.* 8 (1946) 659.
[23] BENTON, A. F. and WHITE, T. A.; *J. Amer. Chem. Soc.* 52 (1930) 2335.
[24] TAYLOR, H. S.; *J. Amer. Chem. Soc.* 53 (1931) 578.
[25] KINGDOM, K. H. and LANGMUIR, I.; *Phys. Review* 24 (1924) 510.
[26] ROBERTS, J. K.; *Proc. Roy. Soc.* A 152 (1935) 445.
[27] RANSLEY, C. E.; *Metallurgical Abstracts* 16 (1949) no. 858.
[28] SPEISER, R., SPRETNAK, J. W. and TAYLOR, J. W.; *Trans. Amer. Soc. Metals* 46 (1954) 1168–1175.
[29] SMITHELLS, C. J. and RANSLEY, C. E.; *Proc. Roy. Soc.* A 150 (1935) 172–197.
[30] SEITH; *Z. Electrochem.* 39 (1933) 538.
[31] SEITH and HOFER; *Z. Electrochem.* 40 (1934) 318.
[32] LAIDLER, K. J.; *Pittsburgh Internat. Conf. on Surface Reactions*, Corrosion Publishing Co. Ltd., Pittsburgh, U.S.A., 1948.
[33] HURD, D. T.; *Chemistry of the Hydrides*, John Wiley (New York); Chapman and Hall (London), 1952.
[34] HUME-ROTHERY, W. and RAYNOR, G. V.; *The Structure of Metals and Alloys*, Inst. Metals, 1954, pp. 216–218.
[35] PETCH, N. J.; *Progress in Metal Physics*, Vol. 5, Pergamon Press (1954) 1–52.
[36] GRIFFITHS, A. A.; *Phil. Trans.* A 221 (1920) 163–198.
[37] INGLIS, C. E.; *Trans. Inst. Naval Arch.* 55 (1913) 219.
[38] SACK, R. A.; *Proc. Phys. Soc.* 58 (1948) 729.
[39] ELLIOTT, H. A.; *Proc. Phys. Soc.* 59 (1949) 208.
[40] OROWAN, E.; Welding Research Supplement. March 1955, pp. 1575–1605.
[41] OROWAN, E.; *Trans. Inst. Engrs.* Shipbuilding in Scotland (1945) 165.
[42] ZENER, C.; *Fracturing of Metals*, Amer. Soc. Metals, 1948, p. 3.
[43] CHANG, H. C. and GRANT, N. J.; *J. Metals* N.Y. 8 (5) (1956) 544–551.
[44] STROH, A. N.; *Phil. Mag.* 46 (380), pp. 968–972.
[45] STROH, A. N.; *Proc. Roy. Soc.* A 223 (1954) 404.
[46] ESHELBY, J. D., FRANK, F. C. and NARBORO, F. R. N.; *Phil. Mag.* 42 (1951) 351.
[47] PETCH, N. J.; *J. Iron St. Inst.* 174 (1953) 25.
[48] GREENWOOD, G. W. and QUARRELL, A. G.; *J. Inst. Metals* 82 (1954) 551.
[49] GILMAN, J. J.; *J. Appl. Phys.* 27 (11) (1956) 1262–1269.
[50] MOTT, N. F.; *Engineering* 16 (Jan. 2nd, 1948).
[51] GILMAN, J. J.; *Trans. Amer. Inst. Min.* (*Metall.*) *Engrs.* (1955) 1252.
[52] WESSEL, E. T.; *Proc. Amer. Soc. Test. Mater.* 49 (1957), pp. 149–169.
[53] BECHOLD, J. H.; *Acta. Met.* 3 (2) (1955) 249.
[54] ROBERTS, C. S., CARRUTHERS, R. C. and AVERBACH, B. L.; *Trans. Amer. Soc. Metals* 44 (1952) 1150.
[55] VREELAND, T., WOOD, D. S. and CLARKE, D. S.; *Trans. Amer. Soc. Metals* 45 (1953) 650.
[56] GEIL, G. W. and CORVILLE, N. L.; *Trans. Inst. Min.* (*Metall.*) *Engrs.* 197 (1953) 213.
[57] WESSEL, E. T.; *J. Metals N.Y.* 9 (7) (1957) 930–935.
[58] COTTRELL, A. H. and BILBY, B. A.; *Proc. Roy. Soc.* A 62 (1949) 49.
[59] COTTRELL, A. H.; *Dislocations and Plastic flow in metals*, Clarendon Press, Oxford, 1953.
[60] SIEVERTS, A.; *Z. Metallkunde* 21 (1929) 37.
[61] ARMBRUSTER, M.; *J. Amer. Chem. Soc.* 65 (1943) 1043.
[62] SIEVERTS, A., ZAPFE, G. and MORITZ, H.; *Z. Physik. Chem.* A 183 (19) (1938–1939).

VOL. 9 1961

(63) BUZZARD, R. W. and CLEAVES, H. E.; Dept. of Commerce. Nat. Bur. Standards, N.B.S. circular 511 (1951).
(64) SEABROOK, J. B., GRANT, N. J. and CARNEY, D.; *Trans. Amer. Inst. Min. (Metall.) Engrs.* 188 (1950) 1317–1321.
(65) HOBSON, J. D. and SYKES, C.; *J. Iron St. Inst.* 169 (1951) 209–220.
(66) SIMS, C. E. *et al.*; *Amer. Inst. Mech. Engrs.* Tech. Pub. 2454 (1948).
(67) ROGERS, H. C.; *Acta Met.* 2 (1954) 617.
(68) CRACKNELL, A. and PETCH, N. J.; *Acta Met.* 3 (2) (1955) 200.
(69) COTTRELL, C. L. M.; *Nature, Lond.* 170 (4338) (1952) 1079–1080.
(70) ZAPFFE, C. A.; *Materials and Methods* 32 (1950) 58–62.
(71) BARNETT, W. J. and TROIANO, A. R.; *J. Metals N.Y.* 9 (4) (1957) 486–494.
(72) BELL, W. A. and SULLY, A. H.; *J. Iron St. Inst.* 178 (1954) 15–18.
(73) PETCH, N. J. and STABLES, P.; *Nature, Lond.* 169 (1952) 842–843.
(74) PETCH, N. J.; *Phil. Mag.* 1 (8th Series No. 4) (1956) 331–337.
(75) DE KAZINSKY, F.; *J. Iron St. Inst.* 177 (1) (1954) 85–92.
(76) VAUGHAN, H. G. and DE MORTON, M. E.; *J. Iron St. Inst.* 182 (4) (1956) 389.
(77) VAUGHAN, H. G. and DE MORTON, M. E.; *British Welding Journal* 4 (1) (1957) 40–61.
(78) BASTIEN, P. and AZOU, P.; *Proc. First World metallurgical Congress.*, Amer. Soc. Metals (1951) 535.
(79) PLUSQUELLBEC, J., AZOU, P. and BASTIEN, P.; *C. R. Acad. Sci., Paris* (1957) 1195–1197.
(80) ROGERS, H. C.; *Acta. Met.* 4 (1955) 114–117 and 5 (1957) 112–113.
(81) MORLET, J. G., JOHNSON, H. H. and TROIANO, A. R., *J. Iron St. Inst.* (1958) 37–44.
(82) SIMS, C. E.; *Trans. Amer. Inst. Mech. Engrs.* (1950) 188.
(83) MORLET, J. G., JOHNSON, H. H. and TROIANO, A. R.; *Trans. Met. Soc. Amer. Inst. Mech. Engrs.*, August 1958, 529–538.
(84) CHANG, P. L. and BENNETT, W. D. G.; *J. Iron St. Inst.* 170 (1952) 208–213.
(85) MCQUILLAN, A. D.; *Proc. Roy. Soc.* A 204 (1950) 309–325.
(86) GIBB, F. D. R. and KRUSCHWITZ, H. W. JNR.; *J. Amer. Chem. Soc.* 72 (1950) 5365–5369.
(87) GIBB, F. D. R. and KRUSCHWITZ, H. W. JNR.; *J. Amer. Chem. Soc.* 73 (1951) 1751–1755.
(88) MCQUILLAN, A. D.; *J. Inst. Metals* 8 (1951) 1355.
(89) LENNING, G. A., CRAIGHEAD, C. M. and JAFFEE, R. I.; *J. Metals* 6 (1954) 367–376.
(90) HÄGG, R. M. and SHIPKO, F. J.; *J. Amer. Chem. Soc.* 78 (1956) 5155–5159.
(91) GIBB, P. D. R., MCSHARRY, J. J. and BRAGDON, R. W.; *J. Amer. Chem. Soc.* 73 (1951) 1751.
(92) HÄGG, R. M.; *Z. Phys. Chem.* (1931) 433–454.
(93) GULBRANSEN, E. A. and ANDREW, K. F.; *J. Metals N.Y.* 1 (1949) 741.
(94) JAFFEE, R. I.; *J. Metals N.Y.* (2) (1955) 247.
(95) CRAIGHEAD, C. M., MYLER, W. S. and MARTIN, D. C.; *J. Metals N.Y.* (1952) 1317–1319.
(96) LIU, T. S. and STEINBERG, M. A.; *Trans. Amer. Soc. Metals* 50 (1958) 455–477.
(97) BERGER, L. W., WILLIAMS, D. N. and JAFFEE, R. I.; *Trans. Met. Soc. A.I.M.M.E.* 212 (4) (1958) 509–513.
(98) BURTE, H. M. *et al.*; *Metal Progress* (1955) 115–119.
(99) CRAIGHEAD, C. M., LENNING, G. A. and JAFFEE, R. I.; *J. Metals N.Y.* 8 (8) (1956) 923–928.
(100) RIPLING, E. J.; *J. Metals N.Y.* 8 (4) (May 1956) 502–503.
(101) JAFFEE, R. I., LENNING, G. A. and CRAIGHEAD, C. M.; *J. Metals N.Y.* 8 (1956) 907–913.

[102] WILLIAMS, D. A. and JAFFEE, R. I.; *Materials and Methods* (1956) 96–97.
[103] BURTE, H. M. *et al.*; U.S.A.E.C. Report No. WADC–TR–54–616 (*un*classified).
[104] HUBER, O. J., GATES, J. E., YOUNG, A. P., POBERESKIN, M. and FROST, P. D.; *J. Metals N.Y.* 9 (5) (1957) 918–923.
[105] BROWN, J. T. and BALDWIN, W. M. JNR.; *J. Metals N.Y.* 6 (2) 1954.
[106] HÄGG, G.; *Z. Phys. Chem.* 11 (1930) 439.
[107] SIEVERTS, A. and GOTTA, A.; *Z. Anorg. Chem.* 187 (1930) 155.
[108] HALL, M. N. A., MARTIN, S. L. H. and REES, A. L. G.; *Trans. Faraday Soc.* 41 (1945) 306.
[109] MARTIN, S. L. H. and REES, A. L. G.; *Trans. Faraday Soc.* 50 (1954) 343–352.
[110] GULBRANSEN, E. A. and ANDREW, K. F.; *J. Electrochem. Soc.* 101 (11) (1954) 560–566.
[111] GULBRANSEN, E. A. and ANDREW, K. F.; *J. Metals N.Y.* 7 (1) (1955) 136–144.
[112] MALLET, M. W. and ALBRECHT, W. H.; *J. Electrochem. Soc.* 104 (3) (1957) 142–146.
[113] EDWARDS, R. K., LEVESQUE, P. and CUBICCIOTTI, D.; *J. Amer. Chem. Soc.* 77 (5.3.55) 1307–1311.
[114] EDWARDS, R. K. and LEVESQUE, P.; *J. Amer. Chem. Soc.* 77 (5.3.55) 1312–1316.
[115] BEVINGTON, C. F. D., MARTIN, S. L. and MATHEWS, D. H.; *Proc. Internat. Conf. of Pure and Applied Chemistry* 1, 1947.
[116] MUHLENKAMP, G. T. and SCHWARPE, A. D.; U.S.A.E.C. Report No. BMI 845 *un*classified.
[117] YOUNG, A. P. and SCHWARTZ, C. M.; U.S.A.E.C. Report No. BME 1100 *un*classified.
[118] SIDHU, S. S. and MCGUIRE, J. C.; *J. Appl. Phys.* 23 (1952) 1237.
[119] YOUNG, A. P. and SCHWARTZ, C. M.; *Trans. Met. Soc. Amer. Inst. Mech. Engrs.* 309–310 (June 1958).
[120] FROST, B. R. T.; *J. Inst. Met.* 82 (1953–1954) 456–462.
[121] FROST, B. R. T. and MASKREY, J. T.; *J. Inst. Met.* 82 (1953–1954) 171–180.
[122] RUNDLE, R. E.; *J. Amer. Chem. Soc.* 69 (1947).
[123] SPEDDING, F. H., NEWTON, A. S., WARF, J. C., JOHNSON, O., NOTTORF, R. M., JOHNS, I. S. and DEANE, A. H.; *Nucleonics* 4 (1949) 4.
[124] BURKE, J. E. and SMITH, C. S.; *J. Amer. Chem. Soc.* 69 (1947) 2500.
[125] GUERON, J., YAFFE, L.; *Nature, Lond.* 160 (1947) 575.
[126] GIBB, P. R. T., MCSHARREY, J. J. and KRUSCHWITZ, H. K.; *J. Amer. Chem. Soc.* 74 (1952) 6203–6207.
[127] MULFORD, R. N. R., ELLINGER, F. and ZACHARISSEN, W. H.; *J. Amer. Chem. Soc.* 76 (1954) 297.
[128] MATTRAW, H. C.; *J. Phys. Chem.* 59, 93–94.
[129] DAVIES, W.; U.S.A.E.C. Report No. KAPL 1548 (1956) *un*classified.
[130] SHULMAN, N., ANDERSON, J. S. and BLAKEY, R. E.; U.K.A.E.A. Report No. A.E.R.E. C/R 846 declassified.
[131] MALLETT, M. W. and TRZECIAK, M. J.; *Trans. Amer. Soc. Metals* 50, pre-print no. 36.
[132] BALDWIN, W. M. JNR.; *The Metal Molybdenum*, A.S.M. (1957) 279.
[133] CLAUSS, A. and FORESTIER, H.; *C.R. Acad. Sci., Paris* 246 (1958) 3241–3243.
[134] HUBER, H., KIRSCHFELD, L. and SIEVERTS, A.; *Ber. dtsch. chem. Ges.* 59 B (1926) 2891.
[135] KINCHFELD, L. and SIEVERTS, A.; *Z. Electro. Chem.* 36 (1930) 123.
[136] SIEVERTS, A. and BERGNER, E.; *Ber. dtsch. chem. Ges.* 44 (1911) 2934.
[137] HAGEN, H. and SIEVERTS, A.; *Z. Anorg. Chem.* 185 (1930) 225.
[138] MARTIN, E.; *Arch. Eisenhüttenw.* 3 (1929–1930) 407.
[139] SIEVERTS, A. and BRUNIG, K.; *Arch. Eisenhüttenw.* 7 (1933–1934) 641.
[140] PETCH, N. J. *Phil. Mag.* 3 (1958) 1089.

VOL. 9 1961

[161] COTTRELL, A. H.; *Trans. Amer. Inst. Mech. Engrs.* 212 (1958) 192.
[162] PETCH, N. J.; *Fracture*, Technology Press of Massachusetts Institute of Technology, John Wiley and Sons (N.Y.) and Chapman and Hall (London), 1959.
[163] KUNZ, F. W. and BIBB, A. E.; U.S.A.E.C. Report No. KAPL 2002 (1959) 10 pp. *un*classified.

CONTENTS OF PREVIOUS VOLUMES IN THE PROGRESS IN METAL PHYSICS SERIES

VOL.
9
1961

VOLUME 1

Progress in the Theory of Alloys G. V. RAYNOR
Theory of Dislocations A. H. COTTRELL
Crystal Boundaries R. KING and B. CHALMERS
Age Hardening of Metals G. C. SMITH
Hardening Response of Steels E. H. BUCKNALL and W. STEVEN
Preferred Orientation in Non-Ferrous Metals T. L. RICHARDS
Diffusion of Metals in Metals A. D. LE CLAIRE

VOLUME 2

Order-Disorder Changes in Alloys H. LIPSON
Rate Process in Physical Metallurgy I. I. BETCHERMAN
Anisotropy in Metals W. BOAS and J. K. MACKENZIE
Developments in Magnesium Alloys H. G. WARRINGTON
Internal Strains and Recrystallization R. W. CAHN
Researches on the Polygonization of Metals A. GUINIER and J. TENNEVIN
Polygonization in Strongly Deformed Metals C. CRUSSARD, F. AUBERTIN, B. JAOUL and G. WYON

VOLUME 3

Crystallography of Transformations J. S. BOWLES and C. S. BARRETT
Properties of Metals at Low Temperatures D. K. C. MacDONALD
Recent Advances in the Electron Theory of Metals N. F. MOTT
Twinning R. CLARK and G. B. CRAIG
Ferromagnetism URSULA M. MARTIUS
Quantitative X-ray Diffraction Observations on Strained Metal Aggregates G. B GREENHOUGH
Recrystallization and Grain Growth J. E. BURKE and D. TURNBULL
Structure of Crystal Boundaries B. CHALMERS

VOLUME 4

Internal Friction in Metals A. S. NOWICK
The Mechanism of Oxidation of Metals and Alloys at High Temperatures KARL HAUFFE
Gases in Metals C. R. CUPP
The Theory of Sintering G. A. GEACH
Theory of Dislocations A. H. COTTRELL
Diffusion in Metals A. LE CLAIRE
Nucleation J. H. HOLLOMON and D. TURNBULL

VOLUME 5

The Fracture of Metals N. J. PETCH
Geometrical Aspects of the Plastic Deformation of Metal Single Crystals R. MADDIN and N. K. CHEN
The Structure of Liquid Metals B. R. T. FROST
Report of Precipitation H. K. HARDY and T. J. HEAL
Solidification of Metals URSULA M. MARTIUS

VOLUME 6

The Effect of Hydrostatic Pressure on the Electrical Resistivity of Metals A. W. LAWSON
The Filamentary Growth of Metals H. K. HARDY
The Austenite : Pearlite Reaction R. F. MEHL and W. C. HAGEL
Recent Advances in Knowledge Concerning the Process of Creep in Metals A. H. SULLY
The Mechanism of Evaporation O. KNACKE and I. N. STRANSKI
Mosaic Structure P. B. HIRSCH

VOLUME 7

Equilibrium, Diffusion and Imperfections in Semiconductors J. N. HOBSTETTER
The Physical Metallurgy of Titanium Alloys R. I. JAFFEE
Thermodynamics and Kinetics of Martensitic Transformations LARRY KAUFMAN and MORRIS COHEN
The Stored Energy of Cold Work A. L. TITCHENER and M. B. BEVER
The Properties of Metals at Low Temperatures H. M. ROSENBERG

VOLUME 8

Work Hardening of Metals L. M. CLAREBROUGH and M. E. HARGREAVES
Grain Boundaries in Metals F. WEINBERG
X-ray Studies of Deformed Metals B. E. WARREN
Substructures in Crystals Grown from the Melt C. ELBAUM
Defects in Pure Metals W. M. LOMER

VOL.
9
1961

PROGRESS IN MATERIALS SCIENCE VOLUME 9
(INCORPORATING PROGRESS IN METAL PHYSICS)
GENERAL EDITOR: BRUCE V. CHALMERS

The Structure and Properties of Solid Solutions

by
J. M. SIVERTSEN and M. E. NICHOLSON
Department of Metallurgy, University of Minnesota, Minneapolis 14, Minnesota.

PERGAMON PRESS
OXFORD · LONDON · NEW YORK · PARIS

N

PERGAMON PRESS LTD.
Headington Hill Hall, Oxford
4 & 5 *Fitzroy Square, London, W.*1

PERGAMON PRESS INC.
122 *East 55th Street, New York* 22, *N.Y.*
Statler Center 640, 900 *Wilshire Boulevard,*
Los Angeles, California

PERGAMON PRESS S.A.R.L.
24 *Rue des Écoles, Paris V*e

PERGAMON PRESS G.m.b.H.
Kaiserstrasse 75, *Frankfurt-am-Main*

VOL.
9
1961

Copyright
©
1961
PERGAMON PRESS LTD.

Library of Congress Card Number 49—50107

Set in Times New Roman 10/12pt. and
made and printed in Great Britain at Page Bros. (Norwich) Ltd.

PROGRESS IN MATERIALS SCIENCE

(INCORPORATING PROGRESS IN METAL PHYSICS)

PUBLISHER'S NOTE

THE twelve years that have elapsed since the publication of the first volume of PROGRESS IN METAL PHYSICS has seen a great increase in the rate of publication of papers in this, as in most other fields of science, and realization that the physics of metals is an important part of, but not the whole of, the science of materials, a field of considerable practical and theoretical importance.

It is becoming extremely difficult, if it is not already impossible, for most scientists to keep up-to-date in their own and closely related fields by reading all the relevant original papers; one approach to the solution of this problem is the provision of adequate up-to-date critical review articles. For these reasons the Editor and the Publisher of PROGRESS IN METAL PHYSICS have decided to broaden the subject matter to include the whole of the field of the Science of Materials, and, in order to ensure maximum availability, to publish each article as a separate entity; thus, an individual subscriber need no longer purchase a whole volume in order to obtain some of the articles. This new procedure will make it possible to publish each article within five months of its receipt by the Editor.

VOL.
9
1961

THE STRUCTURE AND PROPERTIES OF SOLID SOLUTIONS

CONTENTS

1. Introduction 305

2. The Electronic Structure of Solid Solutions 306
   2.1 The formation of solid solutions 307

3. Theoretical Models of Solid Solutions 310
   3.1 Friedel's model 311
   3.2 Henry's model 316
   3.3 Varley's model 317
   3.4 Thermochemistry of solid solutions 317

4. Strain Energy, Atom Size and Lattice Spacings 325
   4.1 Atomic size and lattice spacings 326
   4.2 Strain energy contributions in solid solutions 332

5. Structure of Solid Solutions 334
   5.1 Formation of lattice defects and their interactions 335
   5.2 Observations of solid solution structure 343

6. Physical Properties and the Electronic Structure of Solid Solutions 350
   6.1 X-ray intensity and neutron diffraction experiments 351
   6.2 Electronic specific heats 355
   6.3 The electrical conductivity of solid solutions 361
   6.4 Final comments 373

Bibliography 374

VOL.
9
1961

THE STRUCTURE AND PROPERTIES OF SOLID SOLUTIONS

J. M. Sivertsen and M. E. Nicholson

1. Introduction

Although the concept of a solid solution in metals was described as far back as 1860 by Matthiessen, it was not until the exposition of the Phase Rule by Gibbs in about 1900 that the concept of a metallic solid solution became generally recognized. After the initial concept had been formulated, few developments in the theory of solid solutions occurred until X-rays were applied to the study of metal structures. Since that time, the development of the theory of solid solutions has advanced rapidly in two different stages.

During the decade before World War II, several significant advances were made. The first was due to Hume-Rothery, who set forth the factors which control the structure and properties of solid solutions. The second advance was the concept and theory of ordering in solid solutions set forth by Bethe and others. The Hume-Rothery rules were empirically determined and implied that the factors which controlled the structure of metals were the electronic structure of the solid and the apparent size of the solute and solvent atoms. Also during this period, the electron theory of metals developed rapidly, as a result of the work of Mott and Jones, Wigner and Seitz, J. C. Slater, and others. Applying the electron theory of metals to the problem of alloy formation resulted in significant advances in the theory of solid solutions during this period.

Recently the theory of solid solutions has again undergone significant improvements. This progress has resulted from the advances in two fields of metal physics. Significant developments have been made in the electron theory of metals and major innovations have been introduced which picture real crystals as being structures which contain singularities or imperfections superposed on an ideal lattice structure. Because these developments are particularly significant to the proper understanding of solid solutions, we feel it is appropriate to review the present state of affairs in metallic solid solutions.

The purpose of this review is to describe those aspects of the foundations and recent developments of the electron theory of solids which lead to a more complete understanding of primary solid solutions. The discussion will begin with a short review of the important physical factors in the theory of solid solutions. This will be followed by a discussion of the more recent advances in the theory and applications. The remainder of the report will be concerned with the current views on the structure and properties of real

solid solutions, i.e. solid solutions showing deviations from ideality. One of the principal points of discussion will be the deviation in behaviour of real solutions relative to the simple ideal ones.

2. The Electronic Structure of Solid Solutions

The electron structure of primary solid solutions is derived from the electron structure of metals which serve as solvents. As a result, it is of primary importance to clearly understand the electronic structure of the pure metals. Two excellent reviews of the electron theory of metals have appeared in this series. In *Progress in Metal Physics*, Vol. I, Raynor summarized the status of the theory of alloys as of the end of World War II. Of particular interest to the present discussion are Raynor sections on the electronic theory of alloys and the section on lattice spacing of alloys. In volume III of *Progress in Metal Physics*, Mott discusses the aspects of electron theory which are relevant to crystal imperfections. In addition, introductory presentations of the electron theory of metals have recently been made by Hume-Rothery [1] and Raynor.[2] For the purpose of this discussion, it appears necessary to summarize some of the basic concepts of the electron theory of metals.

VOL. 9 1961

The electron theory of alloys can be described by saying that an alloy will assume that type of crystal structure in which there are enough *low energy* states to accommodate all of the electrons in the crystal. An electronic structure which will do this can be described principally by a knowledge of the following:

(i) the range of allowed energies (band widths) over which the outermost or *chemical valence electrons* are distributed. These "bands" of allowed energies arise from the interactions between atoms as they are brought together to form the crystal. Such interactions cause the valence electron states of the free atom to become a *band* of energy states in the crystal separated by gaps or forbidden energy ranges.

(ii) the form of the distribution of the electrons over the energy ranges of the bands (the density of states or N(E) curve). This distribution is defined as the number of allowed energy states per unit volume of the metal. The effect of band overlap is that N(E) curves are additive in the overlap region; see Fig. 1.

(iii) the type of wave-function to be ascribed to the electrons, especially for alloys where the electrons from the conduction band may occupy either *bound* or non-localized states.

(iv) the relative numbers of electrons with positive or negative spins . . . important in ferromagnetism.

(v) the sign, numbers, and mobilities of electrical charge carriers . . . important in transport processes.*

* An important quantity which depends upon the electronic structure is the concept of an E_{max}. E_{max} is the topmost filled energy level at 0°K (and is called the Fermi level). It has the significance of being equal to the Gibbs' free energy per electron.

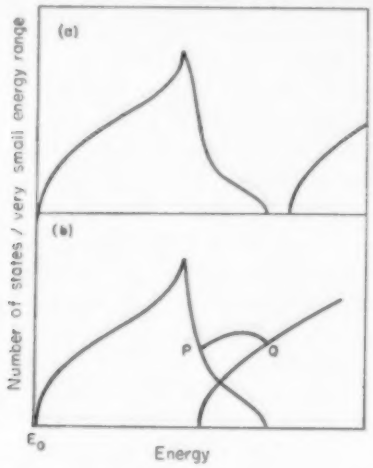

FIG. 1. The density of states curves $N(E)$ for neighbouring energy bands showing (*a*) no overlap or (*b*) overlap; after RAYNOR, vol. I, *Progress in Metal Physics*.

An exact formulation of the electronic structure of a pure metal is clearly impossible. However, the use of certain simplifying assumptions makes possible a reasonably accurate description of these quantities for pure metals. By considering the influence of a solute atom on electronic structure of the pure metal, one is able to obtain some idea of the electronic structure of a primary solid solution.

If a theory of solid solutions is adequate, then it should be possible to explain their structure and properties from an understanding of their electronic structure. Some properties are easier to evaluate from a knowledge of the electronic structure than others because they can be related to a single structural aspect of a solid solution. It is convenient to relate properties to one of the following: (1) the vibration of atoms about their equilibrium positions (2) valence electrons (3) core electrons (4) lattice imperfections. When properties are related to more than one of the features of a solid solution mentioned above, real difficulties are encountered. Attention in this review will be principally centred about properties which are related to the valence electrons and those related to lattice imperfections.

2.1 *The Formation of Solid Solutions*

Of primary concern to the theory of solid solutions is, "What happens when a solute atom is added to the solvent matrix?" From an energetics point of view, the addition of a solute atom produces a change in the electronic energy of the solid, ΔE. If the ionization energy of the solute atom is greater than that of the solvent, then the ion-core of the solute will attract a valence electron more strongly than will a solvent atom. This will result in an accumulation of charge at the solute ion at the expense of the electronic

charge distributed over the rest of the lattice. These charge "shifts" may result in either a "polarization" of the conduction band near the solute atom or the localization of some of the valence electrons in "bound states". The opposite situation is expected if the ionization energy of the solvent is greater than that of the solute. The immediate effect in either case is that the potential field will become smoothed out by the valence electron charge shifts.

Taking into account these charge pile-ups, the energy change, ΔE, resulting from the addition of a solute atom depends upon the following effects:

(1) Ionic attraction. The solute and its solvent neighbours may become oppositely charged and contribute an ionic term to the cohesion. Such terms favour order as in the case of copper–gold but are less important for larger inter-atomic separations, as in the silver–gold system. The larger the electrochemical differences between solute and solvent, the larger the ionic terms.

(2) Ionic repulsion. The electrostatic repulsion between the solvent neighbours of the solute leads to a positive ΔE. There are also attractive Van der Waals' terms but they are assumed negligible.

(3) Coulomb self-energy. The Coulomb self-energy of the valence electrons changes due to the charge redistribution caused by the solute ion fields.

(4) The change in average energy $E_0 + E_F$ of the conduction electrons.* This may be a decrease or an increase, depending on the ion fields of the solutes and the average valence electron density in the solid.

(5) Classical elastic strain energy. The lattice strain energy induced when a solute atom of size which differs from that of the solvent is introduced into the lattice. (For convenience this will not be considered at this time. See section 4.2).

Of the electronic factors 1–4 above, (2) and (3) tend to compensate (1) so that most of ΔE will be due to changes in $E_0 + E_F$. One might expect that ΔE will have opposite signs at opposite ends of the phase diagram because of the relative values of ionization energies of solute and solvent. However, this does not appear always to be the case since it has been shown recently that the energies of solution *may* have a negative electronic contribution at both ends of the phase diagram.

The energy change, ΔE, is due to the modification of the electronic energy states by the solute. As was pointed out in the previous paragraph, the charge distribution is changed around a lattice site occupied by a solute atom. The charge density, and therefore the electrostatic field of the crystal, are not longer perfectly periodic. The solute ion produces a perturbing field, V_p, which will tend to modify the state of motion and energy of the valence electrons. SLATER and KOSTER,[3] extending a method introduced by WANNIER,[4] treated this problem by considering a crystal whose electrostatic potential is period *except* for a localized non-periodic force. They were able to show that the solution to such a problem can be expressed in terms of

* E_0 is the energy of the state at the bottom of the conduction band, i.e. the state $k = 0$; E_F is the "mean Fermi energy" or the average kinetic energy of the conduction electrons.

VOL. 9 1961

the original functions of the unperturbed periodic lattice. Their most interesting general result is that of the effect of the perturbing potential V_p, localized at an atomic site, on the allowed energy band structure. If V_p is less than a certain value, they found that the energy values are distributed in about the same manner as they are in the perfect pure solvent. If V_p is greater than this critical value, one of the energy levels forms a discrete state (called a bound state) by separating from the energy band. This discrete state separates from the bottom or the top of the band, depending on the sign of V_p; that is, if it is attractive or repulsive. The result is that the discrete state tends to be localized at the solute. The presence of such discrete states should be seen from their effect on the physical properties of the solid solution. Figure 2 shows the alternative possibilities of the effect of solute perturbation of the N(E) curve.

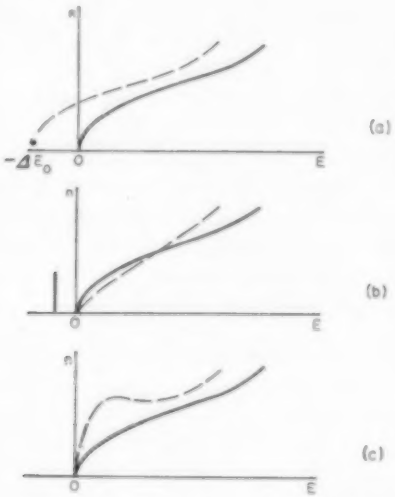

FIG. 2. The band structure of a pure solvent (continuous line) and for an alloy (broken line). (*a*) Rigid band approximation; (*b*, *c*) possible real structures for a dilute solid solution, with and without energy states lying in between allowed energy bands of the pure solvent; after J. FRIEDEL.[65]

Several conclusions may be drawn from the above. In the case of a random distribution of solute atoms, if the nuclear charge of the solute atoms differs by only one or two from the charge on the solvent atoms, then the energy levels will be relatively unaffected; at most, only slight shifts would occur. The wave functions will be modified in such a fashion as to tend to neutralize the impurity charge. For greater differences in nuclear charge, discrete states will separate from the band structure, either above or below it. If the distribution of the solute atoms is periodic (e.g. a supper-lattice), each energy band will split into Brillouin zones whose limits occur at the Bragg reflections for the super-lattice (see Fig. 3). Evidence for such qualitative behaviour may be seen from its effects on properties.

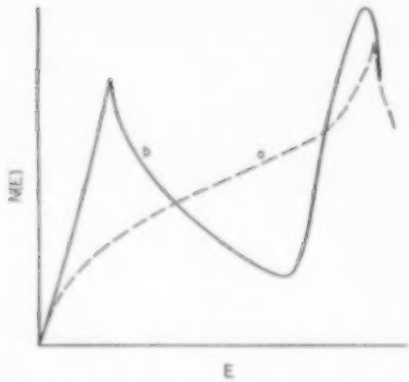

FIG. 3. Illustrating the $N(E)$ curves for (*a*) the Disordered Structure; (*b*) the Ordered Structure; after J. NICHOLAS, *Proc. Phys. Soc.* A66 (1953) 201.

VOL.
9
196

3. THEORETICAL MODELS OF SOLID SOLUTIONS

The success of any physical model of a solid solution depends upon how well its predictions of structure and properties agree with experimental observations. The results of experimental observations indicate that there are certain physical factors which strongly influence the solution structure and properties and therefore are important to any theory. These factors have been empirically determined by Hume-Rothery and are:

(*a*) the valence electron concentration and the relative valency of solute and solvent.
(*b*) the relative atomic sizes of solute and solvent.
(*c*) the difference in electrochemical character of the pure solute and solvent.

Factor (*a*) leads to such valency effects as the dependence of some phase boundaries on the average number of electrons per atomic site and the dependence of the sign of the curvature of the ΔH^M vs. composition curves on the sign of the relative valence difference. Factor (*b*) leads to size effects which (due to relative size differences between solute and solvent) result in elastic distortion of the solvent lattice by the solute atoms. Factor (*c*) leads to ionic interactions between solute and solvent atoms and also possible mutual polarization of the inner electron shells of the Van der Waals' type; such interactions favour compound formation. Usually these factors are treated separately; a good approximation when only one of them is important. The following discussion will attempt to bring out the nature and degree of success of recent calculations of the energies of solution of certain systems. The effect of the different Hume-Rothery factors is considered separately.

Generally, when small amounts of metal *B* are dissolved in a metal *A*, the resulting solid solution has the same crystal structure as *A*, and is formed by

B atoms replacing A atoms in the lattice. The energy of solution, Q_B, of a B atom in an A solvent is related to the electronic energy change, ΔE, by the relation

$$Q_B = \Delta E + (E_B - E_A) \quad . \quad . \quad . \quad . \quad . \quad . \quad (1)$$

where E_A and E_B are the average energies per atom of pure A and pure B respectively. In this process we retain the same zone description for the solid solution that was used for the pure metal A. Changes in the zone structure will occur when the electron atom or e/A ratio, which varies with the concentration of solute B, increases the electronic energy to the extent that a lower energy could be gained by a change in crystal structure.

3.1 *Friedel's Model*

The first step in a theory of solid solutions is the determination of the functional form of V_p. Recently J. FRIEDEL[5] has proposed a model of a solid solution which explains with some success the various properties of a solid solution in terms of its valency factors. He assumed that the perturbation, V_p, produced in a gas of valence electrons by a positive charge Z, is obtained by solving Poisson's equation under Fermi-Thomas assumptions.* The charge Z in this case represents the difference in chemical valence between the solute and solvent atoms. Friedel's treatment of the effect of the size differences between atoms of the solute and solvent elements is considered separately in section (4.2). The chemical factors are not considered by Friedel except by means of a cyclic process introduced at the end of this section.

The alloys which Friedel considered were alloys of copper, silver and gold with polyvalent elements. The valences were assumed to be the normal chemical ones with the exception of the transition elements. For transition elements Friedel assumed that nickel, palladium and platinum behave as if they were zero-valent, while cobalt, rhodium and iridium should have valency -1, iron, ruthenium and osmium a valency of -2, and so on. In this scheme nickel dissolved in copper should show a $Z = -1$, and zinc dissolved in copper will have a $Z = +1$ while copper dissolved in zinc will show a $Z = -1$. Similarly, Z is $+2$ when indium is dissolved in copper and is -2 when copper is dissolved in indium; values of Z for other elements are obtained analogously.

Friedel treated alloys in both the dilute and finite composition range. For dilute solutions there is assumed to be no interaction between solute atoms so that the alloy consists of independent centres of perturbation randomly dispersed throughout the solvent matrix. The results obtained are

* An introductory discussion of the Fermi-Thomas approximation is given in the *Wave Mechanics and Application* by N. Mott and I. Sneddon, Oxford University Press, 1950. An excellent treatment of this model applied to impurities in metals is given by LEE, P. and MARCH, N., *Phil. Mag.*, vol. 2, ser. 8, p. 1226 (1957).

$$V_p = \frac{Z}{r} e^{-qr}, \quad q^2 = 4\pi N_0 (E_{max}), \quad . \quad . \quad . \quad . \quad . \quad (2)$$

where $N_0 (E_{max})$ is the density of states at the Fermi surface. r = the radial distance from the solute and q is a measure of the screening radius; $q^{-1} \cong 1$ Å. Using this form of V_p, Friedel showed that the whole conduction band is displaced rigidly and there is no shift of the Fermi level on the absolute energy scale; i.e. $\delta E_{max} = 0$. The amount that the band is shifted is given by

$$\delta E_0 = \frac{1}{\text{vol.}} \int V_p \, \text{d(vol.)} \quad . \quad . \quad . \quad . \quad . \quad . \quad (3)$$

which is the space average of V_p. A δE_0 at the bottom of the band will add a positive or a negative term to Q_B depending on its sign; see Fig. 2.

The above result is just the case of the JONES[6] "rigid band" model. The "rigid band" model was applied by Jones in describing the theoretical basis for the Hume-Rothery factors. In considering the α/β solubility limits for copper, silver and gold-based alloys, Jones assumed that all of the valence electrons go into the conduction band and that all the energies except E_{max} remain unchanged for the two phases. This means that the level to which the energy bands are filled in the two structures essentially determines the relative free energies of the two phases. Figure 4 shows the N(E) curves

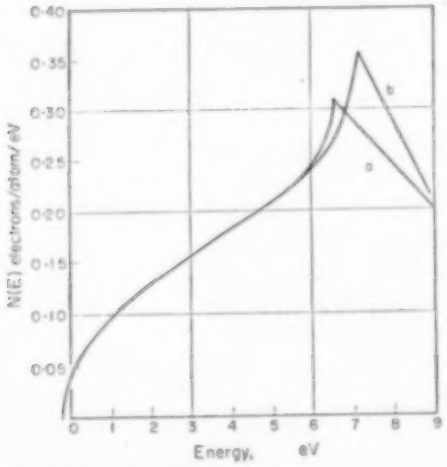

FIG. 4. Curves showing the number of states per unit energy range as a function of energy (*a*) for the FCC structure, (*b*) for the BCC structure; after RAYNOR *loc. cit.*

for both structures and Fig. 5 represents the energy difference between the α(FCC) and β(BCC) phases as a function of the e/A or valence electron/atom ratio. It follows that the phase whose N(E) is filled up to the lower E_{max} is the more stable phase. At $e/A = 1{\cdot}4$ electrons/atom, the slope of the free energy curve of the α-phase is equal to that of the β-phase and therefore

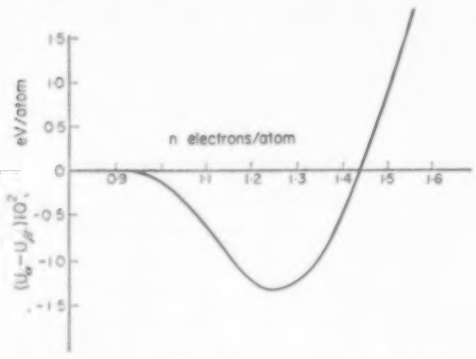

FIG. 5. The difference between the Fermi energies of the FCC and BCC structures as a function of the number of electrons per atom; after H. JONES, *Proc. Phys. Soc.* 49 (1937) 250.

would represent the solubility limit of α. The article by G. Raynor in volume I of this series lists the α-solubility limits in terms of e/A for copper, silver and gold alloys. Although this model shows good agreement with experiment, it neglects the actual non-periodicity of the lattice due to the solute ion fields and the fact that there are electron–electron interactions.

Friedel's model apparently agrees with Jones' "rigid band" model for alloys like silver–cadmium and copper–zinc at dilute concentrations because V_p is sufficiently small. This causes the result that the *screening* charge comes uniformly from the conduction band and hence no bound states exist. Experimental evidence seems to support this interpretation. In the case of copper, the addition of a solute with an odd value of Z, such as zinc, should lead to an increase in the paramagnetism or a decrease in diamagnetism of the alloy if *bound states* are formed. This follows from the anti-symmetry of the electronic states. Actually, just the opposite result is observed; adding zinc to copper causes an increase in the diamagnetism of the alloy.[7] This would suggest that in this alloy *no bound state* is formed. On the other hand, the addition of magnesium to copper or lead to silver[8] should introduce fairly strong perturbations into the copper or silver lattices and hence the formation of bound states is to be expected. That this is the case may be inferred from the known increase in paramagnetism of these alloys as more solute is added.

Friedel has given the following interpretation of the effect of "bound states" on the Hume-Rothery rules: As *bound states* are formed levels move out of the bottom of the conduction band with the top of the band moving down towards the Fermi level; i.e. states are removed from the band. However, states may enter from the band above the conduction band. Thus, states may be added as fast as they are removed. Friedel suggests that new states may be added just fast enough to preserve the Hume-Rothery rules.

For the case of finite concentrations of solute atoms, the solute interactions

were considered in a self-consistent manner to determine the radius R_0, of the spheres of influence of the impurities. R_0 was found to be less than 5 atom distances for most metals. Table 1a lists Friedel's results for copper, aluminium, thallium and nickel. One should note that for the transition

TABLE 1a

Typical values of R_0 and c_0

	Cu	Al	Tl	Fe	Ni
q	1·13	1·4	1·0	3·2	4·75
R_0/r_s	3·3	2·4	2·8	1·2	0·8
c_0 per cent	3·0	7·5	4·5	60	100

R_0 = the radius of the sphere of total screening at infinite dilution.
r_s = the radius of the atomic sphere.
c_0 = the concentration at which impurities interact appreciably.
(after FRIEDEL[5])

metals iron and nickel, R_0 is less than one atomic spacing. This means that solutes like iron or nickel will interact only weakly even at large concentrations; the heats of solution should be small. Generally, the solutes will interact at concentrations of a few atomic per cent and higher. The solute interactions will then result in a heat of solution Q_B, that is concentration dependent. The Fermi level will also be shifted upward on the energy scale as the solute concentration is increased.

At finite concentrations, $a\delta E_{\max}$ becomes appreciable and hence contributes a term to the energy of solution. The effect on Q_B due to the rise in $E_{\max}$ with concentrations is approximately given by

$$\delta Q_B = \frac{2(p + Zc)\, Zq'^3\, R^2}{3c(q'R - 1)\exp(q'R)} \qquad (4)$$

$$q' = \frac{1}{[1 - 3\mu/(2\pi k_{\max})]^{\frac{1}{2}}}$$

where p is the number of conduction electrons per atom in the crystal, μ is the effective mass of the electrons, and q' is the screening constant q corrected for exchange. Since $Q_B = (1/N)\{\mathrm{d}(\Delta H/\mathrm{d}c)\}$, δQ_B is effectively the curvature of the ΔH vs. c curve for a solid solution. If we may neglect the effects of polarization and consider only valence differences Z, then for $Z < 0$ solute atoms will cluster, and for $Z > 0$ unlike neighbours are favoured, i.e. a tendency for short-range order. This follows from the fact that the curvature of ΔH vs. c has the same sign as Z.* Experimental results for aluminium–copper, [9] aluminium–silver, [10] aluminium–zinc, [11] and aluminium–magnesium ($Z < 0$)[12] agree with this prediction. Cases where $Z > 0$,

* See Friedel,[5] (*Adv. in Physics*), p. 474.

VOL. 9 1961

e.g. aluminium–tin,[13] and magnesium–lead[12] show no clustering. Gold–nickel[13] and copper–platinum[14] are exceptions to the above rule, but this may be due to the size effect. Calculations of δQ_B for the copper–zinc and the aluminium–zinc systems both show the correct sign but only copper–zinc shows good agreement with experiments, even when corrected for size effects (see Fig. 6).

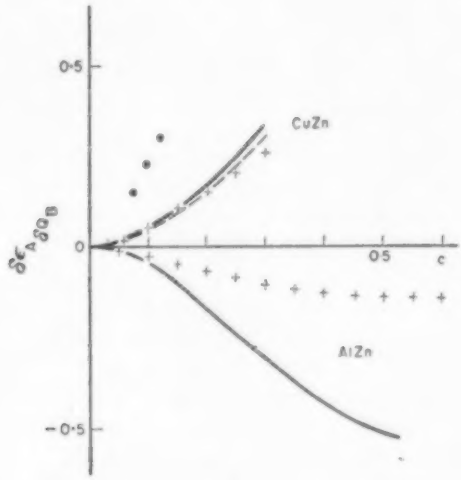

FIG. 6. The change in energies of solution with concentration for Cu–Zn and Al–Zn (in *e.V.*/atom); continuous line—theoretical curve; dashed line—correction for size effect; crosses—experimental values; points—displacement of the optical absorption edge in Cu–Zn; after J. FRIEDEL.[5]

Friedel was unable to determine the absolute values of the heats of solution for dilute alloys by means of the techniques reported above. However, by making use of a cyclic process previously described by Mott (see volume III of this series) he was able to obtain approximate agreement with experiment:

For substitutional alloys A–B with p conduction electrons per atom in A, the energy of solution of B is obtained below:

(1) Evaporate a B atom and ionize it p times.
(2) Substitute the B^{p+} ion for an A^{p+} ion.
(3) Re-combine the A^{p+} with the p free electrons and put the A atom back on the A metal.

The energy of solution given by this cycle is

$$Q_B = E_B - E_A + I_B - I_A + \epsilon \quad . \quad . \quad . \quad . \quad . \quad (5)$$

where ϵ represents the average energy change per electron for the conduction electrons as a result of the alloying. Friedel neglects the term ϵ but adds a small correction term for the size effect, E_A and E_B are the cohesive energies

and I_A and I_B the ionization potentials of A and B respectively. The results of calculations made by this method are reported by Friedel and show reasonably good agreement with experiment; see Table 1b.

TABLE 1b

Energies of Solution for A–B alloys

	Q_B(eV/*atom*)	*Experimental*
Cu–Zn	− 0·4	− 0·35
Ag–Cd	− 0·3	− 0·33
Ag–In	− 1·9	− 0·45
Ag–Sn	+ 0·5	− 0·25
Ag–Sb	+ 0·6	− 0·02
Au–Hg	− 1·5	− 0·56

(after FRIEDEL[51])

VOL. 9 1961

3.2 *Henry's Model*

A more recent calculation of Q_B and ΔH has been reported by HENRY[15] using the Sommerfeld free electron-in-a-box model. This approach is a modification of an exact self-consistent calculation made by Huang in 1948. V_p was chosen to be a square-well potential whose depth is the difference between the Sommerfeld potentials $V_A^\circ - V_B^\circ$ of the two metals A and B. This model applies strictly to monovalent solutes and solvents as it stands. Second order corrections to the perturbed energy levels were calculated taking account of the charge shifts around the solute to obtain self-consistency. The charge accumulations were calculated by a method due to Lennard-Jones. The second order values for the solution energy of gold in silver, corrected for self-consistency and assuming zero volume changes in the alloy amounted to about − 0·1 eV per atom which is the right order of magnitude. The general expression obtained has the form

$$\frac{1}{N}\frac{\mathrm{d}(\Delta H)}{\mathrm{d}c} = Q_B = \frac{(V_p + q\phi)^2}{W_A^\circ} \quad . \quad . \quad . \quad . \quad . \quad (6)$$

for dilute solutions. q = the accumulated charge at the solute, ϕ = the average potential per unit charge at the surface of the solute ion and W_A° = the average electronic energy of the solvent. The screening charge comes uniformly from the lattice and tends to smooth out the potential at the solute. The case of finite concentrations was not considered.

In order to apply this model to monovalent-polyvalent systems, that is cases for $Z = \pm 1$ or ± 2, Henry assumes that the Z "excess" electrons of a polyvalent solute are *in bound states* and that only the energy of the one electron that replaces the solvent electron will be altered appreciably. For the case of a polyvalent solvent he treats the solvent as a monovalent atom. Then assuming no size effect he obtains an expression for Q_A or Q_B which

has the same form as that in Eqn. (6) above. The net result of this is that he calculates heats of solution for monovalent-monovalent and monovalent-polyvalent systems which are negative at both ends of the composition range. The data reported by Kleppa on the heats of mixing of polyvalent solutes in copper, silver and gold do not seem to agree with this.

3.3 *Varley's Model*

A slightly different approach has been taken by VARLEY[16] in treating the electronic structure of solid solutions. He proposes that the electrons of metal A and metal B lie in two different sets of energy levels which become superposed when the alloy is formed. This would give a single band structure of non-uniform density. The electrons in the solid solution are transferred from the band with the higher Fermi level to the band with the lower Fermi level. As the unoccupied levels of the lower band are filled, a reduction in energy occurs for the alloy relative to that of the two pure components and hence contributes to a negative heat of mixing only. This, of course, does not agree with fact. In addition, the charges accumulated in this process predict ordering energies for super-lattices far in excess of those that are observed. On the other hand, MOTT[17] has shown that the screening charges computed by the Thomas–Fermi method lead to values of the right order of magnitude in the case of beta brass.

3.4 *Thermochemistry of Solid Solutions*

Having discussed the essentially electronic approaches to a theory of solid solutions, the agreement between the calculations of solution properties and thermochemical measurements of these properties will be considered next. The comparisons will be limited to the work of Oriani and Kleppa who have performed the most systematic thermochemical investigations of alloys.

Much of the recent work of KLEPPA[18] deals with determinations of the heats of mixing of alloys of copper,[19] silver,[20] and gold,[21] with cadmium, indium, tin and antimony, and with thallium, lead and bismuth.[22] In order to separate out the various effects of atomic size, chemical affinity and valence it will be useful to expand the integral excess thermodynamic functions as a power series of the mole fraction of solute, x_2. If we follow KLEPPA,[18] we obtain

$$\Delta F^{xs} = \Delta F^{M} - \Delta F^{M}_{id} = Ax_2 + Bx_2^2 + \ldots \quad . \quad . \quad . \quad (7)$$

A and B are represented as being temperature dependent, where

$$A = a - \alpha T$$

and

$$B = b - \beta T$$

a, b, α, and β are excess heat and entropy "constants" for temperature, T. At dilute concentrations a equals the partial molar heat of solution of the solute and $2b$ represents the limiting curvature of ΔH^{M}. a will depend upon

the choice of reference state while b does not. According to the quasi-chemical theory, when $a < 0$ the solutes repel each other and order is favoured. When $a > 0$ the solutes attract each other and clustering occurs. The quasi-chemical approximation also requires that $-\mathbf{b} \cong a$.

In order to compare theory and experiment it is necessary to separate valence effects from those due to atomic size and chemical affinity. The effect of atomic size differences is to tend to give positive a's and negative b's. For strong chemical interactions one would expect negative a's and positive

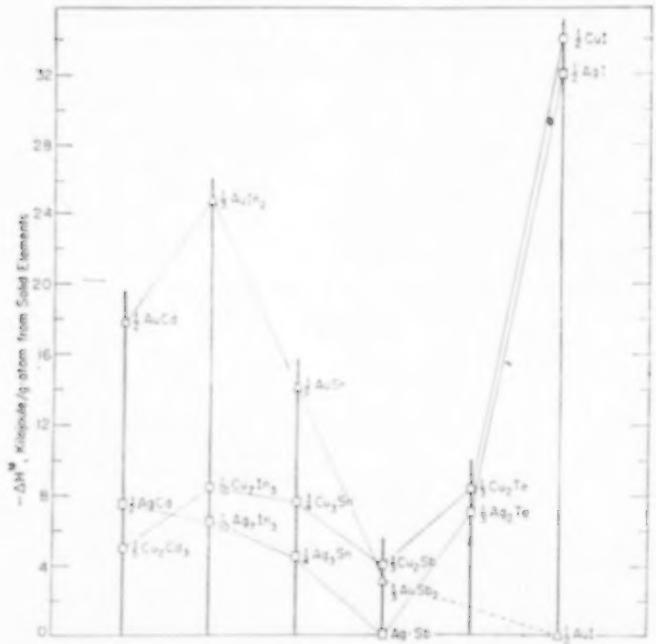

FIG. 7. The Extreme Values of heats of formation for solid "compounds" of Cu, Ag and Au with Cd, In, Sn, Sb, Te and I; after O. KLEPPA.[38]

zero or negative b's depending on the strength of the interaction. Therefore, to reduce the effects of atomic size, experimental determinations should be made at elevated temperatures, near or above the melting point of the alloy. For systems such as gold or silver alloyed with cadmium, indium, tin or antimony the size effect should be relatively small anyway. On the other hand, to obtain some measure of the chemical interaction, the maximum values of $-\Delta H^M$ for the whole composition range should be considered after the fashion of Kleppa; see Fig. 7.

One of the most important valence effects is that predicted by Friedel. He found that if size and electrochemical differences are negligible the limiting curvature of the ΔH^M vs. c curve is determined by the difference in

VOL. 9 1961

valence between solute and solvent. Therefore, as we have mentioned previously Eqn. (4) solutes with $Z < 0$ give a negative curvature while those with $Z > 0$ give a positive curvature. The data reported by Kleppa (see Figs. 8, 9, 10) for the alloys of gold and silver with indium, cadmium, tin and antimony (except gold–tin) may be interpreted as confirming Friedel's prediction of the curvature of ΔH^M vs. c. Calculations of the curvature by Friedel's theory agree with the determinations of b within the experimental error. It is also noteworthy that the value of b for the silver–indium system is roughly twice that for the case of cadmium in silver. This result is again in line with Friedel's predictions. Friedel himself calculated the values of the screening constant q' using the proper V_p and compared these with values of q' determined by fitting the experimental data of Kleppa for ΔH^M vs. c with his curvature formula. The results shown in Table 2 are quite satisfactory. Data reported for the copper–cadmium, –indium, –tin and –antimony systems show no valence effect because of the low solubilities of these elements in copper and the large size differences resulting in significant

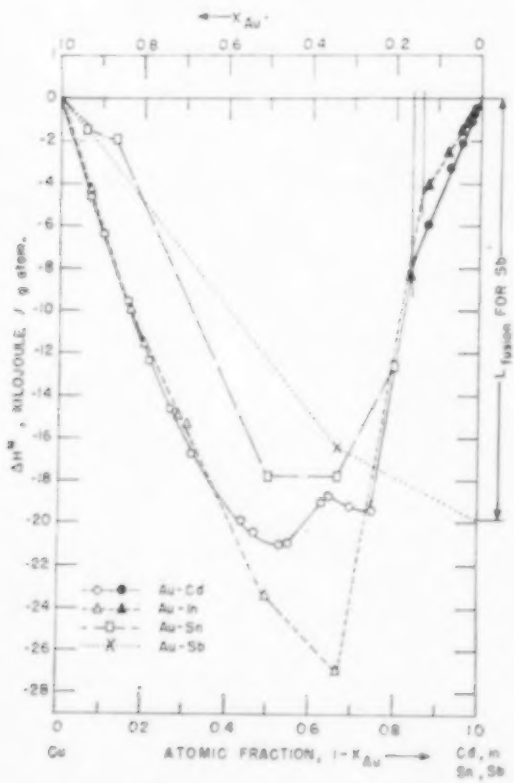

FIG. 8. Composite graph of heats of formation for alloys of Au with Cd, In, Sn and Sb from solid Au and liquid alloying components; after O. KLEPPA.[21]

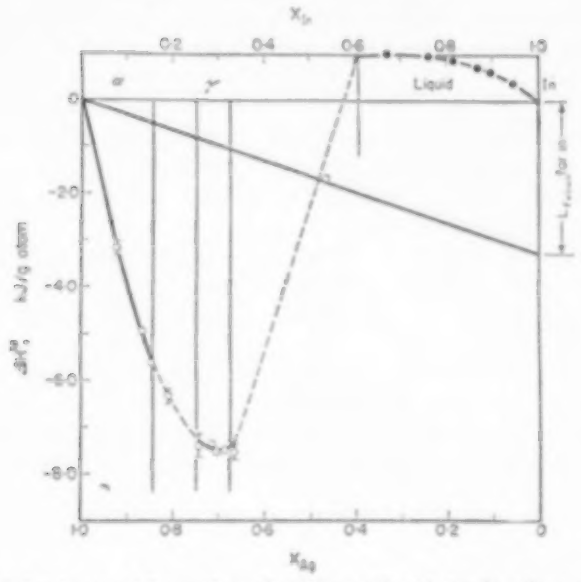

FIG. 9. Molar heats of formation of solid and liquid Ag–In alloys at 450°C; after O. KLEPPA.[20]

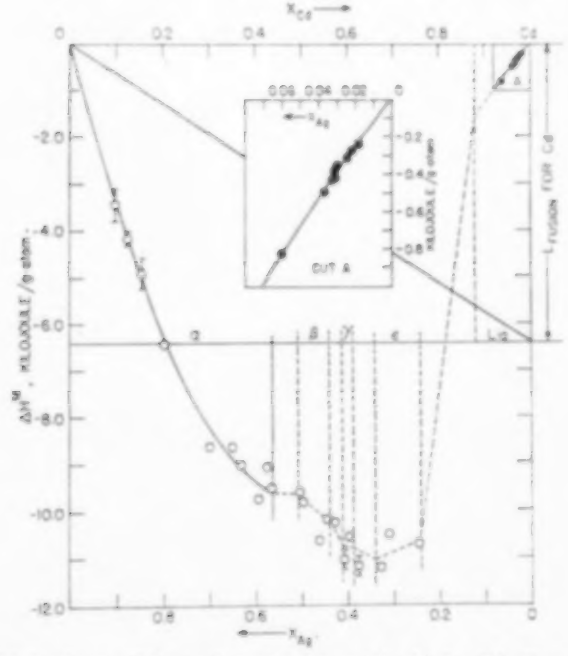

FIG. 10. Molar heats of formation of solid and liquid Ag–Cd alloys at 450°C; after O. KLEPPA.[20]

VOL. 9 1961

TABLE 2

Comparison of Experimental and Theoretical Screening Constants (after FRIEDEL[51])

	q	q'	q_{exp}
Cu–Zn	0·96	1·64	1·65
Ag–Cd	0·90	1·78	1·80
Al–Zn	1·09	1·55	1·75
In–Ag	1·02	1·59	1·75
Sn–Ag	1·05	1·57	1·70

positive contributions to a. Finally, Kleppa indicates that the Hume-Rothery "relative valance" rule holds for the systems silver–cadmium, –indium and –tin but does not appear to hold for the case of gold–cadmium, –indium and –tin. The case of silver–antimony does not seem to fit into Hume-Rothery's scheme since the two limiting heats of solution and the two limiting solubilities are comparable. Kleppa further reports thermochemical data taken for the systems solid copper, silver and gold dissolved in liquid thallium, bismuth and lead. Although the agreement with Friedel's theory is not as clear for these systems, the curvatures of the heat of mixing curves have the expected negative values except for the case of gold in lead; see Table 3.

TABLE 3

Heat Data (Kilojoules at 450°C) for Liquid Solutions of copper, silver and gold in Low-Melting Metals

		Cd	*In*	*Sn*	*Tl*	*Pb*	*Bi*
Cu	a	− 12	0	− 1	34	28	19
	b	(− 5 to − 10)	(− 10 to − 20)	− 13·7			
	− b/a			− 14			
Ag	a	− 24	− 4	4	15	13	13
	b	0	− 11·7	− 13·3	− 30	− 26	− 25
	− b/a	0	− 3	3·5	2	2	2
Au	a	− 61	− 46	− 33	− 2	− 8	2
	b	0	0	8·4	− 0·7	8·6	− 5·3
	− b/a	0	0	0·25	− 0·3	1	2·7

(All data referred to supercooled, liquid solutes; after KLEPPA.[18])

In considering the applicability of the Jones' "rigid band" picture of a solid solution Kleppa attempts to analyze his curves of the heat of formation of α-silver–cadmium to determine if there is an "additional" curvature in the region analogous to $e/A = 1{\cdot}36$–$1{\cdot}40$. Such an effect would be expected since the density of states curve should fall off rapidly once the Fermi surface touches the (111) faces of the first Brillouin zone. No such curvature was

observed but it was presumed that measurements of the electronic specific heats carried out at 1°K might present more definite evidence. Recent experiments quoted by M. COHEN,[24] however, indicate that the Fermi surface should *touch the zone boundaries* in pure copper, and therefore, such a curvature effect should occur at lower e/A values.

An interesting aspect of Kleppa's measurements is the strong similarity in the chemical bonding character of the copper and silver alloys of cadmium, indium, tin and antimony.[18] It was also noted that the maximum values of ΔH^M occurred at equivalent compositions (i.e. e/A values of 1·5 to 1·8). On the other hand, gold shows a much greater bonding to cadmium, indium and tin. This is to be expected since gold is much more electronegative than copper and silver. On the basis of the calculations and Kleppa's results, Friedel's theory is the only one successful in predicting valence effects in solid solutions. The results of calculations of heats of mixing show only fair agreement with experiment for all three models.

Friedel's theory is most successful when applied to solutions of polyvalent

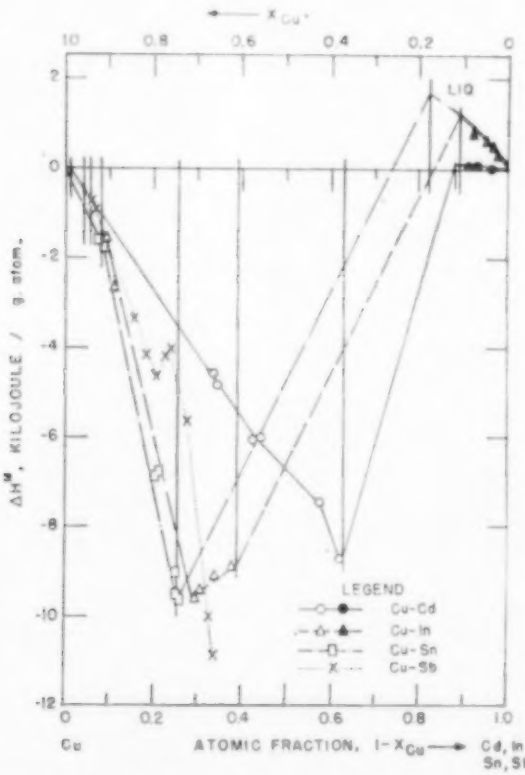

FIG. 11. Composite graph of heats of formation of alloys of Cu with Cd, In, Sn and Sb from solid Cu and liquid alloying components; after O. KLEPPA.[19]

VOL.
9
1961

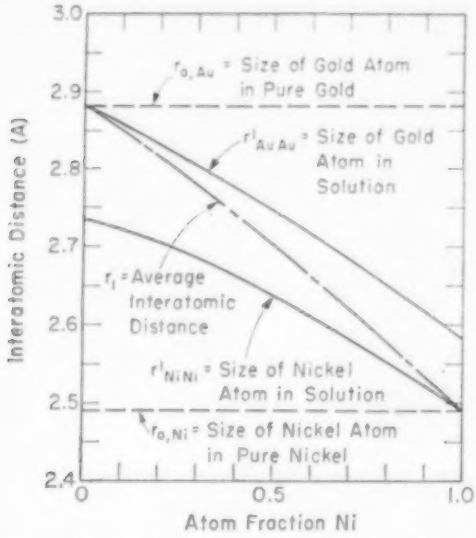

FIG. 12. Interatomic distances in Au–Ni solid solution; after B. AVERBACH.[101]

metals dissolved in copper, silver or gold. The results of Kleppa indicate that the curvature rule breaks down for the case of alloys of polyvalent metals with each other. This is probably due to the complicated band structure and the high e/A ratios for these materials. The major weaknesses in the Friedel model are due to the basic assumptions of this model; he assumed

(1) that the one-electron model of a solid applied to metals and alloys.

(2) that band theory can be applied to alloys having random distributions of atoms.

(3) that the surfaces of constant energy are nearly spherical in k-space except when they nearly touch the Brillouin zone boundaries. For the case of copper, silver and gold the Fermi surface is assumed nearly spherical.

(4) the rigid band model of an alloy; i.e. the shape of the density of states, N(E), is unaffected by alloying.

Assumption (1) may be criticized on the grounds that important Coulomb and exchange interactions between the electrons are being neglected. However, the work of BOHM and PINES,[128] SLATER and KOSTER,[3] MOTT,[7] and others offers some fundamental justification for the one-electron model. The validity of assumption (2) is not at all well established, although, if the atoms of a disordered alloy are sufficiently close together that the atomic wave functions of neighbouring atoms overlap, one part of the material is, on the average, just like any other part. This should then allow that the wave functions and energy values can still be described by a quasi-continuous dependence of energy on momentum; i.e. an energy band picture applies. On the other hand, recent measurements of the anomalous skin effect reported by PIPPARD[23] indicate that the Fermi surface in Cu is touching the zone boundaries and that it is highly anisotropic; a result which raises strong

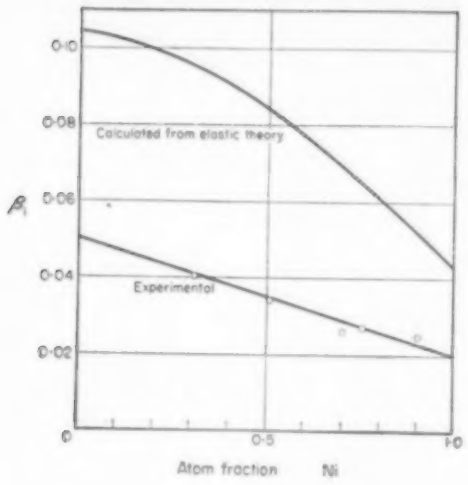

FIG. 13. Atomic size effect coefficients in the Au–Ni system; after B. AVERBACH.[101]

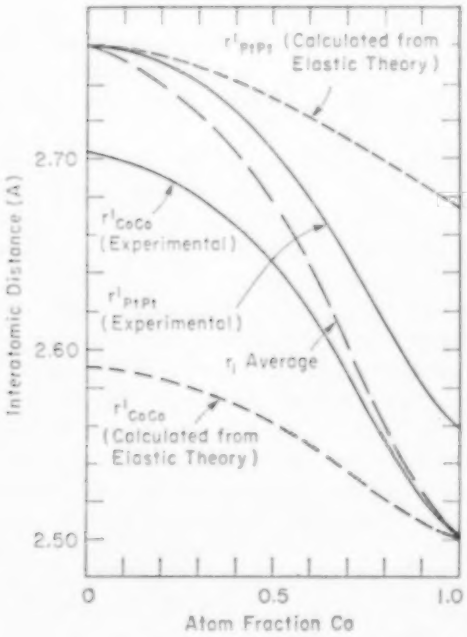

FIG. 14. Interatomic distances in Co–Pt solid solutions; after B. AVERBACH.[101]

VOL. 9 1961

doubts about assumption (3). Assumption (4) is also questioned by COHEN [24] in a recent report. His arguments are based on Pippard's anomalous skin effect data together with some electronic specific heat data for several copper-based alloys.[23] Cohen feels that an energy band in copper is deformed on alloying and that the specific heat effects observed are due to the pulling away of the Fermi surface from the zone faces. An independent agreement with these results can be seen from the measurements of the stacking fault probabilities of copper-based alloys. The discussion in section 5.1 will consider this point.

4. ATOM SIZE, LATTICE SPACINGS, AND STRAIN ENERGY

When a solute atom is added to a solvent lattice, the lattice is strained. The lattice strain may be described as consisting of a uniform lattice expansion or contraction plus various local distortions. Such a solid solution lattice is depicted in two dimensions in Fig. 15. In general the atoms are not located in the average lattice sites but instead are displaced varying amounts from them. In such an arrangement the vectors between atoms are not all multiples of the average lattice vectors. Instead they are functions of the number of interatomic distances between atoms and the identity of the atoms at the ends of the vector and those lying in between. The average lattice spacings, which as the name implies, are the spacing between planes of the ideal lattice, which are calculated from the Bragg reflections. The amount the

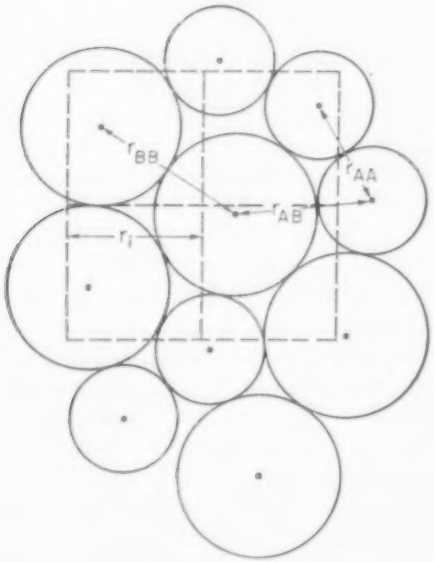

FIG. 15. Interatomic distances in a Solid Solution showing the displacement of atomic centres from average lattice sites; after B. AVERBACH.[101]

average lattice contracts or expands is a function of the difference in size between the solvent and solute atoms. However, it is not possible to determine the true atom sizes from a measurement of lattice spacing. It is clear from Fig. 15 the only measure of the true size of an atom is the distance between like nearest neighbours. The lattice distortions produced by the addition of a solute atom add to the crystal internal energy. This energy is called strain energy. Before one can calculate the lattice strain energy, it is necessary to have a quantitative knowledge about the lattice distortions. The measurement of these strains will be discussed first and the lattice strain energy relations will be discussed in a subsequent section.

VOL. 9 1961

4.1 *Measurement of Lattice Spacing and Atom Size*

As early as about 1920, it was recognized that the lattice spacing of a solid solution was altered by the addition of an atom of different size than the solvent atom. Based on a study of inorganic salts having complete solid solubility and the same crystal structures, Vegard [26] concluded that the change in lattice spacings was entirely due to the size difference of the atoms based on the size they possessed in their elemental form and that the atoms did not change their size upon alloying. He therefore concluded that the lattice spacing of the solid solution varied as follows:

$$d = d_2 - C_1(d_2 - d_1) \quad . \quad . \quad . \quad . \quad . \quad . \quad (8)$$

where d_1 and d_2 are the lattice spacings of the pure component and C_1 is the atomic concentration of component 1. In 1928 Vegard claimed that this relation applied to metal solid solutions as well as inorganic salts. However, as accurate lattice spacing data became available it became evident that almost all metal solid solutions deviate from the behaviour suggested by Vegard. The simple assumptions of Vegard were not valid.

When it was realized that Vegard's law did not hold for metal solid solutions a long period of the investigation of solid solutions using X-ray lattice spacing measurements was begun. These measurements are based on Bragg lattice reflections. From the nature of the diffraction process, the principal contribution to Bragg lattice reflections are those which arise from terms having large values of the lattice vectors connecting pairs of atoms. Therefore, measurements based on these reflections are average or mean lattice spacings.* A measurement of average or mean lattice spacings clearly does not provide sufficient information for one to calculate individual atom diameters directly. Instead it is only possible to measure the general dilatation or contraction of the lattice as a result of alloying. From a study of lattice spacing measurements, it is possible to determine the general influence of a solute element on lattice dilatation. Notable studies of this sort were those of AXON and HUME-ROTHERY [33] RAYNOR, [35] and OWEN. [34]. From their work it was concluded that a change in solute atom size usually occurs if (1) the

* For a detailed discussion of this point see WARREN and AVERBACH [100].

compressibility, (2) the valency, or (3) the electro-negativity of the solute differs from that of the solvent atom.

The influence of the compressibility differences between solute and solvent has been investigated both by ESHELBY[28] and FRIEDEL.[32] From elasticity theory Friedel concludes that for atoms which have approximately the same size and different compressibilities the average atomic diameter may be expressed as follows:

$$\frac{r - r_1}{r_1} = \frac{r_2 - r_1}{r_1}\left(\frac{\alpha + \chi_1/\chi_2}{\alpha + 1}\right) c; \alpha = \frac{(1 + \nu)\chi_1}{2(1 - 2\nu)\chi_2} \quad . \quad . \quad (9)$$

where r_1, r_2 are the atomic radii and χ_1, χ_2 are the compressibilities of the solvent and solute respectively, c is the atomic concentration of the solute and ν is Poisson's ratio. From this equation it is evident that the only instance where one would expect to observe a Vegard's law relation for atoms of different atomic diameters, is in the case where the compressibilities of the two components are equal. Friedel analyzed alloy systems with complete miscibility and found that the deviations agreed with predictions of the above equation. However, the quantitative agreement was not very good. Friedel concluded that the lack of agreement might be attributed to data of insufficient accuracy to yield better agreement or that the error was due to other physical influences which alter the apparent diameter of the atoms of the solid solution.

In their study of solid solutions, AXON and HUME-ROTHERY[33] considered the influence of the so-called V_e effect and the relative ionic radii of solvent and solute atoms on the apparent atomic diameter* of the solute. They described the V_e effect as a valency effect. However, both of these effects can also be considered as manifestation of differences in compressibility between solute and solvent. The V_e effect was based upon the relative "volume" of a valance electron of solute and solvent. If the volume of the valence electron for the solute atom is greater than that for the solvent atom, then the apparent diameter of the solute atom will be smaller than the atomic diameter for the elemental solute atom. AXON and HUME-ROTHERY[33] described the V_e effect as occurring as a result of equalizing the "pressure" of the electron gas. Thus when lithium ($V_e = 21{\cdot}3$ kX^3) is alloyed with aluminum ($V_e = 5{\cdot}5$ kX^3) the apparent diameter of lithium is reduced from its elemental atomic diameter.

AXON and HUME-ROTHERY[33] suggest that the apparent atomic diameter of a solute is also a function of the relative ionic radii of the solute and solvent. Where the ionic radius of the solvent is greater than the ionic radius of the solute, the apparent diameter of the solute is greater than its elemental atomic diameter. This is explained on the basis that the ionic cores are comparatively incompressible. Therefore, if the ionic core of the solute is larger than that of the solvent, then its apparent atomic diameter will be larger because the solute is less compressed than the solvent. It is reasonable

* The apparent atom diameter of a solute atom is obtained by extrapolating a curve of lattice spacing vs. composition in the dilute solute regions to 100 per cent solute.

to assume that as the ionic radius approaches the value of the atomic diameter, the compressibility decreases. If this is the case, then the suggestion of Axon and Hume-Rothery is in accord with Friedel's analysis of the influence of compressibility in Vegard's law, assuming the atom size of solute and solvent are approximately the same. If the compressibility of the solute is less than that of the solvent then a positive deviation from Vegard's law occurs, i.e. the AAD (apparent atomic diameter) of solute is greater than the AD (atomic diameter).

The work of Axon and Hume-Rothery also demonstrated the effect of electro-negativity on the apparent atom diameter of the solute. As the difference in electro-negativity increased the apparent atom diameter decreased. However, for the effect to be significant the differences in electro-negativity have to be considerable.

VOL. 9 1961

The influence of valence on lattice spacing is manifested in one of two ways. First, in univalent solvents, adding a solute of higher valency to the solvent thereby increasing the electron/atom ratio of the solid solution frequently produces a positive deviation from Vegard's law. Second, in certain alloy systems changing the electron/atom ratio by the addition of a solute of different valency produces curves of lattice spacing versus concentration which exhibit distinct changes in slope. These have been attributed to an electron overlap of the Brillouin Zone boundary. These two valency influences will be discussed separately.

The influence of valency on the mean lattice spacing of univalent solvents has been studied by OWEN,[34] RAYNOR,[35] and AXON and HUME-ROTHERY.[33] OWEN[34] studied the alloys of copper, silver and gold with zinc, gallium, germanium, and arsenic, and cadmium, indium, tin and antimony. Owen concluded that as the valency increases, the lattice spacing increases in a generally linear way. Owen made no correction for the diameters of the various solute atoms since they are all approximately the same within the same period. He concluded that $\Delta a/a \sim \Delta V$ where $\Delta a/a$ is the lattice distortion and ΔV is the valency difference between solute and solvent. OWEN[34] recognized this as a trend from one solute element to the next, but he apparently considered that the atom size of solute was not a function of concentration.

In 1948 RAYNOR[35] showed that the apparent atom diameter* was not only a function of the difference in valency between solute and solvent but also a function of the electron/atom ratio. He found that for monovalent solvents the observed lattice spacing differed from the lattice spacing predicted by Vegard's law as if the atomic diameter of the solute differed from its elemental diameter by Δr. He found

$$\frac{\Delta r}{(e-1)} = K\,(V_{\text{solute}} - V_{\text{solvent}}) \quad . \quad . \quad . \quad . \quad . \quad (10)$$

* The apparent atom diameter of a solute atom is obtained by extrapolating a curve of lattice spacing vs. composition in the dilute solute regions to 100 per cent solute.

where e is the electron/atom ratio, V_{solute}, and V_{solvent} are the valencies of the solute and solvent respectively, and K is a proportionality constant. In the calculation he assumed that the atomic diameter was unchanged by alloying.

Recently PEARSON[25] has suggested that the above relation obscures the basic relation between the change in lattice spacing due to valency and the valency difference ($V_{\text{solute}} - V_{\text{solvent}}$). This occurs because $(e - 1)$ is itself a function of valency difference. When the solvent is monovalent

$$(e - 1) = \frac{n_a}{n_a + n_b}(V_a - V_b) \quad . \quad . \quad . \quad . \quad . \quad (11)$$

If this relation is introduced into the above equation then it becomes

$$\Delta r = \frac{n_{\text{solute}} + n_{\text{solvent}}}{n_{\text{solute}}} = K(V_{\text{solute}} - V_{\text{solvent}}) \quad . \quad . \quad . \quad (12)$$

As pointed out by Raynor, this is the same relation as that found by LINDE[36] for the change in resistance of solid solutions as a function of valence.

RAYNOR[35] found the lattice spacing relations for polyvalent solvents varied as a function of valency qualitatively in the same manner as was observed for monovalent solvents, however, as yet a quantitative treatment for the polyvalent solvents has not been developed.

In order to determine the actual size of an atom in solid solution it is necessary to measure the interatomic distance between like nearest neighbours. As pointed out above this is not possible using the Bragg reflections. In 1951 such a determination was made. It was based upon a knowledge of the lattice spacing of the solid solution and the diffuse scattering due to local atomic displacements. WARREN, AVERBACH, and ROBERTS[102] assumed that in general the atoms of a solid solution are not on the average lattice sites. The distance between atoms which are only a few atom diameters apart is a function of the arrangement of the atoms and their size. The X-ray scattering from such pairs of atoms depends on the differences in scattering power of the atoms and their position. Such scattering does not contribute to the Bragg reflections. If the atoms are arranged at *random*, the Laue monotonic diffuse scattering results. However, if the atoms are not randomly distributed but instead, exhibit short range order or clustering, a modulation will be produced in the diffuse scattering. A further modulation is produced which is a function of the atomic diameter of the atoms in solid solution. The parameter which relates the modulations in the diffuse intensity to atomic size is:

where

$$\beta_i = \frac{1}{(\eta - 1)}\left\{\left(\frac{m_B}{m_A} + \alpha_i\right)\epsilon^i_{BB}\,\eta - \left(\frac{m_A}{m_B} + \alpha_i\right)\epsilon^i_{AA}\right\}$$

where

$$\eta = \frac{f_B}{f_A};\ f_A = \text{scattering factor of } A \text{ atoms}$$

m_A = mol fraction of A atoms
m_B = mol fraction of B atoms.

$$\epsilon^i_{AA} = \frac{r^i_{AA} - r_i}{r_i}; \quad \epsilon^i_{BB} = \frac{r^i_{BB} - r_i}{r_i}$$

r_i = average interatomic distance to the ith neighbour, calculated from the alloy lattice parameter.

r^i_{AA} = distance between an A atom and another in the ith shell.

r^i_{BB} = distance between a B atom and another in the ith shell.

$\alpha_i = 1 - \frac{P_A}{m_A}$; P_A = probability of finding an A atom in the ith shell about a B atom.

The calculation of atomic size by this method does not involve assumption of atom shape. The value obtained from the calculation is a nearest neighbour distance for like atoms $r_{AA}{}^1$ and $r_{BB}{}^1$.

Since the work of Warren, Averbach and Roberts, several solid solution systems[37] [51] [103] have been studied. These show that the atoms in solid solution vary in size as a function of composition. The two atoms of the solid solution tend to approach the size of an atom whose size is calculated from the average lattice parameter. For the gold–nickel system see Fig. 12. The lattice distortions calculated from X-ray data are less than that calculated for a system where the atom sizes are calculated from compressibility data. More recently Borie* calculated the actual sizes of atoms in solid solution using another method of X-ray measurement. His method involves considering the displacements of the atom centres from the sites of the average lattice in an anologous way to the measurement of dynamic displacements associated with thermal motion. Of course the static displacements do not vary with temperature. Such an analysis was first made by HUANG.[29] In his analysis Huang assumed the solute atoms behaved as elastic centres randomly distributed in the solvent lattice. The distance between two atoms was assumed to depend upon the distribution of solute atoms in the vicinity of this lattice vector between the two atoms concerned. Huang did not take into consideration the identity of the atoms at the ends of the lattice vector. As a result Huang predicted a reduction in Bragg intensities by a factor exp $(-\beta^1 \sin^2\theta/\lambda^2)$ and a diffuse scattering term. His analysis, however, did not yield a modulation in the diffuse scattering. By taking into account the identity of the atoms at the ends of the lattice vector Borie predicts a reduction of the Bragg intensities, a diffuse scattering similar to temperature diffuse scattering and a modulation of the Laue monotonic scattering identical with that of Warren, Averbach and Roberts size factor parameter β_1. Borie's treatment not only includes the diffuse scattering effects of Warren, Averbach, and Roberts but also relates the atomic displacements to the Bragg intensities through his factor B^1. This quantity is related to the difference in volume between each of the atoms and the mean atomic volume.

* Borie's work essentially includes both of the cases treated by WARREN, AVERBACH and ROBERTS[103] and of HUANG[29]; see Herbstein, F., Borie, B. and Averbach, B., *Acta Cryst.* 9 (1956) 446.

VOL. 9 1961

The measurements of static displacements involves a calculation which does not depend upon the difference in scattering power of the atoms as is the case of β_1. It is therefore possible to make measurements on such important solid solutions as α-brass.

The large changes in atomic radius still have to be explained. Only a small part of the change in atomic radii, at least in the Au–Ni system, appears to be due to the compressibility of the atoms. Since both atoms increase in diameter as the composition varies from nickel to gold one might suggest this is a valency effect. Work of Rudman and Averbach in silver–aluminum shows that there is no significant change of atomic radii of the atoms as a function of composition in this system. Therefore, it appears unlikely that the pronounced change in atomic radii beyond the compressibility effect are valence effects.

The lattice spacings of certain metal systems change abruptly in a way which has been associated with changes in the electron/atom ratio of the alloys and Brillouin Zone overlap. For example, in hexagonal close packed metals, several instances have been observed in which the curve of the "c" lattice parameter as a function of composition exhibits an abrupt change in slope. In these cases it has been noted that there is no corresponding abrupt change in the "a" lattice parameter curve. This has been attributed by RAYNOR[39] and HUME-ROTHERY and RAYNOR[40] to Brillouin Zone overlap. (See *Progress in Metal Physics*, Vol. 1, Raynor, *Advances in the Theory of Alloys*, p. 1.) These breaks have been interpreted as occurring at electron/atom concentration where there is the beginning of overlap of electrons across the faces of the second Brillouin Zone. This overlap occurs across the face which is perpendicular to the *c*-axis and thus causes a contraction of the zone in the *c*-direction. This reciprocal lattice contraction in turn produces an expansion in the *c*-direction of the real crystal lattice. This effect has been noted in the η-phase in the Cu–Zn system and in six magnesium rich terminal solid solutions.

Recently[41] [42] three of the magnesium systems have been remeasured and the original lattice parameter measurements have not been confirmed. In two cases (Mg–Pb) and (Mg–Al) no break was found and in the third (Mg–In) the effect was much smaller and at a composition other than that which would correspond to a Brillouin Zone overlap. In the light of this recent evidence WALKER and MAREZIO[41] suggest that none of the lattice parameter data on these particular magnesium base solid solutions can serve as satisfactory evidence of the onset of electron overlap of the Brillouin Zone.†

† The original one-electron theory of the effect of electron overlap on lattice distortions is due to H. Jones (*Proc. Roy. Soc.* A144 (1934) 225); (*Proc. Roy Soc.* A147 (1934) 396). More recent work by Goodenough (*Phys. Rev.* 89 (1953) 282), extends the theory a little further to the case of the 3/2 electron compounds. Even more recently, McClure (*Phys. Rev.* 98 (1955) 449), included electrostatic and exchange energy terms in his treatment of the HCP distortion effects and was able to show that they are important to the problem.

4.2 *Strain Energy Contributions in Solid Solutions*

The distortional energies of solid solutions associated with the elastic strains produced by solute atoms of different size than the solvent atoms have been computed by a number of authors (see the work of PINÉS,[43] LAWSON,[44] CRUSSARD,[45] ESHELBY[46] and FRIEDEL.[47]) All of them approach the problem in common by applying the methods of classical elasticity. Some of these treatments consider that the elastic calculation represents a contribution to the internal energy of the alloy, whereas others assume that the elastic energy is truly a free energy term. If the latter viewpoint is true, as seems likely, differentiation of the free energy with respect to temperature yields an entropy contribution.

FRIEDEL[47] has treated the problem for both dilute and finite concentrations. Friedel's method of calculation involves the determination of the work done if one is able to fix the dissolved atom on a given lattice point. To obtain a value characterizing a reversible process, a term is added which gives the entropy of position. This result is identified as the free energy of solution associated with the introduction of a solute atom of different size into the solvent matrix. The configurational entropy term used in this calculation is the random one. However, since diffuse X-ray scattering measurements indicate that few if any solid solutions are random, the assumption of a random distribution of atoms is not warranted. The major advantage of assuming such an elastic model is that it provides a reasonable theoretical explanation for the large positive values of ΔH^M that have been obtained for certain alloys systems (e.g. gold–nickel and cadmium–zinc). Since the temperature variation of the strain energy corresponds to a large positive entropy of solution for the alloy, Friedel has shown how its existence may be observed by studying the temperature dependence of the elastic constants of the alloy. According to Friedel

$$\Delta S = -\frac{\partial(\Delta F)}{\partial T} = \frac{\Delta F}{1+\alpha}\left(\frac{\partial \chi'}{\chi' \partial T} + \alpha \frac{\partial \chi}{\chi \partial T}\right) \quad . \quad . \quad . \quad (13)$$

where $\alpha = (a - r_s)/(r_s^1 - a)$, r_s = solvent radius, r_s^1 = solute radius, a = lattice parameter and χ, χ' = solvent and solute compressibilities respectively. Corroborating behaviour has been observed in cadmium–zinc[52] and gold–nickel[50] alloys, which have large size factors.

In order to obtain a more satisfactory experimental determination of the strain energy contribution LUMSDEN[48] and WAGNER[49] have suggested that a comparison of the relevant experimental thermodynamic quantities of the liquid and the solid solutions may yield a satisfactory measure of this quantity. ORIANI[50] chose the gold–copper and gold–silver systems since e/A stays constant, to test this idea using a galvanic-cell technique to measure the thermodynamic properties of these systems in the liquid and solid phases. Table 4 lists for comparison the enthalpies of formation of the solid and liquid alloys determined by Oriani and others. Since the strain energies are usually assumed to disappear with melting, because the atoms are more loosely

VOL. 9 1961

TABLE 4

Solution Energies of Solid and Liquid Solutions

	ΔH_S	ΔH_L
(0·4)Cu–(0·6)Au	− 1100[a],−1450[b] − 1250[c]	− 1500[d]
(0·4)Ag–(0·6)Au	910[a]	− 1000[a]
(0·5)Cd–(0·5)Mg	− 1300[e]	− 2000[f], − 1670[k]
(0·4)Ni–(0·6)Au	+ 2600[g]	(1650)[j], 1800[c]
(0·5)Ag–(0·5)Cu		2000[j], 2400[c]
(0·98)Ag–(0·02)Si		300[c]
(0·8)Cu–(0·2)Zn	− 1400[k]	− 1200[k]

(after ORIANI[54])

ΔH_S is the enthalpy of formation of a solid solution from its solid components.
ΔH_L is the enthalpy of formation of a solid solution from its liquid components.

a. ORIANI, R.; *Acta Met.* 2 (1954) 608.
b. ORR, R. and HULTGREN, R.; Mineral Research Laboratory Report, (Berkeley), June 15, 1956.
c. ORIANI, R. and MURPHY, W.; (by direct calorimetry) to be published.
d. ORIANI, R.; *Acta Met.* 4 (1956) 15.
e. TRUMBORE, F.; *J. Amer. Chem. Soc.* 76 (1954) 6417.
f. KAWAKAMI, M.; *Sci. Rep. Res. Insts. Tohoku Univ.* 19 (1930) 521.
g. SEIGLE, L., COHEN, M. and AVERBACH, B.; *Trans. A.I.M.E. J. Metals* 4 (1952) 1320.
j. EDWARDS, R. and DOWNING, J.; *J. Phys. Chem.* 60 (1956) 108.
k. *Selected Values for the Thermodynamic Properties of Metals and Alloys*—Minerals Research Laboratory, University of California.

bound in the liquid, a considerable difference in ehthalpies of formation should be observed for solid and liquid. As Oriani points out, this is not the case and hence it seems unreasonable to attribute a large "misfit" energy to the elastic strains in the lattice. Independent agreement with the above results were obtained by RUDMAN[51] on comparing the "atomic size" coefficient, β_1, evaluated by elasticity theory with that determined experimentally from X-ray diffuse scattering measurements;[37] (see Fig. 13). It was found that the calculated sizes are much larger than the measured sizes of atoms in solution. This results in much lower "misfit" energies for real solid solutions as compared to those calculated from an elastic model.

The major difficulties in strain energy calculations seem to arise when one attempts to put the *concept* of atomic size on a quantitative basis. BRAGG[53] and ORIANI[54] have also pointed out that if the solute atom is smaller than the solvent there will be a decrease in ionic repulsion energy which probably is greater than the positive strain energy involved in the relaxation of the lattice around the solute. FRIEDEL,[55] assuming a Gruneisen solid, shows that the energy for such a case is still positive. NOWICK[56] further points out that one should also take into account surface terms which again should favour a positive energy term. At present there appears to be no satisfactory elastic

model to account for atomic size effects in solid solutions and the relatively large positive values of ΔH^M observed in some alloy systems with large size differences.

5. Structure of Solid Solutions

In discussing the formation of solid solutions in terms of the electronic and the atomic size factors it was shown that the presence of solute atoms in the matrix leads to certain irregularities in the crystal both electronic and structural. The electronic disorder arises from the fact that the electronic charge distribution is no longer truly periodic in the crystal when solute atoms are present. Structural disorders can arise from the difference in size between solute and solvent atoms which produce the Huang effects. The atoms no longer reside on the average lattice sites (see Fig. 15). Elastic distortions are produced when these "point" imperfections are introduced. However, solid solutions may exhibit additional irregularities in the lattice

VOL. 9 1961

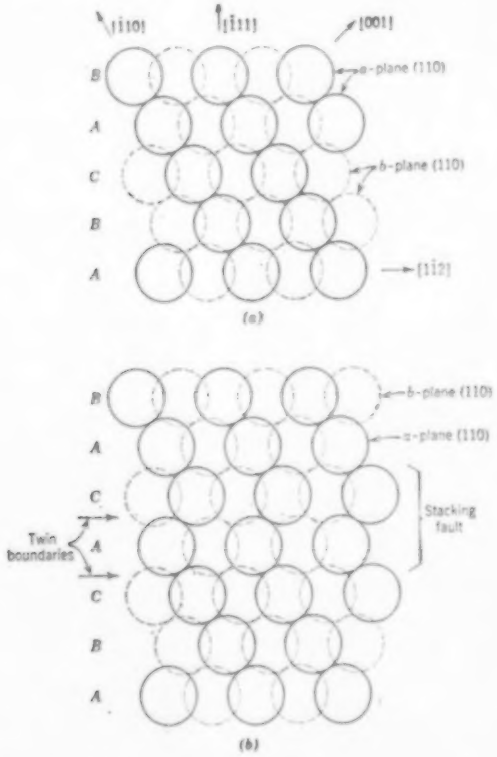

FIG. 16. Stacking Fault in FCC structures: (*a*) (110)-planes without Stacking Fault, (*b*) With Stacking Fault. The letters ABC refer to stacking of (111)-planes; after SEEGER.[89]

structure due to the presence of other types of "imperfections" with different properties. The study of these imperfections[57] is necessary to complete description of the structure and properties of solid solutions.

The presence of imperfections like vacancies, interstitials, and dislocations in the crystal will alter the distribution of internal magnetic and electric fields which influence the valence electrons. Individual defects may also interact with each other or with solute atoms to create more complex defects. For example, the mosaic structure of crystals may be described in terms of specific configurations of interacting dislocations; vacancies may interact to form di-vacancies or even pores; vacancies and solute atoms may interact with enhancement of solute diffusion resulting; vacancies and solute atoms may also interact with dislocations and affect the mechanical properties of alloys. The formation and their influence on the properties of solid solutions of several of the more common defects will be described in the following sections in terms of the electronic structure of the solid alloy.

5.1 *Formation of Lattice Defects and Their Interactions*

A consideration of solid solutions is not complete without a discussion of imperfections such as vacancies, interstitial atoms and dislocations. A detailed discussion of these is beyond the scope of this review. However, several aspects of these imperfections will be discussed. These are the formation of defects, how the solute distribution is affected by defects, and the influence of defects on structure sensitive properties except for the mechanical properties. For a detailed discussion of the mechanical properties of solid solutions and their structure sensitivity the reader is referred to the articles by Cottrell and Parker in the ASM seminar volume on *The Relation of Properties to Microstructure*.

The nature of the problem of formation of defects in a lattice is similar to the calculation of the energy of solution of a solute atom in a solvent matrix. In fact, Dexter has treated the vacancies in a pure metal lattice as solute atoms of zero valence. The calculation of the energy of formation of a vacancy in a solid solution of finite concentration is a problem of considerable difficulty that has not been attempted. However, a reasonably approximate value might be calculated for dilute alloy concentrations assuming a "rigid band" model and following the treatment given by FUMI[58] for vacancy formation in the noble metals. Fumi, following Friedel, assigned a $Z = -1$ to this "solute". Q_f, the energy of formation is largely an electronic energy and is treatable as such. For monovalent metals, the energy change of an electron gas in a sphere of metal is just the energy required to remove a positively charged ion together with its electron from the centre of the metal and place it on the surface of the metal. The free valence electrons will have their own wave functions modified in the region near the vacancy. The perturbing potential, V_p, was treated by Fumi in the same fashion as Friedel to determine the charge accumulation at the vacancy. The change in electronic energy was found to be

$$E_{el} = (2/3)\, E_{max}$$

There are, however, two corrections to be made, (*a*) one energy due to the change in density of the electron gas ($= 2E_{max}/5$), and (*b*) one energy due to the repulsive interactions between ion-cores near the vacancy ($= 0{\cdot}3$ eV). Subtracting these corrections from E_{el} Fumi obtained

	$(2/5)E_{max}$	$(2/3)E_{max}$	Q_f
Copper	2·84 eV	4·73 eV	1·60 eV
Silver	2·20 eV	3·67 eV	1·17 eV
Gold	2·20 eV	3·68 eV	1·18 eV

VOL. 9 1961

Since $\delta E_{max} = 0$ for dilute solutions Q_f should be about the same for dilute solutions as for pure metals.

For interstitials Q_f should contain an elastic distortional term as well as an electronic term. No attempts have been made to evaluate an energy of formation for interstitials in a solid solution although reasonable estimates have been made by BROOKS[59] and others[60] for pure monovalent metals. For dilute solutions we would again expect about the same values of Q_f as for the pure solvents. Rough estimates give an energy of formation of an interstitial in the noble metals to be about 5 eV and may be considered a reasonable value for dilute solutions of these solvents.

The energy of formation of a dislocation is nearly all elastic energy. However, the electronic structure of the solid solution influences the problem considerably through its effect on (*a*) the elastic constants and the lattice spacings, and (*b*) the shape of the dislocation. The elastic energy calculations have been considered by Cottrell in volume I of this series while calculations of the elastic constants have been treated by Mott in volume III. Therefore, these two problems will not be considered here; the present discussion being limited to the problem of the shape of the dislocation. This discussion will follow that originally given by Seeger.

A particularly interesting feature of dislocations in close-packed lattices is the possibility that a dislocation may dissociate into two partial dislocations of opposite sign, which enclose regions of stacking fault between them. A stacking fault is a break in the stacking order of the ideal close-packed lattice which still maintains the number and distance of nearest neighbours (see Fig. 16). No calculations of energies required to form stacking faults have been made using the electron theory. However, SEEGER[61] has discussed qualitatively the dependence of the stacking fault energy on the electronic structure of the solid solution. The resulting estimates give good agreement with experimental findings.

As Seeger points out the electrons in closed shells will give rise to interactions mainly between neighbouring ions (overlap and Van der Waals' types). Since both the number and spacing of nearest neighbours are the

same in the stacking fault as in the perfect crystal there should be only a small contribution to the increase in energy in the stacking fault by the core electrons. The conduction electrons on the other hand will be perturbed by faults in the Brillouin zone reflecting planes and the corresponding change in the shape of the Fermi surface if it approaches the zone boundaries. The direction of the change introduced by the stacking fault results in an increase in energy, otherwise the crystal structure would be unstable. In monovalent metals like copper, silver and gold the filled conduction electron states presumably do not even touch the Brillouin zone boundaries so their energy will hardly be affected by the position of the zone boundaries. On the other hand, the Fermi distribution of electrons in polyvalent metals like aluminium, magnesium, zinc and cadmium will touch and overlap the boundaries of the first Brillouin zone and thus the possibility arises of a strong increase in energy in the presence of a stacking fault. In light of the above considerations low stacking fault energies are to be expected for metals like copper, silver and gold and the close-packed modifications of the alkali metals (e.g. hexagonal close-packed lithium). We should expect high stacking fault energies for aluminium, magnesium, zinc and cadmium.

The estimation of stacking fault energies for transition metals is more complicated. This is due to the fact that Van der Waals' and homopolar forces due to *d*-electron interactions between nearest and next nearest neighbours are important. For metals like iron, cobalt, nickel, ruthenium, rhodium, palladium, osmium, iridium and platinum a systematic study by Seeger of the energetically favourable structures of these metals shows that both the FCC and HCP structures are energetically favourable. (By "energetically favourable" it is meant that the cohesive energy of the meta stable structure differs by not more than 0·3 per cent from the cohesive energy of the stable structre.) Taking into account both *d*- and *s*- electrons, it was shown that the number of *d*-electrons/atom determines which are favourable structures. Vanadium, niobium, tantalum, chromium, molybdenum and tungsten had energetically favourable HCP structures but not FCC structures. The same is true for titanium, zirconium and hafnium. If both close-packed structures are energetically favourable, the stacking fault energy is expected to be low; if only one of them is favourable, the stacking fault energy will be high. The known facts of transition metal allotropy and stacking fault energies agree with these conclusions. Cobalt has been shown by Barrett to have low stacking fault energies. The fact that annealing twins are so easily formed in nickel indicates a low stacking fault energy for nickel.

A different approach to stacking fault energies is based on forces between next nearest neighbours; since it is there, not the nearest neighbour interactions that are affected by stacking disorders in close-packed structures. Following this model it is useful to picture a stacking fault in a close-packed structure as a thin twin crystal bounded by two coherent (111) twin boundaries. One then would estimate the stacking fault energy to be just twice the twin boundary energy. Comparison of the data for copper and aluminium show

that the stacking fault formation in aluminium requires 5 times as much energy as for copper, therefore stacking fault formation should be favoured in copper as compared to aluminium. Recently, direct evidence of the presence and shape of dislocations in metals and solid solutions has been observed. Whelan, Hirsch, Horne and Bollmann, using a transmission electron micrographic technique, have been able to observe the presence of dislocations in aluminium and in a FeCrNi stainless steel, which had been previously deformed about 10 per cent. Both structures are face-centred cubic yet show completely different dislocation shapes. In aluminium the dislocations are unextended while in the stainless steel alloys the presence of "extended" dislocations containing regions of stacking fault was observed directly. This is just the result that one would predict on the basis of Seeger's predictions of stacking fault energies.

VOL. 9 1961

The ideas brought forth by Seeger applied with regard to the case of solid solutions appear to be supported by the well-known result that annealing twins occur more frequently in zinc-rich alpha-brass than in pure copper. Furthermore, Seeger's hypothesis also is supported by investigations of the occurrence of stacking faults in heavily cold-worked copper and alpha-solid solutions of copper; the most detailed investigations are those of SMALLMAN and WESTMACOTT, of C. S. BARRETT and of WARREN and WAREKOIS.[63] [64] [62] Warren and Warekois showed that the frequency of stacking faults increased with increasing zinc content of an alpha-brass alloy. Barrett has observed a similar behaviour to occur in copper–silicon alloys. The work of Barrett and Massalski on copper–zinc alloys of composition just beyond the alpha-phase boundary is also in agreement with these results. These data are most easily interpreted as being due to an increasing extension of the stacking fault ribbons of extended dislocations and therefore a *decreasing* stacking fault energy with *increasing* solute content. Such a result is completely unexpected if one is inclined to accept Friedel's picture of the energy band structure of these alloys. Since in his model we presume that the Fermi surface in pure copper is not touching the zone boundaries, we would expect the Fermi surface to approach the zone boundaries as we increase the solute content of the alloys. This means an *increase* in stacking fault energy is to be expected with increasing solute content rather than the observed *decrease* in stacking fault energy. The question may be partially resolved for dilute concentrations if we accept COHEN'S[65] extension of PIPPARD'S[67] original proposal about the Fermi surface in pure copper. Essentially, he proposes that (in light of Pippard's results) the Fermi surface is touching the zone boundaries in pure copper and that the band structure is distorted with increasing solute concentration. He states there are then two competing effects on alloying. They are (*a*) a change occurs in the energies at the centres of the Brillouin zones faces, and (*b*) the band structure is filled up as e/A increases. (*a*) tends to result in making the Fermi surface pull away from the Brillouin zone faces while (*b*) produces the opposite effect. Measurements quoted by COHEN[66] and performed by PIPPARD[67] on pure copper are said to favour an initial

contact of the Fermi surface with the zone boundaries so that alloying will cause the Fermi surface to pull away from the zone boundaries, i.e. (*a*) predominates. Therefore, in light of Seeger's arguments, it can be seen how the energies[68] of stacking faults in copper alloys decrease initially with increasing solute concentration. The situation is reasonably clear for copper-based solid solutions as a result of the measurements of Smallman and Westmacott. They measured the relative shift of the (111) and (200) pair of Bragg reflections produced by stacking faults on the (111) planes of alloys of copper with nickel, zinc, aluminium, tin and germanium.† Measurements of the peak shifts produced on deformation of these alloys allowed them to determine the stacking fault probabilities using the analysis of Warren and Warekois. The results of their experiments on materials deformed at room temperature are shown in Table 5. One conclusion that may be drawn from

TABLE 5

Stacking Fault Probabilities α versus Composition and Electron Concentration for copper-base Solid Solutions

	Atomic per cent	$\alpha \times 10^5$	e/A
Cu		3·3	1·0
Ni		1·65	
Cu–Ni	50 per cent	5·0	·5
Cu–Zn	14 ,,	7·0	1·14
	27 ,,	20·0	1·27
Cu–Al	5·7 ,,	10 to 11·7	1·12
	11·0 ,,	29·0	1·22
	17·0 ,,	40·0	1·34
Cu–Sn	2·5 ,,	5 to 6·6	1·08
	4·5 ,,	14·5	1·14
	7·1 ,,	34·0	1·21
Cu–Ge	2·5 ,,	5·0	1·08
	5·0 ,,	14·5	1·15
	7·2 ,,	31·7 to 37·0	1·22

(Measurements made at room temperature; after SMALLMAN and WESTMACOTT[62])

their results is that the variation of stacking fault probabilities and hence stacking fault energies in copper, silver and gold at low solute concentrations may be a function of the e/A ratio rather than the particular solute element. Of particular interest is the fact that the stacking fault probability vs. (e/A) passes through a minimum at $e/A = 1{\cdot}0$, namely pure copper, providing we accept the valence scheme proposed by Friedel and discussed earlier in section 3.1. This would seem to be further corroboration of Cohen's proposal that the Fermi surface just touches the zone boundaries in pure copper. The lack

† The original stacking fault calculations were performed by M. Patterson (*J. Appl. Phys.* 23 (1952) 805). He was able to show that stacking faults on the (111) planes of FCC materials produce a line broadening and a small shift of the diffraction lines.

of sufficient data in the case of gold and silver prevent any generalization concerning these metals. It is suggested that a study of stacking fault probabilities in silver- and gold-based solid solutions might lead to a better understanding of the possibilities of contact between the Fermi surface and the zone boundaries in the pure materials.

The interaction of imperfections and solute atoms produces several distinct changes in the structure of solid solutions. In addition, these interactions affect those properties, which are structure sensitive, such as the electrical resistance, thermal conductivity, yield strength and certain magnetic properties (the susceptibility and remanence). The solute atom-defect interactions can occur in several ways; the most important ones involve solute atoms and dislocations, and are

(*a*) chemical interaction between solute atoms and the stacking faults associated with *extended* dislocations;

(*b*) elastic interaction between solute atoms and the dilatational strain field round a dislocation, which are most important for interstitial solutes;

(*c*) electrical interaction between the charge potential produced by the dilatational field of the dislocations and solute atoms of different valence than the solvent.

Other effects, primarily due to valence and atomic size, have been discussed previously in this section and in 3.1 and 4.1, and lead to

(*d*) an increase in the width of extended dislocations with an increase in e/A ratio (important in noble-metal base alloys);

(*e*) a change in the energies of formation and motion of vacancies with a change in the electronic energy of the alloy;

(*f*) changes in the lattice parameter of the matrix when a solute atom is added.

The chemical interaction[69] associated with the segregation of solute atoms at stacking faults arises because of the difference in chemical bonding of the two close-packed modifications of the crystal. The stacking fault region, which is HCP in an FCC lattice, can be treated as a separate phase with definite boundaries. It then follows that the thermodynamic theory of heterogeneous equilibrium predicts a solute atom concentration which is different in an FCC matrix from that in the HCP region of the stacking fault; analogous results are obtained for the case of stacking faults in HCP systems. It has been shown that the strain energy of the system dislocation plus solute atom is lowered as the solute moves into the region of the dislocation.[70] This in effect produces an attractive elastic interaction (*b*) between the dislocation and the solute atom which pulls the solute atom into the dislocation. Since the elastic and electrical interactions both depend on the dilatational field of the dislocation they are of similar character except for the valency dependence of the electrical interaction. COTTRELL *et al.*[71] considered the electrical interaction (*c*) and showed that the electronic charge should be redistributed about the dislocation to maintain a constant Fermi level

VOL.
9
1961

throughout the alloy. An electric dipole is formed which can interact with solute atoms of valence different from the solvent. For the case of copper-based alloys it was shown[71] that the elastic interaction (b) is from 3 to 7 times greater than the electrical interaction. No account was taken of screening terms. The electrical interaction is usually considered unimportant except in the case of ionic crystals.

Although the chemical, elastic and electrical interactions give rise to attractive forces which tend to pull solute atoms into the dislocation region, the physical basis for the formation of such clusters is different in each case. Saturation occurs for the clusters formed by chemical interaction as a result of heterogeneous equilibrium established between the stacking fault and the matrix.[69] COTTRELL and BILBY,[70] COCHARDT *et al.*[72] and WEBB[73] have shown that the elastic strain field of the dislocation becomes saturated if too many solutes are put into a small volume element dV near the dislocation. The effect is presumably important only when atomic misfit energies are large; that is, for the case of interstitial solutes. Recently, THOMSON[74] has criticized the concept of the saturability of the elastic strain field of the dislocation by considering the case of point singularities in an isotropic elastic medium. Neglecting non-linear terms he shows that the total interaction energy between the solute atoms and dislocations is linear in the local density of solute in any element of volume dV, and hence does not saturate. This result follows from the linearity of the equations of elasticity theory and is quite general. Thomson concluded that the most important forces governing saturation are the short-range chemical and non-linear forces, which are just the forces which lead to precipitation. Therefore, the study of saturation is just equivalent to a consideration of the nucleation of precipitates in a solid, which is not easily treated by elasticity theory. Cottrell's treatment of the electrical interaction should also lead to an electrostatic energy density which is linear in the solute particle density and therefore does not saturate.

Electrical resistance, a structure-sensitive property, is readily influenced by the atomic arrangement in the solid solution. Due to the wave-like behaviour of electrons any deviation from the perfect periodicity of a crystal lattice will result in the scattering of the free conduction electrons[75] and hence contribute to the electrical resistance. Therefore, dislocations,[76] vacancies,[77] random solute atom distributions[78] and stacking faults[78] will contribute to a "residual" resistance upon which is superimposed any short-range order or clustering effects. Resistometric studies of the ordering kinetics of copper–gold and other alloys exhibiting long-range order[79] emphasize the sensitivity of the resistivity to changes in short- and long-range order in solid solutions. The effect of the size of clusters of solute atoms or small ordered clusters is to cause "resonances" in the electron scattering and hence maxima in the electrical resistance when the cluster sizes are approximately equal to the Fermi wavelength of the conduction electrons.[80] Data reported for aged Duralumin,[81] copper–palladium[82] and gold–nickel[83] alloys agree with this result. Because of the structure sensitivity of the electrical

resistivity it is difficult to interpret the resistivity of solid solutions in terms of specific models. A similar problem exists for all of the electron transport properties (thermal conductivity, thermoelectric power, galvanomagnetic effects etc.), since defects, clusters and the degree of local order influence the scattering of electrons which in turn result in contributions to the transport properties.

The effect of lattice defects on the strength of metals and alloys has been studied extensively by COTTRELL,[85] MOTT and NABARRO,[84] PARKER[86] and others.[87] [88] They have shown that solute atoms, randomly distributed, segregated as clusters at dislocations or in the matrix, markedly affect the mechanical properties (for example, the yield joint phenomena observed in alloys, solid solution hardening etc.). FISHER and HART[87] have pointed out the importance of precipitate particles and of resistance by alloys to short-range order changes in the strengthening of concentrated solid solutions. The interaction of dislocations with other defects is also of primary importance as in the case of strain hardening resulting from the pile-up of dislocations at grain boundaries. However, it is only recently that consideration has been given to the influence of vacancies on the strengthening of metals and alloys. In principle, it would seem that vacancies, like solute atoms, should be attracted to dislocations to form atmospheres, therefore producing effects similar to those produced by solutes segregated at dislocations and in dispersed clusters in the matrix. For this reason, the work on vacancy hardening has been done on pure metals to avoid masking of the vacancy effects by those due to solute atoms. COTTRELL[89] has reported on some recent experiments dealing with the hardening effects due to vacancies produced by quenching and irradiation.[90] [91] Quench hardening is very similar to radiation hardening in its characteristics, both resulting in the pinning of dislocations as shown by internal friction experiments.[92] [93] The hardening due to quenched-in vacancies may be produced by either (*a*) changes in the core structure of dislocations or (*b*) sessile dislocations created by the collapse of vacancy clusters. COTTRELL[89] considered possibility (*a*) basing his model on the movement of jogs produced in edge dislocations by the precipitation of vacancies[90] and their annihilation at the dislocation cores. KIMURA, MADDIN and KUHLMANN-WILSDORF[89] have proposed that the excess vacancies cluster and then form sessile dislocation loops when the clusters collapse. These loops can cause hardening if they act as sources requiring high stresses to activate them. A more probable cause has been described by THORNTON and HIRSCH[94] as resulting from the interaction of glissile dislocations with the loops which will cause them to climb and glide on unfavourable slip planes, such as (100) planes in FCC crystals. Recent experimental studies by HIRSCH and SILCOX[95] have produced positive evidence of the formation of dislocation loops in aluminium and tetrahedral stacking faults in gold as the result of the collapse of vacancy clusters. Such configurations are to be expected for metals having high and low stacking fault energies respectively. This must be considered as strong evidence

VOL.
9
1961

favouring the ideas of KIMURA *et al.* and of Thornton and Hirsch. It is reasonable to assume that solution hardening effects due to vacancies should be similar to those due to solute atoms in alloys.

The heat of solution is an important chemical property which is apparently structure sensitive. KLEPPA[10] has observed a marked influence of the state of local order on ΔH^M. As a consequence of this structure dependence solute-dislocation interactions should particularly influence the solution energies measured for systems showing small solubilities. The only attempts made to observe this effect have been for the case of interstitial solutes.[96] A problem related to that of solution energies is the effect of solute atoms on the energy of formation and migration of vacancies.[97]† Recent quenching experiments by PEARSON and BRADSHAW[97] made on dilute platinum-based alloys indicate that these quantities do not differ significantly from those measured for the pure platinum metal. For the case of alloys of high concentration work on gold–cadmium alloys reported by WECHSLER[98] indicate a much lower energy of vacancy formation for the alloy as compared to the values obtained for pure gold. This problem is complicated by the fact that these alloys become ordered at low temperatures. The most important consequences of the effect of solute atoms on vacancy formation should be their influence on atomic diffusions* and high temperature creep behaviour in alloys.[99]

5.2 *Observations of Solid Solution Structure*

During the last ten years studies of the coherent diffuse X-ray scattering, including small angle scattering, have produced significant advances in the understanding of the structures of solid solutions. (See the review articles by WARREN and AVERBACH[100] and AVERBACH[101] in the ASM Seminar series.) The most fruitful studies have been carried out by studying the non-Bragg scattering of X-rays by solid solutions although in certain important situations neutron diffraction produces very valuable information.

If a beam of monochromatic X-rays falls on a solid solution crystal diffraction, effects from the crystal will consist of two parts; the sharp Bragg reflections and the diffuse scattering. The Bragg reflections give the average crystal structure of the sample; the size and shape of the unit cell and the average atomic positions in the cell. The occurrence of diffuse scattering will be due to any deviation from the ideal crystal periodicity, such as imperfec-

† The association of vacancies and solute atoms in alloys was suggested years ago by R. P. Johnson (*Phys. Rev.* 56 (1939) 814) on the basis of diffusion data in dilute alloys. More recently, Desorbo, Treaftis and Turnbull (*Acta Met.* 6 (1958) 401), and Federighi (*Acta Met.* 6 (1958) 379) have shown that the rapid kinetics of low temperature aging processes are probably due to quenched-in vacancies trapped in vacancy-solute clusters.

* The importance of solute-vacancy interactions has been considered experimentally and theoretically in some detail by D. Lazarus, L. Slifkin and th co-workers at the University of Illinois. See D. Lazarus, ASM Seminar volu "Impurities and Imperfections", p. 107 (1955).

tions (dislocations, vacancies and lattice vibrations), or solute atoms having different size and atomic scattering factors than solvent atoms.

WARREN, AVERBACH and ROBERTS[102] have shown that the diffuse X-ray intensity (uncorrected for thermal scattering) due to short-range order and size effects is given (in electron units) by

$$\frac{I_{\text{diff}}}{Nx_Ax_B(f_A-f_B)^2}=\sum_{m,n}\alpha_n \exp(i\vec{k}\cdot\vec{r}_{mn})+\sum_{m,n}\beta_n\, i\vec{k}\cdot\vec{r}\exp(i\vec{k}\cdot\vec{r}_{mn}). \quad (14)$$

where the α_n are the short-range order coefficients for the nth shell of atoms around a B atom. The β_n are the size effect parameters. The β_n are usually too small to be measured for other than nearest neighbours; i.e. $n = 1$ is the important term, although in certain systems β_2 is also important. The x_A and x_B are the mole fractions of A and B; the f's are the atomic scattering factors; r_{mn} is the distance to an A atom at the mth position in the nth shell of neighbours surrounding a B atom. The short-range order coefficients α_n have been defined[100] so that if $\alpha_n = 0$ the solution is random; if α_n is negative unlike neighbours are preferred and if positive like neighbours are preferred. If α_1 is negative, unlike *nearest* neighbours are preferred and if positive, like *nearest* neighbours are preferred. To illustrate this behaviour and its effect on I_{diff}, a plot of I_{diff} is shown in Fig. 17 for solutions which show complete randomness, short-range order ($\alpha_1 < 0$) or clustering ($\alpha_1 > 0$). Despite the popularity of the concept of a "regular" solution among thermochemists diffuse scattering measurements indicate that a random distribution of atoms is hardly ever observed in real solid solutions. There is either a

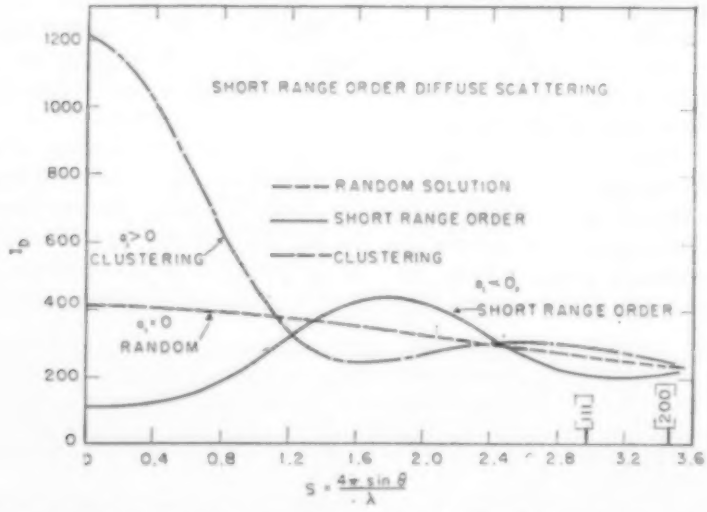

FIG. 17. Diffuse Powder Pattern intensities calculated for solutions which exhibit Randomness, Short-Range Order, and Clustering; after WARREN and AVERBACH.[100]

tendency towards short-range order or towards clustering in agreement with Friedel's valency curvature rule.

The coefficient β_n was derived by WARREN[102] by assuming that the inter-

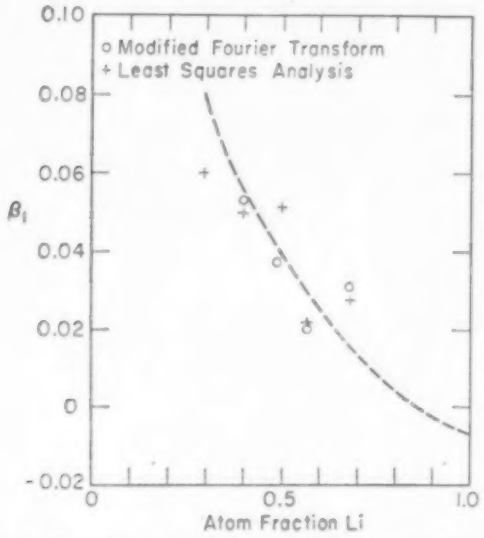

FIG. 18. Atomic Size Effect coefficients β_1 for the Li–Mg system; after HERBSTEIN and AVERBACH.[103]

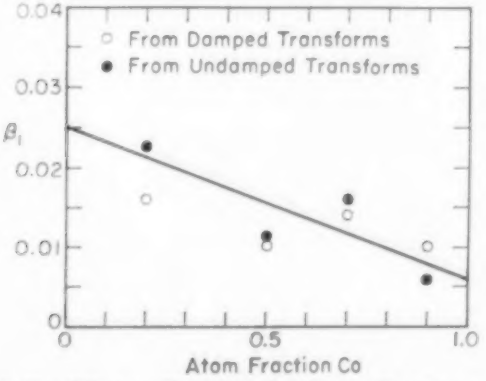

FIG. 19. Atomic Size Effect coefficients β_1 for the Co–Pt system; after RUDMAN and AVERBACH.[51]

atomic separations for nearest neighbours will be of three kinds, r_{AA}, r_{BB}, and r_{AB}, depending on the pair of atoms being considered. These are defined by

$$\begin{aligned} r_{AA}^n &= r_n(1 + \epsilon_{AA}^n) \\ r_{BB}^n &= r_n(1 + \epsilon_{BB}^n) \\ r_{AB}^n &= r_n(1 + \epsilon_{AB}^n) \end{aligned} \quad \ldots\ldots \quad (15)$$

where r_n is the average interatomic distance to the nth neighbour calculated from the alloy lattice parameter. $\epsilon_{AA}^n = (r_{AA}^n - r_n)/r_n$, and so on. One important result of the size effect measurements is that it was shown that the size of an atom in the lattice depends upon the composition of the solid solution (see Figs. 18, 19), and that the atoms no longer reside on the average

TABLE 6

Short-range Order Coefficients of Aluminium–Zinc and Aluminium–Silver Alloys

		No. of Zn atoms in first shell at 400°C		
x_{Zn}	α_1	*Random*	*Observed*	*Difference*
0·10	0·08	1·2	1·1	0·1
0·15	0·11	1·8	1·6	0·2
0·20	0·13	2·4	2·1	0·3
0·30	0·15	3·6	3·06	0·54
0·40	0·156	4·8	4·05	0·75
0·50	0·16	6·0	5·04	0·96

Effect of Temperature

		No. of Zn atoms in first shell for (0·9)Al–(0·1)Zn		
Temp. °C	α_1	*Random*	*Observed*	*Difference*
300	0·09	1·2	1·09	0·11
400	0·08	1·2	1·10	0·10
500	0·075	1·2	1·11	0·09

		No. of Ag atoms in first shell at 540°C for (0·9)Al–(0·1)Ag alloy		
	α_1	*Random*	*Observed*	*Difference*
(0·1)Ag	0·15	1·2	1·02	0·18

(After RUDMAN and AVERBACH, *Acta Met.* 2 (1954) 576)

Note: The X-ray data indicate that the Al, Ag and Zn atoms have almost identical sizes and thus there is no strain energy contribution; the occurrence of positive values of α_1 indicated a preference for clustering of like atoms.

lattice sites. This result is deduced from the fact that β_1 is found to be non-zero. The ϵ's which are determined from values of β_1, represent local displacements from the average lattice sites. Measurements have been made of α_1 and β_1 of a number of systems and are summarized in Table 6 and Figs. 20, 21, 22. The values of α_1 are useful in calculating the number of unlike nearest neighbour bonds in the solid solution. Knowing the ϵ's and the number of unlike bonds, the elastic strain energy and the chemical contributions to the

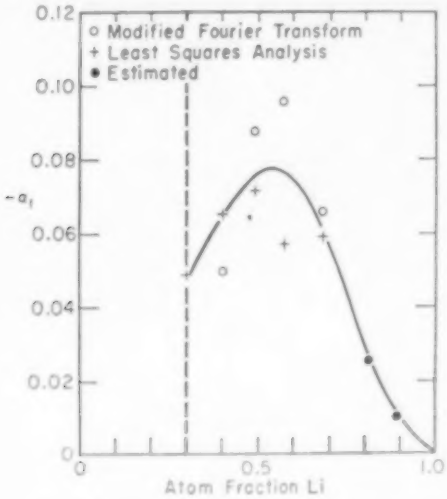

FIG. 20. Short-Range Order coefficients α_1 for the Li–Mg system: after HERBSTEIN and AVERBACH.[103]

heat of mixing ΔH^M can be calculated by the Quasi-chemical theory and compared with experiment. The general agreement is not too good and in some cases the experimental α_1 and β_1 contradict the theoretical predictions, notably in the case of gold–nickel and copper–platinum. The difficulties in these two cases appear to arise from the size for gold–nickel and possible polarization of the *d*-electron shells in the copper–platinum. An interesting effect has been observed in lithium–magnesium alloys. A minimum in the lattice parameter vs. composition curve was observed which suggests that the LiMg distance is less than the mean of the LiLi and MgMg distances (see Fig. 23). Normally, it is assumed that an atom has the same size (for a given solute concentration) irrespective of the identity of its nearest neighbours and hence the LiMg distance should be equal to the mean of the LiLi and the MgMg distances. The size effect data obtained by HERBSTEIN and AVERBACH[103] are interpreted on the basis that the lithium and magnesium atoms retain their pure metal sizes but that because of possible ionic interactions due to charge shifts the LiMg distance is shorter than the average and should be preferred. Measurements of α_1 by Herbstein agree with this result (see Fig. 20).

It has been shown that the atomic displacements associated with the thermal lattice vibrations also contribute to the diffuse scattering. Careful measurements of the temperature diffuse scattering component should permit determinations of the changes in the vibrational spectrum on solid solution formation. These vibrational changes and hence changes in the Debye Θ-temperature are reflected in the entropy of mixing terms of the

alloy. At present, data have been reported for only a few systems[104] [100] and seem to agree well with elastic constant data.

In Eqn. (14) it is shown that I_{diff} is proportional to $(f_A - f_B)^2$. This means that for alloys like copper–zinc and iron–copper and chromium–nickel* the

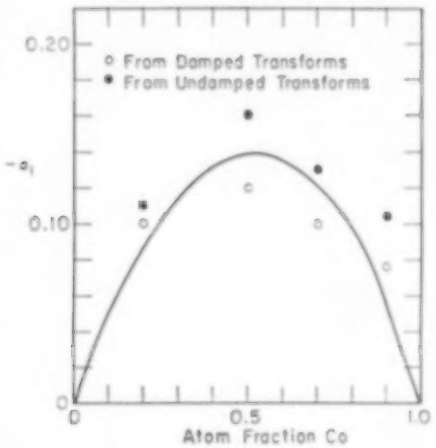

FIG. 21. Short-Range Order coefficients α_1 for the Co–Pt system; after RUDMAN and AVERBACH.[51]

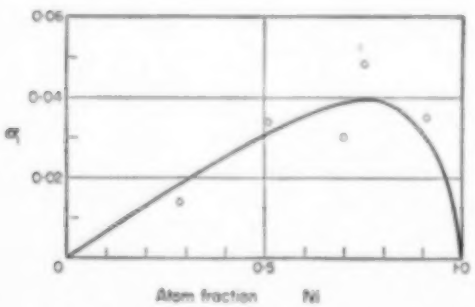

FIG. 22. Short-Range coefficients α_1 for the Au–Ni system; after FLINN *et al.*[97]

X-ray diffuse scattering intensity due to short-range order and size effects will be difficult to observe. (Studies of long-range order in these materials will also be difficult.) On the other hand, neutron scattering factors will be quite distinct for such materials and hence neutron diffraction will be of considerable help in such studies. There are some differences between the

* For example, recent neutron diffraction studies[108] have resolved the question as to whether an ordered structure exists at the Ni_3Cr composition or not; there is apparently no ordering.

VOL. 9 1961

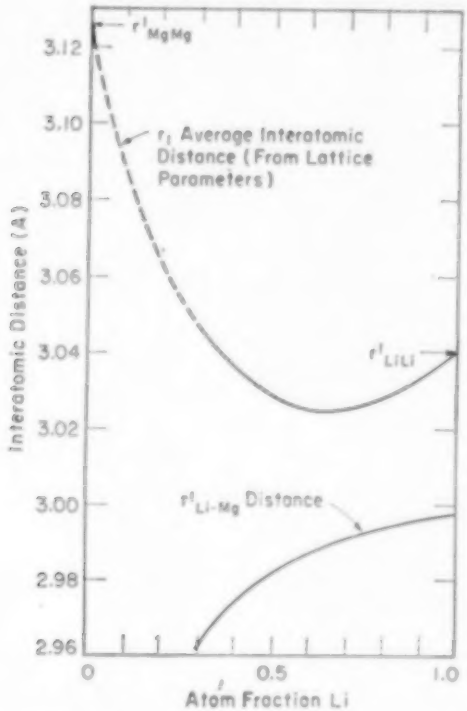

FIG. 23. Interatomic Distances for the Li–Mg system; after HERBSTEIN and AVERBACH.[103]

scattering of X-rays and neutrons by atoms which must be accounted for in order properly to interpret the data. X-rays are scattered only by the electrons in the atom while neutrons are primarily scattered by the short-range nuclear forces. A notable exception occurs when the iron-core electrons impart a permanent magnetic moment to a constituent atom of the alloy. Since the neutron possesses a magnetic moment, it can interact with the atomic moments so that there will be a superposition of scattering effects due to both the magnetic and the nuclear force interaction. In some cases the magnetic interaction may be comparable to or even exceed the nuclear interactions. This offers the possibility of obtaining ordering information about crystalline magnetic systems as well as the usual short-range and long-range order information. The work of SHULL and WILKINSON[105] on transition metal alloys iron–cobalt, cobalt–chromium, iron–chromium, nickel–iron, and ordered Ni_3Mn permitted the observation of magnetic disorder and of super-lattice formation. Careful studies of the magnetic disorder scattering by these workers indicate there are differences in the magnetic moments of the various atomic species and that also these atomic magnetic

moments differ from the values known to exist in the pure element form. A change in composition is found to alter the individual moments although an explanation in terms of electron concentration is not well established. As an example, it was found that the Fe magnetic moment is decreased by adding chromium. In the case of Ni_3Fe the magnetic scattering indicates that the individual atomic moments are determined by the composition and not by the state of chemical order in the alloy. Therefore it appears that the local electron concentration surrounding an atom is not as effective in determining its magnetic moment as is the overall e/A concentration of the alloy.

Recently attention has been focussed on the possibility of obtaining information on the nature of the physical structure of metals and alloys by means of electron transmission micrographic techniques and by diffuse neutron scattering techniques. The studies of Hirsch *et al.* using the micrographic technique have already been reported in the discussion of stacking faults. Other investigators[95] [107] have recently applied these micrographic techniques to the study of vacancy clustering in the noble metals and the clustering of solute atoms in copper–aluminium alloys. The work of WEISS *et al.*,[108] and ATKINSON and others[109] indicate that the ease of neutron transmission through materials and the ease of obtaining long-wavelength beams are especially advantageous for the making of small-angle scattering studies of dislocations in metals.

VOL. 9 1961

6. PHYSICAL PROPERTIES AND THE ELECTRONIC STRUCTURE OF SOLID SOLUTIONS

Measurements of certain physical properties of metals and their solid solutions will complement theoretical treatments of solid solutions by rendering information about important features in their electronic structure and hence test the appropriateness of certain solid solution models. Some of the more promising experiments and their significance are listed below and will be discussed in the following sections:

(*a*) X-ray line intensity and neutron diffraction experiments. Measurements of the absolute intensities of the Bragg lines will give information about the spatial distribution of electrons about atomic sites. Neutron diffraction experiments will, in principle, reveal the strengths and orientations of atomic magnetic moments in a crystal.

(*b*) Electronic specific heat measurements. Determination of the linear temperature term, γT, in the specific heat will give the form of the density of states curve in the neighbourhood of the Fermi surface.

(*c*) Electrical resistance measurements. In principle, measurements of the electrical resistance should give information about the form of the N(E) curve in solid solutions since the transition probability for a given perturbation is proportional to the density of states at the Fermi surface.

6.1 *X-ray Intensity and Neutron Diffraction Experiments*

In a recent report WEISS and DEMARCO[110]† describe the X-ray determination of the atomic scattering factors of several pure solid transition elements (Cr, Fe, Co, Ni, and Cu). From these data they were able to determine the outer electron configurations of the atoms in the pure solids. This report promises innovations in our thinking regarding the electronic structure of the above metals. Their experimental procedure involved (i) a measurement of the "absolute scattering factor" from which is subtracted the "Argon core", which was calculated by self-consistent field techniques. The result leaves the contributions to the scattering factor due to the 3*d*, 4*s* and 4*p* electrons. The radial extension of the charge of the 4*s* and 4*p* electrons is such that their contribution to the scattering factor is negligible. (ii) to obtain absolute scattering factor data, corrections must be made for primary and secondary extinction, surface roughness of the specimen, dispersion, thermal diffuse scattering, absolute counting and the absorption coefficient. Assuming the residual scattering factors (i.e. after making the necessary corrections and subtracting the "Argon core") are due to the 3*d* electrons only, for the lowest angle Bragg reflection, then the peak alone is sufficient to determine the number of 3*d* electrons. The results for chromium, nickel, cobalt, iron and copper are given below

	3d electrons		*4s/4p electrons*	
	(*solid*)	(*atom*)	(*solid*)	(*atom* 4*s*)
Cu	9·8 ± 0·3	10·0	1·0	1·0
Ni	9·7 ± 0·3	8·0	0·5	2·0
Co	8·4 ± 0·3	7·0	0·6	2·0
Fe	2·3 ± 0·3	6·0	5·7	2·0
Cr	0·2 ± 0·4	5·0	5·8	1·0

One should note the marked discrepancy between these results and the known 3*d* configurations for the free atoms.

Recent neutron diffraction experiments performed by SHULL and WILKINSON[105] on some transition metals and their alloys have yielded important information about the magnetic crystal systems found in these materials. Measurements of diffuse neutron scattering allow one to determine an upper limit on the magnitudes of atomic moments which are uncorrelated in orientation. Elements belonging to Groups V-A and VI-A have been examined and show an upper limit of about $0{\cdot}2\mu_B$. Measurements of the

† A more recent publication by Batterman (*Phys. Rev. Letters* 2 (1959) 47) reports what appear to be discrepancies in the results of Weiss and DeMarco for Fe. The difficulty seems to arise from the corrections to be made for extinction as there is no reliable theoretical method of doing this. Batterman used cold-worked specimens in order to make extinction effects negligible. He obtains a value of 6·2 ± 0·4 3*d* electrons per Fe atom which is in good agreement with calculations made using free atom wave functions.

magnetic disorder scattering indicate that the magnetic moments of the alloy constituents differ and that a change in the chemical composition of the alloys alters the individual moments; see Figs. 24, 25, 26. This would seem to indicate that the e/A and not the local surroundings determines the moment on a particular atom. Since it was found that for all alloy systems studied, a magnetic form factor dependence on scattering angle matches that for pure iron satisfactorily, it can be assumed that the magnetic shells

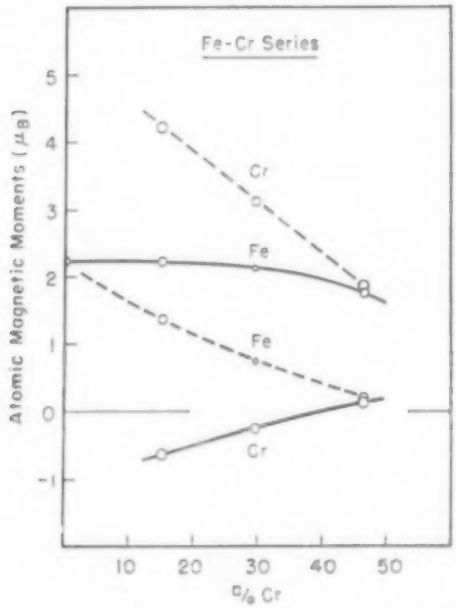

FIG. 24. The Atomic Magnetic Moments present in Fe–Cr alloys (Disordered); alternative values are shown on dashed lines; after SHULL, "Theory of Alloy Phases", A.S.M., p. 279, 1956.

responsible for the atomic moments in the alloys do not differ much among the various transition elements included in the experiments. A particularly interesting result was observed for the cobalt–chromium system, which deviates markedly from the Slater-Pauling average magnetic moment curve. This anomalous behaviour has been interpreted as due to the introduction of anti-ferromagnetic chromium atoms into the cobalt lattice and thus would result in a large decrease of the magnetization. This picture was refuted by the data observed for the magnetic disorder scattering since it was about forty times smaller than had been predicted.

Recently, several authors have proposed schemes for the electronic structures of the transition elements based on the data of Shull and Wilkinson and of Weiss and DeMarco. One of them, that due to MOTT and STEVENS,[120] will be discussed in connection with spin-disorder contributions to electrical

VOL. 9 1961

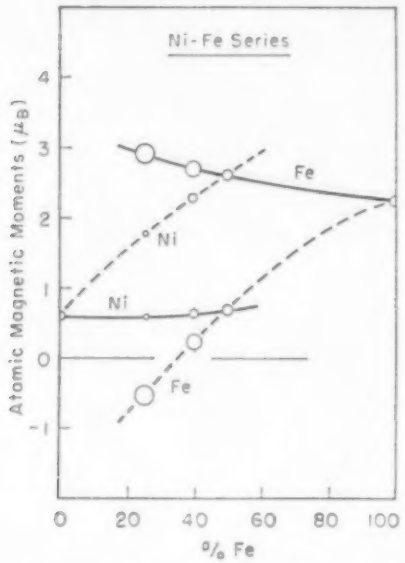

FIG. 25. The Atomic Magnetic Moments present in Fe–Ni alloys (Disordered); alternative values are shown on dashed lines; after SHULL, *loc. cit.*

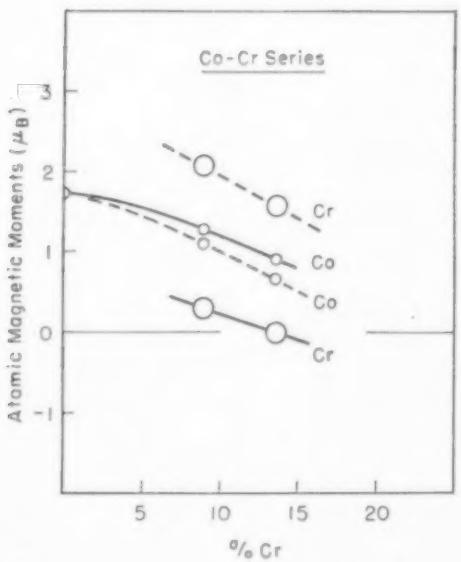

FIG. 26. The Atomic Magnetic Moments present in Co–Cr alloys (Disordered); alternative values are shown on dashed lines; after SHULL, *loc. cit.*

resistivities. Another more recent model has been proposed by Lomer and Marshall in order to explain the magnetic behaviour of binary ferromagnetic alloys. LOMER and MARSHALL[111] propose that we consider the transition metals and their alloys to have the following *electronic structure*:*

(1) The valence electrons are divided into two classes, 4*c* and 3*d* electrons in 4*s* or 4*p* states which serve as conduction electrons distributed over the metal, and *d*-electrons concentrated near each atom.
(2) For some metals, the number of *d*-electrons is a whole number, but in others two different states may be in dynamic equilibrium with the conduction band.
(3) In alloys whose components have the same density of free electrons, each atom retains approximately the *d*-electron configuration of the pure metal.
(4) In alloys where conduction electron densities differ, the number of *d*-electrons may change to decrease the difference. Manganese and iron in high-*d* solvents become high-*d* atoms; Nickel and cobalt in low-*d* solvents tend to lose one or two electrons.
(5) Alloys whose solvent has equilibrium between conduction and *d*-states will have one *d*-state filled by each additional conduction electron added by alloying.

Lomer and Marshal proposed that as the nuclear charge increases and electrons are added to the "argon core" from potassium to chromium, there are practically no electrons in 3*d*-states; they are practically all conduction electrons. At chromium the 3*d*-levels begin to fill and at Co there is a sudden change to a structure with a high number of 3*d*-like electrons and few conduction electrons. This structure is assumed to persist through copper to gallium with filled $(3d)^{10}$ shells. Elements to the left of Fe in the periodic table are "low-*d*"; those to the right are "high-*d*" elements.

Dilute (neglecting solute interactions) binary alloys of the transition elements are grouped into four categories; low-*d* with low-*d*, and high-*d* with high-*d*, low-*d* in high-*d* and high-*d* in low-*d*. In the first two groups each atom retains the configuration of its pure solid. For low-*d* elements in high-*d* solvents some low-*d* elements retain their *d*-structure, but iron and manganese change over to high-*d* structures. High-*d* elements like nickel and cobalt in a low-*d* solvent lose one or two *d*-electrons, the other (like copper and zinc) retain their normal *d*-structure. The magnetic moments in these alloys will be almost entirely that of the 3*d*-electrons. In the case of iron it is noted that conduction electron density changes do not influence the magnetic moment. This is interpreted to mean that the 3*d*-electrons in iron are not in equilibrium

* In this proposed scheme the magnetic properties are assumed to be due essentially to the spin moment of the *d*-electrons only. The interactions between magnetic moments of near-neighbour atoms in a crystal are unknown even as to sign. The magnetic moments of solute elements may be parallel or antiparallel to the moment of a ferromagnetic solvent.

VOL. 9 1961

with the conduction band. On the other hand, there is such equilibrium in the case of cobalt and nickel since the *d*-electron spin moments are suppressed when conduction electrons are added to the system. In iron, cobalt and nickel any *d*-electron spins carried by the solute atoms may contribute either ferromagnetically or anti-ferromagnetically to the total moment. A further conclusion reached by Lomer and Marshall is that the electronic structure *is not* appreciably affected by the crystal structure. They feel that the nuclear charge is the main determining variable (together with the appropriate boundary conditions for the metal) in fixing the electron distribution around the atom. The chemical nature of the nearest neighbours and their arrangement are considered to be of secondary importance. The crystal structure is chosen to be that *most appropriate* to the electronic structure, rather than *vice versa*, for iron, nickel and cobalt. The slight influence of chemical effects is perhaps due to the narrow range of electronegativity of iron, cobalt and nickel. It is not presumed that chemical effects would be unimportant for other solvents. On the basis of this model Lomer and Marshall were able to get quantitative agreement with neutron diffraction experiments carried out on ferromagnetic alloys. Similar agreement with values of the saturation magnetization of these alloys was obtained. Discrepancies were observed for the systems iron–manganese and cobalt–aluminium; both systems have primary solubilities of less than 5 per cent. A smaller degree of success was obtained for alloys of the metals in the later periods. Some difficulty was encountered in fitting the platinum group metals into this scheme. The agreement with data for other properties such as the electrical resistivity and electronic specific heats is fair and is particularly good for cobalt and nickel.

6.2 *Electronic Specific Heats*

One quantity which controls a number of properties of solid solutions is the density of states at the Fermi level, $N(E_{max})$. The low temperature measurements of the linear term in the specific heat of the solid, γT, can be related to $N(E_{max})$ by the following expression derived from the electron theory of metals,

$$C_{el} = \gamma T = \frac{\pi^2 k^2}{3} N(E_{max})\, T,\ k = \text{Boltzmann's constant.}$$

Therefore, measurements of the electronic specific heat coefficient, γ, of alloys will be helpful in interpreting the electronic structure of solid solutions, particularly for dilute solutions. The specific heat measurements are usually carried out at temperatures low enough so that the vibrational terms of the lattice represent only small corrections to the total specific heat in the region of 1° to 4·2°K.

It has been proposed that measurements on dilute alloys of a metal with its nearest neighbours in the Periodic Table would allow one to describe the density of states curve for the metal over small energy ranges above and below the normal Fermi surface; implying the assumption that the band

structure is unaffected by such alloying. HOARE, MATTHEWS and WALLING,[112] and HOARE, KOUVELITES and MATTHEWS[113] have studied Pd-rich Pd-Ag and Pd-Rh alloys in this manner. The results of their specific heat and magnetic susceptibility* measurements for the palladium–silver system indicate a

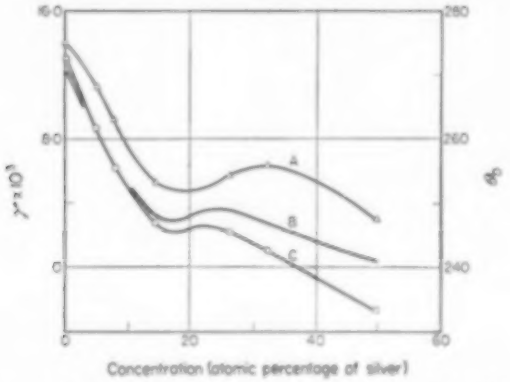

FIG. 27. Values of γ and θ_D versus concentration for Pd–Ag alloys; (*a*) characteristic temperature θ_D; (*b*) corrected γ values; (*c*) experimental data; after HOARE *et al.*[112]

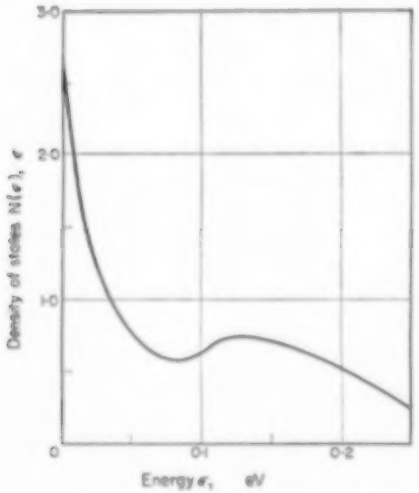

FIG. 28. Band form for Pd as deduced from specific heat measurements; after HOARE *et al.*[112]

decrease in $N(E)$ with silver concentrations as shown in Figs. 27, 28, 29. ELCOCK *et al.*[114] in discussing the palladium–silver data of Hoare *et al.* indicated that the assumption of a parabolic *d*-band is not correct. Data

* The free electron paramagnetic susceptibility is also proportional to the density of states at E_{max}, $N(E_{max})$.

VOL. 9 1961

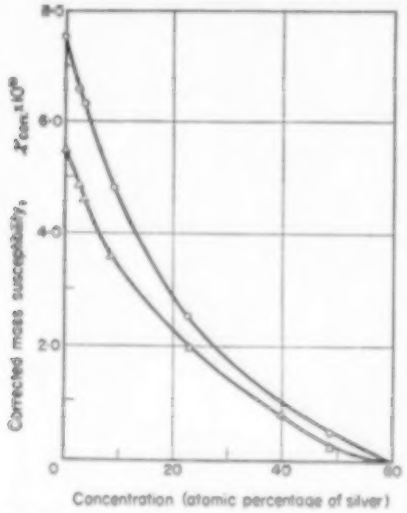

FIG. 29. Susceptibility corrected for core diamagnetism versus concentration for Pd–Ag alloys at 20° and 290°K; Δ, 290°K; ○, 20°K; after HOARE *et al.*[112]

reported for the palladium–rhodium system indicate an increase in the electronic specific heat with the addition of small amounts of rhodium to palladium. This would seem to indicate that E_{max} for pure palladium lies just above a peak in the $N(E)$ curve.

A much more systematic approach to the problem was recently undertaken by WEI, CHENG and BECK[115] for the BCC chromium–iron and chromium–manganese systems. Specific heat curves in the temperature range 1·6° to 4·2°K are reported. The linear temperature coefficient γ is plotted as a function of electron concentration in Fig. 30. A large peak was observed at (·81 Cr)–(·19 Fe) with a γ-value more than ten times that for pure chromium. Measured values of the γ for pure iron are in excellent agreement with data previously reported for iron.[117] Similarly, high γ-values were found also in the chromium–manganese system at corresponding e/A ratios. It is attractive to interpret the data in terms of only the density of states and the electron concentration. However, a correlation of these results with other types of measurements would be desirable. It is well that this important work is continuing. Independent results for the composition (·44 Cr)–(·56 Fe) have been reported by HOARE and MATTHEWS[118] and fit very nicely on the specific heat curve reported by Wei, Cheng and Beck for the chromium–iron alloys.

Experiments similar to those of Wei *et al.* have been performed by RAYNE[116] to determine the electronic contribution to the specific heat in the copper–zinc and copper–germanium systems. The results of these measurements are shown in Fig. 31. They seem to indicate that the Fermi surface in pure copper is not touching the zone boundaries and therefore appear to contradict the

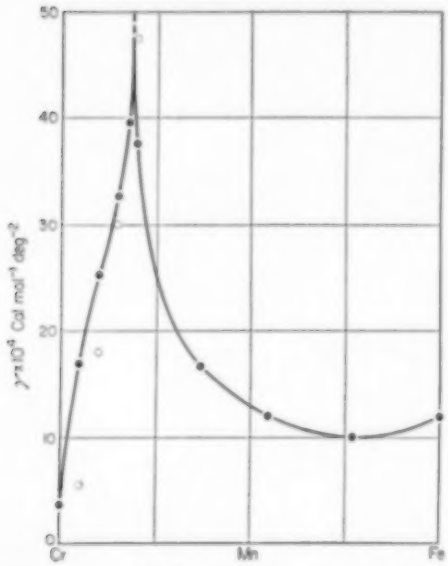

FIG. 30. Low temperature specific heat values versus electron concentration for BCC Cr–Fe and Cr–Mn alloys; after WEI, CHENG and BECK.[115]

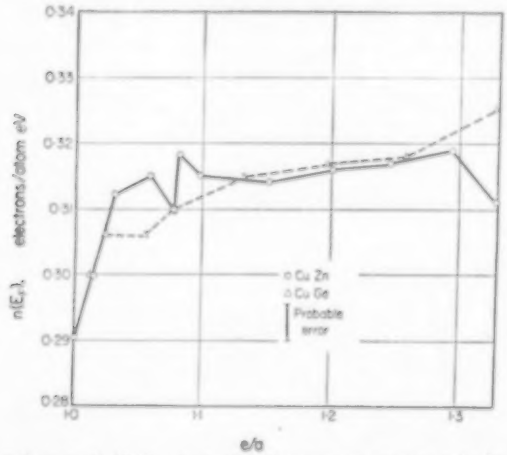

FIG. 31. Dependence of $N(E_{max})$ on the electron-to-atom ratio in Cu–Zn and Cu–Ge alloys as determined experimentally from the electronic specific heat measurements; after RAYNE.[116]

magnetic susceptibility data reported by HENRY and ROGERS,[119] the anomalous skin effect measurements on pure copper reported by Pippard and recent electronic specific heat and optical constant data quoted by COHEN[66] for copper. An interesting aspect of Rayne's results is that up to $e/A = 1{\cdot}1$ the specific heat curves for copper–zinc and copper–germanium agree quite closely. However, for e/A values $> 1{\cdot}1$ the two curves show deviations from

each other with copper–germanium showing an increase in $N(E)$ while copper–zinc shows a decrease in $N(E)$. This effect has not been explained. It is quite apparent from even Rayne's data that the Fermi surface in Cu-Zn overlaps the zone boundaries at an e/A value below 1·1. This is somewhat in line with the value 1·04 proposed by Cohen and is considerably less than that predicted by the original Jones "rigid-band" model, which was estimated to be about at $e/A = 1{\cdot}36$ for the case of spherical energy surfaces. One reason for this large discrepancy lies in the fact that the electrons in copper are not truly free and hence the assumption of spherical energy surfaces is not a valid one.

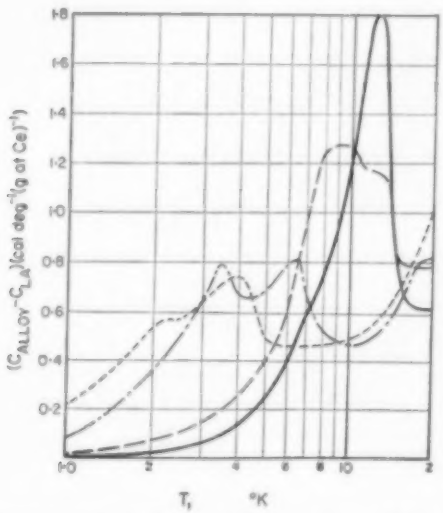

FIG. 32. Excess heat capacities of Ce–La alloys/g-atom of Ce; ———— pure Ce; ——— ——— 78·9 per cent Ce; ——— — ——— — 37·6 per cent Ce; 27·0 per cent Ce —— —— —— ——; after ROBERTS and LOCK.[121]

In the case of transition metals and their alloys the problem of overlapping bands complicates the interpretation of specific heat measurements at 1°K since the bands may or may not be in dynamic equilibrium. The question of equilibrium is important since it determines whether the 3*d* states in metals of the first long period (Ti-to-Ni) can be described in terms of a band model or not. The recent work of MOTT and STEVENS,[120] based on Weiss's 3*d* electron count, indicates that in certain cases a band picture of the 3*d* states is not correct.

Because of the complexity of their atomic structures there has been little or no attempt to calculate the band structure of the rare earth elements and their alloys. However, recent experimental studies of the thermal, magnetic and electrical properties of these materials have lead to some interesting heuristic models of these metals. ROBERTS and LOCK[121] have recently

measured the low temperature specific heats and magnetic susceptibilities of alloys of the cerium–lanthanum system; see Figs. 32 and 33. The specific heats were measured over the range 1·5° to 20°K. The magnetic susceptibility measurements were carried out over the range 1° to 300°K.

Pure cerium shows a single anomaly at 12·3°K which splits into two anomalies in the alloys. These two anomalies move to lower temperatures as the per cent solute is increased (see Fig. 32). The occurrence of the lower temperature anomaly is accompanied by a change in the magnetic properties of the alloys (a maximum occurs in the susceptibility of the most concentrated alloy that was studied and a temperature-independent paramagnetism

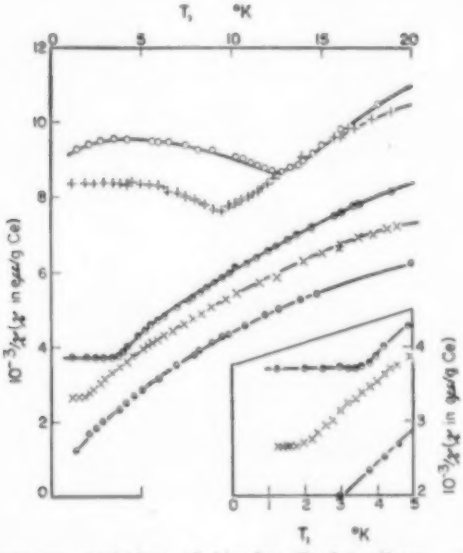

FIG. 33. Temperature variation of $1/\chi$ for Ce–La alloys; ○ ○ pure Ce; + + + 78/9 per cent Ce; 37/6 per cent Ce; × × × 27/0 per cent Ce; ● ● 5/03 per cent Ce; after ROBERTS and LOCK.[121]

occurs in the next two). This has been explained on the basis that antiferromagnetism[121] occurs as the result of 4*f* electron interactions. The fact that a double specific heat anomaly is observed results from a two-stage ordering of the 4*f* electronic orbitals.

The magnetic susceptibilities for all cerium–lanthanum alloys obey a Curie-Weiss law, $\chi = C/(T - \theta)$. The Curie constant C, for this system increases monotonically with increasing amounts of La. The increase in the Curie constant indicates that the population of 4*f* states increases with the amount of lanthanum in solution to about 2 or 3 electrons/cerium atom.*

* The increase in the effective moment of the cerium atoms in the dilute alloys is supposed to arise from a tendency for transitions from the outer valency (5*d* or 6*s*) states to unfilled 4*f* states.

VOL. 9 1961

It is interesting to note that the filling of the 4*f* states of cerium occurs in a manner apparently similar to the filling of 3*d* states of low-*d* elements by high-*d* elements of the first long period.

6.3 *The Electrical Conductivity of Solid Solutions*

The classical free-electron theory* gives the electrical conductivity of a metallic material to be

$$\sigma = \frac{e^2 \tau \, N_{eff}}{m} \quad . \quad . \quad . \quad . \quad . \quad . \quad . \quad . \quad (16)$$

where N_{eff} is the effective number of free electrons per unit volume, e is the electronic charge, m is the electron mass, and τ is the mean-free-time between scattering processes for the electron. From the above τ and N_{eff} must be calculated from quantum theory to obtain the correct value for τ. If we apply wave mechanics we find that

$$N_{eff} = \frac{m}{\hbar^2} \frac{1}{4\pi^3} \int \left(\frac{\partial E}{\partial k}\right)^2 \frac{dS}{|\text{grad } E|} \quad . \quad . \quad . \quad . \quad . \quad . \quad (17)$$

where the integral is taken over the Fermi surface. Looking at Eqns. (16) and (17) it is evident that the conductivity of a metal or an alloy will depend upon two factors:

(*a*) the reciprocal of the probability per unit time that an electron makes a transition or change in energy state as a result of a scattering process; this quantity is equal to τ;

(*b*) the area of the Fermi surface of the "free" conduction electrons.

Therefore, if factors (*a*) and (*b*) are to determine the electrical conductivity of a given material we must know the electronic structure of the solid. We shall develop this idea by considering the origins of the scattering processes which result in a finite electrical resistivity for a solid solution.

In a solid solution, a finite resistance arises from some disorder in the crystalline array of atoms, i.e. deviations from a perfect crystalline structure. This disorder may be caused by thermal vibrations of atoms, and random and non-random distributions of solute atoms, vacancies, or dislocations. In the pure metals at ordinary temperatures, thermal lattice vibrations cause most of the electron scattering and lead to a linear temperature dependence of the resistivity. For the case of binary alloys showing complete solid solubility, the conductivity is a U-shaped curve if plotted as a function of composition (see Fig. 34).[75] Furthermore, the temperature coefficient for the solid solutions will always be below that of the solvent metal.[75] However, the resistivity as a function of temperature may show relationships which differ markedly from the normal linear behaviour that one finds for

* An excellent introduction to theories of electrical conductivity is given in Chap. VII, *The Theory of the Properties of Metals and Alloys* by Mott and Jones; Chap. I, *Progress in Metal Physics*, vol. VI by A. W. Lawson gives a concise review of the results of the theory of electric conduction in metals.

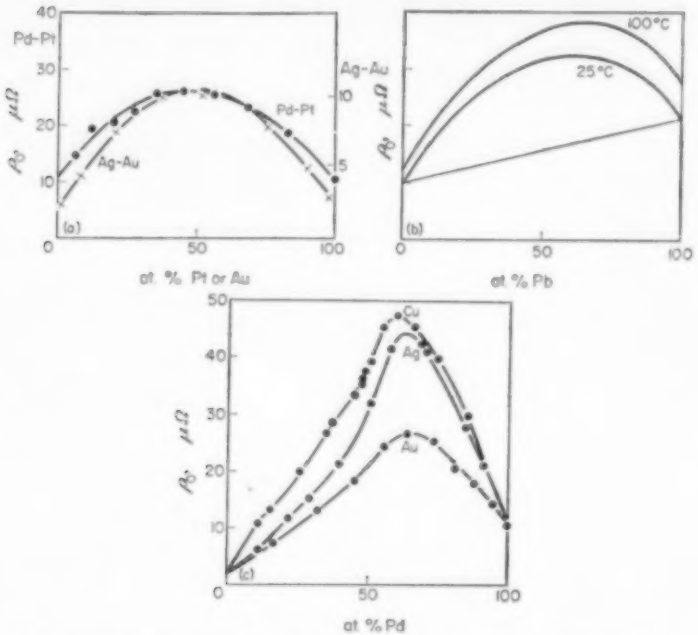

FIG. 34. Electrical resistance for alloys showing a continuous range of solid solutions; (*a*) × × Ag–Au at 0°C, after BECKMAN, Thesis, Upsala (1911); . . . Pt–Pd at 0°C, after GEIBEL, *Zeits. f. an. Chem.* 70 (1911) 240. (*b*) In–Pb at 25° and 100°C, after KURNAKOW and ZEMCZUZNY, *Zeits. f. an. Chem.* 64 (1909) 149. (*c*) Alloys of Cu, Ag and Au in Pd at 0°C; Cu–Pd, Ag–Pd after SVENSSON, *Ann. d. Physik* 14 (1932) 699; Au–Pd after GEIBEL, *loc. cit.*

pure metals. This is particularly true for solid solutions containing transition metals or alloys having magnetic or crystallographic transformations. A corollary to this would be the marked decrease in the resistivity observed for alloys exhibiting substantial ordering.

Some of the most interesting results have been found for the case of dilute solute concentrations; that is, solutions where the solute concentration is so small that the solute atoms do not intact with each other. For dilute solutions then we may write the resistivity as

$$\rho = \rho_{th} + \rho_a \quad . \quad . \quad . \quad . \quad . \quad . \quad . \quad . \quad (18)$$

where ρ = the observed resistivity, ρ_{th} = the resistivity due to thermal vibrations and ρ_a = the resistivity due to electron scattering by the solute atoms. To take account of structural defects like vacancies, dislocations, etc., we may include an additional term expressing the contributions due to these imperfections. The sum of the contributions from the solute atoms and structural defects is usually called the "residual resistance", and is treated as constant in temperature. Eqn. (18) is generally called MATTHIESSEN'S[75] rule and is based on the assumptions that

VOL. 9 1961

(*a*) the temperature is high enough so that all thermal scattering is elastic;
(*b*) the thermal and impurity scattering may be treated independently; showing no interferences;
(*c*) the temperature dependent resistivity is independent of the concentration of solute atoms or imperfections;
(*d*) addition of solute atoms whose valence differs from that of the solvent does not change the N_{eff}.

Actually, none of these assumptions holds strictly as will be indicated in the following discussion. A general calculation of σ means that we must calculate τ and N_{eff} by the methods of the electron theory.[75] In calculating τ it is found that τ is inversely proportional to V_p the difference in potential between the actual lattice and the potential which would exist if the lattice were perfect. Again we have a problem which centres about the determination of a perturbing potential V_p and the electron distribution interacting with it.

MOTT[122] was the first to attempt a calculation of V_p due to solute atoms and treated the case of dilute solutions of silver, gold, zinc, gallium, tin and arsenic in copper. He assumed that all the valence electrons go into the conduction band. An excess contribution to the resistivity arises because the electrons are scattered by the screened Coulomb field of the charges of the solute ion-core. Applying the Fermi–Thomas conditions he determined the scattering potential V_p to be

$$V_p = \frac{Z}{r} e^{-qr}$$

where Z = the excess valence charge of the solute; $Z = +1$ for zinc and $+2$ for gallium. The result obtained for the increment in resistivity per 1 atomic per cent of solute was expressed in the following form

$$\Delta\rho = \frac{2\pi}{100} \frac{z^2e^2m^2}{3\pi^2\hbar^2} V_0 f(y) \qquad (19)$$

$$y = \frac{q^2\hbar^2}{4m^2v^2}, \quad f(y) = \ln(1+y) - \frac{1}{1+y}$$

where e = the electronic charge, m = the electron mass and V_0 is the atomic volume. For the case of monovalent solutes in monovalent solvents the field of the ion-core of e.g. silver or gold in copper is taken to be the difference in the energies between the bottom of the conduction band of the pure metals. Effects due to atomic size were neglected although one expects the addition of a larger ion in the lattice will produce a larger distortion than a smaller ion and hence contribute more to the value of $\Delta\rho$. The above result gives good qualitative agreement for noble metal solvents in general, as can be seen from the results of Linde. LINDE[123] observed that the electrical resistivity is increased with the addition of dilute concentrations of substitutional solute atoms in the following manner:

(i) ρ varies linearly with composition.
(ii) $\Delta\rho = \alpha + \beta Z^2$.

Where $\Delta\rho$ = the resistivity increment for 1 atomic percent of solute, Z = the difference in chemical valence between solute and solvent and α and β are constants. Relation (ii) is just that derived by Mott. Unfortunately, Mott had to assume that $q = 0{\cdot}3$ Å in order to obtain good numerical agreement with experimental results. This is obviously not reasonable on the basis of Friedel's results for screening. The theory also does not apply well for $Z < 0$ since it predicts the same behaviour as is obtained for $Z > 0.(5)$. Actually measured values of the resistivity for transition elements as solutes show unexplained irregularities in their resistivity increment (e.g. from Ti-to-Ni irregular resistivity increments result). The effects observed are also much larger for transition element solutes in the noble metals than are those observed for the case of zinc, gallium, germanium and arsenic (see Fig. 35). This behaviour has been attributed by MOTT [120] to the narrow 3*d* band with its high density of unoccupied states.

The explanation given by MOTT [120] depends on the fact that the transistion probability for the scattering of a conduction electron from an initial state to some final state in the Fermi surface is proportional to the density of states

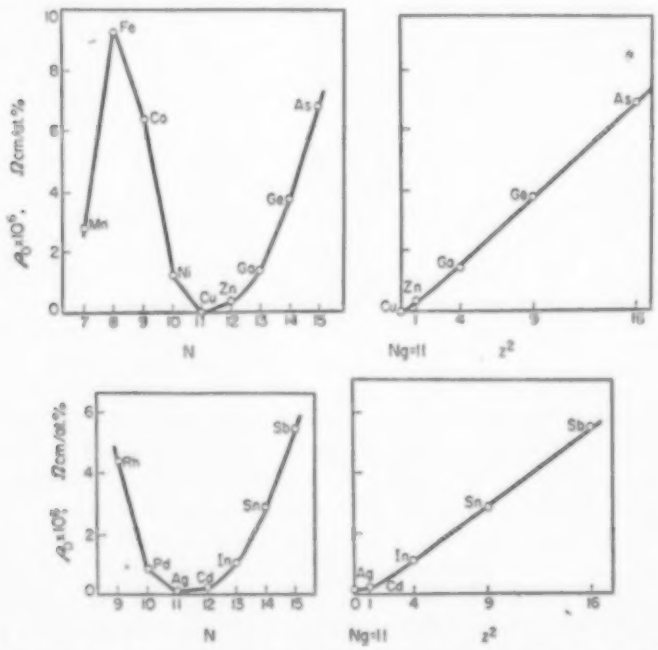

FIG. 35. Increase in resistance of Cu due to one atomic per cent of various metals in solid solution. N is the number of electrons outside an inert gas shell; Z is equal to $(N - 11)$; after LINDE.[133]

at the final state in the Fermi surface. Since the density of states in the *d*-band at the Fermi surface is much higher than the density of *s*-states at E_{max}, the probability for an electron to jump from an *s*-state to a *d*-state is greater than for an ordinary scattering event involving only *s–s* transitions. It should be pointed out that the *s*-electrons scattered into the *d*-band do not stay there. The number of *s–d* transitions is equalled by the number of *d–s* processes so that the net effect is an *s–s* scattering with *d*-states serving as *intermediate* states.

Recently, marked deviations from Matthiessen's rule have been observed for the case of dilute concentrations of transition metals in copper, silver and gold. Certain alloys of finite concentration along with the pure transition and rare earth elements have exhibited similar phenomena. COLES,[124] MOTT[120] and others attribute this to an additional scattering process which is due to the presence of unpaired electron spins localized on particular atoms. Such a process leads to the possibility of the conduction electrons changing their spin states during the scattering process. Therefore a *spin-disorder* scattering can arise from the exchange interactions between the conduction electrons and the unpaired electrons localized on particular atoms if the unpaired spins are randomly oriented.[124] Intuitively this mechanism seems to be the probable one in certain cases, since it is well known that the transition elements do possess permanent spin moments and that exchange interactions are most important in these metals. If the metal or alloy undergoes either ferro- or anti-ferromagnetic ordering of the unpaired spins a marked decrease in resistivity is observed. Resistivity anomalies are observed at the magnetic ordering temperatures if localized spins are present; e.g. the case of the rare earth elements like dysprosium, holmium and erbium[125] as well as the transition elements iron, nickel, cobalt, manganese and titanium (see Figs. 36, 37, 38). Actually, neither *s–d* processes nor spin-disorder scattering will account for all of the resistivity anomalies by themselves. But, in certain cases one or the other will predominate, which can be so determined from the data on the temperature dependence of the resistivity, e.g. *s–d* scattering will predominate where the unpaired spins partly fill as band as in the case of cobalt and nickel. Such is not the case for iron and the rare earth elements.

Spin-disorder resistivity differs from *s–d* scattering in that it is temperature independent above the Néel (or Curie) point. On this basis, we may expand Matthiessen's rule to include spin-disorder by including a term for it in the "residual resistivity". To simplify the discussion we follow COLES[124] in writing Matthiessen's rule as

$$\rho = \rho_{th} + \rho_a = (P_{th} + P_a)\, F$$

where P_a and P_{th} are the perturbations produced by atomic and thermal disorder; F is a factor depending upon the conduction electron configuration, the number of carriers, effective masses and the densities of states to which the electrons are scattered. If ordering occurs in the alloy and the zone of the

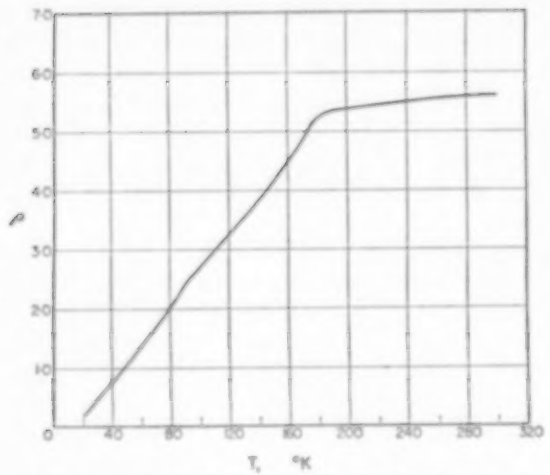

FIG. 36. The electrical resistivity of dysprosium ($\mu\Omega$-cm); after LEGVOLD *et al.*[185]

disordered phase is half full then F increases since the Fermi electrons are now close to the band edge and are therefore less free; e.g. the Hall coefficient of Cu_3Au changes from $-$ to $+$ on ordering.[126] P_a will decrease and will mask the increase in F (since $P_a \gg P_{th}$). Now, if the alloy has localized uncompensated spins the ρ now becomes

$$\rho = (P_a + P_s + P_{th})\, F \quad . \quad . \quad . \quad . \quad . \quad . \quad (20)$$

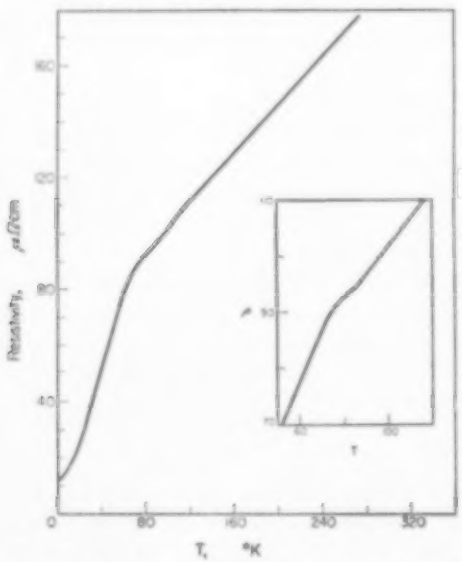

FIG. 37. The electrical resistivity of erbium ($\mu\Omega$-cm); after LEGVOLD *et al.*[185]

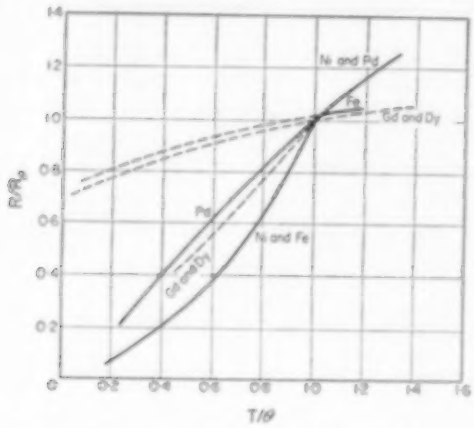

FIG. 38. Reduced electrical resistance of some ferro- and paramagnetic metals; θ is the Curie temperature and R_θ the resistivity there. Ni and Pd, after GERRITSEN;[143] Fe, POWELL, *Proc. Phys. Soc. London*, 51 (1939) 416; Gd and Dy, after LEGVOLD.[125]

This expression is not valid if P_a is large (case of complete disorder). P_s will then be due to both spatial and orientation disorder. Eqn. (20) will be valid only for a spatially ordered array of spins. If the alloy is disordered, spin-disorder will exist well below the Néel (or Curie) point since the spins aligned parallel will be spatially disordered.

The *s–d* scattering processes are explained by the collective band model which predicts the spontaneous magnetization which is observed when magnetic ordering takes place. A collective band model does not allow separation of the resistivity into atomic, spin and thermal contributions since the states to which *s–d* transitions occur are different above and below the Curie (or Néel) temperatures. Because of this, electrical resistivity measurements should give information as to the proper type of wave function to attribute to the magnetic electrons. Exchange interactions could lead to a polarization of the conduction band to states above the Fermi surface of the unpolarized configuration.[127] Thus even the localized spin model may depend upon the degree of magnetic order. In general though, such effects appear to be unimportant.

A comparison of the resistivity vs. temperature data for a number of materials should serve to illustrate more clearly the nature of the processes involved and their relation to the electronic structure of the materials. The rare earths furnish the simplest examples of spin-disorder scattering and of *s–d* scattering. Gadolinium is paramagnetic above 290°K and becomes ferromagnetic below this temperature. The temperature dependence of the resistivity shows an almost linear decrease between 35°K and 290°K (125). Above the Curie point there is a temperature-independent contribution = 120 $\mu\Omega$ cm/°K. KASUYA[129] and others[130] [131] have explained this in terms

of spin-disorder effects. The localized electrons derive their net spin moments from the unfilled 4*f* shell; a similar situation holds for the other rare earths. Dysprosium, holmium and erbium show a slightly different effect. These elements show anti-ferromagnetic ordering with Néel temperatures at 175°, 132° and 84°K.[125] At lower temperatures ferromagnetic transitions occur at 85°, 19·4°, and 19·9°K.[125] The results for dysprosium in Fig. 36 indicate a spin-disorder scattering process which is independent of the *type* of magnetic ordering. Erbium, and α-manganese decrease much less rapidly than is to be

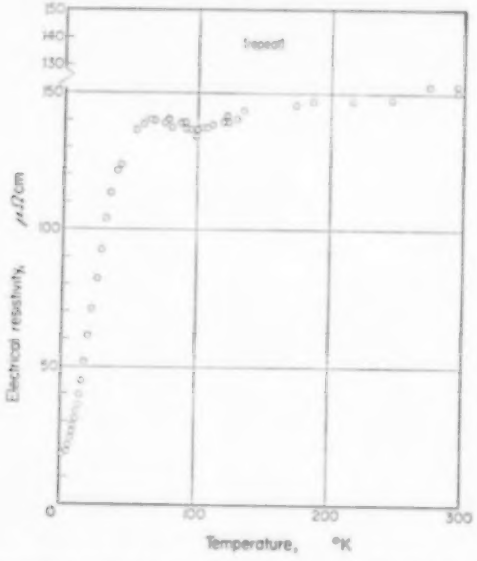

FIG. 39. The electrical resistivity of α-Mn ($\mu\Omega$-cm); after White and Woods.[135]

expected from the onset of magnetic ordering. FRIEDEL[131] attributes this effect to short-range ordering that is analogous to the critical scattering of neutrons in iron near its Curie point. It is not known why this effect does not occur in gadolinium. It is also more difficult to separate the temperature-dependent from the temperature-independent terms than it is for gadolinium.

For similar Debye temperatures and similar conduction electron distributions, some similarity should be observed for the temperature coefficients of resistivity of the rare earths. However, again as in the case of the transition metals, irregularities are observed for the rare earth series and hence we may not describe these elements as differing only in their 4*f* electron configuration.[126]

It has been pointed out that the spin-disorder scattering in alloys can also be sensitive to the amount of atomic order as well as the orientation order of spins. For this reason it is not generally possible to determine whether localized wave functions or a collective band model should be used for the

3d electrons of the transition metals. In some cases, magnetic and electrical data indicate that the localized wave functions would be correct. For example, if the atomic ordering temperature is above the magnetic ordering temperatures then most of the resistivity of the alloy will be due to P_sF over certain ranges of temperature. If the alloy orders magnetically in the anti-ferromagnetic sense then the Brillouin zones of the atomically ordered material will be further subdivided. Au_3Mn is an example of an ordered anti-ferromagnetic alloy [132] where P_sF accounts for most of the high temperature resistance. On the other hand, because Ni_3Cr shows no long-range order no large P_sF term is observed for Ni_3Cr. [133]

Another interesting case is that of Ni_3Mn. [134] It may be more appropriately described in terms of localized spin moments in the manganese atoms, with much smaller localized or collective moments associated with the nickel atoms. Neutron diffraction studies show it to be atomically ordered with a ferromagnetic ordering occurring at 580°C (see Fig. 40). Most noteworthy

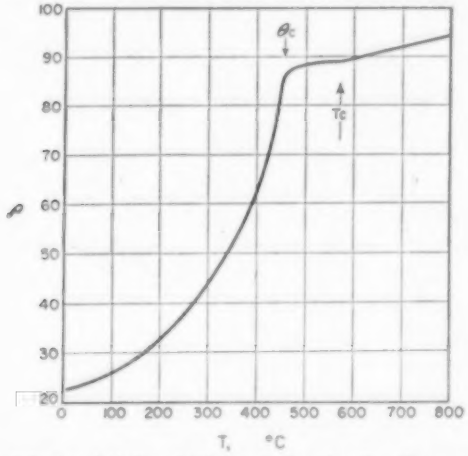

FIG. 40. The electrical resistivity of Ni_3Mn ($\mu\Omega$-cm); after KAYA and NAKAYAMA, *Proc. Phys-Math. Soc. Japan* 22 (1940) 126.

is the slight increase of resistance on atomic ordering (long-range order). Assuming the simple model above we note that a large P_sF term increasing below the long-range order point will easily compensate the decrease taking place in P_aF when P_a, the atomic disorder perturbation, falls to some small value. F will only need to increase about 15 per cent on atomic ordering if P_s is as large as it is in Au_3Mn. At the Curie point, of course, there will be a sharp decrease in P_s and hence the resistivity as the temperature decreases. The ordering temperatures are too close together to allow comparison of the $P_{th}F$ term above and below the long-range order point. However, the slope of the resistivity-temperature curve is smaller than that for pure nickel above the Curie point and would seem to indicate that *s–d* scattering is not as important in Ni_3Mn as it is in pure nickel.

A detailed explanation of the physical properties and alloying behaviour of the transition metals depends on a satisfactory description of their electronic structures. This is not possible as yet, although recent X-ray scattering data reported by WEISS[110] indicates a possible description. MOTT and STEVENS[120] have proposed a reasonable classification of the types of wave functions to be considered for the transition metals based on Weiss's results:

A. a simple Bloch type of 3*d* character,
B. hybridized states of *d*, *s*, *p* character of Bloch type,
C. functions not of the Bloch type localized at particular atoms.

Type A functions belong to a narrow band containing part of E_{max} and hence contribute to conduction. Type B functions belong to a broad band containing part of E_{max} and serve as conduction electron states. Type C functions do not contribute to E_{max} and are non-conducting. Mott and Stevens say that nickel and palladium contain a band of type A states overlapped by a conduction band of free electron states. Iron and manganese are assumed to contain some type C non-conducting states, with outer electrons being in type B states. Chromium is stated as containing some type A which contribute to conduction, overlapping 3*d* states. Earlier elements in the second and third transition groups show no magnetic ordering and neither do those of the first group. Nickel and palladium, the end members of the first and second groups possess a collective band of type A states overlapped by a band of almost free-electron character. This accounts for the similarity in the behaviour of the two.

The complex cubic α-manganese structure exhibits a resistivity-temperature behaviour with one significant feature.[135] The resistivity *rises* when magnetic ordering first takes place and reaches a maximum about 20° below the Néel point (see Fig. 39). This is similar to the behaviour for dysprosium. A critical scattering theory due to short-range order effects has been proposed by Elliot (to be published) but it predicts the maximum to occur *at* the Néel point. However, COLES[124] points out that if magnetic ordering decreased the freedom of the conduction electrons more rapidly at first than it decreased the P_s (spin-disorder) perturbation, such an increase would occur.

Since *s*–*d* scattering plays the predominant role in the resistivities of nickel and palladium, and because of the similarity in their electronic structures, their alloys should show effects determined largely by the variation of the spontaneous magnetization of the *d*-band holes. SCHINDLER *et al.*[136] measured the electrical resistivities in this system and their departure from the simple parabolic form led OVERHAUSER and SCHINDLER[137] to relate the departure to a variation in the relative magnetization and the band form.

Mott and Stevens concluded that on the basis of Weiss's X-ray data iron has two 3*d* electrons and 6 electrons in type B states. Since, in their picture, nickel has 0·5 electrons in the 4*s* band and 9·5 electrons in type A 3*d* states there should be marked differences between the behaviour of iron and

VOL.
9
1961

nickel. Since the α/ϑ transformation in iron occurs just above the Curie point a detailed comparison of the high temperature resistivities of iron and nickel is not possible. However, Mott and Stevens proposed an experiment designed to allow a more detailed comparison of the two metals. The experiment to be described has recently been performed by Coles (to be published). The resistivity of iron is assumed to include a spin-disorder term while that of nickel does not. Therefore if solute elements are added to the two metals whose influence on their band structure is negligible then the effect is just the same as adding another term P_aF to the resistivity of the two pure metals.[120] Ruthenium was added to iron and palladium was added to nickel to obtain such circumstances. The new term P_aF should have a larger value above the Curie temperature than at 0°K for nickel, but will be the same at both temperatures for iron. The resistivity behaviour predicted by Mott and Stevens is shown in Fig. 41. The results of the experiments confirm the predictions for iron and nickel.

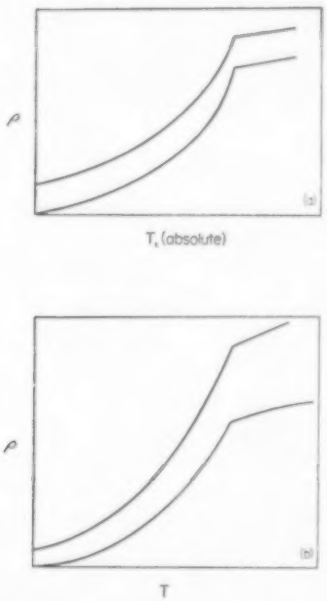

FIG. 41. Predicted behaviour of the electrical resistivity of iron and nickel alloys. (*a*) Fe and Fe–Ru; (*b*) Ni and Ni–Pd; after MOTT and STEVENS.[120]

In closing the discussion of spin-disorder resistivity it will be informative to look at the interesting effects produced by the dilute concentrations of transition metals in copper, silver and gold.[138] Solid solutions of manganese in copper[139] have received the most attention, but solutions of chromium and iron in gold and manganese in silver produce similar effects. The most interesting portion of the resistivity-temperature curves is in the very low temperature regions (see Fig. 42). The alloys are paramagnetic at high

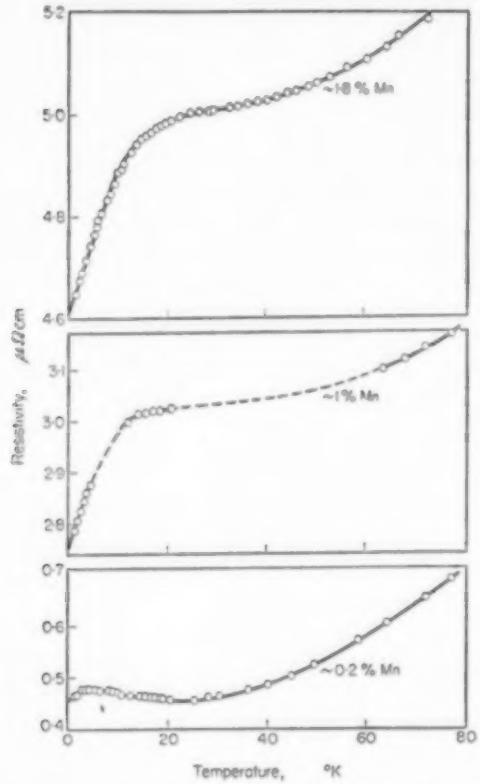

FIG. 42. Low temperature electrical resistivity of dilute Cu–Mn alloys; after SCHMITT and JACOBS.[139]

temperatures with susceptibilities described by a Curie-Weiss type law. Manganese has been theoretically described as having usually a $3d^5$ configuration; susceptibility measurements indicate something closer to $3d^6$. At very low temperatures alloys with as little as 0·1 per cent managanese become anti-ferromagnetic. Alloys with concentrations of greater than 1 per cent manganese[140] show a steady decrease on cooling through the Néel point although the atomic disorder limits the low temperature limit of the resistivity. Solutions of less than 1 per cent manganese concentration show more complex behaviour. This is due to the fact that the magnetic ordering temperature occurs close to a temperature where a minimum in the resistivity occurs. There has been no adequate explanation given yet although an indirect exchange interaction between manganese ions via the conduction electrons seems possible and not inconsistent with data reported on the nuclear resonance absorption in these alloys. Such interactions could lead to a "resonance scattering" of the Fermi electrons[141] and hence to maxima in the observed resistivity at lower temperatures. This prediction would

agree with maxima observed in the resistivity just below the minimum for some still more dilute alloys. Another promising alternative[142] would be to attribute the maximum-minimum low temperature effects to the grain boundaries which would serve as sites for the precipitation of the solutes. These regions of high solute density would serve to present large potential barriers tending to make the passage of conduction electrons more difficult at lower temperatures.

6.4 *Final Comments*

The particular choice of properties for discussion in this review has been an arbitrary one. There are a number of other measurable quantities which may be related to (*a*) the shape of the Fermi surface, (*b*) the width of the conduction band, or (*c*) the wave functions of the conduction electrons. An example of type (*a*) experiments would be the anomalous skin effect which is interpretable solely in terms of the geometrical shape of the Fermi surface.[144] Type (*b*) experiments, such as X-ray emission spectroscopy, lead to a measure of the energy band widths of the conduction states;[145] it is even possible that the shape of $N(E)$ curves may be deduced from the data for simple systems. Type (*c*) experiments are "resonance" experiments such as (1) nuclear spin resonance or (2) electron spin resonance experiments from which one may deduce the symmetry of the conduction electron wave functions.[146] No discussion will be given of these phenomena although a further study of them promises to be fruitful in advancing the state of knowledge of the structure and properties of solid solutions.

It is apparent from the recent experimental and theoretical studies reported that the effect of solute atoms on the band structure of the solvent metal is complicated even for the case of the simple noble metals copper, silver and gold. COHEN and HEINE,[23] in their discussion of the alpha-solid solutions of copper, silver and gold, indicate a possible approach which could restore order to present concepts of alloy formation. They assume a specific band model for the noble metals and then propose that adding a solute increases the electron-to-atom ratio while simultaneously changing the form of the band structure. The key feature of their model is the dependence on the energy gap between the conduction band and the next higher energy band. The energy gap is estimated by relating it to the atomic *s–p* excitation energies of solute and solvent. The importance of the energy gap results from the dependence of the curvature of the Fermi surface on the magnitude of the gap. General trends in band structure with position in the periodic table can then be interpreted in terms of the *s–p* excitation energies and the atomic volume, which increase as one moves down or to the right of the table. For copper-base alloys a large atomic volume means a small Fermi energy, while an increasing atomic number means an increase in *s–p* excitation in copper alloys; both favour a small energy band gap, which favours a spherical energy surface. It is this effect which Cohen and Heine believe causes a breakdown in the "rigid band" model of solid solutions.[6]

The original explanation of the Hume-Rothery rules was given by Mott and Jones (*loc. cit.*) in 1936. Assuming spherical energy surfaces for E_{max} they were able to apply the rigid band model to copper, silver and gold-base alloys. Phase transformations were shown to occur if the density of states were to drop sharply. This will happen at $e/A = 1{\cdot}36$ for spherical energy surfaces. For the case of polyvalent solutes alloyed with Cu the high s–p excitation energy of the solutes causes the energy gap to decrease and the Fermi surface to become more spherical. Therefore, the original explanation of the Hume-Rothery valence rule is probably correct even though contact occurs in pure copper. A similar situation probably holds for silver since optical and thermal data quoted by Cohen indicate the Fermi surface is spherical in silver.

On the other hand, an increase in the average s–p excitation energy of gold-base alloys will cause an increase in the band gap due to a different symmetry character of the electron wave functions at the band edges. This means that the Fermi surface in Au which is already distorted (Cohen[23]) becomes more distorted. Such an effect would cause a breakdown in the Hume-Rothery rule for α to β phase changes. The e/A value at which transformation occurs should then be lower because of the considerable contact of the Fermi surface with the zone boundaries in pure gold, which increases with alloying. Cohen and Heine point out that this explanation provides better agreement with the observed solubility limits than does the explanation based on the effect of the electrochemical factor.

VOL.
9
1961

BIBLIOGRAPHY

[1] HUME-ROTHERY, W. and RAYNOR, G.; *The Structure of Metals and Alloys*, Institute of Metals, 1954.

[2] RAYNOR, G.; *The Band Structure of Metals*, Rep. on Prog. in Phys., The Physical Society, Vol. XV, 1952.

[3] SLATER, J. and KOSTER, G.; *Phys. Rev.* (1954) 94, p. 139; 95, p. 1167; 96, p. 1203.

[4] WANNIER, G.; *Phys. Rev.* 52 (1937) 191.

[5] FRIEDEL, J.; *Phil. Mag.* 43 (1952) 153; *J. Phys. Radium* 14 (1953) 561; *Advanc. in Phys.* 3 (1954) 446.

[6] JONES, H.; *Proc. Roy. Soc.* A144 (1934) 396; *Proc. Phys. Soc.* 49 (1937) 250.

[7] MOTT, N.; *Prog. Met. Phys.* Vol. III, p. 76, Pergamon Press, 1952.

[8] DAVIS, W. and KEEPING, E.; *Phil. Mag.* 7 (1929) 145; SPENCER, J. and JOHN, M., *Proc. Roy. Soc.* A116 (1927) 61; ENDO, H.; *Sci. Rep. Tohoku Univ.* 14 (1925) 479.

[9] MEYERING, J.; *Rev. Metall.* 49 (1952) 906; GUINIER, A.; *Acta Cryst., Camb.* 5 (1952) 121.

[10] KUBASCHEWSKI, O. and EVANS, E.; *Metallurgical Thermochemistry*, Pergamon Press, 1951; WALKER, C., BLIN, J. and GUINIER, A.; *C.R. Acad. Sci., Paris* 235 (1952) 254.

[11] RUDMAN, P., FLINN, P. and AVERBACH, B.; *J. Appl. Phys.* 24 (1953) 365.

[12] GUINIER, A.; *Acta Cryst. Camb.* 5 (1952) 121.

[13] AVERBACH, B., FLINN, P. and COHEN, M.; *Acta Met.* 2 (1954) 92.
[14] WALKER, C.; *J. Appl. Phys.* 23 (1952) 118; KUBASCHEWSKI, O. and EVANS, E.; *Metallurgical Thermochemistry*, Pergamon Press, 1951.
[15] HENRY, W.; *Canad. J. Phys.* 36 (1958) 611.
[16] VARLEY, J. O.; *Phil. Mag.* 45 (1954) 887.
[17] MOTT, N.; *Proc. Phys. Soc.* 49 (1937) 258.
[18] KLEPPA, O.; *Det. Kgl. Norske Vid. Sels. Skr.* (1956) NR 6.
[19] KLEPPA, O.; *J. Phys. Chem.* 60 (1956) 852.
[20] KLEPPA, O.; *J. Phys. Chem.* 60 (1956) 846.
[21] KLEPPA, O.; *J. Phys. Chem.* 60 (1956) 858.
[22] KLEPPA, O.; *J. Phys. Chem.* 60 (1956) 446.
[23] PIPPARD, A. B.; *Phil. Trans. A*, 250 (1957) 325; COHEN, M.; *Phil. Mag.* 3 (1958) 762.
[24] COHEN, M. and HEINE, V.; *Advances in Physics*, 7 (1958) 395.
[25] PEARSON, W. B.; *Lattice Spacings and Structures of Metals and Alloys*, Pergamon Press, London, 1958.
[26] VEGARD, L.; *Zeit. für Physik* 5 (1921) 17; *Zeit für Kristall.* 67 (1928) 148.
[27] MEHL, R. F. and MAIR, B. J.; *J. Amer. Chem. Soc.* 50 (1928) 55.
[28] ESHELBY, J. D.; *Solid State Physics*, vol. 3, 79, Academic Press, 1956.
[29] HUANG, K.; *Proc. Roy. Soc.* A190 (1947) 102.
[30] MILLER, P. and RUSSELL, B.; *J. Appl. Phys.* 24 (1953) 1248.
[31] MILLER, P. and RUSSELL, B.; *J. Appl. Phys.* 23 (1952) 1163.
[32] FRIEDEL, J.; *Phil. Mag.* Ser. 7, 46 (1955) 514.
[33] AXON, H. and HUME-ROTHERY, W.; *Proc. Roy. Soc.* A193 (1948) 1.
[34] OWEN, E. A.; *J. Inst. Metals* 73 (1947) 471.
[35] RAYNOR, G. V.; *Trans. Faraday Soc.* 45 (1949) 698.
[36] LINDE, J. O.; *Ann. Phys.* 15 (1932) 219.
[37] FLINN, P., AVERBACH, B. and COHEN, M.; *Acta Met.* 1 (1953) 664.
[38] RUDMAN, P. and AVERBACH, B.; unpublished work.
[39] RAYNOR, G. V.; *Proc. Roy. Soc.* A174 (1940) 457.
[40] HUME-ROTHERY, W. and RAYNOR, G.; *Proc. Roy. Soc.* A177 (1940) 27.
[41] WALKER, C. B. and MAREZIO, M.; *Acta Met.* (to be published).
[42] VON BATCHELDER, F. and RAECHLE, R.; *Phys. Rev.* 105 (1957) 59.
[43] PINES, B. J.; *J. Eksp. Teor. Fisiki*, 11 (1941) 147.
[44] LAWSON, A. W.; *J. Chem. Phys.* 15 (1947) 831; *Trans. Amer. Soc. Metals* A42 (1950) 85.
[45] CRUSSARD, C.; *Metaux et Corros.* 25 (1950) 203.
[46] ESHELBY, J. D.; *J. Appl. Physics* 25 (1952) 1249.
[47] FRIEDEL, J.; *loc. cit.*
[48] LUMSDEN, J.; *Thermodynamics of Alloys*, Inst. of Metals, 1952.
[49] WAGNER, C.; *Acta Met.* 2 (1954) 242.
[50] ORIANI, R.; *Acta Met.* 4 (1956) 15.
[51] RUDMAN, P.; *Theory of Alloy Phases*, p. 311, Amer. Soc. for Metals, 1956; Sc.D. Thesis MIT, 1955.
[52] LUMSDEN, J., *loc. cit.*; AVERBACH, B., FLINN, P. and COHEN, M.; *Acta Met.* 2 (1954) 92.
[53] BRAGG, L.; *Les Electrons dans Metaux*, Solvay Conf., 1954, discussion of Friedel's paper.
[54] ORIANI, R.; *J. Phys. Chem. Solids*, 2, 327, Pergamon Press, 1957.
[55] FRIEDEL, J.; *Les Electrons dan Metaux* 183, Solvay Conf., 1954.
[56] NOWICK, A. S.; *J. Phys. Chem. Solids* 5 (1958) 147.
[57] SEITZ, F.; *Imperfections in Nearly perfect Crystals*, Report on the Poconos Conf., p. 1, John Wiley, 1952.
[58] FUMI, F.; *Phil. Mag.* vol. 45, ser. 7 (1955) 1007.
[59] BROOKS, H.; ASM Seminar series "Impurities and Imperfections", p. 1, 1955.

[60] LOMER, W. and COTTRELL, A.; *Phil. Mag.* 46, ser. 7 (1955) 711; PANETH, H.; *Phys. Rev.* 80 (1950) 708; HUNTINGTON, H.; *Acta Met.* 2 (1954) 554.
[61] SEEGER, A.; *Phil. Mag.* 46, ser. 7 (1955) 1194; SEEGER, A.; *Les Electrons dan Metaux*, Report of 10th Solvay Congress, p. 391, 1955; *Dislocations and Mechanical Properties of Crystals* (Lake Placid Conf. Report), p. 243, John Wiley, 1947.
[62] SMALLMAN, R. and WESTMACOTT, K.; *Phil. Mag.* 2, ser. 8 (1957) 669.
[63] BARRETT, C. S.; *Trans. A.I.M.E.* 188 (1950) 123; BARRETT, C. and MASSALSKI, T.; *Symposium on the Mechanism of Phase Transformations*, Inst. of Metals, 331, Report No. 18, 1956.
[64] WARREN, B. and WAREKOIS, E.; *Acta Met.* 3 (1955) 473.
[65] COHEN, M. and HEINE, V.; *Advanc. Phys.* 7 (1958) 395.
[66] COHEN, M.; *Phil. Mag.* 3, ser. 8 (1958) 762.
[67] PIPPARD, A.; *Phil. Trans.* A250 (1957) 325.
[68] SIVERTSEN, J.; (to be published).
[69] SUZUKI, H.; *Sci. Rep. Res. Inst. Tohoku Univ.* 4A (1952) 455.
[70] BILBY, B. A.; *Proc. Phys. Soc.* A63 (1950) 191; COTTRELL, A. and BILBY, B.; *Proc. Phys. Soc.* A62 (1949) 49.
[71] COTTRELL, A., HUNTER, S. and NABARRO, F.; *Phil. Mag.* 44 (1953) 1064.
[72] COCHARDT, A., SCHOEK, G. and WIEDERSICH, H.; *Acta Met.* 3 (1955) 533.
[73] WEBB, W. W.; *Acta Met.* 5 (1957) 89.
[74] THOMSON, R.; *Acta Met.* 6 (1958) 23.
[75] PEIERLS, R. E.; *The Quantum Theory of Solids*, Oxford University Press, 1955; JONES, H.; *Handbuch der Physik*, XIX, 1956.
[76] HUNTER, S. and NABARRO, F. R.; *Proc. Roy. Soc.* 220A (1953) 542; HARRISON, W.; *J. Chem. Phys. Solids.*
[77] DEXTER, D. L.; *Phys. Rev.* 87 (1952) 768; JONGENBURGER, P.; *Phys. Rev.* 90 (1953) 710.
[78] KLEMENS, P. G.; *Austral. Journ. Phys.* 6 (1953) 122; SEEGER, A.; *Can. Journ. Phys.* 34 (1956) 1219.
[79] LIPSON, H.; *Progress in Metal Physics*, Vol. 2, p. 1, Pergamon Press, 1950.
[80] MOTT, N.; Discussion of Gayler's Report, *J. Inst. Met.* 60 (1937) 267.
[81] GAYLER, M. L.; *J. Inst. Met.* 60 (1937) 249.
[82] JAUMOT, F. and SAWATZKY, A.; *Acta Met.* 4 (1956) 118.
[83] SIVERTSEN, J. M. and WERT, C. A.; *Acta Met.* (to be published).
[84] MOTT, N. and NABARRO, F. R.; Report on the Strength of Solids, Physical Society, London, p. 1, 1948; MOTT, N.; *Proc. Phys. Soc.* B64 (1951) 729.
[85] COTTRELL, A.; Report on the Strength of Solids, Physical Society, London, p. 30, 1948; COTTRELL, A.; ASM Seminar series *Relation of Properties to Microstructure*, p. 131, 1954.
[86] PARKER, E. R.; ASM Seminar series *Relation of Properties to Microstructure*, p. 30, 1954.
[87] FISHER, J., HART, E. and PRY, R.; *Acta Met.* 1 (1953) 336; FISHER, J. C.; *Acta Met.* 2 (1954) 9; HART, E.; *Relation of Properties to Microstructure*, ASM, p. 95, 1954.
[88] SEEGER, A.; *Dislocations and Mechanical Properties of Crystals*, p. 243, John Wiley, 1957; also papers by H. SUZUKI; J. GARSTONE and R. HONEYCOMBE; C. S. BARRETT; in Section III of this report.
[89] COTTRELL, A.; "Vacancies and Other Point Defects in Metals and Alloys", Inst. of Metals Monograph and Report Series No. 23, p. 1, 1958.
[90] LI, C. H., WASHBURN, J. and PARKER, E.; *Trans. A.I.M.E.* 197 (1953) 1227; MADDIN, R. and COTTRELL, A.; *Phil. Mag.* 46 (1955) 735; KAUFFMAN, J. and MESHII, M.; *Bull. Amer. Phys. Soc.* 2 (1957) 145; KIMURA, H., MADDIN, R. and KUHLMANN-WILSDORF, D.; *Bull. Amer. Phys. Soc.* 3 (1958) 122.

VOL.
9
196

[91] MAKIN, M. J.; U.K. Atomic Energy Research Estab. Report, M/R 2023, 1956; BARNES, R. and HANCOCK, N., U.K. Atomic Energy Research Estab. Report (to be published), 1957.
[92] THOMPSON, D., HOLMES, D. and BLEWITT, T.; *J. Appl. Physics* 26 (1955) 1188; THOMPSON, D. and HOLMES, D.; *J. Appl. Phys.* 27 (1956) 713.
[93] BARNES, R. and HANCOCK, N.; U.K. Atomic Energy Research Estab. Report (to be published), 1957.
[94] THORNTON, P. and HIRSCH, P.; *Phil. Mag.* 3 (1958) 738.
[95] HIRSCH, P. and SILCOX, J.; *Growth and Perfection of Crystals*, p. 262, John Wiley, 1958; HIRSCH, P., SILCOX, J., SMALLMAN, R. and WESTMACOTT, K.; *Phil. Mag.* 3 (1958) 897.
[96] DARKEN, L. S.; (unpublished work).
[97] ALFRED, L. and MARCH, N.; *Phil. Mag.* 2, ser. 8 (1957) 985; PEARSON, S. and BRADSHAW, F.; *Phil. Mag.* 2 (1957) 1387.
[98] WECHSLER, M.; *Acta Met.* 5 (1957) 150.
[99] MCLEAN, D.; "Vacancies and Other Point Defects in Metals and Alloys", Inst. of Metals Monograph and Report Series No. 23, p. 159, 1958.
[100] WARREN, B. and AVERBACH, B.; A.S.M. Seminar series *Research Techniques in Physical Metallurgy*, p. 95, 1953.
[101] AVERBACH, B.; A.S.M. Seminar series *Theory of Alloy Phases*, p. 301, 1956.
[102] WARREN, B., AVERBACH, B. and ROBERTS, B.; *J. Appl. Phys.* 22 (1951) 1493.
[103] HERBSTEIN, F. and AVERBACH, B.; *Acta Met.* 4 (1956) 407.
[104] COLE, H. and WARREN, B.; *J. Appl. Phys.* 23 (1952) 335.
[105] SHULL, C. and WILKINSON, M.; *Rev. Mod. Phys.* 25 (1953) 100; *Phys. Rev.* 97 (1955) 304; SHULL, C.; Report on the 10th Solvay Conf., *Les Electrons dans Metaux*, p. 227, 1955; A.S.M. Seminar series *Theory of Alloy Phases*, p. 279, 1956.
[106] ROBERTS, B. and SWALIN, R.; *Trans. A.I.M.E.*, p. 845, 1957.
[107] NICHOLSON, R., THOMAS, G. and NUTTING, J.; *Brit. J. Appl. Phys.* 9 (1958) 25.
[108] WEISS, R., ANTAL, J. and DIENES, G.; *Phys. Rev.* 99 (1955) 1081.
[109] ATKINSON, H. and HIRSCH, P.; *Phil. Mag.* 3 (1958) 866.
[110] WEISS, R. J. and DEMARCO, J. J.; *Rev. Mod. Phys.* 30 (1958) 59.
[111] LOMER, W. and MARSHALL, W.; *Phil. Mag.* 3 (1958) 185.
[112] HOARE, F., MATTHEWS, J. and WALLING, J.; *Proc. Roy. Soc.* A216 (1953) 502.
[113] HOARE, F., KOUVELITES, J. and MATTHEWS, J.; *Nature, Lond.* 170 (1952) 537.
[114] ELCOCK, E., RHODES, P. and TEVIOTDALE, A.; *Proc. Roy. Soc.* A221 (1954) 53.
[115] WEI, C., CHENG, C. and BECK, P.; (to be published).
[116] RAYNE, J.; *Phys. Rev.* 108 (1957) 22; *Phys. Rev.* 110 (1958) 606.
[117] KEESOM, W. and KURRELMEYER, B.; *Physica* 6 (1939) 663.
[118] HOARE, F. and MATTHEWS, J.; *Proc. Phys. Soc.* 71 (1958) 220.
[119] HENRY, W. and ROGERS, H.; *Phil. Mag.* 2 (1956) 237.
[120] MOTT, N. and STEVENS, K.; *Phil. Mag.* 2 (1957) 1364.
[121] ROBERTS, L. and LOCK, J.; *Phil. Mag.* 2 (1957) 811.
[122] MOTT, N.; *Proc. Camb. Phil. Soc.* 32 (1937) 281.
[123] LINDE, J. O.; *Annalen der Physik* 10 (1931) 52; ibid. 14 (1932) 353; ibid. 15 (1932) 219.
[124] COLES, B. R.; *Adv. in Physics* 7 (1958) 1.
[125] SPEDDING, F., LEGVOLD, S., DANNE, A. and JENNINGS, L.; *Progress in Low Temperature Physics*, North Holland Publishing Co., p. 368, 1957; LEGVOLD, S., SPEDDING, F., BARSON, F. and ELLIOTT, J.; *Rev. Mod. Physics* 25 (1953) 129.
[126] KOMAR, S. and SIDOROW, J.; *J. Phys. Moscow* 4 (1941) 552.
[127] PRATT, G.; *Phys. Rev.* 81 (1957) 440.
[128] PINES, D.; *Solid State Phys.*, Vol. 1, p. 367, Academic Press, 1955.
[129] KASUYA, T.; *Prog. Theo. Phys. (Japan)* 16 (1956) 58.

(130) YOSIDA, K.; *Phys. Rev.* 107 (1957) 396.
(131) FRIEDEL, J. and DEGENNES, H.; *J. Phys. Chem. Solids* 5, 1958.
(132) MEYER, A.; *C. R. Acad. Sci.* (*Paris*), 244 (1957) 2028.
(133) TAYLOR, A. and HINTON, K.; *J. Inst. Metals* 81 (1952) 169.
(134) SHULL, C. and WILKINSON, M.; *Rev. Mod. Phys.* 27 (1955) 304.
(145) WHITE, G. and WOODS, S.; *Canad. J. Phys.* 35 (1957) 346.
(136) SCHINDLER, A., SMITH, J. and SALKOVITZ, E.; *J. Phys. Chem. Solids* 1 (1956) 39; *Phys. Rev.* 108 (1957) 921.
(137) OVERHAUSER, A. and SCHINDLER, A.; *J. Appl. Phys.* 28 (1957) 544.
(138) GERRITSEN, A. and LINDE, J.; Leiden Commun. No. 285c and d; *Physica* 17 (1951) 573, 584; Leiden Commun. No. 290d; *Physica* 18 (1952) 877.
(139) SCHMITT, R. and JACOBS, I.; *Physica* 17 (1951) 584; ibid. 18 (1952) 877.
(140) OTTER, F.; *J. Appl. Phys.* 27 (1956) 196; BACON, G., DUMUR, I., SMITH, J. and STREET, R.; *Proc. Roy. Soc.* 241 (1957) 223.
(141) KORRINGA, J. and GERRITSEN, A.; *Physica* 19 (1953) 457.
(142) LANE, C. T.; *Phys. Rev.* 76 (1949) 304.
(143) GERRITSEN, A.; *Handbuch der Physik* 19 (1956) 187.
(144) PIPPARD, A.; *Les Electrons dans Metaux*, p. 123, 20th Solvay Conference, 1954.
(145) SHAW, C. H.; *Theory of Alloy Phases*, A.S.M. seminar series, p. 13, 1956.
(146) KITTEL, C.; *Les Electrons dans Metaux*, p. 159, 20th Solvay Conference, 1954; BLOEMBERGEN, N.; *Canad. J. Phys.* 34 (1956) 1299.

VOL.
9
1961

OL.
9
961